

2012 Photonics Asia[®]

5–7 November 2012

Technical Abstracts

www.spie.org/pa

Location

Beijing International Convention Center
Beijing, China

Conference

5–7 November 2012



SPIE

Connecting minds. Advancing light.



Photonics Asia®

Sponsored by:



Cooperating Organizations:

Tsinghua University
Peking University
Zhejiang University
Beijing Institute of Technology
Beijing University of Posts and
Telecommunications
University of Science and Technology
of China
Tianjin University
Nankai University
Changchun University of Science
and Technology
University of Shanghai for Science
and Technology
Capital Normal University
Huazhong University of Science and
Technology
Beijing Jiaotong University
Shanghai Institute of Optics and Fine
Mechanics, CAS
Changchun Institute of Optics Fine
Mechanics and Physics, CAS
Institute of Semiconductors, CAS
Institute of Optics and Electronics, CAS
Institute of Physics, CAS
Shanghai Institute of Technical Physics,
CAS
China Instrument and Control Society
Optoelectronics Technology Committee,
COS
SPIE-China Committee
Japan Optical Society
Korea Optical Society
Australia Optical Society
Singapore Optical Society

Supported by:

China Association for Science and
Technology (CAST)
Department of Information of National
Nature Science Foundation, China
(NSFC)

General Chairs:



Eustace Dereniak, SPIE President,
University of Arizona



Bingkun Zhou, COS President,
Tsinghua University

General Co-Chairs:

Arthur Chiou, National Yang-Ming University
Zhizhan Xu, Shanghai Institute of Optics and
Fine Mechanics, CAS
Jianlin Cao, China Ministry of Science and
Technology
Junhao Chu, Shanghai Institute of Technical
Physics, CAS

Technical Program Chairs:

Songlin Zhuang, University of Shanghai for
Science and Technology
Xingde Li, Johns Hopkins University

Technical Program Co-Chairs:

Qiming Wang, Institute of Semiconductors,
CAS
Xu Liu, Zhejiang University
Daoyin Yu, Tianjin University
Qihuang Gong, Peking University
Tianchu Li, National Institute of Metrology
Wei Huang, Nanjing University of Posts and
Telecommunications

Local Organizing Committee Chair:

Guangcan Guo, University of Science and
Technology of China

Local Organizing Committee Co-Chairs:

Guoqiang Ni, Beijing Institute of Technology
Shusen Xie, Fujian Normal University
Xiaomin Ren, Beijing University of Posts and
Telecommunications
Ying Gu, PLA General Hospital
Huilin Jiang, Changchun University of
Science and Technology

General Secretary:

Qihuang Gong, Peking University

Local Organizing Committee:

Yan Li, Chinese Optical Society/Peking
University
Zhiping Zhou, Peking University
Changhe Zhou, Shanghai Institute of Optics
and Fine Mechanics, CAS
Qingming Luo, Huazhong University of
Science and Technology
Chongxiu Yu, Beijing University of Posts and
Telecommunication
Hongda Chen, Institute of Semiconductors,
CAS
Yongtian Wang, Beijing Institute of
Technology
Yiping Cui, Southeast University
Xuping Zhang, Nanjing University
Feijun Song, Daheng Corp.
Cunlin Zhang, Capital Normal University
Yanting Lu, Nanjing University
Yuejin Zhao, Beijing Institute of Technology
Chunqing Gao, Beijing Institute of
Technology
Tiegen Liu, Tianjin University
Xiaocong Yuan, Nankai University
Weimin Chen, Chongqing University
Zhongwei Fan, Academy of Opto-electronics,
CAS
Hanyi Zhang, Tsinghua University
Lan Wu, Zhejiang University
Yongsheng Zhang, University of Science and
Technology of China
Hong Yang, Peking University
Xiaoying Li, Tianjin University
Lin Zhai, Chinese Optical Society

Contents

Click on the conference title and you will be taken to the page

8551	High-Power Lasers and Applications VI	4
8552	Semiconductor Lasers and Applications V	16
8553	Optics in Health Care and Biomedical Optics V	26
8554	Quantum and Nonlinear Optics II	54
8555	Optoelectronic Devices and Integration IV	68
8556	Holography, Diffractive Optics, and Applications V	85
8557	Optical Design and Testing V	101
8558	Optoelectronic Imaging and Multimedia Technology II	123
8559	Information Optics and Optical Data Storage II	146
8560	LED and Display Technologies II.	153
8561	Advanced Sensor Systems and Applications V.	158
8562	Infrared, Millimeter-Wave, and Terahertz Technologies II . . .	174
8563	Optical Metrology and Inspection for Industrial Applications II	193
8564	Nanophotonics and Micro/Nano Optics.	205

SPIE would like to express its deepest appreciation to the symposium chairs, conference chairs, program committees, session chairs, and authors who have so generously given their time and advice to make this symposium possible.

The symposium, like our other conferences and activities, would not be possible without the dedicated contribution of our participants and members. This program is based on commitments received up to the time of publication and is subject to change without notice.

Conference 8551: High-Power Lasers and Applications VI

Monday - Wednesday 5 -7 November 2012

Part of Proceedings of SPIE Vol. 8551 High-Power Lasers and Applications VI

8551-2, Session 1

Theoretical and experimental investigation of Rb-Ar excimer pumped alkali laser characteristics

Desheng Yue, Wenyu Li, Hongyan Wang, Zining Yang, Xiaojun Xu, National Univ. of Defense Technology (China)

Diode Pumped Alkali Laser (DPAL) has been identified as one of the most promising high energy lasers due to its combination of solid-state laser's compactness, high efficiency and gas laser's easy thermal management. However, commercial diode laser stack typically emits with spectral widths of 1000 GHz, which must be narrowed down 2 orders magnitude to match alkali atom's absorption bandwidth. And the small hydrocarbon molecule added in DPAL to accelerate P3/2 and P1/2 state mixing may react with alkali atoms at elevated temperature.

Recently, Excimer Pumped Alkali Laser (XPAL) was proposed to solve the two disadvantages. By pumping alkali-rare gas atomic collision pairs, named excimer's broad blue spectral satellites, commercial diode stacks could be directly used, and the hydrocarbon would not be needed any more. The Cs-rare gas XPAL had been thoroughly studied by group of University of Illinois with short pulsed dye laser, while the Rb-rare gas XPAL's report is rare.

In this paper, theoretical and experimental study of Rb-Ar four level XPAL was put forward. A self-made 10 nanosecond pulsed optical parametric oscillator was acted as the surrogate pump source, and successful lasing in 780nm was realized in a broad spectra range centered at 755nm. A time dependent rate equation model was carried out to study the Rb-Ar laser's threshold and cw running characteristics. It was found that due to the extreme low absorption cross-section of blue wing satellites, much higher pump intensity than DPAL is needed to get population inverted. To realize high efficient cw running, high efficient absorption of pump light must be assured.

8551-3, Session 1

Gas dynamic effect in high-energy fluid diode pumped alkali vapor laser

Yao Xu, Wenyu Li, Hongyan Wang, Zining Yang, Xiaojun Xu, National Univ. of Defense Technology (China)

In the field of high energy lasers, diode pumped alkali laser has become one of the high lights in recent years. Our team has done abundant researches on spectral linewidth narrowing for diode pumping lasers, side-pumped DPAL model setting with flowing medium, etc, both theoretically and experimentally. And we obtained 795nm Rb vapor laser by using a volume Bragg grating stabilized diode laser bar on Jul, 2011.

With the aim to improve the power of DPAL, one of the hotspots today is to solve the heat sinking problem by using cycled flowing medium method. However, gas dynamic effects haven't been taken into consideration in all these methods. In this paper, a one dimensional heated pipe flow model is set to discuss the influence that alkali active media heat source brings to the thermodynamics parameters of the gas. We discover that due to the small size of the volume source, the heat giving out per volume is huge which notably affects the velocity, temperature and the density of the active medium along the direction of the flow. As a result, the rectangular cross section of the pipe needs to be redesigned. With the help of fluid dynamics software based on limit volume method, we calculate the influence a MW light field brings to the volume source and analyze the boundary layer effect. These work can be a reference to the researches on high energy fluid diode pumped alkali vapor laser.

8551-4, Session 1

Competition between spontaneous radiation and ionization in the process of resonance enhanced multi-photon ionization

Guiyin Zhang, Haiping Li, Haiming Zheng, North China Electric Power Univ. (China); Hui Ji, North China Electric Power University (China)

With the coming forth of high power laser, the technique of resonance enhanced multi-photon ionization (REMPI) spectroscopy has become one of the important methods for studying the high excited energy levels and the dynamics of chemical reaction of atoms and molecules.

Photo-ionization probability is an important factor in the practical use of REMPI. To a certain experimental condition, it depends on the competition between spontaneous radiation and ionization of the excited particles. In this work, we investigate the influence of laser resonance detuning, Rabi frequency and ionization rate on spontaneous radiation and ionization in the process of REMPI with the theory of density matrix equation. A model of three energy level system is adopted. It is found that the spontaneous radiation and ionization probability increase with the decrease of laser resonance detuning. They get to the maximum when resonance detuning is zero. The line width of spontaneous emission will decrease with the increase of ionization rate due to the competition between spontaneous radiation and ionization. In addition, the spontaneous radiation and ionization probability increase with Rabi frequency until gets to saturation. Laser resonance detuning has no influence on the saturation value. It only influences the Rabi frequency for saturation. If Rabi frequency increases further after saturation, the spontaneous radiation will decrease because of the phenomena of energy level splitting in strong laser field. Now that resonant absorption and large laser intensity can increase the ionization probability greatly, so we must select suitable laser frequency and large laser intensity in the practical use of REMPI, in order to get optimum detection result.

8551-5, Session 2

Variation of thermal lens curvature type between the convex and the concave lens for zigzag slab laser

Xing Fu, Qiang Liu, Mali Gong, Tsinghua Univ. (China)

In this letter, we investigate the thermal lensing along the direction of heat removal in a zigzag slab laser by numerically computing its temperature distribution, the OPD profile and the focal length of the thermal lens. Particular attention is paid to the dependence of the curvature type of the thermal lens on the number of bounces. As the number of bounces increases consecutively, the curvature type of the thermal lens in the slab thickness direction oscillates between the concave lens and the convex one, but not in an alternate manner. The reason is disclosed that for the convex lens case, the average temperature along the route, through which the ray on the edge of the main lobe aperture travels is much lower than that at the center. The formation of the concave lens can be well explained in a similar way. In addition, we conclude that the beamlet with a larger number of bounces experiences weaker thermal lensing but more serious wavefront deformation due to the large side lobe portion in the curve of optical path difference.

The analysis and the discussion provide a good reference for the design of slab parameters and the selection of the number of bounces. Furthermore, multiple zigzag slabs with different curvature types of thermal lenses can be placed in a cavity or lined up as a multi-stage amplifier, which may compensate the thermal lensing and the wavefront deformation, thus improving the beam quality.

8551-7, Session 2

Nonlinear imaging properties of two parallel gain-typed wirelike scatterers

Jie Huang, Yonghua Hu, Hunan Univ. of Science and Technology (China)

Based on the optical path model for nonlinear imaging, we systematically investigated the propagation of flat-topped Gaussian beam which is modulated by two parallel gain-typed wirelike scatterers through computer simulation. It is found that hot image for each scatterer can be formed, with the hot image plane several centimeters behind the predicted conjugated plane obtained by the approximate theory for attenuation-typed scatterers. When compared with the case where only one scatterer exists, the hot image intensity can be relatively smaller under certain parameters. Moreover, it is found that the object distance, i.e. the distance from the scatterer plane to the incident surface of the Kerr medium slab, has an important influence on the propagation properties and results in some new phenomena. Firstly, under certain object distances, the evolution of the maximum intensity of the beam has one prominent peak before that for hot image, where the on-axis location is dozens of centimeters ahead of the hot image plane, and as the size of the scatterers increases, the distance between these two planes decreases at first, then increases and decreases at last; the value of this peak increases at first and then decreases. The intensity distribution corresponding to this peak shows that, there is an intense fringe, which is the most intense fringe in the plane, at the middle point of the line connecting the two scatterers, indicating that it is a unique result of the interaction of the two scatterers. Second, under some other object distances, the evolution of the maximum intensity of the beam also has one prominent peak before that for hot image, but there are two fringe pairs corresponding to each scatterer in the intensity distribution.

8551-8, Session 2

In-situ measurement based on prior calibration with analogist samples for laser cladding

Jichang Liu, Yaoting Wu, Lei Wang, Hunan Univ. (China)

A system, consisting of a CCD camera, a frame grabber and a computer, is developed to in-situ measure the molten pool parameters during laser cladding based on prior calibration with analogist samples. The signals acquired during laser cladding vary with change in substrate material or clad material, so that, in order to gain the true data of the molten pool parameters, calibration of the instrument must be performed for every set of substrate and clad materials. In this study, a new strategy for on-line acquisition of molten pool parameters is presented. Before measurement of the objective molten pool, cladding is performed to get some analogist samples of the same materials as those used to generate the objective molten pool. The width of a certain segment of the clad bead on the analogist sample is gauged to calibrate the CCD camera-grabbed image of the molten pool which solidify to this segment of the clad bead. The pool width in the grabbed image can be confirmed to the gauged bead width times the scaling because the width of the clad bead segment must be equal to the width of the related pool. It is assured which type of area in the grabbed image is located on by the pool, and the CCD is calibrated for this set of substrate and clad materials. After calibration, the CCD system is applied to in-situ measure the molten pool parameters during laser cladding. In the presented experiments, the measured values agree well with the actual ones.

8551-9, Session 2

Low threshold cholesteric liquid crystal based laser with temperature-tunable characteristics

Yongjun Liu, Feiru Wang, Xiaoqi Liu, Harbin Engineering Univ. (China)

In cholesteric liquid crystal based laser, the periodic helical structures of cholesteric liquid crystal is used to replace resonator and laser dyes to laser medium. With proper orientation treatment and pump light, high monochromaticity laser of 5nm has been gained. the threshold and power are discuss in the paper. By changing pumping light, exit light gets weak, then the threshold measurement of laser is done. To gain high power and low threshold laser, improvement measures are proposed and texted, such as experiment temperature, thickness of liquid crystal layer and angle of pumping light. Among these, the experiment temperature also affect the wavelength of exit light by changing helical pitch and refractive index of cholesteric liquid crystal. At the temperature from 30°C to 43°C, the wavelength changes observantly, gradually and slowly. At the same time the transmissions of cholesteric liquid crystal at different temperature are texted to verify relationship between the wavelength of exit light and transmissions spectrum. Though this, we can conclude the wavelength of exit light always at the right fall edge of transmissions spectrum. Low threshold cholesteric liquid crystal based laser with temperature-tunable characteristics can be obtained by altering the experiment condition above.

8551-10, Session 2

Analysis of convective heat transfer coefficient for SG-II Prototype

Zhiyuan Ren, Jianqiang Zhu, Zhigang Liu, Hongbiao Huang, Shanghai Institute of Optics and Fine Mechanics (China)

The forced convective heat transfer coefficients during the period of thermal recovery for laser slab on the multi-segment amplifies of SG-?is analyzed. We have simulated the parameters including coolant gas and the geometry of amplifier with computational fluids dynamics (CFD) method. Based on the simulated results, we attained the optimized parameters such as the flow rate, the temperature and the type of gas, the diameter of inlet jet, the quantity of inlet jet, the distance between the inlet jet and the laser slab, the spray angle of inlet.

8551-11, Session 3

Ultra-fast ytterbium fiber laser operating at low repetition rate (*Invited Paper*)

Jean-Bernard Lecourt, Simon Boivinnet, Yves Hernandez, Multitel A.S.B.L. (Belgium)

Ultra-fast lasers operating at 1 μm have been used in a lot of industrial applications such as micromachining. Among all the available sources, the recently developed All Normal Dispersion (ANDi) mode-lock fiber lasers are of particular interest because they are compact, alignment-free and able to deliver high pulse energy. In this study, we report a Polarization Maintaining (PM) ANDi all-fibered laser passively mode-locked with a SESAM exhibiting high modulation depth (25%) and ultra-fast relaxation time (~500 fs). We have focused on the possibility to operate with both ultra-short pulses (<1 ps) and low repetition rate (<10 MHz), thus a great care has been taken to manage chromatic dispersion and spectral filtering in the cavity. We observed that a strong spectral filtering is required to operate with stable and ultra-short optical pulses in a highly dispersive cavity. The built laser is a unidirectional ring cavity composed of PM components (optical coupler, multiplexer and circulator), PM fiber Bragg gratings and PM Yb-doped fiber pumped

by a single-mode 976 nm laser diode. The repetition rate has been set to 7.7 MHz, corresponding to the cavity roundtrip. The laser delivers picoseconds highly chirped optical pulses that are compressible down to about 800 fs (Fourier transform limit). The optical spectrum is centered at 1065 nm with a bandwidth of 2 nm. The output power is 4.7 mW leading to a pulse energy of 0.6 nJ.

8551-12, Session 3

Single mode linearly polarized high power fiber laser at 1120 nm

Jianhua Wang, Shanghai Institute of Optics and Fine Mechanics (China) and National Univ. of Defense Technology (China); Lei Zhang, Jinneng Hu, Yan Feng, Shanghai Institute of Optics and Fine Mechanics (China); Jinbao Chen, National Univ. of Defense Technology (China)

We will report our recent progress in developing 1120nm Yb-doped fiber laser. QCW fiber laser at 1120nm with about 100 W peak power was realized, which was successfully used for achieving single frequency Raman fiber amplifier at 1178nm with a peak power of 40W. The polarization extinction ratio of 16dB was measured. At the same time, high power fiber amplifier at 1120nm will be also researched for Raman amplifier. As far as we know, this is the first detailed report about 100W-class Yb-doped linearly polarized single mode fiber laser at 1120nm. In this paper, we will detailed analyze the factors impacting on Yb-doped fiber emitting at 1120 nm.

8551-13, Session 3

High average/peak power all fiber pulse laser from picosecond to microsecond regime

Xiaolin Wang, Pu Zhou, Zhiqun Gong, Hanwei Zhang, Rumao Tao, Xiaojun Xu, National Univ. of Defense Technology (China)

We demonstrated four types of high power/energy all fiber pulse laser in master oscillation-power amplification configuration at 1 μ m wavelength from ps to μ s regime. The picosecond pulsed amplifier is based on an active phase modulated mode-locked seed laser, and more than 196.5W average power, 0.96 μ J pulse energy at ps regime is obtained. The 10ns amplifier is based on intensity modulated single-frequency pulse seed, and 0.5mJ pulse energy, 32.4kW peak power pulses at 15ns regime is obtained, which is considered to be the highest peak power in single-frequency pulse fiber laser. The 100ns pulse amplifier is based on a Q-switched seed laser, 6.2mJ, 33.8kW peak power pulses at 170ns is obtained. The fourth one is based on an active phase modulated Q-switched laser, more than 100W average power and 5mJ pulse energy at μ s regime is obtained. The fiber core/cladding diameters in the final stage amplifier of the four types of amplifiers are of 50/400 μ m, 50/400 μ m, 30/400 μ m, and 30/400 μ m, respectively. In experiment, we coiled the fiber to an appropriate diameter and strip off the high order mode as well as pump light to improve the beam quality. The measured beam quality M² in the 10ns and 100ns amplifiers are both about 3, and the measured beam quality M² in the ps and μ s amplifiers are about 1.5. All pulse amplifiers work steadily without any distinct nonlinear effects such as Stimulated Brillouin and Raman scattering.

8551-14, Session 3

Yb³⁺-doped fiber laser operating at long wavelength

Hanwei Zhang, Pu Zhou, Hu Xiao, Xiaolin Wang, Xiaojun Xu, National Univ. of Defense Technology (China)

Yb³⁺-doped fiber lasers (YDFL) have an important advantage of possessing a broad emission spectrum range (970 nm-1200 nm). Most of recent research of YDFL focuses on the wavelength range between 1030-1120 nm. Exploring the operation of long wavelength (> 1120nm) may increase the number of applications. For example, YDFL operating at 1150-1180 nm is quite attractive for creation of yellow light sources for medicine and astronomy by frequency doubling technique. YDFLs with the emission wavelengths in the wavelength 1120-1160 nm can be defiantly used as pump source for Ho-doped fiber laser emitting in the 2 μ m region.

In this paper, we will report an YDFL operates at a long-wavelength of 1137 nm. The laser cavity consists of a pair of fiber Bragg gratings (FBG) and a piece of highly-doped Yb³⁺-doped fiber. The central wavelength of both FBG is 1137nm, and the reflectivity of which is 99.62% and 39.74%, respectively. The highly-doped Yb³⁺-doped fiber had a core diameter of 5 μ m and cladding diameter of 125 μ m, the absorption coefficient of this highly-doped Yb³⁺-doped fiber could be more than 500 dB/m at 976 nm. The laser cavity is pumped by an YDFL operates at 1040 nm. Experimental results show that the YDFL could work at long-wavelength band and operates at 1137 nm efficiently. The 1137 nm YDFL had a pump-limited maximal output power of 276 mW and the ASE centered at 1080 nm is suppressed by a factor of more than 20 dB.

8551-15, Session 3

Femtosecond fiber lasers for biomedical solutions

Jian Liu, Lihmei Yang, PolarOnyx, Inc. (United States)

For the past few years, femtosecond (fs) fiber lasers have been growing in popularity over conventional solid state lasers. A turn-key fs fiber laser solution offers unprecedented features of compactness, low maintenance, and low power consumption. Many types of fs fiber lasers have been developed for biomedical applications covering optical coherence tomography (OCT), multi-photon imaging (MPI), coherent anti-stoke Raman spectroscopic imaging (CARS), Raman spectroscopic imaging, nonlinear spectroscopy, confocal microscopy, cell dissection, nano surgery, and more.

Several methods have been used to generate passive mode locking femtosecond pulses for fiber lasers: nonlinear polarization rotation, carbon nanotube, and saturable absorbing mirrors SESAM. All these methods can obtain stable mode locking operation with a reasonable performance and qualification. By adding amplifiers after the seed fiber oscillator and in cooperating with pulse shaping, spectral shaping and polarization shaping techniques, output power from 100's of mW to 100's Watts can be obtained with pulse duration compressible to less than 100 fs. For majority of biomedical applications, power level of several Watts is sufficient while most of the requirements are within 100 mW.

In this paper, we will discuss pulse shaping, spectral shaping and polarization shaping techniques used in fs fiber lasers and present experimental results for femtosecond fiber lasers operating at wavelengths of 1 μ m, 1.55 μ m, and 2 μ m, and their harmonic generations including second harmonic generation (SHG), third harmonic generation (THG), and fourth harmonic generation (FHG). Applications in biomedical imaging and diagnose will be present.

8551-16, Session 3

Properties of a double-clad erbium-doped fiber pumped by 355-nm laser system

Junqing Zhao, Shuangchen Ruan, Shenzhen Univ. (China)

Erbium-doped fibers often pumped by 980 nm laser diodes or 1480 nm pump lasers, in order to construct high-efficiency fiber lasers or fiber amplifiers. Besides that, five other absorption bands except the one centered at ~490 nm, between 480 to 1500 nm, have also

been investigated using corresponding pump sources. However, the absorption bands fallen in the ultraviolet (UV) region have never been experimentally investigated using a corresponding pump laser, up to now, although their existences have been theoretically predicated.

We experimentally investigated, for the first time to our knowledge, the fluorescence properties of a home-made double-clad erbium-doped silicate fiber (DC-EDF) using a 355 nm laser system as pump source. Broad fluorescence spectra covering most visible region, from 450 to 850 nm, and part of near-infrared region, from 1400 to 1700 nm, were generated from the DC-EDF with different lengths and at different pump powers. The different excited transition lines, fallen in a wide spectrum range from visible region to near-infrared region, were analyzed mainly based on the energy-level system of erbium ion. In our experiments, the excited central wavelengths after 8 m DC-EDF, at the pump power of ~860 mW, were 474.34 nm, 505.34 nm, 559.08 nm, 670.76 nm, and 1555.25 nm, respectively. All the obtained central wavelengths had different red-shifts compared to the original transitions of erbium ions. Phenomena including spectrum red-shifts and fluorescence-line-width broadenings, especially in the near-infrared region, occurred as the DC-EDF lengthening, which were qualitatively analyzed. For contrast, a piece of ~13.7 cm long highly doped single mode (SM) Liekki Er 110-4/125 EDF and an erbium-ytterbium (Er-Yb) co-doped crystal were also excited by the same pump laser. The results showed that the excited fluorescence spectra of DC-EDF and SM-EDF had much larger spans than those of Er-Yb co-doped crystal, i.e. line-broadenings. A qualitative analysis was given to indicate the possible mechanisms behind the differences between them. This work demonstrated a new route to pump erbium-doped fibers, as well as to get more excited fluorescence lines; thus, it will find wide potential applications in wider-wavelength-range fluorescence sources and new-wavelength-emitted fiber lasers.

8551-17, Session 4

Design and modeling of 10-kW level single-side-pumped slab laser amplifier chain

Xing Fu, Mali Gong, Tsinghua Univ. (China)

We report a novel design of solid-state laser amplifier chain based on Nd:YAG gain mediums, by lining up multiple single-side-pumped slabs in an unique manner. The scheme takes advantage of the excellent power scalability of the side-pumping configuration, and allows a reduction in cost and complexity comparing to the conventional way, by decoupling the cooling and pumping interfaces and thus avoiding water sealing application and water contamination to the crystal.

The pump system is designed with optimization, while the main focus is the feasibility of efficient power scaling through the amplifier chain. Specifically, influences of ASE effects on the amplifier performance (power scaling, beam quality and transverse mode profile) are described in detail, considering the re-amplification of ASE along the slab chain. A point design at 10 kW power level with a total extraction efficiency of 46% is presented with a well-developed numerical modeling.

8551-18, Session 4

LD-pumped 30W high beam quality 1064 nm laser at a 500-Hz repetition rate

Zhen-xu Bai, Ming-Liang Long, Gang Li, Beijing Univ. of Technology (China)

A LD-side-pumped Nd:YAG all-solid-state two voltage supplied Q-switched nanosecond laser was demonstrated. The laser cavity is a plane-to-plane linear cavity. Fundamental mode 1064 nm in center wavelength with pulse width tunable from 5ns to 20ns was obtained at the repetition rate of 500 Hz. The oscillator was scaled up to 30 W through 3 stages Nd:YAG amplifiers at the pulse-width of 6 ns with the divergent angle less than 3 mrad, and the single pulse energy fluctuation was less than 1.16% in 1 hour operation.

8551-20, Session 4

Is diamond a good material for wavelength conversion at high power?

Richard P. Mildren, Ondrej Kitzler, Aaron McKay, Hua Liu, Macquarie Univ. (Australia)

The recent availability of high-quality and low-cost synthetic crystal diamond has stimulated major activities in several areas of optics including laser source development. Although the use of diamond in Raman lasers has prevailed only in the last 5 years, it has already enabled the highest efficiency and output power for several of the prominent laser design configurations. With the thermal conductivity of diamond being two-orders of magnitude higher than most other laser host materials, and its low thermal expansion coefficient, diamond holds substantial promise for enabling Raman-functional devices with greatly enhanced power handling capacity. The external cavity Raman laser is a conceptually simple approach to wavelength shifting a pump laser source, and for increasing beam brightness. Diamond external cavity Raman lasers have yielded the highest powers, as far as we aware, with 25 W pulsed and 10 W cw. However, the output power limitations of external cavity diamond Raman lasers are yet to be elucidated. In this paper, we summarize the current state-of-the-art in high average power external cavity Raman lasers in pulsed and continuous wave formats. We also review progress in external cavity diamond Raman lasers operating in picosecond, nanosecond and continuous wave temporal regimes. By considering thermal lensing, and thermal-gradient induced stress, we investigate the design issues when scaling output power and estimate power limits. We show the high thermal conductivity, low thermal expansion coefficient and high flexural strength of diamond, combine to ameliorate these three effects to enable relatively straightforward order-of-magnitude power increases.

8551-21, Session 5

The technologies on lidar range profile, Doppler spectra, and range Doppler image for target recognition

Mingjun Wang, Xianyang Normal Univ. (China)

The characteristics laser scattered from target with rough surface has been an increased interesting and need for further utilizing these theories and experiments to study the laser radar imaging technologies for past several decades. And with the development of laser detected technologies in aerospace and air industry, more and more many aero and air crafts is of decisive influence on our national contravallation, intercommunism, civilian industries and other applications, for acquisition, tracking, limited discrimination, aim point selection, and performing their different tasks. The Range Resolved Doppler Imaging (RRDI) Lidar will be a research hotspot in aerospace and national defence fields. In this paper, we comprehensive review previous works on Lidar RRDI of the target including the experiments, simulations and features which are useful for target discrimination. The problems of the Lidar imaging system are analyzed to solve in experiment and model. The developed achievements of Range profile, Doppler spectra and Range Doppler imaging Lidar are reported in detail. As special examples, the Laser range Profiles and Range Resolved Doppler imaging features of a cone and cylinder are respectively shown. Our works can be used for laser applications as well as target recognition and discrimination.

8551-23, Session 5

Phase monitor in coherent beam steering system

Dengcai Yang, Dayong Wang, Zhiyong Wang, Beijing Univ. of Technology (China)

Coherent beam steering system(CBSS) attract great attention for its amazed advantages. CBSS provides an elegant means for achieving the inertialess, high-resolution random access beam steering and many other advantages, so it is widely studied by researchers for numerous applications, including laser radar, laser projection displays and high power laser process .

In CBSS, One of the key technologies is the phase monitoring. After monitoring the phase of each beam. Then the phase difference of adjacent beam is controlled. The combination beam is steered for the variation of the adjacent beam phase difference. So how to measure the phase different is very important in the CBSS. In this paper, A approach is provided to measure the phase difference between the adjacent two beams. In this approach, a M-Z interferometer is used. The adjacent two beams as the two branches of the interferometer respectively. It monitor the phase difference between adjacent two beams in the CBSS through measurment the output of the interferometer. The output of the interferometer is calculated theoretically. It is assumed p1,The test value of the interferometer is assumed p2. The phase difference is calculated through the theoretical(p1) and practical(p2) test value. Even the steering of the CBSS can be calculated from the adjacent two beams phase difference. Still we can control the beam phase through the closed loop circuit. In this paper, we design the M-Z interferomtor and set up it. And still the measurment circuit is designed and set up. In this experiment, we test the output of the inerferometer above ten hours. The output is very stable. And the variation of the output less than 0.04dB.

8551-24, Session 5

A high-power structured light vision system used for remote fast and effective obstacle detection of automated vehicle in off-road environment

Xiao Kang, Wei Zhu, Li Tian, KeJie Li, MaoSong Zhang, Jing Jiang, Beijing Institute of Technology (China)

How to achieve remote fast and effective obstacle detection in off-road environment is a key and difficult part of the automated vehicle navigation. As a non-contact measurement method, structured light vision system is widely used in the industrial measurement for its high precision, fast speed and active-controlled characteristics. In this paper, a high-power structured light vision system, which is composed of a high-power 12W 808nm continuous point light source laser with the divergence angle 2.4mrand, fast piezoelectric ceramics steering mirror of PI and the high sensitivity industrial camera of DALSA with the narrow-band filter plate of 808nm, is used for the remote fast and effective obstacle detection in off-road environment. The light spots emitted by the laser are projected to the steering mirror continuously and are formed the line structured light in the ground through the fast swing of the mirror. The image of the light stripe is obtained by the camera. When there is an obstacle, the distortion of the light stripe in the image will occur, which is used to obtain the position and size information of the obstacle through fast image processing. Experiment results show that, with the high-power laser, the system can detect the obstacle which is in front of the vehicle with the distance of 120m. Detection time of this system can reach 10ms and detection accuracy can reach 5cm which meet the automated vehicle remote fast and effective obstacle detection requirement in off-road environment at the speed of 120km/h.

8551-6, Poster Session

Q-switched quasi-concentric laser resonator with line-shaped end-pumping profile: power-insensitive operating point and symmetrized TEM00 output

Xing Fu, Qiang Liu, Mali Gong, Tsinghua Univ. (China)

We put forward a quasi-concentric laser resonator configuration employing a line-shaped end-pumping profile (QRLE).A thermal lensing modeling of the QRLE is developed, including the quartic phase deformation and the dependence of the thermal focal power on the TEM00 mode size at the thermal lens.Based on the calculation, we found that the dynamic operating point of the QRLE depends on both the resonator condition and the thermal effect condition. Furthermore, we predicted that the operating point in the subcritical region is insensitive to power fluctuation, i.e., the QRLE with extremely short cavity length is capable of stable operation. The validity of our prediction was well confirmed by theoretical modeling and experimental realization.

Compared to conventional resonator designs, the QRLE resonator design produces the fundamental mode output with an LD bar instead of the fiber-coupled pump source and realizes good stability with short cavity length, demonstrating a clear advantage of both low cost and compactness. Based on the QRLE configuration, we produced >12 W pulsed TEM00 output, with the repetition rate of 30 kHz and optical-optical efficiency of 27%. The laser output mode is elaborately symmetrized in two directions in terms of beam quality, waist radius, and waist position.

8551-19, Poster Session

Modeling of distributed-side-pumped slab lasers: power scaling by adding slab units

Xing Fu, Qiang Liu, Mali Gong, Tsinghua Univ. (China)

We present a novel distributed-side-pumped configuration for power scaling of solid-state slab lasers, which combines the advantages of both end-pumped and side-pumped geometries, realizing large absorption length and large pump area at the same time. In the distributed-side-pumped slab laser, the long gain medium can be divided into multiple segments (slab units), each of which adopts an end-pumped like geometry, thus the pump uniformity and the utilization ratio of the whole slab are greatly improved comparing to the end-pumped scheme. Furthermore, this configuration decouples the pump windows from the cooling areas, avoiding the necessity of water sealing the optical surfaces.

The parameters of gain medium and pumping system are carefully optimized, while numerical calculation of thermal effects for composite slab and homogeneous slab are compared. An oscillator based the Nd:YAG slab that includes 5 slab units, is expected to produce CW output at 1kW level, with the optical-optical efficiency of 52.6%. By adding more slab units, the distributed-side-pumped slab laser can be enhanced easily and efficiently.

8551-22, Poster Session

The research of adaptive optics technology for Fourier telescopey

Changming Lu, Gao Xin, Tang Jia, Jianjun Wang, Beijing Institute of Tracking and Telecommunication Technology (China)

Previous experiments in both the lab and field have verified that the Fourier Telescopy (FT) technique to imaging geostationary targets is both viable and robust. By theory analysis and numerical calculation of power dispersal and atmosphere's affection, it is proved that the Adaptive Optical (AO) System for the transmitter subsystem of FT is necessary. A special AO system is designed for FT. The AO system includes two wavefront sensors (WFS), a deformable mirror (DM) and an actuator command computer. The AO system can use laser guide stars, GEO itself or star as reference star. Two wavefront sensors have different functions. One WFS is used to measure the wavefront of the reference star's wavefront after it's broadcast through the atmosphere, the other WFS is used to measure the transmitted laser's wavefront before it leave the telescope. The actuator command computer syn-calculate the DM's distortion value according to two waveront sensors'

measure results and figure out the drive voltage of every actuator. The AO system of Fourier Telescoping will realize two functions. On the one hand, it will improve the transmitted beam's quality, decrease the laser's size formed at the side of the GEO object and increase the centralization of the transmitted beam. On the other hand, the AO system will alter transmitted beam's wavefront, make its value is equal to wavefront distortion induced by atmosphere turbulence, but having reverse direction, so the AO system will decrease the infection to the uplink beam caused by atmosphere turbulence.

8551-25, Poster Session

Study on laser ranging to medium-long range moving target

Zhi-Chao Wu, Xiuli Zhang, Xi'an Technological Univ. (China);
Lixin Zu, Beijing Chengxin Science and Technology Ctr. (China)

In view of the high precision ranging needs of military, civilian, laser ranging to medium-long range moving target is studied. We adopted three high power diode arrays with symmetric distribution side pumped Nd:YAG ceramic crystal. According to the thermal focal length of laser material, we optimized the cavity structure and designed reasonable cooling system. In our experiment, the cavity dumping technology and the pockels effect of KD*P crystal were used for high pulse repetition rates, short pulse durations. So, under repetition rate of 1 kHz and single pulse pumped energy of 144 mJ, the high peak power and the short pulse durations are obtained, which have improved the ranging precision to some extent. By using the time to digital conversion chip TDC-GP2 and related circuit, the precise measurement of laser flight time is measured. Finally, laser ranging about 5 km moving target is realized, and the ranging precision is less than ± 2 m. The results formed the basis for the further development of the high precise and long range moving target laser ranging.

8551-41, Poster Session

Treatment of numerical overflow in simulating error performance of free-space optical communication

Fei Li, Anhui Institute of Optics and Fine Mechanics (China) and Univ. of Science and Technology of China (China); Zaihong Hou, Yi Wu, Anhui Institute of Optics and Fine Mechanics (China)

Gamma-Gamma distribution model was widely used in numerical simulations of free-space optical communication system. The simulations were often halted by numerical overflow error due to excessive parameters. Based on former research, two modified models were presented utilizing scientific calculation software and program. Factors of original model where overflow arises were transformed into corresponding logarithmic formats adopting substitution and recurrence, and numerical overflow in the process of calculation was eliminated. Through numerical calculation the practicability and accuracy of modified algorithms were proved and the advantages and disadvantages of the two algorithms were listed. The proper algorithm should be chosen according to practical situation. The two algorithms were also applicable to other numerical models based on gamma-gamma distribution such as outage probability and mean fade time of wireless optical communication.

8551-42, Poster Session

Parameters optimization of the beam clean-up system based on stochastic parallel gradient descent method

Sanhong Wang, Junfeng Cui, Taiyuan Satellite Launch Ctr.

(China); Haotong Ma, Yonghui Liang, Qifeng Yu, National Univ. of Defense Technology (China)

In a high-power laser, the system aberrations and the dynamic aberrations caused by thermal absorption degrade the beam quality. The diffraction losses incident to these aberrations will reduce the laser's output power. Adaptive optics (AO) technique based on a stochastic parallel gradient (SPGD) algorithm can be used to compensate for the wavefront distortions in real time to clean up the laser beam. In such a beam clean-up system, a deformable mirror is controlled by the SPGD algorithm to optimize a scalar beam quality metric. According to the algorithm, statistically independent small random perturbations are simultaneously applied to all the control channels of the deformable mirror in each iteration step, and the stochastic approximation of the corresponding gradient component of the beam quality metric is subsequently measured. So the convergence speed of this algorithm is faster than that of the conventional gradient descent algorithm. However, the parameters of the gain coefficient and the amplitude of the perturbation still need to be optimized to improve the final convergence state and speed of the SPGD algorithm. A simulation system of the beam clean-up based on SPGD was built up to be used to study the optimizing and scaling method of the two parameters. Beam clean-up experiments with the simulation system were conducted for a team of typical aberrations measured in a real laser. The results show that the convergence property of the SPGD algorithm is improved after the parameters being optimized.

8551-43, Poster Session

Numerical analysis of thermal effects in micro-evaporator cooling module

Siqiang Fan, Peng Zhang, Yiping Liang, Teli Dai, Yu Zhang, Chongqing Normal Univ. (China)

At present, the cooling ways of LD with high power are mainly two types, freezing by the cooling water going through micro channel and freezing by the gasification of liquid nitrogen. Both of them have deficiency. The first type needs special freezing machine which can produce cooling water. Besides, the efficiency of cooling is quite low. The latter type needs plenty of liquid nitrogen as consumable materials. The micro channel cooling module uses the theory of normal cooling with single compressor and adopts Freon as its freezing medium. Strong difference in temperature which has high efficiency of heat dissipation will take place between the micro channel tube and the heating surface of LD if the compressor, freezing machine and steamer are small enough. In the paper, the temperature of LD heating surface and steam tube is defined at 25 degree and minus 10 degree respectively. The range of temperature of micro channel will be worked out according to the Numerical analysis of Matlab.

8551-44, Poster Session

High-power Q-switched Yb-doped double-cladding fiber laser

Zhenhua Yu, Yanrong Song, Beijing Univ. of Technology (China)

The Q-switched lasers could form optical pulses with higher pulse-energy and longer pulse-duration than mode-locked pulses and have established their role in the application fields that do not require ultrafast speed. Recently, single-walled carbon nanostructures have realized a novel paradigm of the passive saturable absorbers with the advantages of wide operating range, simple manufacturing process, and extremely high nonlinearities than the normal Q-switched technology. But most of single-walled carbon nanostructures used in the Q-switching or mode locking experiments were mixed with polymer. This kind of saturable absorbers has been suffered from high nonsaturable loss and low damage threshold. Here, we present a saturable absorber based on pure single-walled carbon nanotubes without polymer, which was directly deposited on the core surface of

one Ytterbium-doped double-cladding fiber end by optically driven deposition method to obtain a higher output power. A linear-cavity was employed and a 1.5m long Ytterbium-doped double-cladding fiber played the roles of both gain fiber and the cavity. The two fiber ends were used as the cavity end mirrors. When a 20-W 976-nm fiber coupled diode laser was pumped from one end of the Ytterbium-doped double-cladding fiber, 1.3W of maximum power was obtained at the wavelength of 1070 nm. 385 ns of pulse duration with a wide range of pulse-repetition rate from 90KHz to 540KHz were demonstrated.

8551-45, Poster Session

Properties of all-fiber supercontinuum generation by all-normal-dispersion dissipative soliton ytterbium fiber lasers

Li Wuyi, Jian Wu, Jintong Lin, Beijing Univ. of Posts and Telecommunications (China)

Recently, widely broadened supercontinuum (SC) generation has been demonstrated using ultrashort pulses and photonic crystal fibers. The SC generated with this technique is a coherent ultrawideband source that emits light from the small cores of the fibers, allowing the beam to be delivered and tightly focused. The SC is also useful for advanced new applications, such as optical frequency combs and ultrahigh-resolution optical coherence tomography. We realize the flattening and extending of a low-threshold all-fiber broadband SC source based on the use of the highly nonlinear photonic crystal fiber (HNL-PCF) in combination with a passively mode-locked Yb-doped fiber laser. Passively mode-locked fiber laser operating in the all-normal-dispersion (ANDi) regime with high peak power is great important to generate ultrafast pulses near 1 micron. In this paper, we report the dissipative soliton operation of an Yb-doped ring fiber laser without dispersion compensation and an additional filter that is passively mode-locked by nonlinear polarization rotation (NPR). The formation of the dissipative soliton pulse is a self-consistent result of various effects in the laser cavity. The spectral broadening resulting from the normal group velocity dispersion (GVD) and nonlinear phase accumulation is balanced by gain saturation and narrowing. A 619 mW, 487 fs high-power ultrashort pulse was generated at 1060 nm in Yb-doped fiber-chirped pulse amplification system. We show that the use of the HNL-PCF with a zero dispersion wavelength close to the pump laser wavelength leads to efficient generation of nonlinear broadening. SC wave with the 20 dB bandwidth of ~1200 nm has been obtained.

8551-46, Poster Session

Oxygen partial pressure influence on the character of InGaZnO thin films grown by PLD

Lu Yi, Li Wang, Jiangbo Chen, Yulin Gan, Beijing Univ. of Technology (China)

Amorphous oxide semiconductors (AOSs) are promising for emerging large-area optoelectronic applications because of capability of large-area, uniform deposition at low temperatures such as room temperature (RT). Indium-gallium-zinc oxide (InGaZnO) thin film is a promising amorphous semiconductors material in thin film transistors (TFT) for its excellent electrical properties. In our work, the InGaZnO thin films are fabricated on the SiO₂ glass using pulsed laser deposition (PLD) in the oxygen partial pressure altered from 1 to 10 Pa at room temperature (RT). The targets which were prepared by mixing Ga₂O₃, In₂O₃, and ZnO powder at a mol ratio of 1: 7: 2 before the solid-state reactions in a tube furnace at the atmospheric pressure. The targets were irradiated by an Nd:YAG laser(355nm). Finally, we have three films of 270nm, 230nm, 190nm thick for 1Pa, 5Pa, 10Pa oxygen partial pressure. The product thin films were characterized by X-ray diffraction (XRD), atomic force microscopy (AFM), Hall-effect investigation. The comparative study demonstrated the character changes of the structure

and electronic transport properties probably occurred as a fact of the different oxygen partial pressure used in the PLD.

8551-47, Poster Session

Passive Q-switched Nd:YCOB laser with a single-walled carbon nanotube saturable absorber

Jian Li, Yanrong Song, Zhenhua Yu, Cuicui Tian, Yanlin Li, Beijing Univ. of Technology (China); Yonggang Wang, The Hong Kong Polytechnic Univ. (Hong Kong, China)

A passively Q-switched Nd:YCOB (Nd³⁺:YCa₄O(BO₃)₃) laser was demonstrated at the wavelength of 1055 nm employing a single-walled carbon nanotube saturable absorber (SWCNT-SA).Nd:YCOB crystal was grown by the Czochralski method, and its structure was measured by using a four circle X-ray diffractometer. The transparent spectrum from 200 to 2600 nm was measured at room temperature. The fluorescence spectrum near 1.06 um showed that the main emission wavelength of Nd:YCOB crystal was centered at 1060.8nm. SWCNT-SAs exhibit not only high nonlinear optical effect comparable to that of SESAMs but also low nonsaturable loss and high damage threshold. Moreover, by configure different concentrations of SWCNT-SA solution, we could dropped the liquid on different types of mirror to produce different types of absorber mirrors. We put 10mg of SWCNT powder into 10ml sodium dodecyl sulfate (SDS) aqueous solution. Then the SWCNT aqueous solution was ultrasonically agitated and centrifuged 10000r/min for 10 minutes. After that, the SWCNT dispersion was diluted and poured onto a glass substrate to evaporated at atmosphere or in oven. Using a single-walled carbon nanotube as saturable absorber (SWCNT-SA) (we dropped SWCNT-SA fluid on the reflect mirror), a passively Q-switched Nd:YCOB (Nd³⁺:YCa₄O(BO₃)₃) laser was realized at 1055nm pumped by a 808 nm diode laser. A 242 mW output power were obtained at the pump power of 9W in a plano-concave cavity. The slope efficiency is 27%, the repetition rate is 22.7kHz.The duration is 2μs and the energy could reach 10.7μJ.

8551-48, Poster Session

The fabrication, optical properties research, and application in the Q-switched Yb doped double cladding fiber laser of single-walled carbon nanotubes

Cuicui Tian, Yanrong Song, Zhenhua Yu, Jian Li, Yanlin Li, Beijing Univ. of Technology (China); Yonggang Wang, The Hong Kong Polytechnic Univ. (Hong Kong, China)

The single-walled carbon nanotubes can be used as saturable absorber in Q-Switched and mode-locked lasers recently.The different concentration and different ultrasound time of dispersed single-walled carbon nanotubes could get different parameters of the absorber and then could influence the characteristics of the pulsed laser. The optical infrared absorption spectrum of all different kinds of single-walled carbon nanotubes have been measured respectively. The influence of the concentration and ultrasound time on the single-walled carbon nanotubes' absorption rate were discussed. Along with the increasing of the concentration and ultrasound time the single-walled carbon nanotubes'absorption rate increases proportionately. The structure and morphology of the single-walled carbon nanotubes were investigated by the atomic force microscope (AFM) and scanning electron microscopy (SEM) respectively. Atomic Force Microscope exhibited the single-walled carbon nanotubes' strip shape microstructure of different sizes. As we can see in the photographs the single-walled carbon nanotubes' diameters are from about a few tenths of nm to a few nms unequally. There was more obvious aggregation of SWCNTs at the higher concentration under the scanning electron microscopy. We use the single-walled carbon nanotubes saturable absorber (SWCNTs) in the

Yb doped Q-switched double cladding fiber laser, a duration of 650ns pulses were obtained at the center wavelength of 1037 nm, the average output power of 1.3w with the pump power of about 10w.

8551-49, Poster Session

Temperature distribution of laser crystal in LD end-pumped Nd:YAG/LBO blue laser

Lei Zhang, Shijiazhuang Univ. of Economics (China)

It is well known that diode-pumped solid-state laser have provided many excellent advantages such as smaller cubage, stable power and longer using-life. Still, it is more difficult to obtain higher stable output power because of the strong thermal effects caused by the heat deposited in laser crystals. The thermal distribution is determined by the pumping light distribution. With the high power pumped, the heat caused by radiationless transition and absorb through the laser crystal influences the optical behaviour of the laser crystal which makes the resonator unstable, and greatly limits the maximum pump power. There are three aspects caused the thermal effect of laser crystal: refractive index variety, end-face distortion and double-refraction stress of laser crystal. The threshold value and output power are seriously influenced by the distribute radius and total departure of pumping light, so the temperature distribution of laser crystal is one of the most important factors which influence the quality of output light.

In this study, LD End-pumped Nd:YAG/LBO solid state Blue Laser is realized by even hollow cavity. The temperature distribution in different cooling system was studied. A thermal distribution model of Nd:YAG/LBO crystal was established. Based on the calculation, the temperature distribution and deformation of laser crystal in different cooling system were obtained. The results show that the temperature decreases from the pump end to the launch end exponentially. When the pumping power is 2 W and the radius of pumping beams is 320 μ m, a biggest output power 46.3 mW of blue light is achieved, giving an frequency doubled optical conversion efficiency of 2.3%. The temperature distribution and end face distortion of the laser crystal are lowest by using side directly hydrocooling method. The study shows that, the side directly hydrocooling method is a more efficient method to control the crystal temperature distribution and reduce the thermal effect.

8551-50, Poster Session

Evolution of damage morphology in InSb irradiated with ultrashort laser pulses

Amit Garg, Acharya Narendra Dev College (India); Surendra K. Bansal, Univ. of Delhi (India)

We report here the evolution of laser damage morphology in polished InSb as a function of increasing energy and number of pulses using ultrashort laser pulses. The laser pulses used in the present studies are of 50 femtosecond duration having a repetition rate of 10 Hz with a central wavelength around 800 nm. Damage primarily occurs in the form of surface removal with no crater formation. The morphology shows periodic structuring in the form of ripples and grains. Microcrater formation is observed only at a very high fluence. The results are discussed in light of various ablation theories.

8551-51, Poster Session

Numerical analysis of beam quality's influence on coherent combination of multiple laser beams

Yi Tan, Xinyang Li, Institute of Optics and Electronics (China)

A numerical simulation model for coherent combination of multiple rectangular beams, square beams and circle beams has been

developed. The factor β of single beam which was with wavefront aberration of Zernike polynomials from two to twenty-one and its combination was obtained by numerical calculation through fast Fourier transform (FFT). The influence of piston on coherent beam combination was analyzed when each beam has wavefront aberration of Zernike polynomials from two to twenty-one. We demonstrated that the influence of piston was small if other aberrations were high. The relationship between the average of single beam's factor β and factor β of its coherent combination was also obtained by numerical calculation. A fitting formula was used to fit the discrete number. By this way, an expression of the relationship was acquired. Fitting coefficients between numerical calculation and theoretical result were compared and the affecting factor of the difference was analyzed. We concluded that fitting coefficients of numerical calculation result was smaller than theoretical result because of beam's arrangement and filling ratio.

8551-52, Poster Session

Effect of a self-injected electron bunch on the laser wakefield and electron acceleration in the bubble regime of the laser-plasma interaction

Ming-Ping Liu, Nanchang Univ. (China)

The effect of a self-injected electron bunch from background plasma on the laser wakefield and electron acceleration in the bubble regime of the laser-plasma interaction is investigated by theoretical analysis. The test electron bunch weakens the space-charge electric field of the laser wake. The wakefield structure is strongly modified and the bubble elongates as the density of the self-injected electron bunch increases. The subsequent plasma electrons can be self-injected into the evolving bubble with higher initial longitudinal momentum. As a comparison we perform particle-in-cell simulations and it is found that the results from theoretical model are consistent with simulation results.

8551-53, Poster Session

Narrow linewidth, wavelength stable Er/Yb co-doped fiber MOPA source operating at 1547.8nm

Hongxin Su, Xiaoming Li, Fuyun Jiao, Lijing Xu, Xu Li, Hebei Univ. (China)

High-power optical sources with narrow linewidth and stable wavelength are of great importance in a wide range of applications. Owing to the potential of high efficiency and high power level operating in the eye-safe wavelength region around 1.55 μ m, Er³⁺/Yb³⁺ co-doped fiber lasers (EYFLs) have attracted much attention in recent years. Though DBR configuration which uses fiber Bragg grating (FBG) as the reflector to form resonator has been widely used in EYFLs for the sake of compactness and wavelength stability, FBGs are not very effective for wavelength selection in high power and multimode fiber lasers, because the wavelength for the reflectivity peak varies with the effective refractive index of the mode and the temperature in the fiber core due to heat accumulation. In this paper, we demonstrate the output characteristics of an optical source based on Er³⁺/Yb³⁺ co-doped double-clad fiber (EYDCF) in a master oscillator-power amplifier configuration. In the experimental setup, a DFB diode laser with linewidth less than 0.02nm and power up to 10 mW serves as the master oscillator. The amplifier is composed of a 10m long EYDCF, two isolators at both input and output terminals, and a 975nm pump diode connecting with the EYDCF via a side-pump fiber coupler. A maximum output power of 1.16W is obtained in a backward-pumping configuration. The gain of the fiber amplifiers is up to 30.7dB. The wavelength centered at 1547.8nm with a spectral width no more than 0.02nm shows long-time stability.

8551-55, Poster Session

Diode-pumped composite YVO4/Nd:YVO4/ YVO4 mode-locked laser with ring resonator

Guoxi Huang, Shenzhen Univ. (China)

Some investigates fast physical phenomena, but the nanosecond pulse duration of Q-switched lasers is often not sufficient. Such investigations require mode-locked picosecond laser sources. Since the first observation of the self-mode-locking phenomenon in a Ti:sapphire laser much attention has been given to both experimental and theoretical investigations of self-mode-locked lasers. And the same phenomenon was observed in the Nd:YVO4 laser, which can obtain a mode-locked picosecond laser. It is expected that the output pulse width of mode-locked laser could be more narrow when inset a saturable absorber into the ring resonator, such as Semiconductor Saturable Absorber Mirror (SESAM). The self-mode-locking mechanism is now attributed to the optical Kerr effect inside the Ti:sapphire crystal; thus the mechanism is termed Kerr-lens mode locking (KLM). However, the presence of spatial hole burning in standing-wave resonators limits the efficiency and frequency characteristics of the lasers. As ring lasers sustain oscillation of travelling-wave rather than standing wave, they can eliminate spatial hole burning in the gain medium and enable the lasers to work in the less longitudinal modes. The less longitudinal modes could weaken the mode-locking, but the long length ring resonator can increase the number of longitudinal modes. Compared with the standing-wave resonators mode-locked laser, the ring laser has the smaller gain dispersion, which could be easier to obtain the narrower mode-locked pulse width. With rapidly development of laser diode pump technology, there are many advantages of diode pumped solid state lasers, such compact structure, high efficiency and long service life. They make mode-locked laser technology more practical.

In this paper, we report unidirectional ring resonators composite YVO4/Nd:YVO4/YVO4 mode-locked laser. We present the results of our research on the mode-locked ring laser. By optimizing the resonator, a mode-locked picosecond ring laser at 1.06 μm was achieved.

8551-57, Poster Session

Effects of passivation of nitrogen plasma on photoluminescence of GaAs substrates

Yunhua Wang, Lu Zhou, Xin Gao, Baoxue Bo, Changchun Univ. of Science and Technology (China)

GaAs is one of the most important compound semiconductor materials as substrates for 940nm semiconductor lasers, which has a wide direct energy band gap, high electron and hole mobility, and high saturation drift velocity, etc. The band gap of GaAs is 1.424 eV, corresponding to an emission wavelength of 940nm with high radiation efficiency. However, GaAs is a binary compound semiconductor materials, surface state with high density usually exists at the oxygen-exposed surface and acts as non-radiative recombination centers resulting in rigid pinning of the Fermi level, which has a negative effect on the lifetime and reliability of the lasers. So, in order to eliminate the undesirable effect of the surface state on 940nm semiconductor lasers, in this paper, the GaAs substrate samples were treated by Nitrogen plasma at different plasma cleaning process simulating the laser facet, and then to deposit a SiO₂ passivation layer by radio frequency magnetron sputtering to avoid reoxidation or recontamination of the surface. We introduced N plasma by gas glow discharge, and the fluorescence properties of GaAs substrates were analyzed using RPM2000 rapid photoluminescence mapper. The results showed that the sample was treated under the conditions of sputtering power 10W, N₂ flow 25sccm, cleaning time 15min, the luminous intensity was increased by 63.61% compared with before passivating. The optimized result illustrates that the plasma cleaning process can help to effectively remove the attached contaminants and the native oxides.

8551-58, Poster Session

Nano-gold colloids prepared by microwave synthesis method and its SERS activity

Lan Wang, Fujian Normal Univ. (China)

A novel method for rapidly synthesized Au colloidal under microwave irradiation was present in this paper. Size of the Au nanoparticles varied from 30 nm to 60 nm along with varying mol fractions by chloroauric acid solution reduced with sodium citrate. The prepared Au nanoparticles were characterized by transmission electron microscope (TEM) and ultraviolet-visible (UV-Vis) spectrophotometer. It is found that the nanoparticle size and shape are highly dependent on the reaction time and the molar ratios of the reducing agent. By the SERS measurements of R6G, 4-MBA and BSA, this Ag colloid is shown to be an excellent SERS substrate with good stability and biocompatibility. As the fabrication process of this SERS substrate is simple and inexpensive, this method may be used in large-scale preparation of substrates that can serve as an ideal SERS substrate in biomedical application.

8551-59, Poster Session

STK and application in simulation of the space laser communication network

Jianing Wang, Jingyi He, Yue Yang, Changchun Univ. of Science and Technology (China)

Laser communication with its large capacity communication, strong confidentiality, structure of light and other advantages is becoming research focus. Space laser communications networking technology is communications network of bi-directional, multi-directional network, which is made of satellites, ground station, near the space vehicle and so on. This paper uses the STK (Satellite Tool Kit) on a visibility analysis of the laser communication in satellite network between different or bits. Simulation results demonstrate the two-dimensional or three-dimensional chart.

8551-60, Poster Session

Characteristic research of the waveguide by nanosecond laser pulses on LiNbO3

Zigang Zhou, Southwest Univ. of Science and Technology (China)

The damage threshold and morphology of optical material have been investigated by 800nm, 76MHz, 30fs laser pulses, in 50 magnification and 0.65 numerical aperture (NA) objective in the Z-LiNbO₃ crystals. The influence of several experimental parameters, for example energy per pulse, a ser scanning speed, or repeat time on writing quality and the characters of relative microstructures has been analyzed and studied in theory. The damage structural change, from small refractive index changes to micro explosion structure in LiNbO₃ induced by high intensity nanosecond laser is studied. Nonlinear interactions of nanosecond laser and transparent material are discussed.

The subsurface morphology of the processed structures inside the LiNbO₃ was obtained by a Nikon optical microscope. Particularly, we find that the wider width of the buried channel with the increase of energy per pulse, repeat time and the reduce of scanning speed. It was caused by the avalanche ionization and multi-photon absorption of lithium on the processed area, and which is also lead to the refractive index change rang by the writing conditions. The result shows that the propagation of optical waveguide could achieve ideal effect when the energy per pluse is under 300mW, the scanning speed is from 0.05mm/s to 0.2mm/s, and the focus depth is from 350 μm to 400 μm . At last, in this approach, the insertion loss of 1?4 optical splitter is less than 1dB/cm.

8551-62, Poster Session

An equivalent method to analyze the electrical effect induced by laser plasma

Yunjing Ji, Chunyong Wang, Bao-Min Bian, Nanjing Univ. of Science and Technology (China)

Electrical effect induced by laser plasma in air is measured using a tiny probe placed in close to a metal target. Analysis shows that the resulting signal wave varies with detection distance. Based on the testing system, an equivalent circuit model was proposed to analyze the formation mechanism and evolution of the electrical signal and its dependence on the probe distance. The observed signal peak polarity overturn was also analyzed and explained. Finally, our method provides an explanation for the effects of the testing angle on the probe signals according to the time and space evolution of the laser plasma.

8551-26, Session 6

Mode-locking characteristics of all-solid-state mode-locked laser with graphene saturable absorber

Jieyu Wang, Li Wang, Beijing Univ. of Technology (China)

Ultrafast laser sources have always been an attractive field in laser research and are acquired mostly from the mode-locked lasers by SESAM currently. However, the fabrication of SESAM is very complex and costly, and the saturable absorption band is limited. Graphene is a promising saturable absorber for broadband saturable absorption due to the gapless linear dispersion of Dirac electrons. Thus it is widely investigated in experiments in recent years. Nevertheless, there are few theoretical research about the saturable absorption of graphene that should be important for designing the scheme of the experiments.

In this paper, the saturable absorption of graphene is studied by numerical method. By using the experiment data and assuming the characteristics of monolayer graphene are uniform, the parameters of saturable absorption, such as saturable fluence and saturable absorption coefficient, i.e., modulation depth, are derived from a simple two-level saturable absorber model. With these data, based on theoretical mode of suppressing Q-switched mode locking and combining with all-solid-state Yb:YAG laser, the critical pump power of suppressing Q-switched mode locking is studied. It can be seen that saturable fluence and modulation depth increase with the number of layers. The critical pump power will decrease when the number of layers, transmittance of the output mirror and beam waist on graphene decrease, while cavity length increase, and it contribute to suppress Q-switched mode locking. The minimum critical pump power will be obtain if the crystal length is 1.9mm and beam waist on gain medium is about 67 μ m. Compare with SESAM, graphene is a better choice to generate stable mode-locked laser.

8551-27, Session 6

Nonlinear graphene photonics: saturable absorption for ultra-fast laser photonics and large Kerr nonlinearity for graphene based Kerr photonics

Han Zhang, Hunan Univ. (China)

Graphene as an ideal two-dimensional form of carbon shows wonderful nonlinear photonics property. By performing the open and close aperture Z-scan technique, we are able to ambiguously identify the saturable absorption and Kerr nonlinearity effect for the first time, which corresponds to the imaginary and real part of the third order optical nonlinearity in graphene. Owing to its linear energy band structure, graphene exhibits broadband saturable absorption with attractive

laser photonics applications. Herein, we review the state of the art in this rising field: graphene passively mode locked/Q-switched fiber or solid state lasers from near infrared, telecommunication to mid infrared wavelength band. Very recently, we experimentally confirmed the large Kerr nonlinearity in graphene, which indicates several interesting Kerr based photonics applications including: self and cross phase modulation, optical Kerr switcher, four wave mixing generation, Kerr soliton, and so on. Both the saturable absorption and large Kerr nonlinearity in graphene renders it as an attractive nonlinear optics material platform, with either fundamental or application importance.

8551-28, Session 6

Experimental and simulation research of passive mode-locking fiber laser based on a single-walled carbon nanotube saturable absorber

Pan Zhu, Mei Sang, Ke Liu, Xiaolong Wang, Tianxin Yang, Tianjin Univ. (China)

Single-walled carbon nanotubes has been widely used in the research of passive mode-locking fiber laser, researchers often observed the existing of soliton pulses in the experiment of mode-locking laser. However, few people studied the process how mode-locking pulses evolve into soliton pulses, while they are propagating in the laser cavity. Here, we report a passive mode-locking laser based on single-walled carbon nanotubes saturable absorber experimentally and a numerical simulation based on a modified non-linear Schrodinger equation, which is used to analyze the procedure of soliton pulse evolution in the fiber laser. The physics of passive mode-locked fiber lasers comprises a complex interaction of gain, dispersion and nonlinear effects. In the experiment of mode-locking laser based on single-walled carbon nanotubes saturable absorber, which approaches the working regime of dispersion managed soliton lasers, we obtained 1.2ps mode-locking pulses sequence successfully, whose repetition rate is 8.366 MHz, and the Center wavelength of the spectrum with obvious Kelly sideband is 1562.3nm. The existence of solutions in a dissipative nonlinear cavity comprising a periodic combination of two distinct nonlinear waves is likely to be applicable to various other nonlinear systems. In the simulation, we find that the mode-locked pulse propagates self-similarly in the gain fiber with normal dispersion, soon afterwards for very small anomalous-dispersion segment lengths it approaches dissipative soliton lasers, then gradually transforms into a regular soliton in the rest of the cavity, where the dispersion is anomalous.

8551-30, Session 6

Coherent beam combination of seven high power fiber amplifiers with an all-optical feedback loop

Houkang Liu, Bing He, Jun Zhou, Chi Liu, Liyun Hao, Shoujun Dai, Yunrong Qi, Xiaolong Chen, Shanghai Institute of Optics and Fine Mechanics (China)

We demonstrated a coherent beam combination of seven high power all-fiber polarization-maintaining amplifiers channels with an all-optical feedback loop. Every single channel has four stages amplifiers and the output power of a main amplifier reached about 50 W with an optical-to-optical conversion efficiency of 80%. A broadband laser diode with a central wavelength of 1064nm is used as seed for seven amplifiers channels before the feedback loop been established. Spectrums of output beams are detected before and after phase locking. Thanks to self-organization properties of the all-optical feedback loop, many low loss longitudinal modes are successfully selected for phase locking when the system is in closed loop. There are no stimulated Brillouin scattering, which is a main limitation of power scaling in active coherent beam combination, and other detrimental nonlinear effects.

Seven output beams of main amplifiers are space coupled via seven collimators and carefully arranged in a hexagonal laser array in the near field by using a homemade mirrors array module. The space duty ratio is up to 65%, which is helpful to improve power of central lobe in beam combination. Once the all-optical feedback loop is established, the phase of seven fiber amplifiers is locked steadily in a very short time. The pleasing visibility of interference patterns in the far field is more than 90%. The total combined power is 352 W. Undoubtedly, the all-optic feedback loop technique has the potential to boost passive coherent beam combination to higher power and larger number of amplified channels with low cost, compact configuration, and simple phase-locking mechanism.

8551-31, Session 6

Phase and spectrum control requirements of high intensity laser beam combining

Yanqi Gao, Shanghai Institute of Laser Plasma (China)

Because of the limited optical element aperture, damage threshold, gain bandwidth, and so on, the output capability of a single laser beam is limited seriously. The coherent laser beam combine offers an excellent method to improve the peak intensity which could be gotten greatly. Aiming at getting the general requirements of the coherent beam combine for large aperture laser facilities, this work devotes to modeling the influences of the phase factors and spectrum factors on the combine results. The effects of the phase factors, including the beam configuration, piston error, and tip/tilt error, are studied analytically and numerically. It is found that the expressions of the intensity in the focal plane can be written as three parts, the scale factor, a point spread function (PSF), and a grid function (GF), for the ideal beam combine and beam combine with piston error. Every part has its special physical meaning, and decides different characteristics of the combined focus. For the beam combine with tip/tilt error, though the expression of focal spot intensity can not be separated like the above situations, every part still has obvious physical meanings. The results show that the beam configuration can not affect the Strehl ratio of the combined beam, but it influences the FWHM of the main peak and the ratio of the main peak and the side peak. The piston error affects the grid function greatly, including its maximum value, transverse translation, and shape. For the two beam combine, a piston error less than $2\pi/5$ rad is suitable. For multi-beam combine, the standard deviation of the piston error should be no more than $2\pi/10$ rad. The tip/tilt error affects the superposition degree of the focal spots of the combined elements directly. A requirement of $0.5\sim 1$ rad for the standard deviation of the tip/tilt error is adequate. The effects of the spectrum factors, including the longitudinal chromatism, high order dispersion, and residual chirp, are studied analytically and numerically. Results show that the above spectrum factors have significant influences on the short pulse coherent beam combine, and must be controlled carefully when the pulse is shorter than 1ps.

8551-32, Session 7

Fiber coupled high-power multi-mode diode pump lasers

Tao Wang, Oclaro Technology (Shenzhen) Co., Ltd (China)

This paper summarizes complete fiber coupled diode pump laser products and solutions mainly used in fiber laser application, while covering both Yb and Tm systems. The combination of various power ratings, wavelength ranges and packaging platforms on single/multi emitters, and mini-bars offer flexible options to customers by enabling flexibility of emitter or bar fiber coupling solutions during the system design. Some of key features of pump diodes will be normally considered like brightness, driving current, pumping efficiency, system cooling requirements, diode protection, reliability, and cost. Advanced packaging technologies on diverse platforms assure the most cost effective, high coupling and reliable solutions to the customers.

Oclaro's high power diode laser products are built with the same manufacturing standard, and some even share a common platform, as telecom products which enable high power diode laser high reliability and stringent qualification requirements for industrial customers. The low cost packaging solution also offers customers an attractive \$/W margin for pump diodes which is the most critical and cost consuming component in the fiber laser system. Single emitter, multi emitters and mini-bar fiber coupled platforms are fully developed internally and mature for mass volume manufacturing with these advanced packaging technologies. These factors lead to more explosive growth in the fiber lasers market share.

8551-33, Session 7

A ridge waveguide quantum well AlGaAs/GaAs laser design

Marziyeh Nazari, Islamic Azad Univ. (Iran, Islamic Republic of); Mohammad Mahdi Oskoie Tabrizi, Sharif Univ. of Technology (Iran, Islamic Republic of)

An advanced structure of AlGaAs laser diodes has been designed using the simulation software.

Simulation results suggest that the thicknesses of SCH layers, inner cladding and outer cladding layers should be changed in order to give low loss, narrow far-field divergence angle and high confinement factor. The Thickness of the etch stop layer is optimized to give the required effective lateral refractive index. At the end the channel width and ridge width are also optimized to obtain single lateral mode.

The aim of our study was three folds: (1) to provide the comprehensive analysis and calculations to design a ridge waveguide laser. In the simulations, the thicknesses of SCH layers, inner cladding layers and outer cladding layers are varied in order to observe variations of far-field divergence and the total confinement factor as functions of layer thicknesses. Comparison among loss, narrow far-field divergence and high confinement factor are made to optimize layer thicknesses, (2) The thickness of an etch stop layer is optimized to achieve the required lateral effective refractive index difference, and also the far-field divergence of the ridge waveguide laser, (3) the channel width and ridge width are designed to maintain single lateral mode and low loss by using the three layer dielectric slab waveguide calculations.

8551-35, Session 7

Linewidth-tunable laser diode with double volume Bragg gratings for rubidium laser pumping

Zhiyong Li, Institute of Electronics (China) and Graduate Univ. of Chinese Academy of Sciences (China); Rongqing Tan, Institute of Electronics (China); Cheng Xu, Lin Li, Wei Huang, Institute of Electronics (China) and Graduate Univ. of Chinese Academy of Sciences (China)

In the research field of diode pumped alkali laser (DPAL), one of the critical issues is matching the linewidth and central wavelength of the pumping diode laser with that of the alkali vapor's absorption line. Due to the radial temperature gradient in the active medium of high power alkali laser system, the diodes with ultra-narrow linewidth may not pump efficiently than diodes with wider linewidth. With double volume Bragg gratings (VBG), we achieved a laser diode (LD) with linewidth tunable while the output power changed no more than 1% during the adjustment. The temperature of the VBGs was controlled by thermo-electronically coolers respectively. Because VBG's central wavelength shifts with temperature while the bandwidth maintains the same, adjusting the temperature differences between the two VBGs resulted in different bandwidth of the feedback to the LD. As a result, linewidth of the LD with double VBGs can be tunable in a large range. Through controlling the temperature differences, the linewidth of the LD, which

was 1.8 nm before adding the two VBGs, was tunable from 90 pm to 200 pm while the output power changed little. By changing the VBGs' temperature simultaneously, central wavelength of the linewidth-tunable LD was tunable from 779.40 nm to 780.10 nm. Since the tunable range covered the Rb D2 absorption line, the LD will help to choose the pumping source for high-power alkali vapor laser system.

8551-36, Session 8

High-average-power eye-safe diamond Raman laser

Aaron M. McKay, Ondrej Kitzler, Hua Liu, David Fell, Richard P. Mildren, Macquarie Univ. (Australia)

Diamond is a highly attractive laser material due to its exceptional material properties, which in most cases, outclasses competing materials. Its high thermal conductivity, low thermal expansion and wide transparency make CVD-grown diamond especially commendable for high-average power laser applications. Already diamond, in comparison to more mature Raman crystalline materials, has demonstrated the highest recorded output powers for both pulse and continuous wave operation. In addition, when combined with well-established Nd laser technology, the 1332 cm⁻¹ Raman frequency in diamond provides a convenient and efficient route to the eye-safe spectral region via its second Stokes shift. In this paper, we report an external cavity Raman laser using a 10-mm-long low-loss CVD diamond pumped by a 35 W q-switched side-pump Nd:YVO₄ laser with approximately 22 ns pulses at 36 kHz pulse repetition frequency. Our diamond Raman laser, lasing near 1485 nm, had in excess of 10 W and efficiencies greater than 50%. This represents a substantial improvement in power when compared to other crystalline Raman lasers operating in this eye-safe region. The thermal lens strength was estimated for an external cavity diamond Raman laser which were also compared to those using KGW with similar pumping and resonator conditions. This direct comparison between KGW and diamond in similar resonators gives insight to potential thermal design issues when scaling to higher Raman output powers and estimates possible power limitations.

8551-37, Session 8

Solar pumped laser with the grooved Nd:YAG

Dan Fang, Changchun Univ. of Science and Technology (China)

As the global climate is warming, the earth environment is deteriorated gradually. It is desired to exploit renewable energy and clean energy. The ultimate renewable energy source might be the solar energy, which is far from fully utilized. The power density of solar on earth is so low that it can't achieve to pump laser. To surpass the lasing threshold, the solar has to be highly concentrated. A Fresnel lens as primary concentrator instead of the large-dimensional paraboloidal mirrors collects the solar radiation in 1m² efficient areas. Sunlight concentrated is coupled into the conical chamber pumping grooved Nd:YAG laser media in 8mm-diameter and 100mm-length. The pumping cavity is designed to combine end-pumping to side-pumping, in which the pumping light comes from many directions, which could compensate the drawbacks of single end-pumping or side-pumping. The cooling effect is improved on grooved crystal rod, which changes the state of the fluid motion into turbulence. By comparing grooved rod to ordinary rod, the output laser power and beam quality is by 25%. In our experiment, laser output of 25 W has been achieved and the collect efficiency is 25 W/m² with the grooved laser rod.

8551-39, Session 8

LD dual-end-pumped CW Tm:YLF laser

Xinyu Chen, Changchun Univ. of Science and Technology (China)

Continuous wave Tm:YLF laser by 792nm LD dual-end-pumped is presented. Based on the rate equation of quasi three level, we analyzed the pump threshold and the slope efficiency of the laser system. At the same time, according to ABCD Matrix theory, we analyzed the stability condition and the pattern matching of the plano concave resonator. We contrast the pump threshold, the slope efficiency and optical conversion efficiency when different output mirror transmittance of 15% and 23% is applied. The pump threshold is lower of the 15% transmittance output mirror than that of the 23% transmittance output mirror, while the slope efficiency of the 23% transmittance output mirror is a little higher than that of the 15% transmittance output mirror. Besides, the laser beam quality are measured using output mirrors with different radius of curvature of 150mm, 200mm and 300mm when we apply different output mirror transmittance of 15% and 23%, respectively. For all the experiments, the Tm:YLF laser crystal keeps 18°C and the temperature control method is water cooling. When we applied L shape plano concave resonator, the length of the resonator is 135mm, the radius of curvature output mirror is 300mm and the temperature of the Tm:YLF laser crystal is 18°C, we observed the central laser wavelength is 1908. The threshold power is 6.8W. The highest output power reaches 21.6 W when the totally input pump power is 53.9W. And the optical conversion efficiency and the slope efficiency is 48.1% and 40.0%, respectively. The experimental results are coincide with the theory.

8551-40, Session 8

High-power single-frequency Nd:YVO₄ green laser by self-compensation of astigmatism

Yaohui Zheng, Shanxi Univ. (China)

High-power single-frequency solid-state green lasers can be used for a variety of roles, such as pumping of Ti:sapphire or dye lasers, precision measurement, and high-resolution laser spectroscopy. However, the power scaling and beam quality are limited by thermal effect of the gain medium.

In order to quantify the influence of the thermal effect and to find an optimal resonator scheme, the value of the thermal focus in Nd:YVO₄ crystal is measured by using a probe beam technique. The measuring results show that a strong astigmatism of the thermal lens of Nd:YVO₄. With a laser diode of the wavelength of 888nm as the pump source, the thermal effect in the pumping progress is mitigated greatly. By orienting the c-axis of the Nd:YVO₄ crystal in the tangential plane of the ring cavity, the astigmatism introduced by the thermal lens and the ring cavity can be mutual-compensated. Due to the mitigation and compensation of the thermal effect, scaling the single-frequency laser to higher output power, whilst retaining the excellent performance. We obtain a high power intracavity frequency-doubling single-frequency green laser, with maximum output power of 25.3 W, with 32.2% of the optical-optical conversion efficiency with respect to absorbed pump power. To the best of our knowledge, this is the highest output power and conversion efficiency of single-frequency Nd:YVO₄ laser by intracavity frequency-doubling. The power stability of the green laser at 25.3 W is better than ±0.4% for 8 h.

Conference 8552: Semiconductor Lasers and Applications V

Monday - Tuesday 5 -6 November 2012

Part of Proceedings of SPIE Vol. 8552 Semiconductor Lasers and Applications V

8552-1,

Quantum dot lasers and relevant nanoheterostructures

Alexey E Zhukov, Natalia V. Kryzhanovskaya, Artem V. Savelyev, Alexey M. Nadtochiy, Ekaterina M. Arakcheeva, Fedor I. Zubov, Vladimir V. Korenev, Saint-Petersburg Academic Univ. (Russian Federation); Mikhail V. Maximov, Yuri M. Shernyakov, Marina M. Kulagina, Ilia A Slovinskiy, Ioffe Physical-Technical Institute (Russian Federation); Daniil A Livshits, Innolume GmbH (Germany); Alexandros Kapsalis, Charis Mesaritakis, Dimitris Syvridis, University of Athens (Greece); Alexander Mintairov, University of Notre Dame (United States)

Microring and microdisk structures ($d = 3-6 \mu\text{m}$) comprising $1.3 \mu\text{m}$ InAs/InGaAs quantum dots have been fabricated and studied by micro-PL and NSOM. Ground-state lasing was achieved well above room temperature (up to 380 K). Effect of inner diameter on threshold characteristics was evaluated. Spectral and power characteristics of QD stripe lasers operating in two-state lasing regime have been studied in a wide range of operation conditions. It was demonstrated that neither self-heating nor increase of the homogeneous broadening are responsible for quenching of the ground-state lasing beyond the two-state lasing threshold. It was found that difference in electron and hole capture rates strongly affects light-current curve. Modulation p-type doping is shown to enhance the peak power of GS lasing transition.

8552-2, Session 1

Ultrafast nonlinear dynamics in semiconductor optical amplifiers for optical signal processing (*Invited Paper*)

Yong Liu, Ligong Chen, Xiu Zheng, Shangjian Zhang, Rongguo Lu, Univ. of Electronic Science and Technology of China (China)

Semiconductor optical amplifiers (SOAs) have been broadly used as nonlinear elements for all-optical signal processing, where the nonlinearities in the SOAs have been utilized. To increase the operating speed of the SOA-based optical switches, it is crucial to understand the ultrafast nonlinear dynamics in the SOAs. The gain dynamics of the SOA has been extensively studied. However, the phase dynamics and chirp dynamics are not as clear as the gain dynamics. We present the investigation results on the nonlinear phase and chirp dynamics in SOAs. Time-resolved gain and phase dynamics of a quantum well SOA are measured using 2 ps pump pulses into an integrated Mach-Zehnder interferometer switch under a co-propagation arrangement. Ultrafast component in the phase recovery is clearly observed. We explain the ultrafast phase dynamic by using a field propagation numerical model that includes the impact of sub-picosecond intra-band effects of the SOA. In addition, we numerically investigate the chirp properties of the SOA in all-optical switches, and analyze the influences of chirp dynamics upon the detuned-filtering-based optical switches that extract the ultrafast chirp component to realize more than 160 Gbit/s optical switching. The results are very useful for SOA-based ultrafast optical signal processing in photonic networks.

We present the investigation results on the nonlinear phase and chirp dynamics in semiconductor optical amplifiers (SOAs). Time-resolved gain and phase dynamics of a quantum well SOA are measured using 2 ps pump pulses into an integrated Mach-Zehnder interferometer switch. Ultrafast component in the phase recovery is observed. We also numerically investigate the chirp properties of the SOA, and analyze the influences of chirp dynamics upon the detuned-filtering-based optical switches that extract the ultrafast chirp component to realize more than

160 Gbit/s optical switching. The results are very useful for SOA-based ultrafast optical signal processing in photonic networks.

8552-4, Session 1

An open-path semiconductor laser transmissometer for smoke opacity measuring (*Invited Paper*)

Peng Shi, Ke Du, Institute of Urban Environment (China)

Opacity is an efficient gauge to evaluate obscuring effect and Particles characteristics of smoke. An open-path laser transmissometer has been fabricated to quantify the light opacity of smoke, which is operated in field environment. The 532nm laser emitted out from semiconductor laser diode has been modulated as square wave pulses by an electronic oscillator based on 555 integrated circuit chip. An optical transceiver module has been developed which is based on an off-axis parabolic mirror and a retro-reflector. The laser is expanded to parallel light beam and diverted to open atmosphere by a 90 degree off-axis parabolic mirror. After transmitted the smoke, light beam is reflected back on the same light-path by the retro-reflector. A Fast Fourier Transform Filtering algorithm combining with modulating of laser has been developed to exclude the Mie scattering effects of sunlight by particles in the smoke. The returned light and light from laser source are both detected by two photodiode detectors; detected signals are converted by A/D convertor and then sent to the computer via a USB cable. The opacity of smokes which consisted of fugitive dust is measured by both Laser Transmissometer Method and Digital Optics Method in filed campaign in Xiamen, china. There are 91% of the individual absolute opacity difference values from April 26 that are $< 15\%$, and Laser Transmissometer has much high temporary resolution than Digital Optics Method.

8552-5, Session 2

VCSELs for exascale computing, computer farms, and green photonics (*Invited Paper*)

Werner H. Hofmann, Philip Wolf, Technische Univ. Berlin (Germany); Wei Li, Technische Univ. Berlin (Germany) and Institute of Semiconductors (China); Philip Moser, Gunter Larisch, Technische Univ. Berlin (Germany); James A. Lott, VI Systems GmbH (Germany); Dieter Bimberg, Technische Univ. Berlin (Germany) and King Abdulaziz Univ. (Saudi Arabia)

The copper-induced communication bottleneck is inhibiting performance and environmental friendliness of today's supercomputers. Vertical-cavity surface-emitting lasers (VCSELs) are ideally suited to solve this dilemma. Global players like Google, Intel, HP or IBM are now going for optical interconnects based on VCSELs. The required bandwidth per link is given by Amdahl's balanced system law and depends on the architecture of the data center. According to Google, a band-width of 40 Gb/s has to be accommodated in the future. IBM demands 80 Tbps interconnects between solitary server chips in 2020. We recently realized ultra-high bit rate VCSELs up to 49 Gb/s suited for such optical interconnects emitting at 980 nm. These devices show error-free transmission at temperatures up to 155°C and operate beyond 200°C. Serial data-rates of 40 Gb/s were achieved up to 75°C. Record high energy efficiencies close to 50 fJ/bit could be demonstrated for lasers emitting at 850 nm. The devices were fabricated using a full three-inch wafer process, and the apertures were formed by proprietary in-situ controlled selective wet oxidation. All device data were measured, mapped and evaluated by our proprietary fully automated probe station. The bandwidth density of our present

devices is scalable from reasonably 100 Gbps/mm² to a physical limit around 15 Tbps/mm². Still more energy-efficient devices dissipating less heat are mandatory for further up scaling of the bandwidth. Novel metal-clad VCSELs enable to reduce the footprint for ultra-short range interconnects by 1 to 2 orders of magnitude enabling a similar increase of device density and bandwidth.

8552-6, Session 2

Retrieving alpha factor of semiconductor lasers from a self-mixing interference waveform (*Invited Paper*)

Yan Gao, Yanguang Yu, Jiangtao Xi, Univ. of Wollongong (Australia)

As an active research field, the self-mixing interferometry (SMI) based on semiconductor lasers (SLs) is a highly promising and emerging technique for non-contact sensing and parameter measurements of SLs. The basic structure of an SMI system consists of an SL, a lens and an external target. When a portion of reflected light from the target travels back to the laser cavity, a new lasing field is built up leading to both amplitude and phase modulations. The modulated optical output power, which is detected at the rear facet of laser diode, is called a self-mixing signal which carries the information of both the target and SL's feature parameters. Alpha factor, also known as linewidth enhancement factor, is one of the most important SL's feature parameters. It characterizes the characteristics of SLs, such as the linewidth, the chirp, the injection lock range and the dynamic performances. This paper presents a new method for retrieving alpha of SLs by making use of a self-mixing interference waveform. According to the well-known Lang-Kobayashi (L-K) theory, the self-mixing interference waveform is shaped by multiple parameters, including the alpha, the optical feedback level factor (denoted as C) and other parameters related to the oscillation of the external target. In this work, we build a set of new equations based on the SMI model derived from the L-K theory, which can be used to calculate the alpha value. In existing SMI based methods for measuring the alpha, there are two restrictions: the external target is set in a single harmonic vibration and the C is limited within a certain narrow range. The proposed method is able to relieve these two limitations. The associated simulations and experiments are carried out for verifying the proposed method.

8552-7, Session 2

High-temperature operating 795-nm VCSELs for 87Rb chip-scale atomic clock

Yongqiang Ning, Changchun Institute of Optics, Fine Mechanics and Physics (China)

This paper reports the design and growth of high-temperature operating 795-nm VCSELs with compressively strained InAlGaAs-AlGaAs multiply quantum well (MQWs) which improves the power and modulation performances at 358K. Compositions and thickness of the InAlGaAs MQWs are optimized for operation at elevated temperatures. Temperature sensitivity of the threshold current is estimated by the temperature dependence of cavity-mode gain over a broad temperature range (25oC-150oC).

VCSEL samples with three 6nm In_{0.125}Al_{0.14}Ga_{0.735}As-Al_{0.3}Ga_{0.7}As QWs and 32/45 pairs Al_{0.25}Ga_{0.75}As/Al_{0.9}Ga_{0.1}As p/n-type DBR are grown by metalorganic vapor phase epitaxy (MOVPE) in an Aixtron 200/4 reactor on exactly oriented (001) GaAs substrates. Temperature dependent DBR reflectivity spectra and photoluminescence (PL) showed a temperature-shift of 0.298nm/K for peak wavelength of PL and 0.062nm/K for central wavelength of DBR reflectivity spectra. Cavity mode wavelength is spectrally aligned with peak wavelength of PL at 80oC (353K) which agrees with the calculated expectation.

A self-consistent VCSEL model based on quasi 3D finite element analysis accounting for the electrical, optical, and thermal

characteristics and their close interaction is provided by the photonic integrated circuit simulator in 3D (PICS3D) software. The temperature distribution contour is solved for the proposed structure with 4μm aperture device under a driving current of 2 mA at temperatures of 358K and 300K. It is obviously shown that the proposed VCSEL demonstrates a single-mode output power more than 0.4mW and a 3dB bandwidth more than 6.8 GHz even at 358K, which meets the two most requirements of single mode output and high speed modulation at high temperature.

8552-8, Session 2

Cavity optimization of 1.3 micron InAs/InGaAs quantum dot passively mode-locked lasers

Tianhong Xu, Paolo Bardella, Ivo Montrosset, Politecnico di Torino (Italy)

Performance optimization of monolithic 1.3 micron InAs/InGaAs quantum dot (QD) passively mode-locked lasers of 3 mm long and 10 QD layers have been investigated systematically using the Finite-Difference Traveling-Wave (FDTW) model by changing simultaneously the length of the saturable absorber (SA) and the cavity reflectivity.

Our numerical model describes in a rigorous way the dynamics of the field propagating in the Fabry-Perot cavity consisting of a gain section and a SA and the dynamics of the associated carrier distributions in QD-based lasers. ML lasers designed with help of this model have shown outstanding performances respect to more traditional structures.

In this work, we demonstrate that instead of the typically used low value of the output facet reflectivity (5% to 1%), an appropriate higher value of it with a proper length of the SA allows to achieve performance improvement. Reduction in pulse width from 4.4 ps to 930 fs and increase in the product of the peak power and the average power (figure of merit) from 0.012 W² to 0.2 W² were obtained. Clear design guidance are extracted, which can be also exploited in the design of lasers with different length or QD layers.

Furthermore, we put in evidence that the pulse shape formation is determined not only by the gain/absorption saturation energy, but also by the cumulative longitudinal gain/absorption saturation effects which are related to the length of the gain/SA sections.

Our simulation results also confirm that reducing the ratio between the unsaturable losses and the saturable losses would benefit the ML performances of a laser.

8552-9, Session 2

The characteristics of spectral in vertical-cavity surfacing-emitting lasers based on defect layer structure

Bao Lu Guan, Beijing Univ. of Technology (China)

one-dimensional (1D) photonic crystal (PC) such as Bragg reflectors spontaneously form a photonic band gap (PBG), which widens considerably as the dielectric contrast increases, and would exhibit vivid Bragg reflecting walls at the design wavelengths when the periodicity of the dielectric matches the wavelength of the laser. The PBG feature of the PC has attracted considerable interests for multi-wavelength laser devices and display devices. It is possible to realize a dual-wavelength VCSEL with a single defect layer such as AlGaAs by employing a two-mode asymmetric 1D PC device structure. Here, we have proposed an inexpensive multibeam control method using an asymmetric-PC structure with defect layer to get two or more wavelengths simultaneously from a high-gain VCSEL. It is pointed out that the defect layer matching in the composite mirror of a PC and asymmetric-PC structure could provide an extremely large difference in the reflectivity between the two mode states. The EL spectrum of the GaAs/Al_{0.9}Ga_{0.1}As asymmetric 1D PC structure with Al_{0.8}Ga_{0.2}As

defect layer shows that one of the modes is centered near 980 nm and the other near 930 nm. The full width at half maximum (FWHM) of the dual-wavelength are 1 nm and 2.2 nm, respectively and the total optical thickness of the microcavity device is about 4.5π . This structure can be fabricated after growing an ordinary QW laser structure with a standard epitaxial method. It is very simple and suitable for multibeam control. In the field of nonlinear optics, this laser may be used as the source in spectroscopy and communications.

8552-10, Session 3

Design and optimization of the microwave structures for multi-channel PICs' packaging using flip-chip method and LTCC substrate *(Invited Paper)*

Wei Han, Frank Hudson Peters, Tyndall National Institute (Ireland)

In order to meet the high-speed, high-density, and low cost packaging scheme for the future broadband and multichannel PICs, we have designed and optimized the packaging scheme using LTCC based flip-chip technique. In this paper, the microwave model was built for the LTCC substrate and the flip-chip structure using 3D distributed EM method, in which different signal feeding structures were designed to control the transmission loss and RF reflection. The RF crosstalk as well the isolation was also investigated to provide an optimum signal integrity situation for high-density integration which will also provide the design rules for the PIC fabrications. Finally, the LTCC substrates were made and assembled with the dummy chips to validate our design.

8552-11, Session 3

Holding beam injection for improving self-induced polarization rotation in a semiconductor optical amplifier *(Invited Paper)*

Shangjian Zhang, Yali Zhang, Rongguo Lu, Shuang Liu, Yong Liu, Univ. of Electronic Science and Technology of China (China)

Gain recovery is critical to ultrafast dynamics of a semiconductor optical amplifier (SOA), which determines the working speed and output quality of SOA-based all-optical signal processing functionalities. It has been reported that slow gain recovery might lead to serious signal distortions, pattern effects and degradation of extinction ratio (ER), and limit the operating speed to be lower than 40 Gbit/s in high-speed communication systems. We propose a scheme to improve the performance of self-induced polarization rotation (SPR) in a semiconductor optical amplifier by holding beam injection. It is found that the gain recovery time of TE and TM modes can be largely reduced through an appropriate holding beam injection, with which the response of SPR in the SOA for ultrafast signal can be speeded up. As an example of validation, we apply a holding beam in the SPR-based optical power equalization. Simulation shows that both the distortion of Return-to-zero (RZ) signal and the overshoot of Non-return-to-zero (NRZ) signal due to the slow gain recovery of the SOA can be significantly suppressed. After the power equalization, an extension ratio (ER) improvement of 10 dB and 7 dB of RZ and NRZ has been obtained respectively, and both signals can reach high quality with the Q factor of eye-diagram over 20.

A scheme for improving the self-induced polarization rotation (SPR) in a semiconductor optical amplifier (SOA) based on holding beam injection is proposed. Gain recovery of TE and TM modes can be largely accelerated through an appropriate holding beam injection, with which the response of SPR in the SOA for ultrafast signal can be speeded up. Holding beam injection is employed in SPR-based optical power equalization as an example of validation, in which the distortion of RZ (return-to-zero) and the overshoot of NRZ (non-return-to-zero) signal are

largely suppressed, and the extension ratio are improved by 10 dB and 7 dB, respectively.

8552-12, Session 3

Single facet slotted Fabry-Perot laser and its application in photonic integrated circuits *(Invited Paper)*

Hua Yang, Tyndall National Institute (Ireland)

to meet the exponentially growing demands on data transmission capacity, dense wavelength division multiplexing (DWDM) technology which multiplexes a number of optical carrier signals onto a single optical fiber by using different wavelengths has been adopted by optical communication systems and more channels and components are introduced to improve the functionality. Monolithic photonic integration circuits (PICs) in InP have provided an effective solution to realize multiple channels and advanced functions in the system level with compact size, lower power consumption, simpler coupling and packaging, higher reliability as well as lower cost. In these systems, single mode lasers, typically distributed feedback (DFB) or distributed Bragg reflector (DBR) lasers, are the indispensable components for generating the optical signals. However both require submicron gratings which must be generated using time consuming and costly ebeam or holographic lithography.

Slotted FP lasers using the optical perturbation by one or multiple slots etched into the ridge waveguide of the Fabry-Perot lasers to select the desired mode have been demonstrated as single mode and tunable. And by properly designing the multiple slots to provide enough reflection necessary for lasing, single facet or facetless slotted lasers can be realized which are suitable for monolithic integration in the PIC. These lasers are based on a single epitaxial growth with a simple fabrication process in which traditional photolithographic techniques can realize the feature size of the slots of $1\mu\text{m}$. In this paper, we demonstrate a single facet slotted FP laser with single mode and tunability and its application in the PIC.

8552-13, Session 3

Opto-electronic hybrid integrated platform for high-speed applications

Wei Han, Tyndall National Institute (Ireland)

In this work, a broadband Optoelectronic Modulator Module was developed to enable the fabrication of 40G broadband, low-cost, and compact transceivers for telecommunications. In order to examine the microwave performances of the proposed module, the equivalent circuit method and 3D distributed electromagnetic model are employed. In this module, an opto-electronic device such as a high-speed EAM modulator is integrated with a RF interconnection circuit. A Kovar heatsink with multistep structure is designed for ease of optical coupling using a laser welding process. In order to control the high frequency resonances and improve the signal integrity, AlN based subcircuits are designed to feed the RF and DC signals separately. The interconnection networks between the opto-electronic device and high-speed transmission lines are carefully investigated to optimize the microwave performances. The influence of the packaging for this opto-electronic integration platform on the microwave performance is also analyzed in detail. The simulation results obtained and successful fabrication of a transmitter module demonstrate that the proposed platform can meet the requirements for high-speed WDM or TDM systems.

8552-14, Session 3

High-power narrow far-field broad-stripe semiconductor lasers with second-order metal grating feedback

Li Qin, YongYi Chen, Peng Jia, YongQiang Ning, Lijun Wang, Changchun Institute of Optics, Fine Mechanics and Physics (China)

In order to obtain high power semiconductor lasers with narrow far-field and improve the quality of the output beam, a broad-stripe distributed feedback semiconductor laser with second-order metal surface gratings emitting around 940 nm is fabricated, based on the holographic photolithography and wet etching technology. The second-order metal gratings are located at the metal/semiconductor interface in the p-Al_{0.2}GaIn_{0.49}P cladding layer, with 960 μm x 142 μm grating area, and the metal gratings also act as ohmic contact of the p side, which differs from traditional DFB-LDs. The grating period is 287 nm, the grating depth is 100 nm, and the duty cycle is 0.5.

The characteristics of the semiconductor laser with second-order metal surface gratings are tested under room temperature continuous-wave conditions without any temperature-control device. For the laser with second-order metal gratings, the powers is 700 mW, spectral linewidth (FWHM) is less than 0.1 nm, lateral far-field angle (FWHM) is 2.7° and the vertical far-field angle (FWHM) is 16.7° at the current of 1.5 A. For the laser without gratings at a current of 1.5 A, the spectral linewidth is 1.3 nm, the lateral far-field angle is 7.3° and the vertical far-field angle is 36°, both worse than lasers with second-order metal surface gratings.

To improve the output characteristics, the DFB laser structure with second-order metal surface gratings was optimized by using the modified coupled-wave equations and COMSOL multiphysics.

In conclusion, because of the integration of second-order metal surface gratings, the spectrum is narrowed and the far-field angles are reduced greatly. This opens the way for the realization of watt-scale high-power second-order metal surface grating edge-emitting and surface-emitting lasers with high beam quality.

8552-15, Session 3

InGaAsP/InP DFB laser array monolithically integrated with MMI combiner and SOA

Li Ma, Institute of Semiconductors (China) and Tsinghua Univ. (China); Hongliang Zhu, Institute of Semiconductors (China); Minghua Chen, Tsinghua Univ. (China); Can Zhang, Baojun Wang, Institute of Semiconductors (China)

We developed compact (2.5mmx0.5mm) four-channel 1.55 μm range InGaAsP/InP wavelength-selectable microarray distributed feedback laser diodes (DFB-LD's) with a monolithically integrated multimode interference (MMI) optical combiner and a semiconductor optical amplifier (SOA). The lasing wavelengths of four channels were changed by varying width of ridge waveguides from 2 μm to 3 μm and the four channels can operate separately or simultaneously. Metal-organic Chemical Vapor Deposition (MOCVD) was used for crystal growth and a butt-joint technique was used to integrate the active MQW and passive waveguide. Separation between two adjacent lasers was set at 100μm. The sine S-bends were 850-μm-long. The MMI coupler is 24-μm-wide and 316-μm-long. The length of SOA was 600μm. 1st order gratings were fabricated by normal holographic exposure and a CH₄:H₂:O₂ reactive ion etching (RIE) dry etching process. A shallow ridge waveguide was used for lasers and amplifiers and a deep ridge waveguide was used for the multimode interference optical combiner and S-bend waveguide to reduce bending and radiation losses. The 250-nm-thick InGaAs contact layer was removed by a dry etching process from electrical isolation areas, the S-bend and MMI regions in order to obtain electrical isolation and reduce the absorption loss. At 25°C, the lasing wavelengths of the four channels were 1549.965nm, 1551.105nm, 1552.255nm and 1553.015nm, respectively. Side

mode suppression ratios of more than 35dB were obtained. A typical threshold current was around 35mA when the length of DFB LD was 690μm. Output power of 1.86mW could be achieved when the injection current of DFB LD and SOA were both 100mA at 25°C.

8552-16, Session 4

Time delay signatures of chaotic output in 1550nm VCSELs with variable-polarization double optical feedback (*Invited Paper*)

Ping Xiao, Zheng-Mao Wu, Jia-Gui Wu, Long Jiang, Guang-Qiong Xia, Southwest Univ. (China)

In the last two decades, the optical chaos based on semiconductor lasers (SLs) has received considerable attention for its applications in secure communications, fast physical random bit generation and chaotic radar etc. Since high dimension chaos can be relatively easily obtained by introducing time delay (TD) feedback, external delay feedback SL (EDF-SL) system has been regarded as a main candidate in optical secure communication and physical random bit generation. However, the chaotic output of an EDF-SL system usually retains obvious TD signatures, which inevitably affects the statistical performance of random bit sequences and also may provide a possible clue to the encryption attackers in chaos cryptosystem. Hence, the TD signature suppression becomes crucial both for improving the statistical performance of random bit sequences and for ensuring the cryptosystem security.

In this paper, we theoretically investigate the TD signatures of chaos output in a 1550nm vertical-cavity surface-emitting laser (VCSEL) with variable-polarization double optical feedback (VPDOF) by using self-correlation function (SF) and permutation entropy (PE). Through simulating the influences of polarized angle, feedback strength and injection current on the TD signatures, the optimal parameters setting for the TD signature suppression have been specified. We believe that this work would offer a high-efficiency, simple and practicable TD signature suppression scheme for high speed random bit generation and chaos cryptosystem.

8552-17, Session 4

Photonics-assistant spectra shaping of ultra-wideband signals for dynamic spectrum access in cognitive network (*Invited Paper*)

Jianyu Zheng, Ninghua Zhu, Lixian Wang, Jianguo Liu, Hui Wang, Yuanxin Du, Institute of Semiconductors (China)

The dynamic control for the spectra of the Ultra-wideband (UWB) signals, which is the key for implementing the dynamic spectrum access in the cognitive radio, is still a challenge due to the limited processing speed of the electronic devices. In this paper, we have summarized our recent work about controlling the spectrum shape of the UWB signals in optical domain, in addition to review the other groups' related research work. The experiment setups and results based on nonlinear dynamics of the optoelectronic oscillator, transfer response of the phase or polarization-to-intensity convertor and four-wave-mixing of the nonlinear optoelectronic device will be described in detail respectively, in which the controllable frequency suppress for the optical UWB signals at specific frequency positions were implemented. Particularly, the UWB pulse with the special shape, which corresponds to the 5-GHz band-rejection in frequency domain, was generated in order to avoid the interference between UWB and Wireless Fidelity system in practice. In addition, the UWB signals whose center frequency could be continuously tuned and converted up to the frequency range of millimeter wave were generated by utilizing the polarization modulator based optical switch. The areas for future development and the challenge of implementation of these techniques for the applications in practice will also be discussed.

8552-18, Session 4

Design of laser echo data acquisition system based on USB2.0

Fuzhou Shang, Yong Song, Qun Hao, Wenlong Zhang, He Sun, Beijing Institute of Technology (China)

As a new kind of PC Bus interface specification, USB is widely used in data collection system. The technology of FPGA has its own particular advantages, which has been widely used in the fields of data acquisitions and image manipulation etc.

While collecting the echo signal of the laser and detecting object with a single APD, the data acquisition system based on the technology of FPGA and USB2.0 was designed in this paper.

Firstly, the proposed research project of 3D-imaging radar is explained. The project uses a 905nm pulsed laser diode as the laser source and detects object with a single APD to obtain instance images. The hardware of the data acquisition system including APD, NE5210 amplifier, FPGA controller and USB interface circuit was designed and also analyzed.

Secondly, the architecture of the USB was deeply analyzed firstly, and according to the scheme of the data acquisition system, the detailed hardware and software design was introduced. In the hardware section, the interface between the CY7C68013 and FPGA was introduced. In the software section, the whole communication process of CY7C68013 in the slave FIFO mode were expounded; and the testing result of the firmware was listed at the end of the firmware part; the design process of the driver for the USB was introduced here; Finally the application software used to exhibit the curves and save data was designed.

Finally, the hardware and the software of the system were debugged, the results of debugging were given and analyzed.

8552-19, Session 5

The modeling of comb spectrum stability in quantum dot lasers (*Invited Paper*)

Artem V. Savelyev, Mikhail V. Maximov, Alexey E. Zhukov, Saint Petersburg Academic Univ. (Russian Federation)

Lasers emitting low-noise broadband spectra formed by more than dozens narrow spectral lines (comb lasers) are very promising for a numerous applications. Though it has been shown experimentally that quantum dot lasers have a unique property to generate stable multimode spectrum, the origin of it remains unclear. Still the stability of the spectrum is the key issue for understanding laser dynamics and further calculations of the laser properties. The goal of this paper is to explain the stability of quantum dot laser spectrum in terms of interplay between homogeneous and inhomogeneous broadening and spatial interaction of longitudinal modes. It examines three aspects of stability: modeling convergence, Lyapunov's conditions and robustness to small spectral losses variation. It is shown that the spatial mode interaction is the major mechanism that ensures the spectral stability in the presence of large homogeneous broadening. Moreover, if the latter is taken into account assuming spatial uniformity no solutions stable in the mentioned means could be obtained. These results could be the starting point in studying quantum dot laser's dynamical properties such as intensity noise.

8552-20, Session 5

40-Gbps random bit generation by oversampling chaos from an injected semiconductor laser (*Invited Paper*)

Xiao-Zhou Li, Sze-Chun Chan, City Univ. of Hong Kong (Hong Kong, China)

Random bit generators are applicable to a wide range of areas including numerical simulation, encryption, and secure communication, where a high generation speed is often preferred. Semiconductor lasers in chaotic oscillations have recently been utilized for random bit generation with bit rates on the order of gigabits per second, far exceeding those obtained from conventional electronics. However, in previous works, the chaotic waveforms were usually generated from semiconductor lasers subject to optical feedback. The existence of the internal feedback round-trip delay times had often led to residual peaks in the autocorrelation at multiples of the delay times, which were detrimental to the randomness quality of the outputs. Different approaches such as high-resolution analog-to-digital conversion, bandwidth enhancement, and complicated post-processing were realized to improve the randomness to sufficient quality, which inevitably sacrificed the simplicity of the setups. Recently, as an alternative, we have demonstrated random bit generation using a semiconductor laser subject to optical injection in lieu of optical feedback. The approach inherently avoids existence of any problematic delay time. In this paper, we further report on oversampling the chaotic signal that is recorded by an oscilloscope with 2.5-GHz bandwidth and sampled at 10 GHz, which is twice the Nyquist rate. This allows retention of 4 least significant bits per sample point. After a bitwise exclusive-or operation, output bits generated at 40 Gbps is shown to pass the National Institute of Standards and Technology Special Publication 800-22 statistical tests of randomness. Oversampling significantly alleviates the requirements on the electronic bandwidths.

8552-21, Session 5

Raman spectroscopy system with hollow fiber probes

Binghong Liu, Yi-Wei Shi, Fudan Univ. (China)

A simple Raman spectroscopy system was realized using a flexible hollow waveguide (HW) as laser emitting fiber and another HW as signal collecting fiber. A silver-lined capillary waveguide has flat transmission characteristic in the visible and near infrared wavelength region longer than 500nm and little optical background fluorescence noise without intrinsic Raman scattering compared with silica optic fiber during transmission, which would be of great significance to the detection in low frequency Raman shift region. The complex filtering and focusing system was thus unnecessary. The Raman spectra of CaCO₃ and polythene were obtained using our simple system with reasonable signal to noise ratio without any lens and were compared with the results detected by commercial optic fiber probe. In addition, we used Ag HW as sample cell to detect liquid phase sample, we adopt a 6cm Ag HF cell and direct forward butt-coupling system construction. Experiment results show that such HW and simple system construction can obtain very high signal to noise ratio induced by increasing optical length between sample and laser light. We also give the elementary theoretical analysis of using HW as sample cell, the parameters of the fiber which would affect the system were discussed. HW plays a good performance for Raman detection and thus is allowed to be a potential commercial fiber probe and sample cell.

8552-22, Session 5

All-optical sampling towards high-speed optical analog-to-digital conversion

Shangjian Zhang, Yali Zhang, Rongguo Lu, Shuang Liu, Heping Li, Yong Liu, Univ. of Electronic Science and Technology of China (China)

All-optical sampling attracts considerable attention due to its crucial applications in high-speed optical analog-to-digital conversion. Several fiber-based optical sampling schemes have been demonstrated, such as self-phase modulation, cross-phase modulation, four wave mixing and Raman soliton self-frequency shifting. These schemes can provide ultra-fast sampling speed, but suffer the high operating power and

performance instability. Semiconductor-based signal processing is promising because of low power consumption, high nonlinear efficiency and potential large-scale integration. We propose and demonstrate an all-optical sampling scheme using a single semiconductor optical amplifier, in which the analog optical signal is sampled through the nonlinear polarization rotation arising in the semiconductor optical amplifier. In the experiment, 40 GSa/s all-optical sampling for 2.5 GHz analog optical signal is successfully demonstrated with commercially available fiber-pigtailed components. The all-optical sampling shows the fundamental conversion efficiency of 1.35 and the total harmonic distortion of 2.01% at the operating power of 5 mW. In the full characterization, the output sampling signal demonstrates very good signal quality with the signal-to-noise ratio (SNR) of 38.1 dB and the Signal to Noise and Distortion Ratio (SINAD) of 29.75 dB, which shows an equivalent effective-number-of-bit (ENOB) of 4.65. Our scheme requires only one semiconductor optical amplifier and has low power consumption, which shows much potential for the high-speed optical analog-to-digital conversion.

8552-23, Session 5

0.5Gbits/s message bidirectional encryption and decryption based on two synchronized chaotic semiconductor lasers

Jia-Gui Wu, Zheng-Mao Wu, Tao Deng, Xi Tang, Li Fan, Yi-Yuan Xie, Guang-Qiong Xia, Southwest Univ. (China)

Chaotic cryptography is an attractive technique for information secure transmission at the physical layer. In particular, the optical chaos communication using semiconductor lasers (SLs) has received intensive attention because of its high relaxation oscillation frequency (several GHz) and direct compatibility with existing optical fiber networks. In past years, many valuable theoretical and experimental works have been performed on unidirectional information secret transmission based on SL chaotic synchronization. However, such a unidirectional communication is dissatisfactory, and bidirectional or multidirectional secure communications are always highly expected. In order to implement bidirectional chaos communication, various system configurations have been proposed, where most of them are based on the chaos synchronization between two mutually coupled SLs (MC-SLs). Usually, some additional measures must be adopted to strengthen the stability of chaos synchronization in such a MC-SLs system. Very recently, we have experimentally reported a novel chaos synchronization scheme between two independent SLs driven by a common signal. Different from a MC-SLs system, there is no direct coupling between the two synchronized SLs, which are only linked by a common mediating SL.

In this paper, based on our recent reported chaos synchronization scheme mentioned above, we propose and experimentally investigate a bidirectional chaos communication system. Preliminary experimental results show that the robust chaos synchronization between two authorized SLs can be experimentally realized. Based on this chaos synchronization, by using the synchronized chaos signals as communication carriers, two pseudo-random data streams with a rate of 0.5Gbits/s can be encrypted into the chaotic carriers and be effectively decrypted on both ends of the communication channel.

8552-24, Poster Session

The influence of sampling duty cycle fabrication error in an SBG semiconductor laser on its lasing wavelength

Yating Zhou, Changzhou Institute of Technology (China) and Nanjing Univ. (China); Weichun Li, Rui Liu, Linlin Lu, Yuechun Shi, Xiangfei Chen, Nanjing Univ. (China)

In order to investigate the influence of the sampling duty cycle fabrication error on the lasing wavelength of an SBG semiconductor

laser, a monolithic integrated laser array is fabricated. In this laser array, there are 56 π equivalent phase shift (EPS) SBG semiconductor lasers laid out adjacently to each other in the same bar. Except the sampling duty cycle of these lasers are designed and fabricated from 0.21 to 0.76 successively with a step of 1%, the cavity length, the sampling period and seed grating period for each laser is the same. Furthermore, both the two end facets of every laser are coated with ant-reflection coating (reflectivity 1%).

For these SBG lasers, the -1st channel is selected as the lasing channel. Furthermore, for each laser the work temperature is controlled at 25 oC by a thermoelectric cooler while the injection current is set as 70 mA keeping constant. In order to eliminate the impacts of random end-facet phases on the lasing wavelengths of these lasers, linear fitting curves of the lasing wavelengths versus sampling duty cycles is utilized.

The experimental results show that when the sampling duty cycle varies from 0 to 100%, the lasing wavelength of an SBG semiconductor laser increases about 0.5 nm. Due to the fabrication error of the sampling duty cycle being not less than 2%, the lasing wavelength tolerance that do not exceed to 0.01 nm, which can be ignored in an actual WDM system.

8552-25, Poster Session

Thermal effects of pulsed pumping in semiconductor disk lasers

Peng Zhang, Teli Dai, Yiping Liang, Siqiang Fan, Yu Zhang, Chongqing Normal Univ. (China)

It has been demonstrated experimentally that pulsed pumping can significantly improve the thermal management in an optically-pumped semiconductor disk laser, and the output power of semiconductor disk lasers under pulsed pumping can be upgraded to times of those under continuous pumping. This paper presents numerical analysis of the thermal effects of the pulsed pumping in semiconductor disk lasers, so to theoretically disclose the details of the thermal processes of the pulsed pumping. In the simulation, the parabolic heat conduction equation, which is widely employed to describe the transient thermal transfer processes, is solved under cylindrical coordinates by the use of the finite element method, a time-dependent heat source of periodic laser pulse train is assumed, and the maximum temperature rise in the multiple quantum wells active region is focused. The influences of the pulse shape, the repetition rate, and the duty cycle of the pumping laser pulse train on the maximum temperature rise and the heat flux are investigated respectively, and the results are compared with the case of continuous pumping, i.e., the solutions of the time-independent, elliptical steady heat conduction equation. To verify the applicability of this numerical modeling, some simulation results are compared with reported data, and the theoretical results are in good agreement with the experiments.

8552-27, Poster Session

A multiple excitation technique for fluorescence rejection in Raman spectroscopy base on external cavity diode laser

Hongwu Zhou, Zhijian Cai, Jianhong Wu, Soochow Univ. (China)

Raman spectroscopy is widely used in food-safety inspection, material identification, chemical analysis and biomedical test. However, its applications are often limited by fluorescence disturbance. So, it's necessary to suppress the fluorescence background in Raman spectroscopy, especially for biochemical Raman analysis. An obvious characteristic difference between Raman signal and fluorescence is that fluorescence spectrum is not sensitive to the change of excitation wavelength while Raman signal will shift along with the excitation wavelength in the spectrograph. Based on this principle, a Shifted excitation Raman difference spectroscopy (SERDS) technique is

recently developed for suppressing fluorescence, which has shown good performance and broad suitability. Compared with other fluorescence rejection methods such as laser bleaching method and time resolved spectroscopy technique, SERDS has the advantages of low cost, minimum sample selectivity and good compatibility with the existing Raman instruments. The prevailing SERDS system usually takes two closely-spaced excitation wavelengths to illuminate the sample alternatively, and uses two spectra to generate the first-order difference spectrum, where the fluorescence background will be cancelled out. The difference spectrum will then be processed by a deconvolution algorithm to reconstruct the normal Raman spectrum. However, only two wavelengths are not sufficient to remove the fluorescence background completely and the data reconstruction by first-order difference spectrum could be disturbed by electronic noises. In order to reject the fluorescence better and to improve the signal-to-noise ratio further, multiple excitation and higher-order difference spectroscopy method could be used. In this paper, a multiple excitation SERDS method for Raman fluorescence rejection is proposed. A tunable laser system, which was constructed by a home-made Littrow grating external cavity diode laser, was incorporated in a Raman instrument to achieve multiple wavelength excitation. And the high-order difference spectrum was generated to remove fluorescence background. A robust algorithm based on iterative deconvolution with multiple constraints was specifically developed for Raman spectrum reconstruction. In this paper, the details of system design and algorithm procedure were illustrated, and the simulation and experiment results were presented, which demonstrated that this system could effectively reject the fluorescence disturbance and greatly improve the signal-to-noise ratio of Raman measurement.

8552-28, Poster Session

Low threshold 980-nm tunable vertical-cavity surface-emitting lasers

Shi Guozhu, Baolu Guan, Beijing Univ. of Technology (China)

Because of large, mode-hop free tuning range, low power consumption, high integration density and the compatibility with current optoelectronic fabrication processes, wavelength tunable vertical-cavity surface-emitting lasers (VCSELs) have been of great interest in various applications including optical networks, bio- or chemical molecular sensing technology, such as absorption spectroscopy, fiber Bragg grating measurement and trace gas monitoring. Short-wavelength tunable VCSELs can serve as efficient and low cost transmitters for wavelength-division multiplexing in the short distance reconfigurable optical interconnect to provide larger bandwidth.

We present an electrostatic actuated 980nm tunable VCSEL based on two-chip assembly method. The half-VCSEL and the mechanical part of the laser are fabricated separately and are assembled in a final packaging step which allow for independent optimization of the two components to achieve optimum device performance for desired application. From the measured result, we obtain the maximum output power is 4.56mW with 14 μ m diameter oxide aperture in continuous operation and the continuous tuning range is 6.8nm. Confocal laser scanning microscope is used to detect the flatness and smoothness of the MEMS membrane. The very smooth interface is fabricated between the membrane and air gap in the resonance cavity owing to separate optimization of the two parts of device, resulting in the threshold current as low as 0.6mA. The free-spectral range of 42 nm and the threshold gain versus air gap and resonance wavelength for experimental configuration are obtained from theoretical calculation. A large tuning range performance of the 980nm VCSEL is predicted by improving resonance cavity design and fabrication process.

8552-29, Poster Session

Wavelength tunable VCSELs based on voltage-dependent birefringence of liquid crystal

Wang Qiang, Baolu Guan, Beijing Univ. of Technology (China)

Tunable vertical-cavity surface-emitting lasers (VCSELs) have become one of the key optical sources in optical interconnect, spectroscopy, sensor techniques based on fiber Bragg gratings, especially in the dense wavelength division multiplexing (DWDM) system, owing to their advantages, for instance, low cost, low consumption, easy fiber coupling, large and mode-hop-free continuous wavelengths tuning range. VCSELs incorporating micro-electro-mechanical systems (MEMS) structure for various actuation mechanisms, such as electrostatic, thermal and piezoelectric actuation have been presented in recent years. However, the MEMS movable mirror layers of wavelength tunable VCSEL is fragile, instable and easily influenced by mechanical vibration which will deteriorate the tunable performance. Here, we present a widely tunable 850nm-range VCSEL structure based on the voltage-dependent birefringence of the liquid crystal. An intracavity liquid crystal layer is imbedded between the top DBR and the active region as an electro-optic index modulator. Al_{0.98}Ga_{0.02}As oxidation layer is employed above the active region for current and optical confinement. Because of the voltage-dependent birefringence of nematic liquid crystal, tunable VCSEL with an intracavity liquid crystal layer is designed to develop the tunable performance and stability. Tuning efficiency of 5.4nm/V and 20-nm tuning range are obtained from theoretical calculation. With increasing the thickness of liquid crystal layer, the tuning efficiency increases, nevertheless, the optical loss in resonance cavity also increases. So we found that 1837nm is the most suitable thickness for compromise. Furthermore, the material gain characteristics of the GaAs/Al_{0.3}Ga_{0.7}As quantum well and electric field intensity in the structure layers are investigated, respectively. Our study can provide insight into tunable VCSELs design and optimization.

8552-31, Poster Session

A novel four-section DBR tunable laser with dual-wavelength lasing

Liqiang Yu, Lingjuan Zhao, Dan Lu, Hongliang Zhu, Jiaoqing Pan, Institute of Semiconductors (China); Yan Li, State Key Lab. of Inf. Photonics & Opt. Commun., Beijing Univ. of Posts & Telecommun. (China); Wei Wang, Institute of Semiconductors (China)

A novel dual-wavelength DBR laser is fabricated and investigated. The DBR laser has four parts, a front gain section, a phase section, a DBR grating section, and a rear gain section. The device material was grown on an n-InP substrate by the metal organic chemical vapor deposition. The active region has separate confinement heterostructure with strain-compensated InGaAsP-InGaAsP multiple quantum wells. The wavelength detuning between the passive waveguide and the active region is achieved by the quantum well intermixing (QWI) technique. The facets of both sides were left as cleaved, and optical output from the front gain section was measured.

When the current injected into the front gain section is above the threshold current, the device is working in single mode. Then dual-wavelength can be obtained by adjusting the current injected into the rear gain section. The wavelength detuning of two modes is about 0.73 nm, which corresponds to a beating frequency of 93 GHz. The length of the front gain section, phase section, DBR grating section, and the rear gain section are 250 μ m, 150 μ m, 150 μ m, and 250 μ m, respectively. When the laser is working on dual-wavelength lasing, the power difference between the two modes can be less than 1 dB, and the side-mode suppression ratio (SMSR) can achieve about 36 dB. Moreover, the dual-wavelength can be tunable at the same time when the current injected into the DBR grating section is adjusted. The device can achieve a tuning range of at least 3 nm. Then when we maintain

the current injected into the DBR grating section and tune the front gain section and the rear gain section, the wavelength can be tuned slightly, which is due to the currents induced the effective cavity length change of the laser diode.

8552-33, Poster Session

Numerical simulation on output performance of continuous-wave Raman silicon lasers

Hongxin Su, Lijing Xu, Xiaoming Li, Fuyun Jiao, Xu Li, Hebei Univ. (China)

The potential of silicon as a photonic material for light generation has attracted a great deal of attention owing to the demand for photonic components that can be fabricated in a standard CMOS process. Because Si is not naturally capable of accomplishing efficient radiative recombination, stimulated Raman scattering (SRS) in silicon-on-insulator (SOI) waveguides has been discovered as an effective way for optical amplification and lasing in SOI planar lightwave circuits, and both pulse and continuous-wave (cw) Raman silicon lasers have been demonstrated experimentally in recent years. To understand the physical process of SRS lasing in SOI waveguides and to optimize the performance of cw Raman silicon lasers, in this paper numerical simulation on the output characteristics of cw Raman silicon lasers with different parameters is performed based on power propagation equations in SOI waveguides and boundary conditions. The output powers as functions of the launched pump power, the gain length, the reflectivity of the output end, and the effective mode area of the SOI waveguide are presented. It is shown that two-photon absorption (TPA) and free-carrier absorption (FCA) lead to a significant reduction to the output power of cw Raman silicon lasers, which is in good agreement with the experimental reports. Numerical analysis predicts that in the absence of TPA and FCA there are optimum values for the silicon waveguide length, the effective mode area and the output end reflectivity, respectively. The results can be used in the design of cw Raman silicon lasers with high efficiency.

8552-34, Poster Session

The amplified spontaneous emission in EDF with small pulse pump

Wang Fu, Chongqing Wu, Lanlan Liu, zhi wang, zhenchao sun, yaya mao, Beijing Jiaotong Univ. (China)

Abstract: The Active Spontaneous Emission (ASE) is the important noise source for EDFA, affecting the EDFA based fiber laser seriously. The theory and practice have shown that the ASE is closely related with pump methods, so the study on the ASE of EDF under the condition of the pulse pumping has important academic significations. What's more, the mode-locked laser based on EDFA fiber ring could be pumping by the pulse to realized mode-lock, and the ASE will impact its characteristics. In this paper, the effects of pump pulse with different width and amplitude on the ASE were investigated by the theoretical and experiment methods.

Beginning with the carrier density rate equation, we can get each level of the distribution of the number of particles carriers along with the change of time. based on the relationship between the average number of photons of the spontaneous radiation and the number of particles carriers distribution. An approximate analytical solution of output ASE noise average is derived when pump signal is small. Building an experimental system, the results show that the output amplitude of ASE is proportional to the input width of pump pulse when the pump pulse is small. It's also shows that the output amplitude of ASE is proportional to the input amplitude of pump pulse. The new phenomena can be used for the all-optical measurement of a pulse width.

8552-35, Poster Session

A high-power laser diode driver and collimating optical system design for laser 3D imaging

Wenlong Zhang, Qun Hao, Yong Song, Fuzhou Shang, He Sun, Tengfei Li, Beijing Institute of Technology (China)

In the paper, a design of driving circuit and collimating optical system used for 3-D (three-dimensional) imaging device have been proposed. It can improve the detecting range and precision of semiconductor laser 3-D imaging.

Propose the scheme of main driving circuit based on the model of capacitor charging and discharging. To get a high peak power laser pulse with short pulse width and fast rise time, high speed power MOSFET is used in the laser diode driver. Analyses on main influence of the driving circuit are proposed. According to the corresponding equation of the discharge circuit, which can be regarded as the null-input-response series-would RLC circuit, the energy storage capacitor C has been calculated. The parasitic inductance L is deduced, which is the most influence of output waveform. In addition, the DC-DC circuit which transforms the low input voltage to an DC high voltage is designed, simulated and tested. Experimental results show that the maximum output peak current can be up to 20A when the energy capacitor C is charged by DC-DC converter of 280V and the pulse width is around 100ns.

According to semiconductor laser's far field divergence characteristic, the aspheric collimation part has been designed by optical design software ZEMAX. Far field beam trace and collimation are simulated. The results of the simulation indicate that the RMS divergent angle is 0.318mrad and the spot is more uniform, which can improve the efficiency of energy. The proposed system provides a basis for further study of the three-dimensional laser imaging system.

8552-36, Poster Session

A balanced-detector optical heterodyne detection for local-oscillator excess-noise suppression

Jie Yang, Zhaohui Hu, Yuchi Zhang, BeiHang Univ. (China)

A semiclassical approach is used to calculate the principle and the signal-to-noise density ratio for heterodyne detection utilizing two optical detectors. These calculations show that excess-noise in the local-oscillator can be canceled and the balanced-detector optical heterodyne detection requires less local oscillator power compared with the traditional single-detector optical heterodyne detection. An experimental demonstration of excess-noise cancellation is reported.

8552-37, Poster Session

Speckle characteristics of a broad-area laser diode

Shengtao Zhang, North Univ. of China (China); Xuyuan Chen, Vestfold Univ. College (Norway); Pengfei Zhao, Wenhong Gao, Yunbo Shi, North Univ. of China (China)

The speckle measurement setup consists of a semiconductor laser diode (LD), a polarizer, a rectangular aperture, a scattering screen and a CCD with lens. The laser diode used is the blue laser product of Nichia with center wavelength of 450nm. The intensity of the incident laser light onto a diffuser is controlled by using polarizer or adjusting input current. The rectangular aperture with dimensions of 10mm*10mm close to diffuser is used to select different parts of laser light field as illumination spot. The distance between rectangular aperture and

laser diode without depolarization is set to 465nm. The CCD with the pixel size of 5.6um*5.6um is used to capture the speckle pattern, and the lens with focus length of 50mm has an F number of 22. The laser light field formed on the plane surface of the rectangular aperture has dimensions of 430mm*30mm. The speckle contrast of the different parts selected by aperture is measured, which has the values from 0.92 to 0.96. However there is no obvious trend (turn up or down) along the movement of rectangular aperture. So when the laser diode operates at its typical power output condition, the speckle contrast measured approximately equals 1, while the speckle contrast is depressed about to 0.2 when the laser diode operates with low driving current.

8552-38, Poster Session

Research on the performance of optical communication system based on PoISK with balance detection

Dan Liu, Zhi Liu, Puyao Wang, Xin Zhou, Changchun Univ. of Science and Technology (China)

The paper proposes polarization shift keying (PoISK) technology based on analysis polarization characteristics of the optical wave. Polarization shift keying (PoISK) technology is a new standard digital modulation technique in optical communication field. In this paper, atmospheric laser communication system based on circular polarization shift keying (CPoISK) with balanced detection is constructed, we use the left and right circularly polarization states of optical wave representation logic signal '0' and '1'. Simulate and contrast OOK systems and PoISK system with single receiver and CPoISK system with balance detection, analysis of the performance of communication systems. The results showed that, optical communication based on CPoISK has a unique advantage in the field of free-space optical communication. Waveform amplitude of signal received by CPoISK system with balance detection is tow times OOK system and PoISK system with single receiver. And in the same simulation parameters, the performance of CPoISK system with balance detection is far superior to the OOK system see from eye diagram, and the bit error rate of CPoISK system is also decrease tow order of magnitude. From this we can see that, Atmospheric laser communication system based on PoISK can effectively improve the performance of the communication system, and it has broad space for development and application in the free space optical communication field in the future.

8552-39, Poster Session

Three-dimensional finite element modelling of conductive silver ink tracks thermally cured on flexible substrates by repeating irradiations of Nd:YAG laser at the wavelength of 532 nm

Liwei Fu, Shuo Shang, Eamonn Fearon, Stuart Edwardson, Geoff Dearden, Kenneth Watkins, Univ. of Liverpool (United Kingdom)

Particulate silver inks are made of three basic components: silver flakes, resin complex, and organic solvent, and they are finding increasing use in the direct manufacture of electronic circuitry applications such as conductive traces on Printed Circuit Boards (PCBs), the antennas on Radio-frequency identification (RFID) tags, and the grid wires on strain gauges. Curing by repeating laser irradiations at the wavelength of 532 nm is advantageous for reasons of fast processing speed, good curing quality due to a reduced track's electrical resistivity by multiple passes

of laser beam scan and protection of heat-sensitive polymer substrate due to its high transparency to the wavelength at 532 nm.

This work presented in this paper is a 3-D Finite Element Modelling (FEM) based investigation into a DPSS Nd:YAG laser with a top-hat beam curing a particulate silver ink track on top surface of Polyethylene terephthalate (PET) substrate at the wavelength of 532 nm. Key physical properties of materials have been defined in heat transfer module within COMSOL multiphysics 4.0 environment, a Time-dependent solver has been chosen for modelling a 3 pass curing mechanism, which the first pass of laser scan removes the solvent, the second pass cross links the resin complex, and the third pass increases the degree of inter-particle connections as a result of resin complex further cross links. The modelling results have been compared to the experimentation for evaluations and suggested sets of working parameters that optimizing the balance between fast processing speed and good curing quality in industrial manufacturing.

8552-40, Poster Session

Adaptive optics system based on magnetic fluid spatial light modulator applied in laser communication

Xiaolong Ni, Changchun Univ. of Science and Technology (China)

Abstract: Laser communication is a potentially attractive technology that can offer intrinsically high data rates and resistance to jamming, and facilitates low probability of interception and low probability of detection. In laser communication system, the wavefront aberrations caused by atmospheric turbulence cause many negative influence. This paper presents a new method based on magnetic fluid spatial light modulator (MFSLM) to cancel dynamic wavefront aberrations in laser communication system. MFSLM have been found particularly suitable for imaging systems where they can be used to compensate for the complex optical aberrations. Experimental results showing the performance of a multi-channel closed-loop adaptive optics system are presented. The resulting distortions lead to enhance signal power and decreased bit error rate (BER).

8552-41, Poster Session

Study on the optical antenna for laser communication network

Fu Qiang, Changchun Univ. of Science and Technology (China)

with the urgent needs of the development of high-resolution observation techniques and high data rate transmission of information, studying all-optical network the high-speed laser communication is imminent.

This article describes the advantages of a space laser communication technologies and development trends, optical antenna for laser communication network, to provide a new way on space laser communication link network.

8552-42, Poster Session

Performance comparison study of modulation in laser communication system

Jianhua Liu, Fu Qiang, Changchun Univ. of Science and Technology (China)

There were many ways of modulation in the laser communication system. In order to verify that PolSK modulation was the most suitable technology for space laser communication system, we analyzed the implementation principle of several signal modulation ways in this paper. By combining the theoretical analysis and software simulation, we make an analysis and comparative study through five aspects in the function of the PolSK modulation and the traditional modulation ways, including transmission rate in the unit, bandwidth requirements, transmission capacity, the average power utilization and error performance. The results indicated that PolSK modulation possess a higher transmission rate in the unit, a lower bandwidth requirements, and a larger transmission capacity. The most important thing was that PolSK modulation mode had a superior performance and a strong anti-air channel interference activity compared with the traditional modulation in a weak turbulence conditions. So PolSK modulation mode was suitable for laser communication system.

Conference 8553: Optics in Health Care and Biomedical Optics V

Monday - Wednesday 5 -7 November 2012

Part of Proceedings of SPIE Vol. 8553 Optics in Health Care and Biomedical Optics V

8553-1, Session 1

Optical imaging for mouse brain connectivity (*Invited Paper*)

Qingming Luo, Britton Chance Ctr. for Biomedical Photonics (China)

This presentation will give an overview of optical imaging for mouse brain connectivity, and will focus on progress of my group on MOST for brain connectivity.

8553-2, Session 1

Imaging neurons with inertia-free beam steering of the femtosecond laser pulse (*Invited Paper*)

Shaoqun Zeng, Britton Chance Ctr. for Biomedical Photonics (China)

We will show how the femtosecond laser pulse changes its characteristics after passing an angular device, and how this information is used to implement an inertia-free beam steering, and how such techniques can be used to measure the fast neuronal activity and to achieve high throughput high resolution imaging for neuronal connectivity studies.

8553-3, Session 1

Integrated on-chip lens applied to microfluidic chips (*Invited Paper*)

Qin Li, Yingying Zhao, Xiaoming Hu, Dongfang Yang, Beijing Institute of Technology (China)

The optical signal on microfluidic chip is hard to be collected. On-chip microlens is the potential choice to improve the collecting efficiency. Optical fiber assembled on chip also can increase the signal detection quality. Therefore, the combination of optical fiber and microlens could get much stronger signal on chip. However, the matching between optical fiber and microlens is a tough work. And if we hope to design the one-off chip for medicine test, the fabricating cost of chip should be considered. This article introduced a simple, inexpensive fabrication method to make polymer and air integrated microlens to increase the couple rate of optical fiber. This small element can improve the optical signal detection and could be used to a blood cell counting system based on microfluidic chip. Compared to other established protocols, this procedure allows a simple, miniaturizing and inexpensive microlens fabrication with high reproducibility. The on-chip microlens was designed by Zemax software and tested by numerical simulation to optimize the parameters. The air microlens was produced by using direct lithograph of SU-8 resist. The couple effect showed that the single microlens was possible to reduce the beam divergence of optical fiber. So the export light beam can be focused into a very small point to satisfy the needs of excite the fluorescence of cell. On the other hand, the strength of emission or scattering light coupled into optical fiber also could be increased by the help of the on-chip microlens. The fabrication method does not require any assembly process or external driving forces. To fabricate the polymer and air microlens with different focus, we only need to change the figures on masks. This technique can be used in a variety of applications owing to its ability to achieve customized microlens for specific applications.

8553-4, Session 1

Motion compensation of optical mapping signals from beating rat heart slices (*Invited Paper*)

B. Stender, Univ. zu Lübeck (Germany); M. Brandenburger, Fraunhofer Research Institution for Marine Biotechnology EMB (Germany); B. Wang, Z. X. Zhang, Xi'an Jiaotong Univ. (China); Alexander Schlaefer, Univ. zu Lübeck (Germany)

Introduction

Monitoring the state of myocardial tissue over time is essential to quantify the effects of new pharmacological substances or to perform toxicity tests. The use of mammalian cardiac tissue slices as multicellular model has already been demonstrated, [1, 2, 3]. Typically the slices are grown on a microelectrode array (MEA) to record electrophysiological signals. Another option to measure cardiac excitation with high spatial resolution is optical mapping, [4]. We introduce a technique to noninvasively record simultaneously optical mapping data and motion of the rat heart slices.

Methods

A rat heart was excised and cut into short-axis slices. The slices were stained with Di-4-ANEPPS and placed in warm oxygenated Tyrode's solution. The heart slices were beating first autonomously and then voltage controlled stimulated. Optical mapping data were recorded for each slice with 295fps during both phases.

The motion of the rat heart slices was determined from the images in four steps: First the translation was determined using a 2D affine registration algorithm. Due to the radial nature of the periodic slice contraction we decided to perform a coordinate transformation to polar coordinates on the affine registered images. In the third step the deformation was calculated using a nonrigid B-Spline registration. Finally the resulting images were transformed back to cartesian voxel positions. The approach was implemented in Matlab.

Results

We compared traces of the fluorescence difference signal with and without compensation of the detected motion. We could determine a significant reduction of motion artefacts. In addition the temporal trace of the myocardial deformation was similar to the course of force signals recorded during previously performed experiments with rat heart slices.

Conclusion

Optical mapping of cultured rat heart slices in combination with optical motion tracking makes it possible to monitor the myocardial viability state of a multicellular model with high spatial resolution. Future work will focus on evoked arrhythmia.

References

- [1] M. Brandenburger, J. Wenzel, R. Bogdan, D. Richardt, F. Nguemo, M. Reppel, J. Hescheler, H. Terlau, and A. Dendorfer, "Or-ganotypic slice culture from human adult ventricular myocardium", *Cardiovasc. Res.* 93(1):50-59, 2012.
- [2] A. Bussek, E. Wettwer, T. Christ, H. Lohmann, P. Camelliti, U. Ravens, "Tissue slices from adult mammalian hearts as a model for pharmacological drug testing", *Cell. Physiol. Biochem.* 24:527-536, 2009.
- [3] W. Habeler, S. Pouillot, A. Plancheron, M. Puceat, M. Peschanski, C. Monville, "An in vitro beating heart model for long-term assessment of experimental therapeutics", *Cardiovasc. Res.* 81:253-259, 2009.
- [4] Eds. D.S. Rosenbaum, M. Jalife, "Optical Mapping of Cardiac Excitation and Arrhythmias", Futura Publishing Company, New York, 2001.

8553-5, Session 2

Multifunctional activatable microbubbles for multimodal imaging and image-guided therapy (Invited Paper)

Ronald X. Xu, The Ohio State Univ. (United States) and Univ. of Science and Technology of China (China) and Chongqing Medical Univ. (China)

Background: The therapeutic outcome of many anti-cancer drugs is very low. The poor clinical outcome is partially caused by the low drug delivery efficiency to the tumor site via the Enhanced Permeability and Retention (EPR) effort and is further complicated by tumor hypoxia that increases the tumor resistance to chemotherapies.

Method: We have fabricated multifunctional drug-loaded microbubbles for image-guided active delivery of oxygen and drugs to the tumor site with the increased efficiency. The microbubbles were fabricated by various processes such as micro-emulsification, co-axial electrospray, and co-axial flow focusing. The surface of the microbubbles were modified for cancer targeting. Anti-cancer drugs, imaging agents, and oxygen were loaded in the microbubbles. Upon exposure to ultrasound pulses, the microbubbles were broken and the therapeutic/imaging payloads were released. Optical and ultrasonic imaging tools were used to monitor the microbubble activation process.

Results: Both lipid and poly lactic-co-glycolic acid (PLGA) microbubbles were fabricated and tested. The surface of the microbubbles were conjugated with various cancer-targeting ligands, such as a CC49 antibody(targeting TAG-72 antigen), an anti-VEGF antibody (targeting VEGF), and a Luteinizing Hormone Releasing Hormone analog (targeting LHRH peptide). Oxygen, gene, and anti-cancer drugs were encapsulated in the microbubbles. Upon exposure to 1 MHz ultrasound pulses, the oxygen and the therapeutic payloads were released from the microbubbles. The activation process was monitored by ultrasound and fluorescence imaging.

Conclusion: The multifunctional activatable microbubbles can be potentially used for image-guided active delivery of anti-cancer therapies.

8553-6, Session 2

Scanning optical microscope for samples introducing spatially varying aberrations into the illumination beam (Invited Paper)

Bosanta R. Boruah, Abhijit Das, Indian Institute of Technology Guwahati (India)

Scanning optical microscope such as a laser scanning confocal microscope, when employed to image biological specimens, often suffer from specimen induced aberrations. The aberrations in turn reduce image contrast and degrade the signal to noise ratio. Hence the illumination beam needs to be pre-corrected for the specific aberrations to be introduced by the sample in order to retrieve the image quality. It is easy to construct a microscope that has a single pre-corrected illumination beam profile for the entire image frame. Unfortunately specimen induced aberrations may vary from region to region such that one pre-correction profile may not produce the best image over the entire field of view. Hence in such cases the illumination beam needs to be pre-corrected using phase profiles that may vary from region to region. In this paper we describe the design of a scanning optical microscope with binary hologram based beam scanning where the illumination beam can have phase profiles that can vary from pixel to pixel. The binary hologram is implemented by a liquid crystal spatial light modulator (LCSLM). For a given specimen we first measure the various aberration co-efficients introduced by the specimen on a pixel to pixel basis. The measured aberration co-efficient matrix is then used to construct an appropriate hologram for each of the pixels in the imaged area. The sequence of holograms when displayed on the LCSLM, lead to an illumination beam scanning over the sample, that

has a region specific correction phase profile. We will present here preliminary experimental results obtained using proposed system.

8553-7, Session 2

Fluorescence holography with two spheric waves produced by a spatial light modulator

Shaoqun Zeng, Britton Chance Ctr. for Biomedical Photonics (China); Xiaomin Lai, Huazhong Univ. of Science and Technology (China)

Holographic fluorescence imaging is very promising as it can obtain three-dimensional fluorescence imaging without scanning. However, current method usually recorded holograms far from the image plane, with the fluorescence decays when spreading broadly. Here we show the fluorescence holography with two spheric waves shows high signal-to-noise (SNR) ratio over other configuration such as one plane wave and one spheric wave. This provide better performance in fluorescence imaging for the biological samples.

8553-8, Session 2

Parallel localization of multiple emitters for fast localization microscopy

Yina Wang, Wuhan National Lab. for Optoelectronics (China); Zhen-li Huang, Huazhong Univ. of Science and Technology (China)

Using the strategy of separating close-packed fluorescence emitters into hundreds or even thousands of image frames, localization-based super-resolution fluorescence microscopy naturally scarifies its temporal resolution to obtain ultra-high spatial resolution, thus limits the versatility of this technique in studying dynamic processes inside living samples. A possible approach to minimize this limit is high-density localization microscopy, which increases the density of active emitters so that each image frame samples more molecules. Recently, a number of high-density localization methods have been reported that can retrieve emitter positions when multiple emitters overlap. However, all these methods suffer from either weak localization performance or slow image processing speed, thus obstruct widely uses of these methods in localization microscopy.

In this talk we will introduce a new high-density localization method, termed PALMER for "Parallel Localization of Multiple Emitters via Bayesian information criterion Recommendation". This method comes from the combination of GPU parallel computation, multiple-emitter fitting, and optimal model recommendation via Bayesian Information Criterion (BIC). Compared to DAOSTORM, a representative high-density localization method, the PALMER method shows an overall better localization accuracy performance and an order of magnitude faster analysis speed. Meanwhile, compared to conventional localization microscopy, high-density localization microscopy based the PALMER method allows a speed gain of up to ~14-fold in data acquisition with the same desired Nyquist resolution. We believe that this PALMER method has great potentials in pushing forward the field of fast localization microscopy.

8553-9, Session 2

Coherent fiber supercontinuum laser for nonlinear biomedical imaging

Haohua Tu, Yuan Liu, Univ. of Illinois at Urbana-Champaign (United States); Xiaomin Liu, Jesper Lægsgaard, Dmitry Turchinovich, Technical Univ. of Denmark (Denmark); Stephen Boppart, Univ. of Illinois at Urbana-Champaign (United States)

The last decade has witnessed an increased application of femtosecond (or picosecond) solid-state lasers and closely related optical parametric oscillators (or amplifiers) in label-free biomedical imaging. Representative techniques include multiphoton autofluorescence, stimulated Raman scattering, stimulated emission, and nonlinear absorption. With the rapid advancement of ultrafast spectroscopy, similar molecular specific nonlinear imaging techniques will continue to emerge. However, ultrafast solid-state lasers are often bulky, expensive, and alignment-sensitive, restricting these techniques to dedicated optical laboratories. Also, daily laser operation demands training and experience far beyond that of regular clinical staff. To translate these techniques to the clinic (e.g., point-of-care diagnosis and imaging), there is a critical need to replace the solid-state lasers with portable, low-cost, low-maintenance, and environmentally-stable fiber lasers.

Unfortunately, conventional ultrafast fiber lasers have narrow gain bandwidth, so that the emission is typically limited to a few discrete wavelengths of rare earth dopants, such as ~1040 nm (Yb), ~1550 nm (Er), and ~2000 nm (Tm). To address this key limitation, we have developed a supercontinuum source based on dispersion-engineered photonic crystal fibers, which converts 1040 nm femtosecond pulses (pump) to a targeted wavelength (signal) anywhere inside the UV-visible-IR region of 350-1700 nm. In sharp contrast to traditional supercontinuum generation that loses coherence between the pump and signal, this source preserves the coherence, and thus behaves like a fiber analogue of optical parametric oscillators. The demonstrated frequency up- and down-conversion of a fixed-wavelength ultrafast fiber laser facilitates the envisioned clinical translation of this coherent fiber supercontinuum source for nonlinear biomedical imaging.

8553-10, Session 2

Wide field-of-view microscopy with Talbot pattern illumination

Jigang Wu, Guangshuo Liu, Shanghai Jiao Tong Univ. (China)

Wide field-of-view (FOV) microscopy is useful for high-throughput applications because of the capability to obtain large amount of information from a single image. One way to implement a wide FOV microscope is to scan the sample with a two-dimensional focus grid. The transmission or reflection of the focal spots can then be used to reconstruct the sample image. This scheme is effectively a parallel scanning optical microscope (SOM), where the FOV depends on the area of the focus grid and the imaging resolution depends on the spot size of the foci. We use the Talbot image of a two-dimensional aperture grid as the focus grid and developed a wide FOV microscope. Preliminary experimental results show the capability of our microscope to acquire wide FOV images of US air force target and green algae samples.

Because the diffraction of incident beam by the aperture grid contains complicated angular frequencies, the focal spots in Talbot pattern cannot be approximated as Gaussian beams as in conventional SOM. We characterized the focal spots in Talbot pattern and studied the evolution of the full width at half maximum (FWHM). We also simulated the SOM imaging under Talbot pattern illumination using the razor blade and the US air force target as the sample objects, and compared the results with those performed with Gaussian beams as illumination. Using several foci searching algorithms, the optimal focal distances were found to be shorter than the theoretical Talbot distances. The simulation results were consistent with the experiment results.

8553-11, Session 3

Interstitial laser irradiation in photoimmunotherapy (*Invited Paper*)

Wei R. Chen, Univ. of Central Oklahoma (United States); Xiaosong Li, First Affiliated Hospital, Chinese PLA General Hospital (China); Jessica Goddard, Univ. of Central Oklahoma

(United States); Roman Wolf D.V.M., Eric Howard, Univ. of Oklahoma Health Sciences Ctr. (United States)

In situ photoimmunotherapy was developed to treat metastatic cancers. It uses a combination of laser irradiation and modifier-based immunotherapy, to induce tumor-specific immune responses. Previously, in situ administration of a light-absorbing dye has been used to achieve non-invasive, selective laser photothermal destruction of tumor cells, as an integral part of the photoimmunotherapy. To extend the applications of photoimmunotherapy for deep tumors and/or tumors in internal organs, we developed interstitial laser irradiation using a cylindrical diffuser. The thermal effect of the interstitial photoimmunotherapy was studied using magnetic resonance thermometry and its immune effect was studied using an animal model with metastatic mammary tumors. Our results indicated that interstitial irradiation could be controlled to induce the desired thermal effects. In combination with the immunotherapy, interstitial irradiation is effective in the stimulation of host immune responses to fight against local and metastasized tumors.

8553-12, Session 3

Indirect photobiomodulation in functional networks (*Invited Paper*)

Timon Cheng-Yi Liu M.D., South China Normal Univ (China); En-Xiu Wei, Xiang-Bo Yang, South China Normal Univ. (China)

Photobiomodulation (PBM) is a non-damaged modulation of laser irradiation or monochromatic light (LI) on a biosystem function. It depends on whether the function is in its function-specific homeostasis (FSH). A FSH is a negative-feedback response of a biosystem to maintain the function-specific conditions inside the biosystem so that the function is perfectly performed. A function in its FSH or far from its FSH is called a normal or dysfunctional function. The process of a function from dysfunctional to normal is called functional normalization. Low level LI (LLL) can not directly affect a normal function, but may self-adaptively modulate a dysfunctional function until it is normal. A normal function in its FSH is maintained by a network of subfunctions which mainly include its FSH-essential subfunctions (FESs) and its FSH-non-essential subfunctions (FNSs). For a biosystem in a FSH, all the FESs of the normal function are normal, but only some of FNSs are normal. The quality of a FSH is also called the functional fitness of the normal function. The more the normal FNSs of a normal function and the higher the FNS fitness, the higher the functional fitness of the normal function. Through redundant pathways, LLL may self-adaptively modulate a dysfunctional FNS of a normal function until it is normal and the normal function is then upgraded. This PBM is called indirect PBM (iPBM). The iPBM on tumor cells, myoblast cells and fibroblasts and their applications will be reviewed in this paper.

8553-13, Session 3

Blue light rescues mice from fatal pseudomonas aeruginosa burn infections: efficacy and mechanism (*Invited Paper*)

Tianhong Dai, Massachusetts General Hospital (United States)

Blue light has attracted increasing attention due to its intrinsic antimicrobial effect without the addition of exogenous photosensitizers. However, the use of blue light for wound infections has not been established yet. In this study, we demonstrated the efficacy of blue light at 415 nm for prophylaxis of lethal *Pseudomonas aeruginosa* burn infection in mice. In vitro study indicated that an average 7.64-log₁₀-cycle reduction in the colony forming units of *P. aeruginosa* was achieved after 109.9 J/cm² blue light had been delivered to *P. aeruginosa* suspensions. Transmission electron microscopy revealed apparent steps in blue light mediated damages to *P. aeruginosa* cells. Fluorescence spectroscopy suggested that coproporphyrin III or/and uroporphyrin III are the intracellular photosensitizing chromophores

associated with the blue light inactivation of *P. aeruginosa*. In vivo study using bioluminescence imaging technique showed that a single exposure of blue light at 55.8 J/cm², applied at 30 min after bacterial inoculation to the infected mouse burns, reduced bacterial burden in mouse burns by an approximately 100-fold ($P < 0.0001$). Survival analysis revealed that blue light prophylaxis increased the survival rate of infected mice from 18.2% to 100% ($P < 0.0001$).

8553-15, Session 4

Recent advances on photodynamic therapy dosimetry (*Invited Paper*)

Buhong Li, Fujian Normal Univ. (China)

Photodynamic therapy (PDT) is an emerging therapeutic modality based on the generation of highly reactive singlet oxygen through interactions of photosensitizer, light, and molecular oxygen. As PDT techniques continue to develop and find more potential clinical indications and other new applications, robust dosimetry becomes a critical factor for achieving satisfied treatments. In this review, the advantages and limitations of each available PDT dosimetric method will be presented. In particular, we highlight the recent advances in optical monitoring technologies for real-time clinical PDT dosimetry, and the singlet oxygen luminescence dosimetry will be emphasized in details. Finally, the future challenges in clinical PDT dosimetry will be discussed.

8553-16, Session 4

Efficacy of gallium phthalocyanine as a photosensitizing agent in photodynamic therapy for the treatment of cancer

Kaminee Maduray, Durban Univ. of Technology (South Africa)

Photodynamic therapy (PDT), also known as photoradiation therapy is a revolutionary treatment aimed at detecting and treating cancers without surgery or chemotherapy. It is based on the discovery that certain chemicals known as photosensitizing agents or photosensitizers (e.g. porphyrins, phthalocyanines, etc.) can kill cancerous cells when exposed to low level laser light at a specific wavelength [1]. The focus of this study is to investigate the photodynamic effect and cellular uptake of gallium phthalocyanine using human colorectal adenocarcinoma cells (Caco-2). Caco-2 cells will be treated with different concentrations of gallium phthalocyanine and laser irradiated. Post-irradiated cells will be incubated for 24 hr before measuring cell viability. Cellular uptake studies will be performed by incubating the cells with the gallium phthalocyanine, and lysing them into solution to measure the gallium phthalocyanine fluorescence emission. The results showed an increase in fluorescence intensity of emission peaks at longer incubation times, indicating a greater uptake of gallium phthalocyanine by Caco-2 cells at 24 hr in comparison to 30 min.

It is well documented that the gallium induces chromatin condensation which is an early step of cell death (apoptosis). Therefore, the photodynamic effect of gallium phthalocyanines will be investigated further.

[1] Brown, SB, Brown, EA, and Walker I 2004, The present and future role of photodynamic therapy in cancer treatment, *The Lancet Oncology*, vol. 5, pp. 497-504.

8553-17, Session 4

Efficient photodynamic therapy against *Staphylococcus aureus* using [Ru(bpy)₂(dppn)]²⁺, a novel cationic photosensitizer

Yucheng Wang, Nankai Univ. (China) and Chinese PLA General

Hospital (China); Ying Wang M.D., Ying Gu, Chinese PLA General Hospital (China)

[Ru(bpy)₂(dppn)]²⁺, one of Ru(II) polypyridyl complexes, present inner dicationic charge and high ¹O₂ quantum yield. In this study, the synthetic compound was used as photosensitizer (PS) to photoinactivate a reference strain of *Staphylococcus aureus* ATCC 25923. Bacterial suspensions consisting of 10⁸ colony-forming units (CFUs) per milliliter were incubated with PS of different concentrations (0.025 μM ~ 25 μM). After a 30 minutes period, the suspensions were exposed to 457 nm laser light, determined by the absorption spectra of the PS in PBS, with a power density of 40 mW/cm² for 10 minutes (energy density of 24 J/cm²). PS group, light group and the blank control were also concerned. Viability of bacteria was determined by pour plates. The Log₁₀ reductions were calculated and killing effects in photodynamic inactivation (PDI) group were analysed contrast to the blank control. We observed that neither the laser light nor the PS per se had any inhibitory effect on the viability of the bacteria. PS at low dose (0.025 μM) followed by illumination yielded no significant decrease in the viable number. PS at 0.25 μM and 2.5 μM with irradiation induced reductions of 1.69 Log₁₀ and 5.97 Log₁₀, respectively. PS at 10 μM and 25 μM combined with light brought viable bacterial cells down to undetectable levels (reductions > 7 Log₁₀). We concluded that with the PS of appropriate doses, [Ru(bpy)₂(dppn)]²⁺ mediated PDI inactivated *S. aureus* efficiently. At the concentration of 2.5 μM, bactericidal activity was reached where the viability of bacteria fell more than 3 Log₁₀ based on previous researches.

8553-18, Session 4

Mechanistic study of apoptosis induced by low-irradiance light delivery photodynamic therapy

You H. Zhao, Ren Jie, Ying Gu, Chinese PLA General Hospital (China)

Photodynamic therapy (PDT) is an approved therapeutic procedure that exerts cytotoxic activity towards tumour cells by irradiating photosensitizers with light exposure to produce reactive oxygen species (ROS). In contrast to conventional PDT treatment that low-irradiance light delivery PDT has been reported to be more effective to eradicate tumor. Purpose: To investigate the mechanism of this phenomenon.

Experimental Design: Hela cells were co-incubated with Photofrin (5 μg/ml) in complete growth medium in the dark. After 16 h of incubation, the cells were irradiated at 3 mW/cm² or 30 mW/cm² with identical light dose (3 J/cm²). For the control group, cells were incubated in the same medium without Photofrin or light. Cellular ROS generation was assayed with DCF. Mitochondrial depolarization under PDT treatment was labeled by TMRM (tetramethylrhodamine, methyl ester). In order to image single cells, the confocal laser scanning microscope system was used.

Results: The fluorescence intensity of DCF in the cells irradiated at 3 mW/cm² was significant higher than cells irradiated at 30 mW/cm². The fluorescence intensity of TMRM in the cells irradiated at 3 mW/cm² was decreased quicker than the cells irradiated at 30 mW/cm².

Conclusions: In contrast to that conventional PDT treatment that low-fluence light delivery PDT is more effective to induce ROS generation and damage mitochondria.

8553-19, Session 4

Water-soluble benzylidene cyclobutanone dyes for two-photon excited photodynamic therapy

Qianli Zou, Technical Institute of Physics and Chemistry (China) and Graduate Univ. of the Chinese Academy of Sciences (China); Hongyou Zhao, Chinese PLA General Hospital (China);

Yuxia Zhao, Technical Institute of Physics and Chemistry (China); Ying Wang M.D., Ying Gu, Chinese PLA General Hospital (China); Feipeng Wu, Technical Institute of Physics and Chemistry (China)

Two-Photon Excited Photodynamic Therapy (TPE-PDT) is a novel phototherapy technology, which attracts much attention in recent years due to its advantages of deep biological tissue penetration and highly-selective targeting damage. Conventional clinical PDT drugs were used in early TPE-PDT studies. However, their two-photon absorption (TPA) cross-section values were too small to be suitable clinically. In last decade, a great number of compounds with large TPA cross-section values were reported. However, most of them are hydrophobic, can not be used as photosensitizer directly for TPE-PDT.

In this study, a series of polyethylene glycol-functionalized benzylidene cyclobutanone dyes (Q1-Q4) for TPE-PDT were synthesized. Detailed characterization and systematic studies of these molecules, including linear and nonlinear photophysical properties, lipid/water partition coefficients, reactive oxygen yields, and in vitro photodynamic therapy (PDT) activities, were conducted and compared with our previously reported cyclopentanone derivatives (B2, B3) side-by-side. All these dyes are water-soluble and two of them (Q3, Q4) are completely miscible with water. The singlet oxygen yields of Q1-Q4 are in the range of 0.76 to 0.78 in toluene, which is about three times larger than the cyclopentanone derivatives. These dyes are found to have large TPA cross-section values, for example, 801GM for Q4 at 820nm in toluene. All the studied dyes showed no obviously dark toxicity up to 10 μ M, at which concentrate almost all cells were killed under one-photon light irradiation. TPE-PDT activities were also successfully demonstrated in in vitro cell experiments using 800nm laser. Owing to the simple synthesis route and the capability of two-photon reactive oxygen sensitizations, we believe these new synthesized dyes will be good candidates for TPE-PDT applications in the future.

8553-20, Session 4

Monitoring microcirculation flow rate changes of port wine stains after photodynamic therapy by laser speckle imaging

Jie Ren, You H. Zhao, Ying Gu, Chinese PLA General Hospital (China)

Background and Objective: Microcirculation change is an important aspect in the study of photodynamic therapy (PDT) damage effects. Laser speckle imaging (LSI) is a new technology developed in recent years for the detection of microcirculation flow rate. In this study, we aimed to monitor the microcirculation flow rate changes of Port Wine stains (PWS) after PDT by LSI.

Cases and methods: A female PWS patient with a purple erythema located in the right lower jaw was involved in this study. The patient was placed in the supine position, and remained stationary in the testing process. The speckle images were accessed at pre-treatment, at post-treatment 0, 5, 10, 15, 20, 25, 30 min, and at the first return visit after 2 months. Finally, the speckle images of the PWS regions and the control regions were analyzed by the RTLBI software.

Results: The flow rate values decreased in both the PWS region and the control region after PDT. The differential flow rate values between the PWS region and the control region have a sharp decline at 0 min after PDT, and then rise slowly in the 0-30 min after PDT. There was little difference in the flow rate values at the first return visit compared to the values accessed at 30 min after treatment.

Conclusion: LSI can be used for monitoring the microcirculation flow rate changes of PWS after PDT. As a specific indicator, the differential flow rate values have certain significance in evaluate the microcirculation changes of the PWS regions.

8553-21, Session 5

Tissue optical clearing: enhanced imaging and therapy (*Invited Paper*)

Valery V. Tuchin, N.G. Chernyshevsky Saratov State Univ. (Russian Federation) and Univ. of Oulu (Finland) and Russian Academy of Sciences (Russian Federation)

The main limitations of optical diagnostics and phototherapy are the low penetration depth of light beams and/or low image contrast, because of high tissue scattering. The following optical diagnostic modalities are suffering strongly from a high scattering: Doppler and speckle blood flow measuring techniques, optical coherence tomography (OCT), confocal microscopy, SHG imaging, multi-photon spectroscopy, polarization imaging, and Raman spectroscopy. Optical clearing due to reduction of tissue scattering ability is an attractive method for controlling of optical properties of a variety of tissues. This technology provides many benefits for successful application of optical methods in biomedicine. 1-3 Even for optical diffusion imaging, in-depth blood flow monitoring using diffusion wave spectroscopy, and other principally scattering-based techniques, reduction of scattering of the upper layers of tissues also could be useful to provide more flexibility in getting quantitative information about tissue lesions and functioning. One of the optical clearing approaches is based on impregnation of tissue by an immersion liquid which refractive index is higher than refractive index of interstitial fluid (ISF) and/or tissue dehydration (losing water).

In this paper optical clearing of different tissues will be analyzed in the framework of receiving of more precise and valuable information from reflectance spectroscopy, polarization measurements, Raman spectroscopy, confocal microscopy, and optical coherence tomography (OCT), as well as from nonlinear spectroscopies, such as two-photon fluorescence and second harmonic generation (SHG). In vitro, ex vivo, and in vivo spectroscopic, polarization, and OCT studies of human tissues will be presented. Optical clearing agents and delivery techniques, as well as tissue enhanced permeation, will be discussed. Some important applications of optical immersion technique in dermatology, ophthalmology, gastroenterology, and some other medical fields will be demonstrated.

References

1. V.V. Tuchin, Optical Clearing of Tissues and Blood, PM 154, SPIE Press, Bellingham, WA, 2006.
2. V.V. Tuchin, A clear vision for laser diagnostics, IEEE J. Select. Topics on Quantum Electronics, 13, ? 6, pp.1621-1628, 2007
3. Elina A. Genina, Alexey N. Bashkatov, and Valery V. Tuchin, Tissue optical immersion clearing, Expert Rev. Med. Devices 7(6), 825-842 (2010)

8553-22, Session 5

Advances in optical clearing of tissue in vivo (*Invited Paper*)

Dan Zhu, Britton Chance Ctr. for Biomedical Photonics (China)

The optical technology has provided significant tool for molecular imaging and medical diagnosis with high sensitivity and resolution, and has been a focus of life science and engineering. However, the high scattering in turbid biological tissues limits the penetration of visible and near-infrared light in tissue, which affects its applicability in preclinical and clinical medicine, and other life science. The tissue Optical clearing technique based on immersion of tissues into optical clearing agents (OCAs) with high refractive indices, hyperosmolarity and biocompatibility allows one to effectively control optical properties of tissues, leads to essential reduction of scattering, and therefore enhance the depth to which light penetrates in tissue, and currently attracts great attentions. This technique, combined with various optical techniques has shown a great potential for improving the capabilities of optical imaging, diagnosis and therapeutic treatments. Especially, when tissue optical clearing technique was applied on investigating the brain

or central nervous system, the tissue micro-structural information were obtained with high resolution by using of microscopy imaging, which has produce significant breakout in neuroscience field. However, the final purpose of optical clearing technique is to apply in vivo animal or even human.

During the last several years, we have focused our research interest on optical clearing of tissue in vivo, including skin and skull. In order to develop some safe, effective and reliable optical clearing methods to perform in vivo, non-invasive subcutaneous imaging or cortex neuroimaging, we mainly paid attention to mechanisms of tissue optical clearing and biocompatibility of OCAs. Firstly, we explored the physical or physiological mechanisms, and found that higher refractive indices of OCAs improve optical clearing efficacy as long as OCAs do not change the structure of sample. For the in vivo skin optical clearing, there was a noticeable concentration-dependent decrease in dermal thickness and collagen fiber diameter, and increase in fiber regularity, which is different from in vitro skin optical clearing. Secondly, we paid attention to the dynamical function and morphology of blood vessels caused by OCAs, the negative effect on blood vessel or skin depends on the dose of OCAs and type. Topical application of a mixture of thiazone and the OCA can make skin transparent and improve visualization of subcutaneous microvessels. Combined with optical imaging technology, we will be able to improve image contrast and resolution. The optical clearing methods could be used for non-invasive optical diagnosis of peripheral blood vessel disease.

Recently, we developed an innovative optical clearing agent of skull which can establish a stable transparent cranial window without craniotomy. The preliminary investigations show that there is neither short-term nor long-term effect on cortical blood vessel distribution. Combining optical clearing technique of skull with laser speckle temporal contrast analysis, we not to visualize cortical blood flow at high resolution, which was not previously possible with the use of OCAs alone. Post-imaging treatment with saline allowed the skull recovery. We believe that combining the transparent cranial window with multi-photon microscopy or other optical imaging techniques will help to study cortex neural activity in vivo, which is very beneficial for neuroscience research.

8553-23, Session 5

Autofluorescence in single molecule fluorescence imaging

Yanqiao Huang, Austin Tomaney, Paul Lundquist, Pacific Biosciences (United States)

Single molecule fluorescence imaging has found broad application in biomedical research areas such as in situ molecule tracking, conformational study of biomolecules, and DNA sequencing. Low light levels demanded by single-molecule observations are limited to extremely low signal levels and the SNR requirements are quite demanding. In many systems, autofluorescence from the optical system and from sample substrates constitutes the dominant noise source and determines the fundamental SNR limitations for achieving single molecule sensitivity. However, the optical modeling of autofluorescence is not straightforward, and little quantitative data is available for even commonly used optical materials.

In this manuscript we present an approach to detailed optical simulations of this important noise source and the ultimate SNR resolution of a specific optical system, along with guidelines for the design of optimal instrumentation. Specific optical designs that have been constructed are characterized and comparisons between measured autofluorescence levels and theory are presented. We also propose an intrinsic metric for the evaluation of optical materials, including the separation of bulk and surface contributions and spectral information, and a measurement methodology to separate distinct coefficients as they impact to system noise levels. A quantitative comparison of commonly used optical glasses and crystals is presented along with an analysis of the importance of sample preparation and handling both in material characterization as well as for the construction and maintenance of optical instrumentation maintaining single-molecule sensitivity.

8553-24, Session 5

Design of an affordable fluorescence confocal laser scanning microscope for medical diagnostics

Christin Bechtel, Technische Univ. Dresden (Germany); Jens Knobbe, Heinrich Grüger, Hubert Lakner, Fraunhofer-Institut für Photonische Mikrosysteme (Germany); Günter Huber, Univ. Hamburg (Germany)

Confocal fluorescence microscopes are a promising imaging tool in medical diagnostics due to their capability to selectively survey cross-sections of individual layers from 'thick' samples. Non-invasive depth resolved investigation of neoplastic skin disorders is one example among other applications.

However these microscopes are at present uncommon in medical practice. This is due to their main application area in research. The instruments dealt with here are generally complex, stationary units and are accordingly cost-intensive.

It is for this reason, we have designed a robust and portable MEMS based confocal fluorescence microscope with a field of view of 500 μ m. This has been made possible by the integration of a 2D micro-scanner mirror developed at Fraunhofer IPMS. A variable acquisition depth of cross-sectional images of the fluorescence specimen is enabled by an integrated z-shifter.

With the use of commercially available optics an optical demonstrator set up has been realized. To characterize and to demonstrate the ability of this system for visualization and analysis test measurements were performed. The resolution of the microscope is better than 228 lp/mm determined by 1951 USAF resolution test target. Images of various biological samples are presented and optical sectioning capabilities are shown. A comparison of the measured with the predicted system performance will be given.

8553-25, Session 5

Multiview hyperspectral topography of tissue structural and functional characteristics

Shiwu Zhang, Univ. of Science and Technology of China (China) and The Ohio State Univ. (United States); Peng Liu, Univ. of Science and Technology of China (China); Jiwei Huang, The Ohio State Univ. (United States); Ronald X. Xu, The Ohio State Univ. (United States) and Univ. of Science and Technology of China (China)

Accurate and in vivo characterization of structural, functional, and molecular characteristics of biological tissue will facilitate quantitative diagnosis, therapeutic guidance, and outcome assessment in many clinical applications, such as wound healing, cancer surgery, and organ transplantation. However, many clinical imaging systems have limitations and fail to provide noninvasive, real time, and quantitative assessment of biological tissue in an operation room. To overcome these limitations, we developed and tested a multiview hyperspectral imaging system.

The multiview hyperspectral imaging system integrated the multiview and the hyperspectral imaging techniques in a single portable unit. Four plane mirrors are cohered together as a multiview reflective mirror set with a rectangular cross section. The multiview reflective mirror set was placed between a hyperspectral camera and the measured biological tissue. For a single image acquisition task, a hyperspectral data cube with five views was obtained. The five-view hyperspectral image consisted of a main objective image and four reflective images. Three-dimensional topography of the scene was achieved by correlating the matching pixels between the objective image and the reflective images. Three-dimensional mapping of tissue oxygenation was achieved using a hyperspectral oxygenation algorithm. Our multiview hyperspectral imaging technique was under quantitative validation in a wound

model, a tissue-simulating blood phantom, and an in vivo biological tissue model. Preliminary validation results have demonstrated the technical feasibility of using multiview hyperspectral imaging for three-dimensional topography of tissue functional properties. This research is sponsored by National Institute of Standards and Technology (60NANB10D184).

8553-26, Session 6

Recent advances in optical coherence tomography (*Invited Paper*)

Zhijia Ding, Chuan Wang, Yi Shen, Tong Wu, Liangming Huang, Lan Wu, Chixin Du, Zhejiang Univ. (China)

This paper reports our recent advances in optical coherence tomography at Zhejiang University.

A high speed swept source OCT system is reported, where spectral calibration is conducted by use of the phase from a Mach-Zehnder interferometer, and full-range imaging is realized by wave-number carrier frequency. With evenly divided phase signal, arbitrary number of uniform sampling can be realized. Wave-number carrier frequency of the spectral interference signal is introduced by a double-pass transmissive dispersive optical delay line. High carrier frequency in the spectral interference signal corresponding to a distance shift is exploited to obtain full-range OCT imaging. Instantaneous coherence function is introduced for complete description of the spectral interference signal. The performance of the established full-range imaging system is well above conventional one-side offset approach with increased SNR and especially suitable for high-speed SS-OCT system.

A high speed spectral domain Doppler OCT system is reported. The developed spectral domain Doppler OCT system is applied to monitor cerebral blood flow velocity changes in a rat. An animal model with a cranial window is used, and by application of a drug, light, and electric stimulations, changes in blood flow velocity of the pial artery in sensory cortex are measured in real time. The results show significant differences in blood flow velocity before and after drug administration or light and electric stimulations, demonstrating the feasibility of DOCT in cerebral microcirculation study. Furthermore, a method based on higher order cross-correlation is proposed in the spectral domain Doppler OCT system to fetch the Doppler information on flow velocity within area under low signal-to-noise ratio (SNR). Experimental results demonstrate that the proposed method can significantly suppress noise, thus rendering it suitable for flow measurement under low SNR cases. Since noise is significantly suppressed, the proposed method is much less vulnerable to low SNR and is more reliable for qualitative Doppler imaging.

8553-27, Session 6

Intra-operative OCT devices for clinical translation (*Invited Paper*)

Yu Chen, Chia-Pin Liang, Jaydev Desai, Univ. of Maryland, College Park (United States); Cha-Min Tang M.D., Rao L. Gullapalli, Univ. of Maryland School of Medicine (United States)

Stereotactic procedures that require insertion of needle-based instruments into the brain serve important roles in a variety of neurosurgical interventions, such as biopsy, catheterization, and electrode placement. A fundamental limitation of these stereotactic procedures is that they are blind procedures in that the operator does not have real-time feedback as to what lies immediately ahead of the advancing needle. Therefore, there is a great clinical need to navigate the instrument safely and accurately to the targets. Towards that end, we developed a forwarding-imaging needle-type optical coherence tomography (OCT) probe for avoiding the hemorrhage and guiding neurosurgical interventions. The needle probe has a thin diameter of 0.7 mm. The feasibility of vessel detection and neurosurgical guidance were demonstrated on sheep brain in vivo and human brain ex vivo.

In addition, we further reduced the probe size to 0.3 mm using an optical Doppler sensing (ODS) fiber probe that can integrate with microelectrode recording (MER) to detect the blood vessels lying ahead to improve the safety of this procedure. Furthermore, to overcome the field-of-view limitation of OCT probe, we developed an MRI-compatible OCT imaging probe for neurosurgery. MRI/OCT multi-scale imaging integrates micro-resolution optical imaging with wide-field MRI imaging, and has potential to further improve the targeting accuracy.

8553-28, Session 6

Phantom testing of a novel endoscopic OCT Probe: a prelude to clinical in-vivo laryngeal Use

Taran Tatla, Jing-Yin Pang, Northwick Park Hospital (United Kingdom); Ramona C. Cernat, George M. Dobre, Paul J. Tadrous, Adrian Bradu, Univ. of Kent (United Kingdom); Grigory V. Gelikonov, Valentin M. Gelikonov, Institute of Applied Physics (Russian Federation); Adrian Podoleanu, Univ. of Kent (United Kingdom)

Optical Coherence Tomography (OCT) involving low-coherence infrared light interferometry allows micron-scale image resolution, providing tissue detail up to 2-3mm deep. A unique international collaboration, involving otolaryngologists and experts in biomedical optics used a 1300 nm SS-OCT imaging system which incorporates a miniaturised probe and passed it in tandem with a flexible fibreoptic nasoendoscope into the larynx to interrogate the characteristics of normal versus diseased tissue. The novel OCT probe (rigid part: 15mm long, diameter 1.9mm) was designed and constructed at the Institute of Applied Physics, Russia. The probe tip was passed into a disposable latex endosheath (outer diameter 5.5mm, inner diameter 5.2mm), alongside a flexible fibreoptic nasoendoscope (diameter 3.7 mm) coupled to a USB digital camera connected to its eye-piece. An ex vivo OCT image dataset was acquired as a baseline using a desktop 1300nm TD-OCT imaging system. Here we present pre-clinical data from a novel miniaturised OCT probe utilised for endoscopic imaging of laryngeal mucosa. We tested the feasibility, robustness and safety of this system on an anatomically correct manikin, which was the Trucorp Aisrim Advance Larynx. Following validation of the system ex vivo, we plan to extend the use of this assembly to a patient cohort to assess patient tolerability, practicality, clinical efficacy and accuracy. The ability to extract histological information from OCT imagery holds great potential to guide surgical biopsies, direct therapy and monitor disease.

8553-30, Session 7

Anatomic correlate to the hyper-reflective inner/outer segment band in retinal optical coherence tomography (*Invited Paper*)

Xincheng Yao, The Univ. of Alabama at Birmingham (United States)

Given the excellent capability to identify morphological changes at individual functional layers of the retina, optical coherence tomography (OCT) has increasing application in eye disease detection. Early studies have disclosed four hyper-reflective OCT bands at the outer retina, i.e. photoreceptor side. Anatomic sources of these four OCT bands have been typically attributed as follows: first (1st) band at the outer limiting membrane (OLM); second (2nd) band at the photoreceptor inner/outer-segment (IS/OS) junction; third (3rd) band at the posterior tip of the OS; and fourth (4th) band at the retinal pigment epithelium (RPE). Anatomic correlates of the 2nd and 3rd bands remains controversial. The 2nd OCT band is widely attributed to the IS/OS junction, which cell biologists consider the connecting cilium (CC) between these structures. However, comparative alignment of OCT bands with an anatomically correct model of the outer retina suggested an alternative

correlate, i.e., the IS ellipsoid, to the 2nd OCT band. This study was to experimentally test the anatomic correlate to the 2nd OCT band. In order to achieve sub-cellular resolution in both lateral and axial directions, a rapid line-scan OCT (LS-OCT) was developed. The LS-OCT combined technical merits of our recently demonstrated electro-optic phase modulator (EOPM) based functional OCT and line-scan confocal microscopy. Quantitative comparison of histological images and LS-OCT images revealed that dominant source of the signal reported as the 'IS/OS' OCT band actually originates from the IS. We speculate that the IS ellipsoid, which consists of abundant mitochondria, or the CC extended into the IS may contribute to the observed 2nd OCT band signal.

8553-31, Session 7

Imaging of coronary arteries and respiratory airways ex vivo using micro-optical coherence tomography (μ OCT)

Linbo Liu, Harvard Medical School (United States) and Massachusetts General Hospital (United States); Joseph A Gardecki, Brett E. Bouma, Guillermo J. Tearney, Massachusetts General Hospital (United States)

Understanding pathophysiology processes in coronary arteries and respiratory airways requires knowledge of tissue anatomy at the cellular and sub-cellular level. Unfortunately, methods for visualizing coronary arterial wall and respiratory mucosa at high resolution are limited. We have developed a novel imaging technique termed μ OCT which obtains images with a resolution of $2 \mu\text{m} \times 2 \mu\text{m} \times 1 \mu\text{m}$ (x, y, z) in tissue. We used the μ OCT system to image fresh human coronary arteries prosected from explant (donor) hearts, cultured human bronchial epithelial (HBE) cells, and freshly explanted swine tracheas. Preliminary results show that μ OCT is capable of visualizing most of sub-cellular structures associated with coronary artery diseases (CAD) and mucociliary clearance (MCC) in three dimensions in intact human tissues. Future development of μ OCT for imaging in vivo could open up new opportunities for studying CAD and respiratory airway diseases in human patients.

8553-32, Session 7

In vivo integrated photoacoustic ophthalmoscopy, optical coherence tomography, and scanning laser ophthalmoscopy for retinal imaging

Wei Song, Harbin Institute of Technology (China) and Northwestern Univ. (United States); Rui Zhang, Harbin Institute of Technology (China); Hao F Zhang, Northwestern Univ. (United States); Qing Wei, Northwestern University (United States) and Northwestern Univ. (United States); Wenwu Cao, Harbin Institute of Technology (China) and The Pennsylvania State Univ. (United States)

Photoacoustic ophthalmoscopy (PAOM) is an emerging ophthalmic imaging technology that measures optical absorption properties of the retina. By delivering short laser pulses onto the posterior segment of the eye and detecting laser-induced photoacoustic (PA) signals with an unfocused ultrasonic transducer, PAOM non-invasively images retinal/choroidal vascular networks and retinal pigment epithelium (RPE) melanin at a high contrast due to the strong optical absorption of hemoglobin and melanin. Fluorescein angiography (FA), autofluorescence-scanning laser ophthalmoscopy (AF-SLO), and spectral-domain optical coherence tomography (SD-OCT) are widely used in the ocular research, but they predominantly rely on fluorescence/scattered photons from the retina. Because retinal physiology and pathology are always associated with multiple optical

contrasts, the integration of PAOM with the well-established ophthalmic imaging techniques permits the complementary evaluation on the retina. We built a multimodal imaging platform of PAOM, SD-OCT, and FA for in vivo imaging of wild-type rat eyes, which revealed the optical absorption, optical back-scattering, and fluorescence properties in the retina. Further, an integrated PAOM, SD-OCT, and AF-SLO was developed for imaging mice eyes because mice have more attractive advantages of widely available genetically defined strains, well-characterized genome, and well-established techniques for genetic manipulation. The multimodal capability was demonstrated by imaging transgenic Nrl-GFP mice that express green fluorescent protein (GFP) in photoreceptors. Our integrated ophthalmic imaging system provides more comprehensive information of the retina, and therefore it holds potentials for benefiting clinical diagnosis and fundamental investigation of major blinding diseases.

8553-33, Session 8

Studying the role of macrophages in circulating prostate cancer cells by in vivo flow cytometry (*Invited Paper*)

Xunbin Wei, Shanghai Jiao Tong Univ. (China)

Metastasis is a very complicated multi-step process and accounts for the low survival rate of the cancerous patients. To metastasize, the malignant cells must detach from the primary tumor and migrate to secondary sites in the body through either blood or lymph circulation. Macrophages appear to be directly involved in tumor progression and metastasis, but the role of macrophages in affecting cancer metastasis has not been fully elucidated. Here, we have utilized a novel technique, namely in vivo flow cytometry (IVFC) to study the depletion kinetics of circulating prostate cancer cells in mice and how depletion of macrophages by the liposome-encapsulated dichloromethylene diphosphonate affects the depletion kinetics. Our results show the different depletion kinetics of PC-3 cells between macrophage-deficient group and the control group. The number of circulating tumor cells (CTCs) in macrophage-deficient group decreases in a slower manner compared to the control mice group. The differences in depletion kinetics indicate that the absence of macrophages facilitates the stay of prostate cancer cells in the circulation. In addition, our imaging data suggest that macrophages might be able to arrest, phagocytose and digest PC-3 cells. Therefore, the phagocytosis may mainly contribute to the depletion kinetic differences. The study here might provide new insights in anti-prostate cancer therapy.

8553-34, Session 8

Monitoring heart and respiratory rates at radial artery based on PPG

Cheng Wang, Univ. of Shanghai for Science and Technology (China)

To develop an apparatus for simultaneous monitoring of heart and respiratory rates using photoplethysmography (PPG) and Fast Fourier Transform algorithm (FFT). The PPG waveform was measured at the radial artery with an original based on diffuse reflectance mode photoplethysmographic device. A FFT algorithm was used to extract heart and respiratory information from the PPG waveform. The results good agree with conventional method. The correlation coefficient of heart rate and respiratory rate obtained using PPG waveform and conventional method, which are 0.988 and 0.976, respectively. The PPG waveform and FFT algorithm can contribute to quicker and more accurate measurement of human heart rate and respiration rate. A portable watch-like device can be made via this method and be utilized to monitor heart and respiratory rates in hospitals or daily life care.

8553-35, Session 8

Noninvasive monitoring traumatic brain injury based on an annular transducer array

Diwu Yang, Hunan Univ. of Technology (China)

A photoacoustic imaging system with an annular transducer array was designed for noninvasive in vivo monitoring of traumatic mouse brain. The annular transducer array consists of 256 elements arranged along a 300-deg arc with a 50-mm radius of curvature, using piezocomposite technology for high sensitivity and signal-noise-ratio. An 8-channel data acquisition system is applied to capture the photoacoustic signals using multiplexing and a limited-view filtered back projection algorithm is used to reconstruct the photoacoustic images. Traumatic lesions accompanying with hemorrhage in the mouse cortical surface were accurately mapped and a series of photoacoustic images of morphological changes were also obtained during rehabilitation process of a mouse brain with traumatic brain injury. Compared to other imaging systems, the imaging system overcomes the shortcomings of the long data acquisition time and requiring rotating transducer.

8553-36, Session 8

Simulating the demyelination of a nerve fiber by action potential encoded second harmonic generation

Hong-Pin D. Yang, Zhihui Luo, Xinguang Chen, Yimei Huang, Shusen Xie, Fujian Normal Univ. (China)

Demyelination is the main underlying factor responsible for some neurological diseases. The primary clinical diagnostic methods in identifying demyelination include magnetic resonance imaging (MRI), analysis of cerebrospinal fluid (CSF) and visual evoked potential (VEP). However, these methods have limitations of sensitivity and/or accuracy. In this paper, we simulated the demyelination of a nerve fiber by action potential encoded second harmonic generation (SHG), which may greatly improve the sensitivity and accuracy. The dynamics of action potential propagation in a multi-internode demyelinated nerve fiber, including successive internodes and intermittent internodes was simulated. We found that the attenuation and delay of action potential could obviously change, while the refractory period would increase for a demyelinated nerve fiber. In addition, under the same demyelinated conditions, i.e. the same thickness and number of the demyelination, the peak of SHG signals attenuated much more along successive injured internodes than intermittent injured internodes. Demyelination in a nerve fiber could be revealed through the dynamics of action potential recorded by optical SHG signals. Our study indicates that action potential encoded SHG could be a powerful tool for examining the demyelination induced by autoimmune diseases, or many metabolic and inflammatory disorders.

8553-37, Session 8

The diagnosis of CTCL by color image enhancement technique

Shih-Jie Dai, Hsiang-Yuan Tan, Ta-Wei Chien, National Chung Cheng Univ. (Taiwan); Yu-Ping Hsiao, Chung Shan Medical Univ. (Taiwan); Hsiang-Chen Wang, National Chung Cheng Univ. (Taiwan)

Cutaneous Lymphoma is a heterogeneous group of extranodal non-Hodgkin's lymphoma, which is the most common cutaneous T-cell lymphoma, known as the general academic with CTCL (Cutaneous T-cell Lymphoma). Such symptoms for the majority of plaque are only a slight redness, peeling, but some parts will have skin atrophy to form a reticular pigmentation. Some patients will be accompanied by skin sensation abnormalities, such as tingling phenomenon. In addition,

some patients there will be local depigmentation of the skin pigment. Sometimes, physician may be mistaken for white spot or systemic Pityriasis alba. Recently, methods of the CTCL diagnosis are using the excision biopsy, blood tests, and ultrasound scans. In this study, we use multi-spectral image technology to reproduce new images of the abnormal tissues. The objects for visual perception enhancement focus on the CTCL for coordinating with doctor's diagnosis.

8553-38, Session 9

Identification of non-neoplastic and neoplastic gastric polyps using multiphoton microscopy (Invited Paper)

Jianxin Chen, Shanghai Jiang, Fujian Normal Univ. (China); Deyong Kang, Meifang Xu, Fujian Medical Univ. (China)

Gastric polyps can be broadly defined as luminal lesions projecting above the plane of the mucosal surface. They are generally divided into non-neoplastic and neoplastic polyps. Accurate diagnosis of neoplastic polyps is important because of their well-known relationship with gastric cancer. Multiphoton microscopy (MPM) based on two-photon excited fluorescence (TPEF) and second harmonic generation (SHG) is one of the most important recent inventions in biological imaging. In this study, we used MPM to image the microstructure of gastric polyps, including fundic gland polyps, hyperplastic polyps, inflammatory fibroid polyps and adenomas, then compared with gold-standard hematoxylin-eosin(H-E)-stained histopathology. MPM images showed that different gastric polyps have different gland architecture and cell morphology. Dilated, elongated or branch-like hyperplastic polyps are arranged by neck cells and columnar epithelial cells. Inflammatory fibroid polyps are composed of small, thin-walled blood vessels surrounded by short spindle cells. Fundic glands polyps are lined by parietal cells and chief cells, admixed with normal glands. Gastric adenomas are generally composed of tubules or villi of dysplastic epithelium, which usually show some degree of intestinal-type differentiation toward absorptive cells, goblet cells, endocrine cells. Our results demonstrated that MPM can be used to identify non-neoplastic and neoplastic gastric polyps without the need of any staining procedure.

8553-39, Session 9

Collagen fiber spatial orientation mapping using polarization-sensitive SHG microscopy

Vladimir A. Hovhannisyan, National Taiwan Univ. (Taiwan); Po-Sheng Hu, National Taiwan Univ (Taiwan); Chen-Yuan Dong, National Taiwan Univ. (Taiwan)

Ability to characterize and quantify 3D structural organization of tissue fibers using non-invasive optical microscopy is important for the functional characterization of the extent of disease progression. Polarization dependence of the second harmonic signal from optically nonlinear tissues and other noncentrosymmetric materials provides information on characteristic orientations and degree of structural organization not available from intensity measurements alone. However, azimuth (or lateral) angle of collagen fiber orientation was the only orientation parameter quantified in previous studies. Here we suggest a simple approach for determining both the azimuth and elevation angles, and spatial orientation mapping of second harmonic generated structures.

Using dependences of the effective second-order nonlinear susceptibilities for producing SHG signal components with parallel and perpendicular polarizations on the azimuth (β) and elevation (δ) angles [1], the expressions for β and δ are derived [2], and pixel-resolution mapping of collagen fiber spatial orientation in tendon, cornea, and skin was demonstrated using SHG polarization-resolved microscopy. The new approach may be used for analyzing of biological tissues in vivo. Spatial orientation mapping method provides additional information about fiber organization, and may be incorporated into nonlinear optical

imaging systems.

[1] A. Erikson, J. Örtgren, T. Hompland, C. de Lange Davies, and M. Lindgren, *J. Biomed. Opt.* 12, 044002 (2007).

[2] V. A. Hovhannisyann, P.S. Hu, H.-Y. Tan, S.J. Chen, C.Y. Dong, *J. Biophotonics* 5, (2012).

8553-40, Session 9

Measuring intracellular calcium dynamics of HeLa cells exposed to nitric oxide by fluorescence microplate reader

Yimei Huang, Jiangxu Chen, Hongqin Yang, Liqin Zheng, Yuhua Wang, Hui Li, Shusen Xie, Fujian Normal Univ. (China)

Nitric oxide (NO) has been reported to promote or inhibit cancer cell proliferation and metastasis. NO appears to have an effect on inducing calcium transients, which participates in essential cellular signaling in the physiological and pathological processes. Our work was intended to study the effects of exogenous NO on intracellular calcium dynamics of HeLa cells measured by a fluorescence microplate reader with Fluo-3, a calcium fluorescent indicator. Results showed that after NO donor was injected into the wells, intracellular Ca²⁺ fluorescence intensity changed significantly comparing to that of the control group. Moreover, the calcium transients activated by NO were likely to be due to extracellular calcium influx. These would be helpful to further recognize the roles of NO involving in cancer cell proliferation and metastasis.

8553-41, Session 9

Morphological and metabolic changes of cultured DRG neurons induced by adenosine using confocal microscopy[confocal laser scanning microscopy] imaging

Liqin Zheng, Jiangxu Chen, Yuhua Wang, Yimei Huang, Hongqin Yang, Yanding Zhang, Shusen Xie, Fujian Normal Univ. (China)

Adenosine exerts multiple effects on pain transmission. However, the mechanism is still controversial. This study was performed to use confocal microscopy to evaluate whether adenosine could affect dorsal root ganglia (DRG) neurons in vitro and test which P1 receptor mediate[mediates]s the effect of adenosine on DRG neurons. After adding adenosine with different concentration, we compared the morphological changes of cultured DRG neurons by quantifying the axonal length, soma size and the ratio of nucleus and cytoplasm. And the metabolic changes were also in comparison by the real time imaging of ATP (NAD(P)H, FAD), calcium and mitochondria membrane potential using confocal microscopy after adding adenosine with different concentration. The results showed that the effect of 500μM adenosine on the morphological and metabolic changes of DRG neurons was more significant than others. Furthermore, four different P1 receptor antagonists were used to study which receptor mediated the influences of adenosine on the cultured DRG neurons. All the antagonists, except adenosine A1 receptor antagonist (DPCPX), had no or little effect on the DRG neurons. The above studies demonstrated that adenosine may be involved in the signal transmission on the sensory neurons and the adenosine A1 receptor mediated the transmission.

8553-42, Session 10

Novel optical detection of bladder cancer cells

Jhe-Ming Yang, Tsung-Chih Lin, Ching-Te Huang, Chun-Ping

Jen, Hsiang-Chen Wang, National Chung Cheng Univ. (Taiwan)

Bladder cancer is one of the common malignant tumors of the urinary system. One of them is transitional cell carcinoma, accounting for more than 90% of all bladder cancer. In this study, the detection of the degrees of transitional cell carcinoma was demonstrated by multi-spectral image technique. The spectral difference with the degree of the bladder cancer was discussed. For more exactly verify the degree of the bladder cancer, the Raman spectroscopy of various bladder cancer was measured. Finally, the different degrees of the bladder cancer will be mark and display through color image reproduction.

8553-43, Session 10

Optical methods for knee osteoarthritis detection

Yanping Chen, Chunbin Li, Xiong Ma, Xiamen Univ. (China)

Osteoarthritis is one of the most common diseases nowadays. One with serious damage of osteoarthritis would get disabled of joint, and life quality decreased. Optical methods for knee osteoarthritis detection were reviewed in this paper. Firstly, the advantages and disadvantages of some common imaging diagnostic techniques, such as X-ray, CT and MRI, were briefly summarized. Then three kinds of typical optic methods for the detection were introduced emphatically, which are coherence tomography (OCT), diffuse optical tomography (DOT) and photoacoustic tomography (PAT). After the introductions of some features of these three optical imaging methods on OA detection, this paper briefly forecasts their application prospects in early OA detection.

8553-44, Session 10

Noninvasive screening for diabetes using skin fluorescence

Yikun Wang, Anhui Institute of Optics and Fine Mechanics (China); Shandong Ye, Chengsong Ye, Anhui Medical Univ. (China); Yuanzhi Zhang, Fei Li, Anhui Institute of Optics and Fine Mechanics (China); Gong Zhang, Univ. of Manitoba (Canada); Ling Zhu, Yong Liu, Anhui Institute of Optics and Fine Mechanics (China)

Advanced glycation end-products (AGEs) are biochemical end-products of non-enzymatic glycation. The accumulation of AGEs in tissue has been implicated in the progression of diabetes mellitus and related complications. Some AGEs fluoresce and accumulation of AGEs in tissue can be assessed noninvasively through optical spectroscopy. A portable device for noninvasive assessment of AGEs using skin fluorescence and reflectance spectrum has been developed, and noninvasive screening for diabetes has been evaluated with it. Results indicated that the noninvasive technology assessing skin AGEs is more sensitive at screening diabetes than either fasting plasma glucose or glycated hemoglobin A1C. These results suggest that noninvasive assessment of skin AGEs may be an effective tool to identify individuals with diabetes mellitus. Besides, the noninvasive technology yields immediate results, and since measuring skin fluorescence and reflectance spectrum require no blood draws or subjects fasting, the developed device may be well suited for diabetes opportunistic screening.

8553-45, Session 10

Nonlinear optical imaging characteristics of colonic adenocarcinoma using multiphoton microscopy

Nenrong Liu, Rong Chen, Jianxin Chen, Fujian Normal Univ.

(China)

Colorectal cancer is the third most common malignancy, and the most common colorectal cancer cell type is adenocarcinoma which accounts for 95% of cases. Early detection is important. Multiphoton microscopy (MPM) is a noninvasive optical method with high resolution and high sensitivity, can obtain detailed microstructures of biotissues at submolecular level. In this study, MPM is used to image microstructure varieties of human colonic mucosa and submucosa with adenocarcinoma. The distortion of glands, loss of collagen, and distribution of cancer cells in cancerous tissues are clearly monitored, which are tightly relevant to the clinical pathology of early colorectal cancer. The morphological and pathological differences between normal and cancerous can be effectively distinguished using the MPM. And some parameters, such as gland configuration, SHG/TPEF intensity ratio, and collagen orientation and so on, should serve the indicators of early colorectal cancer. The exploratory results show that it's potential for the development of multiphoton mini-endoscopy in real-time early diagnosis of colorectal cancer.

8553-46, Session 10

Molecular application of spectral photo-acoustic imaging in pancreatic cancer pathology

Minalini Lakshman, Clinton W. Hupple, VisualSonics Inc. (Canada); Ines Lohse, Ontario Cancer Institute (Canada) and Campbell Family Cancer Research Institute (Canada); David W. Hedley, Ontario Cancer Institute (Canada) and Campbell Family Cancer Research Institute (Canada) and Univ. of Toronto (Canada); Andrew Needles, Catherine Theodoropoulos, VisualSonics Inc. (Canada)

Spectral imaging is an advanced photo-acoustic (PA) mode that can discern optical absorption of contrast agent(s) in the tissue micro-environment. This advancement is made possible by precise control of optical wavelength using a tunable pulsed laser, ranging from 680-970 nm. Differential optical absorption of blood oxygenation states makes spectral imaging of hemoglobin ideal to investigate remodeling of the tumor microenvironment- a molecular change that renders resistance to standard cancer treatment.

Approach: Photo-acoustic imaging was performed on the Vevo® LAZR system (VisualSonics) at 5-20 Hz. Deep abdominal imaging was accomplished with a LZ250D probe at a center frequency of 21MHz and an axial resolution of 75 μm . The tumor model was generated in an immune compromised mouse by surgical implantation of primary patient derived tumors, in the pancreas.

Results: Spectral imaging for oxygen saturation at 750 nm and 850 nm characterized this tumor with a poorly oxygenated core surrounded by a well oxygenated periphery. Multispectral imaging identified a sub region in the core with a four-fold signal exclusively at 750 and 800 nm. A co-registered 2D image of this region was shown to be echogenic and calcification was suspected. Perfusion imaging with contrast enhanced ultrasound using microbubbles (Vevo MicroMarker® contrast agents, VisualSonics) identified functional vessels towards this sub region. Histology confirmed calcification and vascularization in the tumor core. Taken together, non-invasive characterization of the tumor microenvironment using photo-acoustics rendered spectral imaging a sensitive tool to monitor molecular changes representative of progression of pancreatic cancer that kills within 6 months of diagnosis.

8553-63, Poster Session

A simulation method of polarization-sensitive optical coherence tomography based on a polarization-sensitive Monte Carlo program and a sphere cylinder birefringence model

Dongsheng Chen, Nan Zeng, Celong Liu, Hui Ma, Graduate School at Shenzhen, Tsinghua Univ. (China)

In this paper, we present a new method to simulate the signal of polarization-sensitive optical coherence tomography (PS-OCT), by using a sphere cylinder birefringence tissue model and a polarization sensitive Monte Carlo program developed by our lab. Using the program and the model, we can simulate complicated tissue containing anisotropic microstructures and various polarization imaging and measurement systems. In this simulation program, the detecting area and angle range and the scattering times of the photons are three main conditions used to screen out the photons contributing to various imaging methods. We study the effects of these three factors on the signals of PS-OCT through simulation using our program, and simulation results show that the scattering times of the photon is a key factor to simulate a right PS-OCT signal, and detecting area and angle range are less important but necessary. By comparison of our simulation with Extended Huygens Fresnel (EHF) method and experimental results, we set a proper screening regularity of PS-OCT photons. Meanwhile, we also make some research on the influence of two anisotropic sources in tissue on PS-OCT imaging: cylindrical scatters and tissue birefringence. In previous work, we have reported that fiber structure and birefringence effect in tissue caused by molecular inherent characters can generate optical anisotropy, and experiments and simulations of PS-OCT show that the retardation measured by PS-OCT comes from birefringence effect. In this paper, we explain further the regularities of anisotropic structure characterization by PS-OCT, through comparison of the different imaging regularities of anisotropic sphere scatters and anisotropic cylindrical scatters.

8553-73, Poster Session

Temperature changes in the pulp chamber during cavity preparation with Er:YAG laser

Xianzeng Zhang, Shusen Xie, Fujian Normal Univ. (China)

To examine the temperature changes in the pulp chamber during cavity preparation with the Er:YAG laser (2940 nm), a total 20 intact molars teeth were divided into 5 groups for cavity preparation with different radiant exposures at 4Hz and 8Hz with and without water spray. the total time of irradiation was 40 sec. Cooling was done with a water spray (3 mL/min). It showed that the temperature in the pulp increased with the increasing of radiant exposure and pulse repetition rate. The highest rise of temperature in the pulp was achieved with 20 J/cm² and 8 Hz(19.83°C). For all the sample without water spray, the rise of temperature was exceed 5°C. In contrast, with water spray, the temperature rise in the pulp can be firmly controlled under 1°C. The highest rise of temperature appeared at 8Hz and 20J/cm². It also indicated that the influence of energy on temperature increase was stronger than that of frequency

8553-79, Poster Session

Second harmonic generation imaging of skin wound healing and scarring in a rabbit ear model

Yiyan Tang, Affiliated First Hospital Fujian Medical Univ. (China); Xiaoqin Zhu, Fujian Normal Univ. (China); Shuyuan Xiong, Fujian

Medical Univ. (China); Jianxin Chen, Fujian Normal Univ. (China)

Skin wound healing and scarring in rabbit ears was examined by second harmonic generation (SHG) microscopy. Rabbit ear wound model was created by punching from the ventral surface with removal of epidermis, dermis and perichondrium. The samples were collected weekly, and cut into 100 μm thickness sections for SHG imaging. SHG imaging system was operated at 810 nm, producing SHG signals at half the excitation wavelength 405 nm. A Plan-Neofluar objective ($\varnothing 40$ and NA=0.75) was employed for focusing the excitation beam into tissue samples and was also used to collect the backscattered intrinsic SHG signals. Our results showed apparent difference in collagen content and microstructure at various wound healing and scarring time points. It suggested that SHG signals from collagen can serve as a good indicator for characterization of wound status. With the advancement on miniaturization, microscopy based on SHG will become a valuable tool for monitoring the wound healing and scarring in vivo, and help to guide the improvement of scar appearance with appropriate and subtle modulation during wound healing based on better understanding of scarring response mechanism.

8553-80, Poster Session

Study of human plasma protein fraction by combining membrane electrophoresis with surface-enhanced Raman spectroscopy

Jing Wang, Juqiang Lin, Zufang Huang, Fujian Normal Univ. (China); Yonghong Shao, Shenzhen Univ. (China); Peng Lu, Wei Shi, Jinyong Lin, Rong Chen, Fujian Normal Univ. (China)

Surface-enhanced Raman spectroscopy (SERS) is emerging as a powerful method in the characterization of biological materials. Recently SERS was successfully applied for blood plasma analysis and obtained good results. However, the effect of blood types on these studies was not discussed adequately in previous reports. In this study, membrane electrophoresis based SERS method was carried out to study these effects. The plasma proteins were firstly purified by membrane electrophoresis and then mixed with silver colloids to perform SERS spectral analysis. We use this method to analyze the blood plasma of normal samples and cancerous samples, where the cancerous samples were obtained from patients ($n = 28$) with pathologically confirmed gastric cancer and the normal samples were obtained from healthy volunteers ($n = 48$). Principal component analysis (PCA) was then performed on the spectra of these two groups, respectively. PCA plots calculated from these two groups have similar results and reveal that the data points as a representative of different blood types clustered together in a small region, meaning that these plots can not be distinguished by any clear delineation between different groups. It's more likely that the expressions of alleles which are relative to blood types do not result in distinct differences in the SERS spectra. These suggest that blood types have little effect on the SERS analysis of blood plasma.

8553-81, Poster Session

Detection of recombinant membrane receptor protein expression in living transgenic HEK293 cells using Raman spectroscopy

Juqiang Lin, Jing Wang, Zufang Huang, Wei Shi, Jinyong Lin, Peng Lu, Rong Chen, Fujian Normal Univ. (China)

Raman spectroscopy can be used for noninvasively measuring changes in cellular activity in single living cells without further labeling/modification or denaturing of the target. G-protein coupled receptor 120 (GPR120) is an orphan G-protein-coupled receptor playing functions as a sensor for dietary fat in the gustatory and digestive systems. In this study, we recorded Raman spectra of single HEK293 cells at the

different induction concentration during the G-protein coupled receptor 120 (GPR120) proteins in transformed HEK293 cells were induced by addition of doxycycline. We found that the intensity of the GPR120 protein-associated spectra from single HEK293 cells is depend on the dose of inducer and increased accordingly, which correlates with the accumulation of GPR120 proteins inside the cells. Moreover, principal components analysis (PCA) of the spectra revealed that the data points for the different treatments of HEK293-GPR120 cells form distinct, completely separated clusters with the receiver operating characteristic (ROC) area of 1, while for the HEK293 cells form a little overlap clusters with the ROC area of 0.815. These findings demonstrated that Raman spectroscopy combined with mathematical methods has sufficient sensitivity for real-time, noninvasive, and quantitative monitoring of biological processes in single living cells.

8553-82, Poster Session

Surface-enhanced Raman spectroscopy study of radix astragali based on soxhlet extractor

Peng Lu, Juqiang Lin, Nengrong Liu, Fujian Normal Univ. (China); Yonghong Shao, Shenzhen Univ. (China); Jing Wang, Wei Shi, Jinyong Lin, Rong Chen, Fujian Normal Univ. (China)

Radix Astragali, one of the most important Chinese traditional medicine, is sweet in taste with a slightly warm property in nature and manifests its the therapeutic actions in the spleen and lung meridians. But in herbal medicine market, counterfeits are very popular which are not only useless to sufferers, but also may cause chronic toxicity. So, it is very important for us to distinguish and identify Radix Astragali though one relatively more precise and quicker quality analysis way. Among other things, high sensitivity, flexibility, and "fingerprints" sensing capability make Surface-enhanced Raman Spectroscopy (SERS) a very powerful method for the characterization of Radix Astragali. In this study, Radix Astragali were firstly extracted through continuous circumfluence extraction method and then mixed with silver nanoparticles for SERS detection. Among the Raman spectrum we have obtained, most Raman bands due to Radix Astragali extraction solution are found at 440~520 cm^{-1} and 950~1490 cm^{-1} . Importantly, two main peaks of Radix Astragali spectrum are found at 729 and 1327 cm^{-1} which belong to the vibration bands of adenine and C(6)-H2 respectively. The preliminary results show that SERS combining with continuous circumfluence extraction method may be a direct, accurate and rapid detection method of Radix Astragali.

8553-83, Poster Session

Photo-induced electron transfer between dendritic zinc(II) phthalocyanine bearing carboxylic terminal groups and methyl viologen

Yuhua Wang, Jiangxu Chen, Lishan Huang, Shusen Xie, Hongqin Yang, Yiru Peng, Fujian Normal Univ. (China)

Dendritic phthalocyanines have been emerged as a new kind of promising biomaterial for biological imaging, since they exhibit excellent photophysical properties, such as a large absorption cross-section, red fluorescence emission and photosensitizing properties. In this study, the intermolecular electron transfer between carboxylic dendritic zinc(II) phthalocyanine bearing carboxylic terminal groups: tetra-[3,5-di-[3,5-di-(4-carboxylic benzyloxy) benzyloxy] benzyloxy] zinc(II) phthalocyanine (G1-Znpc(COOH)16) and methyl viologens(MV2+) was studied by steady-state fluorescence and UV/vis spectroscopy. The effect of different concentrations of MV2+ on intermolecular electron transfer was investigated. The results show that the fluorescence emission of this dendritic phthalocyanine could be greatly quenched with an increasing amount of MV2+ upon excitation at 610 nm. The Stern-Volmer constant(Ksv) of electron transfer is 0.792 $\times 10^3(\text{L}\cdot\text{mol}^{-1})$. The

quenching coefficient K_q is $1.61 \times 10^{11} (\text{L} \cdot \text{mol}^{-1} \cdot \text{s}^{-1})$, which is higher than the normal value for dynamic quenching. This indicates that the fluorescence quenching of this dendritic phthalocyanine by MV2+ is mainly through a static quenching mechanism. Our study suggests that this novel dendritic phthalocyanine is an effective new electron donor and transmission complex and could be used as a potential biosensor conjugated with suitable fluorescence quencher.

8553-84, Poster Session

Cutaneous pain and threshold induced by 1.32 μm laser stimulus with different pulses duration

Jiarui Wang, Zai-fu Yang, Beijing Institute of Radiation Medicine (China); Guang yuan Yu, Chinese PLA General Hospital (China)

To study cutaneous pain and detection threshold induced by 1.32 μm laser stimulus in human. The skin of lateral margin of forearm was irradiated by a 1.32 μm Nd: YAP laser. This study was performed with 3 healthy adult volunteers. The energy of each pulse and whether the subjects felt a painful sensation after each stimulus were recorded. The pain threshold was defined as the laser dose at which the subjects reported a painful sensation to 50% of stimulus deliveries. The pain thresholds were determined under 3 different pulse duration. The stimulus evoked two kinds of perceptions simultaneously, one of which was thermal sensation and the other was pinprick sensation. As a result the pain thresholds were determined to be 4.0mJ/mm², 5.4mJ/mm² and 5.03mJ/mm² respectively under the stimulating condition of 4.0mm beam diameter and 8ms, 0.1s and 1s pulse duration. The threshold of cutaneous pain elicited by 1.32 μm laser stimulus does not change significantly with increasing pulse duration when the exposure time in the range of 8ms~1s.

8553-85, Poster Session

Distinction of gastric cancer tissue based on surface-enhanced Raman spectroscopy

Jun Ma, Hanjing Zhou, Longjing Gong, Shu Liu, Zhenghua Zhou, Ocean Univ. of China (China); Weizheng Mao, Qingdao Municipal Hospital (East) (China); Ronger Zheng, Ocean Univ. of China (China)

Gastric cancer is one of the most common malignant tumors with high recurrence rate and mortality rate in China. This study aimed to evaluate the diagnostic capability of Surface-enhanced Raman spectroscopy (SERS) based on gold colloids for distinguishing gastric tissues. Gold colloids were directly mixed with the supernatant of homogenized tissues to heighten the Raman signal of various biomolecule. A total of 56 samples were collected from normal (30) and cancer (26). Raman spectra were obtained with a 785nm excitation in the range of 600-1800 cm^{-1} . Significant spectral differences in SERS mainly belong to nucleic acid, proteins and lipids, particularly in the range of 653, 726, 828, 963, 1004, 1032, 1088, 1130, 1243, 1369, 1474, 1596, 1723 cm^{-1} . PCA-LDA algorithms with leave-one-patient-out cross validation yielded diagnostic sensitivities of 90% (27/30), specificities of 88.5% (23/26), and accuracy of 89.3% (50/56), for classification of normal and cancer tissues. The receiver operating characteristic (ROC) surface is 0.917, illustrating the diagnostic utility of SERS together with PCA-LDA to identify gastric cancer from normal tissue. This work demonstrated the SERS techniques can be useful for gastric cancer detection, and it is also a potential technique for accurately identifying cancerous tumor, which is of considerable clinical importance to real-time diagnosis.

8553-86, Poster Session

Error analysis of image acquisition by moving objective lens

Hongxia Xie, Hua Chen, Guangxi Univ. (China); Yi Cai, Fengjuan Yang, Guangxi University (China)

Abstract: In the digital confocal microscopy technology, voltage ceramic is used to drive axial moving of objective lens to collect image slices, which is simple and flexible, easy to control and will get a large precision. But as a result of the movement, the corresponding parameters of the system like magnification and numerical aperture, even the point spread function changes, which will bring error to the image restoration.

According to the principle of optical imaging, we obtained that with the moving of the objective lens, the magnification and numerical aperture changed a little, and the PSFs of different positions were very similar, for example, look at the central value of the PSFs, compared with that of the initial PSF when the lens did not start to move, the biggest relative rate of change is 1.86×10^{-5} . While MSE is the mean square error of those PSFs and the initial PSF, and the biggest MSE is 4.99×10^{-9} , all of the differences are very small.

In the simulation experiment, it can be found that the restoration result of image slices collected by moving objective lens is very close to the restoration result of image slices collected by moving the biologic cell on the loading platform, and the image clarity were both significantly improved. So, using the initial PSF to restore the image slices collected in these two ways, the difference is quite small.

Therefore, all of the results above can verify the feasibility of moving lens to collect image slices.

8553-87, Poster Session

Reverse propagation properties of light wave in tapered micro-nano fiber for cell endoscopy

Deshan Zhou, Jingang Zhong, Jinan Univ. (China)

Over the past decade, as the progress of manufacturing technology and biological sensors, micro-nano optical fiber makes living cell monitoring possible. Due to its unique optical propagation feature and sharp tip, tapered micro-nano optical fiber is often used as probe to penetrate into cell for internal detection. The tiny size also can greatly reduce the damage to the cell.

Lately, an American scientist and his research team have further developed this probing technique and put forward a kind of endoscope used for single-cell internal structure. However, this "endoscope" only leads the exciting light into cell membrane through optical fiber, which is different from the traditional endoscope. If we can reversely export optical signal from the tapered fiber, it will contribute to confirm the position of the fluorescent labels more accurately. Consequently, it is necessary to discuss the reverse propagation of optical wave in tapered micro-nano optical fiber.

In this paper, we use Finite Difference Time Domain (FDTD) algorithm to simulate the propagation of light wave back and forward in fiber taper, respectively. The results indicate that most of the light is still in core when reverse propagation. At the same time, in the subsequent experiment the conclusion is further proved. Based on this feature, the light signal in living cell can be easily guided out and the real meaning "endoscopic" for cell detection would be realized.

8553-88, Poster Session

Diiblock copolymer micelle deliver substituted aluminum phthalocyanine for enhancement intracellular photodynamic

Zhe Chen, Fujian Normal Univ. (China)

Phthalocyanines (Pcs) and their substituted derivatives had been intensively investigated as the second generation photosensitizers for photodynamic therapy (PDT) of malignant cancer or or macular degeneration. The solubility and aggregation of Pc played important roles on the in vitro distribution and efficiency to generate singlet oxygen. By introducing amphiphilic long spacer chains substituted groups in the periphery of Pc ring, we hope to improve the solubility in organic solvent, inhibit the self-aggregation, and extend the reactive scope of interaction with proteins of this Pc. In this paper, A novel tetra-carboxylaminohexanoic sulfonyl aluminium phthalocyanine 1 was synthesized. Its structure was characterized by elemental analysis, IR, ¹H NMR and MS. Polyion micelle (PIC) between the 1 and amphiphilic triblock copolymer poly(L-lysine)- block-poly(ethylene glycol) (PLL-b-PEG) was formed via an electrostatic interaction between the positively charged poly(L-lysine)(PLL) segment and negatively charged periphery of the 4. Atom force microscopy (AFM) showed that 4-loaded PIC formed a spherical nanocarrier micelle with approximately 100 nm in diameter. The fluorescence intensity and lifetime of 4-loaded PIC were significantly enhanced by the incorporation 1 into PIC nanocarrier. The time-dependent intracellular uptake amount and in vitro photodynamic photocytotoxicity of the 1 within the nanocarrier were drastically improved compared with the 1.

8553-89, Poster Session

Polyion complex micelles incorporating poly(aryl benzyl ether) dendritic phthalocyanine: effective photosensitizers for enhanced photodynamic therapy

Kuizhi Chen, Sining Zhen, Ming Yu, Yiru Peng, Fujian Normal Univ. (China)

Photodynamic therapy(PDT) is an effective method for treatment of several diseases, including choroidal neovascularization, CNV) and solid tumors. Creating new PSs or their formulation plays a crucial role in the development of PDT. Among the various photosensitizers (PSs) investigated, phthalocyanine have been found to be highly promising. Recently, phthalocyanines and their metal complexes encapsulated into the interior core of dendrimer bearing hydrophilic surface groups have been prepared and reported on their prominent nature on high aqueous solubility, avoiding aggregation as well as interesting photophysical properties. In order to obtain higher PDT efficacy, the selective delivery of PSs to the target tissue was also very necessary. Amphiphilic triblock copolymer PLL-b-PEG-b-PLL had gained increased interest, due to its small size, thermodynamic and kinetic stability in vivo, higher drug-loading capacity and good biocompatibility.

In this paper, a new series of phthalocyanines zinc (II) carrying four poly(aryl benzyl ether) dendritic substituents (G_n= n-generation dendrimer, n=1-2) with carboxylic acid functionalities, and polyion complexes (PICs), which is formed via an electrostatic interaction between the negatively charged periphery of anionic dendritic phthalocyanine zinc (II) and positively charged poly(L-lysine) (PLL) segment of triblock copolymer poly(L-lysine)- block-poly(ethylene glycol)-block-poly(L-lysine), were prepared for use as effective photosensitizers for photodynamic therapy.

Atom force microscopy (AFM) and transmission electron microscopy (TEM) showed that dendritic phthalocyanines formed core-shell -type nanoparticles with a relatively high polydispersity. The photophysical characteristics of dendritic phthalocyanines and their corresponding micelles were strongly depend on the generation of photosensitizers. Electrostatic assembly resulted in a red-shift of the Q band of the

phthalocyanine core, reduced fluorescence intensity and prolonged fluorescence lifetime. The incorporation of dendrimer phthalocyanines into PIC nanocarriers led to an appreciable increase in time-dependent intracellular uptake amount, yet inversely correlated with the generation. Alternatively, the in vitro photocytotoxicity of dendrimer phthalocyanines within the nanocarriers increased with an increase in the generation despite a decrease in the cellular uptake.

8553-90, Poster Session

Ultra-long scan depth optical coherence tomography for imaging the anterior segment of human eye

Dexi Zhu, Meixiao Shen, Ming Li, Wenzhou Medical College (China)

Most people over 45 years old had to face to the common health problem of presbyopia, which reduce the ability of accommodation. The mechanism of accommodation has not been clarified yet because the modality of anterior segment of eyes can't be precisely monitored during accommodation. Optical coherence tomography (OCT) is a low coherence interferometric imaging technology and widely applied in ophthalmology for the features of high speed, high resolution and non-invasive to eye. But the scan depth of current OCT is limited (less than 5 mm), causing it can't been used in accommodation research. In this paper, we developed a novel spectral domain OCT with ultra-long scan depth for imaging the entire anterior segment of human eye. A scan depth of 11 mm and an axial resolution of 10 um are achieved based on the specially designed spectrometer of OCT system, thus the entire anterior segment from front surface of cornea to the posterior surface of crystalline lens is included in one picture. In order to compensate the drop of signal to noise ratio (SNR) through the OCT image, the optical distance in reference arm was adjustable to acquire two images with displacement of zero delay line. These images were overlapped finally to generate one picture with no SNR drop. We demonstrated that using this ultra-long scan depth OCT, the changes of anterior segment were clearly observed in vivo during the eye accommodation.

8553-91, Poster Session

A high-density localization of active molecules for super-resolution microscopy

Xin Liu, Qimei Liao, Gang Li, Junyan Rong, Hongbing Lu, Fourth Military Medical Univ. (China)

The super-resolution microscopy techniques based on single-molecule switching, e.g., stochastic optical reconstruction microscopy (STORM) or (fluorescence) photoactivated localization microscopy ((f)PALM), can achieve 20-30 nm spatial resolution, which provide a powerful way to understand molecular processes in live cells. However, to obtain high spatial resolution, the super-resolution microscopy requires accumulating enough single-molecule switching events, which need the long imaging time. As a result, the low imaging speed limits the use of the technique in live cell imaging, especially in dynamic live cell imaging. To improve the temporal resolution without sacrificing the spatial resolution, an efficient approach is to increase the density of activated fluorophores in each image frame. However, the high-density of activated fluorophores in each frame leads to them overlap each other. As a result, the existing single-molecule localization method is difficult to solve the problem. To overcome the limit, in this paper, based on the compressed sensing theory, we propose a high-density localization method, which is implemented by minimizing the total variation (TV) of image frame. To evaluate the performance of the proposed method, the numerical simulations are performed. The results demonstrate that compared with the previous reported localization method, the proposed method greatly can reduce the imaging time, while keeping a similar imaging quality.

8553-92, Poster Session

Observation of water diffusion in human skin with optical coherence tomography

Feng-Yu Chang, Chih-He Yang, Kung-Min Lin, Chang Gung Univ. (Taiwan); Chih-Hsun Yang M.D., Chang Gung Memorial Hospital (Taiwan); Yuan Ouyang, Meng-Tsan Tsai, Chang Gung Univ. (Taiwan)

Optical coherence tomography (OCT) has been widely used for biomedical applications due to noninvasive, depth-resolves, and high imaging speed natures. In this study, a swept-source OCT (SS-OCT) is used for dermatology studies. Here, time-resolved OCT images of the water diffusion process in the skin that illustrate the changes in the attenuation coefficient of the skin due to the increased water concentration are presented. In our experiments, the water concentration in the skin was increased by soaking the hand in water, and the same region of the index fingertip was scanned and measured with the OCT system and a commercial moisture monitor every 3 min. To quantitatively analyze the process of water diffusion and the increased water concentration detected by OCT, the attenuation coefficients of the skin, including the epidermis and dermis layers, were evaluated based on the Beer-Lambert law. Based on the Beer-Lambert law, the attenuation coefficients of the water concentration in the skin's epidermis and dermis layers can be evaluated during water diffusion. Furthermore, the evaluated attenuation coefficients were compared with the measurements by using the commercial moisture monitor. From the results, the evaluated attenuation coefficients show the same trend with the measured moisture from the commercial product when the skin was soaked into the water. In contrast to the measured results of the commercial moisture monitor, OCT can provide three-dimensional structural images of the skin and characterize its optical properties, which together can be used to observe morphological changes and quantitatively evaluate the water concentration in different skin layers.

8553-93, Poster Session

Quadratic triangular element for diffuse optical tomography

Xuanxuan Zhang, Yong Deng, Jun Xu, Zhaoyang Luo, Hui Gong, Qingming Luo, Huazhong Univ. of Science and Technology (China)

The forward problem of Diffuse optical tomography (DOT) can be described by diffuse equation generally which is an approximation of Boltzmann transport equation at the situation of high scattering and low absorption. Diffuse equation is a typical partial differential equation (PDE) which can generally be solved by analytical method or numerical method. Analytical method can give an exact solution of PDE, but only available for infinite or semi-infinite medium or other certain regular geometries. On the contrary, numerical method is only able to obtain approximate solution of PDE but have no limitation on the shape of medium. Finite element method (FEM) is a major numerical approach for PDE. It uses Galerkin method to attain an approximate solution on an arbitrary mesh. The type of mesh in FEM is optional, but fine meshes consisting of linear element are often chose. However, although the linear element could improve the time consumption for calculation, its accuracy is much lower than that of the high order elements at the same size of mesh. In this paper, we investigate the differences between the linear and quadratic triangular element in the forward problem of diffuse optical tomography. The results show that the quadratic element is a better compromise between high accuracy and low time consumption compared to the linear element. This means high order element is a better choice for diffuse optical tomography.

8553-94, Poster Session

Fractional laser microablation as an enhancer for skin optical clearing

Ekaterina A. Kolesnikova, Darya Tuchina, Elina A. Genina, Leonid E. Dolotov, Alexey N. Bashkatov, N.G. Chernyshevsky Saratov State Univ. (Russian Federation); Valery V. Tuchin, N.G. Chernyshevsky Saratov State Univ. (Russian Federation) and Institute of Precise Mechanics and Control (Russian Federation) and Univ. of Oulu (Finland)

We are proposing a new method for enhancement of optical clearing agent delivery into the skin using fractional laser microablation of the skin surface. Fractional laser microablation was used to overcome the protective skin barrier. The Palomar Lux2940 erbium laser (Palomar Medical Products Ltd., USA) was used as a light source. Its parameters were the following: the wavelength 2940 nm, the pulse energy from 0.8 to 1 J. The pulses possessed a spike structure (from one to three spikes per pulse depending on the energy) with the spike duration of 5 ms. The microchannels were produced by means of a probe that allowed microablation of skin areas as multiple dots. In vitro and in vivo studies have shown that laser fractional ablation enhance the penetration depth and diffusion rate of PEG-300 and mineral oil in the skin tissue. The diffusion measurements were performed using the Spectral Radar OCT System OCP930SR 022 (Thorlabs Inc., USA) at a wavelength of 930 nm. The values of permeability and diffusion coefficients of the investigated chemicals in the tissue are presented.

8553-95, Poster Session

Three dimensional manipulations of cells using holographic optical tweezers

Tao Tao, Jing Li, Yang Lin, Univ. of Science and Technology of China (China)

Optical tweezers technology can be used to trap particles ranging in size from tens of nanometers to several hundreds micrometers with trapping forces from fN to nN. It is characterized with non-touch, no harm to the sample, operation in the liquid environment and so on. Therefore, it has been applied in the area of life science to manipulate cells, stretch DNA, etc.

Recently, more attention has been paid to the application of optical tweezers on single cell analysis. In order to avoid regarding individual behavior of single cell as colony behavior, statistic investigation on a number of related cells is needed while single cell is studied. This requirement can be satisfied by using holographic optical tweezers to manipulate multiple cells simultaneously. In addition, the study has proved that hepatocytes cultured as a monolayer can quickly lose special functions, whilst those same cells in a quasi 3D collagen matrix retain their normal functions for weeks in culture. So, culture and differentiation of cells are influenced by distribution position, proximity and number of the nearby biological particles. Holographic optical tweezers can produce multiple traps which can be controlled individually, and can create new and complex 3D micro-structures. It provides experimental tools to study functions and behaviors of single cell in multi-body structures.

A holographic optical tweezers system is presented with yeast cell as trapped objects, experiments on 3D trapping and manipulation of multiple cells and building 3D structures are performed in it.

8553-96, Poster Session

Photoacoustic measurement for glucose solution concentration based on tunable pulsed laser induced ultrasound

Zhong Ren, Guodong Liu, Zhen Huang, Dengji Zhao, Jiangxi Science and Technology Normal University (China)

Noninvasive blood glucose concentration(BGC) measurement has become a research hotspot. Up to now, some noninvasive BGC measurement methods have been researched. e.g. near-infrared spectroscopy, Raman spectroscopy, fluorescence detection, OCT. Although some progresses have been achieved, many problems are still in researching, such as, strong light-scattering disturb for tissues, individual difference and complexity of human system. However, photoacoustic(PA) spectroscopy have better advantages than others because of the detected ultrasonic waves instead of photon, which overcomes the drawback of scattering light and has higher contrast and resolution. In this paper, a custom-built tunable OPO pulsed laser induced ultrasonic system was established. In this system, the focused ultrasound transducer was used to detect PA signals of glucose. In the experiment, forward PA detection mode was employed. To determine the characteristic wavelength of glucose, the tunable wavelength of OPO laser was adjusted from 1300nm to 2400nm with interval of 10nm. And the distilled water and five different concentrations of glucose aqueous solutions with 50, 100, 150, 200 and 250mg/dl were measured. Experimental result shows that the PA profiles of glucose solutions are highly consistent to other literatures' reports. By mean of the difference of PA peak-to-peak values between glucose solutions and distilled water, several wavelengths, i.e. 1410nm, 1510nm, 1890nm, 2020nm and 2130nm are relatively determined as optimal wavelengths. And the prediction error of glucose concentration by means of fitting algorithm is less than 0.28mmol/L, which is too much better than that of other methods. Therefore, the PA method has large potential value in BGC measurement.

8553-97, Poster Session

Preliminary study on the estimation of epidermal melanin content using diffuse reflectance spectra

Ying Wang M.D., Chinese PLA General Hospital (China); Xiaohua Liao, Fujian Metrology Institute (China); Ying Gu, Chinese PLA General Hospital (China); Rong Chen, Fujian Normal Univ. (China)

Objectives: The object of this study is to characterize the epidermal melanin content of Chinese skin by diffuse reflectance spectra, and evaluate the melanin content change after photodynamic therapy for port wine stains.

Methods: Firstly, diffuse reflectance spectra of normal transplant skin flap skin were measured in vivo in eighteen mildly burned patients before surgery, and Fontana-Masson stain was made in the pathological sections. Epidermal melanin contents were analyzed by image analysis software. Then, least squares fitting was performed to the experiment points from 620-700nm, and the slope of this straight line which corrected with the melanin content was calculated. A semiquantitative relationship between epidermal melanin contents and the slope values was established. Further, diffuse reflectance spectra of PWS patients with various degree of pigmentation were measured, and epidermal melanin contents were estimated approximately. In addition, Monte Carlo algorithm was utilized to investigate the light distribution character of 532 nm laser deposited in PWS skins with various degree of pigmentation.

Results: The epidermal melanin contents estimated with Fontana-Masson stain in these eighteen patients was 5~20%. The slope values were -0.00158 to 0.000592, and reduced with melanin content increasing. The slope value of PWS patient with pigmentation was

smaller than PWS without pigmentation. The 532 nm laser deposited in PWS skin with high degree of pigmentation is much lower than PWS without pigmentation.

Conclusions: Diffuse reflectance spectra have the potential to be applied in establishing the epidermal melanin content and the degree of pigmentation.

8553-98, Poster Session

Expansion of scattered phase matrix based on Zernike polynomials

Haishui Ye, Zhishan Gao, Qianwen Wang, Kexin Bao, Xiaowei Yang, Nanjing Univ. of Science and Technology (China)

Multiple scattering and absorption in biological tissue occurs that scattered light's polarization changes as incident angle and tissue's physical performance when beam bounds to spherical particles in the turbid media. Combined with the classical Mie scattering, radiative transfer equation (RTE) is also introduced to describe dynamic energy conservation. It has been demonstrated that RTE can in fact be derived from the electromagnetic theory of multiple wave scattering in discrete random media under certain simplifying assumption. Obviously, the key is to solve RTE. There exists three variables in the RTE, including polar angle, azimuthal angle and normalized penetrate depth. In order to solve this equation with double integral on polar angle and azimuthal angle, the first step is to introduce proper method to isolate the azimuthally dependency from polar angle, commonly including Fourier series and Legendre polynomials expansion. In this paper, we put forward a novel phase matrix expansion with Zernike polynomials, which represents the probability of scattering events. Specifically, orthogonal Zernike polynomial in square integral region has been derived from Gram-Schmidt orthogonalization. The results show that it can provide a new improved strategy for the solution of radiative transfer equations in Discrete-Ordinate Method (DOM), and the final solution for scattered lights' polarization greatly coincide with the results from Spherical Harmonic Method (SHM). Besides, we also extend this orthogonal decomposition of scattered phase matrix to more orthogonal basis.

8553-99, Poster Session

Optical-resolution photoacoustic microscopy for imaging blood vessels in vivo

Yi Yuan, South China Normal Univ. (China)

An optical-resolution photoacoustic microscopy system was designed and fabricated by integration of a two-dimensional scanning galvanometer, an objective lens, an unfocused ultrasound transducer and a sample stage for imaging blood vessels in vivo. The lateral resolution of the system was measured to be ~5 μm . In vivo blood vessels of mouse ear were clearly shown and the injured blood vessels were also monitored. The experimental results demonstrate that galvanometer-based photoacoustic microscopy holds clinical potential in detecting lesion of blood vessels.

8553-100, Poster Session

Optical characters of prostate using nonlinear optical microscopy

Shulian Wu, Hui Li, Xiaoman Zhang, Fujian Normal Univ. (China)

The incidence rate of the prostatic hyperplasia is increasing in near decade, early detection is important for preventing the prostatic cancer (PCa). In this study, the imagines of prostate and cavernous nerves were carried out using intrinsic fluorescence and scattering properties of the tissues without any exogenous dye or contrast agent based on

nonlinear optical microscope. The texture feature and optical property of the interfibrillar substance in prostate tissue were extracted and analyzed for characterizing the prostate structure. It will be the feature parameter to differentiate the normal, the inflammation or cancer of prostate tissue in clinical with the application of miniature endoscope nonlinear optical microscope in vivo.

8553-101, Poster Session

Crystalline lens surgery: cutting quality and safety evaluation of femtosecond laser pulses

Jiaying Zhang M.D., Chinese PLA General Hospital (China); Rui Wang, Institute of Physics (China); Bin Chen, Hongyou Zhao, Ying Gu, Chinese PLA General Hospital (China)

A femtosecond laser-induced crystalline-lens micro-cut procedure for alleviating presbyopia has received attention recently. We determined the efficiency and safety of this promising strategy using optical measurements of the distribution of pulse energy as light passes through the eyeball. Laser pulses of 35 fs in duration were used to perform in vitro cutting of porcine lens. The transmittance through the refractive media was measured to be 69%~84% according to different input energies. Our data illustrate the theoretical feasibility and safety of the procedure. The results recommend the use of nanojoule laser pulses combined with high numerical aperture optics.

8553-102, Poster Session

Effect of apertures in ultrasound-modulated optical tomography with photomultiplier tube

Lili Zhu, Shubing Ran, Zhiyuan Lin, Hui Li, Fujian Normal Univ. (China)

Improving signal to noise ratio in ultrasound-modulated optical tomography (UOT) is a research topic. Laying apertures in front of a photomultiplier tube (PMT) can reduce the ambient noise collected by the PMT, and efficiently improve the signal to noise ratio of UOT. In addition, the effective area of detection and the off-axis position of the PMT would be varied by changing the aperture size and position in front of the PMT. Experimental results indicated that the modulation depth of ultrasound-modulated signal is dependent on the area of detection. The greater the detector area, the smaller the modulation depth. The modulation depth also depended on the off-axis position of the PMT from the optic axis. In particular, the modulation depth did not reach the biggest value when the PMT just placed on the optics axis. Choosing appropriate size, position of aperture, can improve modulation depth and image contrast.

8553-103, Poster Session

The tapered-tip single fiber optical tweezers and its multi-trapping

Xiaolei Guo, Zhihai Liu, Yuanheng Zhao, Libo Yuan, Harbin Engineering Univ. (China)

Since 1986 Ashkin presented the concept about optical trapping, the optical tweezers have been rapidly developed in the following years. Especially, in the area of bioscience, optical tweezers have become one of the most effective tools in doing research on single cells and biomacromolecule because of its ability of controlling nano-scale particles without contacting and damaging them.

The early fiber optical tweezers using two or more optical fibers guiding light beams to build a large gradient for trapping. Then as the need for

further, these technology mentioned below could not trap particles by only one optical fiber.

Now there many structures of single optical tweezers. In the experiment the researchers found that some of these optical tweezers could trap multi-particles simultaneously. Actually the conventional optical tweezers also has this ability of trapping multi-particles. But it is difficult to observe this phenomenon because the viewing field of the conventional optical tweezers is perpendicular to the trapping direction. So there is no further research on it. The trapping direction of the fiber optical tweezers exists in the focal plane of the imaging. And it makes the research of the multi-particles trapping meaningful

We propose a novel tapered-tip single fiber optical tweezers, which can realize micro particles multi-trapping. The theory analysis about multi-trapping was finished with the finite difference time domain (FDTD) method. The theory and experiment results showed that the particle refractive index affects the multi-trapping obviously.

8553-104, Poster Session

Scattering properties of normal and cancerous tissues from human stomach based on phase-contrast microscope

Hui Zhang, Zhifang Li, Hui Li, Fujian Normal Univ. (China)

In our experiment, all fresh tissue specimens from human stomach were frozen and cut on a microtome (HM550, Microm) to a thickness of 5-um. These unstained tissue slices are microscopic phase objects, its structural information mostly reflect in the refractive index, not amplitude contrast. So we use a phase-contrast microscope (TS100, Nikon) to measure variations in refractive index and observe structural information of each slice. All phase-contrast images were acquired with taken at magnifications of 100x, 200x, 400x with a CCD camera (TCA-5.0C, Tucsen).

Next, images were processed by Matlab software. Mie scattering theory suits for spherical particles as a conventional model. In order to study scattering properties of normal and cancerous tissues, therefore, we analyze phase-contrast images using multiscale mathematical morphology. Creating disk structure elements, and opening operation with a series of various radius on image, we can obtain particle size distribution of tissues.

Assume scattering of light in biological tissue can be seen as separate scattering events by different particles, total scattering properties can be equivalent to as scattering sum of particles with different diameters. According to classical algorithm of Mie scattering providing an exact solution, scattering properties parameters of tissue including scattering coefficient, reduced scattering coefficient, mean cosine of scattering angle, phase function can be calculated.

Compared with normal tissue, we found that scattering coefficient and reduced scattering coefficient of cancerous tissue is significantly higher, mean cosine of scattering angle is approximately equal, scattering phase function is different especially in the backscattering area.

8553-105, Poster Session

Retrieval of atmospheric visibility from multi-axis differential optical absorption spectroscopy

Haijin Zhou, Univ. of Science and Technology of China (China); Wenqing Liu, Fuqi Si, Anhui Institute of Optics and Fine Mechanics (China)

The multi-axis differential optical absorption spectroscopy (MAX-DOAS) technique is being widely used in the monitoring of trace gases column density. In this paper, a retrieval method of visibility from O4 slant column density measured with MAX-DOAS is present. O4 slant column density is sensitive to the change of aerosol properties, and aerosol properties determines the atmospheric visibility. The relationship

of atmospheric visibility and O4 slant column density is analyzed, and a retrieval algorithm to convert the O4 differential slant column density into the surface mixing ratio with the information of visibility is described. MAX-DOAS observation is carried out at HeFei, and atmospheric visibility is retrieved successfully. The visibility measured with MAX-DOAS shows good agreement with the result obtained with visibility meter, proving the feasibility of the retrieval method. This research presents a simple and effective monitoring method of visibility with MAX-DOAS, expands the application of MAX-DOAS technique.

8553-106, Poster Session

Monte Carlo Simulation of Photon Coherent Behavior in Half Infinite Turbid Medium by Scaling Method

Lin Lin, Guangdong Medical College (China); Mei Zhang, Huazhu Liu, Dongguan University of Technology (China)

A method of coherent measuring optical parameters of scattering medium is presented based on Monte Carlo simulation. The condensed scaling method is introduced to accelerating process of calculation. A tri-layer structure BP-artificial neural network is developed for reverse calculation of scattering and absorption coefficients of medium. Fat emulsion and stain mixture of Intralipid™ and India ink are taken as scattering and absorbing sample for coherent measurement by fiber Michelson interferometer. Results of experiments have shown linear relation between scattering or absorption coefficients and concentration of Intralipid™ or India ink. The method is helpful to nondestructive testing components of turbid material.

8553-107, Poster Session

In vivo detection of hemoglobin oxygen saturation and carboxyhemoglobin saturation variations with photoacoustic microscopy

Zhongjiang Chen, Yang Sihua, Da Xing, South China Normal Univ. (China)

Almost all pulse oximeters in common use measure tissue light transmission at two wavelengths (two colors) to estimate arterial hemoglobin saturation. If any other light absorbers are present in the blood, the pulse oximeter's calibration may be invalid. The carboxyhemoglobin (HbCO) is the most life-threatening in blood in CO poisoning. In this study, a method for noninvasive detecting hemoglobin oxygen saturation (SO₂) and carboxyhemoglobin saturation (SCO) in subcutaneous microvasculature with multi-wavelength photoacoustic microscopy is presented. Blood samples mixed with different concentrations of carboxyhemoglobin were used to test the feasibility and accuracy of the photoacoustic microscope comparing with the blood-gas analyzer. Moreover, fixed-point detection of SO₂ and SCO in mouse ear was obtained, and the changes from normoxia to carbon monoxide hypoxia were dynamically monitored in vivo. Experimental results demonstrate that multi-wavelength photoacoustic microscopy can detect SO₂ and SCO, which has future potential clinical applications.

8553-108, Poster Session

Photoacoustic imaging of prostate cancer using cylinder diffuse radiation

Wenming Xie, Hui Li, Li Li, Fujian Normal Univ. (China)

Prostate cancer is one of diseases with high mortality in man. Many clinical imaging modalities are used for the detection, grading and

staging of prostate cancer, such as ultrasound, CT, MRI, etc. But they lacked adequate sensitivity and specificity for finding cancer in transition or central zone of prostate. To overcome these problems, we propose a photoacoustic imaging modality based on cylinder diffuse radiation through urethra for prostate cancer detection. The related parameters, such as resolution, imaging depth and so on, were employed with this system. Finally, in vitro canine prostate as a sample was imaged. The results demonstrate the feasibility for detecting prostate cancer.

8553-109, Poster Session

Realization of the ergonomics design and automatic control of the fundus cameras

Chiliang Zeng, Zexin Xiao, Shichao Deng, Xinye Yu, Guilin Univ. of Electronic Technology (China)

The design principle of ergonomics design in fundus cameras should be extending the agreeableness by automatic control. Firstly, a 3D positional numerical control system is designed for positioning the eye pupils when patient doing fundus examinations. This system consists of a electronically controlled chin bracket for moving up and down, a lateral movement of binocular with the detector and automatic focusing of the edge of the eye pupils. Secondly, a auto-focusing device for the object plane of patient's funds is designed, which collects the patient's fundus images automatically whether their eyes is ametropic or not. Finally, a moving visual target is developed for expanding the field of the fundus images.

8553-110, Poster Session

Laser speckle contrast imaging for early acute myocardial ischemia of rat

Biyang Yu, Hui Li, Fujian Normal Univ. (China); Haiyu Chen, Fujian Medical Univ. (China); Shusen Xie, Fujian Normal Univ. (China)

Nowadays, cardiovascular diseases that threat to human life and health have become main diseases with an obvious rising incidence. Myocardial ischemia is the most of the focus on cardiovascular diseases. The change of microcirculation blood flow and the process of myocardial ischemia are closely related. Laser speckle contrast imaging provides full-field and real-time investigation of microcirculation blood flow in vivo with several outstanding characteristics that including non-contact, noninvasive and high speed imaging. An acute myocardial ischemia model of rat is established by the ligation of the left anterior descending branch in this study. Images that reflect blood flow of the front wall of left ventricle in different ligation time are attained by laser speckle contrast imaging. And some data for evaluating myocardial ischemia degree are obtained used laser speckle contrast imaging.

8553-111, Poster Session

Study the effect of temperature on optical properties of biological tissue-simulating phantom based on OCT

Youwu He, Hui Li, Fujian Normal Univ. (China)

In the basic research area, people would like to study the effects of temperature on optical properties measurement of tissue-simulating sample and vitro tissue. Many methods has been used such as near-infrared spectrum technology and CCD diffusing reflection measurements etc. In our research, we use optical coherence tomography (OCT) technology to study the effect of temperature on the optical properties of biological tissue by using intralipid as an example. OCT imaging is based on the differences of backscatter light, in the

model, OCT is assumed to detect light that only scattered once, and thus the decay of the OCT signal with depth function follows the Beer-Lambert law. According to the Beer-Lambert law, we can easily obtain information on sample scattering properties. Put the sample in the electric heating constant temperature pot (working accuracy: $\pm 0.5^\circ\text{C}$), and we measure the optical properties in the temperature range of 25-40°C. The temperature span is 5°C. The results show that obvious decrease can be observed with increasing temperature in the reduced scattering coefficient. The results were in contrast with those reported results on the study of ex vivo tissue, and they were coherent. The results demonstrate that OCT is an effective and novel method to study the effect of temperature on optical properties of biological tissue.

8553-112, Poster Session

Miniature interferometer for refractive index measurement in microfluidic chip

Minghui Chen, Univ. of Shanghai for Science and Technology (China); Martial H. Geiser, Frederic Truffer, Univ. of Applied Sciences Western Switzerland (Switzerland); Chengli Song, Univ. of Shanghai for Science and Technology (China)

The design and development of the miniaturized interferometer for measurement of the refractive index or concentration of sub-microliter volume aqueous solution in microfluidic chip is presented. It is manifested by a successful measurement of the refractive index of sugar-water solution, by utilizing a laser diode for light source and the small robust instrumentation for practical implementation. Theoretically, the measurement principle and the feasibility of the system are analyzed. Experimental device is constructed with a diode laser, lens, two optical plates and CMOS. Through measuring the positional changes of the interference fringes, the refractive index change are retrieved. A refractive index change of 10^{-4} is inferred from the measured image data. The entire system is approximately the size of half a deck of cards and can operate on battery power for long time.

8553-113, Poster Session

Study for noninvasive determination of optical properties of bio-tissue using spatially resolved diffuse reflectance

Dongqing Peng, Fujian Normal Univ. (China) and Jimei Univ. (China); Hui Li, Fujian Normal Univ. (China)

The optical characteristic of absorption and scattering of irradiated tissue determine light spatial distribution and the subsequent biological effects, which can decide the dosimetry for laser medical applications. Based on the measurement of diffuse reflectance obtained by Monte Carlo simulation, the optical properties of bio-tissue were determined through the nonlinear least-square algorithm with spatially resolved diffuse reflectance theory in the first. and the data scope, data space, even start value for the nonlinear regression were discussed in detail. Then, a laser scattering imaging system based on digital camera was designed by ourselves for measurement radial distribution of diffuse reflectance light at 632.8nm from several bio-tissues. The absorption and reduced scattering coefficients are derived by nonlinear fitting of diffusion equation with the relative distribution data of diffuse reflection light intensity. The results were compared with the reported results and show the feasibility of theoretical model and experiment method. Study indicate that the appropriate regression of noninvasive measurement of radial dependence of the diffuse reflectance and a more accurate light diffuse reflectance theoretical model are required to provide the possibility to obtain the optical parameters of biological tissues.

8553-114, Poster Session

Development of an in situ magnetic beads based RT-PCR method for electrochemiluminescent detection of rotavirus

Fangfang Zhan, Xiaoming Zhou, South China Normal Univ. (China)

Rotaviruses are double-stranded RNA viruses belonging to the family of enteric pathogens. It is a major cause of diarrhoeal disease in infants and young children worldwide. Consequently, rapid and accurate detection of rotaviruses is of great importance in controlling and preventing food- and waterborne diseases and outbreaks. Reverse transcription-polymerase chain reaction (RT-PCR) is a reliable method that possesses high specificity and sensitivity. It has been widely used to detection of viruses. Electrochemiluminescence (ECL) can be considered as an important and powerful tool in analytical and clinical application with high sensitivity, excellent specificity, and low cost. Here we have developed a method for the detection of rotavirus by combining in situ magnetic beads (MBs) based RT-PCR with ECL. RT of rotavirus RNA was carried out in a traditional way and the resulting cDNA was directly amplified on MBs. Forward primers were covalently bounded to MBs and reverse primers were labeled with tris-(2, 2'-bipyridyl) ruthenium (TBR). During the PCR cycling, the TBR labeled products were directly loaded and enriched on the surface of MBs. Then the MBs-TBR complexes could be analyzed by a magnetic ECL platform without any post-modification or post-incubation, which avoid some laborious manual operations and achieve rapid yet sensitive detection. In this study, rotavirus from fecal specimens was successfully detected within 2 h, and the limit of detection was estimated to be 104 copies/ μl . This novel in situ MBs based RT-PCR with ECL detection method can be used for pathogen detection in food safety field and clinical diagnosis.

8553-115, Poster Session

ERK-dependent activation of Sp1 is required for low-power laser irradiation-induced vascular endothelial cell proliferation

Jie Feng, Da Xing, South China Normal Univ. (China)

Angiogenesis participates in developmental and pathological neovascularization, during which proliferation of vascular endothelial cells is a crucial procedure. The role of low-power laser irradiation (LPLI) in promoting cell proliferation has been widely spread in clinical for decades of years. Therefore, the effect of LPLI on proliferation may offer clinically therapeutic options to facilitate angiogenesis. However, the underlying mechanisms are not fully elucidated. Here, we report that LPLI activates ERK/Sp1 (Extracellular signal-Regulated Kinase / Specificity protein 1) pathway to upregulate VEGF expression and promote vascular endothelial cell proliferation. Using a Sp1 luciferase reporter and chromatin immunoprecipitation analysis, we demonstrate for the first time that LPLI enhances DNA-binding activity and transactivation activity of Sp1 on VEGF promoter. The results from real-time single-cell analysis suggest that ERK translocates from cytoplasm to nucleus following LPLI. More importantly, activated ERK by LPLI phosphorylates Sp1. FRET method and co-immunoprecipitation reveal that the interaction between ERK and Sp1 is gradually increasing. In addition, selective inhibition of Sp1 by mithramycin A or shRNA suppresses the effect of LPLI on the promotion of vascular endothelial cell cycle progression and proliferation, which is also significantly abolished by inhibition of ERK with PD98059, a specific inhibitor of MEK. These findings provide a novel link between LPLI and endothelial proliferation, an essential procedure of angiogenesis, supplying potential therapy strategies for vascular pathologies through ERK/Sp1 signalling pathway with LPLI.

8553-117, Poster Session

Iterative reconstruction for bioluminescence tomography with total variation regularization

Wenma Jin, Peking Univ. (China); Yonghong He, Beijing Aerospace Control Ctr. (China)

Bioluminescence tomography(BLT) is an instrumental molecular imaging modality designed for the 3D location and quantification of bioluminescent sources distribution in vivo. In our context, the diffusion approximation (DA) to radiative transfer equation(RTE) is utilized to model the forward process of light propagation.

Mathematically, the solution uniqueness does not hold for DA-based BLT which is an inverse source problem of partial differential equations and hence is highly ill-posed. In the current work, we concentrate on a general regularization framework for BLT with Bregman distance as data fidelity and total variation(TV) as regularization.

Two specializations of the Bregman distance, the least squares(LS) distance and Kullback-Leibler (KL) divergence, which correspond to the Gaussian and Poisson environments respectively, are demonstrated and the resulting regularization problems are denoted as LS+TV and KL+TV. Based on the constrained Landweber (CL) scheme and expectation maximization(EM) algorithm for BLT, iterative algorithms for the LS+TV and KL+TV problems in the context of BLT are developed, which are denoted as CL-TV and EM-TV respectively. They are both essentially gradient-based algorithms alternatingly performing the standard CL or EM iteration step and the TV correction step which requires the solution of a weighted ROF model. Chambolle's duality-based approach is adapted and extended to solving the weighted ROF subproblem. Numerical experiments for a 3D heterogeneous mouse phantom are carried out and preliminary results are reported to verify and evaluate the proposed algorithms. It is found that for piecewise-constant sources both CL-TV and EM-TV outperform the conventional CL and EM algorithms for BLT.

8553-118, Poster Session

Imaging the morphological change of tissue structure during the early phase of esophageal tumor progression using multiphoton microscopy

Jian Xu, Fujian Normal Univ. (China); Deyong Kang, Meifang Xu, Fujian Medical Univ. (China); Jianxin Chen, Fujian Normal Univ. (China)

Esophageal cancer is one of the most common cancer and leading cause of cancer death worldwide. Like most other cancers, early detection is important to improve the quality of life in patient and reduce mortality. Multiphoton microscopy (MPM) is becoming a novel optical tool of choice for imaging tissue architecture and cellular morphology by two-photon excited fluorescence. In this study, we used MPM to image the morphological change of tissue structure during the early phase of esophageal tumor progression, including human normal esophagus, carcinoma in situ, and early invasive carcinoma. We extracted the diagnostic features to distinguish between normal and cancerous esophagus tissue, such as the appearance of cancerous cells, the absence of the basement membrane. We also quantitatively described the differences of morphology between normal and cancerous cells. These results correlated well with the paired histological findings. With the advancement of clinically miniaturized MPM and the multi-photon probe, combining MPM with standard endoscopy will therefore allow us to make a real-time in vivo diagnosis of early esophagus cancer at the cellular level.

8553-119, Poster Session

Low-power laser irradiation protects mitochondrial function and inhibits MPP+-induced neuron loss through the activation of PGC-1[alpha]

Juan Wang, Shengnan Wu, Da Xing, South China Normal Univ. (China)

Parkinson's disease (PD) is a pervasive neurodegenerative disease which results from the loss of the dopaminergic neurons in the substantia nigra pars compacta. 1-methyl-4-phenylpyridinium (MPP+) induced mitochondrial dysfunction and oxidative stress have been implicated in PD model. Previous studies show that low-power laser irradiation (LPLI) can reverse MPP+-induced decrease of mitochondrial membrane potential and neurons loss. However, the underlying mechanisms are unknown. In the present study, we first reported that LPLI promoted peroxisome proliferator-activated receptor γ coactivator 1 (PGC-1 α) expression and activation, which decreased the number of neurons undergoing apoptosis, and significantly reduced the excessive reactive oxygen species in MPP+-exposed neurons. Inhibition of PGC-1 α expression by siRNA significantly abolished the effect of LPLI. We also discovered that MPP+-induced neurons toxicity declined the phosphorylation of cAMP-responsive element-binding protein (CREB), a main regulator of PGC-1 α expression, which was recovered by LPLI in an extracellular signal-regulated kinase (ERK) dependent manner. Therefore, LPLI protects neurons from MPP+-induced apoptosis through ERK/CREB/PGC-1 α pathway. These data provide a new clue that PGC-1 α may be a potential target for the PD therapeutic manipulation with LPLI treatment.

8553-120, Poster Session

Amplification-free detection of miRNA via an ECL chips system

Weipeng Liu, Xiaoming Zhou, South China Normal Univ. (China)

MicroRNAs play pivotal roles in many fundamental aspects of life, such as plant and animal development, tissue differentiation, metabolic modulation and cell proliferation control. As miRNA with the characteristics of small size, easy degradation and low abundance, a simple, rapid and specificity method to measure the concentration of miRNA is required. Herein, we present an Electrochemiluminescent Chips system for rapid microRNA detection based on the base stacking hybridization and magnetic beads(MB) enrichment technology. In this design, integrating the microfluidic system with Electrochemiluminescent detection makes it easy to assemble the multiple assay steps (e.g., sample preparation, incubation, washing and detection) and let the device convenient to carry. This method is very fast, we can detect miRNA-21 in 15 min with a 10 μ L sample volume. Moreover, in this experiment the detection limit was 0.1 nM or 1 μ g total small RNA(20-200 nt) from human tissues, and the linear range from 0.1 nM to 50 nM. It also exhibited excellent selectivity over a series of interference miRNA, which display a high level of expression in cancer cell. These results suggest that this method might have potential for cancer diagnosis at the point of care.

8553-121, Poster Session

Label-free and sensitive fluorescence detection of nucleic acid, based on combination of a graphene oxid /SYBR green I dye platform and polymerase assisted signal amplification

Xiao Zhu, Da Xing, Xiaoming zhou, South China Normal Univ.

(China)

A new label-free isothermal fluorescence amplification detection for nucleic acid has been developed. In this paper, we first developed a novel sensitive and specific detection platform with an unmodified hairpin probe (HP) combination of the graphene oxid (GO) / intercalating dye, which was relied on the selective principle of adsorption and the high quenching efficiency of GO. Then for the application of this new strategy, we used Mirco RNA-21 (Mir-21) as the target to evaluate this working principle of our design. When the target was hybridizing with the HP and inducing its conformation of change, an efficient isothermal circular strand-displacement polymerization reaction was activating to assist the first signal amplification. In this format, the formed complex conformation of DNA would interact with its high affinity dye, then detached from the surface of GO after incubating with the platform of GO/intercalating dye. This reaction would accompany with obvious fluorescence recovery, and accomplish farther signal enhancement by a mass of intercalating dye inserting into the minor groove of the long duplex replication product. By taking advantage of the multiple amplification of signal, this method exerted substantial enhancement in sensitivity and could be used for rapid and selective detection of Mir-21 with attomole range. It is expected that this cost-effective GO based sensor might hold considerable potential to apply in bioanalysis studies.

8553-122, Poster Session

Histopathologic change of rabbit retinal injury induced by continuous 1.319 μ m laser

Jiarui Wang, Zaifu Yang, Academy of Military Medical Sciences (China)

Objective To explore the characteristics and histological change of rabbit retinal after irradiation of continuous 1.319 μ m laser in different exposure time. **Methods** A Nd: YAG laser was used to deliver 1.319 μ m laser to the retinas of 15 pigmented rabbits. The exposure time was 0.1s, 1s and 10s respectively. The irradiated site and its instantly change was obtained by ophthalmoscope. The histological evaluation and recordance were performed at 1h, 24h, 48d, 3d and 7d after irradiation. The eyeballs was fixed in Davidson's fixative solution. **Results** White coagulation macula with unsharp borderline and dispersion of pigments was discovered immediately after irradiation. There occurred new injury macular after 24h which showed retina buninoidly eminence, retinal structure derangement, RPE swelling, photoreceptor collapse and ganglion cells degeneration or dropsy. When the exposure time was 10s the corneal and crystalline lens were damaged simultaneously. **Conclusion** The mechanism of the retinal injury induced by continuous 1.319 μ m laser is photothermal damage mainly with heat production by absorption the energy of laser. It suggested that the degree of the damage depends on both the exposure time and irradiation dose which become more serious with larger dose at given exposure time.

8553-123, Poster Session

Photoacoustic spectroscopic differences between normal and malignant thyroid tissues

Li Li, Wengming Xie, Fujian Normal Univ. (China); Shuqiang Chen, Fujian Medical Univ. (China); Hui Li, Fujian Normal Univ. (China)

The thyroid is one of the main endocrine glands of human body, which plays a crucial role in the body's metabolism. Thyroid cancer mortality ranks only second to ovarian cancer in endocrine cancer. Routine diagnostic methods of thyroid diseases in present clinic exist misdiagnosis and missed diagnosis to varying degrees. Those lead to miss the best period of cancer treatment--early. Photoacoustic spectroscopy technology is a new tool, which provides an effective

and noninvasive way for biomedical materials research, being highly sensitive and without sample pretreatment. In this paper, we use photoacoustic spectroscopy technology to detect the absorption spectrum between normal and malignant thyroid tissues. The result shows that the photoacoustic spectroscopy technology could differentiate malignant thyroid tissue from normal thyroid tissue very well. This technique combined with routine diagnostic methods has the potential to increase the diagnostic accuracy in clinical thyroid cancer diagnosis.

8553-124, Poster Session

Ex-vivo endoscopic laryngeal cancer imaging using two forward-looking fiber optic scanning endoscope probes

Ramona C. Cernat, Univ. of Kent (United Kingdom); Taran Tatla, Jingyin Pang, Paul J. Tadrous, Northwick Park Hospital (United Kingdom); Grigory V. Gelikonov, Valentin M. Gelikonov, Institute of Applied Physics (Russian Federation); Yuying Y. Zhang, Johns Hopkins Univ. (United States); Adrian Bradu, Univ. of Kent (United Kingdom); Xingde Li, Johns Hopkins Univ. (United States); Adrian Podoleanu, Univ. of Kent (United Kingdom)

Larynx cancer is one of the most common primary head and neck cancers. For early-stage laryngeal cancer, both surgery and radiotherapy are effective treatment modalities, offering a high rate of local control and cure. Optical coherence tomography (OCT) is an established non-invasive optical biopsy method, capable of imaging ranges of 2-3 mm into tissue. By using the principles of low coherence light interferometry, OCT can be used to distinguish normal from unhealthy laryngeal mucosa in patients. Two forward-looking endoscope OCT probes with different sizes in a sweeping frequency OCT configuration (SS-OCT) were compared in terms of their performances (transversal resolution, sensitivity, and signal to noise ratio) for ex-vivo laryngeal cancer imaging.

The setup configuration of the first OCT probe unit was designed and constructed at the Institute of Applied Physics RAS, Russia (diameter of 1.9 mm and the rigid part at the distal end is 1.5 cm long). The second OCT endoscope probe was constructed at the Department of Biomedical Engineering at Johns Hopkins University, USA, using a tubular piezoelectric actuator with quartered electrodes in combination with a resonant fiber cantilever (diameter of 2.4 mm, and rigid part of 4.5 cm.)

B-scan images of diseased laryngeal tissue using the two OCT configurations were aquired and compared with OCT images obtained in a 1310 nm SS-OCT classical non-endoscopic system. The work presented here is an intermediate step in our research towards in-vivo endoscopic laryngeal cancer imaging.

8553-125, Poster Session

Glucose and temperature sensitive luminescence ZnCdS nanoparticles

Elena K. Volkova, Vyacheslav I. Kochubey, Julia G. Konyukhova, N.G. Chernyshevsky Saratov State Univ. (Russian Federation)

We have investigated changes in the luminescence characteristics of ZnCdS semiconductor nanoparticles depended on temperature and glucose concentration.

ZnCdS nanoparticles were synthesized from a mixture of aqueous solutions of cadmium chloride (CdCl₂) and zinc chloride (ZnCl₂) by addition of sodium sulphide solution at room temperature. The nanoparticles were not stabilized. The ZnCdS nanoparticles solution was added into aqueous glucose solution. Photoluminescence intensity of the particles strongly depended on glucose concentration by adding glucose oxydase. The degree of luminescence quenching is

proportional the glucose concentration.

The luminescence spectra also changes with temperature. Its amplitude decrease and luminescence maximum shifts into long-wave spectral region.

8553-126, Poster Session

Characterization of muscle drawing and injury by polarization-sensitive optical coherence tomography

Dongsheng Chen, Nan Zeng, Celong Liu, Hui Ma, Graduate School at Shenzhen, Tsinghua Univ (China)

In this paper, we study muscle elastic drawing and injury using our lab's polarization-sensitive optical coherence tomography (PS-OCT) instrument and polarization sensitive Monte Carlo program. First, we acquire two-dimensional PS-OCT images of elastic drawn and injured muscle, injury processes including dehydration and hydrolysis, using our instrument, and from the images, we extract such information of the muscle as extinction coefficient, integral reflectivity, depolarization coefficient and birefringence and so on, which is changing when muscle is being elastically drawn or injured. In order to further understand and demonstrate the relation between the information above, extracted from experiments, and the degree of muscle elastic drawing or injury, we do some corresponding simulations by our lab's Monte Carlo program, which is based on a sphere cylinder birefringence model and can simulate complicated tissue containing anisotropic microstructures and various polarization imaging and measurement systems. For muscle elastic drawing, we find that integral reflectivity sometimes increases and decreases as muscle's elastic drawing continues, and through simulation we are unable to find the relationship between extinction coefficients and muscle elastic drawing. As for muscle injury, we simulate two processes: dehydration and hydrolysis. We find that as dehydration deepens, the birefringence of muscle is increasing but getting slowly and the integral reflectivity is decreasing, and as hydrolysis deepens, the birefringence is decreasing and the integral reflectivity is almost decreasing linearly. Through the analysis above, we demonstrate the validity of those parameters to characterize muscle elasticity and fiber structure and explain its potential for assessment of muscle injury.

8553-127, Poster Session

Analysis on the characteristics of glucose solution based on terahertz time domain spectroscopy system

Zhao-feng Jiang, Wei Liu, Capital Normal Univ. (China)

With the rapid development of terahertz time domain spectroscopy (THz-TDS) technology, the coherence detection of terahertz pulse allows to obtain the samples' phase and amplitude information. Obviously, glucose is the most prevalent organic compound in nature and is also a major source of metabolic energy. So it is especially necessary to measure and analyze the properties of the glucose solution. The systematical measurement for glucose concentration is the basis of diagnosing symptom, directing the medicine's usage and observing an effect. THz-rays have lower photon energies, which they have no chance to generate ionizing radiation, and this make the higher precision analysis of glucose solution without any damage possible. Therefore, it has an important scientific and medical value in researching glucose solution and finding an accurate measurement method of the concentration. In 2006, M. Nagel, etc, in Germany utilized reflection coherent terahertz waveguide to present the results of alcohol solution and study the relationship between concentration and refractive index, the extinction coefficient.

In this letter, our work is focused on what the quantitative relationship between the concentration of aqueous glucose solution among

refractive index and absorption coefficient based on THz transmission spectroscopy system. Compared with reflection mode, it has an obvious advantage, which is that transmission measurement consists in data processing's simplicity. What's more, it is easy to realize high precision parameters survey. And it is helpful to get the characters of biological liquid sample in the far-infrared spectral region.

8553-47, Session 11

Dynamics of two-photon two-color transitions in flurophores excited by femtosecond laser pulses (*Invited Paper*)

Oleg S. Vasyutinskii, Peter S. Shternin, Andrey G. Smolin, Ioffe Physico-Technical Institute (Russian Federation); Karl-Heinz Gericke, Stefan Denicke, Sebastian Herbrich, Technische Univ. Braunschweig (Germany)

We present the results of theoretical and experimental studies of the polarized fluorescence in flurophores excited by two-photon two-color (2P2C) laser pulses. Quantum mechanical expressions describing the fluorescence polarization have been derived under the condition of isotropic rotation diffusion for arbitrary polarization of each of the three photons involved in the photoprocess.

The experiment has been carried out on p-terphenyl dissolved in cyclohexane/ paraffin and with indol dissolved in methanol. The fluorescence was produced within a 2C2P excitation scheme utilizing simultaneous absorption of two femtosecond laser pulses in the 400-440 nm and in the 800-880 nm spectral range. Using different combinations of the photon polarizations we extracted seven time-dependent molecular parameters from experiment. The analysis of the obtained experimental data was based on the ab initio calculations of the vertical excitation energies and transition matrix elements and allowed for determination of the whole structure of the two-photon absorption tensor, fluorescence lifetime, and rotational correlation times. This gives information on possible two-photon excitation channels and interaction of flurophores with surrounding solute molecules.

1. P. S. Shternin, K.-H. Gericke, O. S. Vasyutinskii, *Molecular Physics*, 2010, 108, 813.

2. S. Denicke, K.-H. Gericke, A. G. Smolin, P. S. Shternin, O. S. Vasyutinskii, *J. Phys. Chem. A* 2010, 114, 9681.

8553-49, Session 11

Dual color CW STED nanoscopy with a Ti:Sapphire oscillator

Yujia Liu, Shanghai Jiao Tong Univ. (China); Eric Alonas, Philip J. Santangelo, Georgia Institute of Technology (United States) and Emory Univ. (United States); Dayong Jin, James A. Piper, Macquarie Univ. (Australia); Qiushi Ren, Peng Xi, Peking Univ. (China)

Fluorescent microscopy has become an essential tool to study biological molecules, pathways and events in living cells, tissues and animals. Meanwhile even the most advanced confocal microscopy can only yield optical resolution approaching Abbe diffraction limit of ~200 nm. This is still larger than many subcellular structures, which are too small to be resolved in detail. These limitations have driven the development of super-resolution optical imaging methodologies over the past decade.

In stimulated emission depletion (STED) microscopy, the excitation focus is overlapped by an intense doughnut-shaped spot to instantly de-excite markers from their fluorescent state to the ground state by stimulated emission. This effectively eliminates the periphery of the Point Spread Function (PSF), resulting in a narrower focal region, or super-resolution. Scanning a sharpened spot through the specimen renders images with sub-diffraction resolution. Multi-color STED imaging can present important structural and functional information for

protein-protein interaction.

In this work, we presented a dual color, synchronization-free STED microscopy with a Ti:Sapphire oscillator. The excitation wavelengths were 532nm and 635nm, respectively. With pump power of 4.6 W and sample irradiance of 310 mW, we achieved super-resolution as high as 71 nm. A series of biological specimens were imaged with our dual-color STED.

8553-50, Session 11

LOSOM: Phase relief imaging can be achieved with confocal system

Tong Peng, Hao Xie, Yichen Ding, Peking Univ. (China); Weichao Wang, Shanghai Jiao Tong Univ. (China); Zhiming Li, Wenzhou Medical College (China); Dayong Jin, Macquarie Univ. (Australia); Yuanhe Tang, Xi'an Univ. of Technology (China); Qiushi Ren, Peng Xi, Peking Univ. (China)

Confocal laser scanning microscopy (CLSM) has become one of the most important biomedical research tools today due to its noninvasive and 3-D abilities. It enables imaging in living tissue with better resolution and contrast, and plays a growing role among microscopic techniques utilized for investigating numerous biological problems. In some cases, the sample was phase-sensitive, thus we introduce a novel method named laser oblique scanning optical microscopy (LOSOM) which could obtain a relief image in transparent sample directly.

Through the LOSOM system, mouse kidney and Hela cells sample were imaged and 10x, 20x and 40x magnify objective imaging results were realized respectively. Also, we compared the variation of pinhole size versus imaging result. One major parameter of LOSOM is the distance between fluorescence medium and the sample. Previously, this distance was set to 1.2 mm, which is the thickness of the slide. The experiment result showed that decreasing d can increase the signal level for LOSOM phase-relief imaging. To study this effect quantitatively, we set each depth of 0.17mm by designing a stack of hollow coverglasses, and the result demonstrated the signal strength versus the fluorescence medium distance.

The LOSOM technic could be used in multiple well plate cellular imaging. In this study, the imaging result of cells with different density in multiple well plate was attained. We also monitored the cell division process of onion by LOSOM. Both the results indicated the LOSOM technic may supply a novel phase sensitive optical image method.

8553-52, Session 11

Design of control system of a real-time confocal scanning laser microscope

Yaohuan Zhao, Peking Univ. (China); Xusan Yang, Xi'an Univ. of Technology (China); Tingting Wang, Peking Univ. (China); Haojie Li, Xi'an Univ. of Technology (China); Peng Xi, Peking Univ. (China)

Here we used a single Complex Programmable Logic Device to generate the control and synchronization signals for real time confocal microscopy. The CPLD can generate the pixel clock, H-Sync, V-Sync, and the saw-tooth control signal of the oscillating galvanometric mirror. The CPLD can automatically track the possible drift of the polygon scanner velocity and adjust H-sync and V-sync signals accordingly to eliminate the instability of the image. Taking advantage of the programmable capability of CPLD, our confocal setup can be easily tuned to work on fast frame rate, or high resolution mode for a variety of applications.

8553-53, Session 12

Photo-acoustic excitation and detection of guided ultrasonic waves in bone samples covered by a soft coating layer

Zuomin Zhao, Univ. of Oulu (Finland); Petro Moilanen, Univ. of Jyväskylä (Finland); Pasi Karppinen, Univ. of Helsinki (Finland); Mikko Määttä, Univ. of Oulu (Finland); Timo Karppinen, Edward Hægström, Univ. of Helsinki (Finland); Jussi Timonen, Univ. of Jyväskylä (Finland); Risto Myllylä, Univ. of Oulu (Finland)

Photo-acoustic (PA) excitation was combined with skeletal quantitative ultrasound (QUS) for multi-mode ultrasonic assessment of human long bones. This approach permits tailoring of the ultrasonic excitation and detection so as to efficiently detect the fundamental flexural guided wave (FFGW) through a coating of soft tissue. FFGW is a clinically relevant indicator of cortical thickness. An OPO laser with tunable optical wavelength, was used to excite a photo-acoustic source in the shaft of a porcine femur. Ultrasonic signals were detected by a piezoelectric transducer, scanning along the long axis of the bone, 20-50 mm away from the source. Five femurs were measured without and with a soft coating. The coating was made of an aqueous gelatin-intralipid suspension that optically and acoustically mimicked real soft tissue. An even coating thickness was ensured by using a specific mold. The optical wave length of the source (1250 nm) was tuned to maximize the amplitude of FFGW excitation at 50 kHz frequency. The experimentally determined FFGW phase velocity in the uncoated samples was consistent with that of the fundamental antisymmetric Lamb mode (A₀). Using appropriate signal processing, FFGW was also identified in the coated bone samples, this time with a phase velocity consistent with that theoretically predicted for the first mode of a fluid-solid bilayer waveguide (BL1). Our results suggest that photo-acoustic quantitative ultrasound enables assessment of the thickness-sensitive FFGW in bone through a layer of soft tissue. Photo-acoustic characterization of the cortical bone thickness may thus become possible.

8553-54, Session 12

ICG-loaded microbubbles for multimodal biliary imaging in cholecystectomy

Kinshuk Mitra, The Ohio State Univ. (United States); Shufang Chang, Chongqing Medical Univ. (China); Scott Melvin M.D., The Ohio State Univ. (United States); Ronald X. Xu, The Ohio State Univ. (United States) and Univ. of Science and Technology of China (China)

Bile duct injury during a cholecystectomy is an iatrogenic accident ranking among the leading sources of medical malpractice claims against surgeons. Intraoperative fluorescence imaging has been used for real-time non-invasive detection and prevention of bile duct injury. However, commonly used Indocyanine Green (ICG) is not an ideal contrast agent for biliary imaging in cholecystectomy. We encapsulated ICG in PEGylated poly(lactic-co-glycolic acid) (PLGA) microbubbles by a modified double-emulsion process. Microbubble-assisted biliary imaging was tested in both tissue simulating phantoms and an ex vivo tissue model. The tissue simulating phantoms simulated different surgical scenarios and the simulated biliary structures were imaged by a fluorescence imaging module in a Da Vinci surgical robot. As to the ex vivo model, liver, gall bladder, common bile duct, and part of duodenum were dissected freshly from domestic swines. Simultaneous hyperspectral and fluorescence images were acquired after regional injection of ICG-loaded microbubbles. Our benchtop and animal tests showed that ICG-loaded MBs are superior to ICG as a fluorescence contrast agent for image-guided cholecystectomy. This work was supported by OSU Center for Minimally Invasive Surgery and the National Center for Research Resources (NCRR Award Number: UL1RR025755).

8553-55, Session 12

Multimodal imaging of ischemic wounds

Shiwu Zhang, Univ. of Science and Technology of China (China) and The Ohio State Univ. (United States); Surya C. Gnyawali, Jiwei Huang, The Ohio State Univ. (United States); Wenqi Ren, Univ. of Science and Technology of China (China); Gayle Gordillo M.D., Chandan Sen, The Ohio State Univ. (United States); Ronald X. Xu, The Ohio State Univ. (United States) and Univ. of Science and Technology of China (China)

The wound healing process involves the reparative phases of inflammation, proliferation, and remodeling. Interrupting any of these phases may result in chronically unhealed wounds, amputation, or even patient death. Quantitative assessment of wound tissue ischemia, perfusion, and inflammation provides critical information for appropriate detection, staging, and treatment of chronic wounds. However, no method is available for noninvasive, simultaneous, and quantitative imaging of these tissue parameters. We integrated hyperspectral, laser speckle, and thermographic imaging modalities into a single setup for multimodal assessment of tissue oxygenation, perfusion, and inflammation characteristics. Advanced algorithms were developed for accurate reconstruction of wound oxygenation and appropriate co-registration between different imaging modalities. The multimodal wound imaging system was validated by two ongoing clinical trials approved by OSU IRB. In one clinical trial, the oxygenation and the perfusion maps of a healthy subject's upper extremity were continuously monitored during post occlusive reactive hyperemia and compared with standard measurements. In the other clinical trial, a wound of 3mm in diameter was introduced on a healthy subject's lower extremity and the healing process was continuously monitored by the multimodal imaging setup. Our experiments demonstrated the clinical usability of multimodal wound imaging. This research is sponsored by National Institute of Standards and Technology (60NANB10D184) and US Army Medical Research Acquisition Act (W81XWH-11-2-0142).

8553-56, Session 12

Microfabrication of multifunctional microcapsules for multimodal imaging and image-guided therapy

Ting Si, Univ. of Science and Technology of China (China); Leilei Zhang, The Ohio State Univ. (United States); Guangbin Li, Univ. of Science and Technology of China (China); Ronald X. Xu, The Ohio State Univ. (United States)

With the recent advances in multimodal imaging and image-guided therapy, optimizing the design and fabrication of biodegradable carriers for the delivery of drugs and imaging agents become more and more important. Multifunctional microcapsules encapsulate several imaging and therapeutic agents in the same biodegradable carrier for simultaneous detection and treatment of the diseases. Commonly used microfabrication processes, such as double emulsion, have multiple limitations, such as the low encapsulation efficiency and the loss of bioactivity for the encapsulated biological cargos. To overcome these limitations, we carried out both experimental and theoretical studies on coaxial atomization of PLGA microcapsules. The process combined coaxial electrospray with flow focusing techniques. It was characterized by the formation of a coaxial liquid jet in the core of a high-speed co-flowing gas stream under an axial electric field and the breakup of the liquid jet into fine microcapsules. On the experimental side, the device of the coaxial atomization was developed and tested. On the theoretical side, a classical normal mode method was used for instability analysis of the coaxial jet based on the experimental parameters. The microcapsules were fabricated under different process conditions. The effects of the process parameters on morphologic and size characteristics of the microcapsules were studied. The reported research represents the first step toward quantitative control and

optimization of the coaxial atomization process for the fabrication of multifunctional microcapsules in multimodal imaging and image-guided therapy. This project was sponsored by Natural Science Foundation of China (Project No. 11002139 to Si), National Cancer Institute (Grant No: R21CA15977 to Xu), and Ohio Lion's Eye Research Foundation (Fellowship support to Zhang).

8553-57, Session 13

Electromagnetic scattering from biological tissue

Zhisong Tong, Olga Korotkova, Univ. of Miami (United States)

After the development of the optical biomedical technology, the underlying mechanism for the interaction of light with tissue has been illustrated that light scattering is not due to discrete particles but rather to continuous refractive index variation at the microscopic level in tissue. The proposed mathematical models of the experimentally fitted spectrum of index inhomogeneities provide a path to investigate the second-order statistical properties of light on interaction with (propagation through or scattering from) tissue and accelerate the progress of applications of biomedical optics. For example, with the help of models, some studies show that for most biological tissues the spectrum of the backscattered light is blueshifted with respect to the spectrum of the incident light, although the overall trend of red spectral shifting is observed for forward scattering. The above studies about scattering from tissue are confined to cases in which the incident field is scalar. Hence, it is not possible to account for changes in those characteristics of the scattered field, which are based on full electromagnetic description of stochastic fields, such as, for instance, the degree of polarization.

Based on the recently built electromagnetic scattering theory, of both deterministic and random nature, and the relationship between the refractive index correlation function and correlation function of the scattering potential, we carry out the analysis in terms of the cross-spectral density matrices of the field scattered from tissue, from which one can determine its spectral density, spectral degree of polarization, and momentum distribution, etc.

8553-58, Session 13

Optical-tracker-based 3D reconstruction for endoscopic environment

Bo Yang, Ya Zhou, Xiaoming Hu, Qiaona Xing, Junqin Lin, Beijing Institute of Technology (China)

Endoscopic surgery is increasing for minimally invasive treatment in recent years. But the conventional two-dimensional endoscope technique cannot provide three-dimensional information for surgeon. Lacking depth and other 3D information often made doctors have to carry out the surgery depending heavily clinical experience. In order to solve the above described issues, a novel method is proposed.

An 1394 camera is used to capture images. The improved SIFT algorithm, which is based on SIFT (Scale-invariant feature transform) and improved according to the characteristics of the endoscopic images, is applied to extract and match feature points from the endoscopic images. The algorithm can effectively solve the problem that few feature points can be get from endoscopic images. After enough feature points are gotten, the depth information of the matching points is calculated with the help of an optical tracking system. The camera is in conjunction with a tracking marker, and the sensor can receive the infrared light reflected by the marker, therefore the position and orientation of the endoscope can be obtained easily. From the above work, a set of point cloud of the structure which needs to be reconstructed is produced. As the discrete 3D points cannot show the real structure in the field of endoscope vision because the shape of the surfaces have been lost. How to establish a visual model from points cloud is also discussed. In this paper, the Delaunay triangulation algorithm is used for surface reconstruction. The proposed approach is

evaluated on sequence digital images gotten from the 1394camera and experimental results show that the approach is effective.

8553-59, Session 13

Quantification of the scattering and absorption coefficients of two-layered tissue models with hyperspectral imaging and Monte Carlo modeling

Kung-Bin Sung, Hsiang-Chen Pi, Hsi-Hsun Chen, Kuang-Wei Shih, Yu-Hui Su, Herbert Hsieh, National Taiwan Univ. (Taiwan)

Diffuse reflectance spectroscopy has been increasingly used to noninvasively quantify optical properties of tissue and has the potential to detect epithelial dysplasia which is a precursor of many cancers. For stratified squamous epithelial tissues, however, dysplasia-associated changes in the epithelium and the underlying stroma may have opposite effects on reflectance and therefore, reduce the contrast between normal and dysplastic tissues. We have developed a movable hyperspectral imaging system with an imaging fiber bundle to measure spatially-resolved reflectance spectra. To improve the sensitivity of measured reflectance to the optical properties of predominately forward-scattering thin epithelium, we propose to use a beveled fiber bundle whose end surface is flush with the tissue surface. Compared to the frequently used probe design in which the source and/or detection fibers are tilted to increase the overlap between illumination and collection cones, our proposed probe geometry facilitates miniaturization of the probe for endoscopic applications. The sensitivity of the proposed probe is analyzed with a scalable Monte Carlo (MC) code that is capable of obtaining a full spectrum in a single MC run. The MC code is also used in an iterative curve fitting algorithm to extract the optical properties of two-layered numerical tissue models and tissue mimicking phantoms. Both the simulations and experiments show increased sensitivity to epithelial scattering coefficient and improved accuracy of quantifying the epithelial optical properties. Quantification of the optical properties of oral mucosa in vivo is demonstrated to prove the feasibility to improve noninvasive detection of dysplasia in stratified squamous epithelium.

8553-128, Session 13

Photoacoustic imaging: a potential new tool for arthritis (Invited Paper)

Xueding Wang, Univ. of Michigan Health System (United States)

The potential application of photoacoustic imaging (PAI) technology to diagnostic imaging and therapeutic monitoring of inflammatory arthritis has been explored. The feasibility of our bench-top joint imaging system in delineating soft articular tissue structures in a noninvasive manner was validated first on rat models and then on human peripheral joints. Based on the study on a commonly used adjuvant induced arthritis rat model, the capability of PAI to differentiate arthritic joints from the normal was also examined. With sufficient imaging depth, PAI can realize tomographic imaging of a human or a small-animal joint as a whole organ noninvasively. By presenting additional optical contrast and tissue functional information such as blood volume and blood oxygen saturation, PAI may provide a unique opportunity to enable early diagnosis of inflammatory joint disorders, e.g. rheumatoid arthritis, and to monitor therapeutic outcomes with improved sensitivity and accuracy.

8553-61, Session 14

Enabling technologies towards noninvasive “optical biopsy” at subcellular and molecular level (Invited Paper)

Xingde Li, Wenxuan Liang, Johns Hopkins Univ. (United States); Meredith Akins, The Univ. of Texas Southwestern Medical Ctr. at Dallas (United States); Jiefeng Xi, Yongping Chen, Qi Mao, Kristine Glunde, Johns Hopkins Univ. (United States); Ming-Jun Li, Corning Incorporated (United States); Katherine Luby-Phelps, Mala Mahendroo, The Univ. of Texas Southwestern Medical Ctr. at Dallas (United States); Zaver Bhujwala, Johns Hopkins Univ. (United States)

This talk will report our recent developments of translational biophotonics imaging technologies towards visualization of tissue histology in situ, in vivo and in real time at subcellular resolution and with molecular specificity. We will first discuss the nonlinear optical endomicroscopy technology which enables “optical biopsy” at true histology resolution. This technology can translate multiphoton microscopy to clinical practice. Secondly we will present a fast-track approach for overcoming one key bottleneck in translating optical molecular imaging to clinical practice by developing near-infrared fluorescent nanocapsules using only FDA approved materials. Representative applications of the reported technologies will be presented.

8553-62, Session 14

Sophisticated model of the human eye for the matching and the analysis of vision power variations between the cataract intraocular lens and corneal after refractive surgery

Chung-Jen Ou, Hsiuping Institute of Technology (Taiwan); Han-Yin Sun, Chung Shan Medical Univ. (Taiwan)

At the present time, the clinical physicians encountered an argument: patient proceed the cornea-reshape surgery like Orthokeratology, with cataract and glaucoma, sometimes do not currently know how to match the artificial lens to achieve optimal vision qualities. In addition, not every hospital or local doctor owns a high wavefront detection system with optical/mechanical simulation experiences that can simultaneously measure wavefront and predict the possible consequences caused by such surgery uncertainty. In this report, we discuss the formulae for the doctor about the matching between the artificial lens surgery with the cataract and glaucoma. Software simulation on the constructed human eye and the wavefront detection is the key to complete this task.

In conclusion, we introduce simple components to correct higher order aberration of the human eye with these deceases and the surgery treatment. Although we realize and expect that these simple components cannot eliminate all the aberration of the patients - however, they can provide necessary information to a portable device and send it back to the simulator to understand the present situation of the patients for the next step diagnosis.

8553-64, Session 14

Investigating the backscattering characteristics of individual normal and cancerous cells based on experimentally determined three-dimensional refractive index distributions

Jing-Wei Su, Wei-Chen Hsu, Chih-Chiang Chang, Kung-Bin Sung, National Taiwan Univ. (Taiwan)

During dysplastic progression of epithelial tissues it is believed that epithelial cells introduce changes of sub-cellular structures which alter the light scattering properties of the cells. In particular, backscattering properties are sensitive to subtle changes in the sub-cellular structures of the cells. The finite-difference time-domain (FDTD) simulation tool can be used to investigate the spectral and angular backscattering characteristics of cells due to structural changes, thereby increasing the understanding of the changes in light scattering properties associated with dysplasia. However, the quantitative investigation of three-dimensional (3D) sub-cellular structures of living cells has been limited by the lack of appropriate microscopy techniques. Recently, we developed digital holographic microtomography (DH μ T) based on arbitrary phase-shifting interferometry in Mach-Zehnder configuration and optical diffraction tomography algorithms to determine the 3D quantitative refractive index (RI) distributions of living cells. In this study, we utilize the DH μ T to quantify the RI distributions of normal and cancerous epithelial cells of skin and oral cavity. We then investigate the spectral and angular backscattering characteristics of the cells using the measured 3D RI distributions in FDTD simulations. The preliminary statistical results show that cancerous cells present higher average values of nuclear and nucleolar RI and a higher standard deviation of cytoplasmic RI than normal cells. The backscattering cross section of the cancerous cells is significantly higher than that of the normal cells, mainly attributed to the higher average RI value and more heterogeneous sub-cellular structures of the cancerous cells.

8553-65, Session 14

Cost-effective approaches for high-resolution bioimaging by time-stretched confocal microscopy at 1 μ m

Terence Wong, Yi Qiu, Andy K. S. Lau, JingJiang Xu, Antony C. S. Chan, Kenneth K. Wong, Kevin K. Tsia, The Univ. of Hong Kong (Hong Kong, China)

Optical imaging based on time-stretched process has recently been proven as a powerful tool for delivering ultra-high frame rate (> 1 MHz) which is not achievable by the conventional image sensors. Together with the capability of optical image amplification for overcoming the trade-off between detection sensitivity and speed, this new imaging modality is particularly valuable in high-throughput biomedical diagnostic practice, e.g. imaging flow cytometry. The ultra-high frame rate in time-stretched imaging is attained by two key enabling elements: dispersive fiber providing the time-stretched process via group-velocity-dispersion (GVD), and electronic digitizer. It is well-known that many biophotonic applications favor the spectral window of ~ 1 μ m. However, reasonably high GVD (> 0.1 ns/nm) in this range can only be achieved by using specialty single-mode fiber (SMF) at 1 μ m. Moreover, the ultrafast detection has to rely on the state-of-the-art digitizer with significantly wide-bandwidth and high sampling rate (e.g. > 10 GHz, 40 GS/s). These stringent requirements imply the prohibitively high-cost of the system and hinder its practical use in biomedical diagnostics. We here demonstrate two cost-effective approaches for realizing time-stretched confocal microscopy at 1 μ m: (i) using the standard telecommunication SMF (e.g. SMF28) to act as a few-mode fiber (FMF) at 1 μ m for the time-stretch process, and (ii) implementing the pixel super-resolution (SR) algorithm to restore the high-resolution image when using a lower bandwidth digitizer. By using a FMF (with a GVD of

> 0.2 ns/nm) and a modified pixel-SR algorithm, we can achieve time-stretched confocal microscopy at 1 μ m with cellular resolution (~ 3 μ m) at a frame rate 1.25 MHz.

8553-66, Session 14

Hilbert transform imaging in phase object detection

Shouyu Wang, Liang Xue, Jiancheng Lai, Yang Song, Zhenhua Li, Nanjing Univ. of Science and Technology (China)

Imaging of phase objects such as biological samples owns great significance in qualitative and quantitative detection. Since many biological cells act as phase objects since they own negligible absorption and scattering effects, traditional bright field and dark field microscopy could not clearly show the characteristics of these samples. Many other methods as phase contrast (PC) and differential interferometric contrast (DIC) are applied to reveal the phase distributions. Here, a new method named as Hilbert Transform Imaging (HTI) is proposed for phase object imaging. Compared to PC and DIC methods, HTI focuses on edge information of the phase object in order to reveal the phase changing of the phase distribution. The enhanced edge in Hilbert Transform Imaging could easily determine the shape of the phase samples. Besides, Hilbert Transform Imaging is easy to realize only with 4f system and waveplates. Combining Hilbert Transform Imaging with microscopy, the edge and shape of the biological samples could be demonstrated. Hilbert Transform Imaging is shown to provide highly efficient in biological samples detection for disease diagnosis in vivo and in vitro.

8553-67, Session 15

Fast reconstruction of Raman spectra from narrow-band measurements based on Wiener estimation

Shuo Chen, Yihong Ong, Quan Liu, Nanyang Technological Univ. (Singapore)

Raman spectroscopy has demonstrated great potential in the study of biological molecules in a variety of biomedical applications. But slow data acquisition due to weak Raman signals from these molecules has prevented its wide use especially in an imaging setup. We propose a novel method to reconstruct the entire Raman spectrum from a few narrow-band measurements based on Wiener estimation. This method consists of a calibration step and a test step. In the calibration step, both the Raman spectra and the narrow-band measurements are acquired from given calibration samples and a Wiener matrix is created out of two sets of data. The Wiener matrix is then used in the test step to reconstruct the Raman spectrum from narrow-band measurements acquired on an unknown sample. This method has been tested on Raman spectra from individual cells. In addition to the fast speed, this method has also shown high accuracy in reconstructed Raman spectra. This method represents a new direction to speed up Raman data acquisition in an imaging setup to investigate fast changing phenomena.

8553-68, Session 15

Evaluation of human dentine demineralization of yellow race by Raman spectra

Zhenlin Zhan, Fujian Normal Univ. (China); Wenqing Guo, Haishan Liu, Xianzeng Zhang, Shusen Xie, Fujian Normal Univ (China)

Dental caries, also known as tooth decay or a cavity, is the most

prevalent chronic disease in dentistry, which is seriously threatening human oral health. Generally, a tooth is in a constant state of back-and-forth demineralization and remineralization between the tooth and surrounding saliva. When demineralization exceeds saliva and other remineralization factors, the mineral content is progressively broken down, producing dental caries. If carious lesions could be detected early enough, intervention methods can be applied to reverse the caries process. In this study, the demineralization status at different acid-etch time is monitoring by Raman spectra. Human molar in vitro of yellow race is used in the study and immersed in 0.3% citric acid to simulate the oral natural demineralization. According to acid-etch time, samples are divided into four group: I:5 min, II:10 min, III:20 min and IV:40 min. The normal untreated specimen is set as control group. Raman spectra before and after treatment are measured and analysed. The result shows that Raman spectroscopy could be efficiently used to monitor the demineralization status of human dentin. There is no new constituent formed after demineralization. The peak intensity of inorganic constituent decreases with the increase of acid-etch time, while the trend of organic constituent is opposite. For 10 min, 40 min and control group, there are statistical difference between any two groups.

8553-69, Session 15

Assessment of skin flap viability using visible diffuse reflectance spectroscopy and autofluorescence spectroscopy

Caigang Zhu, Shuo Chen, Quan Liu, Nanyang Technological Univ. (Singapore)

The accurate assessment of skin flap viability is critical to shortening the period of inconvenient immobilization and saving medical cost without compromising the success rate of flap transfer in plastic surgery. Visible diffuse reflectance and autofluorescence spectroscopy have shown excellent potential for assessing tissue viability separately. However, they have not been used in the characterization of skin flap viability at the same time to our best knowledge. In this study, we performed both diffuse reflectance spectroscopy and autofluorescence spectroscopy on a reversed MacFarlane rat dorsal skin flap model in an attempt to identify the additional value of autofluorescence spectroscopy to the assessment of flap viability. Diffuse reflectance and autofluorescence spectra (excited by 405 nm laser light) were measured every four hours over 72 hours after the creation of dorsal flap. The trend in total hemoglobin concentration and blood oxygenation over time estimated from diffuse reflectance spectra agreed with the published data. The trends in total hemoglobin concentration over time estimated from autofluorescence spectra in both survived and died flaps were consistent with those obtained from diffuse reflectance spectra. The shape of fluorescence spectra from flaps that eventually died changed dramatically in the first a few hours. In particular, the single fluorescence peak at around 500 nm was blue shifted and the width of the peak decreased in died flaps. The analysis of intrinsic fluorescence indicates that these observations could be attributed to the changes in the concentrations of tissue fluorophores. Our result suggests that fluorescence spectroscopy could be a valuable complement to diffuse reflectance spectroscopy for the assessment of flap viability.

8553-70, Session 15

Characterization and differentiation normal and abnormal semen samples using micro-Raman spectroscopy

Zufang Huang, Xiwen Chen, Yongzeng Li, Shangyuan Feng, Rong Chen, Fujian Normal Univ. (China)

Male infertility has become a social and medical problem with rough estimation showing that over 10% of male are diagnosed with infertility.

Drop in semen volume and quality has been confirmed with factors such as radiation, food products and drugs. In clinical, the most commonly used method: computer-assisted semen analysis (CASA) has been considered inaccurate and imprecise. Therefore, development of methods that allow for providing morphological and biochemical information of semen samples from cellular or sub-cellular level without causing potential damage is attractive. In our study, a fast and reliable semen sample preparation method is proposed, and then micro-Raman spectroscopy was employed to characterize and differentiate the normal and abnormal semen samples based on their different biochemical components which reflect in their specific Raman spectra differences. As semen consists of two parts, the cellular and noncellular parts, we focused on using micro-Raman spectroscopy combined with multivariate analytical method (PCA-LDA) to characterize and classify the morphologically normal and abnormal-shaped human sperm cells, meanwhile, seminal plasma which acts as the nutritive and protective medium for sperm cells were separated and tested between normal group and abnormal group. Our preliminary results demonstrate that as a powerful tool, micro-Raman spectroscopy has the potential of being used to characterize and classify semen samples.

8553-71, Session 15

Brain cancer probed by native fluorescence and stokes shift spectroscopy

Yan Zhou M.D., The General Hospital of the Air Force, PLA (China); Cheng-Hui Liu, The City College of New York CUNY (United States); Yong He, Beijing Normal Univ. (China); Yi Sun, The City College of New York (United States); Yang Pu, The City College of New York CUNY (United States); Qingbo Li, Wei Wang, BeiHang Univ. (China); Robert R. Alfano, The City College of New York CUNY (United States)

Optical biopsy spectroscopy has many advantages; it is less invasive, rapid, real time and can be potential used in situ diagnosis. This presentation focuses on the diagnosis of human brain cancer in vitro. The native fluorescence, stokes shift and excitation spectra were measured in malignant, benign, normal meningeal tissues and acoustic neuroma benign tissues within wide wavelengths range. The study was performed using PerkinElmer LS 55 fluorescence Spectrometer. Ninety one spectra of fluorescence and Stokes shift were investigated. The fluorescence spectra of the meningeal brain tissues displayed different chromophoric molecules such as ceroids and lipofuscin lipopigments that were identified under the excitation with UV to visible wavelength range.

The basic biochemical component analysis model (BBCA) and a set of algorithms were used to analyze the spectra. Our preliminary analyses of fluorescence spectra showed, for the first time, the relative content of tryptophan and flavin increased, and those of fat, collagen type I and hemoglobin decreased in cancerous tissue compared to normal brain tissues. The ratios of intensity at peak position in the spectra of both fluorescence and stokes shift were found to be different between cancerous and normal tissues. The criteria for distinguishing brain diseases were established. For the typical fluorescence spectra, ratio of I 340nm over I 440nm is larger than 18.50 in meninges cancer tissues while for the typical stokes shift spectra, the values of ratio of I290nm to I341nm is larger than 8.2 in cancer meninges tissues. The database for clinical diagnosis of brain is extended and will be presented.

8553-72, Session 15

Wide bandwidth absorption/scattering spectroscopy for biomedical and industrial applications

Dmitry Khoptyar, Lund Univ. (Sweden); Otto H. A. Nielsen, Technical Univ. of Denmark (Denmark); Arman Ahamed Subash,

Lund Univ. (Sweden); Muhammad Saleem, National Institute of Lasers and Optronics (Pakistan); Stefan Andersson-Engels, Lund Univ. (Sweden)

Diffuse optical spectroscopy (DOS) is an important component of biophotonics toolbox that readily finds its applications in biomedical optics, optical diagnostics and treatments monitoring. DOS is also highly actual in numerous industrial applications such as new product R&D, fabrication process monitoring and quality control. The further advance in applications urges development of the novel DOS instrumentation capable to deliver highly accurate and exhaustive spectroscopic data at high speeds relevant for such time-critical application as real-time treatment response monitoring or in line process control. Recent progress in source and detector technology enables us to design broadband photon time of flight (PTOF) spectrometer for turbid media that is capable to deliver continuous absorption/scattering spectra over visible and close NIR range. In our contribution we report on further progress of instrument performance. By upgrading the source we have recently further extended the spectral range of our instrument which is now stretches from below 500nm up to 1400nm. This facilitates advance structural sample characterization due to extended scattering data available. Implementation of advanced stabilization techniques enables us to attain superior precision in measurements of absorption and scattering coefficient down to 0.5%. Furthermore recent upgrade enables fully automated spectra acquisition at the speed appropriate for real-time industrial and biomedical applications. We illustrate outstanding performance of our instrument by presenting our new results on highly accurate quantitative analysis of pharmaceutical and for industrial control in dairy fabrication. Moreover we also report on application of the spectrometer to monitoring of cardio-vascular activity in real patients.

8553-74, Session 16

Rabbit electroretinograms evoked by 632.8nm laser flash stimuli

Zai-Fu Yang, Bo-Lin Guan, Jiarui Wang, Beijing Institute of Radiation Medicine (China); Hongxia Chen, Chinese PLA General Hospital (China); Xiaona Zhang, Wen-Yuan Zhang, Jinggeng Yang, Beijing Institute of Radiation Medicine (China)

The flash electroretinography is a standard electrophysiological method and widely employed in basic research and ophthalmology clinics, of which the stimulus is usually white flash from dome stimulator. However, little is known about the electroretinograms (ERGs) evoked by monochromatic laser flash stimuli. The goal of this research effort is to quantify the ERGs of dark-adapted New Zealand rabbits evoked by He-Ne laser flash with wavelength 632.8nm. The flash field was either a Maxwellian viewing disc with angular subtense of 20.2, 13.3, 8.5 degree or a collimated beam with 3mm beam diameter at cornea. The stimulus duration was 22ms, 70ms and 220ms. The energy per laser flash varied from 0.5nJ through 0.5mJ. Under the condition of stimulus duration 20ms and angular subtense 20.2 degree, the ERG of New Zealand rabbit was compared with that of Chinchilla gray rabbit. Results showed that the amplitude of b- and a-wave increased, while the implicit time decreased with the increase of laser energy. The b-wave met a platform when the laser energy was high enough. The comparison of b-wave amplitude between different angular subtenses showed that the ERG is dominated by the retinal total energy but not radiant exposure. The comparison between different stimulus durations showed that the ERG is dominated by the retinal laser power and the b-wave amplitude decreases with the increase of stimulus duration. The comparison between pigmented and non-pigmented rabbits showed that the later is more sensitive and the threshold energy for b-wave excitation is about 10 times lower than the former.

8553-75, Session 16

The threshold of vapor channel formation in water induced by pulsed CO2 laser

Wenqing Guo, Xianzeng Zhang, Zhenlin Zhan, Shusen Xie, Fujian Normal Univ. (China)

Water plays an important role in laser ablation. There are two main explanations of laser-water interaction: hydrokinetic effect and vapor channel. The two explanations are reasonable in some way, but they can't explain the mechanism of laser-water interaction completely. In the study, the dynamic process of vapor channel in static water layer induced by pulsed CO2 laser was monitored by high-speed camera. The wavelength of pulsed CO2 laser (Sharplan 30C) is 10.64μm, power ranges from 1W to 30W and pulse repetition rate is 60Hz. The maximum frame rate of high-speed camera is 150000fps. Based on the processing of the photographs attained by high-speed camera, the threshold of vapor channel formation was determined. The study of the mechanism of laser-water interaction will improve the application of laser in surgery, laser machining and other fields.

8553-76, Session 16

Mechanisms of interaction between very high-frequency photoacoustic waves and the skin

Gonçalo Sá, Carlos Serpa, Luis G. Arnaut, Univ. de Coimbra (Portugal)

The enhancement of transdermal drug delivery with ultrasounds is interpreted on the basis of the following mechanisms: 1) temperature increase caused by heat release, 2) cavitation associated with the creation and collapse of microbubbles, 3) microstreaming defined as circulating fluid flow accelerated by oscillating microbubbles, 4) radiation pressure due to the force exerted by the sound wave.

Ultrasonic waves with the center frequencies employed in sonophoresis and ultrasonography (typically from 0.2 to 20 MHz) interact weakly with tissues. The heat dissipated leads to a temperature increase that is quantified by the thermal index of ultrasound. The onset of cavitation, and hence of microstreaming, is characterized by the mechanical index of ultrasound. The role of temperature, transient cavitation and microstreaming in permeabilizing the skin has been thoroughly discussed in the literature. On the other hand, the radiation pressure mechanism was previously disregarded on the basis of: i) calculations on the forces exerted by pressures of millibar amplitudes, 2) the small pressure gradients generated by ultrasound across the stratum corneum (the typical wavelength of ultrasound at 1 MHz is 150 μm whereas the thickness of the stratum corneum is 15 μm).

In this work we employ photoacoustic waves with 1 MPa amplitude and center frequencies of 100 MHz to transiently perturb the stratum corneum. We show that the dynamic acoustic radiation force mechanism can explain the perturbation induced by the photoacoustic waves. Indeed, 15 bar pressure gradients across 5 corneocytes (approx. 5 μm wide) are expected to perturb their structure.

Conference 8554: Quantum and Nonlinear Optics II

Monday - Wednesday 5 -7 November 2012

Part of Proceedings of SPIE Vol. 8554 Quantum and Nonlinear Optics II

8554-1, Session 1

Scalable quantum information processing with atoms and photons

Jianwei Pan, Univ. of Science and Technology of China (China)

No Abstract Available

8554-2, Session 1

Balanced-heterodyne detection of optical squeezing (*Invited Paper*)

Sheng Feng, Chenggang Shao, Huazhong Univ. of Science and Technology (China)

As part of an effort to make use of optical squeezing for detection of sub-shot-noise optical signals, we study the balanced-heterodyne scheme, for which the corresponding spectral density of the photocurrent fluctuations produced at the output of the photo-detector is calculated as the Fourier transform of their autocorrelation function. We show that, for maximal signal-to-noise ratio enhancement by use of squeezed states of light, an optical signal to be measured in this scheme must be carried in the squeezed quadrature of the carrier field. Most importantly, our analysis reveals that "the additional heterodyne noise" can be eliminated in balanced-heterodyne detection under some experimental conditions and, from this, we discuss how this scheme may be exploited in gravitational-wave searching.

8554-3, Session 1

Quantum election based on distributed scheme

Rui-Rui Zhou, Li Yang, Institute of Information Engineering of Chinese Academy of Sciences (China)

We have presented an unconditionally secure authority-certified quantum election scheme based on anonymous quantum key distribution, the scheme ensures the completeness, soundness, privacy, eligibility, unreusability, fairness and verifiability of a large scale election. The voting administrator and the counter are independent parties and we assume they are semi-honest in the scheme. However, this condition is difficult to achieve in practice, because there is no efficient way to guarantee that the two parties will not cooperate forever, and a malicious voting administrator may impersonate the eligible voter to vote. In view of this, we propose a distributed election scheme, in which the voting administrator is made up by two parties who cannot cooperate up to cheat within a certain period of time, thus it solves the dispute between the voting administrator and the voters. In addition, we use an "identity exchange" scheme to conceal the identity of voters. While the election is completed, nobody except the voter himself can match him with his ballot even if the voting administrator and the counter collaborate up to do so. The scheme can also work well with noisy quantum channels and the only condition is that the entities in the scheme cannot cooperate with a certain period of time, this require is reasonable and not difficult to achieve in practice.

8554-4, Session 1

A quantum enhanced lidar with polarized photons

Xiaofei Wang, Bing Zhu, Univ. of Science and Technology of China (China)

Electromagnetic waves with polarization modulation are widely utilized in Radar and Lidar, and they often depend on classical mechanics and Shannon information theory. As such, quantum effects can't be directly dealt with nor used. Since quantum effects can bring quantum positioning system, interferometric quantum radar, quantum illumination and so on. This paper designs a quantum enhanced lidar which transmits polarized photons, and the processes are calculated by the laws of quantum electrodynamics. The polarized photons process photon-atom scattering on the target's surface, and this theoretically brings new results to the classical system: polarized quantum enhanced lidar can gain more targets' characters. In this paper we report simulations and experimental results. The transmitter combines two sets of orthogonal 653nm linearly polarized beams: 00,900,450 and 1350, then attenuate them to photons. The detecting photons and the targets 30 meters away interact in the free space, and different target's characters feed back by the scattered photons. This paper designs a polarized quantum demodulator which makes up of polarizing beam splitter and photon counters to acquire the above feedback. Transmitter and Receiver synchronize their clocks to suppress the noise by the time filtering. The experiments verify that our regime can apperceive different targets and amends the classical system. As such this polarized quantum enhanced lidar gets the similar transmitter and receiver to the BB84 quantum key distribution system, for some targets, our system can achieve utterly confidential target detection in theory.

8554-5, Session 1

Measurement of transition frequencies and magnetic field amplitudes via beating signals in an asymmetric procedure of light storage and retrieval

Qianqian Bao, Bo Fang, Junyan Gao, Jilin Univ. (China)

Coherent control of light propagation dynamics has been greatly investigated in the past few decades according to its important applications in reversible storage and efficient processing of photonic quantum information. It is interesting to note that beating signals have been observed recently as a manifestation of the preserved phase information during light storage and retrieval. Moreover, such interferometric beating observed in a light storage experiment is essential due to its potential application in the fast quantum-limited measurements of atomic transition frequencies and magnetic-field amplitudes. To this end, we present a novel scheme for the dynamic generation and flexible manipulation of beating signals in a tripod-type atomic sample via an asymmetric light storage and retrieval technique based on electromagnetically induced transparency (EIT). In addition, we have demonstrated by numerical calculations and analyzed the efficient scheme in the polariton picture for the beating signals. Furthermore, we interpret how to infer the frequency difference, the relative phase, and their stabilities from the beating signals imposed on a weak probe field. Particularly, we demonstrate that the amplitude B of a magnetic field can be determined from such interferometric beating signals. We expect that our numerical findings could be explored to devise novel photonic devices for manipulating a quantum light field, even at the single-photon level.

8554-6, Session 2

Confined indirect excitons in one and two dimensional magnetic lattices: Bose-Hubbard model and beyond

Ahmed M. Abdelrahman, Byoung Seung Ham, Inha Univ. (Korea, Republic of)

Confined indirect excitons in one and two-dimensional magnetic lattices are promoted to simulate condensed matter systems. Sufficient evaporative cooling allows the trapped clouds of indirect excitons to experience the Bose-Einstein condensation phase transition and exhibit a long-range spatial coherence which causes an inherited phase-locked across all of the coupled sites (single traps). Using an external magnetic bias field a mutual tunneling can be adiabatically exchanged between sites in which case the underline physics of Bose-Hubbard model can be explored such as Mott-insulator and Josephson Effect.

8554-7, Session 2

Towards coherent manipulation of the ground states of single cesium atom confined in a microscopic far-off-resonance optical dipole trap

Wenting Diao, Jun He, Bei Liu, Tiancai Zhang, Junmin Wang, Shanxi Univ. (China)

Coherent control of ground states of single atoms has attracted much attention as it can be used as single quantum bit (qubit). We have efficiently loaded single cesium (Cs) atoms from a large-magnetic-gradient magneto-optical trap (MOT) into a microscopic far-off-resonance optical dipole trap (FORT) which is formed by a strongly-focused single-frequency 1064nm laser beam with the waist radius of 2.3um. The trapping lifetime of single Cs atoms in the FORT can be extended to ~ 130 s by improving the background pressure and adopting a proper laser cooling phase. The relaxation time of hyperfine ground state of single Cs atoms is measured to be ~ 4.6 s. The qubit can be encoded into the two clock states ($|6S_{1/2} F=4, m_F=0\rangle$ and $|6S_{1/2} F=3, m_F=0\rangle$) of single cesium atom. To realize scalability, we will construct a 2D array of microscopic dipole traps by using of 2D arrays of micro lenses.

In the coherent manipulation process of single atom, two phase-locked laser beams with frequency difference of 9.192GHz (hyperfine splitting in cesium ground state) are used to drive the STIRAP in a Lambda-type three-level system consists of cesium $|6S_{1/2} F=4, m_F=0\rangle$ and $|6S_{1/2} F=3, m_F=0\rangle$ long-lived ground clock states and $6P_{3/2} (F=4)$ excited state with the single photon red detuning of ~ 50GHz. The two laser beams is generated by optical injection of an 852-nm extended-cavity diode laser (master laser) to lock the +1-order sideband of a 9-GHz current-modulated diode laser (slave laser). The relative line-width of two phase-locked laser beams has measured ~ 1 Hz by beat-note experiment, which is limited by the resolution bandwidth (RBW) of the radio-frequency spectrum analyzer.

Our ongoing work is preparing the single atom into an arbitrary coherent superposition states of cesium $|6S_{1/2} F=4, m_F=0\rangle$ and $|6S_{1/2} F=3, m_F=0\rangle$ long-lived ground clock states, measuring the Rabi oscillation of coherent manipulation of single atom, and evaluating de-coherence time of atomic qubit.

8554-8, Session 2

Strong coupling of single cesium atoms with TEM₀₀ and TEM₁₀ modes of a high-finesse optical microcavity and applications

Junmin Wang, Pengfei Zhang, Gang Li, Tiancai Zhang, Shanxi Univ. (China)

In our experiment, strong coupling of single cesium atoms with a high-finesse optical cavity (the finesse is ~ 3.3×10^5 and the cavity length is ~ 86 um) has been realized in both cases of using TEM₀₀ and TEM₁₀ modes. The typical parameters for these two cases are $(g_{00}, k, \gamma) = 2\pi \times (23.9, 2.6, 2.6)$ MHz and $(g_{10}, k, \gamma) = 2\pi \times (20.5, 2.6, 2.6)$ MHz, respectively. Obviously the coupling factors (g_{00} and g_{10}) are almost one-magnitude larger than the cavity field decay rate (k) and the transverse atomic dipole decay rate (γ), therefore our system

reaches exactly the strong coupling regime. It means that even only one atom or one photon entering into or escaping from the cavity will completely modify the state of whole atom-cavity system.

Adopting strong coupling of single atoms with TEM₀₀ cavity mode the effective temperature of laser-cooled atoms, which are prepared in a magneto-optical trap (MOT) located just ~ 5 mm above the micro-cavity, can be determined. The vacuum Rabi splitting is measured when cold atoms freely fall from MOT due to gravity and pass through the micro-cavity. From the probe laser's transmission signals of the atom-cavity system the velocity with which individual atom passed through the cavity is obtained. Then the effective temperature is extracted after averaging many single-atom measurements statistically and fitting experimental data theoretically. Obviously this is an alternative method for measuring the cold atoms' temperature.

Employing strong coupling of single atoms with the tilted TEM₁₀ cavity mode the trajectories of individual atoms, which freely fall and vertically pass through the anti-node plane of the cavity, can be precisely tracked. Thanks to the tilted TEM₁₀ mode, instead of TEM₀₀ mode, the degeneracy of symmetric trajectories is eliminated completely. Under the low-field approximation the trajectories of individual atoms passing through the cavity are almost straight lines along vertical direction. This allows us to more precisely determine individual atom's trajectory along the off-axis horizontal direction. Typical spatial resolution of 100 nm is obtained in a measurement time of 10 us, and it is much better than previous measurements.

8554-9, Session 3

Einstein-Podolsky-Rosen entanglement and steering in two-well BEC ground states (Invited Paper)

Qiongyi He, Peking Univ. (China) and Swinburne Univ. of Technology (Australia); Peter D. Drummond, Swinburne Univ. of Technology (Australia); Murray Olsen, The Univ. of Queensland (Australia); Margaret Reid, Swinburne Univ. of Technology (Australia)

We consider how to generate and detect Einstein-Podolsky-Rosen (EPR) entanglement and the steering paradox between groups of atoms in two separated potential wells in a Bose-Einstein condensate (BEC). We present experimental criteria for this form of entanglement, and propose experimental strategies for detecting entanglement using two or four-mode ground states. These approaches use spatial and/or internal modes. We also present higher order criteria that act as signatures to detect the multiparticle entanglement present in this system. We point out the difference between spatial entanglement using separated detectors, and other types of entanglement that do not require spatial separation. The four-mode approach with two spatial and two internal modes results in an entanglement signature with spatially separated detectors, conceptually similar to the original EPR paradox.

In addition, we also develop the concept of genuine N-partite Einstein-Podolsky-Rosen (EPR) steering. This nonlocality is realized as a multiparty EPR paradox, and is the key ingredient for quantum secret sharing. Useful properties emerge that are not guaranteed for genuine multipartite entangled states. We derive criteria to demonstrate multipartite EPR steering for GHZ, W and Gaussian continuous variable (CV) states in experiments.

8554-10, Session 3

Theory of quantum entanglement based on surface phonon polaritons in condensed matter systems

Yang Ming, Zijian Wu, Xikui Hu, Fei Xu, Yanqing Lu, Nanjing Univ. (China)

Condensed matter systems are potential candidates to realize the integration of quantum information circuits. Surface phonon polariton (SPhP) is a special propagation mode in condensed matter systems. In this work, we present a theoretical study of quantum entanglement in condensed matter systems. Firstly, to describe the quantum characters and relative evolution processes of LRSPhP, a canonical quantization procedure is taken. Based on the quantization formulation of the LRSPhP mode, we could obtain the effective interaction Hamiltonian of the coupling process between entangled photons and entangled LRSPhPs. Utilizing the interaction Hamiltonian and the perturbation approximation of the evolution equation, we obtain the state vector of the entangled LRSPhP modes. The entanglement performance of the system is discussed. To a further investigation of our system, the coupling process of entangled photons and entangled LRSPhP is described through the mechanics approach. Finally, the correlation of our system is examined. We aim to providing a whole set of theories to describe entanglement of surface phonon polariton, which may possess huge potential for realizing integrated quantum circuits in condensed matter systems.

8554-11, Session 3

Generation of frequency de-correlated photon pairs by using photonic crystal fiber

Liang Cui, Ningbo Zhao, Kang Gao, Xiaoying Li, Tianjin Univ. (China)

For quantum information processing and quantum state characterization involving quantum interference among multiple sources, frequency de-correlated photon pairs, which can be employed to realize heralded single photon in pure state, are highly desirable. Recently, there are growing interests in generating frequency de-correlated photon pairs via pulse pumped spontaneous four wave mixing in photonic crystal fibers (PCF).

In this paper, after illustrating why the measurable quantity--intensity correlation function $g^{(2)}$ of individual signal (idler) photons can be used to characterize the frequency correlation of photon pairs, we first numerically investigate the dependence of $g^{(2)}$ upon the higher order dispersion of PCF, the intrinsic sinc oscillation of the phase matching function and the chirp of pump pulse. We then accordingly optimize the experimental parameters and experimentally generate photon pairs with minimized frequency correlation. For filter free case, the maximum $g^{(2)}$ of the individual signal photons we obtained is 1.78 ± 0.02 , showing the photon pairs are approximately frequency de-correlated. Moreover, based on the photon pairs, we also demonstrate a heralded single photon source with low noise and approximate single-mode characteristic, whose the heralding efficiency is about 86%, and the intensity correlation of the heralded (signal) photons is suppressed by a factor of more than 80 relative to the classical Poissonian light limit. Although the experimentally measured $g^{(2)}$ is less than the calculated result due to the inhomogeneity of the PCF, the experimental results qualitatively agree with numerical simulations.

8554-12, Session 3

Entanglement storage with self-assembled quantum dot devices

Qin Wang, Nanjing Univ. of Posts and Telecommunications (China); Yongsheng Zhang, Univ. of Science and Technology of China (China)

We give a proposal on using self-assembled single-quantum-dot devices to store entangled photon pairs and retrieve them on demand. We also analyze the possibility of realizing it with current technology. In this scheme, the quantum information can be stored by exciting a coherent superposition of exciton states corresponding to the two polarizations and then mapping the electronic part of that state to the nuclear ensemble, so as to realize a quantum storage in nuclear

ensembles. Finally, the quantum information can be retrieved on demand with the reversed process. We also evaluate the storage fidelity with imperfect experimental conditions and demonstrate that a quite high storage fidelity can still be obtained. Therefore, the proposal may be a feasible avenue in processing entanglement storage in the near future. The scheme is an alternative to the research on utilizing atomic ensembles to realize quantum repeater which is highly desired in quantum communication. Besides, because of the good scalability in self-assembled quantum dot devices, it also has a promising implementation in the field of quantum computing.

8554-13, Session 4

Quantum light sources based on third-order nonlinear waveguides (Invited Paper)

Wei Zhang, Qiang Zhou, Yidong Huang, Jiande Peng, Tsinghua Univ. (China)

Recently, the concept of quantum engineering was proposed and accepted by the academia, driving by the efforts to develop quantum information applications for real use. Many mature technologies traditionally used in laboratories are difficult to meet the requirements of engineering. Hence, new realization schemes of quantum information functions compatible with today's engineering technologies attract much attention. The researches of practical quantum light sources are representative in this direction.

Traditionally, correlated/entangled photon pairs are generated by spontaneous parametric down-conversion (SPDC) in crystals with second-order nonlinearities, which have been widely used in various quantum optics experiments. However, its experimental setup is based on free space optics, which has several drawbacks from the view of engineering, including its high requirement on fine optical alignment and stability of experimental condition, large capacity and unwieldiness, and limited photon collection efficiency in long distance transmission. Spontaneous four-wave mixing (SFWM) in third-order nonlinear medium provides another way to generate correlated/entangled photon pairs, which can be realized in waveguides widely used in optoelectronics and optical communication, showing great potentials in developing practical quantum light source devices.

In this talk, we will introduce our recent works on correlated / entangled photon pair sources and heralded single photon sources based on optical fibers and silicon wire waveguides.

8554-14, Session 4

Hong-Ou-Mandel interference experiment of two independent heralded single photon sources in an optical fiber with birefringence

Tianyi Ma, Qiang Zhou, Wei Zhang, Yidong Huang, Mingquan Lu, Zhenming Feng, Tsinghua Univ. (China)

Single photon sources (SPSs) play important roles in quantum communication and quantum information processing. Spontaneous four wave mixing (SFWM) in optical fibers provides a promising way to realize practical heralded single photon sources (HSPSs), since it is compatible with current techniques of optical communications.

In this paper, two independent HSPSs at 1.5 μm band are realized in one polarization maintaining dispersion shifted fiber (PM-DSF) utilizing its large birefringence. When pulsed pump light passes through an optical fiber, two kinds of SFWM will take place simultaneously. One is scalar processes, in which two annihilated pump photons and generated photon pair are all polarized along the same fiber polarization axis. The other is vector processes, in which two annihilated pump photons are polarized along different fiber polarization axes, either to the two photons of the generated pair. In the PM-DSF, the large birefringence generates obvious walk-off effect on the two pump polarization components, which leads to an effective suppression of

the vector processes. Hence, by proper pump polarization, correlated photon pairs (CPPs) with different polarization directions can be generated independently by the two scalar processes, which can be used to realize two independent HSPSs.

The indistinguishability of the heralded photons generated by the two independent sources is demonstrated by an experiment of Hong-Ou-Mandel (HOM) interference. Using a fiber coupler as the beam splitter, a visibility of HOM dip of 76% is achieved with subtracting the contribution of accidental coincidence counts, showing their potential on quantum information.

8554-15, Session 4

Indistinguishability and semantic security for quantum encryption scheme

Xiang Chong, Li Yang, Institute of Information Engineering of Chinese Academy of Sciences (China)

The definition of security for encryption scheme is an important area of cryptography. In this paper we investigate the indistinguishability and semantic security into quantum context.

In our previous work, we have already defined the indistinguishability for quantum public-key encryption scheme, and have given a necessary and sufficient condition leads to this security. Here we will systematically define the indistinguishability and semantic security for quantum public-key and private-key encryption schemes, and for computational security, physical security and information-theoretic security.

The quantum parameters are continuous variable. In order to give the definition of indistinguishability for quantum encryption scheme, we first give a definition of indistinguishability for encryption scheme with continuous variable based on probability density function, and a definition of indistinguishability based on multi-outputs-circuit. We show that these definitions are equivalent. Then we prove that the indistinguishability based on multi-outputs-circuit is equivalent to ordinary indistinguishability with single-bit-output-circuit. Then we get the definition of indistinguishability for quantum encryption scheme. Similarly we define the semantic security.

The equivalence between computational indistinguishability and semantic security for classical encryption scheme is already proved, but the equivalence for information-theoretic ones is still an open problem. For public-key encryption scheme, there is no information-theoretically secure classical public-key encryption scheme, so we discuss the equivalence between computational indistinguishability and semantic security for quantum encryption scheme and between information-theoretic ones. About private-key encryption scheme, the equivalence between computational indistinguishability and semantic security for quantum encryption scheme and between information-theoretic ones for classical and quantum encryption schemes all are discussed.

8554-16, Session 4

Properties of high quality heralded single photon source based on fibers at 1.5 μm

Qiang Zhou, Wei Zhang, Yidong Huang, Jiangde Peng, Tsinghua Univ. (China)

Single photons are essential resource for quantum communication and quantum information processing, which can carry quantum information to distant locations. A promising scheme for single photon generation is the heralded single photon source (HSPS), which is based on the generation of correlated photon pairs (CPPs). Utilizing the quantum correlation property of the CPPs, one photon of the CPP is detected providing an electrical signal to herald the other photon as a single photon output. Recently, 1.5 μm CPP generation through spontaneously four wave-mixing (SFWM) in fiber has focused much attention, which provides a practical way to realize 1.5 μm fiber-

based HSPS. The quality of a HSPS is described by the preparation efficiency and $g(2)(0)$. In the fiber-based HSPS, the preparation efficiency is determined by the loss of the filtering and splitting system and the noise photons generated by spontaneously Raman scattering (SpRS). Considering the impact of the SpRS can be reduced by cooling the fiber and optimizing the frequency detuning of filtering and splitting system, the loss of the filtering and splitting system may decide a theoretical up-limit of the preparation efficiency.

In this paper, making use of commercial dense wavelength-division multiplexing components, we optimize the frequency detuning and the loss of filtering and splitting system, improving the theoretical up-limit of the preparation efficiency. As a result, a high quality HSPS based on cooled fibers is realized with a preparation efficiency of 80%, while $g(2)(0)$ is 0.06, showing its great potential in the application of quantum information technology.

8554-17, Session 5

Feedforward control of high-power optical frequency comb (*Invited Paper*)

Heping Zeng, Ming Yan, Wenxue Li, East China Normal Univ. (China)

Fiber-based optical frequency comb has become an attractive near-infrared light source for precision spectroscopy, coherent laser ranging and optical frequency metrology due to its compactness, high precision in time and frequency domains and long-term stability. Usually, in order to precisely control the carrier-envelope phase or offset frequency of high-power lasers, either a phase servo loop or a difference-frequency-generation scheme has been employed. However, the two approaches inevitably suffered from the limited feedback bandwidth and the $1/f$ noise, respectively. Recently, a self-referenced feed-forward scheme by using an acousto-optic frequency shifter (AOFS) has been reported to be an effective way of reducing phase noise of a Ti:Sapphire laser to shot-noise-limited level. And we successfully employed the similar scheme stabilizing the CE phase of an ytterbium-doped fiber laser mode-locked by nonlinear-polarization rotation effect.

In this paper, we demonstrate a high-power ytterbium-doped fiber frequency comb centered at 1030 nm by using the self-referenced feed-forward scheme. As a result, the carrier-envelope phase frequency was locked on the laser repetition rate with a relative linewidth of ~ 1.4 mHz. The phase noise and timing jitter (integrated from 4 mHz to 100 kHz) were calculated to be 370 mrad and 120 as, respectively. Meanwhile, by using a large-mode-area (LMA) ytterbium-doped double-clad photonic-crystal fiber amplifier, the laser pulses were amplified up to 7 W with recompressed pulse width of ~ 130 fs.

8554-18, Session 5

Propagation-induced transition from slow to fast light based on coherent population oscillation in a cascaded Erbium-doped fiber structure

Weikun Yu, Shuguang Lu, Lingling Gu, Jin Zhou, Ming Feng, Yigang Li, Nankai Univ. (China)

Controlling the group velocity of light based on coherent population oscillation in optical fibers has become a popular research topic for its many advantages and its potential applications. A change from slow to fast propagation upon increasing the modulation frequency can be realized in a single fiber structure, however, only with narrow bandwidth and small difference between the maximum fractional advancement and the maximum fractional delay.

In this work, we analyze the slow and fast light propagation induced by the coherent population oscillation in a Cascaded Structure. In the first part, we use an erbium-doped fiber pumped at 980nm. Then we use a wavelength division multiplexing to take out the pump beam at

the output of this first fiber and sent the signal to the second part. The power of the signal is controlled by an attenuator. In the second part, we use an erbium-doped fiber without the pump beam. A change from slow to fast propagation at the output of the second fiber can be achieved. We also study the propagation of light in a single fiber structure in the same conditions.

Through compared with the single fiber structure, we found that the change from slow to fast light is more obvious in the Cascaded Structure. The value of delay or advancement is found to depend significantly on the ion density and pump power in the cascaded structure. The bandwidth is larger and the difference is bigger than that in a single fiber.

8554-19, Session 5

Transverse localization of light in weakly modulated photonic lattices based on two-photon photorefractive effect

Zhengguo Xiao, Xiudong Sun, Chunfeng Hou, Harbin Institute of Technology (China)

The discrete diffraction of the incident beam propagates in the weakly modulated photonic lattices formed in two-photon photorefractive materials is investigated. The discrete diffraction patterns in square and hexagonal backbone structure are simulated by beam propagation method(BPM). The effects of the external applied bias field, excitation mode, and intensity of the probe beam on the discrete diffraction patterns are discussed in detail. It is shown, when the refractive index modulation depth of the photonic lattices is high enough the probe beam propagating in the photonic lattices will be localized in transverse dimension for both on-site and off-site excitation, and the probe beam can evolve into discrete spatial soliton under appropriate conditions.

8554-20, Session 5

Double-probe phase grating

ZhiHong Xiao, Suzhou Institute of Nano-Tech and Nano-Bionics (China)

We study atomic phase grating in a four-level system driven by a degenerate probe field and a standing wave field. The simulation results show that the diffraction efficiency of phase grating is greatly improved due to the application of a degenerated probe beam; the first-order diffraction efficiency can reach up to 35%, and the high-order diffraction efficiency of approximate 20% is achieved.

8554-21, Session 5

Two photon absorption related femtosecond filament in methanol solution of Tb (III) complex

MingYuan Xie, YiMin Zhu, YangYi Yang, Fuli Zhao, Sun Yat-Sen Univ. (China); Zhizhan Xu, Shanghai Institute of Optics and Fine Mechanics (China)

Filamentation and supercontinuum generated in the methanol solution of a Tb(III) complex by femtosecond laser pulse from Ti: sapphire system has been investigated for the first time. The dynamics of the filament formation and transmission in solution are also be discussed quantitatively. Such an investigation of the femtosecond filament dynamics is a good complementarity for the propagation of ultrashort laser pulse in complex liquid media. In summary, two spectacular nonlinear phenomena: filamentation and supercontinuum were observed in our study of the methanol solution of a Tb(III) complex by using 800nm 125-fs Ti: sapphire laser pulse with input power ranging

from 3mW to 53mW. The lifetime of the solution is about 20ps. The side emission light of different positions on the filament were measured and the evolution of filament with respect to the input power was analyzed. The dynamic balance between the positive factor of self-focusing and the negative factors including group velocity dispersion, plasma defocusing and two-photon absorption plays an important role in keeping the filament in a long distance, following with a transfer-enhanced process between the bubbles. This investigation of the femtosecond filament dynamics in the methanol solution of a Tb(III) complex is a good complementarity to study the propagation of ultrashort laser pulse in liquid media.

8554-28, Poster Session

The new scheme to generate Airy-Bessel wave packets

Zhijun Ren, Zhejiang Normal Univ. (China)

Counteracting the diffraction and dispersion of wave packets in space and time domain by making use of nonlinear effects of some media, three-dimensional spatiotemporal inspreading soliton waves are generated in nonlinear media. However, the application scopes of three-dimensional solitons is limited because the generation of solitons requires ultrahigh peak powers, which is devastating in some possible applications such as being used to probe biological tissue, etc. In addition, nonlinear solitary waves do not exist in free space. In practical science researches such as imaging in media, microcosm exploration and researching its ultrafast process, it is urgently need a kind of stable linear wave packet without spatiotemporal spread during propagation in free space.

Since Bessel and Airy function is an invariant propagation mode in free space, they can be potentially used not only in spatial but also in temporal domains. As a result, an important scientific innovation is that Airy-Bessel configuration wave packets with particle-like nature, which combine spatial Bessel beams with temporal Airy pulses is first introduced in Nat. Photonics, 4, 103 (2010). Different from nonlinear solitary wave, Airy-Bessel configuration wave packets a kind of stable linear wave packet without spatiotemporal spread during propagation in free space.

In the papers, by studying spatially induced group velocity dispersion (SIGVD) effect during propagation of ultrashort pulsed Bessel beams, we find that Gaussian-Bessel wave packets can evolve as Airy-Bessel in given propagation conditions. The research results are expected to open up one new channel to generate stable linear localized wave packets.

8554-42, Poster Session

Photo-ionization probability of 3+1 resonance enhanced multi-photon process

Guiyin Zhang, North China Electric Power Univ. (China); Mengjun Li, Yidong Jin, North China Electric Power Univ. (United States)

The technique of resonance enhanced multi-photon ionization (REMPI) spectroscopy is one of the important methods for studying the dynamics of photo-ionization. This method depends on the detection of the ions produced in the ionization process. Thus improving the photo-ionization probability is a crucial factor in the practical use of this technique.

In this work, the analytic expression of the ionization probability about 3+1 REMPI process is deduced with the theory of rate equation. The influence of laser intensity, laser pulse duration and collision relaxation rate on the ionization probability is analyzed theoretically. It is found that the ionization probability increases with laser intensity and laser pulse duration until gets to saturation. After that, the ionization probability will oscillate around the saturation value if laser intensity increases further. The amplitude of oscillation increases with laser intensity at first, and

then it will decrease even get to zero after a maximum peak comes out. We attribute the appearance of the oscillation to the phenomena of quantum coherence caused by the energy level splitting in strong laser field. As to the fact that the ionization probability becomes to zero with the increase of laser intensity, it indicates that laser intensity is strong enough so as to make the neutral particles getting to the region of ionization suppression. It is also found that ionization probability decreases near linearly with the increase of collision relaxation rate. But the variation is very little due to the collision relaxation rate is far smaller than the ionization one. So the influence of the collision relaxation rate on ionization probability could be ignored.

8554-43, Poster Session

Conversion efficiency analysis of second harmonic generation of the novel nonlinear crystal RbBe₂BO₃F₂

Rui Sun, Li Wang, Chuanchen Bao, Beijing Univ. of Technology (China)

For the first time, the theoretical conversion efficiency versus the crystal lengths and polarization ratio of second harmonic generation of RbBe₂BO₃F₂ (RBBF) crystal in type I and type II phase matching has been simulated by using the three wave coupled equations and energy conservation law. RBBF crystal is pumped by the fundamental radiation of a Q-switched Nd:YAG laser with the wavelength of 1064nm and the shape of plane wave or Gaussian beam. RBBF is a novel ultraviolet (UV) crystal, which is a member of KBe₂BO₃F₂ (KBBF) family, which has been widely used to produce harmonic generation below 200 nm by its unique features. Compared with KBBF, RBBF crystal has a wide crystalline phase under the existing growth system, and in the ab direction is very easy to grow a large single crystal with transparent area. When the pumped radiation is of plane wave, the conversion efficiency of RBBF crystal in the type I phase matching shows a monotonically increasing trend, and eventually tends to 100%, while the conversion efficiency of RBBF crystal in the type II phase matching varies periodically which could be as high as 78% in the type II phase matching. When the pumped radiation is of Gaussian beam, the conversion efficiency shows a monotonically increasing trend which could be as high as 67% in the type I phase matching, and in the type II phase matching the conversion efficiency varies periodically.

8554-44, Poster Session

Properties analysis of novel nonlinear crystal: CsBe₂BO₃F₂ by frequency doubling

Chuanchen Bao, Li Wang, Rui Sun, Beijing Univ. of Technology (China)

Base on three wave coupled equations and energy conservation law, the frequency doubling properties of CsBe₂BO₃F₂ (CBBF) are analyzed theoretically for the first time. The phase matching angle, effective nonlinear coefficient, walk-off angle and conversion efficiency are simulated in type I and type II phase matching. The difference of the CBBF optical properties between type-I and type-II are elucidated. A wider frequency doubling wavelength range in type-I were obtained, the lowest wavelength limit of CBBF is 201.8 nm in type-I and 268.7 nm in type-II; the effective NLO coefficient in type-I are larger; and the walk-off angle in range of 693.9~2730 nm fundamental wavelength in type-I are smaller. Conversion efficiency at wavelength of 1030 nm was calculated with shape of plane wave or Gaussian wave. The conversion efficiency in type-I increases monotonously with crystal length increasing, while the conversion efficiency in type-II varies periodically with plane wave and fluctuates with Gaussian wave. Meanwhile, the characteristics of the frequency doubling process of CBBF has been compared with KBe₂BO₃F₂ (KBBF) crystal. The lowest wavelength limit of CBBF are larger than KBBF; the effective nonlinear coefficient of CBBF are smaller than KBBF except in the range of 772.3~2500

nm fundamental wavelength in type I, this leads to a lower conversion efficiency; nevertheless, walk-off angles of CBBF are smaller so that it can make up for the disadvantage of effective nonlinear coefficient at some degree. Both shape of conversion efficiencies of CBBF are little lower than KBBF in type-I and type-II.

8554-45, Poster Session

Controlling spatiotemporal chaos of photorefractive ring oscillator with constant bias

XiaoXiao Chen, XiuQin Feng, ZhiHai Yao, Changchun Univ. of Science and Technology (China)

A photorefractive crystal, which is pumped by an external laser beam, is inserted into optical ring cavity, the crystal and the ring cavity together consisting of the photorefractive ring oscillator. photorefractive ring oscillator is a typical nonlinear optical system. With the increasing cavity detuning and absorption loss, bifurcation and chaos phenomena appear gradually. We study the evolutions of spatiotemporal chaos for the system in the one- dimensional and two-dimensional map lattices. As the system parameters are changed, we obtain different patterns such as the frozen random state, the pattern selection state, the defect chaotic diffusion state and fully developed turbulence state in the one- dimensional map lattice system. We can observe symmetry breaking from four corners and the boundaries and finally lead to spatiotemporal chaos in the two-dimensional map lattices system. Then we demonstrate that the global and local constant bias can suppress spatiotemporal chaos in photorefractive ring oscillator by varying the bias strength. The results of numerical simulations present that the constant bias are suitable for not only the photorefractive ring oscillator but also the coupled photorefractive map lattice system. When constant bias is 0.045, the system is suppressed to stable periodic orbits 5, constant bias is increased to 0.05, the system is controlled into stable periodic orbits 3, if constant bias is greater than 0.1, the system is converted into stable periodic orbits 1. Local constant bias can suppress spatiotemporal chaos in spatially localized regions, the rest of the localized regions continue to spatiotemporal chaos.

8554-47, Poster Session

Chaotic characteristic in the BEC system of a 1-D tilted optical superlattice potential with attractive interaction

Zhiying Zhang, Xiuqin Feng, Zhihai Yao, Zuolin Tian, Changchun Univ. of Science and Technology (China)

The dynamics equation of the Bose-Einstein condensation system can be expressed by the nonlinear Schrodinger equation (Gross-Pitaevskii(G-P) equation). The nonlinearity makes it possible to introduce chaos into a quantum system. Chaos plays a role in the regularity of the system and causes instability of the condensate wave function. In this paper, the spatiotemporal evolutions of chaos for the system in BEC trapped a 1-D tilted optical superlattice potential with attractive interaction is researched. The spatial evolution of chaos is shown numerically by resolving G-P equation for the system with the fourth Runge-Kutta(RK) algorithm. The chaotic characteristics in the BEC system are well demonstrated with Lyapunov exponent, chaotic attractor, time series and power spectrum. The results of numerical simulations reveal that as the tilt or the amplitude of the optical superlattice potential of the BEC system is increased, the chaos in the BEC system increases. These elements make the chaotic system more unstable and the phase-space orbit becomes more complex. A method for controlling chaos based on parameter modulating is proposed. Chaotic behaviors can be controlled into periodic behaviors by parameter modulating. The results of numerical simulation show that the BEC system can be converted into different periodic states if we change the modulating frequency and modulating strength. Parameter

region that can be used for controlling chaos is fixed by calculating the Lyapunov exponent. The stability of periodic orbits in the modulated BEC system is illustrated by the results of numerical calculations and phase space outline.

8554-48, Poster Session

Chaos synchronization and communication in unidirectionally-coupled VCSELs with fiber channel

Linfu Li, Guizhou Minzu Univ. (China); Jianjun Chen, Xinjiang Medical Univ. (China)

As one of the microchip lasers, vertical-cavity surface-emitting lasers (VCSELs) exhibit many advantages, such as single longitudinal-mode operation, low threshold current, circular output beam with narrow divergence, low cost and etc. Chaos secure communication has attracted significant attention and got an extensive application in recent years, for its complicated nonlinear dynamics and high sensitivity to the parameters of system. In order to realize the long-distance privacy communications, it also raised the optical chaos communications based on fiber. The influences of the chromatic dispersion and nonlinearity in fiber on the chaotic synchronization have been investigated.

A novel chaotic synchronization configuration is proposed. This system is constructed on the basis of unidirectionally coupled VCSELs and signal transmission in fiber. The transmitter VCSEL is subject to an isotropic optical feedback, the receiver VCSEL is subject to an orthogonal optical injection from the transmitter VCSEL, the chaotic signal transmission in fiber channel is adopted, also message encoding and decoding of the chaotic system have been investigated. The results show that, during to the fiber nonlinear and chromatic dispersion, the amplitude characteristics of chaotic signal are distorted partially and the system synchronization quality will be impaired, but message can be hidden efficiently in the chaotic signal during the fiber transmission with additive chaos modulation (ACM). Better decoding performance is achieved by choosing appropriate matched parameters.

8554-49, Poster Session

Spatial soliton tunneling in longitudinally modulated optical lattices

Qingnan Chen, Yali Qin, Hongliang Ren, Jia Li, Zhejiang Univ. of Technology (China)

Nowadays, theoretical and experimental studies of solitons in optical lattice with nonlinearity have attracted a great deal of attention due to their novel physics and potential applications in diverse branches of science. Wealthy properties of solitons that cannot be observed in homogeneous nonlinear media are discovered in lattice modulated media. Variation of the lattice shape in the longitudinal direction offers a wealth of opportunities to control the evolution of light. Due to transformation in lattice configuration along the longitudinal, a series of novel dynamical regimes including binary switching, soliton tunneling, and tunneling inhibition were discussed. More recently, the tunneling effect of self-similar optical waves has been investigated extensively.

In this paper, we study numerically the dynamics of a beam in a focusing photorefractive nonlinear optical lattice with a longitudinal potential barrier. Such kind of lattice with the refractive index modulation in both transverse and longitudinal directions can be realized by induced optically in photorefractive crystals. Different soliton states are found with different position of the input pulse, which exhibits compression or splitting during transmission. The results also indicate that the intensity of a beam and the transverse modulation frequency of lattice can affect apparently the ability of tunneling. For the same lattice depth, the smaller the transverse frequency of the lattice is and the higher peak intensity the soliton possesses, the easier the soliton tunnels through. However, when we increase the frequency of optical

lattice, the optical beam can successfully pass through the barrier for the relatively small value of lattice depth as well. Otherwise, the beam splits into some filaments when the lattice depth is large enough. In addition, we find that beam can exhibit the behavior of oscillation during transmission and the oscillation frequency of spatial soliton is influenced by the biased field.

8554-50, Poster Session

Ghost interference with pseudo-thermal light

Yin P. Yao, Ren Gang Wan, Shi Wei Zhang, Tong-Yi Zhang, Xi'an Institute of Optics and Precision Mechanics (China)

Ghost imaging (correlated imaging) has been extensively investigated in recent years, both theoretically and experimentally. Meanwhile, ghost interference and diffraction were also studied. By using the second-order or high-order coherence properties of light field and the correlation measurement, ghost imaging was realized with quantum entangled light, pseudo-thermal light and even true thermal light. As a kind of nonlocal imaging system, the seminal light beam is split into two separate optical paths that are spatially correlated. One beam (usually called the test path) is sent to an unknown object and then detected by a bucket detector without any spatial resolution. However, the image of the object can be retrieved when the bucket detector signal is correlated with the signal of a spatial resolving detector in the other optical path (usually called the reference path). In this paper, we firstly prepare the pseudo-thermal source using a laser beam that passes through a rotating ground glass plate, and obtain the parameters about the pseudo-thermal source via Hanbury-Brown-Twiss (HBT) experiment. Then, we perform ghost interference with the pseudo-thermal light. The experimental results show that the quality of ghost interference is influenced by the rotating velocity of the ground glass plate and the light field propagation distance. Furthermore, the distance between the source and the object has effect on the ghost interference when keeping the length of the test path as constant.

8554-52, Poster Session

The effect of pump focusing on the performance of ghost imaging with entangled resource

Ming-Yang Zheng, Lian Chen, Xin-Dong Cai, Feng Li, Ge Jin, Univ. of Science and Technology of China (China)

Ghost imaging, a novel imaging method, has been extensively concerned around the physics community owing to its non-locality. The image of an object can be achieved by coincidence measurement between the bucket detection over the signal path (with object) and the transverse scanning over the idler path (without object). In this paper, the effect of pump focusing on the performance of ghost imaging is studied theoretically and experimentally. As we have known, an idealized plane-wave pump would lead to perfect transverse momentum conservation for a perfect phase-matched crystal. Theoretical results show that the correlation properties of the entangled photon source are destroyed when the conversion crystal is pumped by a focused laser beam.

In our experiment, a 405 nm semiconductor cw laser is used to pump a BBO (beta-barium-borate) crystal cut for type-II non-collinear degenerate SPDC. The two rings of signal and idler light at the degenerate wavelength 810 nm, perpendicular to the pump beam, propagate freely with the intersection in an external angle of 3° with respect to the pump direction. Generally, the fluorescence light in each path need to pass a half-wave plate and an additional BBO crystal to compensate the transverse and longitudinal walk-off introduced by the birefringence of the conversion crystal. However, our experimental results indicate that the "walk off" effects almost have no effect on ghost image. When the pump beam is focused by a lens, the visibility of the image is greatly degraded. But a sharp image could be reproduced

in the configuration first proposed by T. B. Pittman et al. for the case with pump focusing.

8554-53, Poster Session

Two kinds of high-contrast optical filters for the detection of Stokes and anti-Stokes photons from cesium ensemble

Tingting Liu, Qiangbing Liang, Jun He, Tiancai Zhang, Junmin Wang, Shanxi Univ. (China)

Laser-pumped atomic vapor cell and a properly-designed Fabry-Perot etalon can be used as high-contrast optical filters. Especially in the case of generation of quantum correlated Stokes and anti-Stokes photon pairs in a Lambda-type three-level atomic ensemble with Raman excitation, high-contrast optical filters are very important components to pick up single-photon-level optical pulses from strong excitation laser beams. In our experiments, we designed and characterized two kinds of high-contrast optical filters for the detection of Stokes and anti-Stokes photons from cesium ensemble: the laser-pumped cesium atomic vapor cell and the temperature-stabilized coated bulk etalon. Typical peak signal transmission of $\sim 75\%$ and distinction ratio between excitation channel and 9.19GHz-frequency-detuned signal channel of ~ 25 dB are measured for the laser-pumped cesium atomic filter. Typical peak signal transmission of $\sim 84\%$ and distinction ratio between pump and signal channels of ~ 20 dB are measured for the temperature-stabilized bulk etalon filter. To improve the distinction ratio, normally the mixture combination of the laser-pumped cesium atomic filter and the temperature-stabilized bulk etalon filter will be a good choice.

8554-54, Poster Session

Optimization of the experimental parameters of cesium CPT system

Zhi Liu, Jieying Wang, Wenting Diao, Jun He, Tiancai Zhang, Junmin Wang, Shanxi Univ. (China)

Coherent population trapping (CPT) is a quantum interference phenomenon between atoms and coherent light field. The interference process leads the atoms to be driven in a coherent superposition dark state of the two ground states where photons are not absorbed anymore. Based on the Lambda-type three-level atomic system consists of cesium $6S_{1/2}$ ($F_g=3$) and $6S_{1/2}$ ($F_g=4$) long-lived ground states and $6P_{3/2}$ ($F_e=4$) excited state, we have experimentally measured and theoretically analyzed the passive coherent population trapping (CPT) resonances in cesium vapor cells with and without Ne as buffer gas. The impact on the CPT resonance of some experimental parameters, such as laser intensity, relative intensity ratio and longitudinal magnetic field, is investigated. Under the optimized condition, the CPT resonance with full width at half maximum (FWHM) linewidth as narrow as ~ 340 Hz is realized. The FWHM linewidth of CPT signal linearly increases with laser intensity. By measuring this dependence we can extrapolate the coherence relaxation time of the two hyperfine ground states of cesium atoms (the lifetime of the coherent superposition dark state) at zero laser intensity. For the case of cesium cell filled 2 Torr Ne as buffer gas, the coherence relaxation time is ~ 1.06 ms. For the case of pure cesium cell without buffer gas, it is $\sim 17\mu$ s. When increasing the longitudinal magnetic field, CPT resonances are split into 7 resolved components in the $\sigma^+_{\sigma^+}$ (or $\sigma^-_{\sigma^-}$) laser polarization configuration.

These results, as well as those relevant published works, will provide more references for development of high-performance CPT atomic clocks as well as high-sensitive CPT atomic magnetometer. In the next step, we will further reduce the relative phase noise of phase-locked dichromatic lasers and optimize the pressure ratio of Ne buffer gas in the cesium cell and temperature of cesium cells. Expect to get narrower CPT linewidth and better signal-to-noise ratio.

8554-55, Poster Session

Study of the threshold coupling strength for mutually pumped phase conjugator

Lin Ma, Jiang Zhi Guo, Liu Ji Fang, Xidian Univ. (China)

Mutually pumped phase conjugation has many attractive features such as exchanging time-domain information, reflecting spatial information and making incoherent-to-coherent conversion. The action mechanism of a variety of mutually pumped phase conjugator (MPPC) is almost the same. Depending on the number of the grating (or active area) within the crystal can be MPPC is divided into two categories: one interaction region four-wave mixing self-oscillation mechanism and two interactive regions four-wave mixing mechanism. The mechanism is one, two or more four-wave mixing function area to solve difficult theory, make the research of the law of the threshold coupling strength for is not full, and this problem is the key that MPPC can work normally. Its research, that is of theoretical significance but also practical significance.

In the paper, based on the four-wave mixing mechanism and fanning effect, the threshold coupling strength for one interaction region and two interactive regions MPPC is researched in theory. The relation of the the threshold coupling strength for MPPC and the fanning intensity is studied. In the biggest fanning scattered light intensity direction the formation of MPPC requires threshold coupling strength minimum. Due to the more efficient fanning, preset grating in MPPC has the ability to reduce the threshold coupling strength and improve output efficiency. These characteristics predicted by theory have been used to explain the previous experiment phenomenon. MPPC is most likely produced when the two incident beams is consistent. Furthermore, the threshold coupling strength is much lower for one-interaction-region MPPC than two-interaction-regions MPPC. These results have importance for applications and experimental realization of MPPC.

8554-56, Poster Session

Multistability of nanomechanical mirror in atom-assisted optomechanical cavity

Changbao Fu, Jilin Univ. (China)

We study the multistability of nanomechanical mirror by theoretical calculations and numerical simulations in atom-assisted optomechanical cavity. We obtain that the multistability of nanomechanical mirror changes along with original detuning between the transition frequency of atom and the frequency of cavity field for several elastic coefficients of spring. In addition, we find that the multistability of nanomechanical mirror will be increased by two when the level of atom is increased by one.

8554-57, Poster Session

All-optical switching characteristics analysis in an optimized nonlinear Bragg grating with a $[\pi]$ phase shift

Jianjun Chen, Xinjiang Medical Univ. (China); Linfu Li, Guizhou Univ. (China); Murat Hamit, Yanting Hu, Xinjiang Medical Univ. (China); Xiaoxi Fan, Abuduaini Kuduluke, College of Medical Engineer Technology of Xinjiang Medical University (China)

We numerically study the nonlinear switching characteristics of optical pulses transmitted through optimized fiber Bragg grating with a phase shift. The nonlinear coupled-mode equations were solved numerically based on the time-dependent transfer-matrix method. We show that the phase shift grating is superior to the uniform grating in the enhancement. The nonlinear Bragg grating is 3mm long and has a strength of γ , corresponding to the enhancement to be a factor of 15. It shows that the use of phase shift gratings reduces effectively

the switching threshold, but the on-off contrast is generally declined which can be generally improved through the introduction of tapered parameters. In addition, the narrowed transmitted pulse for positive-tapered nonlinear Bragg grating is a Bragg soliton owing to the balance of anomalous group velocity dispersion and self-phase modulation (SPM). From the comparison of the introduction of tapered and chirp parameters, it can be found that the tapered nonlinear Bragg grating with a phase shift is more preferable for achieving the larger on-off contrast.

8554-58, Poster Session

High repetition rate tunable mid-infrared optical parametric oscillator based on MgO:PPLN

Yongji Yu, Xinyu Chen, Chao Wang, Chunting Wu, Guangyong Jin, Changchun Univ. of Science and Technology (China)

High repetition rate nanosecond mid-infrared (3~5 μm) lasers have attracted the interest of scientists in many applications such as military countermeasures, remote monitoring of the special environment, and so on. Quasi-phase matched optical parametric oscillator (OPO) based on periodically-poled crystal can offer a high conversion efficiency and wide wavelength tunability, especially periodically-poled MgO doped lithium niobate (MgO:PPLN) which has a low coercive field and big effective nonlinear coefficient. However, the damage threshold of MgO:PPLN is as low as 10 J/cm² (1064 nm, 10 ns pulse), so raising the repetition rate of the pulse is an effective way to improve the power of the lights generated by OPO. In this paper, we present a mid-infrared OPO with the idler wavelength of 3.86 μm at the repetition rate of 200 kHz, and a high repetition rate electro-optic (EO) Q-switched Nd:GdVO₄ laser with a double-crystal RbTiOPO₄ (RTP) EO modulator is used as the pump source. The OPO is designed as an extra-cavity singly resonant optical parametric oscillator. The threshold value of the OPO system is only 1.3 W at 1.06 μm . When the MgO:PPLN crystal is operated at 90 °C and the pump power is 10.5 W with a repetition of 200 kHz, the maximum average output power of 1.82 W at idler wavelength 3.85 μm and pulse width of 14.3 ns are obtained. The slope efficiency of the 3.85 μm laser with respect to the pump laser is 21.3%. The M² factors of the 3.85 μm laser are 1.84 and 1.76 in the parallel and perpendicular directions, respectively. The mid-infrared tunability of 3.7~3.9 μm can be achieved by adjusting the temperature of MgO:PPLN crystal from 210 °C to 35 °C.

8554-59, Poster Session

Electromagnetically induced absorption in lambda-type three-level system driven by bichromatic coupling field

Zhanfei Yan, Lijun Yang, Lijin Ma, Xiaomin Feng, Shuqing Guo, Hebei Univ. (China)

The probe absorption speciality of the λ -type three-level system driven by bichromatic coupling field and weak probe field is investigated. We obtain the probe absorption spectrum for different frequencies of coupling field by solving the density matrix equation and numerical analysis. For same intensity but different frequency detuning of the coupling field, three electromagnetically induced absorption (EIA) in the absorption profile of probe field are simultaneously observed. We report the dependence of EIA on the frequency of the bichromatic coupling fields. The results show that central EIA always appears at the resonant frequency of probe field, with the constant intensity. The location of the secondary EIA vary with the frequency detuning of coupled field, and the intensity of the absorption peaks decrease with the increasing detuning. Finally, we present an analysis based on dressed states to explain our numerical results.

8554-60, Poster Session

Cerenkov radiations in nonlinear photonic crystal and waveguide

Changdong Chen, Xiaopeng Hu, Jiong Zhou, Nanjing Univ. (China)

By analogy with the Cerenkov radiation from particles, nonlinear Cerenkov radiation (NCR) results from nonlinear polarization driven by light field. The generation as well as modulation of NCR has drawn increasing research interests in recent years. Our research works mainly focus on the experimental realizations of NCR in nonlinear photonic crystals, including frequency up-conversions and down-conversions. The phase velocity of the nonlinear polarization waves can be accelerated with a backward reciprocal vector while decreased with a forward one provided by the structure, thus the characteristics of NCR were modulated. By this means, cascaded Cerenkov third harmonic generation and Cerenkov difference frequency generation were realized. In addition, some novel phenomena, such as mode-coupling Cerenkov sum frequency generation and elastic scattering were observed.

8554-61, Poster Session

The three-photon resonant nondegenerate six-wave mixing via quantum interference

Juan Sun, Jiang Sun, Ying Wang, Hongxin Su, Jinfeng Cao, Hebei Univ. (China)

We study the quantum interference in three-photon resonant nondegenerate six-wave mixing (NSWM) in a five-level system in which the middle level of six-wave mixing and other level are coupled by a strong laser field. The coupling field-dependence of the NSWM signal intensity, and the spectrum of the NSWM with a coupling field, are discussed. We find that in the presence of a strong coupling field, the three-photon resonant NSWM spectrum exhibits Autler-Townes splitting, which reflects the levels of the dressed states. It also leads to either suppression or enhancement of the NSWM signal. Thanks to the enhancement of NSWM signal caused by quantum interference, the dressed state, created by a coupling field, can replace the atom intrinsic level and serve as the middle level of three-photon resonance. Thus the middle level of three-photon resonance can be controlled by a coupling field.

8554-62, Poster Session

Probe correlation and energy gap of Bloch bands in one dimensional optical lattice by matter wave amplification

Xuguang Yue, Xiaoji Zhou, Xuzong Chen, Peking Univ. (China)

Using resonant Superradiant Rayleigh Scattering (SRS), correlations of a Bose gas released from an optical lattice are measured. Conditions are chosen so that, after initial incident light pumping at the Bragg angle for diffraction, superradiant scattering into the Bragg diffracted mode is preponderant due to matter-wave amplification and mode competition. A temporal analysis of the superradiant scattering gain reveals periodical oscillations and damping due to the initial lack of coherence between lattice sites. Such damping is used for characterizing first-order spatial correlations with a precision of one lattice period. Furthermore, We use a coherent Bragg diffraction method to impart an external momentum to ultracold bosonic atoms trapped in a one-dimensional optical lattice. This method is based on the application of a single light pulse, with conditions where scattering of photons can be resonantly amplified by atomic density grating. An oscillatory behavior of the momentum distribution resulting from the time evolution in the lattice potential is then observed. By measuring the oscillating frequencies, we extract multiband energy structures of single-particle

excitations with zero pseudomomentum transfer for a wide range of lattice depths. The excitation energy structures reveal the interaction effect through the whole range of lattice depths

8554-63, Poster Session

Manipulating the momentum state of Bose-Einstein condensate by standing wave pulses

Yueyang Zhai, Xiaoji Zhou, Xuzong Chen, Peking Univ. (China)

We analyze the effects of sequences of standing-wave pulses on a Bose-Einstein condensate. We present a scheme for nonadiabatically loading a Bose-Einstein condensate into the ground state of a one-dimensional optical lattice within a few tens of microseconds, i.e., typically in less than half the Talbot period. We apply a method for flexible manipulation of the atomic momentum states where the standing-wave pulses are less limited in pulse intensities and durations. The experimental observations are in good agreement with a numerical simulation based on band structure theory in an optical lattice.

8554-64, Poster Session

Transient behaviour of EIT and EIA in an optical-radio two-photon coupling configuration

Xiaoli Li, Zicai Yang, Hebei Univ. (China)

Electromagnetically induced absorption (EIA) and transparency (EIT) are quantum interference phenomena due to the interaction of coherent electromagnetic fields and multiple level atom system. They have received sufficient attention for their potential applications in quantum communication storage and quantum calculation. In this paper, a four-level optical-radio two-photon coupling system is firstly established, and a set of density matrix equation of motion is derived using the rotating wave approximation method. Both EIA and EIT can be obtained in this four-level system consisting of an optical-radio two-photon coupling field and a probing field. The formation of EIA and EIT can be showed in terms of a transient state picture in this paper. It can be seen that the optical coupling field in this system has a crucial effect on the forming of EIA and EIT. An EIA is observed under a resonant optical coupling and it evolves into an EIT when there is a detuning. In this paper, the formation of EIA and EIT are studied separately. When both optical coupling field and radio coupling field are resonant, the formation of EIA can be shown from absorption minimum to absorption maximum as time increases. On the other hand, when optical coupling field is off-resonant and radio coupling field is resonant, the formation of EIT can be shown from absorption maximum to absorption minimum as time increases. At the same time, the dependence of the frequency position of EIA and EIT on Rabi frequencies and frequency detunings of two coupling fields is investigated.

8554-65, Poster Session

Resonant optical nonlinearity of Nb-doped silica fiber measured with LPFG interferometer

Litao Wang, Shanghai Univ. (China); Na Chen, Zhenyi Chen, Tingyun Wang, Shanghai Univ. (China)

Recently, specialty fibers with various functional material doping have attracted significant attention due to their unique performance. Nonlinear optical properties, both the resonant nonlinearity and the Raman spectra of specialty fibers have been studied for a number of compositions. In this paper a new kind of Nb-doped silica fiber

is fabricated combining MCVD and atomic layer deposition (ALD) technologies. We measured its optical absorption spectra in the range from 400 nm to 1650 nm with the cut-back method. The Nb-doped fiber shows broadband absorption in the vicinity of 900nm. Then, we measured the Raman spectra of Nb-doped silica fiber under the excitation of 785nm laser. The Raman scattering intensity is enhanced compared with the conventional single-mode fiber. Then, we used Mach-Zehnder Interferometer (MZI) formed by two long-period fiber gratings (LPFG) to measure the resonant nonlinear refractive index of the specialty fibers. Two LPFGs were fabricated by the method of CO₂ laser pulse writing technology. Then, a section of 15cm-length Nb-doped silica fiber was inserted between the LPFG pairs. The fringe visibility of formed MZI reached 9dB. The interference fringe shifts when we launched the 532nm pumping laser into the interferometer. As the launched pumping power increased, the interference fringes shifted toward the longer wavelength. The total fringe shift of the Nb-doped fiber was 0.1 nm with the 532 nm laser at the launched power of 25mW. The resonant nonlinear refractive index of the Nb-doped fiber is estimated to $8.12 \times 10^{-16} \text{m}^2/\text{W}$ around 1537nm.

8554-22, Session 6

Relative delay enhancement of light pulse propagating in nonlinear medium via cavity resonance effect (Invited Paper)

Fang Bo, Jie Wang, Guoquan Zhang, Jingjun Xu, Nankai Univ. (China)

Based on the transverse-phase modulation effect, the analytical expression of the relative delay of a sinusoidally modulated fundamental-mode Gaussian beam passed through a nonlinear medium filled in a thin resonant Fabry-Perot cavity were derived. As examples, the dependences of the relative delay of the signal pulse transmitted from ruby, alexandrite and GbAlO₃ crystals on the experimental parameters were discussed. The results showed that the relative delay of the signal pulses can be significantly improved by several orders of magnitude through the introduction of a resonant Fabry-Perot cavity in the case of weak absorption of nonlinear media. The same maximum relative delay was achieved in the same nonlinear medium for different lengths in the case of impedance matching, which means that micro-cavities made by nonlinear medium have the ability to produce the same amount of relative delay as their macro- counterparts.

8554-23, Session 6

Optical frequency comb generation through quasi-phase matched quadratic frequency conversion in a micro-ring resonator

Zijian Wu, Nanjing Univ. (China); Yang Ming, Nanjing University (China) and Nanjing Univ. (China); Fei Xu, Yan-qing Lu, Nanjing Univ. (China) and Nanjing University (China)

We propose optical frequency comb generation in a monolithic micro-ring resonator. Being different from the previously reported nonlinear optical frequency combs, our scheme is based on more efficient quadratic frequency conversion rather than the third-order nonlinearity. To overcome the phase mismatch, a partly poled nonlinear ring is employed. Cascading second harmonic generation and parametric down conversion processes thus are realized through quasi-phase matching (QPM). In our theoretic model, a half poled Lithium Niobate 'add-drop' ring system is considered. Based on coupling equations, the second-harmonic generation efficiencies are calculated. And two influencing factor, pump power and coupling coefficient between waveguide and ring, are analyzed. Through these analyses, proper coefficients are chosen and the optical frequency comb generation efficiency are calculated. The interactions among 22 different whispering-gallery modes are included. A 56% internal generation efficiency is got from these calculations.

8554-24, Session 6

Soliton spectral tunneling effect in multi-cladding single mode fibers with three zero-dispersion wavelengths

Jungao Hu, Xianglong Zeng, Shaofei Wang, Qianwu Zhang, Tingyun Wang, Shanghai Univ. (China)

When the waveguide dispersion is engineered to make a normal group velocity dispersion (GVD) region located between the two anomalous GVD regions, a sharp switching of the soliton self-frequency shift due to phase-matched dispersion wave occurs from one anomalous GVD region to another, known as soliton spectral tunneling (SST) effect. SST effect is a promising approach to achieve nonlinear wavelength conversion and octave-spanning supercontinuum.

In this paper, we investigate the generation of SST effect in multi-cladding single mode fibers. We design the multi-cladding fibers that can exhibit three zero-dispersion wavelengths. Phase matching between soliton and dispersive waves can be satisfied by engineering the waveguide dispersion curve. Fiber geometries with appropriate refractive index difference and fiber radius are selected to generate this unique dispersion property and the mechanism of multi-cladding fiber exhibiting multi zero-dispersion wavelengths is discussed. The standard split-step Fourier method is implemented to solve the GNLS numerically.

Simulation results show that the SST effect is clearly observed, while the resonant frequency falls in the anomalous GVD region. The center frequency of output pulse in SST effect is investigated numerically and analytically. The detail studies present the phase-matching condition with the dispersive pulses in different engineered dispersion curves of multi-cladding fibers. The simulation results reveal the relationship between the carrier frequency of input pulse and center frequency of the dispersion waves. The predicted results by phase-matching condition are in agreement with extensive numerical simulations. The soliton number N is significant to SST effect, which has a great on the variation of the threshold length.

8554-25, Session 6

The chaotic dynamics of ultra-long erbium-doped fiber ring laser

Juan Zhang, Lingzhen Yang, Naijun Xu, Xiangyuan Zhang, Taiyuan Univ. of Technology (China)

We report an experimental study of chaotic generation in an ultra-long erbium-doped fiber ring laser (ULEDFRL). The 980 nm semiconductor laser (LD) is used to pump an erbium doped fiber (EDF) with 8m long by a 980/1550 nm wavelength division multiplexed coupler (WDM). The polarization isolator (ISO) forces the light to operate in unidirectional. The polarization controller (PC) is used to adjust the polarization state of the light. The total cavity is 752 m. The output coupler with a ratio of 90:10 has 10% of the lasing light for output detection. During the experiment, we adjust the PC under a fixed pump power to make the output power at the maximum value. When the drive current is adjusted from 180 mA to 413 mA, The ULEDFRL shows chaotic oscillation. The experimental results reveal the chaotic laser of the ULEDFRL shows narrow width in the autocorrelation curve, and the full width at half maximum (FWHM) of the autocorrelation curve is 0.125ns. The chaotic laser can be used in the range finder with centimeter-range resolution.

8554-26, Session 7

Study on parametric amplification effect in fiber

Xiuping Sun, Changchun Univ. of Science and Technology (China)

The basic principle of Analysis parametric amplification in fiber was discussed in the paper, as well as basic factors of influence to parametric amplification. Taking the fiber as the carrier and the gain medium, we respectively selected wavelength of 1445nm; 1455nm; 1535nm, as the pumping light, the amplification of 1555nm signal light can be accomplished. Experimental results show that, at a certain wavelength range, fiber optical amplification can be achieved through parametric process.

8554-27, Session 7

SPM and XPM effects on properties of chaos optical fiber fence system based on semiconductor fiber ring laser

Chen Liu, Nian Fang, Lutang Wang, Zhaoming Huang, Shanghai Univ. (China)

The dependence on the initial conditions is one of the key characteristics of chaotic systems. Base on this, a chaos optical fiber fence system has been put forward by employing a semiconductor fiber ring laser (SFRL) as the sensing medium. The output waveform of the SFRL has a framing structure. The traveling time of light in the ring over one cycle is a ring period or a frame. The adjacent-frame waveforms are similar. However the similarity is declined when an external disturbance acts on the sensing fiber. Furthermore the declined degrees are proportional to the locations where disturbances happened in the fiber ring. Therefore the disturbance can be detected and located by the change in the adjacent-frame similarity. This paper presents an improved dynamic model of the chaos optical fiber fence system firstly involved in the SPM and XPM effects of the fiber. A matrix related to the fiber polarization states is introduced to the sensor model that is made up of nonlinear phase shifts of two orthogonal polarization components of the electrical fields of the light in the ring induced by the SPM and XPM effects. We investigate numerically the influence of the nonlinear effects on the sensing properties of the long-range fence system especially in the adjacent-frame similarity. We calculate self-correlation of chaos waveforms to get normalized self-correlation coefficients for judging the change of the adjacent-frame similarity. The simulation results are compared with the ones based on the original model in different ring lengths, which reveals the relation of the adjacent-frame similarity and the SPM/XPM effects.

8554-29, Session 7

The self-bending and interactions of (1+1) dimension spatial solitons in photorefractive crystal

Yali Qin, Jia Li, Hongliang Ren, Hao Wen, Zhejiang Univ. of Technology (China)

Spatial solitons, beams that do not spread owing to diffraction when they propagate, have been demonstrated to exist by virtue of a variety of nonlinear self-trapping mechanisms. Photorefractive spatial solitons can be formed when the diffraction of the beam is exactly balanced by self-focusing due to the photorefractive material nonlinearity at mW power levels. There will be the potential application in all optical communications.

By considering the diffusion effect, we investigate the features of the self-deflection of the screening-photorefractive spatial soliton and the influence of first-order and higher-order space charge field on the propagation characteristics both on the theory and numerical simulation aspects. The results show that the center of the optical beam moves on a parabolic trajectory; As to the higher-order space charge field, the self-bending process is further enhanced by a factor that varies cubically with the applied field. The numerical study shows that the bending distance of the soliton beam center increase, reaching its maximum value at the characteristic temperature by taking into account

the temperature dependence of the diffusion effect and the dark irradiance. Numerical investigations of the screening-photorefractive spatial solitons interaction. The influences of initial phase difference, the intensity and peak separation on the interactions between screening bright solitons are investigated, the results show that the in-phase interaction will result in the separation of two solitons from each other; As for the anti-phase interaction side, two solitons separated each other and deflect simultaneously to the same side. Finally, interactions among multiple solitons are also investigated.

8554-30, Session 8

Ultrafast molecular symmetry breaking dynamics probed by coherent two-dimensional infrared spectroscopy (*Invited Paper*)

Jianping Wang, Institute of Chemistry (China)

Ultrafast two-dimensional infrared (2D IR) spectroscopy can probe fast structural dynamics of molecules in condensed phases under thermal equilibrium conditions. In these systems, a solute molecule constantly changes its shape and symmetry as a result of solvent-solute interactions. Such a dynamical process cannot be easily probed by conventional spectroscopic method. In this work, using a highly symmetric anion, hexacyanocobaltate (Co(CN)₆³⁻), we examined the dynamical symmetry breaking and regaining processes using the 2D IR method. Using the CN stretching mode as the intrinsic structural probe, the symmetry breaking and regaining processes of Co(CN)₆³⁻ were found to closely associated with the localization and delocalization of the vibrational excitations of the CN stretches. In water, glycol and glycerol, such events occurred on the time scales of a few to tens of picoseconds.

8554-31, Session 8

Linear and nonlinear optical properties of liquid solutions of Rhodamine B dye and Au nanoparticles

Fereshteh Hajjesmaeilbaigi, Yasaman Golian, Asma Motamedi, Univ. of Tehran (Iran, Islamic Republic of); Eftekhari Bostandoust Nik, Sharif Univ. of Technology (Iran, Islamic Republic of)

There is considerable interest in understanding optical nonlinearities of dyes for widespread application. The fluorescent yield and lasing efficiency of these organic dyes have been studied extensively. Metallic nanoparticles can strongly influence the optical response of organic and inorganic materials. It has been demonstrated that metals affect the shapes of absorption and emission spectra as well as the kinetics of luminescence decay. Metallic nanoparticles also strongly affect nonlinear response of optical materials. If a mixture of dye solution and metallic nanoparticles is used as a laser medium, the SP-induced enhancement of absorption and emission of dye can significantly improve the laser performance. In this study Au nanocolloid is performed by laser ablation method. Absorption and emission studies were carried out for the laser dye Rhodamine B dissolved in doubled distilled and DI water with and without the presence of gold nanoparticles. Results show the red shift of the fluorescence emission in the case of dye with the presence of gold nanoparticles. Here we report our results on the measurement of nonlinear absorption in Au, Au/Rhodamine B and Rhodamine B using the standard Z-scan technique. The excitation source was 150 mW CW laser at 532 nm. The input beam was focused with 19.5 cm lens and the sample was scanned across the focus using a micrometer translation stage. The beam waist at focus was estimated to be 48 μm and the corresponding peak intensity was estimated to be 3.98×10³ W/cm². We observed the reversed saturable absorption behavior for this peak intensity.

8554-32, Session 8

A nearly-zero ultra-flattened dispersion polarization-maintaining photonic crystal fiber for nonlinear applications

Yani Zhang, Univ. of Glamorgan (United Kingdom); Dun Qiao, Northwest Univ. (China)

The dispersion management and tailoring in highly nonlinear PCFs can be achieved by utilizing the design flexibility in the fiber geometry including the core region and the microstructured cladding, fiber compound material, etc. Specifically, GVD with reduced wavelength dependence, i.e. a flattened dispersion profile is suitable for SC generation in telecommunication window. The preserved polarization state along the fiber is a desired feature for SC generation, as less power is required due to enhanced nonlinear interaction. The polarization maintainability is also important for stable SC generation therefore a fiber design with good polarization-maintaining (PM) characteristics is desired. Specifically, pumping the PM nonlinear fiber with the pumper laser polarization aligned to one of the principle axis, could achieve better power compared to non-PM nonlinear fiber. Moreover, the output is also kept polarized in the PM fiber leading to increased usability of the generated light. To achieve the near-zero ultra-flattened chromatic dispersion in PCFs, several designs have been proposed but lack of the stable polarization-maintaining properties, or involving many design parameters such as different air hole size in the cladding structure, and/or modifications in the core region. The fabrication for low dispersion fibers requires precise control of the geometrical parameters such as air hole shape, core diameter, lattice pitch, etc. For this reason, the research for novel and relatively simple designs of HNL-PCF with polarization-maintaining properties for stable nonlinear applications is necessary. In this work, we employ the index-guiding PCF structure with uniform air-silica lattice, and the defected-core to achieve flattened dispersion profile. Based on the relatively simple structure, we optimize the design parameters to achieve other desirable properties including high nonlinearity and high birefringence. The optimized structure is numerically analyzed by using the full-vector finite difference method (FDM). The boundary conditions are treated with anisotropic perfectly matched layer (APML) to minimize the reflections at the boundary and thus simulate an unbounded region.

8554-33, Session 8

Efficient generation of mid-infrared photons at 3.16 μm by coherent frequency downconversion

E. Wu, Kun Huang, Qian Zhou, Xiaorong Gu, Haifeng Pan, Heping Zeng, East China Normal Univ. (China)

We demonstrated an efficient way for generating a mid-infrared source at 3.16 μm by coherent coincidence downconversion. The signal light at 1.04 μm was frequency downconverted by the synchronized pump pulses at 1.55 μm with a conversion efficiency of 65%.

The experimental scheme mainly consisted of three parts: laser synchronization, frequency downconversion and photon detection. The pump and signal sources were taken from two fiber lasers arranged in the master-slave cavity configuration. In order to emulate the quantum light source, the signal source was attenuated to the single-photon level. The synchronized signal photons and pump pulses of the same polarization were combined and sent into an 50-mm-long MgO:PPLN crystal to facilitate the type I quasi-phase matching. The temperature of the crystal was optimized at 23.5 °C for the grating period of 30.49 μm. The peak conversion efficiency of 65% was achieved at 80 mW. The downconverted mid-infrared light was directed into a monochromator for spectrum measurement. The spectrum was centered at 3.16 μm with a bandwidth of 3.7 nm. Without the incident signal at 1.04 μm, the noise spectrum showed no observable peaks around the target wavelength of the DFG photons.

The mid-infrared source could be applied to sensitive high-resolution spectroscopy of the fundamental absorption band of methane. Moreover, the output mid-infrared light could be spectrally and temporally controlled by engineering the pulse property. Thanks to the preservation of the quantum feature in the coherent frequency downconversion, if nonclassical signal source was implemented, nonclassical mid-infrared light could be generated.

8554-34, Session 8

Large nonlinearity enhancement of Ag/MEH-PPV nanocomposite by surface plasmon resonance at 1550 nm

Cuicui Lu, Xiaoyong Hu, Qihuang Gong, Peking Univ. (China)

Recently, the construction of photonic materials having large nonlinear susceptibility and ultrafast response at 1,550 nm has attracted much attention because of their important applications in the fields of optical computing, optical signal processing, optical interconnection systems, and integrated photonic devices. The third-order nonlinear susceptibilities of traditional semiconductor materials such as Si and GaAs are relatively small. Various approaches, including synthesizing materials with inherently large nonlinear responses at the optical communication range, constructing composite materials based on local-field-enhanced nonlinearity, and forming photonic micro-resonators to enhance the interactions of light and matter, have been proposed for developing such materials. However, the chemical syntheses are very complicated, and it is also very difficult to fabricate high-Q photonic micro-resonators. An alternative method is to construct nanocomposite materials consisting of noble metal nano-particles dispersed in a dielectric matrix. Noble metal nanoparticles possess excellent optical nonlinearity because of their strong quantum size effect. An ultra fast response time can be achieved using fast relaxation of nonequilibrium electrons. We experimentally demonstrate a large third-order nonlinear susceptibility for a nanocomposite made of poly[2-methoxy-5-(2-ethylhexyloxy)-1,4-phenylenevinylene] doped with silver nanoprisms at 1,550 nm, achieved based on nonlinearity enhancement associated with strong surface plasmon resonance. The nonlinear refractive index reaches $-1.37 \times 10^{-12} \text{ m}^2/\text{W}$, which is three orders of magnitude larger than that of pure poly[2-methoxy-5-(2-ethylhexyloxy)-1,4-phenylenevinylene]. An ultrafast response time of 18.7 ps is reached using fast energy transfer from excited states of organic molecules to silver nanoprisms. A low-power and ultrafast nanocomposite photonic crystal all-optical switching is also realized.

8554-35, Session 9

Control of electron localization in the dissociation of H_2^+ using orthogonally polarized two-color sequential laser pulses (Invited Paper)

Feng He, Shanghai Jiao Tong Univ. (China)

Orthogonally polarized two-color sequential laser pulses are used to control the electron localization in the dissociation of H_2^+ . The first single attosecond pulse, whose polarization axis is perpendicular to the molecular axis, excites H_2^+ from $1s\sigma_g$ to $2p\pi_u$, and the time-delayed infrared pulse, whose polarization axis is parallel to the molecular axis, steers the electron between two nuclei. The simulation of the time-dependent Schrödinger equation predicts the control degree of the electron localization can be up to 90% with the current laser technology. To the best of our knowledge, we first reveal that the new mechanism for the asymmetric localization is the mixture of $2p\pi_g$ and $2p\pi_u$ orbitals.

8554-36, Session 9

Linear and nonlinear localized modes in the width-disordered one-dimensional waveguide arrays

Lei Xu, Yi Yin, Fang Bo, Jingjun Xu, Guoquan Zhang, Nankai Univ. (China)

Transverse localization of light in one-dimensional waveguide arrays with width disorder has been studied in both linear and nonlinear regimes. In the linear regime, with the increase in the width disorder level, more and more eigen modes become localized near the band edges. The corresponding eigenvalues penetrate into the semi-infinite bandgap and the first bandgap of the uniform periodical waveguide array, which makes the bands extend and the bandgaps narrow with increasing width disorder level. When one introduces a refractive index defect, i.e., the refractive index of a specific waveguide is higher or less than the surrounding ones, into the disordered waveguide array, localized defect modes will be generated in the semi-infinite bandgap or in the first band gap. These defect modes will be delocalized with the increase of the width disorder due to the interaction with the nearby eigen modes.

In the nonlinear regime, a self-focusing nonlinearity tends to enhance the transverse localization of the nonlinear disordered modes originating from Anderson modes near the edge of the semi-infinite bandgap. While the inverse participation ratio first increases to a maximum in the first bandgap and then decreases and enters the second band for the nonlinear disordered modes originating from Anderson modes near the edge of the first bandgap with increasing self-defocusing nonlinearity. This intriguing light localization behavior may be attributed to the interplay between the nonlinear disordered modes and the eigen modes of the width-disordered waveguide array.

8554-37, Session 9

Evanescence coupling assisted four-wave mixing in a silicon-on-insulator directional coupler

Wei Ding, Institute of Physics (China); Owain Staines, Gareth Hobbs, Andrey Gorbach, Charles de Nobriga, William J. Wadsworth, Jonathan C. Knight, Dmitry V. Skryabin, Univ. of Bath (United Kingdom); Michael J. Strain, Marc Sorel, Richard M. De La Rue, Univ. of Glasgow (United Kingdom)

Four-wave mixing (FWM) has been extensively explored in optical fibers and more recently in on-chip silicon-on-insulator (SOI) waveguides. A phase-matched FWM with a pair of degenerate pump photons generating and amplifying signal and idler photons is referred as modulational instability (MI). Following theory of FWM in waveguide arrays, we utilize evanescent couplings between neighboring waveguides to control the phase-matching condition in FWM. In experiments, a set of single SOI waveguides with the waveguide width decreasing from 380nm to 340nm demonstrate that changing the waveguide group velocity dispersion (GVD) at the pump wavelength of 1532nm from being anomalous to normal makes MI gain gradually disappear. Then, we perform the same experiment with an array of two 380nm-wide SOI waveguide, and demonstrate that for the large separation of 900nm and 800nm, MI gain is present as for the single waveguide; while for the small separation of ~400nm, the gain disappears. This transformation of phase-matching in FWM is attributed to the fact that the coupling induced dispersion changes the net GVD of the symmetric supermode from being anomalous for large separation to being normal for small separation. Our observation illustrates that the coupling-induced GVD can compete and exceed in value the GVD of a single SOI waveguide. This creates a new previously unexplored degree of freedom to control FWM and other dispersion dependent processes on chips.

8554-38, Session 9

Role reversal in a Bose-condensed optomechanical system

Keye Zhang, East China Normal Univ. (China); Pierre Meystre, College of Optical Sciences, The Univ. of Arizona (United States); Weiping Zhang, East China Normal Univ. (China)

We analyze the optomechanics-like properties of a Bose-Einstein condensate (BEC) trapped inside an optical resonator and driven by both a classical and a quantized light field. We find that this system exhibits a nature of role reversal between the matter-wave field and the quantized light field [1]. As a result, the matter wave field now plays the role of the quantized light field, and the quantized light field behaves like a movable mirror, in contrast to the familiar situation in BEC-based cavity optomechanics [2]. We demonstrate that this system can lead to the creation of a variety of nonclassical matter-wave fields, in particular Schrödinger-cat states [3], and discuss several possible protocols to measure their Wigner function [4].

[1] Our work has been published in Phys. Rev. Lett. 108, 240405 (2012) as an editor suggestion.

[2] Brennecke et al., Science 322, 235 (2008); K. W. Murch et al., Nat. Phys. 4, 561 (2008).

[3] S. Mancini et al, Phys.Rev.A 55, 3042 (1997); S. Bose et al, ibid. 56, 4175 (1997).

[4] S. Deléglise et al., Nature 455, 510 (2008); L. Lutterbach and L. Davidovich, Phys. Rev. Lett. 78, 2547 (1997).

8554-39, Session 9

An all fiber source of pulsed twin beams in the telecom band

Xueshi Guo, Nannan Liu, Xiaoying Li, Liang Cui, Tianjin Univ. (China)

or the practical continuous variable quantum information processing, the availability of a simple system to produce large amount of squeezing is vital. In this paper, we present an all-fiber source of twin beams by using a fiber optical parametric amplifier (FOPA). The broadband FOPA consisting of 300 m dispersion shifted fiber and a 10/90 fiber coupler is pumped with a mode-locked fiber laser, and the wavelengths of twin beams with pulse duration of a few picoseconds are in the 1550 nm telecom band. When the seeded parametric gain is about 56, the intensity noises of the amplified signal and generated idler pulses are found to be correlated by 30 dB, while the subtracted noise drops below the shot-noise limit by 3.1 dB (10.4 dB when corrected for losses). To the best of our knowledge, this is the highest noise reduction obtained in a FOPA. Thorough analysis reveals that high-order four wave mixing, Raman effect, and extra noise of the pump and seeded signal are key factors preventing the twin beams from further noise reduction. By engineering the phase matching condition of the FOPA and suppressing the noise of laser system, an even higher noise reduction will be feasible. The investigation shows a pulse pumped high gain FOPA provides an efficient and simple means to generate continuous variable quantum state.

8554-40, Session 9

All-optical format conversion from 16QAM to QPSK based on four-wave mixing in semiconductor optical amplifier

Yueying Zhan, Min Zhang, Mingtao Liu, Xue Chen, Beijing Univ. of Posts and Telecommunications (China)

A scheme of format conversion from optical 16QAM to QPSK signal based on cascaded-FWM in SOAs is proposed. Theoretical analysis and simulations of the scheme are conducted to validate the feasibility of the proposal. Theoretical analysis and simulations of the format conversion scheme are conducted to validate the feasibility of the proposal. In this paper, we present an investigation of format conversion from 16QAM signal to QPSK signal through both theoretical analysis and simulation approaches. A phase conjugated of 16QAM signal is generated after the first FWM process in an SOA. And then the QPSK signal is converted after non-degenerate four wave mixing (ND-FWM) process in another SOA. The performance and the optimum bias current of the SOAs, the pump frequency space and the performance of the 10Gbit/s format conversion system are evaluated and discussed by simulation Theoretical analysis. The proposed scheme can potentially useful in optical switching and the interconnection between backbone network and access network.

Conference 8555: Optoelectronic Devices and Integration IV

Monday - Wednesday 5 -7 November 2012

Part of Proceedings of SPIE Vol. 8555 Optoelectronic Devices and Integration IV

8555-1, Session 1

Making the mid-infrared nano with designer plasmonic materials (*Invited Paper*)

Stephanie Law, Jonathan R. Felts, Univ. of Illinois at Urbana-Champaign (United States); Viktor A. Podolskiy, Univ. of Massachusetts Lowell (United States); William P. King, Daniel M. Wasserman, Univ. of Illinois at Urbana-Champaign (United States)

At short wavelengths (visible or near-infrared), the use of gold or silver as constituent materials in plasmonic or meta-material structures has allowed for the demonstration of a wide variety of novel phenomena. However, the extension of these phenomena to longer wavelengths, such as the mid-infrared (mid-IR), an important wavelength range for sensing and defense applications, requires more than a simple scaling of geometries. This is because at longer wavelengths, the real parts of the permittivities of gold and silver are quite large in magnitude, and these metals behave almost as perfect electrical conductors, giving significantly different near-field behavior for plasmonic and metamaterial structures. However, scaling is possible if new plasmonic materials, whose permittivities at long wavelengths mimic those of gold and silver at shorter wavelengths, can be developed. In this presentation, we will demonstrate that epitaxially-grown, highly-doped semiconductors can be used as designer mid-IR plasmonic materials across a broad range of mid-IR wavelengths. At wavelengths where our materials' permittivity approaches zero, so called epsilon-near-zero (ENZ) wavelengths, we will show that these designer ENZ materials can enhance transmission of light through subwavelength apertures. At longer wavelengths, our materials behave, in the mid-IR, similar to traditional plasmonic metals (gold and silver) at shorter wavelengths. This is evidenced by their ability to support localized surface plasmons, which we demonstrate, using both far field FTIR spectroscopy as well as a novel near-field measurement technique for spectral and spatial mapping of the localized resonances.

8555-2, Session 1

Polymer based plasmonic elements investigated with leakage radiation microscopy (*Invited Paper*)

Douguo Zhang, Univ. of Science and Technology of China (China)

Recently, dielectric loaded surface plasmons (SPs) elements are inducing highly interesting in the field of nano-optics, which are composed of dielectric nanostructures fabricated on a metallic thin film. In this talk, we will present our recent work in this field. Polymer nano-structures are fabricated on a silver film by the EBL and laser interference lithography. These nano-structures are used to manipulate the behaviors of the SPs, such as converging, diverging, and guiding the propagation of SPs in sub-wavelength scale. Dye materials doped PMMA structures are also fabricated on the silver film, which provides a choice to realize active plasmonic elements. On the other hand, the interaction between the fluorescence molecules and SPs will give rise to some new optical phenomena, such as directional fluorescence emission, anisotropic fluorescence emission. We will also introduce some of our recently progress in super-resolution lithography taking advantages of polymer materials.

8555-3, Session 1

Optical interactions between silver nanocubes and two-dimensional silver gratings studied by surface enhanced Raman scattering

Qiang Fu, Univ. of Science and Technology of China (China)

In the present work, we fabricate some different period two dimensional metal gratings through two beams interference photolithography, and synthesis about 50nm silver nanocubes by chemical reduction method. The surface enhanced Raman scattering (SERS) intensity of rhodamine6G in different structures is compared. The results show that the SERS intensity is much weaker when there is only silver film than 2D silver gratings and silver nanocubes composite structure. Furthermore, we find that the SERS intensity on the ridge of the 2D silver gratings is also weaker than that in the groove. We attribute these results to the coupling of localized surface plasmon (LSP) and propagating surface plasmon (PSP) and the electric field enhancement in the cavity (groove).

8555-4, Session 1

Subwavelength dielectric-loaded plasmonic waveguides based on a core-shell structure

Bing Shen, Yongqing Huang, Xiaomin Ren, Qi Wang, Xia Zhang, Xiaofeng Duan, Beijing Univ. of Posts and Telecommunications (China); Dong Zhang, Beijing Univ. of Posts and Telecommunications (China); Jinhua Hu, Beijing Univ. of Posts and Telecommunications (China)

Surface Plasmon Polaritons (SPPs) have attracted great attention due to its ability to break the diffraction limit and thus greatly minimize the dimension of optical devices. In this paper, a new type of subwavelength plasmonic waveguide based on a core-shell structure has been proposed. A three-layer structure in the shape of semi-cylinder arranged on a dielectric substrate forms the proposed waveguide. The inner core layer, middle gap layer and the outer cladding layer is made of metal, dielectric with lower permittivity and dielectric with higher permittivity, respectively. As with the metal properties to tightly confine light near its surface, the middle gap layer serves as the channel guiding the light.

It is demonstrated that a modal area as small as $\lambda^2/3600$ can be achieved in the proposed waveguide, which is far smaller than that in the traditional dielectric-loaded plasmonic waveguide. Meanwhile, a propagation length is calculated as large as $100\mu\text{m}$, large enough for the application of guiding light in Photonic Integration Circuits. Thus a better trade-off in terms of confinement and propagation is achieved in the proposed waveguide. In addition to that, it is demonstrated that a ring resonator based on the proposed waveguide exhibits a perfect performance with a 1.8nm 3dB-bandwidth and 23dB extinction ratio. The simulated results reveal that ring resonator based on the proposed waveguide could exhibit better performance than that based on the dielectric or traditional dielectric-loaded plasmon waveguide with bandwidth larger than 3nm and extinction lower than 20dB.

8555-5, Session 2

Random optical traps enabled by metallic nano-island (*Invited Paper*)

Ho-Pui A. Ho, Zhiwen Kang, Haifei Lu, Haixi Zhang, The Chinese Univ. of Hong Kong (Hong Kong, China)

We report a simple approach to generate plasmonic optical traps in metallic nano-islands generated by annealing nanometer thick gold films. The plasmonic substrate is first immersed in an aqueous medium containing silver nanoparticles and a Raman tag (4-MBA). Upon illuminating the islands with a focused 785 nm laser beam, surface enhanced Raman scattering (SERS) occurs due to the formation of nano-gaps between the silver nanoparticles and the traps. Raman signals from 4-MBT slowly increases with time as the nanoparticles migrate into the optical traps. The trapping process is switchable. This technique might be useful for high sensitivity detection of molecules.

8555-6, Session 2

Heterojunction Si-SiC photodiodes for high-temperature operation

Joel Therrien, Daniel Shmidt, Lian Dai, Univ. of Massachusetts Lowell (United States)

Silicon-Silicon carbide based heterojunction photodiodes were fabricated using a novel process for making semiconductor grade SiC from polymer sources. The diodes were fabricated by spin coating the precursor polymer [Poly(silylenemethylene)], dissolved in hexanes onto a boron doped [100] silicon substrate to produce a film with thickness in the range of 0.5-1 microns. The substrates were heated in an inert atmosphere to 900 °C to pyrolyze the polymer into silicon carbide. The SiC was doped n-type by ion implanting nitrogen with dopant densities in the range of $10^{17}/\text{cm}^3$. The diodes showed excellent rectifying properties with a turn on voltage of ~ 4V. The diodes were tested for open circuit photovoltage and short circuit photocurrent response as a function of temperature. A commercial silicon photodiode was tested under the same circumstances for comparison. At temperatures exceeding 100 °C, the commercial diode was overwhelmed by thermally generated current. In comparison, the heterojunction diode's performance did not diminish for temperatures up to 170 °C.

8555-7, Session 2

A simple ultra-wideband dual-core SPSM PCF

Min Liu, Li Dan, Chongqing Univ. (China)

A simple dual-core single-polarization single-mode (SPSM) photonic crystal fiber (PCF) is proposed. We find that the PCF has simple structure which is easy to manufacture, and the SPSM region is ultra-wide. Also, the wide width of the SPSM region and the short coupling length can be tailored by adjusting the design parameters. The most important feature is that it can obtain simultaneous low-loss transmission of 1.30/1.55 μm in the SPSM region, which is very attractive for optical communication systems. Based on the analysis of the coupling characteristics, we demonstrate that the wavelength division demultiplexer (WDDM) can be realized by using this kind of PCF.

8555-8, Session 2

Multilayer polymeric mode filter using K-resin for optical integrated circuits

Kailash N. Tripathi, Galgotias Univ. (India)

There have been often problems of multimodes in any optical component. Mode Filter is an optical component used to suppress the higher modes and allow the basic mode to propagate undamped. Optical mode filter is an optical waveguide formed by higher refracting material disposed near a flat waveguide core. Two buffer layers are located opposite the waveguide core and one is formed with a thinned region to function as a filter for higher modes being transmitted through waveguide. Thin film multimode waveguides of K-resin were fabricated

by standard dip coating technique on clean microscopic glass slides.

Waveguides were characterized by prism coupling technique using He-Ne Laser. Multilayer structure has also been fabricated using same technique. Four layer dispersion curves have been generated using formulation of Sun and Mullar. Theoretical dispersion curves have been generated for both the polarizations. It has been clearly observed that first few modes are guided for both TE and TM polarization thus can be used as mode filter. The results show good agreement with theoretical ones. Another important result is that four layer optical guides exhibit relatively low propagation losses. It is also suggested that evanescent portions of the field distribution study can lead to evaluate the optical properties of the surroundings and as such can be exploited for sensor applications.

8555-9, Session 2

Compact terahertz wave broadband reflectors based on silicon photonic crystal slabs

Xiaolong Hao, Zexuan Qiang, Zhiyong Chen, Yanmin Zheng, Junzhen Jiang, Fujian Normal Univ. (China); Xiyao Chen, Minjiang Univ. (China); Yishen Qiu, Fujian Normal Univ. (China)

Terahertz (THz) waves with a frequency of 0.1THz-10 THz offer many potential applications like medical imaging, security screening, chemical sensing and astronomy. There is a high need to control THz waves in a compact integrated circuit for these applications, especially for compact THz sources. Broadband reflectors (BBRs) with high reflectivity are the essential components to construct the laser cavity. For visible and near IR, they can be typically realized by using either stacked dielectric films with glassy materials like SiO₂, TiO₂, and ThF₄ or metal films. However, such materials will not work in THz waves due to high absorption loss.

Here, we report a compact THz wave BBR based on the effect of guided mode resonance in photonic crystal slabs (PCSs) where these in-plane guided modes are strongly interacted with vertical radiation modes due to phase matching provided by the periodic lattice structure. By properly controlling the design parameters, very broadband reflectors can be obtained. Square-lattice air-hole PC pattern is fabricated in silicon material due to its high transparency in THz wave. A novel method based on a map of localized bandwidth with defined reflectivity is introduced to analyze the impact of normalized thickness and hole size. The rigorous coupled-wave analysis (RCWA) technique is then applied to analyze its performance. The numerical simulations show that the proposed configuration can offer a broadband frequency range from 2.27THz to 2.89THz with beyond 95% reflectivity.

This work has been partly supported by the Natural Science Foundation of Fujian Province of China under No.2012J01253.

8555-10, Session 2

Absorption modulation enhancement of azo-polymer film induced by plasmonic field

Xiang Xian Wang, Univ. of Science and Technology of China (Chile)

A thin photochromic film on top of the resist layer can be used as a virtual mask to fabricate super-resolution lithography patterns (science 2009,324,917). In this letter, based on the azo-polymer, the absorption intensity of the 365nm LED is modulated by 532nm laser, the modulation degree reaches to 87%. When the metallic nanoparticles are included in the polymer film, the modulation degree is significantly higher than that without the nanoparticles in the same intensity of 532nm laser due to the field enhancement of plasmons' excitation. The absorption modulation features of the polymer film are favorable for the further smaller nanolithography.

8555-11, Session 3

Tabletop ultrafast X-ray “laser” advancing nanophotonics under unprecedented spatial and temporal resolutions (*Invited Paper*)

Xiaoshi Zhang, Kapteyn-Murnane Labs., Inc. (United States)

Bright and short pulse high harmonic generation beams in the EUV and soft X-ray range of the spectrum promises breakthrough for nanoscience and nanotechnology. X-rays are unique in their ability to probe the electronic or spin state with element-specificity in molecules and materials, because the position of the characteristic x-ray absorption edges of individual elements is sensitive to the local environment and structure. Ultrafast x-rays can capture the coupled motions of charges, spins, atoms and phonons by monitoring changes in absorption or reflection that occur near these edges as a material or molecule changes state or shape.

In our labs, we developed table-top, bright, coherent and ultrafast x-ray “laser” source based on high harmonic generation using hollow core fiber. To enhance the efficiency of high harmonic generation, we developed all photonic phase matching technique using counter-propagating light and achieved >140 X enhancement of harmonic generation at ~ 70 eV. This technique can be applied essentially to any harmonic order and potentially enhance the efficiency by many orders of magnitude. Most recently, we demonstrated high harmonic generation into the x-rays of the spectrum by converting 5001 mid IR photons into one X-ray photon at 1.6 keV with spectral bandwidth supporting <1 attosecond (1E-18 s) pulse duration. In the work, we also showed that in order to achieve higher order harmonics, longer driving laser wavelength is desired. Combining all these technologies promises a table-top bright, coherent and ultrafast x-ray “laser”.

Finally, we present a few nano photonics and nano material science applications that were developed at our laboratories using this light source. All these new achievements advance nano photonics and nano material science into the x-ray regime with the capabilities to achieve sub-nanometer spatial and sub-femtosecond temporal resolutions.

8555-12, Session 3

External cavity based single mode Fabry-Pérot laser diode and its application towards all-optical digital circuits (*Invited Paper*)

Bikash Nakarmi, KAIST (Korea, Republic of)

All-optical signal processing is of great interest as they possess many advantages such as electromagnetic interference free, high data rates, transparency and others. All-optical logic gates and combinational circuit are one of the key elements of any optical systems and subsystems including signal processing, computation and control circuits where electromagnetic interference poses a great threat. Various techniques have been proposed for implementing different logic gates and digital circuits which are based on Er-doped optical amplifier and periodically poled LiNbO₃, semiconductor optical amplifier (SOA); and others have been reported based on injection locking of FP-LDs. SOAs are more popular due to its advantages of speed, integrality and Boolean logic capability. But SOAs require more driving current of about 200 mA and expensive. Besides, SOAs need additional probe beam for realization of optical devices and units.

FP-LD based logic gates are much promising than others as it is simple, less expensive and consumes low power. Single mode (SM) FP-LD possesses more advantages than the commercialized FP-LD as it has self-locking dominant mode which removes the necessity of additional probe beam. Thus, using SMFP-LD provides the simpler and cheaper solution.

In this paper, we introduce different techniques of injection locking for suppressing the dominant mode of external cavity based SMFP-LD which can be used for realizing different digital circuits. Power management schemes are introduced for different forms of injection

locking and are used for realizing all-optical logic gates and some digital combinational blocks at the data rate of 10 Gbps.

8555-13, Session 3

Vector beam fiber laser based on few-mode FBG

Biao Sun, Anting Wang, Lixin Xu, Chun Gu, Hai Ming, Univ. of Science and Technology of China (China)

We propose and demonstrate a single-wavelength all-fiber laser using few-mode fiber Bragg grating, generating high quality vector beams including both cylindrical vector mode TM₀₁ and TE₀₁, and hybrid mode HE₂₁ odd and even mode. And the four polarization states can be switched by adjusting fiber polarization controller in the fiber laser cavity. The fiber laser operates at a single wavelength of 1053 nm with a 3 dB linewidth of less than 0.1 nm, signal-to-background ratio of 50 dB.

8555-14, Session 3

Research on pattern-induced transparent conductive films

Xiaohong Zhou, Zongbao Fang, Heng Zhang, Linsen Chen, Soochow Univ. (China)

Indium tin Oxide (ITO) is widely used in touch panel as conductive material. However, it is fragile and low transparency in low resistance. In this paper, a new non-ITO transparent conductive film (TCF) has been proposed. Micro-nano structured patterns are designed to induce the nano silver particles and can form the circuit of touch panel sensor conveniently. Patterns are fabricated by nano imprinting technology to form micro grooves on flexible films such as PET. And then nano silver particles are filled in the grooves which constitute the conductive area of the TCF. The ratio of the line width to line period can influence the optical transmittance and sheet resistance. The relationship between the optical properties of the TCF and the parameters of the micro grooves such as the depth, the width, and aspect ratio will be investigated. Experiment results show the transmittance can be 87% and the square resistance can be less than 10 Ω/sq. The new material has a good performance for a large scale touch panel display and the fabrication process is high throughput and low cost for touch panel.

8555-15, Session 3

Emission properties of single deep confinement potential QD-cavity system under incoherent excitation

Huan Guan, Peijun Yao, Wenhai Yu, Pei Wang, Hai Ming, Univ. of Science and Technology of China (China)

Single quantum dot-cavity system with a deep confinement potential quantum dot is detailedly investigated, with both s- and p-exciton incoherent pump. Through gradually increasing pump rate (about 0.0001/ps~12/ps), the mean photon number shows a linear-dependence on pump power, the photon probability distribution, characterized by $g(2)(0)$, transforms from antibunching to bunching through Poisson, and the spectra go from the doublet to a singlet, the linewidth shows clear reduction in the lasing region. If we increase pump rate further, the mean photon number decreases monotonically to zero, $g(2)(0)$ reaches its maximum value 2, and all the electrons stack at upper lasing level, indicating thermal light generation. The results show, the deep QD-cavity system under s- and p-exciton pump can generate laser although it is not an ideal coherent light, and with only p-exciton pump considered, in spite of the coherent light generated, this pump method is unreasonable to simulate the experimental conditions for the negligible energy spacing between s-exciton and p-exciton.

8555-17, Session 4

Opto-DMD-based tunable triple-channel-wavelength fiber laser

Di Zhang, Binbin Yan, Kuizhi Huang, Qiang Yang, Beijing Univ. of Posts and Telecommunications (China); Xiao Chen, Minzu Univ. of China (China); Gengxiang Chen, Beijing Jiaotong Univ. (China)

A novel approach employing a digital-micromirror-device (DMD) to achieve a high stable tunable triple-channel-wavelength fiber laser structure is experimentally demonstrated. The control system is maintained by an embedded computer incorporating a FPGA circuit board. A graphical user interface (GUI) is designed for the usage of interaction and calibration. When a required wavelength is entered in the command line on the embedded pc, a corresponding grating image will be generated and loaded to the FPGA board, the pixel data is transmitted to DMD through a low voltage differential signaling (LVDS) interface with high speed. At the same time, the loading mode command is sent to DMD Power and Reset Driver (DAD2000) to reset the pixel array on DMD. As appropriate steering grating is formed on DMD surface, only the needed waveband of the ASE spectra will be selected and coupled into the fiber collimator array, while others are dropped out. There are three gratings can be generated at a time and hence a triple-channel function can be realized. According to a series of experiments, there exists a linear relationship between the digital grating position and output laser wavelength, which makes it quite convenient to determine the linear coefficient just by using the calibration function on GUI when environment has changed. The output power at every channel is regulated separately by a polarization-maintaining EDFA using an automatic power control (APC) system. GUI can analyze the received data from three channels and display the current output power on the control panel. Besides, a required output power can be achieved through the communication between GUI and EDFA. Experimental results show the laser line-width is 0.02nm with a facile tuning ability of 0.08nm per step over C band. The stability is indicated by the output power uniformity of 0.01mw during one hour under room temperature.

8555-18, Session 4

Tunable high-power multi-wavelength double-clad fiber laser

Jie You, Pengbo Xiao, Xin Wang, Long Huang, National Univ. of Defense Technology (China)

Multi-wavelength fiber lasers are under intense research due to their potential in many application fields like wavelength-division-multiplexing communication, fiber-based sensing, ranging, microwave photonics and terahertz generation, etc. In previous literatures, various multi-wavelength fiber lasers have been realized. However, most of which have employed single-clad rare-earth doped fiber pumped with single-mode laser diode, the output power is limited by the available laser diode (600 mW for the time being). Multi-wavelength double-clad fiber laser is expected in many application fields that requires higher laser power.

In this manuscript, we will present our detailed investigation on tunable high power multi-wavelength double-clad fiber laser pumped by high-power multimode laser diode. The fiber laser is constructed in a ring-cavity. A multimode laser diode with 8 watt output power is employed. The active fiber is double-clad Yb-doped fiber, which had a 10 μm core diameter and 125 μm inner cladding diameter. The NA of the core and the inner cladding of the double-clad fiber is 0.08 and 0.46, respectively. The active fiber is clad-pumped by the lased diode via a 7x1 pump combiner (only one pump port is employed). By adjusting the polarization-controller inside the cavity, the laser can operate at single-wavelength, dual-wavelength and triple-wavelength regime. The maximal output power is 5.5 watt and the conversion efficiency is 68.8%. Long-time observation ensures that the laser has an excellent

scalability. The output power can be scaled to multi-tens watt level by adding more pump diodes.

8555-19, Session 4

All-optical QPSK signal regeneration based on XPM in semiconductor optical amplifier

Yueying Zhan, Min Zhang, Beijing Univ. of Posts and Telecommunications (China); Mingtao Liu, Beijing Univ of Posts and Telecommunications (China); Lei Liu, Xue Chen, Beijing Univ. of Posts and Telecommunications (China)

A scheme of all-optical QPSK signal regeneration is proposed which based on cross phase modulation (XPM) in semiconductor optical amplifier (SOA) with subsequent an optical filter. A QPSK signal is generated based on an IQ modulator, and the QPSK signal is distorted after 100km fiber transmission. The QPSK signal is distorted by the negative chirp after fiber transmission due to the group velocity dispersion (GVD) and the self-phase modulation effect of the fiber, and then the distorted QPSK will be regenerated due to the positive chirp which is induced by XPM in the SOA which is discussed by theoretical analysis. In our system, the SOA would works at the deep saturation and the cross gain modulation (XGM) can be mitigated and no phase distortion will be introduced during the amplitude regeneration. From the simulation results, the BER of the regenerated QPSK signal makes better when the clock and distorted QPSK signal power are lower values and the current of SOA is higher value due to the XPM effect in the SOA and the average power of distorted QPSK signal and clock signal are set -5dBm and 10dBm. The amplitude noise of the distorted signal can be suppressed significantly, and the clear and open eye diagrams can be obtained. A power penalty 2.3dB is improved after QPSK regeneration with the receiver sensitivity of -30.7dBm. Simulations and theoretical analysis are conducted to validate the feasibility of the proposal.

8555-20, Session 5

All-optical modulation based on side mode injection locked multi-mode Fabry-Pérot laser diode (*Invited Paper*)

Jianwei Wu, Chongqing Normal Univ. (China)

Fabry-Perot laser diodes (FP-LD) are the most common type of diode laser, where two mirrors are separated by a gain medium. In reality, the FP-LD has attracted significant attention in optical network because of the rich nonlinear, low power consumption, and cost effective. To date, the FP-LD based optoelectronic devices were successfully demonstrated in various applications such as optical switching, logic gates, wavelength conversion, and so on. Even so, some potential applications are not still explored and proposed based on the FP-LD element. To promote its role in optical technology, the FP-LD based all-optical modulation is presented and investigated in this paper, in which the corresponding gain modulation effect is main influence on causing the modulation behavior. Of course, it is well known that all kinds of optical modulation technologies have already reported based on the silicon waveguide, silicon core fiber, and silicon microring resonator, etc. In these literatures, both the high power levels and complex configurations were introduced and presented so that it is very difficult to reduce the power consumption and simplify the device. Compared to the previous reports, the FP-LD based optical modulation can overcome some limitations, in which the modulated outcome signal with large modulation depth can be achieved under the condition of milliwatt power level.

8555-21, Session 5

Comparison on the accuracy and sensitivity of hole-based solar sensor under gray scale and binary configuration

Chung-Jen Ou, Yo Yuan Liu, Hsiuping Institute of Technology (Taiwan)

Solar tracking device becomes the major concerns for energy research and application. The basic hole type mask can provide an easy and elegant approach to activate the sensors below the device. However, the configurations and interactions between the mask arrangement and the light sensors are critical for various applications and the cost effective considerations. Furthermore, details analysis and sensitivities of the illuminating directions are a key success for a more advanced adaptive tracking system. In this paper we report the sensitivity and tolerance of the holes based device. The comparison of the signals for grey scale level and the binary type are demonstrated. We proposed two dimensionless parameters between the mask patterns and the sensors for revealing the performance of the hole based solar sensor. A 0.5 degree accuracy for grey scale type sensor is possible to achieve, however an average of 2 degree tolerance is recommended for grey scale electronic circuits. As for low cost binary type configurations, designed patterns can achieve 5 degree accuracy under the same number of sensors below the mask.

8555-22, Session 5

All-optical amplitude regeneration for PDM RZ-DPSK signal using a semiconductor optical amplifier

Yu Yu, Huazhong Univ. of Science and Technology (China); Dexiu Huang, Wuhan National Lab. for Optoelectronics (China) and Huazhong Univ. of Science and Technology (China)

The amplitude-only regeneration, which is usually simple and cost-effective, is very attractive for the phase modulated signal, since the amplitude noise will transfer to the phase noise due to the Gordon-Mollenauer effect during the transmission. On the other hand, the polarization division multiplexing (PDM) technique also attracts more and more people in all-optical communication system as it can double the spectral efficiency and data capacity.

In this paper, we propose and demonstrate all-optical parallel amplitude regeneration for PDM return-to-zero differential phase-shift keying (RZ-DPSK) signal, using a single semiconductor optical amplifier (SOA). The regeneration is based on the cross-phase modulation (XPM) in the SOA. The input two polarization tributaries are phase modulated by a synchronous optical clock signal with large power and optimal polarization state. A subsequent offset filter is used to extract the specific part of the broadened spectra to perform the noise suppressing function. The PDM RZ-DPSK signal at 2*40 Gb/s can be amplitude regenerated with a power penalty of -1.5 dB.

8555-23, Session 5

Two-wavelength switching in an asymmetric Fabry-Perot resonator with InGaAs/InP based multiple quantum well structure

Lokanath Mishra, Indian Institute of Technology Kharagpur (India); Rajib Pradhan, Midnapore College (India); Prasant K. Datta, Indian Institute of Technology Kharagpur (India)

Wavelength switching between two optical signals at different wavelengths has been studied theoretically in an asymmetric Fabry-Perot resonator (AFPR) operating simultaneously in reflection and

transmission mode. The AFPR, embedded with a semiconductor saturable absorber exhibits high nonlinearity, which makes this device attractive for all-optical signal processing. The bistable characteristic of the device has been studied in reflection and transmission incorporating both optically induced thermal effects and Kerr-nonlinearity. In the present work we have studied the switching of a signal beam at 1549nm by another control beam at the cavity resonance wavelength of 1550nm using bistability of the device. In our simulation we have fixed the input intensity of the signal beam at $I_{in2} = 0.2I_{sat}$, and is operated in reflection mode. Initially the control beam (I_{in1}) is at 'OFF' output state while the signal beam is at 'ON' output state for an input $I_{in1}=0$, operated in transmission mode. On gradually increasing the input power of the control beam the carrier concentration within the cavity increases, this modifies the absorption and refractive index of the saturable absorber, results in change of the output intensities of both signals. The simulated result shows that the output of the control beam switched abruptly from an OFF to ON output state (counter clockwise bistability) at $I_{in1}=1.34I_{sat}$, while the reverse effect observed in case of the signal beam. Due to its comparatively small carrier recombination time (~2ps), the AFPR could be a potential device for high speed switching.

8555-24, Session 5

Optical generation of millimeter-wave based on single-mode fiber ring cavity

Haiyan Chen, Lilin Chen, Cong Chen, Yangtze Univ. (China)

Recently, optical generation of millimeter waves has attracted a lot of attention, due to its high speed, low cost and high reliability. Compared with traditional high-frequency radio and coaxial cable transmission system, The combination of millimeter wave and optical fiber communication, radio over fiber(ROF), is a good solution to improvement of information capacity. One of the key of ROF system is the generation of millimeter wave. With the first microwave was generated by optical inject locked technology in 1985, more and more modulation techniques are found out and applied to millimeter wave generation. High frequency millimeter signal has a big phase noise in heterodyne method. The center wavelength of optical fiber grating must accurately match with the obtained millimeter wave signal wavelength. Recently, optical generation of millimeter-wave based on active ring cavity and microfiber ring resonator was reported by CHU and Yu Zhang etc, respectively. But both of them did not consider the impact of fiber-optic birefringence.

In this paper, a novel photonic generation of millimeter waves based on the birefringence in a single mode fiber ring cavity is studied theoretically. The effects of straight- through coupling coefficients, phase delay factor, loss factor and refractive index difference on millimeter wave signal are discussed.

8555-35, Poster Session

Tunable erbium-doped fiber ring laser based on an all-fiber filter

Xiaochun Ji, Zhigang Cao, Benli Yu, Anhui Univ. (China)

We demonstrate a tunable erbium-doped fiber ring laser based on an all-fiber filter. The filter consists of an optical circulator, a fiber loop mirror (FLM) and a polarizer which is spliced to a segment of polarization maintaining fiber (PMF) at the angle of 45° with respect to the fast axis of the PMF.

In the experiment, the laser oscillates when the pump power is 110mw. The tunable laser is achieved when the PC2 is adjusted in the laser cavity. The wavelength can be tuned from 1553.92 to 1560.1nm at a discrete step of ~0.35 nm, which is related to the wavelength spacing of all-fiber filter, and the side mode suppression ratio is over 38 dB. The output power difference is less than 1.2 dB. The mechanism of tunable wavelength can be explained as below. The light which is reflected by

the FLM returns to the polarizer and converts into linearly polarized light. When in the ring cavity, the polarization states is changed by PC2 and the birefringence effect of fiber in the cavity. The changes of different wavelength are different, and the different wavelength will experience different loss when the light passes through polarizer again. That is to say, the control on the polarization states of the different wavelength by PC2 is equivalent to the control on the loss of different wavelength. Only the wavelength have the lower loss can oscillate. Thus we achieve the tunable erbium-doped fiber laser by adjusting PC2

8555-37, Poster Session

Addressable wide dynamic range and high precision digital control device for adaptive liquid crystal microlenses array

Xin Chen, Huazhong Univ. of Science and Technology (China); Shengwu Kang, Wuhan Polytechnic Univ. (China); Xinyu Zhang, Huazhong Univ. of Science and Technology (China); An Ji, Institute of Semiconductors (China); Changsheng Xie, Wuhan National Lab. for Optoelectronics (China); Tianxu Zhang, Huazhong Univ. of Science and Technology (China)

Traditional optical microlenses have certain limitations because of the fixed optical properties. Current research demonstrates that liquid crystal (LC) is a kind of excellent electro-optic materials, because they have relatively strong electronic and optical anisotropies, and their optical properties can easily be shifted by external electric fields applied. Compared to traditional optical microlenses, the focal length of LC microlenses can be changed with the variance of the alternating signal voltage applied over the LC microlenses. A high precise and relatively wide range adjustable output voltage signal can be utilized to perform well in the controlling of LC microlenses array because the variance of focal length can be set in a relatively large range when the voltage of the signal is changed in a relatively large dynamic region. According to the above demands, a digital control device with a wide-range adjustable precise output voltage is designed and realized. Its output voltage range can be changed continually from 1 VRMS to 48 VRMS, and the voltage output precise is ~10 mVRMS, and the output signal waveform can be chosen as a sinusoidal, triangular, or square wave, and its frequency range can be set from 1Hz to 100 KHz. The realized controlling system has independent 16 channels, which independently control any one of 474 liquid crystal microlenses array, so all the 16 parts of 474 array is addressable, which is very important to performing high performance imaging detection of object in complex circumstance. Using this device fabricated by us, we can independently control the 474 array to focusing partial incident light beams that are interested to detect or recognize object, according to the characteristics of light intensity distribution over the photosensitive array. That means that the LC microlenses is attached with the features of adaptive function and have a broad application perspective for detection and imaging apparatus.

8555-38, Poster Session

Wide FOV receiving device for indoor visible light communication systems based on the MIMO principle

Xue Ming Liu, Nanjing Xiao Zhuang College (China) and Nanjing Univ. of Posts and Telecommunications (China); Zhong-cheng Liang, Xuying Wang, Qiuqi Ju, Nanjing Univ. of Posts and Telecommunications (China)

Visible light communication (VLC) is expected to be the next generation of indoor wireless broadband access technology. In order to achieve high data transmission rates, the multiple input multiple output (MIMO) VLC is proposed to break the bandwidth limitation due to the slow

response time of LED devices, MIMO-VLC offers the potential to transmit data in parallel between multiple sources and detectors. In addition, MIMO processing removes the need for precise alignment of transmitters and receivers, if the channel matrix is known and of full rank. Therefore, MIMO provides a solution to the design of wide field-of-view (FOV) receiving device for indoor VLC system, which is expensive if traditional optical components are used. This paper demonstrates the feasibility of such FOV receiving device with an integrated four-quadrant detector, and discusses the device properties in terms of optimal channel capacity, complexity and robustness to misalignment. A physical model is proposed for system simulation based on the single lens optical transform. The aim of this effort is to design and realize the integrated receiving device of wide FOV for LED visible light communication systems.

8555-39, Poster Session

Liquid crystal microlens with tunable-focus in focal plane driven by low voltage

Shengwu Kang, Xin Chen, Huazhong Univ. of Science and Technology (China)

Many modern optical imaging systems require elements with variable optical power for auto-focus and optical zoom applications, the conventional mechanical approaches are very difficult to implement. New alternative approaches and materials have been explored to replace those mechanical elements. Liquid crystal materials have large electrical and optical anisotropies, and they may provide huge electrically controlled refractive index changes without mechanical movements. Multiple attempts have been done to use this phenomenon for developing tunable focus lenses. To produce lens effect in a LC layer of uniform thickness, it is important to design an electrode pattern capable of creating an axially symmetrical inhomogeneous electric field in the LC layer. A LC lens with one hole-patterned and one planer electrodes was first realized in 1979, its focal length could be continuously varied electrically, since then many kinds of LC lens with various patterned electrode have been developed. Japanese scientists developed a LC lens driven by two voltages. One voltage acts as a bias voltage, while the other one varies to control the focal length. The electrode with a circular hole in the center, being separated from the LC layer by a glass substrate, is divided into four subelectrodes. This LC lens could make focus movable both along and off lens axis, but they need high AC voltage to drive electrode and the two AC voltages must be in phase. The reason is that the upper electrode is separated with LC layer by glass substrate, which increases the driven voltage. Another problem is that the diameter of circular hole is large. According to these problems, a LC lens with new electrode pattern is designed and realized. The ITO low and top electrodes are placed face to face, they are separated by glass spacer, and LC is injected between them. Because the two electrodes face the LC layer closely, this design could decrease driving voltage largely. The low electrode is designed with one hole-pattern. The top electrode is four circle patterns. The diameters of hole and circle are 500um and 160um respectively. Each circle electrode can focus respectively in the different place in plane, when the four circle electrodes are driven by different voltage at the same time, the focus could move off-axis in focus plane, the voltage varies from 0 to 20V. So we realize a LC microlens with tunable-focus in focal plane driven by low voltage.

8555-40, Poster Session

A no adhesive and temperature-independent package for fiber Bragg grating pressure sensor

Hui Wang, Hui Wang, Jun Zhu, Hao Yin, Zhao Zhang, Benli Yu, Anhui Univ. (China)

In this study, an innovative temperature-independent and no adhesive

package for FBG pressure sensor was designed. The FBG sensor package structure to compensate for temperature deviation by mechanical properties of different metal materials; It was metallized package with no adhesive using an plating method and laser welding process. The sensor can be effective to achieve the temperature compensation, and to avoid the problems of the aging and high-temperature failure of the adhesive. Strain sensing experiment obtain good symmetry and linearity within the range of $-30\% \sim 80\%$.

8555-41, Poster Session

Linearly-polarized Yb-doped fiber laser based on 45-degree fiber Bragg grating

Shenggui Fu, Xiaojuan Liu, Gongxiang Wei, Liping Guo, Xiaolu Ge, Shandong Univ. of Technology (China)

Tilted fiber Bragg gratings (TFBGs) have drawn a great deal of interests in recent years for their special structure and advanced properties. 45 degree TFBGs have been proved to be of excellent polarization characteristics.

In the paper, a 45 degree TFBG was fabricated in photosensitive fiber successfully using phase mask technique. The polarization-dependent loss characteristic of the TFBG was experimentally researched in the paper using a special measurement system. The measurement results showed that the 45 degree TFBG could act as a polarization possession element. Based on the 45 degree TFBG, a linearly-polarized Yb-doped fiber laser was demonstrated. The polarization-extinction ratio of the output laser is about 30 dB. The output power was about 5mW with the pump power of 120mW. The central wavelength of the laser is 1064nm and the wavelength bandwidth was about 0.1nm. Being a polarization device, the TFBG has the advantages of in-fiber, compact, good polarization capability and low price.

8555-42, Poster Session

Photoemission stability of negative electron affinity GaN photocathode

Junju Zhang, Nanjing Univ. of Science and Technology (China)

With the rapid development of lithographic manufacturing and ultraviolet (UV) detection technology, high performance

UV photocathode is needed urgently. GaN based photocathode has become an attractive candidate due to its wide band gap, stable physical and chemical properties, high quantum efficiency (QE), and low dark current. GaN photocathode activated by Cs/O can reach a higher QE because of the negative electron affinity (NEA), and how to keep photoemission stability of negative electron affinity GaN photocathode further becomes the important part of our study. The spectral response and quantum yield curve of reflection mode GaN photocathode just after Cs/O activation and Cs reactivation was achieved by using the online multi-information measurement and evaluation system. Also the attenuation in photocurrent under the radiation of 300 nm light is measured every hour. The result indicates that GaN photocathode are much more stable than narrow band material. The photocurrent peak increased by 16.8% after Cs reactivation which demonstrates the reason of the QE attenuation is the Cs desorption on the Cs₂O adlayer of surface. This can be explained by a double dipole layer model of GaN(Mg):Cs₂O whose stability determines the stability of GaN photocathode.

8555-43, Poster Session

Laser-induced damage threshold of CCD in nanosecond, picosecond, and femtosecond regimes

Junyan Hou, Beijing Track and Communication Technology Institute (China)

Nanosecond, picosecond and femtosecond laser pulse induced damage thresholds on CCD are investigated in this study. The thresholds of laser-induced damage on CCD are calculated theoretically for three pulse widths based on the thermal damage model. An axisymmetric mathematical model is established for the transient temperature field of the CCD. Experiments are performed to test the damage thresholds of CCD at various pulse widths. The results indicate that the damage thresholds obviously increase with the increasing of laser pulse width. Additionally, the experimental results agree well with theoretical calculations and numerical simulation results.

8555-44, Poster Session

Research on the impact of extreme environment on the FBG-based tensile strain monitoring for CFRP composite structure

Hong-yue Liu, Nanjing Univ. of Aeronautics and Astronautics (China) and Southeast Univ. (China); Da-kai Liang, Nanjing Univ. of Aeronautics and Astronautics (China); Qing-guo Fei, Southeast Univ. (China)

From the sensitivity of the FBG center wavelength changing with strain variations on the surface of CFRP composite, we investigate the correlation between the mechanical properties of the CFRP composite tensile specimen and extreme environments (high, low temperature and hydrothermal environment), that is, the tensile strain of CFRP specimen after different temperature or hydrothermal environment changes and a certain residual strain occurs. By combining FBG and the effect monitoring of CFRP structure caused by environmental factors, a FBG-based monitoring method for mechanical properties of composite after extreme environments is proposed. The tensile strain on the surface of CFRP specimen after high-temperature is slightly larger than the one before, and there is a certain residual strain; there is little effect on the tensile strain of CFRP specimen after low-temperature; the residual strain coming from hydrothermal environment is larger. The experimental results numerically showed that the FBG-based mechanical properties monitoring of CFRP specimen has good accuracy for a wide area.

8555-45, Poster Session

Three-dimensional modeling of nematic liquid crystal micro-optics structures with complex patterned electrodes

Xing Rong, Huazhong Univ. of Science and Technology (China); Shengwu Kang, Wuhan Polytechnic Univ. (China)

Liquid crystal (LC) is a kind of special liquid material composed of molecules with weak orderly orientation distribution. Generally, the functional liquid crystal devices demonstrate both the birefringence characteristics and special electro-optic property, in which LC molecules can be easily driven and controlled by the external electrical fields applied. The obvious advantages of LC device are the low signal voltage, very low power consumption and the electrically tunable optical property. Currently, it is very attractive to make the micro-optics structure using liquid crystal material. A micro-optics structure can make the incident field turned into the anticipated optical output field. In

order to design and fabricate the micro-optics structure, it is important to study the relationship between the anticipant optical output field and the external electrical fields formed by complex patterned electrode plates. So the first step is to calculate the distribution of LC directors which determine the distribution of refractive index in LC layers.

In this paper, a three-dimensional (3-D) over-relaxation method is proposed to model the dynamic response behavior of liquid crystal (LC) directors in nonuniform electric fields. The method is based on Frank-Oseen continuum elastic theory by using a vectorial representation. This method can deal with liquid crystal structures with arbitrary patterned of electrodes, and it is quite computational stability. Different numerical results obtained according the method are as follows: (1) the nematic LC structures with different patterned electrodes applied by a constant voltage, and (2) the nematic LC structures with different thickness of LC layer, and (3) the nematic LC structures with different signal voltage. The typical results include the distribution of LC directors in LC layers, the distribution of electric potential in LC layers, and the distribution of phase retardation. The results show that the method can be used to effectively predict the formation of disclination lines, which has a strong impact on the performance of LC micro-optics structure.

8555-46, Poster Session

Photoelectric response performance of nano-graphene film over infrared substrates

Jinhui Gong, Huazhong Univ. of Science and Technology (China)

The development of graphene technology indicates that the graphene, a single atomic-layer of carbon, is a novel two-dimensional material with extraordinary optical, electronic, and structural properties. With the special gapless band structure and spectral bandwidth, graphene can be used in the next generation of IR photodetection and novel material in other important opto-electronic application. In this paper, we demonstrate the fabrication and the measurement of special nano-graphene-detectors for IR radiation. We transfer graphene onto different infrared wafer including germanium, GaAs, silicon, and quartz. The system consists of the transferred graphene film over different wafer and metal electrodes that is fabricated on graphene sheet. With the zero band structure, graphene generate electron-hole pairs over a broad range of wavelength including UV, visible range, IR and THz wavelength. In our studies, the current-voltage relation of the system (certain direct voltage is applied on through the two metal electrodes) is measured before and after IR laser irradiation.

As tested, graphene has high optical transmittance in the visible, IR, and THz wavelength range. We research the current-voltage performance of the system. When the graphene structure is illuminated by laser beam of 1.1 μm wavelength and 0.9W power, an inflection point and current gain can be discovered. Because of the low light absorption of graphene, the photocurrent of the system is limited in about 1-3mA/W under certain voltage. We hold the point that the graphene and semiconductor form a certain kind of energy Band gap, which affect the photocurrent generation.

8555-47, Poster Session

Giant laser-induced thermoelectric voltage in c-axis inclined Na_xCoO_2 thin films

Shufang Wang, Zilong Bai, Hebei Univ. (China); Shanshan Chen, Zilong Bai, Hebei University (China)

Layered cobalt oxide thin films exhibit large light-induced thermoelectric voltage effect due to anisotropic Seebeck effect and have a great potential for light detector applications. In this paper, we have prepared c-axis inclined Na_xCoO_2 thin films by the topotaxial conversion method and studied its light-induced thermoelectric voltage effect by using an ultraviolet pulsed laser as light source. The incidence direction of the laser beam was directly perpendicular to the film surface. The laser

spot was located at the centre position between the two electrodes and its diameter was about 2 mm. The induced lateral voltage signals were recorded using a digital oscilloscope of 500 MHz bandwidth terminated into 1 Mohm. A giant open-circuit voltage signal with the peak voltage V_p of tens of voltage was observed when the film surface was illuminated by the 308 nm pulsed radiation, and the V_p increased linearly with the inclination angle as well as the laser energy on the film. The results demonstrate that the c-axis inclined Na_xCoO_2 thin film has a great potential application in the detection of weak ultraviolet pulsed radiation.

8555-48, Poster Session

Drift error analysis of atomic spin gyroscope

Shuangai Wan, Jiancheng Fang, Yao Chen, BeiHang Univ. (China)

Sensitive gyroscope is used in a wide range of applications, particularly in inertial navigation. In recent years, with the rapid development of quantum manipulation and modern optic manipulation technique, the advantages such as high precision and compact size offered by the atomic spin gyroscope, have attracted a number of researchers to these fields. Now the atomic spin gyroscope is believed to be the development trend for the high precision and compact gyroscope in future. The atomic spin gyroscopes are mainly composed of optical system, signal detection circuitry, magnetic shielding and magnetic compensation system, which produce errors under working conditions inevitably. Understanding the influence of magnetic field and light field on the performance of atomic spin gyroscope is important during the design of such devices. The basic principle of atomic spin gyroscope was reviewed and the analysis of error sources presented began with the coupled Bloch equations describing the dynamics of atomic spin gyroscope including magnetic field, light shift and pump-probe non-orthogonality. It was shown analytically that the first order effects of the transverse magnetic fields imperfections can be eliminated by turning the longitudinal magnetic field on the magnetic field compensation point. The effects of longitudinal magnetic field and light shift imperfections with other terms zeroed contributed only to scale factor of the atomic spin gyroscope. Furthermore, the effects magneto-optical crystal and magnetic shielding due to temperature drift were described and according approaches to suppress these errors were also proposed.

8555-49, Poster Session

Coupling characteristics between fundamental mode square waveguide and fiber

Fuyuan Guo, Lianhuang Li, Hua Zheng, Yi Wang, Jinrui Ke, Tianguai Dai, Fujian Normal Univ. (China); Xiaoming Lin, Fujian Normal University (China)

For the sake of clarifying the rationality of the Gaussian approximation for fundamental mode square waveguide and fiber, the relationship between the beam propagation factor (M^2) and the structure parameter is discussed. As the beam propagation factors of fundamental mode square waveguide and fiber are very close to the unit in a certain range of the normalized frequency, it is rational that the mode field distributions of fundamental mode square waveguide and fiber are expressed by the Gaussian functions approximately.

As the mode field half width defined by second order moment is greater than the identical concept defined by differential operator, it is difficult to confirm which one of them would work better, so the mode field half width defined by equivalent matching efficiency for fundamental mode square waveguide or fiber is recommended, it is the geometrical mean of the mode field half widths defined by second order moment and differential operator.

The coupling characteristic between fundamental mode square

waveguide and fiber is depended on their mode field matching characteristic. Base on the overlap integral formula of coupling efficiency and the mode field half width defined by equivalent matching efficiency, the approximate optimal structure parameters of this couple system is suggested. And Base on the overlap integral formula of coupling efficiency and the real mode field distributions of fundamental mode square waveguide and fiber, the real coupling efficiency between fundamental mode square waveguide and fiber is presented.

8555-50, Poster Session

Variable doping narrow-band response GaAlAs photocathode the preparation method of the research

Yuan Xu, Nanjing Univ. of Science and Technology (China) and Nanyang Institute of Technology (China); Xinlong Chen, Jing Zhao, Benkang Chang, Nanjing Univ. of Science and Technology (China); Youtang Gao, Nanyang Institute of Technology (China)

In order to avoid the low sensitivity common problem of 532nm sensitive narrow-band response photocathode, variable doping narrow-band response GaAlAs photocathode structure is designed. The photocathode is composed of GaAs substrates, Ga_{1-x}Al_xAs buffer layer, Ga_{1-x}Al_xAs doping concentration gradient emissive layer and GaAs protection layer from bottom to top. Among them, exponential doping method is applied to Ga_{1-x}Al_xAs unit layer from the bottom to the top. And a preparation methods of GaAlAs photocathode is developed. For the GaAlAs photocathode components which grow well, chemical cleaning, heating purification and (Cs, O) activation are operated, and ultimately Cs / O activation layer is formed on the surface of Ga_{1-x}Al_xAs doping concentration gradient emissive layer. The highest sensitivity of the photocathode peak response is at 532nm, and the photocathode quantum efficiency in 532nm peaks at 36%.

8555-51, Poster Session

Add-drop filters based on asymmetric high-order microring resonators

Dong Zhang, Yongqing Huang, Xiaomin Ren, Xiaofeng Duan, Bing Shen, Qi Wang, Xia Zhang, Shiwei Cai, Beijing Univ. of Posts and Telecommunications (China)

Add-drop filters are key components of Wavelength Division Multiplexing (WDM) communication systems.

Our effort is devoted to a wide free spectral range (FSR) and a flat-top response with a sharp roll-off from passband to stopband. FSR is a key parameter for Add-drop filters, an appropriately FSR should operate within the entire C-band (1530-1562nm). Flatness of the passband and sharp roll-off from passband to stopband are necessary to minimize the pulse broadening.

There are two custom ways to extend FSR. Firstly, the direct way to increase the FSR of a microring resonator is to reduce its radius. However, decreasing the bending radius of an optical waveguide will increase dramatically the bending loss. Secondly, a widely used alternative to extend FSR is Vernier approach, where microrings of different diameters are used to obtain 6-50 fold increase of the FSR of the single resonators. Although Vernier effect is effective in series-coupled ring resonators, spurious interstitial mode may increase when FSR expansion fold is large.

In this paper, an asymmetric high-order microring filter is proposed, the aim is to achieve large extension ratios and adequate suppression of the spurious interstitial mode, meanwhile, a flat-top and steep-side response of filter could be obtained by this approach. Our simulation results showed an extended FSR of 40nm, which can operate within the entire C-band, enlarging the interstitial peak suppression from 5dB

to 35dB and a boxlike filter response with sharp factor(SF) of 0.68. In addition a quality-factor of 2961 and a 3-dB bandwidth of 0.52nm are achieved.

8555-52, Poster Session

Experimental demonstration of a narrow linewidth 1120-nm Yb-doped fiber laser

Xiaojuan Liu, Shandong Univ. of Technology (China)

Because of the heat-dissipation characteristics of fibers and the excellent spatial mode characteristics, fiber yellow lasers are preferred candidates for various applications such as modern medicine, material processing, high-resolution spectroscopy, military applications and laser guide stars (LGS). Especially in the field of LGS, a 589 nm fiber laser with high beam quality and narrow bandwidth (better than 50 MHz) is the key instrument for the astronomical adaptive optics systems. So, in past years, fiber based 589 nm sources have been actively studied. So far, the mainly used methods to obtain 589 nm fiber lasers are double frequency of 1178 nm fiber lasers. Yb-doped silica fiber can lase at 1178 nm, but the gain is poor. Comparably, stimulated Raman scattering (SRS) can convert 1120 nm pump laser to 1178 nm with much higher efficiency. So, in the paper, we experimentally demonstrate a 976 nm LD pumped 1120 nm Yb-doped fiber laser, which will be subsequently used to obtain 1178 nm signal laser in the SRS experiment. The resonator composes a normal single-mode Yb-doped fiber and a pair of fiber Bragg gratings (FBG). The FBG1 is the total reflection mirror with a reflectivity above 99%. The FBG2 is the output coupler mirror with a reflectivity of about 10%. The maximum output power of 1.5 mW is achieved. The central wavelength is 1119.95 nm with a linewidth of 0.2 nm. To realize 1178 nm lasing in the Raman fiber, the output power of the 1120 nm fiber laser must be scaled to a much higher level and this can be realized by applying high power pumping and using double-clad Yb-doped fiber in the subsequent experiments.

8555-53, Poster Session

Hybrid integration of III-V RCE photodetector with CMOS receiver on silicon platform from Associated National Laboratory

Luo Yang, Yongqing Huang, Xiaofeng Duan, Xiaomin Ren, Qi Wang, Xia Zhang, Shiwei Cai, Beijing Univ. of Posts and Telecommunications (China)

In recent years, the combination of III-V semiconductor devices with Si manufacture techniques to develop optoelectronic integrated circuits(OEICs) has been widely studied. In this paper ,the fabrication procedure of a hybrid integration of monolithic InP-base resonant cavity enhanced (RCE) photodetector with silicon CMOS circuits is described. To realize a low-loss , high-data-rate optoelectronic micro system so that create an integration optoelectronic/electronic device is necessary . optoelectronic active devices and processing circuits is attractive in a packaging on a platform. For this project , RCE photodetector is designed using P-I-N diodes with a InP/In_{0.67}Ga_{0.33}As_{0.7}P_{0.3} layers structure with high reflectivity InP/Air gap distributed Bragg reflectors (DBRs). It has a high quantum efficiency of 59% at 1550nm wavelength, the dark current of 2nA at 3V reverse bias, the 3dB bandwidth of nearly 8GHz have been achieved. The processing circuits using a low-cost standard industry CMOS process chip.The monolithic photoelectronic detector and a transimpedance amplifier(TIA) chip are bonded on a Si substrate platform via metal wafer bonding technology. Because of the InP-based photoelectric detector(PD) and CMOS process chip are quite sensitive to temperature and stress-induced degradation, So the bonding metal should be chosen to have high thermal conductivity and stress-relief. We chose Au-Sn20 as the bonding media for large number of experiments. Si substrate not only provide a platform to place devices on it ,but also can as a heat sink for it has a good thermal conductivity. After TO-CAN packaging we test the whole

hybrid integration device on a optical test PCB. A clear transmitter eye diagrams is measured for the total integration device of frequency response.

8555-54, Poster Session

Hermite Gaussian approximation for TE1 mode of dielectric planar waveguide

Ziyun Wang, Lianhuang Li, Fuyuan Guo, Fujian Normal Univ. (China)

Because the Gaussian beam theory is perfect, the Gaussian approximation is used to express some light beam frequently. The normalized frequency is one of the most important parameters of optical waveguide, then, the relation between M^2 factor and the normalized frequency of TE1 mode of dielectric planar waveguide is presented when the half width of core layer is given, the minimum value of M^2 factor is 3.049 and M^2 factor tends to 3.403 when the normalized frequency tends to infinity. As the M^2 factor of TE1 mode of dielectric planar waveguide is close to 3 in the proper rang and the M^2 factor of the first order Hermite Gaussian beam is 3, the first order Hermite Gaussian approximation for TE1 mode of dielectric planar waveguide is reasonable.

The radius of the beam of the first order Hermite Gaussian approximation is expressed by equivalent mode field half width which is the geometrical mean of the mode field half widths defined by second order moment and differential operator. The matching efficiency between TE1 mode of dielectric planar waveguide and the first order Hermite Gaussian beam is good.

A simple fitting expression of M^2 factor and equivalent mode field half width is suggested, the numerical calculation indicates that the maximal relative error of M^2 factor and equivalent mode field half width is less than 2 percent in the proper rang.

8555-55, Poster Session

Analysis and design of a tunable filtering waveguide based on silicon-on-insulator

Fuquan Hu, Yongqing Huang, Xiaofeng Duan, Xu Zhang, Xinye Fan, Xiaomin Ren, Qi Wang, Xia Zhang, Shiwei Cai, Jinhua Hu, Beijing Univ. of Posts and Telecommunications (China)

One of the current research trends in silicon photonics is to integrate many kinds of optical functionalities on a single chip, which can lead to superior or novel functionalities. In this paper, based on Silicon-on-Insulator (SOI) we design a tunable filtering waveguide consisted of a Fabry-Pérot filtering-cavity and a straight waveguide. The Fabry-Pérot filtering-cavity is used for wavelength selectivity and the waveguide is used for light guide, which can be fabricated by utilizing electron beam lithography and inductively-coupled-plasma reactive ion etching (ICP-RIE) technique. The transmission characteristic of the device has been numerically simulated. The result shows that the Full-Width Half-Maximum (FWHM) is inversely proportional to pairs of the DBR. The FWHM decreases as the increase of the pairs of DBR. The peak wavelength is changed by changing the refractive index of DBR or the cavity of the Fabry-Pérot filtering-cavity. In order to tune peak wavelength, we can deposit different materials in the air grooves to change the refractive index of DBR or change the current to change the temperature of the cavity, so the length of cavity can be altered. The result shows that the peak wavelength changed 2 nm when changing the length of cavity by 3 nm. The tunable filtering waveguide can be integrated with waveguide photodetector, and the integrated photodetector will show great importance for the realization of optoelectronic integration circuits, hopeful to be widely used in WDM system.

8555-56, Poster Session

The influence of growth parameters on the formation on InAs/GaAs by MOCVD

Hui Wang, Beijing Univ. of Posts and Telecommunications (China); Qi Wang, Beijing Univ. of Posts and Telecommunications (China); Zhi-Gang Jia, Ying-Ce Yan, Yong-Qing Huang, Xiao-Min Ren, Beijing Univ. of Posts and Telecommunications (China)

InAs/GaAs quantum dots (QDs) have been grown by Metal-Organic Chemical Vapour Deposition (MOCVD) in the Stranski-Krastanow growth mode. We have investigated the influences of growth parameters such as the V/III ratio, growth temperature, QDs deposition thickness and the deposition rate of the overgrowth layer to the QDs qualities. Through the room temperature photoluminescence (PL) spectra, we have obtained the characters of QDs. The growth of QDs is very sensitive to the growth parameters which influence the QDs quality nonlinearly. During our work, a narrowest FWHM but the shortest center wavelength was obtained at the point of 25, when the V/III ratio was increased from 12.5 to 31.25. A redshift in the PL spectra and a broaden FWHM was obtain when the growth temperature was increased from 480°C to 520°C. A narrowest FWHM but a shortest center wavelength was obtained at the point of 3.0ML when the deposition thickness of QDs was increased from 2.7ML to 3.3ML. Overgrowth layer was grown with the deposition speeds of 0.1ML/s and 0.08ML/s, the latter brought a narrower FWHM. In an extensive study of the growth parameters, InAs/GaAs QDs with 80 meV of FWHM at 1.12µm were achieved.

8555-57, Poster Session

Coplanar lumped electroabsorption modulator fabricated on the common n-type InP substrate

Can Zhang, Song Liang, Li Ma, Baojun Wang, Hongliang Zhu, Wei Wang, Institute of Semiconductors (China)

A coplanar lumped electroabsorption modulator (Co-LEAM) based on n-type InP substrate is designed and fabricated, which is convenient to integrate and package with the flip-chip bonding technique. The device shows a high VBR nearly -25 v. The device capacitance is 0.55pf with the back n-electrode and 0.62pf with the coplanar n-electrode, which could satisfy a 10Gb/s bandwidth. The characteristic of extinction ratio is compared with the common LEAM.

8555-58, Poster Session

A polymer-modified PbS quantum dot fiber amplifier excited by evanescent wave

Xiaolan Sun, Libin Xie, Wei Zhou, Shanghai Univ. (China)

A novel polymer-modified PbS quantum dot (QD) optical fiber amplifier was proposed and demonstrated. Fabricated by depositing the PbS QD doped film around the tapered single mode fiber (SMF) coupler, the amplifier can produce a significant gain within the wavelength range between 1450 and 1650 nm by evanescent wave excitation. The PbS QDs were synthesized in an organic phase - by which we can acquire QDs with high quantum yield. Then QDs were transferred into water by polymer modification. Amphiphilic polymers modification will not affect the surface ligands and thus the initial high quantum yield can be retained. Also we can lower the refractive index of film (lower than the refractive index in fiber cladding material) to ensure the confinement of light wave. PbS QD doped film was achieved by mixing PbS QD solution and SiO₂ sol-gel solution. The tapered SMF coupler was fabricated by flame fused taper technique using standard SMF. The tapered region length was about 2 cm, and the waist diameter was about 12 µm. The mixed solution after ultrasound treatment was coated

onto the tapered region of fiber coupler and aged for 3 days at room temperature to obtain an amplifier. The signal produced by 1550 nm semiconductor light emitting diode can be amplified by the PbS QD optical fiber amplifier. With increasing pump (a 980 nm laser) power, the gain increases from 2 dB to about 6 dB gradually.

8555-59, Poster Session

A flat-top steep-edge waveguide photodetector composed of cascaded silicon microring resonators

Jinhua Hu, Yongqing Huang, Xiaofeng Duan, Xinye Fan, Fuquan Hu, Bing Shen, Luo Yang, Qi Wang, Xia Zhang, Xiaomin Ren, Beijing Univ. of Posts and Telecommunications (China)

Optical photodetector with filtering function is one of key elements in Wavelength Division Multiplex (WDM) optical communication system. Microring resonators using silicon-on-insulator waveguide are highly promising for photonics integrated technology due to the excellent filtering functions and the compatibility with complementary-metal-oxide-semiconductor (CMOS) processes. In order to enhance the tolerance of signal wavelength drifting in optical communication system, we proposed a novel photodetector with flat-top steep-edge response, composed of cascaded microring resonators on silicon-on-insulator in this paper. In the photodetector, we used polarization insensitive cascaded silicon microring resonators as optical filter cavity, and used a silicon racetrack resonator bonded in p-i-n chip as optical detecting cavity. We used finite element (FE) mode solver, finite different time domain (FDTD), and transfer matrix method (TMM) to simulate the behavior of the polarization insensitive optical filter. With optimized parameters, the photodetector showed high quantum efficiency, narrow line width and flat-top steep-edge. Comparing with traditional photodetector, this device had more compact and higher integrated level. This photodetector is very suitable for Wavelength Division Multiplex communication system.

8555-60, Poster Session

The tunable demodulator of DPSK based on reflection differential delay interference

Guodong Liu, Chongqing Wu, Yaya Mao, Zhengyong Li, Beijing Jiaotong Univ. (China)

A new scheme of demodulating DPSK signal is proposed based on structure of differential delay interference which is suitable for variable bit-rate and the tuning speed is faster than the existed demodulator. The experimental setup is composed of a circulator, collimator and a total reflecting mirror. The part of light beam incident to collimator reflects on its end as referring beam; the other transmits to the total reflecting mirror and reflecting back to the collimator as detecting beam. Referring beam and detecting beam interfere in the detector. In order to get the best results of interference, according to analysis and measurement, we make the reflectivity of the end of collimator is 40%, the transmittance of collimator is 60%, and the transmittance of reflecting mirror is 100%, so when the detecting beam return to the collimator, the reflecting beam and detecting beam have the equal amplitude. Adjusting the distance between the collimator and the total reflecting mirror by electric translation stage equals to half of transmission length of one bit signal in the air, referring beam and detecting beam carry phases of the adjacent symbols respectively, so the adjacent symbols interfere and then are demodulated. The demodulation of variable bit-rate NRZ-DPSK formats of 10Gb/s and 40Gb/s are demonstrated, the BER after demodulating is lower than 10⁻⁹. The demodulation results of 10Gb/s and 40Gb/s DPSK signal are also compared, it shows that the demodulation system is stable.

8555-61, Poster Session

Design and fabrication of the Y-branch waveguide for optical printed circuit board(OPCB) interconnect

Kang Li, Shanghai Univ. (China); Fufei Pang, Xiaobei Zhang, Tingyun Wang, Shanghai Univ (China)

With the rapid development of the fiber-optic communication technologies, the interconnect system is becoming more and more complex. Traditional electrical interconnect technologies on printed circuit board (PCB) are facing big challenges due to the limitation of bandwidth and data transmission rate and can not meet people's increasing requirements. In recent years, the interconnect technology of the optical printed circuit boards (OPCB) has become more and more mature. Compared with the traditional electrical interconnect technologies, the OPCB technology has the advantages of high data rates, wide bandwidth, low loss and low crosstalk. In this paper, a low loss multimode Y-branch interconnect optical waveguide was designed and fabricated. The transmitting properties of the Y-branch splitter were designed and simulated by using a commercial waveguide simulation software. For a 1 x 2 Y-branch splitter with 50 μ m x 50 μ m channel waveguide, the relationship between insertion loss and splitting angle was calculated. The splitting angle was optimized to realize a compact size of the Y-branch splitter. According to the theoretical result, a multimode Y-branch waveguide was fabricated based on a UV-lithography method on the printed circuit board. To balance the trade-off between the insertion loss and the component size, the Y-branch waveguide was designed of two sections with different splitting angles. An insertion loss of 0.36dB was observed with a 5cm Y-branch waveguide. Based on the low loss and compact size, the multimode Y-shape interconnect optical waveguides will find a wide application in future optical communication interconnect system.

8555-62, Poster Session

High stable single-polarization tunable fiber laser based on Opto-DMD processor and polarization-maintaining fiber devices

Huang Kuizhi, Yan Binbin, Beijing Univ. of Posts and Telecommunications (China); Xiao Chen, Genxiang Chen, Ai Qi, Minzu Univ. of China (China); Wang Kuiru, Beijing Univ. of Posts and Telecommunications (China); Yiquan Wang, Ying Zhang, Minzu Univ. of China (China); Feijun Song, China Daheng Group, Inc. (China); Sang Xinzhu, Beijing Univ. of Posts and Telecommunications (China)

Tunable fiber laser with narrow line-width operation and uniform amplitude output has attracted a lot of research interests because of its potential applications in optical communications, optical instrument testing and optical fiber sensors. A high stable wavelength-tunable fiber laser is experimentally demonstrated by using a digital-micromirror-device (DMD) processor and a polarization-maintaining erbium-doped fiber amplifier (EDFA). The electronic-addressed DMD processor is able to select and couple a waveband from of the polarization-maintaining EDFA back into the fiber ring to generate a narrow line-width laser output. The tunable fiber laser shows a line-width of 0.02nm, a tuning step of 0.08nm over the c-band and a side mode suppression ratio (SMSR) greater than 50 dB. The output power uniformity of 0.01mw is achieved by using the automatic power control (APC) system under room temperature. The center wavelength fluctuation during 1 hour is below 0.02 nm.

8555-63, Poster Session

A photonic instantaneous microwave frequency measurement without ambiguities

Nuannuan Shi, Xiyou Han, Yiyang Gu, Meng Wang, Jingjing Hu, Mingshan Zhao, Dalian Univ. of Technology (China)

Attention has been turned to the approach of photonic microwave frequency measurement with the advantage of large bandwidth, low power consumption, light weight and immunity to electromagnetic interference. Comparing with the traditional electronic methods, photonic approach can realize wide detection bandwidth and real-time operation which has great importance for unknown interceptive signal. For both military and civil applications, it is often required that the radar system has the capability of measuring the frequency of an unknown electromagnetic signal over a large spectral range.

In this paper, a novel technique for instantaneous frequency measurement of unknown microwave frequency based on the phase modulation and intensity modulation is theoretically and experimentally demonstrated. And the experimental results are presented with the measurement error smaller than 200MHz. In the proposed system, two different wavelengths of light are respectively for the phase modulation and the intensity modulation. These two modulated optical signals propagate in two segments of single-mode fibers. The electrical power after photodetection is related to laser power, laser wavelength, fiber dispersion, modulation index and microwave frequency. The above parameters are optimized in order to reduce measurement errors. Based on the output microwave power, three amplitude comparison functions (ACFs) are established to realize frequency measurement ranged from 1GHz to 20GHz. The unknown frequency is measured in the large slope of ACFs. At the same time, three ACFs are combined to realize the unambiguous determination of the microwave signal frequency beyond a single monotonic region of the ACF. Further research is being conducted and the results will be presented in the coming conference.

8555-64, Poster Session

Temperature tuning of the resonant photonic band gap of InAsP/InP Bragg-spaced quantum wells grown by MOCVD

Wei Yan, Wuhan National Lab. for Optoelectronics (China)

In this article, we presented a study of InAs_{0.04}P_{0.96}/InP Bragg-spaced quantum wells (BSQWs), a type of resonant photonic band gap structure (RPBG), grown by metal organic chemical vapor deposition (MOCVD). The quantum wells were characterized by photoluminescence (PL), double-crystal x-ray diffraction (DC-XRD), and reflection spectra. We found that the BSQWs structure grown at 580°C appears to be extremely abrupt, uniform, free of misfit dislocations, and narrow PL line width. By researching the reflection spectra at different temperature, we presented a theoretical analysis of the changes in RPBG, and proposed a new scheme of using the temperature to control the resonant photonic band gap structure.

8555-65, Poster Session

Wideband nearly-zero dispersion in fiberized slot waveguides

Qi Liu, Nanjing Univ. (China)

The dispersion of circular microfiber (CMF) can be reduced or even made anomalous at visible and near-infrared wavelengths. However, it is still a difficult task to achieve dispersion flattening. Combining current mature technology of drawing CMFs and micro-machining, it is possibly easier to realize a so-called fiberized slot waveguide (FSW), a microfiber with a slot inside. Same as the air-hole in PCF, a slotted structure could

provide extra design freedom to tailor the dispersion while keeping a large fraction of the guided mode in a nanometer-wide slot. Here we theoretically investigate the dispersion of the engineered FSWs. Our results show that low dispersion of ± 10 ps/(nm•km) over a 340 nm wavelength range can be realized. It presents great potentials in fiber micro-devices for high-speed optical communications.

8555-66, Poster Session

Micro-cavity lasers with highly directional emission

Changling Yan, Changchun Univ. of Science and Technology (China)

Micro-cavity lasers have attracted a lot of attention due to their low threshold high cavity Q factor and being suitable for high density optoelectronic integration. Optical micro-cavities which can confine light in a small mode volume with high quality factors have become an important platform not only for optoelectronic applications with densely integrated optical components but also for fundamental studies such as cavity quantum electrodynamics and nonlinear optical processes. Micro-cavity lasers have low threshold current densities but their optical power output is very low due to total internal reflection of the whispering gallery modes WGMs and their far-field profiles are isotropic. To overcome the intrinsic problems of microdisk lasers, several types of deformed structures were proposed, which are typically stadium-shaped lasers, bow-tie mode lasers, and spiral-shaped lasers, and the triangle cavity structures have also been reported. Recently, a limaçon-shaped microcavity has been proposed as a promising resonator shape for microcavity lasers with attractive properties such as a directional emission and a high cavity Q-factor. In this paper we compared several kinds of micro-cavity quantum cascade lasers with the limaçon shape cavity, the triangle shape cavity and ellipse shape cavity upon their far-field patterns. Quantum cascade lasers (QCLs) are especially suited for the micro-disk geometry due to their lack of surface recombination and inherently in-plane, transverse magnetic (TM) mode emission. Finally by using quantum cascade lasers material, InP based InGaAs/InAlAs quantum cascade structure with about 10 μ m emitting wavelength, the three kinds of micro cavity lasers are compared about output emission characteristics such as the far-field patterns, threshold current and light output power.

8555-67, Poster Session

Long distance optical printed circuit board for 10Gbps optical interconnection

Shiqiong Chen, Fufei Pang, Kang Li, Shanghai Univ. (China); Jinhua Wu, TTM Technologies, Inc. (China); Marika P. R. Immonen, TTM Technologies, Inc. (Finland); Xiaobei Zhang, Shanghai Univ. (China); Tingyun Wang, Shanghai Univ (China)

Optical printed circuit boards (OPCB) are a very important technique to realize wide band and high speed interconnection between board to board. With rapid increase of capacity in fiber-optic communication system, the layout of OPCB becomes more and more complex, which will increase the size of OPCB largely. Therefore, to realize high-transmission-rate interconnects on a long distance, OPCB technique has become an important trend. In this paper, a long-distance OPCB was fabricated to realize high-speed optical interconnects. The OPCB was made up of polymer optical waveguide fabricated by using an ultraviolet (UV) photolithography technique. The length of OPCB is 30cm long. The minimal transmission loss of the polymer optical waveguide is approximate 5.36dB at 850nm wavelength. Two MT-RJ optical connectors were assembled on the OPCB to realize optical coupling between optical fibers and waveguides. The dependence of coupling loss on misalignment was obtained with different offset value theoretically and experimentally. The minimal total insertion loss is only 8.06dB. With 10 gigabits-per-second (Gbps) optical transceivers as the

input/output module, we connected the polymer waveguide with optical fiber by MT-RJ connector and tested the performance of the OPCB. The data rate of 10Gbps can be transmitted successfully. Additionally, the relationship between the packet loss rate and total loss is also studied. It is found out that when total loss is less than 10.5dB, the whole data which is sent can be received.

8555-68, Poster Session

Negative feedback optical amplification effect based on optical triode

Yuma Fujikawa, Mohamad Syafiq Azmi, Yoshinobu Maeda, Kinki Univ. (Japan)

We demonstrated noise suppression characteristics of negative feedback optical amplifier using an optical triode. The optical triode that constituted by two semiconductor optical amplifiers (SOA) is based on change of gain in a SOA by cross-gain modulation (XGM). In this experiment, input signal light of 10 Gbps modulated NRZ signal with wavelength 1551 nm is used. The input signal light is divided into two by a coupler. One is fed to the first SOA and is used for generating an inverted signal light by XGM. The other and the inverted signal light are fed to the second SOA at the same time. The signal light is amplified with the gain modulation which depends on the inverted signal light. In order to evaluate the effect of gain modulation we measured a relationship of the inverted signal light intensity and bit error rate. Consequently, as the intensity of inverted signal light was increased, the received sensitivity was better. As compared with no inverted signal light, the received sensitivity was improved more than 4 dB. The negative feedback optical amplification effect based on gain modulation improves a extension ratio and a overshoot of output signal.

8555-69, Poster Session

Simulation and parameters optimization of high gain silicon micro-pixel avalanche photodiode

Fangkui Sun, Huaiqi Gu, Lixue Chen, Zhiwei Wang, Harbin Institute of Technology (China)

Avalanche photodiode (APD) is an attractive candidate for the replacement of photomultiplier in photon counting, and it has also been used in many photoelectric detect field include ladar, bio-aerosol detection, fiber communication, and low-light imaging. It can be compact, provides high internal gain. In addition, compared with other direct band gap materials, Si material has much lower inter-band tunneling current, which makes a better noise performance of Si-APD. The internal photocurrent amplification in APD is based on avalanche multiplication process. To get higher gain, the device is often to work in or above the breakdown voltage. With the increasing requirement of APD array integration, the study of high-gain and low operating voltage for APD pixel has become an urgent requirement. The appearance of micro-pixel APD sizes under 100 μ m provides a way to solve this problem. A compact array which meets the requirements could be the duplication of hundreds micro pixels.

In this paper, the silicon avalanche photodiode (Si-APD) size in micron, which was comprised of separate layer of absorption charge and multiplication(SACM) has been studied. The influence of different thicknesses and different doping concentration of the absorption, charge and multiplication layer on the electric field distribution, current-voltage characteristic and breakdown voltage were simulated and analyzed respectively. The structural parameters optimization has been done with the simulation results. The results show that the better gain and low bias voltage can be achieved with layer thicknesses in micro/nano-sized, which can give a high gain of 106 and low bias voltage of 127V. Also the fabrication process conditions has been given.

8555-70, Poster Session

Blue-green reflection-mode GaAlAs photocathodes

Xinlong Chen, Jing Zhao, Benkang Chang, Muchun Jin, Guanghui Hao, Yuan Xu, Nanjing Univ. of Science and Technology (China)

The traditional negative electron affinity GaAs photocathodes have the wide spectral response, which ranges from 400 nm to 1000 nm. The GaAs photocathodes are widely used in the area of night vision, but not applicable for the field of ocean exploration because the seawater is a good window to blue-green light. In order to obtain the suitable photocathode, the p-type zinc (Zn)-doped reflection-mode GaAlAs photocathode samples using exponential-doping technique are grown by metal organic chemical vapor deposition, the Al component of GaAlAs emission layer is designed to be 0.63. After the chemical cleaning, the photocathode samples are heated in vacuum at high-temperature of 650°C and 600°C respectively, the vacuum variation curves during the heat cleaning are measured, which correspond to the desorption of oxides in the surface of GaAlAs emission layer. The (Cs, O) activation for the photocathodes is executed after heat cleaning. Different proportion of Cs and O is performed on the different photocathode samples. The active photocurrent curves of two samples with different heat-cleaning temperature show that the GaAlAs surface treated by higher heat-cleaning temperature is more sensitive to the Cs-O adsorption. The photocathode activated with the larger Cs current has a shorter time to reach the first photocurrent peak, and also obtains a bigger final photocurrent peak. The spectral response curves are measured by the on-line spectral response measurement systems after activation. According to the measured spectral response curves, it could be found that a suitable heat-cleaning temperature and a moderate Cs/O current ratio are very important to prepare high performance GaAlAs photocathode. The prepared reflection-mode GaAlAs photocathodes are response to the blue-green light, and the cut-off wavelength is at about 580 nm.

8555-71, Poster Session

Beam steering based on multi-waveguide shifter

Dengcai Yang, Dayong Wang, Zhiyong Wang, Beijing Univ. of Technology (China)

Laser-phased-array(LPA) system has attracted more and more researchers because of its excellent performance. Including achieving high-resolution ; rapid; flexible beam steering. So it may be used many fields in future such as laser display, laser radar, and high power laser process.

In a LPA system, the performance is mostly decided by three factors, the first is the coherence source array. A perfect coherence sources are needed to achieve high performance combination beam. And the second is the phase control unit, which ensure the beam scanning accuracy and the beam quality. the last is the beam combination unit, which still ensure the far field beam quality. In this paper, an approach of the phase control is discussed theoretically and experimentally.

Recent years, several approaches have been provided to achieve phase shift, such as waveguide, grating, PZT, liquid crystal. Each way has advantage and shortcoming. As some researchers had great progress of the fiber laser and integrated optics in recent years. because the waveguide for phase shift has some advantages, including impact, easy for integration, it is an inevitable trend for all-optical to use waveguide for phase shift in the PLA. In this paper, a multi-waveguide based Lithium Niobate(LiNbO3) is provided. And the multi-waveguide is processed by proton exchange. The phase is shifted by loading the voltage on the electrode crossing the waveguide. In this experiment, a DFB source and four channels waveguide are used. The beam combination unit is one dimension. And the combination beam is detected by CCD. From the experiment, The combination beam scan

with the variation of the voltage. It achieve the beam steering. And the steering angle reach to $\pm 3^\circ$

8555-72, Poster Session

Direct-detection WiMax orthogonal frequency division multiplexing over fiber access networks

Jing He, Hunan Univ. (China); Jinshu Su, National Univ. of Defense Technology (China); Yuan Huang, Hao Liu, Hunan Univ. (China)

The future access networks should provide high bandwidth, improved network flexibility, mobility and cost-effective access. Recently broadband wireless access technology such as WiMax for Wireless Metropolitan Area Networks has become a strong candidate for the last mile wireless connectivity to provide flexible broadband services to end users. According to WiMax standard, the typical cell coverage can extend to 5 km in the atmosphere, with selectable channel bandwidth. However, the WiMax signal distribution would be greatly hindered as signal access inside a long tunnel and indoor. There is a real desire to merge the wireless and optical wire network into a single infrastructure. Previous investigation reported that using radio-over-fiber (RoF) technology to carry the WiMax signal and investigated the performance of WiMax RoF system such as throughput and packet-loss at different link lengths. The transmission limitation and performance of the standard WiMax access in RoF link is demonstrated, but it focus on standard mobile WiMax for the applications in the high speed railway. In the paper, we have demonstrated novel optical-wireless architecture consists of a wireless network and an optical network, and applied IEEE 802.16 standard WiMax OFDM modulation to the optical-wireless architecture by simulation. Based on the constellation diagrams of the received signal and the measured error vector magnitude after direct detection, simulation results show that the proposed system can successfully transmit a high capacity WiMax OFDM signal over 250km SMF without any amplification, which can extend the network converge distance of optical network and serve more end-users who share an optical line terminal link.

8555-73, Poster Session

Optimized parallel energy storage and delivery solar lighting and heating system

Junewen Chen, Chung-Hua Univ. (Taiwan)

We have designed and efficiently developed a parallel energy storage and delivery solar lighting and heating hot water system. The complete system is designed and simulated with practical data to evaluate and optimize the efficiency. A well fabricated solar energy system had been in operation and had achieved best efficiency compares to the other traditional systems. The optimized compulsive circulate controls of the solar heater were investigated in detail. Based on the thermodynamic theories of the solar heating and the solar source various incident angles, we have design a control circuitry that can automatically control as well as maximize the overall efficiency. Our designs also embedded in the system monitoring and protecting capabilities. The integrated system control loop design can accordingly switch the system to have maximum efficiencies. This design results also gave high commercial value.

8555-74, Poster Session

1.65um distributed Bragg reflective (DBR) laser for CH₄ trace-gas sensing

Bin Niu, Hongyan Yu, Liqiang Yu, Jiaqing Pan, Lingjuan Zhao,

Wei Wang, Institute of Semiconductors (China)

The device was fabricated on n-type InP substrate. Strained multiple quantum-well (MQW) material was designed and grown using metal organic chemical vapor deposition (MOCVD). The device is composed with phase section, grating section and gain section. Photoluminescence spectrum peak of the grating section's material was blue shifted by Quantum-well interference (QWI) method.

The device was characterized. Single mode stability and wide tuning range make the device suitable to be used for trace-gas sensing with the technique called Tunable Diode Laser Absorption Spectroscopy (TDLAS). The special wavelength was design for CH₄ trace-gas sensing.

8555-75, Poster Session

Saturable absorption in graphene at 800 nm band

Shunbin Lu, Shuqing Chen, Zhiwei Zheng, Han Zhang, Chujun Zhao, Shuangchun Wen, Hunan Univ. (China)

Graphene exhibits broadband optical saturable absorption due to its linear energy band structure and the Pauli blocking principle. We experimentally demonstrated the saturable absorption in graphene at 800 nm. The graphene sample under investigation, which consists of three layers grown by chemical vapor deposition (CVD) method, is transferred from the copper substrate to the quartz substrate. Two-dimensional Raman mapping shows its high material quality. By performing the balanced twin-detector measurement technology, we are able to characterize the nonlinear optics property of the as-fabricated graphene sample. The incident laser source is based on a Ti: sapphire femto-second laser with a central wavelength of 800 nm, a repetition rate of 1 kHz and a pulse duration of 100 fs. Under strong illumination, we find that the absorption of graphene decreases with the increase of incident power, and by fitting the experimental data with theoretical model, the saturable intensity and the normalized modulation depth are measured to be 7.911 GW/cm² and 10.6%, respectively. The experimental results show that graphene may be a promising saturable absorber, with the potential laser photonics applications such as laser mode locker or Q-switcher, at 800nm band.

8555-76, Poster Session

Model of a series-cascaded fractal topological structure of microring resonator arrays

Xiaobei Zhang, Yingchun Li, Fan Gu, Biyun Jin, Shanghai Univ. (China)

A series-cascaded fractal topological structure of microring arrays is proposed, by introducing fractal topological structures to all-pass microrings. Every unit of this series-cascaded fractal topological structure regard as a series-cascaded microring, thus these units form a special microring arrays by series-cascaded method. Due to resonance occurring in every unit and the whole region of the series-cascaded fractal topological structure, the performance of transmission spectra and delays are improved significantly. Its analytical model is established by the transfer matrix method. Then the characteristics of this structure are investigated by the effects of coupling coefficients and loss. Generally, there are dips with the resonator number in the transmission spectra. As the loss increases, the average intensity decreases. However, the delay becomes interesting positive and negative delays. As the ring-bus coupling coefficient decreases, the dips of the spectrum become degenerated. However, there are several delay peaks with some positive and other negative delays. These kinds of multiple positive and negative delays can be explored for applications in all-optical delay lines.

8555-77, Poster Session

Temperature tunability of hybrid material infiltrated photonic crystal fiber

Yinping Miao, Nankai Univ. (China)

The advent of photonic crystal fibers (PCFs) offers an excellent carrier for the further development of novel functional materials. PCFs, possessing several distinguished characteristics compared with conventional single-mode fibers, have attracted a lot of research interest. It is a special kind of optical fibers with micrometer-sized air holes running along the length of the fiber axis. Infiltration of advanced materials into the air holes of the PCFs would effectively combine their unique optical properties with material features together efficiently and provide opportunity to achieve tunable fibers and relevant photonic devices.

In this paper, Fe₃O₄ nanoparticles were superficially modified by refractive index liquid and then filled in the air-hole of photonic crystal fibers, and based on this structure the temperature-dependent properties of the fluid material and the infiltrated fiber have been investigated. Experimental results show that there exists some self-assembly phenomenon that two-dimensional and grating-like fluid structure form along the fiber axis. Three resonant peaks of the quasi-LPG turn up in the wavelength range from 800nm to 1700nm. Based on the enhanced negative thermo-optical effect of the infiltrated media, the resonant peaks show blue-shift in different degrees as temperature increases. The highest temperature sensitivity reaches 4.4nm/°C at 1610.4 nm, which is 440 times higher than that of conventional fiber grating (~0.01nm/°C). It is possible to acquire composite magnetic fluid with excellent optical property by selecting and optimizing the surfactant of Fe₃O₄ nanoparticles. Through combining the channels of PCF with advanced material, photonic devices have advantages of compact size, high sensitivity and stability, ease of fabrication, etc.

8555-78, Poster Session

Selective etching of metamorphic GaAs/Si and InP/GaAs wafers

Xiong Zhen, Qi Wang, Zhigang Jia, Yingce Yan, Yongqing Huang, Xiaomin Ren, Beijing Univ. of Posts and Telecommunications (China)

Heteroepitaxial growth of GaAs on Si and InP on GaAs plays a very important role in promoting the optoelectronic integrated (OEIC) technology. The threading dislocation density of GaAs/Si and InP/GaAs heterostructures seriously influence the performance of devices. Compared with transmission electron microscopy (TEM) which requires arduous sample preparation, long cycle and high cost, selective chemical etching methods have been widely used to reveal dislocations due to its merits of intuitive results, low cost and simple experimental procedure.

In this paper, GaAs/Si and InP/GaAs wafers growth was performed by low-pressure metal-organic chemical vapor deposition (LP-MOCVD) using a two-step growth method. The wet chemical etching methods were used to characterize the dislocations density. For the GaAs/Si wafer, the chemical etching was performed in molten KOH at temperatures about 350°C and for duration about 1.5min. For the InP/GaAs wafer, the chemical etching was performed in H₃PO₄: HBr (2:1) solution (Huber etchant) at temperatures about 20°C and for duration about 2min. Then, the morphology of the dislocations characteristics of the etch pit density (EPD) were examined with a high-resolution field-effect scanning electron microscope (SEM). There are some ellipse dislocations pits of the GaAs/Si wafer with a density about 2E7cm⁻², and sizes ranging from 700nm to 1500nm in diameter, and there are many sunken dislocations pits of the InP/GaAs wafer with a density about 2E8cm⁻², and sizes ranging from 300nm to 700nm in diameter. So the method has been accurate and convenient to show the dislocations characteristics of metamorphic GaAs/Si and InP/GaAs wafers.

8555-25, Session 6

Rigorous calculation of optical modes and their interference induced power distribution in arbitrary numbered coupled slab waveguides (*Invited Paper*)

Guiru Gu, Xuejun Lu, Univ. of Massachusetts Lowell (United States)

In this paper, we present a simple yet rigorous method based on transmission matrix to calculate the optical modes and power distribution in arbitrary numbered coupled slab waveguides. The optical mode profiles and their refractive indices obtained by this method are identical as those obtained from the BPM method. This method doesn't depend on the grid size and becomes much more efficient than the BPM or CMT for a large number of coupled waveguides. We also prove that the optical modes are orthogonal. Based on the orthogonal property, the coupling coefficients to the optical modes and the interference of the modes are calculated along the waveguides. We found that the optical power distribution among the waveguides obtained by calculating the mode interference is very close to that obtained by the BPM method, suggesting that the optical power distribution among the waveguides as it travels along the waveguides is due to the interference of the optical modes.

8555-26, Session 6

Error analysis and system implementation for structured light stereo vision 3D geometric detection in large scale condition

Li Qi, Xuping Zhang, Jiaqi Wang, Yixin Zhang, Shun Wang, Fan Zhu, Nanjing Univ. (China)

Stereo vision based 3D metrology technique is an effective approach for relatively large scale object's 3D geometric detection. Unfortunately, with the object scale keep on increasing, it's hard to maintain both efficiency and high precision. In this paper, firstly we introduced the structure and detection process of our structured light based stereo vision detection system. The system used a 500mW line-structured laser carried by a motor stage which set up in the middle of the two cameras. Secondly, we made an error analysis for large scale vision detection based in the common parallel camera case. Based on this analysis we find out that the system precision is affected by various factors such as the trigger time difference, the baseline length and the common field of view of the binocular system. After that, we proposed several system design principles in large scale vision metrology applications. The prototype we built implements LVDS interface embedded CMOS sensor and CAN bus to ensure synchronous trigger and exposure. We tested the system in both indoor and outfield experiments, the results of which demonstrate that the precision level can be guaranteed effectively.

8555-27, Session 6

Thermal effects on interconnect crosstalk of optoelectronic transmitter modules

Ikechi A Ukaegbu, Bikash Nakarmi, KAIST (Korea, Republic of)

Optical interconnection technology have been widely studied as one of the most potential technologies to meet the high speed requirements of next generation computer systems. However, most optical and optoelectronic components used in optical interconnection technology, require electrical interconnects for power and signal transmission and these electrical interconnects affect the performance optical link. As clock frequency reaches the gigahertz band with signal transmission rate reaching the gigabit range, signal reliability and performance are

determined by factors such as thermal effects.

Optoelectronic modules are sensitive to temperature changes which has drastic effect on the performance of the modules and can affect them by increasing crosstalk between channels; increasing threshold density which can lead to failure of device; decreasing output power of laser; changing the wavelength of the emitted light; and broadening the spectral line width which affects the speed.

In order to investigate and analyze thermal effects on crosstalk and performance of optoelectronic interconnects, two 4-channel transmitter modules have been designed and fabricated. The modules are a planar and a multi-chip (MCM) transmitter module. The planar module uses the conventional wire-bonding for interconnect between the driver chip and the VCSEL while the multichip module employs the flip-chip bonding technology.

This work therefore presents an analytical model based on interconnect parameters for thermal effects analysis on crosstalk of multi-channel optoelectronic transmitter modules. The model is used to determine the thermal critical frequency, f_{crit} , above which signals become severely deteriorated.

8555-28, Session 6

Monolithically integrated photodetector with flat-top and steep-edge response for wavelength division multiplexing (WDM) systems

Yongqing Huang, Xiaofeng Duan, Xinye Fan, Xiaomin Ren, Qi Wang, Shiwei Cai, Xia Zhang, Beijing Univ. of Posts and Telecommunications (China)

The wavelength selective photodetectors are considered promising candidates for application in high-speed optical communications and interconnections, especially in wavelength-division-multiplexing (WDM) optical communication. Some monolithically integrated wavelength-selective photodetectors have been realized, such as one-mirror inclined three-mirror cavity (OMITMC) photodetector, multiple resonant cavities RCE photodetectors, photodetector arrays with multistep cavity and so on. But many of these devices can't get flat-top steep-edge spectral response that is very important for using in WDM system. A 1550nm monolithically integrated photodetector with flat-top and steep-edge spectral response is reported in this paper. The contradiction among the quantum efficiency, high response speed and the narrow spectral response linewidth each other is overcome by the design of a Si-based multi-cavity Fabry-Pérot (F-P) filter and a cone absorption cavity. In the structure of this photodetector, there are five cavities and six distributed Bragg reflectors (DBRs) for the narrow spectral response linewidth and flat-top and steep-edge spectral response, a cone absorption-cavity with an absorption enhancement effect for high quantum efficiency. Based on this structure, flat-top steep-edge spectral response, high quantum efficiency, high response speed, and a narrow spectral response linewidth can be obtained simultaneously. The $\text{In}_{0.53}\text{Ga}_{0.47}\text{As}$ absorption layer thickness is 200nm. A peak quantum efficiency of 55% at 1549.2 nm, the -0.5 dB band of 0.43 nm, the 25dB band of 1.06 nm, and 3-dB frequency response bandwidth more than 16 GHz, are simultaneously achieved with the active area diameter of 30 μm . The dark current as low as 10nA was obtained at a reverse bias of 3.0V in the device. Compared with other similar photodetectors, this device has good flat-top and steep-edge response and ideal high-speed characteristics can be applied to 100GHz channel spacing DWDM system.

8555-29, Session 6

Polymer planar lightwave circuit based hybrid-integrated coherent receiver for advanced modulation signals

Jin Wang, Yang Han, Zhongcheng Liang, Yongjin Chen, Nanjing Univ. of Posts and Telecommunications (China)

Advanced modulation formats have become attractive candidates for optical transmission systems, because of their increased spectral efficiency, improved dispersion tolerance, lower OSNR requirement and robustness towards nonlinear impairments. Applying coherent detection technique to them makes it possible to electronically compensate the signal impairments. A key issue for a successful deployment of coherent detection technique is the availability of cost-efficient and compact integrated receivers. Such an integrated receiver is composed of an optical 90° hybrid and four photodiodes (PDs) that are better to be integrated. Thus, a practical problem for a coherent receiver is how to realize the optical 90° hybrid, which is cost-efficient and easily integrated with PDs. In this work, three different types of optical hybrids are fabricated with polymer planar lightwave circuit (PLC). Polymer PLC technology is regarded attractive because it offers the potential of fairly simple and low-cost fabrication, and of low-cost packaging. The first type of realized optical hybrid is composed of four 3-dB couplers and an additional phase delay of 90° in one branch; the second type is to use a 2 \times 4 MMI coupler; the third type is composed of one polarization-beam splitter, which is realized by a polarization splitting thin film element (TFE), and two 3-dB couplers. Via 45° turning mirrors, these three optical hybrids are integrated with a PD-array, which comprises four vertical backside illuminated PDs. Their performances, such as the insertion loss, the transmission imbalance, the polarization dependence and the phase deviation will be given. The realization challenges will be discussed.

8555-30, Session 6

InGaN/GaN light-emitting diode on GaN/Si template with AlN/GaN superlattice as interlayer

Fang Ren Hu, Y. J. Wang, H. B. Zhu, Nanjing Univ. of Posts and Telecommunications (China); M. Wakui, H. Sameshima, K. Hane, Tohoku Univ. (Japan)

GaN on Si is attractive for the integration of light-emitting device and Si microelectronics. Also, highly functional and integrated optical Micro-Electro-Mechanical-Systems (MEMS) can be developed, through monolithically integrating silicon three-dimensional structures and microactuators with nitride devices. However, the large differences of lattice constant and thermal expansion coefficient between GaN and Si restrict high quality GaN crystal growth on Si. Lateral overgrowth, nanocolumn crystal and patterned substrate have proved to be effective ways to grow GaN on Si. In our Riber32 molecular beam epitaxy (MBE) system, column crystal growth was deposited to improve the GaN crystal quality. However, it is difficult to fabricate integrated devices using GaN column crystal and Si. GaN/Si template is another effective way to grow GaN on Si. Here we used the GaN/Si template as substrate and deposited InGaN/GaN p-i-n junction structure with AlN/GaN superlattice layers as the interlayer. Different surface microstructure of the p-GaN was affected by the amount of Mg flux. Light-emitting diode was fabricated from the p-i-n junction. The crystal properties of InGaN/GaN p-i-n junction and the related light-emitting diode properties were investigated. The monolithical integration of GaN semiconductor and Si Optical-MEMS would improve the application of GaN-based light-emitting devices in the Optical MEMS.

8555-31, Session 7

Surface-corrugated microfiber Bragg grating (Invited Paper)

Fei Xu, Jun-Long Kou, Nanjing Univ. (China); wei luo, nnajing university (China); Yan-Qing Lu, Nanjing Univ. (China)

There are two steps to obtain as small as possible fiber Bragg gratings. First, it is to taper the fiber and reduce its diameter. A subwavelength-scale microfiber (MF) is the basic element of miniature fiber devices and sub-systems. Then it is to reduce the grating length. For short fiber grating, strong refractive index modulations are necessary. Strong refractive index modulations can be obtained inducing surface corrugation by alternating layers of different materials, one of which can be air. Few techniques have been proposed for the fabrication of surface-corrugated fiber gratings, including photorefractive inscription using etching, femtosecond lasers, and Focused ion beam (FIB). So far, FIB is the most flexible and powerful tool for patterning, cross-sectioning or functionalizing a subwavelength circular MF due to its small and controllable spot size and high beam current density. In past two years, a number of ultra-compact surface-corrugated microfiber Bragg gratings (SCMGs) have been successfully fabricated by FIB milling. The length of FIB milled SCMGs can be as small as tens of micrometers. In addition, there are several novel proposals on SCMG including wrapping a microfiber on a microstructure rod or put a microfiber on a surface-corrugated planar grating. In this chapter, we will introduce recent advances in these ultra-small SCMGs and their characteristics and applications.

8555-32, Session 7

Large area monolithic organic solar cells

Hui Jin, The Univ. of Queensland (Australia); Cheng Tao, Mike Hamsch, Almantas Pivrikas, Marappan Velusamy, Muhsen Aljada, Yuliang Zhang, Paul Burn, Paul Meredith, Centre for Organic Phototics and Electronics, University of Queensland (Australia)

Although efficiencies of > 10% have recently been achieved in laboratory-scale organic solar cells, these competitive performance figures are yet to be translated to large active areas and geometries relevant for viable manufacturing [1]. One of the factors hindering scale-up is a lack of knowledge of device physics at the sub-module level, particularly cell architecture, electrode geometry and current collection pathways. A more in depth understanding of how photocurrent and photovoltage extraction can be optimised over large active areas is urgently needed. Another key factor suppressing conversion efficiencies in large area cells is the relatively high sheet resistance of the transparent conducting anode - typically indium tin oxide [2]. Hence, to replace ITO with alternative transparent conducting anodes is also a high priority on the pathway to viable module-level organic solar cells.

In our paper we will focus on large area devices relevant to sub-module scales - 5 cm ? 5 cm monolithic geometry. We have applied a range of experimental techniques to create a more comprehensive understanding of the true device physics and define sensible boundary conditions for anode sheet resistance that could help make large area, monolithic organic solar cells more viable [3]. By employing this knowledge, a novel transparent anode consisting of molybdenum oxide (MoOx) and silver (Ag) is developed to replace ITO and PEDOT-free large area solar cell sub-modules, acting as both a transparent window and hole-collecting electrode. The proposed architecture and anode materials are well suited to high throughput, low cost all-solution processing [4].

References:

[1] M. A. Green, K. Emery, Y. Hishikawa, W. Warta, E. D. Dunlop, Prog. Photovolt: Res. Appl. 2012, 20, 12.

[2] B. Muhsin, J. Renz, K.-H. Drüe, G. Gobsch, H. Hoppe, Phys. Status Solidi A 2009, 206, 2771.

[3] H. Jin, A. Pivrikas, K. H. Lee, M. Aljada, M. Hamsch, P. L. Burn, P. Meredith, Adv. Energy Mater. 2012, DOI:10.1002/aenm.201200254.

[4] H. Jin, C. Tao, M. Velusamy, M. Aljada, Y. Zhang, M. Hamsch, P. L. Burn, P. Meredith, Adv. Mater. 2012, 24, 2572.

8555-33, Session 7

Improve the open-circuit voltage of organic photovoltaic devices with PCDTBT: PCBM heterojunction

Weimin Li, Jinchuan Guo, Shenzhen Univ. (China)

We fabricated the heterojunction organic photovoltaic devices with PCDTBT as donor and different fullerene derivatives with different LUMO energy levels and side chains as acceptor, and investigated the effect of interfacial morphology and temperature on open circuit voltage. The temperature dependence of current voltage characteristics was analyzed by an equivalent circuit model. The results suggest that open circuit voltage is relatively insensitive to interfacial morphology, and the short circuit current was a function of interfacial area. The origin of open circuit voltage is ascribed not only to the relative the highest occupied molecular orbital level of a PCDTBT and the lowest unoccupied molecular orbital level of different fullerene energy gap but also to the electronic couplings between fullerene and fullerene, PCDTBT and different fullerene.

8555-34, Session 7

Design of planar lightwave interleavers based on Echelle gratings structure

Wenkai Liu, Baoqun Li, Xiaowei Dong, North China Univ. of Technology (China)

Planar lightwave interleavers, playing the multiplexing/demultiplexing function, are the key components in the dense wavelength division multiplexing (DWDM) systems. However, the device design and the processing errors have significant influence on the device performance, such as insertion loss and crosstalk with the increase in the number of the device channels and the decrease in the channel spacing. This paper reports the design procedure of planar lightwave interleavers based on Echelle gratings structure, introduces two methods to eliminate the device aberration which are two-point aberration-free design and elliptical grating facets design respectively. The device crosstalk and insertion loss is relatively large when the interleavers are working at higher diffraction series. Proper aberration Compensation design can effectively reduce the device insertion loss and crosstalk. Aberration compensation design includes two-point aberration-free design and high order aberration compensation design [15]. The two-point aberration-free design can be achieved by changing the location of the center point of Echelle grating facet. Higher-order aberration correction can be achieved by adjust the shape of each grating facet. The device performance compensation has been compared by simulation before and after aberration compensation. The 50/100GHz and 100/200GHz interleavers on the SOI (Silicon-on-insulator) materials are fabricated, whose actual experiment results match quite well with theoretical analysis. What's more, compared with other solutions, the Echelle Gratings Structure planar lightwave interleavers are smaller and more compact. Moreover, Echelle gratings are fabricated with the conventional semiconductor processing, suitable for mass production and reducing component cost, and easily to be integrated with other semiconductor optoelectronic devices to achieve monolithic integration.

Conference 8556: Holography, Diffractive Optics, and Applications V

Monday - Wednesday 5 -7 November 2012

Part of Proceedings of SPIE Vol. 8556 Holography, Diffractive Optics, and Applications V

8556-1, Session 1

Transparent 3D display for augmented reality (Invited Paper)

Byoungho Lee, Jisoo Hong, Seoul National Univ. (Korea, Republic of)

Augmented reality (AR) is a recently developed concept that overlays the artificial data onto various types of sensory input to human from real world. Especially AR display, which deals with the visual information, is actively investigated among various fields. In this paper, we demonstrate the transparent 3D display systems, based on the principle of integral imaging, which are applicable to projection-type AR display or the optical see-through head mounted display (HMD).

Proposed projection-type transparent 3D display is based on the concave half mirror array (CHMA). CHMA is a thin transreflective sheet whose shape is the 2D array of concave mirrors. Supported by the sufficiently thin thickness, CHMA bypasses the real world scene behind the structure. By projecting proper elemental image onto the CHMA, the 3D image is reconstructed by reflection because of concave mirror array structure, resulting in the mixture of 3D virtual image and real world scene.

We will also demonstrate the integral floating system adopting convex half mirror to implement the optical see-through HMD. As will be discussed in the presentation, addressing accommodation response to farther distance, using integral imaging, requires the pixel pitch of display device to be reduced. The convex half mirror effectively reduces the pixel pitch of the display, which, in turn, extends the addressable accommodation response to farther distance resolving accommodation mismatch problem of optical see-through HMD.

In the presentation, viable implementation methods of proposed scheme will be presented. And the characteristics of the proposed methods will be discussed with the implemented prototypes.

8556-2, Session 1

Fourier holographic display system of three-dimensional images using phase-only spatial light modulator

Hao Zhang, Qiaofeng Tan, Guofan Jin, Tsinghua Univ. (China)

We propose a holographic 3D display system which can produce images with adjustable viewing parameters and eliminated zero-order interruption. The 3D scene is generated from a 3D CAD tool, and point source algorithm with anti aliasing technique is used to generate the holograms. A two-step model is introduced in the computing to generate precise Fourier holograms. A phase-only spatial light modulator (SLM) is used in the optical reconstruction, which can replay clear images for 3D diffusive objects. During optical reconstructing, the viewing angle and image size of the system can be adjusted by changing the parameters of the replay lens. A filter is introduced in the replay system to eliminate the zero-order interruption and increase the 3D image quality. Optical experiments are performed, and the results show that our proposed holographic display system can produce noiseless 3D image reconstructions clearly.

8556-3, Session 1

Comparative analysis on light field reconstruction characteristics of autostereoscopic three-dimensional display technologies (Invited Paper)

Jae-Hyeung Park, Chungbuk National Univ. (Korea, Republic of)

Autostereoscopic three-dimensional displays present three-dimensional images to users without requiring special glasses. Motivated by a success of glasses-type stereoscopic three-dimensional displays, various autostereoscopic display techniques have been actively developed in recent years. Multi-view techniques which project different view images to different viewpoints are considered as practical solution in current panel resolution. Integral imaging which reconstructs light ray field without specific viewpoints and holography which reconstructs wave front using coherent optics are also considered as candidate technologies for achieving more realistic three-dimensional displays.

In this presentation, we provide a comparative analysis on image characteristics of these autostereoscopic three-dimensional displays. For a unified comparison, we analyze light field reconstructed by multi-view, integral imaging, and holography. Due to different optical configuration and light source coherency, these techniques reconstruct the desired light field with different spatial and angular sampling, which eventually affects the image quality and viewing limitations. By analyzing light field reconstructed by three techniques, it is expected that not only image characteristics of individual technique can be understood but also optimum technique for a given application can be identified.

8556-4, Session 1

360-degree viewable volumetric 3D floating display system

Wenping Pan, Nanjing Univ. of Aeronautics and Astronautics (China)

A novel spatial three-dimensional (3D) display system is proposed in this paper. The proposed system takes advantages of both volumetric 3D display and floating display technologies. Volumetric 3D display is capable of preserving all physiological and psychological depth cues for human vision system, and presenting 3D images with true physical depth. Floating display has the capability of transferring images from imaging mediums into free space and making penetrable human-computer interaction (HCI) enabled. We studied the optical path for static volumetric display based on spatial matrix of addressable crystal scatters, which are cracked as spatial voxels embedded in a glass cube by a technology called laser induced damage, and designed a GPU-based algorithm for generating depth-coded two-dimensional (2D) images according to the distribution of the scatters. Depth-coded 2D image plays a role on trading off 2D solution of projector in the optical path to get the third dimension for volumetric display. We also studied the scheme for floating display based on convex mirrors and designed several experiments for the prototype evaluation. Experimental results demonstrate that, in the prototype, directly penetrable objects can be displayed with true three dimensions at a refresh rate high up to 60 Hertz, and can be observed from any viewpoints simultaneously by multiple users, without any special viewing aids.

8556-5, Session 2

3D LED display without glasses and viewer responses (*Invited Paper*)

Hirotsugu Yamamoto, Shiro Suyama, Univ. of Tokushima (Japan)

Light-emitting diode (LED) panel is suitable for public television and large digital signage because of its high brightness and low energy consumption. Large LED televisions enable many audiences to enjoy on-the-spot broadcasting of big events, including Olympic games and World cup soccer games. Showing these sports scenes in 3D improves sense of reality and excitement. In this invited paper, we describe our developments of 3D LED display and report movements and accommodation of a viewer when viewing the developed 3D LED display without glasses.

We have developed a stereoscopic large television system by use of a full-color LED panel and binocular cameras. In 1998, we developed a full-color stereoscopic 3D (S3D) LED display with polarization glasses. Then, a full-color S3D display without glasses was realized by use of a parallax barrier. By introducing black regions between LED lamps, viewing zones have been enlarged so that a variety of audiences enjoy the S3D images. We have investigated viewer's perception of depth and movements to evaluate the viewing zones. A new configuration of a parallax barrier, called an aperture grille, has been developed in order to enlarge the viewing angle. We have realized 140-inch full-color S3D LED display without glasses.

As well as reporting the developments of S3D display, we propose a viewing-zone control technique an LED panel. The viewing-zone control architecture is utilized for S3D display without pseudostereoscopic viewing positions and 2D LED display with multiple viewing distances.

8556-6, Session 2

Binocular and multi-view parallax images acquisition for three-dimensional stereoscopic displays

Hongsheng Ge, Xinzhu Sang, Tianqi Zhao, Jinhui Yuan, Junmin Leng, Beijing Univ. of Posts and Telecommunications (China); Ying Zhang, Minzu Univ. of China (China); Binbin Yan, Beijing Univ. of Posts and Telecommunications (China)

Three dimensional (3D) displays have become an attractive frontier research area in the last decade. Except for replicating the light distribution of the 3D scene, the basic idea for the 3D experience is the stereoscopic vision, which means that the viewer observes a scene with two similar but slightly different visions with left and right eyes, and the brain processes the parallax information to be perceived in 3D. The scenes displayed in 3D displays are captured by stereoscopic image acquisition, and the contents obtained by stereoscopic image acquisition are finally shown in 3D displays.

In the paper, two and multiple cameras with the same intrinsic parameters are used to capture a 3D scene from slightly different directions. Not the same as before, we demonstrated that by setting the proper distance between the cameras and the location of the convergent point in this capturing configuration, the displayed 3D scene with the appropriate stereo depth and the expected effect in front of and behind the display screen can be obtained directly. The quantitative relationship between the parallax and the parameters of the capturing configuration with two cameras is presented. The capturing system with multiple cameras for acquiring equal parallaxes between the adjacent captured images for the autostereoscopic display system is also discussed. We have experimented to attest the proposed method. The parallax images captured using the calculated parameters for the 3D display system shows the expected results, which can provide the viewers the better immersion and visual comfort without any extra processing.

8556-8, Session 2

Relationship between individual maximum disparity and individual comfort disparity in visual comfort of stereoscopic 3D contents

Zaiqing Chen, Junsheng Shi, Yunnan Normal Univ. (China); Yonghang Tai, Yunnan Normal Univ (China)

It is well known that some viewers experience visual discomfort when looking at stereoscopic displays. The disparity is a key factor influencing visual comfort, and there is a comfortable disparity for a person. In this paper, we explore the comfort zone of horizontal disparity, which correlates with the optimal viewing distance, as a function of the maximum disparity for an individual. Firstly, the individual maximum disparities of 14 subjects were measured. Then the subjects were asked to rate the comfort levels of a 3D video sequence with different disparity levels, to evaluate the individual comfort disparities. The results show that as the individual maximum disparity increased, the corresponding comfort disparity increased, and we found a correlation coefficient of $r=0.946$. The average ratio between the individual comfort disparity and the individual maximum disparity was approximately 0.72, and this ratio can be used for an individual to determine the optimal viewing distance by a rapid method.

8556-9, Session 3

10-Gbps RSOA-based upstream transmission in WDM-PON with MZI-based equalizers

Ting Su, Beijing Univ. of Posts and Telecommunications (China)

Reflective semiconductor optical amplifier (RSOA) has been utilized extensively in wavelength-division multiplexed passive optical network (WDM-PON). Not only does the RSOA amplify and re-modulate the signals, but it also provides colorless optical network units (ONUs) to realize cost effective wavelength adaptability. However, the modulation bandwidth of RSOA is usually limited to 2.5GHz. In this paper, we propose a 10-Gbps uplink transmission of directly modulated RSOA with the help of Mach-Zehnder Interferometer (MZI) serving as an optical equalizer as well as a periodic filter. The model of RSOA is proved to be able to simulate the commercial RSOA accurately by fitting the dependence of the small signal frequency response (SSFR). The 3dB-bandwidth of RSOA with MZI increases to >10GHz and the equalization effect is improved considerably. The transmission function of MZI is certified to be a two-tap optical equalizer with delay time, coupler factor and initial phase shifts. Given the configuration of the system, proper span of the MZI-induced delay time and initial phase shift have been identified to improve the BER and the eye diagram. A better received sensitivity of -16dBm at BER=1.1?10⁻³ which is the threshold of the Reed-Solomon (255, 223) is obtained after 25-km SSMF transmission. Experimental and simulation results show that the MZI with proper delay time and initial phase shift can improve the transmission performance. We also demonstrate the multiple WDM channels anchored at the 100-GHz can use a single MZI to equalize the upstream signal.

8556-10, Session 3

Performance analysis of a novel super-orthogonal modulation scheme for high speed optical OFDM system

Qi Zhang, Xiangjun Xin, Lijia Zhang, Yongjun Wang, Chongxiu Yu, Nan Meng, Houtian Wang, Beijing Univ. of Posts and Telecommunications (China)

High speed optical communication is one of the research hotspot

about optical communication field in the world at present. A novel super-orthogonal modulation method based on quadrature amplitude modulation (QAM) and frequency shift key (FSK) is proposed for high speed optical orthogonal frequency division multiplexing (OFDM) system. The coding modulation scheme and demodulation-decoding scheme are designed. The frequency spectrum utilization and transmission performance of optical OFDM system with proposed super-orthogonal modulation method is simulated and analyzed. It is also researched that bit error rate change with different code type in optical communication. All the research result will lay the foundation of optical communication realization with high speed, large capacity and high efficiency transmission.

8556-11, Session 4

Frequency shifts of spectral lines induced by scattering of a truncated polychromatic plane wave

Jia Li, Yali Qin, Hongliang Ren, Zhejiang Univ. of Technology (China)

Within the accuracy of the first-order Born approximation and the paraxial assumption of light waves, the analytical expressions are deduced for the spectral density of light waves which scatter from a quasi-homogeneous (QH) medium illuminated by a truncated plane wave. It is shown that once a polychromatic plane wave firstly diffracts through Young's pinholes and then scatters from QH medium, the spectral lines of the resultant field generally displays red shift toward the lower frequency, closely depending on the scattering angle, the correlation length of the scatterer as well as the ratio of the spacing between pinholes to the distance between opaque screens and the scatterer i.e. d/R . It is further indicated that the red shift of spectrum of scattered light would convert into the blue shift of spectral lines provided that the correlation length of the scatterer fulfills an enough small value. Effects of these parameters on the evolution of frequency shifts of spectral lines are specifically analyzed via the numerical approach, respectively. The theoretical results obtained in this paper may be of great significance to various experimental aspects, e.g. the measurement of spectra of scattered light or the determination of the internal structures of unknown scatterer.

8556-12, Session 4

All-optically manipulated plasmonic microscope (Invited Paper)

Rong Wang, Chonglei Zhang, Changjun Min, Jing Bu M.D., Hui Fang, Yong Yang, Nankai Univ. (China); Siwei Zhu, Nankai Univ. Affiliated Hospital (China); Xiaocong Yuan, Nankai Univ. (China)

A dynamic all-optically controlled surface plasmon polaritons (SPP) novel high-performance multi-function optical microscope, combining optical microscopic imaging, bio-sensing and surface enhanced Raman Scattering (SERS) in a single microscopic system, is presented in this talk. This new configuration uses phase shift of SPP standing wave generated from sub-wavelength slit arrays embedded in a thin silver film to achieve super-resolution wide-field microscopic imaging; phase sensitive surface plasmon resonance (pSPR) bio-sensing technology based on differential phase measurement between radially polarized (RP) and azimuthally polarized (AP) beams to obtain an ultra-high sensitivity and a wide dynamic range simultaneously; the coupling between the localized surface plasmon (LSP) of metallic nano-particles and SPP virtual probe with longitudinal electric field to significantly improve the sensitivity of SERS system. With the integration of these three technologies in a single microscopic configuration, the system can achieve wide-field super-resolved imaging of biological specimens, ultra-high sensitivity for molecule detection and real-time monitoring for reaction process of biological samples simultaneously, fulfilling the requirement of multi-parameter multi-function real-time in-situ

measurement of biological samples. The new microscopic scheme has great importance in real-time dynamic study on nano-scale biological living cells, and may therefore leads to a strong impact in the design of next-generation optical microscope.

8556-13, Session 4

Impact of surface waves on the electromagnetic enhancement by a metallic nano-cavity (Invited Paper)

Haitao Liu, Zhiwen Zeng, Nankai Univ. (China)

Enhancement of electromagnetic field has important applications such as the surface enhanced Raman scattering (SERS) [1]. Metallic nano-cavities have been found to be promising structures that can achieve a giant electromagnetic enhancement [2]. It has been shown that nano-apertures under external illumination can launch surface waves such as the surface plasmon polariton (SPP) [3]. Although it has been shown in previous literatures that SPPs can play an active role in the electromagnetic enhancement [4], their exact role in enhancing the field concentration or resonance has not been clarified at a quantitative level. In addition, the impact of another so-called quasi-cylindrical wave (CW) [5] on electromagnetic enhancement is rarely addressed. In this report [6], we consider a T-shaped metallic nano-groove to show the impact of surface waves on the electromagnetic enhancement by a nano-cavity. It is found that a two-fold higher enhancement factor of electric field can be achieved compared with a single bare groove without the top trench. By developing an intuitive model that explicitly incorporates the waveguide mode resonance in the central groove and the launching and scattering of surface waves in the top trench, we quantitatively show that the improved field enhancement is attributed to the coupling of both surface waves that are collected by the top trench into the central groove. The present work can be helpful for clarifying the physics of the surface-wave driving electromagnetic enhancement and for intuitively designing relevant devices.

8556-14, Session 4

Theory on the quasi-cylindrical wave diffracted by a sub-wavelength metallic slit and its enhancement by surface plasmon resonance

Yann Gravel, Yunlong Sheng, Univ. Laval (Canada)

Light scattering by a nano-sized slit engraved in metallic surface is an elementary problem of optical diffraction. In addition to the Surface Plasmon Polariton (SPP) mode, experiments found an extra field close to the slit. Its physical explanation gave rise to debate with confusing names as creeping wave, quasi-cylindrical wave, transient SPP and Norton wave. In fact, the problem involves calculating the field of an electrical dipole on a planar metallic surface and dates back to the work of Sommerfeld, but has no known closed solution. Here, we present, for a nano-slit diffraction, a simple closed form solution consisting of a SPP mode and a scattered field. The asymptotic behaviour of the solution close to the slit corresponds to the extra-field previously observed and takes the form of a flattened cylindrical wave. Farther from the slit, the solution behaves as a first order cylindrical harmonic propagating outward from the slit with a diffraction shadow along the metallic surface. Our solution clearly shows that the observed extra-field is not a surface wave but rather the asymptotic behaviour of the 2D scattered field over the metallic surface. Furthermore, the solution for the scattered field close to the slit shows potential strong resonant enhancement, depending on the materials and incident wavelength. The theory is consistent with previous experimental and numerical results, as well as FDTD simulations, closes the current debate and will be useful in the design of nano-plasmonic devices.

REFERENCES

- [1] W. L. Barnes, A. Dereux, T. W. Ebbesen, "Surface Plasmon subwavelength optics", *Nature* 424, 824-830 (2003);
- [2] S. A. Maier, *Plasmonics: Fundamentals and applications* (Springer, Berlin, 2007);
- [3] G. Gay, O. Alloschery, B. Viaris De Lesegno, C. O'Dwyer, J. Weiner, and H. J. Lezec, "The optical response of nanostructured surfaces and the composite diffracted evanescent wave model", *Nature Phys.* 2, 262-267 (2006);
- [4] G. Gay, O. Alloschery, J. Weiner, H. J. Lezec, C. O'Dwyer, M. Sukharev, T. Seideman, "Surface quality and surface waves on subwavelength-structured silver films", *Phys. Rev. E* 75, 016612 (2007);
- [5] P. Lalanne, J. P. Hugonin, "interaction between optical nano-objects at metallo-dielectric interfaces", *Nature Physics* 2, 551-556 (2006);
- [6] B. Ung, Y. Sheng, "Optical surface waves over metallo-dielectric nanostructures: Sommerfeld integrals revisited" *Opt. Express* 16, 9073-9086 (2008);
- [7] P. Lalanne, J. P. Hugonin, H. T. Liu, B. Wang, "A microscopic view of the electromagnetic properties of sub- λ metallic surfaces", *Surface Science Reports* 64, 453 (2010);
- [8] G. Lévêque, O. J. F. Martin, J. Weiner, "Transient behaviour of surface plasmon polaritons scattered at a sub-wavelength groove", *Phys. Rev. B* 76, 155418 (2007);
- [9] Y. Gravel, Y. Sheng, "Rigorous solution for the transient surface plasmon polariton launched by sub-wavelength slit scattering", *Opt. Express* 16, 21903-21913 (2008);
- [10] A. Y. Nikitin, s. G. Rodrigo, F. J. Garcia-Vidal, L. Martín-Moreno, "In the diffraction shadow: Norton waves versus surface plasmon polaritons in the optical region", *New Journal of Physics* 11, 123020 (2009);
- [11] A. N. Sommerfeld, "Propagation of waves in wireless telegraphy", *Ann. Phys. (Leipzig)* 28, 665-737 (1909);
- [12] J. Zenneck, "Propagation of plane EM waves along a plane conducting surface", *Ann. Phys. (Leipzig)* 23, 846-866 (1907);
- [13] K. A. Norton, "The propagation of radio waves over the surface of the earth and in the upper atmosphere", *Proc. IRE* 24, 1367-1387 (1936);
- [14] R. E. Collin, "Hertzian dipole radiating over a lossy earth or sea: Some early and late 20th-century controversies", *IEEE Ant. And Prop. Mag.* 46, 64-79 (2004)

8556-15, Session 4

Enhanced subwavelength light spot of vertically-tapered metallic aperture based on plasmonics

Junbum Park, Kyungho Kim, Il-Min Lee, Dawoon Choi, Byoungcho Lee, Seoul National Univ. (Korea, Republic of)

We propose an approach that improves the characteristics of a subwavelength light spot with a tapered metallic aperture without increment of the subwavelength spot size. Two advantageous features of the proposed tapered structure are investigated: At first, by enlarging the effective area of the aperture, the structure could collect more light compared to the regular one. Thus the funneled light contributes to the field enhancement. Furthermore, the tapered edges of the exit surface of the aperture provide confined field, a wedge mode, which is bounded strongly and enhances the local electric field around the edge of the aperture. The enhanced characteristics of subwavelength spot in vertically-tapered aperture, including peak intensity, power throughput, and full width half maximum (FWHM) were obtained numerically using finite difference time domain (FDTD) method. The proposed device is fabricated using conventional planar fabrication techniques and focused ion beam (FIB) milling to realize the tapered structure. The relative tapered angle-dependent enhancements are presented with experimental and quantitative demonstrations of the proposed structure.

8556-16, Session 5

Tunable nano-pattern generation based on surface plasmon polaritons (*Invited Paper*)

Chinhua Wang, Soochow Univ. (China); X. Fy, Zhejiang Normal Univ. (China); Yiming Lou, Cao Bing, Soochow Univ. (China)

We present a numerical observation of a tunable 1D and 2D nano pattern generation and photolithography technique based on a surface plasmon resonant cavity formed by a metallic grating and a metallic thin-film layer separated by a photoresist layer. The tuning capability is implemented by varying the cavity length combined with the polarization of the incident light, from which different surface plasmon interferometric patterns with inherently higher optical resolution than that of conventional surface plasmon techniques are generated in the cavity of photoresist layer. The physical origin of the tunability is analytically confirmed by the dispersion relation derived from the cavity system as well as the interferometric behaviors of the surface plasmon polaritons. The technique opens a new possibility to generate tunable ultra-deep subwavelength patterns by using a fixed diffraction-limited mask with capability of large area, deep exposure depth and flexibility of arbitrary 2D patterns.

8556-17, Session 5

Metallic superlens design using the long-range SPP mode cutoff technique

Guillaume Tremblay, Jing Wang, Yunlong Sheng, Univ. Laval (Canada)

In applications of the metallic near-field imaging superlens to nano-scale resolution lithography, the image quality is a critical issue. Moreover, the object as a metal coated photomask forms an additional metal layer, which can also support the Surface Plasmon Polariton (SPP) modes. Although the fundamental Fourier analysis still apply with the transfer function computed by the transfer matrix, the SPP resonance and the SPP waveguide theory, the object field should be computed by the scattering of nano-scaled object detail, which is related to object topographic profile in a complex manner. In the case of metal object, the presence of neighbouring object points impacts the formation of the electrical dipole at that point. As a result, one uses no longer the impulse response, but the two-slit image resolution as a measure of merit. To avoid designing the metallic superlens by random trials in the numerical FDTD method, we find the transfer function of the superlens represents, in many cases, is determined by the SPP waveguide modes along the superlens layer. We propose the long-range SPP mode cut-off technique to flatten the transfer function. We model the metallic superlens with metal object as a dielectric multi-reflecting resonator formed by two metal layers, which are themselves multi-reflecting SPP resonator. We trim the transfer functions of the three resonators by adjusting the thicknesses and the permittivity of each layer to optimize the total transfer function. The genetic algorithm is used for the optimization. Design examples are all confirmed by the real image computed with FDTD.

8556-18, Session 6

Digital holographic display for a single user (*Invited Paper*)

Joonku Hahn, Kyungpook National Univ. (Korea, Republic of); Hwi Kim, Korea Univ. (Korea, Republic of)

Digital holography has been regarded as the technology to realize an ideal three-dimensional display. Even though this technology was invented a number of decades ago, many people think there are still many problems for holographic display to be commercialized. The main problem is that the holographic displays generally need enormous data

capacity in comparison with other traditional display. But spatial light modulators have only small space-bandwidth product. So, there is a trade-off between screen size and field of view in holographic display. There have been two major approaches to achieve a reasonable screen size. One is to increase the space-bandwidth product of spatial light modulators. The other is to sacrifice the field of view to get large screen size. The latter has an advantage to design a system with small spatial-bandwidth product. So it is possible to build a system with spatial light modulators already in market. For this approach, we need to define our target as a holographic display for a single user. In this paper, we will introduce two kinds of digital holographic displays which are recently studied. One is a holographic display with a large-scale spatial light modulator and the other is a holographic display with a small-scale spatial light modulator and projection optics.

8556-19, Session 6

In-line phase shifting digital holography based on LCOS

Spozmai Panezai, Dayong Wang, Jie Zhao, Yunxin Wang, Beijing Univ. of Technology (China)

The phase shifting digital in-line holographic microscopy is a powerful method for 3-D imaging with high resolution and capabilities of tracing moving objects. The phase shifting removes the distortion coming from twin images while optimizing the space-bandwidth product of the detector due to the absence of carrier fringes in the recorded hologram which limits the resolution in case of the off-axis configuration. In this paper the liquid crystal on silicon spatial light modulator (LCOS) is used to introduce the phase modulation in the reference beam in the in-line configuration based on Gabor like setup. In this experiment the object is placed between condenser lens and LCOS, so the wave front diffracted from the object is focused on the LCOS which changes only the phase of the DC term (non diffracted light) of the object's spectrum. So that we will record the phase shifted holograms in time sequence by modulating the LCOS pixel which spatially coincides with DC term. Then the conventional phase shifting algorithm is applied to recover the complex amplitude distribution of the object and it is digitally propagated to the object plane. The obtained experimental results are then compared with the results obtained from Gabor's approach. The comparison will show that the proposed method has a better image quality and even works for a highly non-transmissive object.

8556-20, Session 7

Common-path phase-shifting digital holographic microscopy (*Invited Paper*)

Baoli Yao, Peng Gao, Junwei Min, Xi'an Institute of Optics and Precision Mechanics (China)

Digital holographic microscopy (DHM), combining optical interferometry and microscopy, is a whole-field optical technique for measuring profile, thickness or refractive index distribution of microscopic specimen. It has the advantages of nondestructive, high-resolution, high measurement speed, requiring no extra preparation on specimen. Thus, it has been widely used in biology, medical science, micro-fabrication industry, and so on. To solve the problems of stability, spatial resolution and speed, we investigated the DHM based on common-path configuration and parallel phase-shifting mechanism.

A common-path and in-line point-diffraction interferometer for quantitative phase microscopy is proposed. The magnified tested wave is split by a diffraction grating into two copies. One copy is recast for reference wave through pin-hole filtered in the Fourier plane; the other one is still used as object wave. After diffracted by the second grating, the two waves propagate on-axis into the CCD camera. Achromatic phase-shifting is implemented by linearly moving one of the two gratings in grating vector direction. The setup has advantages of less sensitive to environmental vibration due to the common-path configuration.

A common-path and parallel phase-shifting point-diffraction interference microscopy is proposed based on a cube beamsplitter pair. Together with the parallel phase-shifting scheme, slightly-off-axis interferometry for microscopy is performed, which suppresses dc term by subtracting the two phase-shifting holograms from each other. The setup is stable due to its common-path configuration, and can be used for measuring moving object or dynamic process.

Zernike phase contrast microscopy is extended to perform quantitative phase measurement for microscopic object by combining with the phase-shifting technique. The extended microscopy uses dozens of periodic point-like light sources on a ring for illumination, and corresponding point-like phase-shifters for phase retarding the undiffracted component of object wave. By shifting the phase shifters with different height (to cover the undiffracted components), the phase shifting can be performed. The method has low coherent noise level due to the partially-coherent illumination. Besides, it has higher lateral resolution because of the synthetic-aperture of the oblique illumination.

8556-21, Session 7

A JPEG-based enhanced compression algorithm of digital holograms

Hanming Yu, Zibang Zhang, Jingang Zhong, Jinan Univ. (China)

Digital holography is a successful technique for recording and reconstructing 3-D objects. But digital holograms contain a large amount of information and occupy large amounts of bandwidth and memory space. For the efficient storage and transmission of digital holograms, an appropriate compression algorithm is necessary. We present a JPEG based enhanced compression algorithm of digital holograms as a modified version of the general JPEG encoder. Since digital holograms, unlike general images, are characterized by most of the information concentrated at their first-order component, to compress digital holograms only with their first-order component is available. JPEG is a commonly used method of lossy compression for digital images and based on human visual system. To make the general JPEG fit the character of digital holograms, we propose the JPEG based algorithm to obtain more efficient compression ratio and maintain the compatibility. The algorithm divides digital holograms into 8*8-blocks and performs 2D-DCT(discrete cosine transform) on each of them, as the general JPEG. Then it extracts the low-frequency section where the first-order component locates with an adaptive mask according to the DCT coefficients distribution. Next, the algorithm quantizes the masked coefficients with the general JPEG quantization table and encodes them with Huffman encoding finally. Compatible with the general JPEG, the compressed holograms can be directly decoded by the general decoders. Our simulation and experimental results show that this algorithm has higher compression ratio than the general JPEG and more accurate retrieved phase while the compression is equal.

8556-22, Session 7

Effect of phase-shift step on hologram reconstruction in Fresnel incoherent correlation holography

Hao Chen, Yuhong Wan, Tianlong Man, Zhuqing Jiang, Dayong Wang, Shiquan Tao, Beijing Univ. of Technology (China)

Fresnel Incoherent Correlation Holography (FINCH) enables holograms to be created from incoherent light illumination of 3D objects. The optical setup of FINCH is usually simple and compact owe to its in-line geometry while the reconstruction of hologram suffers from the obstruction of zero-order item and twin image. Phase-shift technology is combined with FINCH in order to obtain zero-order-free and twin-image-free reconstruction. Three-step phase-shifting is adopted in all the publications of FINCH and the application of other multi-step phase-shift technology in FINCH are not investigated yet. The Fresnel holograms are sequentially recorded with different multi-step

phase shift (including four, three, and two-step) to form the complex hologram and the quality of the reconstructed images are compared by simulations and experiments respectively in this study. The quality of the reconstructed images is evaluated by resolution of system and the single-noise ratio(SNR). Although various noise would be induced by the optical elements and the experimental environment in practice, four-step phase-shifting technology still offer the best reconstructed image. According to the results, It's founded that four-step phase-shifting provides the best quality of the reconstructed image but the system resolution is not different from two, three-step phase-shifting. At present, multi-step phase-shifting in FINCH is realized by multi-exposure sequentially, therefore it is not suitable for imaging of the dynamic samples and processes. The feasibility and reconstruction characteristics of multi-step phase-shifting with single-shot in this system is analyzed.

8556-24, Session 7

Detection of silver ions induced morphological changes on E. coli membrane using digital holographic microscopy

Farzaneh Borji Monfared, Ali Mohebbi, Zanjan Univ. (Iran, Islamic Republic of); Ali-Reza Moradi, Institute for Advanced Studies in Basic Sciences (Iran, Islamic Republic of) and Optics and Photonics Research Ctr. (Iran, Islamic Republic of)

The Digital holographic microscopy is a non-destructive and quantitative phase contrast microscopy technique that is suitable for marker-free investigations of living cells and organelles. In this work, we utilize this technique and also conventional video microscopy to detect the dynamic morphological changes of bacteria membrane in presence of silver ions. Silver ions have shown strong inhibitory effects on bacteria and can be used as antibacterial. We used E. coli as a sample and the influences of the ions were compared in terms of the variations in volume and roughness of E. coli for different concentration of silver ions in the buffer and various incubation times. In a controlled experiment using a microinjecting pump the concentration of antibacterial is increased, the movement of a single or a set of bacteria are monitored live, and successive digital holograms are recorded. The recorded holograms by digital camera can be post-processed to three dimensional reconstruction of the samples and measurement of quantitative structural changes in various interacting time of the bacteria.

8556-45, Poster Session

Numerical simulation of polarization dependent characteristics of the structured thin-films phase grating

Yiyu Li, Chuan Hu, Yuchen Wu, Haihua Feng, Jiaojie Chen, Wenzhou Medical College (China)

Diffraction efficiency of the structured thin-films phase grating (STFPG) at the visible wavelength is analyzed by the rigorous coupled wave analysis (RCWA) method demonstrating that the TM polarization can be separated from the 0th transmitted order of the TE polarization by ± 1 st order diffraction. The far field diffraction pattern is simulated by the finite-difference time-domain (FDTD) method to show the polarization beam splitting process of the STFPG at wavelength of 633nm. In the near field, polarization dependent Talbot effect of the STFPG is also elaborated. FDTD simulations reveal that the spatial distribution of the interference fringes forming the self-image of the STFPG can be shifted by a half of grating period by changing the incident wave polarization within a particular wavelength range.

8556-46, Poster Session

A novel iterative computation algorithm for kinoform of 3D object

Xiaoyu Jiang, Pei Chuang, Yantao Zong, Jia Wang, Academy of Armored Force Engineering (China)

A novel method for computing kinoform of 3D object based on traditional iterative Fourier (GS) algorithm is proposed in this paper. Kinoform is a special kind of computer-generated holograms (CGH), which has very high diffraction efficiency since it modulates the phase of illuminated light only and doesn't have disturbance from conjugate image. The traditional GS arithmetic assumes that reconstruction image is in infinity area(Fraunhofer diffraction region), and ignores the deepness of 3D object ,so it can only calculate two-dimensional kinoform.The proposed algorithm in this paper divides three-dimensional object into several object planes in deepness direction and treat every object plane as a target image, then iterative computation is carried out between one input plane(kinoform) and multi-output planes(reconstruction images) .A space phase factor is added into iterative process to represent depth characters of 3D object, then reconstruction images is in Fresnel diffraction region. A lookup table is used to reduce the influence of phase factor operation to the speed of iterative calculation. Optics reproduction experiment of kinoform computed by this method is realized based on liquid spatial light modulator. Mean Square Error(MSE) and Structure Similarity(SSIM) between original and reconstruction image is used to evaluate this method. The experimental result shows that this algorithm computational and convergent velocity is fast and the result kinoform can reconstruct matching object plane in different distance with high precision under the illumination of plane wave. The reconstruction images provide space sense, which has three-dimensional vision effect. At last, the influence of space and shelter between different object planes to reconstruction image is also discussed in the experiment.

8556-47, Poster Session

Combination of electronic speckle pattern interferometry and digital image correlation for 3D deformation measurement

Xinghua Chai, Naiguang Lv, Xiaoping Lou, Beijing Information Science & Technology Univ. (China)

Electronic Speckle Pattern Interferometry (ESPI) and Digital Image Correlation (DIC) are two whole-field , non-contact experimental techniques that enable rapid and highly accurate 3-D measurements of scattering surfaces. Electronic Speckle Pattern Interferometry needs a phase-shifting setup and rotating the whole device for 3-D deformation measurement. These operations are especially inconvenient to data acquisition of deformations in three directions simultaneously and increase the system deviation. Digital Image Correlation using one CCD camera can acquire 2-D information of displacement. Another CCD camera needs recording speckle image simultaneously for 3-D measurement. The matching of images recorded by two CCD cameras may introduce extra deviation. The combination of the two techniques is an effective method to diminish these deviations and simplify experiments. Electronic Speckle Pattern Interferometry setup for out-plane measurement and Digital Image Correlation setup using one CCD camera for in-plane measurement constitute one measurement system. Three dimensions information of deformation can be recorded simultaneously. The former can measure 3-D deformations or shape of complex amplitude in nanometric level. The latter can measure small displacement in micrometric level. Thus matching for measurement ranges and precisions of the two techniques is very important. Key factors effecting the matching including laser wavelength, phase analysis of speckle fringe pattern, sub pixel fitting are discussed in this paper.

8556-49, Poster Session

Speckle reduction by spatial light modulator in digital holography

Puhui Meng, Dayong Wang, Shifeng Chang, Shiquan Tao, Beijing Univ. of Technology (China)

A speckle noise reduction method is proposed in digital holography using angular diversity based on phase only SLM (spatial light modulator) device. Laser as a light source, it has very high coherence, and is widely used in digital holograph systems. Coherent light illuminates the object and interfered by another coherent light called reference light. The interference pattern is recorded by CCD as the hologram. Since the speckle noise phenomena can be found in most of coherent light illumination conditions, so the laser character of the high coherence also brings the speckle noise into digital holography and greatly worsens the quality of holograms. In this paper, we analyzed the SLM device's working principle and discussed the speckle reduction method with speckle theory. This article mainly focuses on the method of changing the angles of the illumination light. We analyzed the relationship between the speckle phenomena and the illumination angle. By compared the maximum modulation angle that SLM device can reach with the essential minimum angle, we proved that phase only SLM device can perfectly modulate the illumination light and reduce system speckle noise in theory. With the help of SLM device, the illumination light could be modulated faster and more accurately than other methods. We constructed a digital holography setup with phase only SLM device. In experiments, a series of results of USAF test target were obtained, and the results showed that the speckle noise in digital holography system was obviously reduced by phase only SLM device and the speckle contrast ratio dropped to 36% of the initial value.

8556-50, Poster Session

Iterative partial quantization method for the error reduction of low-quantized kinoforms

Shiyuan Yang, Seiichi Serikawa, Kyushu Institute of Technology (Japan)

A kinoform with low phase modulation levels is desirable from the point of view for fabrication, but the quantization error will disturb the reconstruction seriously. Various optimization algorithms had been suggested and the iterative stepwise quantization method can reduce the quantization error much with few calculation time. In this study, we suggest an iterative partial quantization method to improve the performance of the conventional iterative stepwise quantization method. The strategy of stepwise quantization is to increase the quantization interval around the quantization values with the general Fourier repetition algorithm to concentrate the phase distribution around the quantization values so that the quantization error can be reduced. It is powerful for the error reduction of low-quantized kinoforms, but the phase distribution could not be concentrated to the phase quantization values completely, especially a number of phase values remain far from the quantization values. We modify the conventional iterative stepwise quantization method by using an iterative partial quantization method to decrease the phase distribution far from the quantization values. The iterative partial quantization method uses the same process of stepwise quantization but only partial points of kinoform phase are quantized. This partial quantization gives a relaxation of kinoform phase constraint in the Fourier repetition. The conventional iterative stepwise quantization process is performed after the iterative partial quantization and the phase distribution far from the quantization values decreases so that the reconstruction error can be reduced.

8556-51, Poster Session

Research of fabricate large scale pulse compression grating by multiple exposure

Chaoming Li, Soochow Univ. (China)

Pulse compression grating plays very important role in the laser confinement fusion system. Along with the development of laser confinement fusion project, more and more large scale gratings are needed. Holographic technology is very important means to manufacture large scale gratings, but the scale of gratings is limited by the recording system. In order to fabricate large scale pulse compression grating, the method by exposure several times to fabricate large scale mosaic gratings is investigated in the paper. The method uses the recorded part of grating as a detecting standard to test the phase situation between the recording light wave and the recorded grating. By using stripes locking system to control the phase of light wave, the goal of manufacture large scale compression mosaic grating have been achieved. At last, the mosaic grating experiment is studied. The grating frequency is 1740lp/mm, the size of exposure unit is 200mm \times 200mm. The experiment results show that the method can achieve high precision alignment, and can be used to fabricate large scale grating.

8556-53, Poster Session

Defect mode in a one-dimensional photonic crystal with a dielectric-superconducting pair defect

Ji Jiang Wu, Jinxia Gao, Shandong Univ. of Technology (China)

The one-dimensional dielectric photonic crystals (PCs) with complex defect layers, consisting of superconducting (SC) and dielectric sublayers are theoretically studied. Transfer matrix method (TMM) has been used throughout this study. The influence of a substitutional defect on the transmittivity spectra is analyzed for normal incidence of light on the structure. The two-fluid model and wavelength-dependent dispersion formula were adopted to describe the optical response of the low temperature superconducting defect sublayer. The pronounced difference in the transmittivity spectra of the photonic crystals with right-handed (RH) and left-handed (LH) positions of the superconducting defect sublayer with respect to the dielectric defect sublayer is demonstrated. We have showed that in contrast to the usual defect modes, the position of the defect modes is nearly invariant with the position of the defect layer from one end to the other end of the PC. It is observed that, for the case of RH SC defect sublayer, the position of the defect mode and the transmittivity at the defect mode frequency strongly depend on the thickness of the superconducting sublayer as well as on the temperature. It is also shown that in contrast to the case of the PCs with RH SC defect, the defect modes of the PCs with LH SC defect sublayer are nearly invariant upon the change of the thickness of the superconducting sublayer and the temperature. This study may be valuable in designing optical devices.

8556-54, Poster Session

Effective design of diffractive optical elements for beam splitting with SA algorithm

Hui Pang, Shaoyun Yin, Qiling Deng, Institute of Optics and Electronics (China); Yongqi Fu, Univ. of Electronic Science and Technology of China (China); Chunlei Du, Institute of Optics and Electronics (China)

Simulated annealing algorithm (SA) can find the global optimal solution and is widely used for solving the stochastic optimization problems

in physics and engineering. Though the SA algorithm could achieve lower uniformity error and higher diffraction efficiency compared to the iterative Fourier transform algorithm in the design of the diffractive optical element (DOE), such as for beam shaping, pattern generation or beam splitting, the time taken by SA algorithm is unacceptable, for the large number of sampling point of DOE designing. By using the character of periodic DOE, an effective method for the design of phase only and quantized DOE for beam splitting with SA algorithm is presented. The relation of the parameters of the DOE including the sampling size, number of sampling point, divergence angle and output field size are analyzed, and the elimination method of high diffraction orders is given. It concludes that when the desired output field size only takes a quarter of the total diffraction field, the high diffraction orders could be eliminated effectively. Simulation result shows that this method could greatly reduce the time of beam splitter's design compared to the original method and keep the higher diffraction efficiency and lower uniformity error compared to the iterative Fourier transform algorithm.

8556-55, Poster Session

Computer simulation and optimization design of the holographic photonic crystal template fabrication process

Ying Liu, Academy of Armored Force Engineering (China)

According to the holographic multi-beam interference theory, three-dimensional (3D) holes structure can be recorded in photosensitive materials and 3D photonic crystals can be generated by filling in high refractive index materials. Among the fabrication approaches of photonic crystals, holographic lithography method has a number of advantages, e.g. ability to create large volume of periodic structures, the uniformity of period, and more degrees of freedom to control the structures. It has been demonstrated theoretically that 3D structures can be obtained by recording the interference patterns generated by four coherent laser beams on photosensitive materials. This technique produced defect free, nanometer-scale structures over large substrate areas in a single step fabrication. However, in four-beam interference approach, many factors in photonic crystals fabrication must be considered. Such as different included angle between two interference beams generates different lattice structure, the polarization directions of the beams affect the contrast of the interference fringes and make the shape and lattice structure changed with the polarization direction adjustment. For these reasons, the included angle between the beams, the polarization states of the beams and the intensity ratio must be adjustment simultaneously in the process of fabricating holographic photonic crystal templates. Based on the theory of lattice pattern simulation with multi-beam interference, the process of generation of holographic photonic crystal templates in photoresist is simulated by matlab program. The incident light direction, beam polarization and light intensity in the optical path of fabricating fcc structure and the exposure and development time in the fabrication process are analyzed theoretically. A set of optimized parameters of the optical path and exposure and development time are presented in this paper.

8556-56, Poster Session

Iterative phase difference constraint method for the speckle elimination of kinoforms

Toshinori Hora, Shuan Yang, Seiichi Serikawa, Kyushu Institute of Technology (Japan)

Speckle noise is a serious problem in the reconstruction of computer-generated holograms (CGHs). Especially for a kinoform (a phase-only CGH), the speckles lead to a large reconstruction error and it is important to eliminate the speckles. The speckles are caused by the isolated zero points in the reconstruction of a CGH, so the speckles can be avoided if there are no isolated zero points. In this study, we suggest a new method that restricts the existence range of the

phase differences between the sampled points of reconstruction. The phase differences have the range of two times the phase period and we restrict them into half of the phase period after wrapping the phase differences. This strategy can successfully avoid the existence of isolated zero points so that speckles can be eliminated. The phase difference constraint process can be incorporated into the general iterative algorithms for the optimization of a kinoform. Speckleless reconstruction can be obtained after a sufficient number of iterations and the also the kinoform conditions are satisfied (i.e., the kinoform amplitude uniform condition and its phase quantization). In addition, this speckleless reconstruction has noise immune when the reconstruction phase noise is under a quarter of phase period. We will show some simulation results to show the effect of the iterative phase difference constraint method for the speckle elimination of kinoforms in our presentation.

8556-58, Poster Session

Optical correlation recognition based on LCOS

Mingchuan Tang, Soochow Univ (China); Jianhong Wu, Soochow Univ. (China)

Due to the characteristics of high-speed and parallelism during the information processing, the real-time optical correlator is widely used for pattern recognition in the fields of missile guidance, spacecraft docking, landing and biometric. The traditional real-time Vander Lugt correlators use LCD or ferroelectric liquid crystal spatial light modulator (FLC) as the matched filter, but the modulation curve of the LCD is coupled, which will reduce the optical efficiency, while the FLC merely has two states (0 and π) leading to a low signal-to-noise ratio. Severing as a phase-only matched filter, LCOS has been adopted in the correlator for the recognition of the letters without distortion. Attributed to the large open rate, uniform amplitude and continuous phase modulation characteristics of the LCOS, the filter will improve the optical efficiency and signal-to-noise ratio substantially. Allowing for the distortions of the object to be identified including rotations, scale changes, perspective changes, which can severely impact the correlation recognition results, in this paper, a modified real-time Vander Lugt correlator based on the LCOS is presented by means of applying an optimization algorithm to the design of the filter so that the correlator can be invariant to the distortions while maintaining good recognition performance. In the frequency domain, the filter is synthesized by the linear combination of the phases of the training images covering a certain distortion, meanwhile the weights of the linear combination are calculated by the successive forcing algorithm, then the new correlator will get the similar recognition results for all the training images. Moreover, the modified filter is dominated by the higher frequency signal based on the combination of the phases, it will have higher identification rate.

8556-60, Poster Session

Design and fabrication of aluminum nanowire-grid polarizer in near-infrared broadband

Qiufeng Jin, Quan Liu, Jianhong Wu, Soochow Univ. (China)

Polarizers and polarizing beam splitters are essential optical devices for most optical systems and optical networks. The infrared polarizers are widely used in the infrared imaging systems as the core components, such as infrared stealth, target acquisition and mine detection, automobile night-vision instrument and other systems. Generally in order to distinguish the object emission from the reflection, infrared polarizers are used as a filter of the infrared camera.

Aluminum is a high-performance functional material used as the metal layer of Sub-wavelength metal wire grid. Holographic lithography is widely used in nano-fabrication process for its larger scale, high efficiency, low cost. But the most severe limitation of holographic

lithography arise when resist exposures are performed on reflecting substrates (Al) which will produce strong standing waves, and it's difficult to yield a well resist profile which can be used as the mask for the post dry etching.

In this paper, a thin layer of Cu, which worked as the substrate of resist for holographic exposure, is deposited on the Al layer, and the standing wave is effectively suppressed. The following aspects are analyzed.

(1) The reflection on the substrate is suppressed with the optimal Cu layer thickness. In the conditions of 413.1nm recording wavelength and 250nm~350nm grating period, the reflectivity of the resist-substrate interface is calculated with a aluminum layer(150nm to 250nm),copper layer(5nm to 50nm).After trade-off between the resist-substrate reflectivity and the final performance of the polarizer, the structure with a Al layer 190nm, and anti-reflection Cu layer 40nm is chose.

(2)According to the optimal thickness of Cu layer, the exposure dose is calculated. The distribution of intensity of incident irradiation in resist during exposure is figured out, and it is shown that the pattern in resist on surface with high reflectivity will suffer standing wave due to the fact that the incidence irradiation interferences with the reflective beam from the resist-substrate interface. Combining with parameter of the lithography process in our laboratory, the concentration of the developer is adjusted and the time of the development is also optimized. Ultimately, the desired start exposure dose is reached.

(3)The affect of the residual Cu layer to the performance of the polarizer is simulated. Optical performance of a bilayer nanowire-grid polarizer is analyzed by FDTD method with a residual Cu layer(5nm to 40nm). The results show that the bilayer nanowire-grid polarizer obtained the TM transmittance>85%, extinction ratio>30dB. No significant difference between the pure aluminum and copper residues grating is found.

8556-61, Poster Session

3D measurement for volume holograms in Fe:Cu:LiNbO₃ crystal by dual-wavelength digital holographic microscopy

Zhirui Gao, Zhuqing Jiang, Yujia Wang, Jiangtao Wu, Yunxin Wang, Beijing Univ. of Technology (China)

The technique of digital holography has experienced substantial developments in the past years as charge coupled device (CCD) and digital image processing technologies progressed.

However, when the optical depth of an object is greater than the wavelength, the phase image contains 2π discontinuities, and numerical unwrapping procedure could not be applied to obtain phase information of the objects which have a high aspect ratio. Two wavelengths are used to produce a longer wavelength called the 'beat wavelength' in dual-wavelength phase unwrapping.

In this paper, the phase-type grating recorded in a 2-mm-thick Fe:Cu:LiNbO₃ crystal is measured by dual-wavelength digital holography. In the experiment, a volume hologram, which is recorded in a 2-mm-thick Fe:Cu:LiNbO₃ crystal by interference of two recording beams at the wavelength of 532 nm, is reconstructed to be imaging by dual-wavelength digital holography. Two lasers of the different wavelengths 660 nm and 671 nm are used to obtain a larger beat wavelength. Each laser output, which is spatially-filtered and collimated, is split into a reference and object beams in an interferometer setup based on the Mach-Zehnder configuration. In dual-wavelength phase unwrapping, two individual phase images are obtained by using each wavelength, respectively, and the phase image for beat wavelength is obtained by subtracting one single wavelength phase image from the other and then adding 2π whenever the resultant value is less than zero. In the final synthetic image, the discontinuities are removed after reduce the noise of the beat wavelength phase image. Thus, a 3D surface profile of the grating is obtained.

8556-62, Poster Session

Improving the phase measurement by the apodization filter in the digital holography

Shifeng Chang, Dayong Wang, Yunxin Wang, Puhui Meng, Jie Zhao, Beijing Univ. of Technology (China)

Since the limited aperture of the CCD target surface, the point spread function of digital hologram reproduction system has high sidelobe, which leads to significant diffraction effects in the reproduction process and reduces the quality of the reconstructed images. In addition, the presence of laser speckle and other noise also make the phase measurement accuracy of the object be decreased.

In this paper, the apodization filter is applied to improve the phase measurement in the digital holographic microscopy imaging system. The sidelobe energy of the imaging system can be reduced by the apodization to suppress the border diffraction. First, a novel reconstruction method based on extension and apodization of the digital hologram is presented, by which the original hologram can be extended through filling the average intensity values of the boundary, and the extended hologram is apodized by use of the constructed window function. Second, the light wave propagation of digital hologram reproduction is explored by numerical simulation to analyze the apodization function on cutting diffraction effects and noise effect. Third, the experimental system of the lensless Fourier transform digital holography is set up, and the apodization method is applied to the structure measurement of a phase grating with the grating constant 300m and depth 150nm. Finally, the results are compared to the detection data given by the light interferometer. Simulations and experiments demonstrate that apodization can effectively reduce the border diffraction and noise effects to improve the phase measurement precision and the quality of the reconstructed images.

8556-63, Poster Session

Rectification of gridline structure in integral image using radon transform and perspective transformation

Bi-yun WANG, Yang Song, An-zhi He, Nanjing Univ. of Science and Technology (China)

Integral imaging is one of the most promising techniques for capturing and displaying the three-dimensional information of the object. Most integral image analysis and processing tasks require each elemental image can be identified with high precision, which is difficult to implement in a real pick-up process. For the acquisition of the three-dimensional information in integral imaging process, the lens array should be aligned precisely with respect to the CCD. In this paper, we present a method to accurately correct geometric distortions triggered by the misalignment between lens array and CCD. The method for calculating the skew angle of deviation and the accurate gridline structure in the three-dimensional integral images is based on the Radon Transform algorithm. Then using projective image transformation, the geometrical distortion in the elemental image set can be rectified. The size and position information of the rectified element images also can be calculated by the gridline structure, which will prevent the image splitting, shifting along the lateral or longitudinal direction, or blurring according to reconstruction distance in the optical or computational reconstruction process.

8556-64, Poster Session

System calibration of road rut detection by linear structured light and binocular vision

Shan Zhao, Yang Song, An-zhi He, Nanjing Univ. of Science and Technology (China)

With the rapid development of national highway construction, increasingly importance has been attached to the quality detection and maintenance work on the highway surface all over the world. Rut is one of the primary damages of the highway, and how to make the precise and fast detection with the depth of pavement rutting is significant. This paper presents a new method for road rut detection, which is based on structured light measurement and binocular stereo-vision. Firstly, the linear structured light is projected onto the road surface and two digital images of surrounding scenery are acquired by two CCD cameras from different point of view. On this basis, three dimensional mathematical model for linear structured light rut detection is established. And then, carry out research deeply on two key technologies including camera calibration and linear structured light system calibration. By being testified, the calibration methods for road rut detection are proved to be feasible. The advantage of this method is that the algorithm can reduce or even eliminate the effects which caused by the bumpy and pitch vehicles and the height is precise enough to meet the requirement.

8556-65, Poster Session

Study on effects of organic solvents on proliferation of Hela cells by digital holography

Liting Ouyang, Dayong Wang, Yunxin Wang, Yizhuo Zhang, Xinlong Wang, Beijing Univ. of Technology (China)

In traditional Chinese medicine anticancer research, many medicinal effective ingredients can only dissolve in higher polar organic solvents, such as ethanol, DMSO and so on. However the organic solvents may affect the accuracy of therapeutic efficacy evaluation. Therefore the study on effects of organic solvents with different concentrations on proliferation of Hela cells is very important in the research of anticancer drugs and cell apoptosis. The digital holography is capable of giving phase-contrast images with high precision, which is suitable for the imaging of transparent living cells. It can not only rule out interference of the staining step on treatment outcome evaluation, but also get the changes of surface topography quantitatively of cell proliferation inhibition. Based on the pre-magnification off-axis Fresnel digital holography, an inverted digital holographic microscope is built. Holograms are recorded by the CCD camera, and the numerical reconstruction and extraction process of phase images is completed in the computer. Then phase-contrast images of Hela cells with different concentrations of organic solvents are given. Based on the analysis of experimental results, Hela cells proliferation was significantly inhibited by methanol, ethanol with concentrations ranged from 20% to 100%, DMSO with concentrations more than 33%. In conclusion, the digital holography is an optimized way for cell biology and traditional Chinese medicine anticancer research, which has very high practical value in the observing and detection of the changes of cell morphology. It can also be used in testing the effectiveness of new drugs against drug-resistant pathogens and cancer. It will contribute to the screening of new drugs.

8556-67, Poster Session

The fabrication of super-hydrophobic surface on the glass

WeiPing Liu, Changsi Peng, Soochow Univ. (China)

The super-hydrophobic surface has captured the attention of many materials scientists recently as there are potential applications in defense, daily life and industrial areas. It exhibits unique performance especially in the self-cleaning, reduced-friction, anti-corrosion, prevention of snow disaster, anticoagulant, and oxidation, etc. Generally, the micro-nano structures have great effects on the wettability of the surface of a material. There are many methods to fabricate micro-nano structures on the surface, such as the sol-gel method, template technology, soft printing method on the polymer,

electrochemical deposition, chemical vapor deposition, independent fitted method, Lithography, mechanical stretching method, etc. Some of the fabricated super-hydrophobic surfaces are uneven and not translucent, which limits applications. Generally, the essential processes in fabricating super-hydrophobic surface are the preparation of the rough surface and subsequent treatment with low surface energy materials.

In the paper, the micron-sized photoresist mask is fabricated via laser interference lithography on the glass substrate and shifted to the glass substrate by reactive ion etching. Then 20nm silver is coated on the sample by electron beam evaporation and subsequently heated by the rapid annealing furnace to make the silver aggregation. At last, the sample is treated under the ethanol solution with 2 mM dodecanethiol. The micro lattice and silver nanoparticles composite structures, which is helpful for obtaining surfaces with super-hydrophobic ability. The routes are simple and easy, which can be also used as a template for roll to roll imprinting technology and be easily realized in its large-scale manufacture.

8556-68, Poster Session

Measurement of the optical fiber refractive index profiling based on digital holography

Duocheng Wang, Sujuan Huang, Zheng Chang, Tingyun Wang, Shanghai Univ. (China)

As development of optical technologies including fiber communication and fiber sensor system, the role of optical fiber has become more and more important. The characteristics of optical fiber are quite important for improving the performance in various applications. Especially, the refractive index of fiber is the most elementary aspect because it describes how light propagates through the medium. Conventional approaches to measure the refractive index of optical fiber have drawbacks such as destruction and low efficiency.

Digital holography is a powerful tool to measure the refractive index because it takes the basic theories of classical holography concerning 3-D information (complex amplitude distribution) of the object wavefront. Besides, it also has advantages of digital processing methods provided by computers. Based on optical fiber Mach-Zehnder interferometer, a new measuring method using digital holography is proposed in this paper. Unlike traditional holography, we use optical fibers as light transmission arms of outputting object light and reference light which simplifies the experimental set by reducing the optical elements. The light emitting from the laser generator is separated into two light beams by a fiber coupler. One beam goes through the fiber sample and the other becomes the reference light. Then several kinds of fiber samples such as multi-mode fiber, polarization-preserving fiber and special fiber are tested and their holograms are recorded by CCD. After the hologram is digitally processed by spectrum filtering, the phase distribution can be reconstructed and extracted with good quality. At last, the experimental results of refractive index profiling of fiber are given, which can be used to further research of fiber characteristics.

8556-69, Poster Session

Factors of influencing the value of the W in the bi-grating diffraction imaging equation

Weiping Zhang, Feng Zhu, Chunzhi Wang, Yanchun Gao, Lei Liu, Guangxi Univ. (China)

The novel bi-grating diffraction imaging effect have been reported for years. By this effect, a clear object image can be seen after the polychromatic beam coming from object is diffracted twice by two gratings.

This paper focuses on factors of influencing the value of W in the bi-grating diffraction imaging equation. And W is approximately equal to 1 when the bi-grating system is under the following ideal conditions.

The two bi-gratings is parallel to each other, and the first one G1 is set in a position where the incidence and diffraction angle of the object beam are same, also the second one G2 is along the middle of the first grating's diffraction beam of a certain diffraction order. But we found that the effect could also appear under some non-ideal conditions and the value of W would change.

The values of W for the bi-grating system were studied under following non-ideal conditions in experiments. G1 is set in a position where the incidence angle of the object beam is larger or smaller than the diffraction angle, and G2 is respectively along optical paths for the red, green and blue lights of the first grating's diffraction beam of a certain diffraction order. The results of changes on W for these conditions are given. It is of profound significance for understanding the effect deeply and promoting the application of it.

8556-70, Poster Session

Electro-holography display using computer generated hologram of 3D objects based on projection spectra

Sujuan Huang, Duocheng Wang, Chao He, Shanghai Univ. (China)

Holography is able to provide the most authentic three-dimensional (3D) illusion to the human eye without the need for special viewing devices. Computer generated holography has become an important technique in 3D imaging, it can yield ideal 3D visual effects even for virtual 3D objects. A new method of synthesizing computer-generated hologram (CGH) of 3D objects from their projection images is proposed. Numerical reconstruction of the hologram has been achieved. Electro-holography display of the hologram can be implemented.

A series of projection images of 3D objects are recorded with one-dimensional azimuth scanning. According to the principles of paraboloid of revolution in 3D Fourier space and 3D central slice theorem, spectra information of 3D objects can be gathered from their projection images. Because there is quantization error of horizontal and vertical directions, in order to make full use of projection spectra, the spectrum information of each projection image is extracted in double circle even four circles form. Spectrum information obtained from all projection images is used to fill the u-v plane. Then the wavefront distribution of 3D object at the Fourier plane is achieved. The complex matrix can be encoded efficiently into CGH of 3D objects based on computer-generated holography using a conjugate-symmetric extension. Experimental results for numerical reconstruction of the CGH at different distance validate the proposed methods and show its good performance.

Electro-holographic reconstruction can be realized by using an electronic addressing reflective liquid-crystal display (LCD) spatial light modulator. The CGH from the computer is loaded onto the LCD. By illuminating a reference light from a laser source to the LCD, the amplitude and phase information included in the CGH will be restored. The 3D objects can be reconstructed in the distance due to the diffraction of the light modulated by the LCD.

8556-72, Poster Session

Holographic two-dimensional photonic crystal of LED decorative illumination

Yidan Zheng, Fujian Normal Univ. (China)

The film of holographic two-dimensional photonic crystal is used for the led illumination system. According to the decorative patterns, the structure sizes of two-dimensional photonic crystal and relevant led Luminaire have been reasonably designed. Then the master mask of two-dimensional photonic crystal is produced with the method of multiple-beam interference. With the experiment of LED illumination, the results show that it is able to meet the expected decorative patterns of LED illumination. While the master mask is used to copy optical coating

of polycarbonate, it will provide a better option for LED decorative illumination under low cost.

8556-73, Poster Session

Theoretical analysis of volume moiré tomography based on double orthogonal gratings for real 3D flow fields diagnosis

Nan Sun, Yang Song, Jia Wang, Zhenhua Li, Anzhi He, Nanjing Univ. of Science and Technology (China)

Moiré tomography has been considered as a powerful diagnostic tool for complicated flow fields due to it is nonintrusive and instantaneous. However, the normal moiré deflectometry, which could generate the partial derivative of the projection data in one direction, cannot meet the requirements of Volume Moiré Tomography (VMT) for real 3-D reconstruction. Moreover, the partial derivative in two orthogonal directions of the projection data is required for VMT. In this Letter, an improved moiré deflected system based on double orthogonal gratings is introduced to solve this problem. The proposed method could obtain the first-order partial derivatives in two vertical directions of the projection in one time. Then the second-order partial derivatives of 3-D Radon transformation of the test field can be obtained by merging the data of these two directions. Theoretical analysis of this improved moiré deflected is given in this letter. Comparing with the normal moiré deflectometry based on double linear gratings, the proposed system is more effective and easier to realize the multi-direction data acquisition. Finally, this improved moiré deflected system is used for reconstruct the temperature distribution of a simulated field.

8556-74, Poster Session

A novel 2D wavelength-time chaos code in optical CDMA system

Qi Zhang, Xiangjun Xin, Yongjun Wang, Lijia Zhang, Chongxiu Yu, Nan Meng, Houtian Wang, Beijing Univ. of Posts and Telecommunications (China)

Chaos OCDMA is very potential in optical access due to its high capacity and security. A novel wavelength-time chaos code for optical code division multiple access system is proposed and constructed from one-dimensional chaos code based on map of Logistic equation. The access performance based on the proposed chaos code is evaluated by comparison with one-dimensional single wavelength chaos code and one-dimensional WDM/chaos code according to capacity, spectral efficiency and bit-error ratio. For two-dimensional wavelength-time chaos code, the usable wavelength number m is larger than its code length L. When m is same, the capacity of two-dimensional wavelength-time chaos code is always larger than that of WDM/chaos code and one-dimensional chaos code. Two-dimensional wavelength-time chaos code always has a higher spectral efficiency than the corresponding WDM/chaos code system when . The bit-error rate increases with the number of the users due to the increased level of inter-user interference. For a fixed bit-error rate, the number of users using two-dimensional chaos code is larger than that of one-dimensional chaos code.

8556-25, Session 8

The formation of large scale reconstructed images through the use of computer generated holograms: colorization

Sumio Nakahara, Kyoji Matsushima, Kansai Univ. (Japan)

We propose and demonstrate a method which constructs large size multicolor images in limited spaces, i.e. tunnels. The traffic

sign image, visibly the same size as the original physical sign, is reproduced using smaller size color holograms with R-,G-,B- laser. Each 20cm square binary type of plane amplitude hologram is made by computer-generation method. Cross-talk images which appear in color reproduction are separated by appropriate alignment of reconstruction beams.

8556-26, Session 8

High-efficient design method of large diffractive optical elements by vectorial field analysis based on boundary element method *(Invited Paper)*

Jun-ichiro Sugisaka, Toyohiko Yatagai, Utsunomiya Univ. (Japan)

An efficient approach to design the structure of diffractive optical elements (DOEs) is presented. Simulation of DOEs with conventional vectorial diffraction methods requires considerably large calculation resources, and cannot apply to DOEs with large apertures. We have developed a multistep difference-field boundary element method. This is a vectorial diffraction method for non-periodic structures, and has an advantage that the amount of memory consumption is almost free from the entire sizes of DOEs. This method firstly divides the groove patterns on a DOE into a flat substrate and small projections on the surface. We start with a field distribution for the flat substrate, and then iteratively update the field distribution by adding the projections one by one. At each step, the necessary discretization is only the dielectric boundaries around the added projection, and can perform with very small memory consumption. For designing a device structure, we add a projection so that the updated field approaches to the desired one. Otherwise we can repeat the step by changing the size or position of that projection. After finding the optimal projection, we add the next projection. When the all projections are added, we can obtain the device structure and the diffracted wave simultaneously. As conventional methods, we do not have to calculate the whole of huge structures many times with large-scale computers. The necessary memory for two-dimensional structure is only around 20 MB, and our method is sufficient with a desktop computer to perform an accurate designing even including the polarization characteristics.

8556-27, Session 8

A parameters study of the multi-plane diffraction iterative algorithm for single-beam phase retrieval

Yuanyuan Sun, Jinan Univ. (China); Zibang Zhang, Jinan Univ. (China); Jingang Zhong, Jinan Univ. (China)

Phase retrieval techniques have been used for the measurement of 3D objects. The phase of the transmitted or reflected light beam is modulated by different characteristics of the object and reveals valuable information. The multi-plane diffraction iterative algorithm is a method of phase retrieval with single beam. Based on numerical phase-error correction system, the method obtains the phase and amplitude of a wave front using wave propagation equation with a sequence of intensity patterns recorded at different planes. We study the three parameters of this method, including the number of iterates and sampled planes and the distance from the first sampled plane to the object, through simulations and experiments. In simulation, the retrieved phase error is reduced with the increase of the number of iterates and sampled planes and the decrease of the distance from the first sampled plane to the object. In practice, the increase of the number of iterates and sampled planes reduces the retrieved phase error just in a certain range. The error induced by the setup or the environment such as aberrations, displacements, especially vertical displacements of planes to record in motion and the spatial nonuniformity of the beam can be

accumulated in the iterative processing, resulting in the deterioration of the retrieved phase. Compromise has to be made for the balance between accuracy and computation time. And the decrease of the distance from the first sampled plane to the object is demonstrated to improve the result in accord with the simulation.

8556-28, Session 8

Slanted volume holographic gratings design based on rigorous coupled-wave analysis *(Invited Paper)*

Ting Li, Liangcai Cao, Tsinghua Univ. (China); Qingsheng He, Guofan Jin, Tsinghua Univ. (China)

Volume holographic gratings are widely used because of the high efficiency and accurate orientation. Slant grating structure can enable optical functions flexibly that cannot be easily reached in traditional grating. So modeling of the slanted volume holographic grating based on rigorous coupled-wave analysis (RCWA) is necessary for practical application. An oblique coordinate system related to the grating fringes simplifies the mathematical analysis. The S-matrix algorithm gives the mathematical results. Based on the periodicity, RCWA can present all the diffraction orders including transmission and reflection. Compared with the traditional approximate scalar theory, the RCWA for the modeling can analyze the angular selectivity and the diffraction efficiency accurately. Obviously, the diffraction details offer all the grating features, thus making the design more accurate for the dedicated grating.

In terms of the slanted vector modeling, many important factors, such as the grating thickness, the relative index, the grating period and many other structure parameters, have been taken into account. Connecting all the impossible determinants, a transmission angle amplifier with the diffraction efficiency close to 100% has been simulated. And the matching grating element has been reached successfully. In the angle response, the highest efficiency approaches 100%, the first-order side-lobe peak is lower than 15% and the main-lobe bandwidth is less than 1 degree. At the same time, a narrow band filters with high reflection at resonance and high rejection has been also introduced.

8556-29, Session 8

Fast generation of hologram from range camera images based on the sub-lines and holographic interpolation *(Invited Paper)*

Peter W. M. Tsang, Wu Chao Situ, Kayton W. K. Cheung, City Univ. of Hong Kong (Hong Kong, China); Ting-Chung Poon, Virginia Polytechnic Institute and State Univ. (United States); Changhe Zhou, Shanghai Institute of Optics and Fine Mechanics (China)

The intensity image and the depth images of a three-dimensional object scene can be captured with a commodity range camera, and converted into a Fresnel hologram. However, for some cameras, the images are subject to radial distortion, and too small to be visible in optical reconstruction. Moreover, the conventional hologram generation process with numerical means is significant. In this paper, we present a fast method to overcome the above-mentioned problems. First, the intensity and the depth images are transformed to reduce the radial distortion. Next, the images are interpolated horizontally, and converted into a sequence of sub-lines. Finally, the sub-lines are swiftly converted into a Fresnel hologram through padding along the vertical direction. The pair of interpolation process effectively increases the size and visibility of the reconstructed image. Although our method can be applied to different kinds of range cameras, we have selected the Swissranger model as a showcase to demonstrate the feasibility of the approach.

8556-30, Session 8

A new way to reconstruct the amplitude distribution of coherent light source

Qiankun Gao, Graduate Univ of the Chinese Academy of Sciences (China); Tuo Li, Liang Qiao, Yali Wang, Graduate Univ. of the Chinese Academy of Sciences (China); Haifei Li, Ordnance Repair Factory of Air Force (China); Yishi Shi, Graduate Univ. of the Chinese Academy of Sciences (China)

In holographic projection, the actual coherent light source is different from the theoretical light source. Therefore it reduces the system's output quality. This light source's variation contains phase and amplitude parts. However, we consider the amplitude part is the main factor. Based on the assumption, a new iteration algorithm is presented to reconstruct the amplitude distribution of the coherent light source. New diffraction optical elements can be designed by using this reconstructed amplitude distribution, which will greatly improve the output image's quality in holographic projection. Both simulation and experimental results demonstrate the effectiveness of this method.

8556-31, Session 9

Dynamic holographic interferometry with matrix LC modulator (*Invited Paper*)

Vladimir Y. Venediktov, Saint Petersburg State Electrotechnical Univ. (Russian Federation) and Saint Petersburg State Univ. (Russian Federation); Sergey A. Pulkin, Saint-Petersburg State Univ. (Russian Federation)

The method of holographic interferometry with increasing sensitivity was applied for measurements of height of nano-steps (from 10 nm and higher) with standard uncertainty about 0.5 nm. The initial microinterferogram with fringes of equal thickness is obtained in Michelson micro-interferometer with nano-step sample in one of arms. That interferogram is registered on CCD - camera and digital interferogram passed on matrix phase modulator with spatial resolution 30 lines/mm. The matrix phase modulator is placed on the exit of two-beam Mach-Zehnder interferometer and illuminated by two plane laser beams. These two beams are diffracted on phase modulator, are focused on and filtered by diaphragm with holes in (+ 1-st) and (- 1-st) order of diffraction. The second digital interferogram with twice increasing sensitivity is obtained on CCD - camera and so on. The increasing of sensitivity is obtained because interference of waves with complex conjugated phases. One can obtain the interference of higher orders too if work with nonlinear interferogram. It is possible to make any carrier fringe space frequency because usage of two plane waves in interferometer. The flatness less than $\lambda/100$, topography of surfaces with height difference less than few nanometers is possible to research with increased sensitivity too. Also we demonstrate the possibilities of Rozhdestvenski Hook method with increasing sensitivity for measuring of oscillator strengths (transition probabilities) for weak atomic transitions. It is important for future development of interference spectroscopy because usual hook method has insufficient sensitivity and allows us to measure oscillator strengths only for resonant transitions from ground state or from metastable states for strong transitions. It's necessary to underline, that holographic interferometric methods with increasing sensitivity are well known but here we demonstrate the possibility of these methods with using of digital interferograms registered on matrix phase modulator.

8556-32, Session 9

Research on fabrication for nanostructures on the surface of GaN

Heng Zhang, Xiaohong Zhou, Zongbao Fang, Soochow Univ. (China)

We demonstrate the fabrication of nanostructures on the GaN surface using a GaN-on-Sapphire substrate, by using a nanosecond diode-pumped solid-state laser (DPSSL wavelength 351nm and pulse duration 20 ns) as light sources. The laser is split into four interfering beams with two diffractive beam splitters and then interfered on the top surface of the sample. Composed by dot array, nanostructures are realized on the GaN surface. The mechanism to form the dot array was analyzed and it was found that the obtained nanostructures had a negative shape of the interference pattern of four laser beams. The reflection losses at the GaN interfaces are suppressed. The light extraction efficiency is significantly improved for the nanostructured GaN layer. This work provides a very practical approach to fabricate freestanding nanostructures on the GaN-on-Sapphire substrate for further improving the light extraction efficiency.

8556-33, Session 9

3D measurement system with two detecting channels using structured light

Shengbin Wei, Changhe Zhou, Shaoqing Wang, Shanghai Institute of Optics and Fine Mechanics (China)

In this paper we propose a 3D measurement system with two cameras using structured light. The modulated light is projected on the object by a projection lens. Two calibrated digital cameras are used to capture the images of projected area on the object separately. According to triangulation, the local 3D point cloud is obtained from the pair of images. The images are captured from different angles to cover the whole profile of the object to obtain corresponding series of local 3D point clouds. The series of local 3D point clouds are then connected to generate the integrated 3D point clouds of the object according to surface connection technique. The 3D point clouds can be exported as the original data, or be rendered to generate a visual result.

We designed a special pattern of structured light to generate distinct artificial corner points on the object. The system was used to measure a plaster statue of Apollo. More than 1.4 million of 3D point clouds are obtained with a depth precision of less than 0.2mm. The system with the advantages of high measuring precision, compact structure and good robustness is highly attractive for applications in 3D measurement, 3D display and so on.

8556-34, Session 9

The influence of squeezing ratio on the birefringence characteristics of photonic crystal fibers

Peng Song, Univ. of Jinan (China)

In recent years, the squeezed photonic crystal fiber with high birefringence has attracted significant attention. The squeezed photonic crystal fiber consists of elliptical air holes and squeezed lattice in the cladding, which both can break the multi-fold rotational symmetry of photonic crystal fibers and introduce high birefringence. The author promoted a model to describe the squeezed degree of photonic crystal fibers and studied the influence of the squeezing on those photonic crystal fibers in previous work. We studied and analyzed the influence of elliptical air holes or squeezed lattice on the birefringence characteristics, respectively. However, the compounded effect of elliptical air holes and squeezed lattice makes the influence of birefringence complicated, which is quite disadvantageous to analyze

and design the high birefringence photonic crystal fibers. In this paper, a novel concept of squeezing ratio is introduced to describe the squeezed degree of photonic crystal fiber with squeezed lattice and elliptical air holes in the cladding. We study and analyze the influence of both of them on the birefringence characteristics based on the supercell lattice method. Then a novel definition of squeezing ratio is presented, which describes the compounded effect of elliptical air holes and squeezed lattice on the birefringence characteristics. Studies show that the birefringence simply varies with the squeezing ratio. So the concept of squeezing ratio can be used effectively to design the high birefringence photonic crystal fibers.

8556-35, Session 10

Three dimensional optical techniques using Dammann gratings (*Invited Paper*)

Changhe Zhou, Shanghai Institute of Optics and Fine Mechanics (China)

This paper summarized our work on three-dimensional optical technologies using Dammann gratings, e.g., three-dimensional Dammann gratings, three dimensional imaging using a Dammann grating, etc.. We developed three-dimensional Dammann grating which can produce three-dimensional array with equal distance and equal intensity with a high-numerical-aperture lens. As we know, a lens usually has a single focal point. Fresnel zone plate can generate several axial focal points, but the intensity between them is unequal. By introducing the concept of Dammann grating into the circular phase plate, we invented Dammann zone plate (DZP) which can produce a series of axial focal points with equal intensity. Combining DZP with a Dammann grating, three-dimensional Dammann array will be generated, which is highly interesting for various applications.

We also built a three-dimensional measuring system using a Dammann grating, with two cameras as the right eye and right eye, respectively. We used a 64X64 Dammann grating for generation of a square array of light spots for parallel capturing the three-dimensional profile of an object. The two cameras and the illuminating part are packaged together. After scanning the object, its three-dimensional profile will be obtained. Experimental results demonstrated the effectiveness of this technique.

8556-36, Session 10

Beam splitters of metal-dielectric reflective grating

Anduo Hu, Changhe Zhou, Hongchao Cao, Jun Wu, Jia Wei, Shanghai Institute of Optics and Fine Mechanics (China)

Beam splitters are important optical components. In this paper, reflective 1x2 and 1x3 beam splitters based on metal-dielectric grating are designed at wavelength of 1064 nm. Alumina, silver, alumina and fused silica films are coated on substrate in sequence from bottom to top. On the top fused silica film, grating with rectangular grooves are etched. The alumina film immediately below the grating is a connecting layer. The thickness of silver is 100 nm. Light is incident from air. In order to realize high efficiency and uniformity, rigorous coupled-wave analysis and simulated annealing algorithm are employed to search the geometric parameters such as period, depth, duty cycle, thickness of connecting layer and incident angle. For a 1x2 beam splitter, the direction of the two diffraction orders is expected to be perpendicular. The optimized 1x2 beam splitter is operated at angle of 37.4 degree and can achieve diffraction efficiencies of 49.1% at the -1st order and 48.9% at the 0th order. The optimized 1x3 beam splitter is operated at angle of 6 degree. The diffraction efficiencies of the -1st, 0th and +1st orders are 32.8%, 32.3% and 33.0%, respectively. To guide the fabrication and operation of the beam splitters, the tolerance of grating depth, duty cycle and angle are analyzed. The optimized beam splitters exhibit high efficiency and good uniformity, which should be useful in practical applications.

8556-37, Session 10

The focusing property of the VLS grating with different types of beams

Chunzhi Wang, Weiping Zhang, Yanchun Gao, Guangxi Univ. (China)

The varied line-space grating (VLS grating) has the ability of self-focusing and eliminating aberration, and it has been used widely in spectral measurement, fiber communication, synchrotron radiation beam regulation, displacement sensing, and etc. Therefore, Study the diffraction characteristics of the VLS grating is of great significance. When VLS grating is used in sensor, in some cases, it needs to be known the focusing property of one VLS grating with different types of incident lights. This article will study on it.

When the incident angle of the incident light changes, the focusing position of diffracted light through VLS grating will be different. This paper will study the differences. Mainly studies how the change of the incident angle of monochromatic plane wave impacts the focusing properties of VLS gratings with same center spatial frequencies and different frequency distributions. And impact of different wavelength of monochrome plane wave. Besides the above work, we will study the changes of the focusing properties of VLS gratings using spherical wave instead of the plane wave and research the change law of the focusing position of the VLS grating with different types of beams.

8556-38, Session 10

Absorption enhancement in thin-film solar cell using grating structure

Jun Wu, Hongchao Cao, Anduo Hu, Jia Wei, Shanghai Institute of Optics and Fine Mechanics (China)

The enhancement of absorption in thin-film amorphous silicon solar cell based on guided mode resonance is theoretically investigated. This is achieved by patterning a grating with waveguide layer in the absorbing layer and an antireflective layer on the top. The optimized grating parameters are obtained by use of rigorous coupled-wave analysis and the simulated annealing algorithm in the visible region. The absorption at normal incidence is higher than 50% in the wavelength range 300-660 nm, and the peak absorption is higher than 95% for both TE and TM polarization. We studied the angle dependence of the integrated absorption spectrum in solar cell structures. The integrated absorption for TM polarization is larger than TE polarization in the angular range of 0-88 degrees. In general, the averaged integrated absorption decreases as the incident angle increases, but it is higher than 60% in the range 0-66 degrees. So it is very weakly dependent on the angle of incidence. A physical understanding of enhanced absorption based on guided mode resonance effect is presented. It is found that the effect can effectively trap light in the absorber layer and enhance absorption in the active layer. Double-groove grating structure is also discussed for the sake of reducing reflection and enhancing absorption. The designed solar cells have high integrated absorption and are weakly dependent on incident angle, which should be of highly practical significance.

8556-39, Session 11

Low-coherence holography with two-spherical waves

Shaoqun Zeng, Britton Chance Ctr. for Biomedical Photonics (China)

Low-coherence holography obtains three-dimensional information without scanning and shows many potential applications. However, current method usually recorded holograms with plane wave as the reference wave. Here we show the holography with two spherical waves exhibits special features over the one with plane waves. These features will facilitate more application in the future.

8556-40, Session 11

Calibration and pre-compensation of direct laser writing system

Feng Zhu, Changhe Zhou, Jianyong Ma, Shanghai Institute of Optics and Fine Mechanics (China)

The Direct Laser Writing (DLW) technique has become a well-established, flexible and multi-functional method of micro- and nano-technology. A DLW system, mainly containing blue light writing module and red light autofocus module, is established and efficiently applied for the fabrication of diffractive optical elements (DOEs). In the DLW system, the stability of the writing beam is always a concern. Although the autofocus module is employed to eliminate the influence of the drifting focus point resulting from ambient vibration, the inherent defocusing error still has a serious impact on the lithography accuracy of the DLW system. As the refractive index of the lithography objective lens with a high numerical aperture (NA, 0.9) for blue light (405nm) differs from that for the auto-focus red light (650nm), the focal planes of the two beams will not coincide. Furthermore, the two beams can't be mounted seriously parallel to the axis of the objective lens in practice. The misalignment will impact the location of the focus point axially and laterally. The above defocusing error is determined experimentally, and then is pre-compensated, which improves the fabrication accuracy dramatically. The relationship between defocusing amounts and line widths of the stripes is obtained, which can be used for writing gratings with different line widths. A 100?100 mm sized fused-silica grating with a period of 2 μm is obtained with the DLW system, and some microscope images are presented to show the effectiveness of the error-eliminating methods.

8556-41, Session 11

Quantitative evaluation of spatial phase light modulator characteristics in Fresnel incoherent correlation holography

Man Tian Long, Yuhong Wan, Hao Chen, Zhuqing Jiang, Dayong Wang, Shiquan Tao, Beijing Univ. of Technology (China)

Fresnel incoherent correlation holography (FINCH) is one of the methods for recording holograms of 3D samples under incoherent illumination. The FINCH combines the theory of spatial self-coherence and the technology of in-line phase-shift technology together to form a complex hologram. A spatial phase light modulator (SPLM) plays an important role as dynamic diffraction optical elements (DOE) and phase shifter. The incoherent light originated from each object point of 3D samples incidents to a SPLM and is split into two beams with different curvature which are spatial self-coherence. A Fresnel interference pattern including 3D information of the objects is captured by an image detector. Three holograms with different phase-shift are recorded sequentially for eliminating the zero-order and twin image, and then a complex valued hologram without bias is obtained by superposing the three holograms. The modulation characteristics of SPLM and phase shift error in FINCH are investigated experimentally in this paper. Phase modulation characteristics are measured when the SPLM under coherent and narrow-bandwidth incoherent illumination respectively base on digital holography technology and phase shift error is analyzed in FINCH due to quasi monochromatic light illumination. The effect of phase shift error on the quality of reconstructed image is also investigated and some measures are proposed to reduce the phase shift error.

8556-42, Session 11

An optically addressed liquid crystal light valve with high transmittance

Dajie Huang, Wei Fan, Xuechun Li, Zunqi Lin, Shanghai Institute

of Optics and Fine Mechanics (China)

We fabricate an optically addressed liquid crystal light valve based on a twisted nematic liquid crystal layer associated to a photoconductive BSO layer. Based on the optical addressing of a continuous layer of liquid crystal, the spatial transmittance distribution of 1053nm coherent light through the light valve has a corresponding relationship with the intensity distribution of 470nm incoherent light projected onto the photoconductive BSO layer. The AC voltage is added to both liquid crystal layer (4.7microns thick) and photoconductive BSO layer (1mm thick) through two transparent electrodes. Resistivity of the BSO layer decreases when the intensity of 470nm address beam increases. When the intensity of address beam projected onto the BSO layer changes, the voltage on the liquid crystal layer changes accordingly, which leads to different anisotropic birefringence of the liquid crystal layer. So the BSO layer enables the intensity of 470nm address beam to locally modulate the polarization of 1053nm read beam. A downstream polarizer enables the polarization modulation to be manifested as an amplitude modulation. As a result, we can control spatial intensity distribution of 1053nm read beam by controlling the intensity of 470nm address beam projected onto the light valve. In our experiment, by controlling the intensity of 470nm incoherent light with a LCOS modulator, the spatial intensity distribution of 1053nm coherent light through the light valve can be controlled correspondingly. Performance characteristic of this light valve has been studied experimentally to ensure its ability of beam shaping for 1053nm coherent light.

Due to the strong interaction between liquid crystal molecules, our device has the advantage of generating non pixelated spatial transmittance. As a transmissive device, it has the advantage of high transmittance(80%) and it can overcome the problem of black-matrix effect compared with the traditional TFT(Thin Film Transistor) liquid crystal modulator.

8556-43, Session 11

Tunable photonic structures from polymer-liquid crystal composites

Irena Drevensek-Olenik, Univ. of Ljubljana (Slovenia)

Liquid crystals are soft materials with large anisotropy of physical properties. This combination provides that huge modifications of their optical refractive index can be induced by relatively low external stimuli. For that reason, liquid crystals are widely used in information displays (LCDs) and in various switching and sensing devices. Incorporation of liquid crystals in polymer structures and composites results in microconfinement effects, which lead to several new interesting optical features and tuning capabilities. Investigations of tuning properties of two different types of polymer-LC composite materials, namely holographic polymer-dispersed liquid crystals (HPDLCs) and light-sensitive liquid crystal elastomers (LS-LCEs), will be reviewed.

REFERENCES:

1. MILAVEC, Jerneja, DEVETAK, Miha, LI, Jianfeng, RUPP, R. A., YAO, Baoli, DREVEN?EK OLENIK, Irena. Effect of structural modifications on the switching voltage of a holographic polymer-dispersed liquid crystal lattice. *Journal of optics*, 2010, vol. 12, no. 1, p. 015106-1-015106-8.
2. DEVETAK, Miha, MILAVEC, Jerneja, RUPP, R. A., YAO, B., DREVEN?EK OLENIK, Irena. Two-dimensional photonic lattices in polymer-dispersed liquid crystal composites. *J. Opt. A, Pure Appl. Opt.*, 2009, vol. 11, p. 024020-1-02420-8.
3. GREGORC, Marko, LI, Hui, DOMENICI, Valentina, AMBRO?I?, Gabriela, ?OPI?, Martin, DREVEN?EK OLENIK, Irena. Kinetics of holographic recording and spontaneous erasure processes in light-sensitive liquid crystal elastomers. *Materials (Basel)*, 2012, vol. 5, no. 5, p. 741-753.
4. GREGORC, Marko, ZALAR, Bo?tjan, DOMENICI, Valentina, AMBRO?I?, Gabriela, DREVEN?EK OLENIK, Irena, FALLY, Martin, ?OPI?, Martin. Depth profile of optically recorded patterns in light-sensitive liquid-crystal elastomers. *Phys. Rev. E*, 2011, vol. 84, 3, p. 031707-1-031707-5,

8556-44, Session 11

Laser beam scanning using binary diffraction holograms

Bosanta R. Boruah, Abhijit Das, Indian Institute of Technology
Guwahati (India)

Laser beam scanning is important in a number of applications such as to detect events or information in a given surface or to induce physical phenomena in a given surface. Laser beam scanning is also at the core of a scanning optical microscope that is routinely used in number of areas. One of the most commonly used beam scanner is a galvo mirror scanner. However galvo mirror scanners suffer from limitations such as short term repeatability and long term thermal drift. Hence for applications requiring large number of scannings over a long duration of time, galvo mirror scanners are not appropriate. A binary hologram displaying a reconfigurable grating profile can give rise to a diffracted beam whose position on a plane is entirely dependent on the hologram profile. Such beam positioning can offer an unlimited repeatability as long as the grating pattern is described identically. Unfortunately such a reconfigurable binary hologram, if used as a beam scanner, will not give uniform step size of the diffracted beam for uniform increase in input spatial frequency used to design the hologram. Further for pixellated hologram planes there is no one-to-one relation between the beam deflection angle and the input hologram frequency. In this paper we propose a binary hologram based optical scanner. We show that it is possible to theoretically suggest the precise location of the diffracted beam from the input hologram frequency. Thus one can generate a set of spatial frequencies of the grating pattern that can provide beam deflection with equal step size. Preliminary experimental results clearly demonstrate our proposed scheme of beam scanning.

Conference 8557: Optical Design and Testing V

Monday - Wednesday 5 -7 November 2012

Part of Proceedings of SPIE Vol. 8557 Optical Design and Testing V

8557-1, Session 1

Developing interface localized liquid dielectrophoresis for optical applications (Invited Paper)

Glen McHale, Northumbria Univ. (United Kingdom); Carl V. Brown, Michael I. Newton, Gary G. Wells, Naresh Sampara, Nottingham Trent Univ. (United Kingdom)

Electrowetting charges the solid-liquid interface to change the contact area of a droplet of a conducting liquid. It is a powerful technique used to create variable focus liquid lenses, electronic paper and other devices, but it depends upon ions within the liquid. Liquid dielectrophoresis (LDEP) is a bulk force acting on the dipoles throughout a dielectric liquid and is not normally considered to be a localized effect acting at the interface between the liquid and a solid or other fluid. In this work, we show theoretically how non-uniform electric fields generated by interdigitated electrodes can effectively convert LDEP into an interface localized form. We show that for droplets of sufficient thickness, the change in the cosine of the contact angle is proportional to the square of the applied voltage and so obeys a similar equation to that for electrowetting – this we call dielectrowetting. However, a major difference to electrowetting is that the strength of the effect is controlled by the electrode spacing and the liquid permittivity rather than the properties of an insulator in a sandwich structure. Experimentally, we show that this dielectrowetting equation accurately describes the contact angle of a droplet of oil viewed across parallel interdigitated electrodes. Importantly, the induced spreading can be complete, such that contact angle saturation does not occur. We then show that for thin films, LDEP can shape the liquid-air interface creating a spatially periodic wrinkle and that such a wrinkle can be used to create a voltage programmable phase diffraction grating.

8557-2, Session 1

Wafer-level micro-optics: trends in manufacturing, testing, packaging, and applications

Reinhard Voelkel, Li Gong, Jürgen Rieck, Dayu Zheng, SUSS MicroOptics SA (Switzerland)

Micro-optics is an indispensable key enabling technology (KET) for many products and applications today. Probably the most prestigious examples are the diffractive light shaping elements used in high-end DUV lithography steppers. Highly-efficient refractive and diffractive micro-optical elements are used for precise beam and pupil shaping. Micro-optics had a major impact on the reduction of aberrations and diffraction effects in projection lithography, allowing a resolution enhancement from 250 nm to 45 nm within the last decade. Micro-optics also plays a decisive role in medical devices (endoscopes, ophthalmology), in all laser-based devices and fiber communication networks, bringing high-speed internet to our homes. Even our modern smart phones contain a variety of micro-optical elements. For example, LED flash light shaping elements, the secondary camera, ambient light and proximity sensors.

Wherever light is involved, micro-optics offers the chance to further miniaturize a device, to improve its performance, or to reduce manufacturing and packaging costs. Wafer-scale micro-optics fabrication is based on technology established by semiconductor industry. Thousands of components are fabricated in parallel on a wafer. This review paper recapitulates major steps and inventions in wafer-scale micro-optics technology. We report on the state of the art in wafer-based manufacturing, testing, packaging and present examples and applications for micro-optical components and systems.

8557-3, Session 1

Optical modulation of polarization state based on an etched single mode fiber with azo-polymer overlay

Weiwei Qiu, Xiujie Tian, Qijin Zhang, Bing Zhu, Univ. of Science and Technology of China (China)

A large modulating range of polarization state at 1550nm is achieved by using an etched single mode fiber (SMF) overlaid with azo-polymer. Most cladding of the SMF is etched off by hydrofluoric acid (HF) to access evanescent field, and then the azo-polymer is used as coating layer for the etched fiber. With irradiation of polarized light, the photo-reorientation of azo-polymer occurs, causing the birefringence in the fiber. This optically induced birefringence results in the change of polarization state which is continuously recorded on the Poincare sphere, making the state of polarization (SOP) tunable by the irradiation of 365nm polarized light. By precisely controlling the refractive indices of the azo-polymer which are 1.4489, 1.4479 in two orthogonal directions, the SOP of propagating light in the etched fiber can be changed significantly by the irradiation of 365nm light with different polarization directions. The SOP changes from right-handed elliptical polarization to left-handed elliptical polarization, also linear polarization is achieved. The trajectory of the SOP can also be recovered to the initial polarization state when irradiated by unpolarized light. The phase shift of the propagating light varies from 28.8 degree to 143.0 degree and the ellipticity varies from 16.2 degree to 55.6 degree during the irradiation. Our experimental results show a simple method of achieving large modulation of polarization state of propagating light by optical control.

8557-77, Session 1

Fabrication method of artificial compound eye

Lifang Shi, Axiu Cao, Yan Liu, Institute of Optics and Electronics (China); Yutang Ye, Univ. of Electronic Science and Technology of China (China); Qiling Deng, Institute of Optics and Electronics (China); Chunlei Du, Chongqing Institute of Green and Intelligent Technology (China)

Optical imaging and detecting are extensively used in biomedical, industrial, and military applications, and there is a continuing trend in the performance improvement of such systems. However, traditional imaging system suffers narrow field of view (FOV). To address this issue, artificial compound eyes has attracted a great deal of research interest, which comprise thousands of integrated optical units called ommatidiums spherically arranged along a curvilinear surface so that each unit points in a different direction. The omnidirectionally arranged ommatidium collects incident light with a narrow range of angular acceptance and independently contributes to the capability of wide field-of-view (FOV) detection. For practical implementations of compound eyes with wide FOV, the requirement of curvature-compatible fabrication schemes is evident. In this work, a method used to fabricate artificial compound eye is presented, where microlens are used as ommatidium. Regular micro-fabrication is adopted to manufacture the planer microlens array pattern. Soft-lithography is used to manufacture the deformed elastomer membrane to obtain opposite concave microlens patterns. 3D Polymer replication is used to transfer the patterns onto the hemispherical dome substrate. Experiments were carried out and an artificial compound eye contain over 20 thousands ommatidiums was fabricated. No expensive equipment and materials are needed in the fabrication process. The 3D polymer fabrication method presented in this work has potential for a broad

range of optical applications, such as data storage and readout, medical diagnostics, surveillance imaging, and light-field photography.

8557-5, Session 2

Aberration retrieval using through focus intensity measurements (*Invited Paper*)

Silvania F. Pereira, Technische Univ. Delft (Netherlands)

The increased interest in qualification methods for lenses may be explained from a number of factors: lens aberrations are known to have an important contribution to linewidth or image displacement in optical projection lithography and it leads to serious limitations in the quality of images in microscopy. Several methods to measure lens aberrations are commercially available based on interferometry, wavefront sensing, and resist printing.

Here, we show an easy assessment tool that would allow rapid control of the quality of these lenses. The measurement is based in obtaining the through-focus intensity distribution of the point spread function of the test lens.

We use two approaches to retrieve the aberrations: a semi-analytical approach based on the solution of the Debye integral using the Extended Nijboer Zernike theory and another approach based on correlation between the through focus images. Experimental results that validate the theoretical expectations are presented.

8557-6, Session 2

Aspheric optics testing with the SCOTS: a reflection deflectometry approach (*Invited Paper*)

Peng Su, James H. Burge, College of Optical Sciences, The Univ. of Arizona (United States)

A software configurable optical test system (SCOTS) based on the fringe reflection or phase measuring deflectometry method was developed for rapidly, robustly, and accurately measuring large, highly aspheric optics.

In its simplest configuration, all that is needed to perform the test is a laptop computer with a built-in camera. The laptop illuminates the test surface with a light pattern on the LCD screen and uses the reflected image to determine the surface gradients.

The SCOTS acts as a Hartmann test in reverse. To obtain large dynamic range, the CCD detector of the Hartmann test is replaced with a flat display and sending light backward, while a pinhole camera takes place the position of the point source in the Hartmann setup. The camera is conjugated with the test mirror. Each valid pixel samples certain region on the mirror, so the classical Hartmann screen is not needed.

We have applied SCOTS to measure many different aspheric optical system such as solar collectors, 8.4m diameter primary mirror segment for Giant Magellan telescope, meter level highly aspheric mirrors of the Hobby Eberly Telescope wide field corrector, X-ray optics, and a 350mm convex aspheric mirror. The results show that the SCOTS has a performance comparable with interferometric methods.

8557-7, Session 2

High-speed zonal wavefront sensing

Bosanta R. Boruah, Indian Institute of Technology Guwahati (India); Biswajit Pathak, Abhijit Das, IIT Guwahati (India)

High speed wavefront sensing is important in applications such as real time optical profile analysis, analysis of fluid dynamics, and ophthalmology. Wavefront sensor can also be used for surface profiling and high frame rate of the sensor will cause the system to be less

susceptible to mechanical vibrations. One of the most commonly used wavefront sensor in such applications is the Shack-Hartmann wavefront sensor (SHWS). It comprises an array of micro lenses which focuses the various zones of an incident wavefront on the detector plane of a digital camera. The incident wavefront profile is measured from the focal spot shifts corresponding to each tiny lens. The speed of such a wavefront sensor depends on the frame rate of the digital camera. Recently we showed that the array of tiny lenses of the SHWS can be replaced by an array of gratings followed by a focusing lens. One advantage of such an arrangement is that the array of focal spots can have reduced number of rows. In this paper we implement such a grating array based zonal wavefront sensor using a ferro electric spatial light modulator (FLCSLM). We show that the gratings in the sensor can be configured in such a way that the focal spots form just one row in the ideal case (i.e. the incident wavefront is plane). We further show that this gives rise to reduced number of effective rows of the digital camera leading to extremely high frame rate. We present here proof-of-concept experimental results using the proposed zonal wavefront sensor setup.

8557-8, Session 2

Test of diffractive optical element for DUV lithography system using visible laser

Zhonghua Hu, Jing Zhu, Baoxi Yang, Yanfen Xiao, Aijun Zeng, Huijie Huang, Shanghai Institute of Optics and Fine Mechanics, Chinese Academy of Sciences (China)

Diffractive optical element (DOE) is widely used to generate various illumination modes in deep ultraviolet (DUV) lithography system. Testing optical performance of DOE under the working wavelength of DUV laser is accurate but complex. Testing DOE using a visible laser make the process more convenient. Additionally, optical alignment of DUV lithography system under assembly is usually carried out with a visible laser, it is more helpful to test the optical performance of DOE in the visible light conditions.

The farfield diffractive pattern distribution is theoretically analyzed with the scalar diffraction theory when the DOE designed for DUV lithography system is tested with a visible laser. The analysis result shows the diffractive pattern distribution of the DOE is enlarged proportionally with a zero-order spike in its center under visible laser condition. Using Matlab program, the diffractive pattern distribution of the DOE is simulated. The simulation result agrees with the theoretical analysis result and indicate the feasibility of the test method.

For test, a He-Ne laser passes through the DOE under test and a fourier lens, the farfield diffractive pattern is generated on a screen. The DOE and the screen is located at the front and back focal planes of a fourier lens, respectively. By image processing, the azimuth, the pole angle and the pole balance can be obtained.

In experiments, the DOE was tested under the working wavelength of 193nm and the results were used as the reference values. Then the DOE was tested under a He-Ne laser and its farfield diffraction pattern was analyzed to calculate its parameters. The experimental results coincide with the reference values. The usefulness of method is verified.

8557-9, Session 2

Wave-front aberrations analysis by Zernike polynomials based on the annular sub-aperture stitching system

Lei Duan, Mei Hui, Cheng Gong, Yuejin Zhao, Beijing Institute of Technology (China)

Large aperture aspheric optical elements with their excellent optical properties, have played a significant role in areas such as aerospace and military imaging systems. Annular sub-aperture stitching method was developed for testing large-aperture aspheric surfaces without

using of any compensating element for measurement. It is necessary to correct measurement of aspheric optical aberrations and create mathematical description to describe wave-front aberrations. This paper presents a method that uses Zernike polynomials to describe the wave-front aberrations of full wave-front and reconstructed wave-front by annular sub-aperture stitching algorithm, in order to prove that the annular sub-aperture stitching method can meet the requirement for high precision and effectiveness.

Zernike polynomials form a complete set of modes that are orthogonal over a circular or an annular pupil. Different modes of wave aberrations with a circular or an annular pupil are accurately described by different weighted sum of Zernike polynomials, and the orthogonal set of Zernike polynomials is suitable to describe wave aberration functions and data fitting of experimental measurements for the annular sub-aperture stitching system. Here, the analysis is proven by computer emulation. Simulation are given to demonstrate to the original full-aperture wave-front of the surface by setting up Zernike coefficient in circular region. According to the division of the sub-aperture, different annular regions wave-front surfaces are acquired by a given coefficient of annular Zernike polynomials. The full-aperture surface are reconstructed by stitching algorithm. At the same time, the imaging quality of the aspheric optical element can be contrasted. The stitching result shows good agreement with the full-aperture result.

8557-11, Session 3

Recent progress on digital holography for 3D display *(Invited Paper)*

Hiroshi Yoshikawa, Takeshi Yamaguchi, Nihon Univ. (Japan)

We have been investigating on digital holography for 3D display, particularly fast calculation of the computer-generated hologram (CGH). The hologram is known as the ultimate 3D display because it has all three-dimensional information and the reconstructed image of the hologram provides the natural spatial effect. However, required pixel number for the practical 3D hologram is much higher than that for 2D images. Therefore, fast generation of CGH is quite important. This talk reviews recent progress on CGH, mainly done by the speaker's group. In addition, output methods such as holographic fringe printers and holographic video displays are also reviewed.

8557-12, Session 3

Three-dimensional display based on phase modulation *(Invited Paper)*

Osamu Matoba, Kobe Univ. (Japan)

Holographic 3D display is known as an ideal 3D display. However, holographic reconstruction creates unwanted reconstruction such as DC term and conjugate of the object wave. These unwanted terms reduces spatial frequency contents of reconstructed 3D object and viewing zone in a 3D display. In this presentation, 3D display based on the modulation of phase distribution of object wave is briefly reviewed. The phase distribution to generate 3D objects in air is obtained by digital holography for real objects or by numerical propagation from computer graphics data for virtual objects. Experimental demonstration using 2K1K phase mode spatial light modulator (pSLM) is presented. We also presented a method for achieving wide viewing angle using single pSLM.

8557-13, Session 3

Parallel phase-shifting digital holography system using a high-speed camera *(Invited Paper)*

Yasuhiro Awatsuji, Takashi Kakue, Tatsuki Tahara, Peng Xia,

Kenzo Nishio, Shogo Ura, Toshihiro Kubota, Kyoto Institute of Technology (Japan); Osamu Matoba, Kobe Univ. (Japan)

Parallel phase-shifting digital holography is a technique capable of high-precision and three-dimensional (3-D) measurement of objects with a single-shot exposure. In this technique, a single hologram containing multiple holograms required for phase-shifting digital holography is optically generated by using space-division multiplexing of holograms. The single hologram is recorded by using an image sensor. The multiple holograms are numerically generated by interpolating the recorded hologram by using a computer. The complex amplitudes of the objects are numerically reconstructed by use of the scheme of phase-shifting digital holography. Not only phase images but also 3-D images of the objects are obtained. We constructed a system of the parallel phase-shifting digital holography consisting of a Mach-Zehnder interferometer and a high-speed camera. The high-speed camera is capable of detecting polarization of light wave pixel-by-pixel. This camera can record holograms consisting of 1024×1024 pixels, 512×512 pixels, 128×128 pixels, and 64×64 pixels, at the rate of 7,000 frames per second (fps), 15,000 fps, 150,000 fps, and 300,000 fps, respectively. Motion picture of 3-D image of two vibrating elastic bands located at different depth was demonstrated at 180,000 fps by the system. Motion picture of phase image of flow of compressed transparent gas sprayed from a nozzle was demonstrated at 180,000 fps. Strange dynamics in the flow was observed in the motion picture of phase image. Also a motion picture of phase image of dynamic change of air induced by a focused femtosecond light pulse in air was recorded at 262,500 fps.

8557-14, Session 3

Digitization and visualization of virtual cultural heritage

Ameng Li, Xiang Peng, Dong He, Hailong Chen, Xiaoli Liu, Shenzhen Univ. (China); Qinqing Zhao, Aimin Hao, BeiHang Univ. (China); Xinghua Qu, Tianjin Univ. (China); Kaibing Xiang, ESUN Co., Ltd. (China)

In recent years, virtual cultural heritage generated by optics and computer graphics methods has become an active research subject that has drawn much attention and interest from communities of optical engineering, computer science and cultural heritage around the world. In this talk, we are going to briefly introduce some of typical research projects regarding virtual heritage undertaken and ongoing in the North America, European Community (EC), Japan and China, from which we can see that the technology of 3D scanning and interaction with high quality graphics plays a central role in virtual heritage. Thereafter we present a new optics-graphics platform for automatically digitizing and presenting the virtual cultural heritage. This platform is designed with a strategy of using an optical scanning network arranged as one-dimensional array consisted of a set of 3D node-sensors. The 3D sensor array works in conjunction with a motorized controlled turntable in our proposed platform architecture. With this dedicated design, we are able to digitize complete 3D virtual heritage with complex geometry and topology while the 3D scanning pipeline, including the acquisition and registration of multiple range images can be implemented in a fully automatic fashion. Furthermore, the texture mapping and blending are also applied for generating photorealistic 3D graphic models of virtual cultural heritages. The architecture design of instrument prototype for scanning hardware and the framework for reconstruction and interaction software are described in this presentation. Furthermore, some of experiment results for digitization and visualization of virtual cultural heritage are shown to demonstrate the effectiveness of proposed platform.

8557-15, Session 3

Basic problems in 3D real-time holographic display

Juan Liu, Jia Jia, Beijing Institute of Technology (China)

A holographic display can reconstruct the whole optical wave field of a three-dimensional (3D) scene, and it is known as the only 3D display technique that can produce all the depth cues. The commercial pixelated spatial light modulator (SLM) is employed in a typical 3D display system. However, the zero-order intensity exists in the image plane because of the pixelated structure of a phase only SLM, which is a typical problem when using a commercial SLM for holographic projection of arbitrary light patterns. To achieve the real time 3D holographic display, there are still two main problems hindering the real time applications of state-of-art holographic 3D projection: one is the enormous computational time, and the other is the limited size and viewing zone of the reconstructed 3D optical image due to the limitations of the total size and its pixel pitch of the SLM. As is well known, higher resolution and smaller pixel pitch of the SLM on which the hologram is loaded will lead to a larger viewing zone and a bigger size of the 3D reconstructed image. Here a technique is proposed theoretically and verified experimentally to eliminate a zero-order beam caused by a pixelated phase-only spatial light modulator (SLM) for holographic projection; we propose a simple technique to enlarge the reconstructed three-dimensional (3D) optical image and shorten the reconstructed distance simultaneously in real time holographic projection using a conventional lens or concave reflecting mirror based on the optical reversibility theorem.

References:

1. Jia Jia, Yongtian Wang, Juan Liu, Xin Li and Jinghui Xie, "Magnification of three-dimensional optical image without distortion in dynamic holographic projection", *Opt. Eng.* 50, 115801 (Oct 27, 2011); doi:10.1117/1.3654163.
2. Dongdong Wang, Nan Zhu, Yongtian Wang, Jinghui Xie, Juan Liu*, "Experimental verification of optical image encryption based on interference", *Optics Communications* 284 (2011) 2485–2487.
3. Nan Zhu, Yongtian Wang, Juan Liu, Jinghui Xie, "Holographic projection based on interference and analytical algorithm", *Optics Communications* 283 (2010) pp. 4969-4971.
4. Hao Zhang, Jinghui Xie, Juan Liu, and Yongtian Wang? "Elimination of a zero-order beam induced by a pixelated spatial light modulator for holographic projection" *Applied Optics* Vol. 48, No. 30, 5834-5841, 20 October 2009.
5. Hao Zhang, Jinghui Xie, Juan Liu, and Yongtian Wang, "Optical reconstruction of 3D images by use of pure-phase computer-generated holograms", *Chinese Optics Letters*, Vol. 7, No. 12, 1-3, December 10, 2009.

8557-16, Session 4

Super-resolving spots for high momentum transfer sub-wavelength scatterometry and imaging (*Invited Paper*)

H. Paul Urbach, Technische Univ. Delft (Netherlands)

By shaping the field in the entrance pupil of a high NA lens, very special focused fields can be obtained. For example, fields which, for a given focused power, give the maximum electric energy density in focus or the maximum force in a given direction on a small particle in the focal point. The corresponding pupil fields can in some cases be obtained in closed forms. In other cases an expansion of the pupil field in Zernike polynomials is convenient. To realize these focused fields, the polarization, amplitude and phase of the pupil fields must be made position dependent. This can be achieved by spatial light modulators.

We shall discuss an number of examples of special focused fields. Furthermore we will discuss the application of focused fields in sub-wavelength scatterometry and high resolution imaging.

8557-17, Session 4

The behavior of branch points in laser propagation through atmosphere

Xiaolu Ge, Anhui Institute of Optics and Fine Mechanics, Chinese Acad (China) and Shandong Univ. of Technology (China); Chengyu Fan, Xiaoxing Feng, Anhui Institute of Optics and Fine Mechanics (China); Chengfeng Li, Xiaojuan Liu, Liping Guo, Gongxiang Wei, Shandong Univ. of Technology (China)

When branch points are present in laser beam wave-front during the propagation in turbulence, the adaptive optics system for atmosphere turbulence compensation will be degraded greatly. The theory of branch-point detection and phase reconstruction is introduced. Numerical experiments are carried out about the temporal and spatial variation of branch points by four-dimension code of laser propagating in atmosphere. The act of branch points' creating and annihilating is emulated when the light wave propagating in atmosphere. The involvement of branch points in some propagating range with time is emulated, too. In the adaptive optics system, the phase of compensating main laser is acquired from the distorted field of beacon laser, so the behavior of branch points in the distorted optical field is simulated when the main laser and beacon laser propagate in the atmosphere with opposite direction at the same time. These computational results indicate that branch points are moving at the movement of a light wave in the space, and they create and annihilate in pairs. The position of branch points in distorted optical field varies with time when the propagating range is fixed. When the condition of laser beam propagating in atmosphere is fixed, the ensemble average of branch points can be definite at the fixed propagating range. The beacon laser produces more branch points than main laser when they propagate in the atmosphere with opposite direction at the same time. So when the branch points in turbulence-distorted optical field are considered, the compensating power of adaptive optics can become much better when the beacon wavelength chosen slightly longer than the wavelength of main laser. The work could provide a reference for further study of laser propagation through atmosphere and adaptive optics system.

8557-18, Session 4

Implementation of controlling the divergence angle utilizing liquid crystal optical phased array

Feng Xiao, Lingjiang Kong, Univ. of Electronic Science and Technology of China (China)

Laser radar has the disadvantage in target detection because of its extreme narrow beam. The efficiency of the laser radar system for detection and tracking will be greatly increased if it can rapidly and accurately control the size of divergence angle of the transmitted laser beam. This paper analyses the propagation properties of the Gaussian beam and the transform function of a lens, then obtain the method to change the size of the divergence angle of a Gaussian beam by using a lens with proper focal length. Then an implementation of tunable liquid crystal lens is proposed in this article based on the principle of optical phased array technology and the electro-optic characteristic of the liquid crystal. Theoretic analysis of the feasibility is made and a liquid lens is fabricated. The device has 1920 electrodes and an aperture size of 10mm. It is driven by a voltage of 5V and each electrode can be controlled independently by AC square-wave voltage. Simulation has been made to demonstrate the liquid lens can vary the length at the range of 0.4m to 10m continuously. A method is also been proposed that uses this liquid crystal phased array tunable lens to modulate the wavefront of an incident Gaussian beam and change the size of divergence angle continuously and rapidly without changing the structure of the device. Experiment has also been done to certify the liquid crystal lens has the capacity to control the divergence of an incident light by varying the focal length.

8557-19, Session 5

New approach to cost-based tolerancing (Invited Paper)

Akira Yabe, Independent Consultant (Germany)

The tolerances are given to keep the performance criteria within the acceptable values in the manufactured lenses. If the tolerances and the performance criteria are given, the yield of the manufacturing can be estimated with the Monte Carlo simulation. The tolerance determines the manufacturing cost. The manufacturing cost should be as low as possible. The cost-based tolerancing is to determine the tolerances accounting for the manufacturing cost. The typical formulation of the cost-based tolerancing is to minimize the cost under the target yield or to maximize the yield under the target cost.

This optimization problem looks complicated and time-consuming when the yield is viewed as a function of the tolerances. The global optimization seems to be necessary, because there are many local minima in the tolerance space. If the discrete values of the tolerances are possible, the problem looks like a combinatorial one.

The number of the combination grows exponentially to the number of the tolerance parameters. The author found the problem is dramatically simplified if the the variances or averages of the critical performance criteria are used as the independent variables of the optimization. The optimal tolerance set can be found with a few trials of the Monte Carlo simulation.

In the cost model, the tolerances may be continuous or discrete. It will be shown that, for the discrete cost model where the choice from 2 or 3 values is possible for a tolerance parameter, the cost optimization can be simplified with the linear programming.

In an example, the curvature, surface separation, refractive index, and Abbe number will be toleranced. The tolerancing of the refractive index and Abbe number will be discussed in detail.

Reference:

"Rapid optimization of cost-based tolerancing", Applied Optics, 51, 855-860 (2012)

8557-20, Session 5

Thermal control design of a multi-channel scanning imagery radiometer (Invited Paper)

Jiang Shichen, Bingting Hu, Xu Tao, Shanghai Institute of Satellite Engineering (China); Ganquan Wang, Shanghai Institute of Technical Physics (China)

The multi-channel scanning imagery radiometer is one of the main payloads of a geostationary earth orbit satellite, which can observe multi spectrum from earth. The radiometer will endure complicated heat flux environment in orbit, and effective thermal design for the instrument is required in order to ensure high quality scanning image.

According to the geosynchronous orbit characteristics and configuration of radiometer, thermal design features are summarized to control the temperature of radiometer by means of heat dissipation, thermal insulation design, isothermal design and active heaters' control. Detailed thermal control design was showed in this paper.

Radiometer thermal model is developed using the NEVEDA and SINDA/G software. Heat flux calculation and temperature calculation were performed for all typical orbital cases, and the numerical temperature results of the radiometer are showed all within the acceptable range for all typical orbital cases. The numerical results verified the validity of the thermal control design.

8557-21, Session 5

Description and implementation studies on field dependent wavefront aberration

Luwei Zhang, Zhaofeng Cen, Xiaotong Li, Zhejiang Univ. (China)

Zernike polynomials has been widely used to fitting lens surface figure error and the wavefront aberration of optical systems ,for its orthogonality in the unit circle and its corresponding relationships with optical aberrations. Because the current extensively used Zernike polynomials is just a function of the aperture ,without consideration of the field factor , it can only represent single field wavefront aberration. This is incomplete for the description of the wavefront aberration, especially for lithographic lens with a large field and high imaging quality.Thus, considering the field factor in the description of wavefront aberration becomes very necessary. This paper presents a convenient and practical method to fit the full field wavefront aberration. A rotationally symmetric optical system has been taken as an example, in the scope of normalized full field, selecting field points close to the Chebyshev polynomial zero points as the interpolation nodes, and applying the Chebyshev polynomial to the fitting of Zernike coefficients of different fields. Meanwhile, taking the Chebyshev polynomial fitting order's influence on the fitting accuracy into account, this paper gives the criterion to determine the best fitting order for different optical systems by comparing and analysing the fitting results of different fitting order. The results show that the fitting method used in this paper is of high accuracy, and the fitting results is very important for the analysis of full field wavefront aberration.

8557-22, Session 5

Simulation analysis of space remote sensing image quality degradation induced by satellite platform vibration

Feng Yang, Xiaofang Zhang, Yu Huang, Weiwei Hao, Baiwei Guo, Beijing Institute of Technology (China)

Satellite platform vibration causes the image quality to be degraded, it is necessary to study its influence on image quality. The forms of Satellite platform vibration consist of linear vibration, sinusoidal vibration and random vibration. Based on Matlab & Zemax, the simulation system has been developed for simulating impact caused by satellite platform vibration on image quality. Dynamic Data Exchange is used for the communication between Matlab and Zemax. The data of sinusoidal vibration are produced by sinusoidal curve with specific amplitude and frequency. The data of random vibration are obtained by combining sinusoidal signals with 10Hz, 100Hz and 200Hz's frequency, 100, 12, 1.9's amplitude and white noise with zero mean value. Satellite platform vibration data which produced by Matlab are added to the optical system, and its point spread function can be obtained by Zemax. Blurred image can be gained by making the convolution of PSF and the original image. The definition of the original image and the blurred image are evaluated by using average gradient values of image gray. The impact caused by the sine and random vibration of six DOFs on the image quality are respectively simulated. The simulation result reveal that the decenter of X-, Y-, Z- direction and the tilt of Z-direction have a little effect on image quality, while the tilt of X-, Y- direction make image quality seriously degraded. Thus, it can be concluded that correcting the error of satellite platform vibration by FSM is a viable and effective way.

8557-23, Session 5

A realization method of full-field point spread function

Hongmei Luo, Zhaofeng Cen, Xiaotong Li, Zhejiang Univ. (China)

Point spread function (PSF) describes the intensity of the diffraction image formed by the optical system for a point source in the field. PSF is frequently used in image quality evaluation of optical system, image restoring and image simulation. The PSF of an optical system varies with the position of the point source and such variance cannot be negligible particularly with the increasing degree of complication of the optical system. Therefore it becomes advantageous to know how each element in the PSF matrix depends on the field.

This paper proposes a realization method of full-field PSF. Firstly the data of several field points of the PSF are obtained by using the optical design software, then the expression for the field dependence of each element in the PSF matrix is gotten by polynomial fitting, thus the PSF matrix of any field, i.e. the full-field PSF is realized.

To verify this method, we choose a real optical system in this context, and compare the PSF adopting the method mentioned above with that obtained in optical design software by ray tracing. The comparison shows that the full-field PSF method is able to obtain the PSF of any desired field in less time and with relatively high accuracy. In addition, the full-field PSF is hopefully applied in computing the significant modulation transfer function (MTF) data in less time using an FFT algorithm, higher accuracy image simulation by the convolution of the input object and the varied PSF.

8557-32, Poster Session

Design and experimental research on miniature fiber-optic displacement sensor

Fei Gao, Jun Yang, Harbin Engineering Univ. (China)

A detecting method based on Fizeau interferometer for fiber-optic displacement sensing is presented to detect high-precision displacement measurement with order of nanometer or sub-nanometer. On the basis of optical interferometry and common-path Fizeau interferometer, micro displacement can be detected by accurately measuring the distance changes between the surfaces of fiber-optic collimator and measuring mirror. Its characteristics are as follows: (1) With common-path interferometer, environmental dependence of energy transmitting fiber to ambient temperature is eliminated, then the effect of ambient temperature variation to the system is reduced; (2) With the method of optical frequency phase-carrier modulation/demodulation instead of electrically controlled phase modulator, the optical path is formed with all-fiber components to improve the application flexibility of the system; (3) By micro fiber-optic collimator with diameter of 1 mm, the overall dimensions of the displacement sensor is greatly reduced, which makes the use of the sensor more flexible. In the paper, the structure and parameters of micro all-fiber common-path fiber-optic displacement sensor is studied, the experimental platform for high-precision displacement calibration is built, and a series of performance tests are completed. Experimental results show: with the displacement length of 0-8 mm, the measuring resolution of the micro fiber-optic displacement sensor can reach 0.1 nm, the measuring dynamic range can get 158 dB, which indicate that the micro fiber-optic displacement sensor has superior performances with high resolution, high precision and large dynamic range.

8557-39, Poster Session

Infrared dual-band telephoto design used in joint transform correlator

Mu Da, Dong Jianing, Chunyun Xu, Changchun Univ. of Science and Technology (China)

On the basis of optical correlation detection, photoelectric hybrid joint transform correlator(JTC) is widely used in military, aviation and intelligentization, etc. It has the advantages of great flexibility and high precision of recognition. However, the optical system which is in front of joint transform correlator(JTC) is applied to receive the infrared radiation of the target. It also has a certain influence on JTC's detecting

precision and tracking ability. Dual band infrared imaging system can receive different wave band of infrared radiation. Therefore, the image quality of optical system plays an important role in the joint transform correlator(JTC).According to the requirements of the joint transform correlator (JTC), the processes of optical design including the allocation of parameters and the selection of initial structure are presented. The infrared dual band coaxial telephoto system is designed for target detection. The system which is composed of four lenses can image in both 3 μm ~5 μm and 8 μm ~12 μm wavebands. The focal length is 200 mm and the relative aperture is 1:3. The system has the characteristics of small volume and compact structure. The optical system image quality is evaluated with ZEMAX optical design software. The results have shown that MTFs of the system are 0.62 and 0.35 for both wavebands respectively at 17lp/mm of spatial frequency which are closed to the diffraction limited curve. The relative aperture, field of view, and focal length are same for both spectral regions. The system meets the requirements of technical specification and improves the ability of JTC in target tracking and recognition.

8557-40, Poster Session

A high-speed and small-volume IR zoom lens using root-exchange theory and DOE element

Liu Lin, Sun Xing, Zhang xing de, North China Research Institute of Electro-Optics (China)

The high-speed and small-volume mid-wave IR zoom lens capable of 16x magnification using a 320 \times 256 IR FPA detector has been described. The system magnification can be continuously adjusted by simply moving two lens groups, which uses the root-exchange theory. The system also contains much less optical material and has a very simple structure by using DOE elements. Based on the characteristics, the chromatic aberration was balanced. Research on the thermal analysis and compensation is considered. DOE elements make the zoom lens maintain its performance when it is operating between 0 $^{\circ}\text{C}$ and 60 $^{\circ}\text{C}$. The results show the high magnification zoom lens design performance, with small volume and light weight. The aberration of the system were well corrected and diffraction limited performance was achieved in required temperature range.

8557-41, Poster Session

Optical design of solar blind ultraviolet warning system

Quanyong Li, Chunyun Xu, Jianing Dong, Changchun Univ. of Science and Technology (China)

Ultraviolet warning technology is one of the important methods for missile warning. "Solar blind region" provides a very effective way to detect the target for missile approaching alarm. In order to find the target by detecting the ultraviolet radiation of missile efflux plasma, ultraviolet optical system design of large field of view and large relative aperture is the key for the technology of ultraviolet detection. From the academic point of view, the structure parameters are determined for 2048 \times 2048 ultraviolet CCD detector according to the requirements of ultraviolet warning system. The refractive ultraviolet warning optical system is designed for 0.24 μm ~0.28 μm waveband with ZEMAX optical design software. The focal length is 41mm, the field of view is 46 $^{\circ}$ and the relative aperture is 1:3.5. In order to ensure the detected energy, aspherical and binary surface are adopted to reduce the aberration and spot size of the system. Within the 0.8 field of view RMS of spot diagram is less than 13 μm . It is smaller than the pixel size 13.5 μm of ultraviolet CCD. The energy concentration is more than 80%. This optical system has long focal length and large relative aperture that meet the energy requirements of warning system. Large field of view can satisfy the range of searching targets. The spot diagram RMS of each field of view is so small that can meet the requirement of

image quality. In addition, the system is composed of six lenses. The structure of it is simple, the volume is small and the application is very convenient.

8557-42, Poster Session

Designing adapted to fabricating of holographic silver gratings

Amir Asgari, Amirkabir Univ. of Technology (Iran, Islamic Republic of); Naser Partovi, NSTR Optic & Laser Research School (Iran, Islamic Republic of); Hooshang Araghi, Amirkabir Univ. of Technology (Iran, Islamic Republic of); Eesa Alidokht, Mohammad Hadi Maleki, NSTR Optic & Laser Research School (Iran, Islamic Republic of)

Some holographic super Gaussian silver gratings were optimized in 700-1100nm bandwidth for stretching and compressing pulse in chirped pulse amplification technology. Accordingly, the genetic algorithm (GA) was employed by Grating Solver software to optimize groove spacing, groove depth and groove shape of the grating; then, the rigorous coupled wave analysis was used to analyze the grating diffraction efficiency (DE) as a function of period, depth, angle of incidence, wavelength and duty cycle. GA and developing model of S.Austin et al. (for designing holographically fabricated periodical structures in a positive photoresist) were used to obtain manufacturing parameters (exposure energy densities, development time, groove spacing and Littrow angle). Accordingly, Kpp1206 photoresist was employed for modeling of grating profile. This paper was devoted to consider super Gaussian gratings. Therefore, approximately identical exposure energy density intervals were used for optimizing grating profile. Two optimized silver gratings (for central wavelengths of 800 and 950nm in the 700-900 nm and 800-1100nm intervals) for TM polarized light in the 1st order (Littrow mount) have been achieved. Following results were obtained: (1) DE>92% in the bandpass of >100nm and approximately $\pm 20^\circ$ difference from Littrow angle in the 700-900nm range and DE_{max}>94.5% at ~830nm. (2) DE>92.5% in the bandpass of >300nm and approximately $\pm 10^\circ$ difference from Littrow angle in the 800-1100 nm range and DE_{max}>95.5% at ~925nm. Moreover, a silver grating for the central wavelength of 1060nm desired for Nd:YAG and Nd:Glass lasers, with DE_{max}~ 97% was obtained. Also, it was found that super Gaussian gratings with the depth of ~170-250nm and duty cycle of ~ 0.3-0.65 have maximum DE in 1064nm.

8557-43, Poster Session

Design of all-reflective zoom optical system of wide field-of-view with 3 mirrors

Lifei Zhang, Jun Chang, Aman Wei, Jiao Cao, Jiao Ouyang, Beijing Institute of Technology (China)

All reflective zoom optical systems have advantages of no color aberration and lightweight which have a wide application prospects in space optical system. All reflective zoom optical systems, which have been designed, all use telephoto construction. And these systems have disadvantages of big obscuration and small field of view. So in order to satisfy of requests the wide spectrum and field of view of space optical system, this paper design a novel all reflective zoom optical system which uses anti-telephoto construction with 3 mirrors. Firstly, using the zoom theory of differential, the initial configuration with 2 zoom ratio was obtained. Then simulating and optimizing the system with Zemax that is software of the optical design, we get a novel all reflective zoom optical system. It has a smaller obscuration and bigger field of view than traditional reflective zoom optical system. At last, the image qualities of this system was evaluated and concluded. And the image qualities of this novel all reflective zoom system is well and the construction of the optical system is reasonable. It can be applied in space optical system.

8557-44, Poster Session

Study of an ultra-short-throw projector optical system design using the aspherical surfaces

Yong Wang, Xuemin Cheng, Tsinghua Univ. (China); Qun Hao, Beijing Institute of Technology (China)

The ultra-short-throw projector has been popular these days because of its advantages of occupying little space to light up a big screen, reducing set up time, etc. The optical systems used in these projectors need to achieve special performance qualities, especially a small projection distance. To get a wide field of view while maintaining high optical performance and compact size, a tilted and decentered optical system used in the ultra-short-throw projector is presented in this paper.

The optical system has the non-rotationally symmetric aberrations brought about by tilted and decentered lens and a large field of view, and vector aberration theory is used to analyze the aberrations and help to produce the initial structure. To add the degrees of freedom in design and reduce the number of lens elements, the aspherical surfaces are designed to correct the aberrations. Thus the relationship between the fields of view and the pupil aberration is discussed to achieve a good image quality. It is demonstrated that the MTF values and the relative illumination could be improved regarding to the optimization of the optical structure parameters in the non-rotationally symmetric optical system. The presented optical system has a projection distance of 300 mm, and the maximum distortion is no more than 5%. Its cost is taken into account as well; its advancements in manufacturing technology facilitate the utilization of aspherical surfaces without adding too much expenditure.

8557-45, Poster Session

Prototype design of an all-reflective non-coaxial optical zooming system for space camera application without moving elements based on deformable mirror

Hui Zhao, Xuewu Fan, Gangyi Zou, Zhihai Pang, Wei Wang, Rui Guo, Yunfei Du, Yu Su, Xi'an Institute of Optics and Precision Mechanics (China)

Nowadays, in order to obtain remote-sensing images with different resolutions, space cameras with different focal length installed on different platforms are used. However, this is not an efficient way for space-borne reconnaissance especially when emergencies happen. If the focal length can be changed, only one camera on a single platform is flexible enough to obtain the required information.

As a long established technique, optical zooming allows us to adopt only one camera to capture images with variable resolution and variable field of view (FOV). The development of this technique undergoes three stages: from refractive system to reflective system, from co-axial system to non-coaxial system, from system with moving elements to system without moving elements.

In this paper, an all-reflective non-coaxial optical zooming system is designed. Considering the sensitiveness of satellite platform to vibrations, traditional zooming technique in which moving elements are indispensable is not suitable. Instead, a deformable mirror (DM) whose curvature radius can be changed electronically is introduced. By carefully selecting the optical power of conventional reflective mirrors surrounding the DM, the overall focal length of the system can be 4x changed with the slight variation of curvature radius of DM. The system performance is approaching diffraction-limited according to diverse criteria and what is the most important is that the maximum stroke of DM is still within its physical limits (less than 9 μ m). The proposal of this prototype is a big progress in optical zooming system design and is very meaningful for space camera application.

8557-46, Poster Session

The design of a stepper motor control-based high-precision varifocal imaging optical system

Bai Xiang, Beijing Institute of Tracking and Telecommunications Technology (China)

With high speed developing Chinese spaceflight project, telescope demands more advanced, requiring the optical zoom system. The excellence of zoom is in despite of the target size or distance changed, it image still appropriate dimension easy to looking. So in recent years we produced telescope almost used zoom. The paper first brief introduces principle and composing the optical zoom system. It is made up of fixed mirrors of foreside, mirrors of variofocus, mirrors of compensation and fixed mirrors of rearward. Then paper introduces often used an optical zoom system of cam frame principle and existed problems. The optical zoom system of cam frame is used cam control mirrors of variofocus and compensation motion, to realize zoom and adjust position of image. But this system has some problems. The problems are big shake of optical axis and high error output of real-time focus length. To these problems we designs a precision optical zoom system, used two step motors replace cam frame to command distance of mirrors of variofocus and compensation motion, and used rolling linear path replace sliding path to control direction of mirrors motion, and used grating ruler replaces potentiometer measured numeral of focal length to realize real-time output. The numeral does feedback signal to realize closed loop control by step motor. The excellences of this new system are precision controlled distance of linear motion, reduced shake of optical axis, precision output of real-time focus length, and high reliability of system. So the new system compared the old system shake of optical axis reduces 90%, alignment accuracy increases 80%. It resolves existed problems of the optical zoom system of cam frame. This precision optical zoom system can accomplishes measure of high-degree of accuracy.

8557-47, Poster Session

Design of cooled athermalized infrared telephoto lens

Yu Zhang, Jiyang Shang, Yue Xu, Wensheng Wang, Changchun Univ. of Science and Technology (China)

With the development of the technology of infrared, infrared optical system has been widely used in many fields, especially in target detection and recognition. While the merit of infrared optical system is that it can not only detect all-weather but also detect the target in the poor conditions such as turbid air or smoke, fog and snow. So IR optical system is much more appropriate to be applied in cluttered and formidable conditions. The change of temperature could degrade image quality of the infrared optical system. So the difficulty and key in the designing of LWIR optical systems for working under temperature range of -60°C ~ 80°C is athermalization. The effective focal length of the infrared optical system should be large enough to ensure the long distance detecting. The relative aperture should be large enough to ensure adequate energy.

In this paper, cooled infrared focal plane arrays is used as infrared detector, the pixel size is $35\mu\text{m}$. The working waveband is $8\text{--}12\mu\text{m}$. Its resolving power is 17cy/mm . The infrared telephoto lens is designed which is composed of four pieces of lenses, it meets the designing requirements and has good image quality. The material which we chose zinc selenide, zinc sulfide and germanium is commonly used in IR waveband. The working temperature range is -60°C ~ 80°C . In order to balance the chromatic aberration and thermal aberration, two aspherical surfaces are used in this cooled athermalized infrared optical system. The effective focal length is 100mm and the F-number is 2. The full field of view is 7.04° . The curve of MTF is close to diffraction limit. Within the working temperature, the value of MTF at 17cy/mm is always large than 0.4. The result shows that the infrared optical system achieved better

athermal performances at the working temperature range. The image quality of the system approaches the diffractive limit. In addition, the optical system has many advantages, such as simple structure, light weight and high reliability. This telephoto lens can be used for infrared target detection.

8557-48, Poster Session

Design of low-distortion single fingerprint acquisition system

Zheming Wu, Tianjin Univ. of Technology (China)

In order to get high resolution and low distortion, a method of aberration correction for the trapezoid distortion of the single fingerprint acquisition optical system is proposed in this paper, which combines nearly telecentric optical path with the inclined plane compensation. With this method, not only the distortion of system can be reduced using the character of telecentric optical path, but also the asymmetric aberration caused by the tilted object plane can be compensated with setting the angles of the fingerprint collecting prism. An actual fingerprint acquisition system is designed also. There is a fingerprint collecting prism and a follow-up lens in the system. The structure parameters including the angles of the prism and the position of the pupil are set with little aberrations and low distortion. The 0.43% maximum grid distortion and the 500dpi resolution of fingerprint acquisition system can be obtained. The optical length of this system is in 45mm, the image sensor is $1/3.5''\text{CMOS}$, the size of object plane is $16\text{mm}\times 18\text{mm}$. The MTF of the system is more than 0.5 at 50lp/mm in the majority of field views. The system is small and Simple. The experimental results show that there is almost no trapezoidal distortion in the actual grid image which is collected and it has been clear enough to be able to distinguish pores on the fingerprint image. The grid distortion and imaging quality of the system almost meet the standard of the FBI fingerprint scanning system.

8557-49, Poster Session

Design of blue LEDs arrays with high optical power

Pengzhi Lu, Bin Xue, Hua Yang, Huaiwen Zheng, Xiaoyan Yi, Jing Li, Junxi Wang, Guohong Wang, Institute of Semiconductors (China)

Technical progress in the field of blue light emitting diodes (LEDs) based on III-V compounds has been breathtaking during recent years around the world. With the rapid development of the device, high optical power is expected from blue LEDs in a wide range of applications such as optical-communications, medical optics and Biomedical optics.

In this paper, an array of blue LEDs with high optical power is presented and discussed. Optical of the novel design is completed with the help of running simulation in TracePro to predict the performance of the module.

Cree XP-E LEDs with a square reflector was used in the novel design. In addition, the length and depth of the reflector was 23.7mm and 20mm respectively.

Optical simulation obtained from TracePro shows that optical output power of the LED array could reach 8130mW with a uniform square spot.

To verify the simulation results, Aluminum substrate, Copper substrate and Aluminum reflector have been made, respectively.

From the relationship between input current (A) and optical power (mW) of the samples with Aluminum substrate and Copper substrate, It can be observed that the optical power of sample 2 was higher than that of sample 1 and it can be attributed to the better thermal dispersion performance of Copper. The optical power of sample 1 and sample 2 was 8126mW and 9445mW at 2A, respectively. The experiment result of sample 1 is consistent with previous simulation. Due to the better

thermal characteristic of Copper substrate, the optical power of sample 2 is even higher than the simulated result.

8557-50, Poster Session

Compact optical imaging system for star tracker with long focal length and perfect thermal adaptability

Yiqun Ji, Hucheng He, Rongbao Shi, Soochow Univ. (China)

Star camera is a kind of astronomic navigation equipment for position and state information acquisition. There are two kinds of star camera, the star sensor and the star tracker. Different from star sensor, star tracker is usually applied for certain star detection, and with small field of view but long focal length. According to the requirement of the customer, a star tracker optical imaging system is designed for Polaris detection. First of all, the determination of key parameters of the optical system is analysis in the paper. Secondly, a suitable configuration is chosen after comparison and the optimally design method is given. Finally, the design result and its performance evaluation are presented. The main index parameters of the designed system are as follow. It works at VNIR (0.6 μm ~1.1 μm) waveband according to the spectrum of the Polaris. Its view field is 0.5 degree. And the focal length is 1000mm and the entrance pupil diameter is 80mm. The optimally designed lens is only 80mm in length. A Macsutov-Cassegrain type based lens with the pre determined parameters is designed imagery tele-centric. The lens is compact and with good performance. And the prominent advantage is its perfect thermal adaptability, which is from -40 to 60 centigrade. Its MTF (Modulation Transform Function) reaches diffraction limit. The spot diagrams after tracing are quit near a circle. And about 80% of the energy is encircled in a CCD pixel. The distortion is less than 1%.

8557-51, Poster Session

Optimization design and error analysis of photoelectric autocollimator

Lei Gao, Bixi Yan, Beijing Information Science & Technology Univ. (China)

A photoelectric autocollimator employing an area CCD as its target receiver, which is specially used in numerical stage calibration is optimized, and the various error factors are analyzed. The autocollimator measuring range is designed between -30' and +30', and the expecting accuracy is less than 2".

By using ZEMAX software, the image qualities are evaluated and optimized to make sure the spherical and coma aberrations of the collimating system are less than 0.2mm and 0.035mm respectively; the RMS radius is close to 6.45 microns, which is identified with the resolution of the CCD, and the MTF is greater than 0.3 in the full field of view, 0.5 in centre field at the corresponding frequency of the imaging system. Then, the tolerance analysis function of ZEMAX is applied to simulate the process of the components' machining and assembly. We take the RMS SPOT RADIUS and Diff. MTF Avg as the criteria of tolerance analysis, and the Monte Carlo analysis shows that 90% of the RMS radiuses are less than 6.45microns and 90% of the MTF are larger than 0.3 and meet the requirement.

The mechanical structure is designed according to the upper tolerance analysis.

At last, the errors of the optical-mechanical system are analyzed and calculated. The result demonstrates that the errors origin mainly from fabrication and alignment, which are all about 04". The principle error is about 0.35" and the aiming error is about 0.2". The error synthesis shows that the instrument can meet the demands of the design accuracy, which is also consistent with the experiment.

8557-52, Poster Session

Design of a front objective in a monocular zoom video microscope

Liao Wenzhe, Xiao Zexin, Guilin Univ. of Electronic Technology (China)

Nowadays, the monocular zoom video microscope is one of the most widely used detection equipment at mainstream position in the electronics industry. The front objective of this kind of microscope is benefit for the enlargement of its magnification. At present, the similar products are mainly designed out by non-coaxial system, which means the optical axes between front objective and objective are un-coaxial. However, the actual front objective of monocular zoom microscope uses coaxial system. So a particular front objective designed for the zoom microscope is imperative. At first, we point out this unique design idea form the special imaging relationship between front objective and objective in zoom microscope. And then we choose the position of entrance pupil, numerical aperture and the layout. At last we enumerated examples of the zoom in and out lenses, and analyze the design methods of their similarities and differences.

8557-53, Poster Session

Design of reflective active zoom systems with four mirrors

Shen Benlan M.D., Jun Chang, Beijing Institute of Technology (China)

The traditional zoom systems usually change the spaces between optical components to realize the variable focal lengths. Based on active optics, a new type of reflective active zoom system with four mirrors is proposed, which is different from the traditional zoom system, and realizes the different focal lengths through changing the curvature radius of two reflectors. The new zoom system consists of an afocal front group with three mirrors, and the fourth mirror used for focusing. The relation among the four mirrors is determined by the Pezval condition. The primary and secondary mirrors are both deformable mirrors, which contribute to the transition among the minimum, middle and maximum focal lengths by the curvature radius variation controlled by the voltage, with the constraint limiting its' change rules. According to the designed system characteristics and the practical requirements, based on 3rd-order aberration theory, a set of Seidel aberration coefficient functions are established, with the constraint limitation. Then the initial construction parameters of the optical system can be achieved. The new active zoom system with four mirrors can realize that the zoom ratio is 3, the focal lengths vary from 100mm to 300mm, the field angle of view range is 2.1°~0.7°, and the wide working band is from the visible to the infrared. At the same time, because of the control flexibility, the active optical zoom system has the potential to be widely applied in remote sensing, life medical and other fields.

8557-54, Poster Session

Design and research of the second parallel optical path of the telescope photoelectric imaging system

Chen Gang, Guilin Univ. of Electronic Technology (China); XingYu Gao, Liu Zhou OVM Machinery Co., Ltd. (China); Dao Yin Yu, Tianjin Univ. (China); Ze-Xin Xiao, Guilin Univ. of Electronic Technology (China)

A second parallel CCD (CMOS) camera imaging system for an telescope objective with the fixed D/f' is proposed. For the direct imaging system that the CCD target surface coincides with the imaging surface of the telescope objective, it shows the outstanding

performance of more than doubled resolution compared with the ordinary telescope objective with the same D/f' . On the base of discussions about the innovative telescope optical imaging system, three design examples are compared and analyzed. The relation between the image field and the optical elements of the second parallel path is clarified, which provides a operable method for readers. This practice has proved that it is a new telescope objective photoelectronic imaging system with broad application prospects.

8557-55, Poster Session

Design and modeling of a new CO₂ laser heater for thin film deposition applications

Mohammad Reza Rashidian Vaziri, Fereshteh Hajiesmaeilbaigi, Mohammad Hadi Maleki, Univ. of Tehran (Iran, Islamic Republic of)

In this paper, we report on designing a new raster-scanned CO₂ laser heater for homogeneous heating of the disk-shaped substrates [1]. This new design aims at concentrating the laser energy near the substrate peripheral edge, which mostly tends to remain cooler than the inner parts during the heating process. Our design benefits from using a CW medical CO₂ laser, which at an affordable price can be found by any research group involved in PLD. The capability of this raster-scanned method for producing a highly homogenous temperature distribution on the disk deposition face has been proved by a comprehensive transient heat diffusion model. Our computational model shows that a minimum temperature standard deviation of 1.5 K is achievable using our heater design for a laser power of 7 W. The capability of producing such great temperature uniformity with our CO₂ laser heater design may be quite of assistance in thin film deposition applications. It can favorably be used in preparation of crystalline thin films where their quality depend on the maintained temperature during the deposition time interval. This heater can also be used for CO₂ laser conditioning of the prepared thin films. Furthermore, a set of experiments have been conducted to measure the substrate temperature. The aim of the measurements was to estimate the emissivity of the substrate material (YAG in our case) which was necessary for solving the heat diffusion equation and for comparing the results with the predicted temperature values obtained from modeling.

[1] M.R. Rashidian Vaziri, F. Hajiesmaeilbaigi, and M.H. Maleki, Opt. Eng. 51(4), 044301 (2012).

8557-56, Poster Session

A new type of wide spectral coverage echelle spectrometer design for ICP-AES

Shoajie Chen, Yuguo Tang, Bayan heshig, Xiangdong Qi, Changchun Institute of Optics, Fine Mechanics and Physics (China); Wenyu Zhu, Changchun Institute of Optics, Fine Mechanics and Physics (China) and Medical Instrument Ltd. of CIOMP (China)

The inductively coupled plasma atomic emission spectrometry (ICP-AES) has always attracted great interest and is widely used for routine elemental analysis. While one drawback of this technique is the fact that conventional Czerny-Turner spectrographs in combination with CCD cameras are very limited either in terms of spectral resolution or in terms of simultaneously detectable spectral range. A cross-dispersion system with echelle grating and prism has therefore been developed, and the spectral image is directed by large area charge coupled device (CCD). This configuration meets the needs of atomic emission spectroscopy well, since it has many benefits including high resolving power, spectral coverage, high sensitivity, and high optical throughput. While, because the limitation of the development of detectors, it is difficult to complete wide spectral coverage measurement. Due to the improvements in optical design, this system can detect the wide

spectral coverage from 180nm to 900nm simply by rotating the prism two times, and these three ranges are 180nm-250nm, 250nm-400nm and 400nm-900nm, with a high resolution 0.008nm@200nm. The detection of different elements only needs to choose appropriate wavelength coverage, thus lots of elements can be analyzed within a quite short time. The novel optical design of this instrument is presented and its merits are discussed in this paper. The optical spectral resolution and the precision of wavelength calibration are found to be satisfactory and within the design goals. Experiments show that the ICP-AES with echelle spectrometer is available to detect multiple elements within a short time correctly, the wavelength precision is better than 0.01nm.

8557-57, Poster Session

Optical system design of polarization imaging spectrometer for ground-based astronomical observation

Lingying Chang, Xi'an Univ. of Posts and Telecommunications (China)

In order to obtain polarimetric hyper spectral observation of the astronomical objects such as stars nebulae and extragalactic, the polarization imaging spectrometer for ground-based astronomical observation was developed. It can be quickly electrically tunable for spectral channels by acousto-optic tunable filters for optical dispersion element with low noise back-illuminated CCD as detector, and the orthogonal polarization O light and E light spectrum image was obtained simultaneously at multidimensional target. In this paper, First, the overall scheme of astronomical observations for polarization imaging spectrometer was introduced, then described the optical parameters of each imaging subsystems. It covers the spectral band from 450nm to 900nm with a spectral resolution near 10nm, and the optical system can provide about 4.1° view field angle. Finally, the design of the optical system was completed by the optical design software CODE-V, which imaging resolution excelled 40 lp/mm when the modulation transfer function (MTF) reaches 0.6.

8557-58, Poster Session

A novel optical beam deflection detection system based on aspheric lens for high-speed atomic force microscope

Jianyong Zhao, Guangyi Shang, Junen Yao, Weitao Gong, BeiHang Univ. (China)

The optical lever method is widely used to detect the cantilever deflection in atomic force microscope (AFM) for its simple mechanism and high sensitivity. How to focus the diode laser beam on the very small cantilever with a spot of several microns in diameter is a key and difficult issue in high speed AFM. An ingenious designed optical beam deflection detection system based on aspheric lens is presented. An aspheric lens which can focus laser beam and correct spherical aberration is fixed by an adjustable bolt above the cantilever. Two laser line beamsplitter cubes are installed back to back over the aspheric lens with a 3mm beam diode laser and a quadrant photodetector separately placed in two sides at the same height. The collimated laser beam is reflected down by the beamsplitter, incident on the aspheric lens at an off-centered position. The outgoing beam is focused onto the cantilever and reflected back onto another part of the aspheric lens. Change in the angle of the reflection caused by cantilever deflection results in a parallel shift of the exiting laser beam after the aspheric lens. The laser beam is reflected onto the photodetector by the other beamsplitter where the cantilever deflection is measured by the difference in current between the top and the bottom elements of the photodetector. Experiment results show that diode laser beam can be focused with a spot of less than 16 microns in diameter, which meet the deflection detection requirement for high speed AFM.

8557-59, Poster Session

Design and theoretical investigation of nanograting for XUV outcoupler

Ying-Ying Yang, Institute of Semiconductors (China); Wei Sun, Laboratory of solid state laser sources, Institute of Semiconductors, Chinese academy of sciences (China); Ling Zhang, Huai-juan Yu, Xue-Chun Lin, Institute of Semiconductors (China)

A nano-periodical highly-efficient blazed grating is fully theoretically investigated for outcoupling extreme-ultraviolet (XUV) radiation. The rigorous coupled-wave analysis (RCWA) method with S-matrix is employed to optimize the parameter of the grating. It would allow conducting high resolution spectroscopy of the 1s-2s transition in He at around 61 nm with extreme precision. The grating is designed to be etched into its top layers as a highly-reflective mirror for IR light and outcoupler for XUV. The XUV diffraction efficiency was determined to be greater than 20% in the range from 36 nm to 79 nm and consistent with the experimental data.

8557-60, Poster Session

Off-axis illumination of lithography tool

Xing Han, Lin Li, Beijing Institute of Technology (China); Bin Ma, Beijing Institute of Technology (China) and Univ. of Rochester (United States)

Lithography tool is a necessary part for LSI and VLSI. Off-axis illumination technology is an effective way to reducing resolution of lithography. This paper introduction the basic components of lithography tool, the principle of off-axis illumination reducing the resolution of lithography and do some research about two implementations of OAI technology.

8557-61, Poster Session

Research on design of a cubic conjugate phase mask having the capability of controlling the bandwidth of wave-front coding system

Hui Zhao, Yingcai Li, Xi'an Institute of Optics and Precision Mechanics (China)

Wave-front coding is a widely known technique used to enlarge the depth of field (DOF) of incoherent imaging system and the phase masks are the key to generate large DOF effect.

Many phase masks have been designed to realize the wave-front coding and the cubic type is the most popular one. In paper [Proc. SPIE Vol.4422 pp.34-42,2001], the authors derived an extended cubic phase mask which not only contained cubic terms, but also had quadratic, unitary and constant terms. Although those terms except the cubic one have no effect in enlarging the DOF, according to our further investigation, the extended cubic phase mask has the capability of changing the system bandwidth, indicating that the mask could play a role of bandwidth selection and this effect is rarely noticed in existing literatures.

In this paper, we make three contributions. First, a new procedure is proposed to derive the extended cubic phase mask. Second, by splitting and re-combining the terms of the phase function, a new phase mask containing two conjugate cubic terms is generated and can be physically realized by shifting and superposing two cubic phase mask having relative displacement in the pupil plane. With the variation of displacement, the system bandwidth can be changed with defocus invariance characteristics unchanged. Third, the results can be

extended to other phase masks and the expected bandwidth selection effect can be obtained by combining two conjugate masks with relative shift together.

The work reported is complementary to the field of wave-front coding.

8557-62, Poster Session

Aberration retrieval for annular pupils using parametric model of point spread function

Xinhua Chen, Weimin Shen, Soochow Univ. (China)

Because of imperfect design and manufacture, performances of optical systems are affected by various aberrations. These aberrations will cause image blur and distortion. Adjustment and calibration of optical system can be performed if its aberrations are known, and this can be realized by measuring its pupil wavefront. Wavefront interferometry and Shack-Hartmann wavefront sensing method are two traditional wavefront measurement methods. Compared with these two methods, image-based wavefront sensing method can determine aberrations directly from image formed by the optical system with no extra hardware. This method has attracted more and more attentions for this unique advantage, and has been successfully applied in many domains such as large telescope alignment, X-ray imaging and so on. For annular pupil, wavefront can be decomposed with annular Zernike polynomials. The coefficients of these polynomials can be retrieved using spot intensity images-based aberration retrieval method. In this paper, we propose an aberration retrieval method for annular pupils using proposed parametric model of point spread function (PSF). With this model, the diffraction integral for annular pupils is expressed with Bessel-series representation and annular Zernike coefficients. Conjugate gradient algorithm is used to retrieve aberration coefficients of annular pupil from the corresponding spot intensity images. The iterative calculations of objective function and its gradient function are required for this algorithm. These calculations are accelerated by using the parametric model's analytical expression instead of Fourier transforms. Numerical simulation and experiment are performed to validate this aberration retrieval method.

8557-63, Poster Session

Analysis on the effect of extinction ratio in birefringent measurement by phase-stepping method

Xusheng Zhang, Haoyu Wang, Chuan He, Beijing Institute of Technology (China)

The analysis on the effect of extinction ratios of linear polarizer and analyser in the birefringent retardation measurement by a five-step phase-shifting method based on plane polariscope setup is presented. The phase stepping method with automatic phase unwrapping algorithm is well known to be one of the most effective ways for whole field photoelastic stress induced birefringence analysis. However, the phase stepping methods having been reported in the past literatures have not addressed the potential errors produced by extinction ratios of linear polarizers. The theoretical analysis on how the extinction ratios of linear polarizer and analyser act in our presented five-step phase shifting method is made and discussed in this paper. Stokes vector and Mueller matrix are used to carry such theoretical analysis. This five-step phase shifting method will not introduce errors of quarter wave plates. Also, when this five-step method is used in stress-induced photoelastic birefringence measurement, the isoclinic angle is not necessary to be obtained prior to the measurement of phase retardation, so the data processing can be simplified and the error of isoclinic angle will not affect the accuracy of phase retardation measurement. The theoretical analysis and experiment in this paper show that extinction ratios of linear polarizer and analyser do not cause significant errors in the presented five-step phase shifting method. Standard mica waveplates with given phase retardations are tested, and the results agree well with

the theoretical analysis and given values. Experimental setup of plane polariscope herein includes the components of a 635nm semiconductor laser, rotatable polarizer and analyser, a switchable-gain amplified silicon photodetector and the compatible 16-bit data acquisition system.

8557-64, Poster Session

Research on surface deformation of lens fastened by adhesive under gravity load and aberration analysis

Shaohua Guan, Institute of Optics and Electronics (China);
Tianmeng Ma, Quanzhong Wei, Institute of Optics and Electronics, CAS (China)

In the design and production of optical instruments, various kinds of adhesive are used to mount optical system instead of screw, platen and other fixed parts. But in the assembly of high-accuracy lens and large-aperture lens, the effect of the curing stress of adhesive and gravity is not be ignored, as a result, research on surface deformation of lens and aberration analysis is necessary.

In order to shorten design cycle and reduce costs, this paper designed a simulation analysis about lens structure fastened by adhesive, which make use of finite element software (Ansys) based on finite element basic theory. The following aspects are the major in this paper:

- The whole assembly model of lens fastened by adhesive was built with Solidworks;
- The lens deformation in two different directions of gravity was analyzed, one was along the axial direction and the other was along the radial direction;
- The Zernike polynomials fitting algorithm was used to fit the surface deformation with Matlab program, and the deformed surface mirror values of PV and RMS was calculated;
- According to the relationship between Zernike polynomials and Seidel aberrations, aberrations induced by gravity load were analyzed;
- Different thickness and different spots of adhesive were considered in the analysis of assembly model.

The simulation results indicated that the surface deformation was within the limits of permission, and proper thickness and spot of adhesive were found. These results can be guideline in the practical assembly work of lens.

8557-65, Poster Session

Stray light analysis of a space patrol

Huiyi Chen, Li Lin, Beijing Institute of Technology (China)

The stray light of a space patrol is analyzed in this paper. The space patrol is used to observe the Earth in space. In the paper the definitions of stray lights in the optical system are introduced and the stray lights are classified based on their sources. After the analyzing the serious harm situations of the stray lights in the optical system is presented. Software Tracepro is used in analysis of stray light. The model of the space patrol is established in the software and stray light simulation and analysis of the space patrol are presented based on the evaluation criterion of maximum irradiance value. Three different situations are discussed. First, sunlight directly irradiates onto the sensitive surface of the detector; second, sunlight enters the system by the reflections of the space patrol's body; and finally sunlight reflecting from the moon's surface irradiates onto the sensitive surface of detector by the reflection of the space patrol's body. In each situation, we respectively calculate different elevation angles in ranges between 15°~45° by the ray tracing method in the solar azimuth of 0° and 30°. Transmission paths of stray lights are obtained by ray tracing data in different circumstances and the important surfaces of the system are found out. Finally, some corresponding stray light suppression measures which can help to reduce harm of stray light are proposed.

8557-66, Poster Session

Analysis and protection of stray light for the space camera at geosynchronous orbit

Xiaorui Jin, Li Lin, Beijing Institute of Technology (China)

Stray light is the general term for all non-normal transmission of light in the optical system. The influence of stray light is different according to optical system's structure. Large area array camera at geosynchronous orbit is facing more serious influence of stray light, especially for the small incident angle of sunlight on the system. It is in dire need of a detailed analysis of stray light of the basic shape of the optical system. In the paper, the influence on the camera used in space from stray light and the necessity to eliminate stray light are presented. The definition of the stray light factor and PST (point source transmittance) is briefed. In tracepro, analysis of the impact of sunlight incident was made at different angles on the space camera, in the case of stray light factor for the quantitative evaluation. The design principle of the inside and outside hood is presented for the R-C (Ritchey Chretien) optical system. On this basis, in order to reduce stray light interference for the space camera, the primary and secondary mirror's hoods were designed. Finally, when sunlight at more than 3° incidence on the space camera, the coefficient of stray light is less than 2%. It meets the engineering requirements.

8557-67, Poster Session

Analysis of thermal shock strength and quality factor with infrared optical domes

Yutang Gao, NanYang Institute of Technology (China)

The development of infrared optical materials is always closely related to the research and exploration of material science. The infrared optical domes bears shock and produces stress when the infrared optical domes mounted on the missile moving at a high speed is shocked by high temperature. According to principle of energy balance in fracture mechanics proposed by D.P.H. Hasselman, the author analyzed the crack extension and derived the relationship between Infrared optical materials window model and thermal shock quality factor. Meanwhile, strong or weak of thermal shock for different samples whether they are thin or thick are compared through the operation of queuing algorithm. The conclusion is the internal surface of the domes isn't heated when the window model is the thermal shock quality factor of thick sample and the heating time is between heating time constant and diffusion time constant. On the other hand, the internal surface of the domes is being heated when the window model is the thermal shock quality factor of thin sample and the heating time is between the two time constants. The most optical domes parts in practice is belong to the thin model. For the thin model, reducing the thickness of optical parts can improve their thermal shock ability but mechanical impact stress factor should be considered comprehensively to design optical parts.

8557-68, Poster Session

Off-axis three-mirror zoom system perturbation analysis

Jiao Ouyang, Jun Chang, Lifei Zhang, Jiao Cao, Aman Wei, Beijing Institute of Technology (China)

Reflective zoom system is widely used in the design of large size, wide spectral, high resolution system due to its great superiority in compacting size, system weight, aperture size, free chromatic aberration and thermo-stability. But for coaxial system, its disadvantage of obstruction renders the FOV (field of view) and light utilization rate unsatisfactory. Thus, to make the secondary and tertiary mirror off-axis is a good choice for optical designers. However, there are two problems in the alignment of off-axis zoom optical system. First, the Seidel aberration theory is not applicable for a system without rotational

symmetry. Second, it is hard to control the misalignment status when zoomed. In this paper, the nodal aberration theory (sometimes is called vector aberration theory) worked out by Thompson is selected to analyze the off-axis three-mirror zoom system. When perturbation is applied to the system, coincident with the alignment in reality, the residual aberration varies along with the movement of secondary and tertiary mirror. As the result, aberration character of misalignment three-mirror-reflective zoom system is provided, which offers guidance for misalignment determination and makes sure of the normal operation of the zoom system.

8557-69, Poster Session

Research on the real-time calibration of the varifocal photoelectric imaging system

Bing Zhou, Fuyu Huang, Yu-dan Chen, Shijiazhuang Mechanical Engineering College (China)

In the varifocal photoelectric image system, the method of moving two batteries of lenses along with the optical axis is usually adopted to vary the system focal length. With this method, the focal length can be changed directly by moving the varifocal lenses, and the image quality can be improved during the zooming procedure mainly by the compensating lenses, whose position is also changed with the shift of the varifocal lenses. However, influenced by the mechanical processing technology, mechanical tolerance, and other factors, the radial deviation between two types of the lenses will be produced unavoidably as they move along with the optical axis in the actual varifocal optical system, which may results in the variance of the optical axis before and after zooming the focal length. This phenomenon is especially serious in the photoelectric reconnaissance and tracking system with a long focal length, and it affects the calculative precision of the target angular coordinates for the succeeding signal processing system.

A real-time system for optical axis of the varifocal photoelectric reconnaissance and tracking system is designed in this paper. Two images are acquired by the DSP processing system before and after zooming the focal length, and the varifocal and shifting coefficients are calculated real-timely through extracting the feature points and affine transform, etc, while the rotation coefficient equals to zero basically. The shifting parameter can be used to calibrate the optical axis, and its calibration precision is less than one pixel. Besides, the varifocal coefficient calculated by the affine transform, whose precision is far higher than that obtained by the mechanism-potentiometer method, can be treated as the output of the precise varifocal coefficient.

The real-time calibration of the varifocal photoelectric image system is realized by the method of electronic processing, and this method has a higher calibration precision, which can reduce the requirement of mechanical processing technology and mechanical tolerance greatly in the production procedure of the photoelectric reconnaissance and tracking system with a long focal length, and can make the system easier to implement.

8557-70, Poster Session

Accuracy analysis of surface figure fitting based on optomechanical-thermal technology

Xifa Song, Li Lin, Yifan Huang, Beijing Institute of Technology (China)

Opto-mechanical-thermal technology is used more and more widely, but few people mentioned the accuracy of surface figure fitting. In this paper, we analyzed the sections that may cause error based on thermal analysis and mechanical analysis. We used error analysis to consider the accuracy of surface figure fitting. We took into account of the error of ABAQUS modeling, the initial error, the error of surface figure fitting, the error of MATLAB and the error of ZEMAX.

And then we gave out the total error, and analyzed which is the dominant error, thus give support for Quadratic optimization design

8557-71, Poster Session

Multi-limit unsymmetrical MLIBD image restoration algorithm

Yang Yang, Information Engineering Univ. (China); Chen Bo, Peking Univ. (China)

A novel multi-limit unsymmetrical iterative blind deconvolution(MLIBD) algorithm was presented to enhance the performance of adaptive optics image restoration. The algorithm enhances the reliability of iterative blind deconvolution by introducing the bandwidth limit into the frequency domain of point spread(PSF), and adopts the PSF dynamic support region estimation to improve the convergence speed. The unsymmetrical factor is automatically computed to advance its adaptivity. Image deconvolution comparing experiments between Richardson-Lucy IBD and MLIBD were done, and the result indicates that the iteration number is reduced by 22.4% and the peak signal-to-noise ratio is improved by 10.18dB with MLIBD method. The performance of MLIBD algorithm is outstanding in the images restoration the FK5-857 adaptive optics and the double-star adaptive optics.

8557-72, Poster Session

Polarization characteristics of a linearly polarized laser beam after hollow light pipe in projectors

PengFei Zhao, Shengtao Zhang, Yanhong Wang, Yunbo Shi, North Univ. of China (China); XuYuan Chen, North Univ. of China (China) and Vestfold Univ. College (Norway)

Abstract: In this work, a multilayered dielectric film of SiO₂ and Nb₂O₅ and metal film of silver are used as reflecting surface to fabricate hollow light pipes separately. And the internal dimensions of the light pipes is 0.157in(4mm)x0.157in(4mm)x1.65in(42mm). Linearly polarized laser beam with wavelength of 532nm enters into the light pipes at the solid angle of 42 degree. After multi-reflection process, laser beam comes out from the light pipe, then, irradiates a screen. With the adjusting of the polarization orientation of the input laser beam from 0 degree to 90 degree, the polarization state of the laser beam after reflection is changed from approximate linearly polarized to partially polarized, which can be observed by rotation the polarizer placed before the screen. And the depolarization ratio of the light pipe coated with metal film is superior to the one coated with multilayered dielectric film. The whole aforementioned experiment process can be well simulated using a commercial available software ZEMAX. The polarization degree of output beam can be calculated according to the simulation data of the PPM (Polarization Pupil Map). Referring to the theoretical dependence of the laser speckle contrast on the laser beam polarization degree, laser speckle contrast from a glass diffuser is measured to exam the simulated result. At last, through the simulation, the effects of the polarization orientation and solid angle of the input laser beam, and dimensions of the light pipe on the polarization degree of output laser light are discussed.

8557-73, Poster Session

Parameters affecting pattern fidelity and line edge roughness under diffraction effects in optical maskless lithography using a digital micromirror device

Manseung Seo, Haeryung Kim, Taehyoung Lee, Tongmyong

Univ. (Korea, Republic of)

In optical maskless lithography in concern, a digital micromirror device plays the role of a digital mask. Due to the spatial/temporal configuration of micromirror arrays/response or the specification of illumination/projection optics, an array of beams reflected off micromirrors may be considered as dispersive pixels. An irradiation process may be considered as a pixel by pixel reflection. Therefore, the diffraction effect may not be negligible. In present study, a systematic integration of an optical maskless lithography system based on binary micromirror reflections is performed in consideration of the diffraction effect. For the approval of the binary reflection off the micromirror, the occupancy limit is employed. Parameters that affect pattern fidelity and line edge roughness under diffraction effects at various occupancy limits is investigated and simulation and experimental results are analyzed. To improve image resolution, a method of dividing an image pixel reflected off a single micromirror into equal-sized sub-pixels on a translating substrate by the superposition of an array of image pixels is adopted. However, the decrease of sub-pixel size through the increase of the dynamic sub-pixelation degree results in a decrease of the scan pitch which directly affects throughput. Thus, to increase throughput while maintaining pattern fidelity and line edge roughness, the dynamic sub-pixelation process is modified by using the hop degree and the lithography system parameters utilizing dynamic sub-pixelation are adjusted. The potential of utilizing adjusted parameters for improving image resolution and further enhancing pattern fidelity and line edge roughness under diffraction effects is demonstrated through simulations and experiments.

8557-74, Poster Session

Wavefront fitting with Zernike polynomials based on total variation regularization method

Lihong Lu, Tianjin Polytechnic Univ. (China); Qingyu Hou, Jinnan Gong, Harbin Institute of Technology (China)

The wavefront of the measured optical surface and system are smooth and continuous. Therefore, the wavefront can be expressed by a linear combination of complete base function, and then the discrete points with wavefront information can be fitted to the actual wavefront precisely. The wavefront function can be achieved by fitting the optical surfaces data using Zernike polynomials because of the corresponding relation between Zernike polynomials and Seidel aberrations, which has been widely used in optical testing and optical design. The accurate fitting coefficients can be achieved by using Least Square, Gram-Schmidt orthogonalization and Householder transformation with the accurate measured values. However, there exist errors on phase values obtaining by optimization algorithm, which cause the instable solution obtaining by the common algorithms. In this paper, the reason of the stable solution cannot be achieved when proceed to fit wavefront by Gram-Schmidt orthogonalization and Householder transformation is deduced in theory. The essence of Gram-Schmidt orthogonalization and Householder transformation is QR decomposition, and the only difference between the two methods is the way to obtain the orthogonal matrix. The Zernike coefficients fitting method based on total variation regularization is presented to suppress the effects of errors in measured data on fitting results. The solving model of Zernike coefficients is developed, and the regularization term is introduced in solving model, then the L-curve method is applied to determine the regularization parameter and the modified steepest descent method is applied to solve Zernike coefficients. The algorithm efficiency is proved by simulation experiment.

8557-75, Poster Session

A model for simulating coherence of laser light caused by Mie scattering

Yanhong Wang, Wenhong Gao, Wenhong Gao, Pengfei Zhao, Xuyuan Chen, North Univ. of China (China)

In this work, in order to study coherent characteristics of the laser light encountering Mie bulk scattering, a model for simulating coherence of laser light caused by Mie scattering has been built up in ZEMAX optical design software, which consists of a linear polarized laser source, scattering medium, an interferometer configuration, and a photo-detector. The linear polarized laser source is of wavelength 0.45 micron. The scattering medium is a particle solution with variable parameters including the index, the particle size, and the solution density. The interference configuration is a Young's double-slit interferometer. By changing the index, the size, and the density of the particle in the solution, respectively, the interference patterns are recorded. We have discovered that the contrast of the interference patterns strongly depends on the particle size and the density.

The results show that the interference fringe contrast changing from 1 to 0.14 has a monotonic decreasing relationship with the particle density from 1000 cm⁻³ to 600000 cm⁻³ when the refractive index was 1.6 and the particle size was 10 microns. The interference fringe contrast decreases from 1 to 0.12 when the particle size increases from 10 to 100 micrometers under the condition of fixed the refractive index 1.6 and the particle density 5000 cm⁻³. However, the interference fringe contrast hasn't changed obviously with altering the refractive index.

We can conclude that the spatial coherence of the laser light can be modulated by design the Mie scatter medium which will not cause the big loss of the light transmission.

8557-76, Poster Session

Fluid mechanics principle about manufacture technology of micro-lens generated on needing positions

Jian Wu Sr., Kuanxin Yu Sr., Beijing Univ. of Technology (China)

In this paper a new fabrication technology of the micro-lens which is generated on needing positions is suggested. Its process is as follows. First a solidifiable ultraviolet optic glue drip is released on the horizontal plane. When the droplet spreads, its shape will change with the face tension. Final the droplet is irradiated by ultraviolet laser in due time and it can be solidified according to the designing shape. The technology doesn't need mould or masks, It is easy, quick and cheap. It has application prospects in astronavigation, military affairs, biology, chemistry and civil affair. In this paper fluid mechanics principle about the optic micro-lens generated on needing positions is researched. A surface equations set of viscous optic glue drip is given. The equations set reflect relationship between coordinates of the surface curve. A numerical calculation method is proposed. Some shape curves and curvature radius curves for different contact angles between the glue and glass base and different character lengths of the glue are given. Methods influencing shapes of the glue drips are discussed. Decreasing contact angles and character lengths can make spreading area to change big and thickness to change small. Adulterating nanometer quartz powder in the glue and milling the glass can change the contact angle and the character lengths. So controlling adulteration concentration and roughness of the glass, the optic micro-lens with ideal shape can be obtained. The research results have directive significance to manufacture of the optic micro-lens generated on needing positions.

8557-78, Poster Session

Fiber ring depolarizer with one degree of freedom

Chunhua Wang, Qing Yang Yu, Li Li, Shengfei Zhang, Shanghai Univ. (China)

Depolarization techniques are an efficient way to solve the polarization turbulence induced impairments in optical sensing systems. The essential of depolarization is to split the light in two orthogonal polarization directions equally in power and make all the split lights incoherent as well. In this paper, a one-degree of freedom (DOF) tunable single fiber ring depolarizer is proposed by specially setting the bend-induced birefringence in the fiber ring to behave as a half-wave plate (HWP) and with the optimal coupling ratio of the coupler. The methods of making and testing the HWP-performance of the fiber ring are analyzed and discussed. Depolarization can be realized by just rotating the fiber ring instead of adjusting the polarization controller within the fiber ring as previous works did. In our experiment, a 12-meter long fiber ring depolarizer is demonstrated to depolarize a Fabry-Perot (FP) laser with 10-meter coherent length. Degree of polarization (DOP) of 1.5% can be easily reached by rotating the whole set of fiber ring. The losses in the ring and the twist-induced birefringence are the key factors that make DOP not equal to zero. Therefore, to reduce the splicing losses and to coil the fiber with the best performance of HWP and fix it are very crucial in fabricating the device. Moreover, if inserting a polarizer ahead of the fiber ring, a full scale one degree of freedom tunable depolarizer can be realized. The features of depolarizer proposed are all-passive, compact, stable and low-cost, and with the ability to depolarize narrow-band spectrum of light.

8557-79, Poster Session

A practical approach for measurement of IR optical system transmissivity

Yi Jian, Zhaoxin Pan, Shiyong Wang, Wang Yu, Luo Yixue, Shanghai Institute of Technical Physics (China)

Transmissivity is a crucial parameter for an optical system, especially for an infrared imaging system, which is commonly used for detecting and tracking dim target. NETD (Noise Equivalent Temperature Difference) is an important indicator for quality of an infrared FPA system, and it is always related with the transmissivity of its optical system, which is dealing with energy transmission of the system. So it is necessary to measure the transmissivity when optical system is fabricated. However it is usually not easily available as visible light optical system, when the structure of IR optics is complex in particular. In this article, a new reliable method for measuring the transmissivity of optical system with cooled infrared detector is introduced. The principle of measurement is based on Etendue conservation and luminance (radiance) conservation when light travels through an ideal optical element. We put a Lambertian blackbody source attached at the cold stop of IR detector of under testing system, and get the grey-scale value of axis point of detector. Afterwards we put on the optical system for the detection and calibrate the optical path for imaging system. Then we put the Lambertian blackbody source at the position of entrance pupil of optical system, and get the grey-scale value of axis point of detector again. With proper calculation with these two grey-scale value, we could get transmissivity of this optical system. A ray tracing simulation is made to show the result for supporting correctness of this approach. A high-aperture Lambertian blackbody source is required for the embodiment of this measurement.

8557-80, Poster Session

Analysis of array image camera modes in the test for dynamical focus position

Juanning Zhao, Xiaona Dong, Limin Gao, Hongguang Li, Xi'an Institute of Optics and Precision Mechanics (China)

The focus spot position is one of the most significant parameters in optical system, especially to the optical system including multiple elements. Many methods based on physical or geometry optics have been investigated to measuring it. However, they are not appropriate to test the altering focus position accurately, or test online. To investigate the position altering of focus spot in high energy laser system, caused by material thermal distortion or environmental turbulence, three array image camera modes (plane mode, plan-mirror mode and wedge-mirror mode) are discussed in this paper. All of them are based on the theory that the altering of focus position can be calculated from the variation of spot size on a certain detecting plan. Each of them has two splitting elements installed vertically to divide the beam into series beams. In this paper, not only the advantages but also the disadvantages have been investigated for each measurement model. As four key factors for the array image camera, the complexity of calculation, the flexibility of operation, the spots adhesion characteristic and the stray light have been respectively analyzed. Through the theoretical analysis, software stimulation, wedge-mirror can works well in dynamical spot measurement for reducing spots adhesion and parasitic light effect. The measure step of this design can reach one quarter of the focal depth; when measure the system of f 1250mm, D 50mm, the accuracy can reach 0.0315mm.

8557-81, Poster Session

The distortion analysis and correction of two-dimensional scanning system in laser differential confocal microscopy

Chao Gao, Dali Liu, Weiqian Zhao, Beijing Institute of Technology (China)

Laser differential confocal technology is applied to lots of fields as an important way of analysis and measurement for its high-resolution imaging capability, unique section imaging capability and multi-parameter capability. Because of its zero vision field imaging, differential confocal technology needs a scan system to image. For its high-response frequency and fast positioning speed, two-dimension vibrating mirror scan system is applied to laser differential confocal microscope system. According to the structural characteristics of two-dimension vibrating mirror scan system, this paper implements systemic research and analysis. In this paper, based on the thin-lens imaging principle, the mathematic model of two-dimension vibrating mirror scan system is built to achieve coordinate tracing of the scan beam and it is found that the scan plots in scanning plane is distributed unevenly, and there are two kinds of distortion, the nonlinear distortion and the pillow-shaped distortion, which will cause the image compress in two dimensions. In order to correct the distortion, this paper proposes an inverse-function method, and verifies the effectivity of the method by Matlab simulation of the system. The provided method can be operated simply and understood easily, can be applied to large-scale calculation correction, which provides an effective way to solve the distortion problem of two-dimension vibrating mirror scan system.

8557-83, Poster Session

Research on the key parameters influencing the anti-vibration capability of time-frequency-domain interferometer

Fanghua Zhang, Qun Hao, Yao Hu, qiudong zhu, Beijing

Institute of Technology (China)

Phase-shifting interferometry is a non-contact precise measuring method for optical surface, but it is highly sensitive to external vibrations. In this paper, a time-and-frequency-domain anti-noise phase-shifting interferometry is used to eliminate the effect of vibrations and improve the precision of measurement. In this measuring system, a large number of phase-shifting interferograms are captured. The temporal intensity array from each pixel is transformed into frequency domain. A series of phase is obtained by frequency spectrum analysis. A linear fitting of the phase series produces the result of original phase. After unwrapping operation, the profile of the testing surface is reconstructed.

The paper focuses on an experimental system for testing the anti-vibration ability of the measuring method. In this system, the laser is both the source and the phase shifter whose wavelength can be modulated by current, and the displacement of the reference mirror propelled by a PZT is used to simulate the environment vibration. A stepped plane mirror is measured. During the measurement, each of the parameters, such as the number of sampling frames, sampling frequency and phase shift frequency, is assigned different values. The testing results are compared with that from a ZYGO phase-shifting interferometer. By analyzing the comparative results, the law of the parameters' influence on system anti-vibration capability can be obtained. According to the law, the optimization parameters can be determined so that the system has the maximum anti-vibration capability.

8557-84, Poster Session

Study of partial coherence measurement of the illumination system in excimer laser lithography based on CCD image sensor

Xiaoyong Liu, Sichuan Univ. (China) and Shi Hezi Univ. (China);
Yiping Cao, Sichuan Univ. (China)

Rapid measurement of the partial coherence is very useful for process engineers to optimize the performance of exposure tool and process condition in optical lithography. In this paper, a novel method of the partial coherence measurement based on CCD image sensor is proposed. A pin-hole is located at the reticule such that the effective source is imaged through the pin-hole via the lens onto the photosurface of CCD camera. Using the simple encircled energy convention, the partial coherence can be calculated through Matlab when the effective source is captured by CCD. This research analysed the parameters of the main components of the measurement system, we mainly study the positioning accuracy along the vertical direction, and the position variation of the spot caused by straightness, parallelism of the mechanical platform and the telecentricity of the illumination system.

The paper presents the statistic results and the sensitivity of the measurement system under conventional illumination and kinds of off-axis illumination modes. All of the simulation results have proved the feasibility and availability of the proposed method.

8557-86, Poster Session

The measurement schemes of PSF of Star Sensor

Xu Yao, Beijing Institute of Technology (China)

In order to measure the MTF of optical system, we should first get the PSF of optical system, then we get MTF through Fourier transform. Based on the influences from the shape of star image and the energy distribution to precision, we analysed the schemes of measuring PSF and concluded that if the purpose of the PSF which is owned to be measured is different from the PSF which is used in the measurement of MTF, we will have different measurements. In theory, the smaller

the detector is, the more precision the result is. As to the PSF of Star Sensor, we will get the highest precision when we choose the scheme of simple scan in principle. However, while adopt photoelectronic detector to detect it directly which is based on the method of sub-pixel interpolation is a compromised scheme. So, in the consideration of the precision of measurement, we should choose the scheme of arrowhead simple scan.

8557-87, Poster Session

Study on the sub-aperture stitching method

Zhengnan Liang, Weirui Zhao, Guangyu Pan, Rong Li, Beijing Institute of Technology (China)

Sub-aperture stitching is a virtual method for measuring large aperture optical Components with low cost and high resolution by a small aperture interferometer.

In this thesis, the theory of sub-apertures titehing15investigatedfirst, including selection of stitching modes and setting of the number of sub-apertures .Secondly, getting the interference fringe of the measured surface through acquisition, using the extracted feature matching points on different sub-aperture unwrapping the phase map stitching process, using the Zernike fitting to obtain the measured surface full bore surface information. under the premise of early positioning by using instruments, reuse of the characteristics of the areas of the mirror for precise positioning, And correctness of the Program is validated by simulation. A platform is established for sub-aperture stitching test, and then the experimental stitching that test the 100mmx100mm optical component by five Planar sub-apertures is Performed. Gives the results of contrast stitching and full aperture detection. Finally, experimental research is conducted on the influence of stitching accuracy by sub-aperture overlapping area and stitching modes. The results show that increasing the sub-aperture overlapping area can enhance the stitching accuracy when the number of sub-apertures is unchangeable, and serial stitching is better than parallel stitching at controlling the stitching accuracy.

8557-88, Poster Session

Smile effect detection for dispersive hypersepctral imager based on the doped reflectance panel

Jiankang Zhou, Soochow Univ. (China); Xiaoli Liu, Jiaozuo Institute of Technology (China); Yiqun Ji, Yuheng Chen, Weimin Shen, Soochow Univ. (China)

Hyperspectral imager is now widely used in many regions, such as resource development, environmental monitoring and so on. The reliability of spectral data is based on the instrument calibration. The smile, wavelengths at the center pixels of imaging spectrometer detector array are different from the marginal pixels, is a main factor in the spectral calibration because it can deteriorate the spectral data accuracy. When the spectral resolution is high, little smile can result in obvious signal deviation near weak atmospheric absorption peak. The traditional method of detecting smile is monochromator wavelength scanning which is time consuming and complex and can not be used in the field or at the flying platform. We present a new smile detection method based on the holmium oxide panel which has the rich of absorbed spectral features. The higher spectral resolution spectrometer and the under-test imaging spectrometer acquired the optical signal from the Spectralon panel and the holmium oxide panel respectively. The wavelength absorption peak positions of every column pixels are determined by curve fitting method which includes Gaussian model simulation and spectral convolution. The iteration strategy and Pearson coefficient together are used to confirm the correlation between the measured and modeled spectral curve. The present smile detection method is posed on our designed imaging spectrometer and the result shows that it can satisfy precise calibration requirement of high spectral resolution imaging spectrometer.

8557-89, Poster Session

Error and compensation of Non-polarization Splitting Prism(NPBS) in single frequency laser interferometer

Yong Wei, Jun Yang, Harbin Engineering Univ. (China)

An online compensation method of non-polarization splitting prism(NPBS) error in single frequency laser interferometer is presented in the paper. Single-frequency laser has been widely used in the field of nano-vibration measurement interferometer for its high accuracy, wide measuring range, and less optical components. We study the effect of polarization characteristics of NPBS with different incident conditions, establish online performance detecting system to study NPBS. Using this system we also study the effect of reflected additional phase of NPBS to single frequency laser interferometer. Changing the location of quarter-wave plate in the interferometer can compensate the additional phase shift caused by the non-ideal of NPBS devices. But this method will lead to the rotation, of polarization azimuth and ultimately make the output signal contrast decrease. Adding a half wave-plate in optical path to joint with quarter-wave plate for the compensation of NPBS additional phase shift, which improves contrast ratio of interference signal and restrains nonlinear errors of single frequency laser interferometer. The results indicate that the method can effectively compensate polarization error of NPBS, improve the quality of interference signal and raise measurement resolution of interferometer. Therefore, the method can be widely used in many fields such as the investigation and preparation of nanometer high-precision laser interferometer.

8557-90, Poster Session

Measurement of physical polarization parameters by system estimation with least-square optimization

Tao Liu, Chunhua Wang, Li Li, Haiyang Zhou, Shenfei Zhang, Shanghai Univ. (China)

In this paper, we propose to obtain physical polarization parameters of optical devices directly by solving nonlinear equations with least square best-fit optimization, instead of decomposing PP parameters form the Mueller matrix measured in advance as previous works did. The proposed scheme is based on the idea of system estimation, where physical polarization parameters are regarded as the systematical parameters to be estimated by using the measured input states of polarization and output states of polarization. The system estimation method performs conveniently in obtaining the polarization parameters of the device under test. Besides, the states of polarization involved in estimation are not restricted on special ones, therefore a polarization state generator simply consisting of a polarizer followed by a rotating wave-plate is used to generate states of polarization for estimation. Simulations based on MATLAB are done and the results show that better estimation precisions can be obtained by involving more states of polarization in estimations. More comprehensive results are obtained by employing system estimation in our simulation. An experiment to approve our simulation is demonstrate, which is mainly constructed with a commercially available polarization state analyzer and a polarization state generator which is comprised simply by a linear polarizer and a rotatable wave-plate. As a sample, the physical polarization parameters of a polarization controller is measured and the estimated errors is within 0.0011~0.01 for all parameters.

8557-91, Poster Session

Evaluation of parallel phase-shifting digital holography by photon counting method

Lin Miao, Kobe Univ. (Japan); Kouichi Nitta, Osamu Matoba,

Kobe University (Japan); Yasuhiro Awatsuji, Kyoto Institute of Technology (Japan)

Parallel phase-shifting digital holography (PPSDH) is one of promising methods to obtain instantaneously three-dimensional (3D) information. The complex amplitude of an object wave is extracted from a patterned interference distribution and then the reconstruction of the 3D object is implemented in a computer by numerical Fresnel propagation or other propagation method. In the measurement of fast phenomenon of a 3D field, the detected power will be decreased. In this paper, we evaluate numerically the number of photons to be required for fast 3D object measurement in PPSDH. In the numerical evaluation, a two-dimensional image with a random phase distribution is used. This random phase distribution increases the sensitivity of reconstruction distance. Photon counting method is applied to obtain the patterned interference distribution under weak illumination. The number of photons at each pixel in an image sensor is generated from Poisson distribution. The interference pattern obtained by the photon counting method is processed by PPSDH and then the reconstruction is implemented by numerical Fresnel propagation. The error of the amplitude and the phase distributions are evaluated by changing the number of photons. This numerical evaluation gives us the minimum number of photons for the fast measurement of PPSDH.

8557-92, Poster Session

The effect of temperature characteristic of Faraday rotator to passively demodulated all optical fiber current transformers

Yuekun Wang, Zhengping Wang, Shuai Sun, Harbin Engineering Univ. (China)

In order to move signal detecting point to the most sensitive position and improve the immunity of the system at the same time, the scheme named passively demodulated all optical fiber current transformer (AOFCT) inserts a Faraday rotator of 22.5° rotation angle between fiber retarder and leading fiber. To improve the performance of this type of all fiber current transformer, after considering the temperature features of a large proportion of Faraday crystals, the effect of the Faraday rotator's temperature properties on temperature stability of the passively demodulated AOFCTs are theoretically analyzed and numerically calculated. The results show that the errors induced by the Faraday rotators are beyond the requested values in the International Standard IEC 60044-8:2002 of International Electrotechnical Commission (IEC) and the State Standard of P.R.China GB/T 20840.8-2007. Finally, to solve this problem, some possible solutions are suggested.

8557-93, Poster Session

Cyclops opening-up fiber for real-time fluorescence sensing

Yi Yang, Donghua Univ. (China); Guanjun Wang, Key Laboratory of Instrumentation Science and Dynamic Measurement (Ministry of Education) (China); Jian Cui, Engineering Training Center, Beijing University of Aeronautics and Astronautics (China)

Compared with traditional fluorescence-based microstructured fiber sensors using filled structure, the opening-up microstructured fibers have shown many advantages for real-time sensing. The design and theoretical study about Cyclops opening-up microstructured fiber is present in this paper. In Cyclops fiber, a large asymmetry hole is placed in fiber cladding. A tri-hole design is adopted for fiber core to enlarge the evanescent field interactions with measured material. This structure is compatible with the traditional stack-draw processing. To make the opening-up structure, chemical etching (with acid) or polishing machining could be used for the asymmetry hole.

The opening depth and shape of large asymmetry hole is important

for real-time sensing response in Cyclops opening-up fiber. The relationship between marching depth in cladding and fluid concentration distribution at different time in evanescent field near fiber core is analyzed numerically based on incompressible Navier-Stokes equations and finite element method (FEM). The results show that the concentration distribution in evanescent field adjacent to fiber core can reach the true value out of cladding below ten seconds by design cladding structure appropriately. The field distribution of fundamental mode and some cladding mode of Cyclops fiber without tri-hole core and with different tri-hole are presented in this paper too. To analyze the sensing error in distributed measurements, the difference in effective index, dispersion parameter and confinement loss about two fundamental non-degenerate modes of the Cyclops fiber are studied. Cyclops fiber show good characters in these aspects compared with wagon wheel (WW) opening-up fiber. In order to evaluate the performance of sensing based on Cyclops opening-up fibers we adopted the modal power fraction (PF) within the sensing region and the effective modal area (A_{eff}) and the fluorescence capture fraction (FCF). The results show the Cyclops opening-up fiber is a competitive candidate for real-time fluorescence sensing.

8557-94, Poster Session

Radiation distribution measurement for forest plant canopies tracing

Xue-fen Wan, North China Institute of Science and Technology (China)

Plant canopies in forest have distinct architectural elements such as tree crowns, whorls, branches, shoots, etc. Since these structures dictate the spatial distribution of leaves, the traditional random assumption can't satisfy Leaf Area Index (LAI) and the Fraction of Photosynthetically Active Radiation (FPAR) measuring with high precision, which are important biophysical parameters required in many ecological and climate models. To obtain precise canopies characteristic, the radiation distribution in forest gap should be tracing. In this paper, a low-cost multi-node method for forest gap radiation distribution synchronous measurement is present. It provides distributed working parameters collecting for each tracing-line. And a Zigbee wireless network is imbedded for communicating between measuring node and host computer.

Using the solar beam as a probe, the measuring nodes collect radiation distribution in forest gap. Each radiation spike is converted into gap size values to obtain a gap size distribution. Low-cost photodiode (FDS-100 in our design) is introduced for radiation spike tracing. A Microchip PIC16F877 MCU is employed for radiation measuring and Zigbee in each node. The collected data is sent to central station by Zigbee wireless network. Solar radiation spike data and other environment parameters (Temperature and Humidity) are forward to host computer. Host computer get potential relationship in tracing-line LAI and FPAR and compute them in long-term through Chen and LeBlanc TRAC theory. A multi-node measuring theory developed from TRAC method is also presented. Instead of tracing-line measuring, an arc nodes installation according to Zenith angle is more efficient for rarefaction arbors such as Banyan and Poplar. An experimental setting with 3 nodes and host computer is tested. The experimental results show our design could be a competitive candidate for radiation distribution measurement for forest plant canopies tracing.

8557-95, Poster Session

Temperature effect of SO₂ ultraviolet differential absorption

Guiyin Zhang, Haiping Li, Haiming Zheng, North China Electric Power Univ. (China)

The technique of differential optical absorption spectroscopy (DOAS) can achieve the real time on-line monitoring of gaseous pollutants

due to its fast response time. It has been used widely in industrial and environmental fields. But when applied DOAS to continuous emission monitoring systems (CEMS) such as in power plant, the differential absorption characteristics of pollution gases will change greatly owing to the flue gas is often with high temperature and high dust. This will bring the influence on the detection results.

This article mainly aims at the temperature effects for SO₂ differential absorption cross section in UV region by recordings of spectra in a heat-pipe cell. The results show that the differential absorption properties change dramatically with temperature. The differential absorption peaks in the region of 280-320nm decrease with the increase of temperature while the valleys will increase. So the entire differential absorption cross section decreases with the increase of temperature, but no wavelength drift and differential absorption structure change appear with temperature. By measuring the differential absorption cross section of ten obvious peaks at different temperature, it is found that the reduction amplitude at different wavelength peak is varied. When the temperature rises from 300C to 3900C, the relative change of the differential absorption cross section peak value at 304.48nm is 60.88%, while it can reach 94.41% at 292.54nm. This shows that it is necessary to consider the temperature effect in the application of DOAS method for measuring the flue gas SO₂, otherwise very big measurement error will be produced.

8557-96, Poster Session

A high-precision method and its implementation of measuring spatial azimuth

Zhiyong Yang, Zhaofa Zhou, Zhili Zhang, Xi'an Research Institute of High Technology (China)

The spatial azimuth measurement system based on magneto-optic modulation polarized light, refers to measuring the spatial azimuth between upper and lower instruments without mechanical connection with the polarized light and Faraday effect, this technology will greatly promote the growth of spacecraft docking and developments of biomedical and other fields. But the measurement precision of the traditional system is low, and the measurement scale is narrow. In order to improve the traditional system, a new method of calculating azimuth directly was present for the first time.

The principle of the traditional system was analyzed, the signal from modulator was filtered with the lowpass, and it was expanded with the Bessel Function, then the signal from modulator was substituted with the Bessel expression whose higher order terms was omitted, therefore there must be signal truncation error, which has influence on the system measurement effect.

In the new method, the signal from modulator did not need being filtered, it was analyzed directly, and its character that there are two extremums whose abscissa is a constant was detected. The relationship between azimuth and the extremums was established, the extremums was sampling with the sampling integral circuit, and the equation between azimuth and the extremums was established.

There are adding roots when solving the equation, in order to omit the adding roots, the extremums was analyzed, and the relationship between the number of extremum and the root of equation was detected, then the rule how to omit the adding roots, which is based on the number of extremums was present, and the model of measuring azimuth based on arc tangent function was acquired. At the same time, the measurement scale of azimuth was widened as the double angle formula was cited. In order to calculate the arc tangent function in the model with hardware, the method of looking-up table was introduced, and the appropriate table according to the system measurement precision was designed. At last the realization scheme of the new method was finished. The measurement precision and scale of the new method in the paper was analyzed with simulation calculation, simulation results show that the measurement precision of the new method is higher and measurement scale is wider, it provide a reference to measuring spatial azimuth in wider scale and high precision, and it has an important theoretical guiding significance.

8557-97, Poster Session

Design and optimization of chopper based on Labview

Guo Li, Capital Normal Univ. (China); Xiaolei Wang, Ministry of Industry and Information Technology (China); Lichun Feng, Cunlin Zhang, Capital Normal Univ. (China)

Chopper is widely used in optical system to produce a series of optical pulses which has particular shape and frequency. A chopper system always has two parts: modulation plate and control box. A tiny photoelectric switch detects the modulation frequency, and the frequency is transmitted to control box by voltage signal. In the control box, detected frequency and target frequency make a comparison. Then a feedback signal is transferred to motor to adjust the rotate speed of modulation plate. With this feedback system, modulation frequency keeps approaching to target frequency and finally reaches it. Now the price of choppers in the market ranges several hundreds to several thousands RMB, depending on its quality. This paper presents a way to make a simple chopper based on Labview. Labview and NI DAQ are widely available in universities. So with this method chopper system can be easily constructed for temporary use. NI DAQ uses counter tools to detect the frequency of modulated laser and produce several feedback signal to drive the location and rotate speed of modulation plate, which leads to the change of modulation frequency and duty. In this sense, NI DAQ plays the role of control box. The program which drives NI DAQ is edited by Labview. Labview use various frames and icons as programming language, instead of traditional code. With this point, the program can adjust to different use and it has an advantage of flexibility. This paper can provide a reference for experiment work in optics and other natural science.

8557-98, Poster Session

Technique of measuring single grating incremental angle

Yu Xiao, Changchun Univ. of Science and Technology (China)

This paper discusses a new method of measuring incremental angle, which uses an arranged matrix of a narrow slit photoelectric cell according to certain logic phase combination replacing the fixed grating in the grating pair. The measuring operation can be accomplished by the coordination to replace between the coder disk and the arranged matrix of the narrow slit photoelectric cell. Thus, there is no need of considering the gap between the slit and the coder disk. The sensibility of the incremental photoelectric encoder to the vibration and the precision requirements of the spars are deduced. Thus the contrast degree of the Moors fringes is enhanced, the subdivision precision is increased and finally the measuring precision and the Stability are all increased.

8557-99, Poster Session

Planar alignment sensor based on Rayleigh interference in two wavelengths

Yao Hu, Beijing Institute of Technology (China)

Precise alignment of planar optical element is common in industry or scientific research. Generally, autocollimator can help solve the parallelism adjustment between planes. As to coplanar alignment of planes, such as mirrors or gratings, interferometer can be used to remove the angular or positional error, and displacement transducers are often used for locking the coplanar condition. In this paper, a planar alignment sensor based on Rayleigh interference in two wavelengths is proposed. It can conduct parallelism and coplane alignment at the same time. Two beams of monochromatic probing lasers from the sensor point normally to the two mirror reflection planes to be aligned.

The reflective beams carrying the angular information back to the sensor are focused by a lens to form a Rayleigh interference pattern at the focal plane. Four-quadrant detector picks up the pattern and outputs angular adjustment signal according to the rotational-symmetry of the pattern. Monochromatic probing laser in another wavelength can tell the coplanar status from the axial-symmetry of the pattern. This is similar with dual-wavelength interferometer. Demonstration experiment shows that the sensor can help achieve angular alignment accuracy within 2 arcsecond and coplanar accuracy of 0.1 micron. With a group of split-image and beam merging prisms, the probed positions on the two surfaces can be adjusted so that the sensor is flexible. This sensor has prospect in industrial online alignment and monitoring.

8557-24, Session 6

Advances in optical design and optimization of miniature zoom optics with liquid lens element (Invited Paper)

Yi-Chin Fang, National Kaohsiung First Univ. of Science and Technology (Taiwan)

Abstract: An optical design of 2X optical miniature zoom lens with liquid lens elements and optimization method: discrete lens groups shifts (DLGS) has been presented in this research. Two liquid elements are applied to minimize the overall length of zoom optics. Moreover, a compensative optimization method with assistance of Genetic Algorithm is introduced in this research with a new concept of DLGS, which not only solve the complicated problem of liquid optics itself but also improve the performance of optics. Genetic algorithms (GA) written in CODE V plays the role at finding out the appropriate parameters such as curvatures, thicknesses, glass materials and etc. Besides, one table with great lens groups shifts by GA would be created to move the lens groups on the optimal positions of different zooms. As a result, the DLGS optimization method associated with the GA optimization improve the zoom lens performance averagely 40% better than traditional ones.

8557-25, Session 6

Ultra-wide to mid-wide angle 3X zoom and focus adjustable lens design for industrial video endoscope

Dongmin Yang, GE Inspection Technologies (United States)

Optical zoom lens design for industrial video endoscope faces big challenges in stringent compactness requirement in both diameter and rigid length dimensions, as well as working in harsh environment such as high temperature so that liquid lens is not an option. Market is strongly demanding industrial video endoscope with optical zoom and focus change capability for better imaging performance at different desired FOV (Field of View) and focus distance. No such product has been commercialized yet. Once it succeeds, it could provide huge benefits for customers to improve inspection quality and productivity. A 3X continuous optical zoom lens design with short focal lengths is presented in this paper. It is capable to change FOV from ultra-wide angle as 120degrees to mid-wide angle as 40degrees. At any zoom position, the focus distance is capable to change from infinity to as close as 5 mm. The whole lens train has max diameter of 4mm, and overall length of 14mm, which makes it practical to be integrated into the mainstream 6mm industrial video endoscope. Image quality in terms of contrast and resolution satisfies or significantly better than today's existing commercial 6mm video endoscope. The design has also considered cost and product ruggedness requests.

8557-26, Session 6

Optical image stabilizing technique based on deformable mirror zoom system

Yuhua Jiang, Qun Hao, Beijing Institute of Technology (China);
Xuemin Cheng, Tsinghua Univ. (China)

Zoom lens is a kind of system whose focal length can be continuously changed, which keeps a stable image plane and a good image quality in zoom process. It has played a significant role in areas such as aerospace and military imaging systems for its quick, continuous target detection and flexible image motion compensation ability. This paper presents a method that uses a deformable mirror in the optical design in order to achieve a quick response, optical image stabilizing (OIS) and miniaturization zoom lens, improving its system performance.

This paper developed the OIS scheme for an off-axis three-mirror anastigmat. The deformable mirror was designed to correct the image blurring and degradation, as carrier movement in the system makes the relative motion between the imaging optical axis and the object. Here we used a two-configuration system before and after motion for the same point target in object. The first configuration is set as carrier motionless and the second configuration tilts a small angle relative to the first one. The secondary mirror uses a deformable mirror as corrector mirror. Then by tracing a set of rays data, calculate the surface parameters of the deformable mirror. Change the shape of the deformable mirror to make the image plane of the second configuration approach the image plane of the first configuration to produce image plane decentration. At the same time, it can correct defocus, image plane tilt and aberration. Finally, we can achieve OIS for the zoom system based on the deformable mirrors.

8557-27, Session 6

Optical system design for a short-wave infrared imaging spectrometer

Han Huang, Xiaotong Li, Zhaofeng Cen, Zhejiang Univ. (China)

A short-wave infrared (SWIR) imaging spectrometer with all reflective elements was designed. The imaging spectrometer is composed of an off-axis three-mirror anastigmatic (TMA) telescope and an Offner spectral imaging system with convex grating. Based on the geometrical optical imaging theory of coaxial three mirror system, the initial structural parameters of TMA telescope were determined. Designed and optimized with ZEMAX software, the off-axis three mirror system had a spectral region from 1.0 to 2.5 μ m, focal length of 343.56mm, relative aperture of 1/3.5, field of view angle of 5°x0.1°, and modulation transfer function approaching to diffraction limit. Using the image space NA of the telescope as the object space NA of the spectrometer, determining the initial configuration by analyzing the astigmatic feature of Offner spectroscopic system, a SWIR Offner spectral imaging system was designed and optimized. Attaching the telescope to the spectrometer, the optical design of a SWIR imaging spectrometer system was finally completed after further optimization. The system has a slit of 30mm, a spectral resolution of 10nm, a smile or keystone of the slit spectral image less than ten percent of a pixel size, and its imaging quality approaches to diffraction limit. The theory of design and the analytical approach that the paper referred to are relatively simple and the design method used is also applied to other spectral region. In addition, ZPL language of ZEMAX is used to simplify the procedure. It is a good way for designing similar imaging spectrometers of excellent quality in a short time.

8557-28, Session 6

Designing an all-reflective long focus and large field-of-view optical system with freeform surface

Qingfeng Wang, Dewen Cheng, YongTian Wang, Yue Liu,
Beijing Institute of Technology (China)

Freeform surface has many advantages in optical design over the conventional spherical or aspheric surface. The appropriate application of freeform surface can not only help to achieve high imaging performance but also make the system light-weight and compact.

All-reflective optical system has been widely used in deep space detection. We studied the application of freeform surface in all-reflective, off-axis optical system and infrared, off-axis optical system was designed which has long effective focal length and large field of view. The freeform surface was employed to get better performance and smaller system size and weight.

The starting point of the design was calculated by the theory of aberration and property of conic. After that we optimized the starting point using the strategy of successive approximation optimization which can reduce the difficulty of optimizing process. Based on the theory of aberration, the best position of freeform surface in the off-axis system was analyzed. At last, a four mirrors optical system with long EFL and large field of view was designed. The system consists of three conic surfaces and one freeform surface. The effective focal length and field of view are 4.5m and 3°, respectively. The volume is as small as 0.5m x 0.5m x 0.7m. The MTF at Nyquist frequency is close to diffraction limit.

By taking consideration of the fabrication and align difficulty of the freeform optical system, we carried out a comprehensive tolerance and alignment analysis. Based on the result of analysis, a process of alignment was proposed to ensure the system can be fabricated in low cost and high performance.

8557-29, Session 7

Measurement of the mirror refractive spectrum of typical roughness surface in the ultraviolet band (*Invited Paper*)

Lu Bai, Zhensen Wu, Yanhui Li, Xidian Univ. (China)

The reflect light of a surface contains many features of the surface. It is usually used as a powerful tool for process in situ or ex situ monitoring because of its non contact and non destructive nature. Recently, with the development of multi-band target detection, the requirement of the measurement data in the multi-band is necessary to analysis the scattering properties of a target. But lots of paper adducible discussed the measurement or model method in the visible to infrared band. Few references discuss about the measurement results of the surface in the ultraviolet band. As there has been increasing interest in the study of scattering and reflective properties in ultraviolet band (200 to 400 nm). Such as ultraviolet space objects detection and subsurface defects short wavelength monitoring in semiconductor industry etc. Researches on the scattering properties in the UV band are necessary. Ellipsometry is a well-known and an extremely sensitive characterization technique which may be used to determine a lot of characteristics of the surface, such as the specular reflection and transmission properties from surfaces and coatings. In this paper, the experiment measuring system is introduced. Scatter measurements of some typical samples in the UV band are performed by using the ellipsometry WVASE 32 made by J. A. Woolam Co. Inc. The mirror-direction refractive measurement results obtained by ellipsometer are analyzed and compared with the measured data from spectrometer.

And these kinds of researches about measuring and analyzing of typical roughness samples in ultraviolet band have significant meanings in a lot of related fields.

8557-30, Session 7

The measurement of optical reflector with complex surface using nano-CMM

Zhichao Wu, Tong Guo, Jinping Chen, Xing Fu, Xiaotang Hu, Tianjin Univ. (China)

Among variety of methods to measure complex surfaces, coordinate measurement is widely used in reverse engineering and measuring complex topography. In this article, a coordinate measuring system based on 3D tactile probe is used to measure a high precision sine surface array. This system can measure complex surface with resolution of 1nm, 3D uncertainty less than 50nm, measuring range of 25mmx25mmx5mm. The probe named Gannen XM can measure the movement of the tip in 3D, so it is more accuracy than trigger probe and 1D analog probe. The probe also applies 3D uncertainty of 50nm and measuring force less than 1mN. The positioning system is based on Nano Measuring Machine (NMM), it uses three interferometers to measure the displacement of the stage with 0.1nm resolution and 10nm uncertainty. The tip of the probe is at the point that the three interferometers' measuring line intersect, so it can reduce the Abbe error as small as possible. A signal acquisition module NI-USB6259BNC is used to acquire the signal of the probe and became the main part of feedback system. There is a sine array reflector sample with about 5 micrometer amplitude and we test it with our 3D coordinate measuring system. The result is compared with data of AFM and the course of deviation is analyzed in the conclusions.

8557-31, Session 7

Wave-front coded optical readout for the MEMS-based uncooled infrared imaging system

Tian Li, Yuejin Zhao, Beijing Institute of Technology (China); Xiaomei Yu, Peking Univ. (China); Liqian Dong, Beijing Institute of Technology (China); Mei Hui, Beijing Institute of Technology (China); Xiaohua Liu, Cheng Gong, Xuhong Chu, Beijing Institute of Technology (China)

The uncooled optical readout infrared imaging system based MEMS has become a researching hotspot. In the space limited system pursuing integration, miniaturization and modularization, the adjustment of optical readout part is inconvenient. This paper proposed a method of wave-front coding to extend the depth of field of the optical readout system, to solve the problem above, and to reduce the demanding for precision in processing and assemblage of the optical readout system itself as well.

This wave-front coded imaging system consists of optical coding and digital decoding. By adding a CPM(Cubic Phase Mask) on the pupil plane, it become non-sensitive to defocussing within an extended range. The system has similar PSFs and almost equally blurred intermediate images can be obtained. Sharp images are supposed to be acquired based on image restoration algorithms, with the same PSF as a decoding core.

For comparing, we designed a traditional optical imaging system as well, which had the same optical performance with the wave-front coding one. Analogue imaging experiments were carried out, using MATLAB, by calculating two-dimension convolution between the object and the defocussing PSFs. One PSF was used as a simple direct inverse filter, for imaging restoration. Relatively sharp restored images were obtained. Comparatively, the analogue defocussing images of the traditional system were badly destroyed.

Using the decrease of the MTF as a standard, we found the depth of field of the wave-front coding system had been extended significantly, to which can never be achieved by any traditional imaging system.

8557-33, Session 8

Enhancing the performance of coaxial three mirror anastigmatic optical system by wavefront coding (*Invited Paper*)

Bo Li, Bing-Long Zhang, Beijing Institute of Space Mechanics and Electricity (China)

Coaxial Three Mirror Anastigmatic(TMA) optical system is used in many space based optical earth observing satellites because it's excellent anti-astigmatic performance. Space environment disturbances such as thermal field change, vibration often causes optical elements to deformation, tilt or position deviation. So the structure stability is one of the key factor to influence the actual performance when coaxial TMA camera run on orbit. A coaxial TMA optical system is designed and optimized that is insensitive to defocus and defocus-related aberrations by adding a designed phase mask based on wavefront coding method. A filter is developed based on wiener filter which can effectively restore the blure produced by phase mask and defocus and magnify the image noise only a little. Finally, the actual performance of optimized imagin system is analyzed by the simulation. The result shows that the fabrication and assembly tolerance of coaxial TMA optical system is relaxed to 2 times, the depth of focus of system is extended to 15 times than before by using wavefront coding, and the imaging quality is almost unchanged, actual performance is enhanced.

8557-34, Session 8

Analysis of the silicon carbide applicable technique in the EO/IR telescope for spaceborne

Haengbok Lee, Agency for Defense Development (Korea, Republic of)

The latest very high resolution optical sensors are WorldView-1 a GSD of 0.45m is available, but also with QuickBird(0.62m GSD), GeoEye-1(0.41m GSD), Pleiades-1(0.5m GSD), EROS-2B(0.7m GSD) and Kompsat Series(Kompsat-1, -2, -3 : 6.6m, 1m, 0.7m GSD respectively) as well as with the other new very high resolution optical space imagery a topographic mapping is possible. The spaceborne telescope assembly, which incorporates the primary mirror and secondary mirrors, optical bench, and metering structure, must retain the alignment after launch and during operation in space. A trend in spaceborne telescopes has been an increase in collection area and in resolution. Both of these demands in performance require larger primary mirror aperture sizes. Since the primary mirror often dominates the mass budget of the telescope, either of these options imply larger mass for the overall system. Major efforts in spaceborne telescopes have inspired research in lightweight optics. Also, metering structure requires high stiffness, high dimensional stability and minimum obstruction of the telescope aperture to get high quality images. Silicon Carbide(SiC) mirrors and structures are becoming more important for high precision lightweight optical applications in space. For space applications, mass density, elastic stiffness and strength related properties are most important. There are many SiC satellites which were applied Formosat-1,-2, THEOS, Pleiades-2, STOP6, 7, Geo-Africa, ASNARO. This paper describes trade studies that explore the structural views for the lightweight primary mirror and the metering structure as well as the sic application in sub-metric class spaceborne telescope.

8557-35, Session 8

The effects of piston error on image quality

Jun Zhang, Weirui Zhao, Feng Yang, Beijing Institute of Technology (China)

The relationship between image quality and piston errors between

adjacent segments in synthetic aperture optical imaging system has been studied. An active segmented cophasing imaging system with a high accurate optical adjustment and control in nanoscale was set up for the study. A Zemax simulation model of the cophasing imaging system was established. Under the condition of a monochromatic and a continuous spectrum halogen light being as the source of the system respectively, diversity piston error were introduced between the segments and then the MTF correspond to each piston error was calculated with the Zemax simulation model. The range of the introduced piston error under each condition is from 0nm to 5000nm, and the error step is 50nm. The MTF correspond to each piston error was recorded, and the curves of MTF's change with the change of piston errors were obtained and analyzed. Meanwhile the experiments have been carried out with the active segmented cophasing imaging system to research the relationship between the image quality and the piston errors. The experimental results are coincident with the results simulated by Zemax. The results of the experiments and simulation show that the image quality of synthetic aperture optical imaging system changes with the increase of the piston error between the segments periodically if the piston error is smaller than the coherent length of the light source used by the synthetic aperture imaging system, and the image quality becomes the worst if the piston error is an odd multiple of π .

8557-36, Session 8

Optical design of multispectral sensor using off-axis three-mirror reflective optics

Tianjin Tang, Huan Li, Beijing Institute of Space Mechanics and Electricity (China)

al mirror, the light incidents into the TMA, then dichroic by the wedge dichroic mirror, one part of the incident light is reflected by the dichroic mirror to the visible and near infrared focal plane; another part of the incident light transmits the dichroic mirror and afocal relay lens to the short and medium wave focal plane.

The optical system is composed of three reflective mirrors and five lens with an F-number of F/4 for visible light channel and F/3 for another channel, the focal length is 680mm and a field of view of 56.1616° ; (CT) 61.6201° ; (AT) for two channels, a working wavelength range of 450~5000nm. The paper also analyses the selection of dichroic schemes. The MTF of each channel at respective fields for multiple wave bands are also given at respective Nyquist frequency, the MTF of visible and near infrared wave bands is over 0.7 at respective Nyquist frequency 50lp/mm and over 0.5 for short and medium wave band at respective 25lp/mm and 12.5lp/mm. The engineering feasibility of the optical system is also analyzed based on the tolerance analysis, the MTF of the camera is also forecasted at the end of the paper.

8557-37, Session 8

Design of a compact four-mirror optical system with wide field-of-view

Aman Wei, Jun Chang, Beijing Institute of Technology (China)

During the development of science and the enhanced demand of scientific research, the demand to optical design is enhancing every day. The study of optical system with wide field of view is a branch of optical design. Compared with the traditional optical system with wide field of view, the reflective optical system had many advantages, such as less weight and without chromatic aberration. The reflective optical system is drawing more and more attention with the above referred to advantages. A method based on Seidel aberration theory to design a four mirror optical system with wide field of view was mentioned in this paper. In this method, Seidel aberration theory was studied in the first step, and the technical parameters of the system were got from the demands, then the technical parameters, such as the diameter of entrance pupil and the field of view were substituted into the Seidel aberration equations. Then we solved the equations with additional limit, and got the initial parameters of system, for example the radius of curvature of each mirror. The example in this article was a design of a compact four mirror system with a field of view of 15° and F number of 5. This example showed that the method based on Seidel aberration theory to design a four mirror optical system with wide field of view is effective and feasible. This kind of compact four mirror system with a wide field of view can be applied to UV light, visible light and infrared light multispectral imaging with the less weight and without chromatic aberration. It can be widely applied to many fields, such as remote sensing and electricity discharge detection.

Conference 8558: Optoelectronic Imaging and Multimedia Technology II

Monday - Wednesday 5 -7 November 2012

Part of Proceedings of SPIE Vol. 8558 Optoelectronic Imaging and Multimedia Technology II

8558-1, Session 1

Real-time interactive projection system based on infrared structured-light method

Xiaorui Qiao, Qian Zhou, Kai Ni, Yang Li, Guanhao Wu, Liang He, Leshan Mao, Xuemin Cheng, Tsinghua Univ. (China)

Interactive technologies have been greatly developed in recent years. However, most interactive projection systems are based on special interactive pens or whiteboards, which is inconvenient and limits the improvement of user experience.

This paper introduced our recent progress on theoretically modeling a real-time interactive projection system. The system permits the user to easily operate or draw on the projection screen directly by fingers. The projector projects infrared striping patterns onto the screen and CCD captures the deformational image. We resolve the finger's position and track its movement by processing the deformational image in real-time. A new way to determine whether the finger touches the screen is proposed. The first deformational fringe on the fingertip and the first fringe at the finger shadow are the same one. The correspondence is obtained, so the location parameters can be decided by triangulation. The simulation results are given, and errors are analyzed.

8558-2, Session 1

A laser-based measurement system for transparent surface forming

Mingyan Li, Xinzhu Sang, Yang Sun, Binbin Yan, Chongxiu Yu, Beijing Univ. of Posts and Telecommunications (China)

In the traditional process, the transparent surface forming just simply relies on the engineer's experience to determine. However, the precise requirements of modern industry stimulate us to find an accurate judgment mechanism rather than manual. To achieve the high precision measurement, this paper presents an optical measurement for the key points of the transparent surface. This system has three modules, a laser, a CCD camera and a computer. They are in charge of exposure, receiving and processing respectively. Transparent surface is placed in an enclosed space, growing slowly from low to high. The laser beam is injected to the transparent surface, CCD receives it on the other side. After passing through the transparent surface, the laser spot images on the camera. Once we connect the camera with the computer, we can see the image change in real time. When the transparent surface grows, the shape of the spot will change accordingly. We detect the change to monitor the height change of transparent surface.

Image processing includes several steps such as median filtering, binarization and ellipse fitting. We present a method to record the change, from which we can calculate the effective axial length. The performance of the algorithm is given. It can process ten images per second, achieving the desired processing speed requirements. After measuring and analyzing large amount of data, the relationship between the change of effective axial length and the height of transparent surface is drawn. It can help us to control the growth of the transparent surface better by analyzing the trends of the curve. By calculating, we obtain the measurement error is 2.725%. The small error ensures the accuracy of measurement.

8558-3, Session 1

Seal imprint verification using edge difference histogram

Jin He, Tianjin Univ. of Technology and Education (China); Hao

Zhang, Liu Tiegeng, Tianjin Univ. (China)

An automatic seal identification method based on the edge difference histogram is proposed. Differences between a sample seal (SS) and a model seal (MS) on geometrical characteristics, such as topological structures, stroke width and stroke position, were wholly reflected by edge difference image. In this paper, edge difference is expressed quantitatively as two parameters, distance between non-overlapped corresponding edges and their lengths. Addition to positions and areas of non-overlapped corresponding edges, statistical property of points on the edges is used to compute the two parameters. To eliminate effects of noises and stamping conditions on the verification result, efficient edge difference that is closely related to the identification is obtained according to the two parameters. A histogram on the product of the two parameters of the efficient edge difference is proposed to constitute the input feature vectors of support vector machine (SVM). SS is classified by SVM as true, false or doubtful. In Experiments, 4810 (2450 genuine and 2360 fake) seal imprints were verified, and the correct recognition rate is 99.42%. Moreover, the classification results can be customized according to the requirements of users. When the false-acceptance error rate and the false-rejection error rate are both required to be close to 0, the rejection rate is about 3%.

8558-4, Session 1

A new 3D imaging lidar based on the high-speed 2D laser scanner

Chunsheng Hu, Zongsheng Huang, Shiqiao Qin, Xingshu Wang, National Univ. of Defense Technology (China)

The research of the 3D imaging lidar is a key area in the field of 3D information acquisition. Laser diode is widely used in 3D imaging lidars because of its low price, small volume and easy usage. To enhance the measuring speed of 3D imaging lidar and to obtain 3D images in high speed under static conditions, we proposed a new 3D imaging lidar with a laser diode and a high-speed 2D laser scanner as the fundamental parts. The laser diode was used to output pulsed laser of high peak power and narrow width. With the proposed new structure, the laser scanner can scan fast in a 2D field by only one asymmetric 16-plane rotating mirror. The characteristics of this scanner included high speed scanning, large scanning field and simple structure. The proposed 3D imaging lidar was mainly composed of a transmitter, a laser scanner, a receiver and a processor. The laser diode was one of the most important parts in the transmitter. This paper introduced here the composition and principle of each important part of the 3D imaging lidar. Some experiments were implemented to evaluate the performance of the lidar, such as scanning field, measuring precision, scanning speed, image resolution and etc. The results showed its scanning field of about 26°×12°, its measuring precision of better than 5 cm (4 m distance), its scanning speed of 30 frames per second and its image resolution of 16×101. It can obtain a 3D image and an intensity image for the given target at the same time.

8558-5, Session 1

A novel high-speed 2D laser scanner for the 3D imaging lidar

Chunsheng Hu, Dejun Zhan, Shiqiao Qin, National Univ. of Defense Technology (China); Xingshu Wang, National University of Defense Technology (China)

The research of 3D imaging lidars is the key area in the field of 3D information acquisition. Laser diode is widely used in 3D imaging lidars because of its low price, small volume and easy usage. In order

to enhance the speed of measurement in the 3D imaging lidar and to obtain 3D images in high speed under static conditions, we proposed a brand new high-speed 2D laser scanner used in the 3D imaging lidar with a laser diode as a key element. This paper discussed the principles and the characteristics of commonly used laser scanners, including symmetric rotating mirror scanners, vibrating mirror scanners, oval line scanners and double optical wedge scanners. We proposed here an asymmetric 16-plane rotating mirror with a new structure, with the ability to scan fast in a 2D field by only one rotating mirror. The principle of scanning and the structure of the rotating mirror were introduced in detail. With the use of this asymmetric rotating mirror, the scanner had some advantages: high speed scanning, large scanning field and high reflectivity. This paper discussed the scanning speed and the resolution of the scanner. Some scanning experiments had been carried out and the results showed that the scanning speed of above 30 frames per second, the scanning field of about $32^{\circ} \times 12^{\circ}$, the vertical resolution of each frame of 16, the laser reflectivity of above 0.9. The proposed laser scanner had wide applications such as groundborne, vehicleborne and airborne 3D imaging lidars.

8558-6, Session 2

Compressive imaging based target locating system for APT in FSO communication

Ping Wei, Jun Ke, Fen Wang, Beijing Institute of Technology (China)

Conventional APT (acquisition, pointing, tracking) acquires 2D images for target locating, and then uses the location to guide signal beam direction for FSO (free space optics) communication. Each image in APT is a bright spot with an all-black background. Therefore, it is spatially sparse and redundant. To reduce the redundancy and increase target locating speed, we study a compressive imaging based APT (CI-APT) system.

In a CI-APT system, linear combinations of object pixels, referred to as features, are measured by a single detector. Hadamard projection is used for collecting features because of its simplicity for implementation. Then from these features, objects are reconstructed with methods such as OMP for target locating. Multiple sets of Hadamard vectors, such as sorted and randomly selected vectors, are analyzed.

To demonstrate the idea, an experimental system using a 0.55" DMD with XGA resolution is built. The DMD driver system is modified to increase the data acquisition speed from 100 to 20K frames per second. A LED is used as the movable bright spot in the all-black background. Objects of size 256x256 and 768x768 are tested. For a 256x256 object with the bright spot located at position (40, 30), reconstructions are obtained using 256, 128, and 64 Hadamard features. The estimated spot location are (39.56, 30.60), (38.43, 28.58), and (41.70, 25.68), respectively. It can be observed that after compressing $256 \times 256 / 64 = 1024$ times, the CI-APT system still works well for target locating. Additionally, in this work, main factors for the experimental system error are analyzed.

8558-7, Session 2

Real-time identification and tracking of infrared markers based on Kalman filter

Qiaona Xing, Dayuan Yan, Xiaoming Hu, Junqin Lin, Bo Yang, Beijing Institute of Technology (China)

Automatic equipment transportation in the wild terrain circumstances is very important in rescue or military. How to realize accurate tracking of a guider is the key to completing the automatic walking for mobile robots. But the existing identification methods are affected greatly by ambient light or the non-unique feature in the environment. Therefore, this paper presents an accompanying system based on the identification and tracking of infrared LED markers which are fixed on the guider's back. This system overcomes the influence of light

conditions on the identification accuracy and makes the tracking target unique in the wild circumstances.

For the limitations of the global search, this paper presents a fast infrared markers' identification algorithm based on the Kalman filter. The Kalman filter predicts where the infrared markers may appear in the next frame by establishing motion model of infrared markers to reduce the searching area of infrared markers, which remarkably improves the identification speed of infrared markers.

The flow of the system is divided into the following steps: (a) Obtainment of the images of the infrared markers by the camera; (b) Image processing; (c) The identification of the infrared markers; (d) Calculation of the centroid of the infrared markers; (e) Calculation of the camera's position; (f) Prediction of infrared markers' area in the next frame by the Kalman filter. Then the above 6 steps are completed in the predicted area. The experimental results show that the algorithm proposed in this paper is effective and feasible.

8558-8, Session 2

Potential fingerprints detection using UV spectral imaging

Wei Huang, Institute of Forensic Science (China); Zhichao Yang, Zhejiang Police College (China); Xiaojing Xu, Institute of Forensic Science Ministry of Public Security (China); Jingjing Guo, Institute of Forensic Science Ministry of Public Security (China)

Spectral imaging technology research is becoming more extensive in the field of examination of material evidence. UV spectral imaging technology is an important part of the full spectrum of imaging technology. Due to the limitations of previous devices, most research has focused on technology of the near-infrared light and visible light. The study of ultraviolet spectral imaging technology is much fewer. This paper summarizes the application of the results of UV imaging technology in the field of evidence examination, explores the common object of potential fingerprints of UV spectra characteristic for the research objectives, which shows the potential traces of criminal using the ultraviolet spectrum imaging method.

This paper finished the experiment contents of the ultraviolet spectrum imaging method and image acquisition system UV spectral imaging technology. The experiment of UV spectral imaging method obtains the image set of the UV spectrum, and formats a pseudo-color images to show the potential traces successfully by processing the set of spectral images; UV spectral imaging technology explores the technology method of obtaining the image set of ultraviolet spectrometer through ultraviolet spectrometer and image acquisition system, and extensive access to the UV spectrum information of potential fingerprints of common objects, and study the characteristics of the ultraviolet spectrum.

In this paper, the experimental UV spectral imaging method for the UV spectral imaging technology provides a reference path to practical experience for future experiments. UV spectroscopic imaging experiments explore a wide variety of UV reflectance spectra of the object material curve and its UV spectrum of imaging modalities, can not only give a reference for choosing ultraviolet wavelength to show the object surface potential traces of substances, but also gives important data for the ultraviolet spectrum of imaging technology development.

8558-9, Session 2

A real-time people counting system by detecting human head-shoulder profile using line structured light

Ping Wei, Jun Ke, Lizhong Wei, Beijing Institute of Technology (China)

People-counting is important for civilian security protection in crowded places such as subway, train station, stadiums, or festival celebration sites. Majority solutions to this problem are based on processing surveillance camera images with sophisticated algorithms. In this work, a novel real-time people counting system is discussed by detecting human head-shoulder profile using line structured light. Compared with image processing approaches, this system is cost-effective, computationally simple, and has higher detection accuracy.

The system is assumed to be installed above an entrance/exit gate with height roughly 2.5 meters. Several line structured light source are spread over the width of the gate, which can be larger than 10 meters. Each source is paired with a CCD camera having a vertically downward view. Then, as people go through the gate, their head-shoulder profiles are captured by the camera. However, instead of using grayscale or color information in the image to extract the profiles, we calculate the depth of the line illuminated by the source from the line's deformation using range finding technique. Then, by correlating the obtained depth signal with a reference human head-shoulder profile, the number of persons passing through the gate is obtained. To avoid the overlapped field of views between adjacent cameras, we expose the cameras and their paired light sources sequentially. Additionally, simply by using another line structured light array, we can detect the direction of each person passing through the gate.

8558-10, Session 2

Video fire detection based on three-state hidden Markov modal and fractal dimension calculation

Bo Lei, Zhijie Zhang, Chensheng Wang, Huazhong Institute of Electro-Optics-Wuhan National Lab. for Optoelectronics (China)

Fire detection based on video surveillance is a very effective method for large area outdoor fire prevention, but the unpredictable place and time makes automatic fire detection a difficult problem. Many papers adopt color based fire detection method, whose results depend greatly on the camera's chromatic rendition ability. Strict color match would cause much false negative detection while loose match would evoke many false positive alarms. We adopt a loose color selection to narrow down possible fire areas, and use frame differential to confirm areas where consequential fire detection should be performed. Pixels in those areas are put into a detection pool where every pixel's temporal color variations are analyzed. Then two three-state hidden Markov modals are used. One is used to exam the brightness variations of those pixels and the other one is used to exam the fire color likeness of them. Fire color likeness of a pixel is measured by color difference from the fire color which at first is a given default value and changes according to the previous fire detection results. The results of these two exams are combined with certain weights to determine whether those pixels belong to fire regions. We use two methods to eliminate false alarms. First one is to check the fractal dimension of detected fire regions, which is useful for some moving fire color like objects, such as wiggling flag. The second one is to perform texture match for nearby fire regions in consecutive frames, which is effective for fire texture like objects, such as light yellow color hay. Experiments proved the promoted method are suitable for real-time outdoor or indoor fire detection in surveillance videos.

8558-11, Session 2

Improvement of single-wavelength based Thai jasmine rice identification with elliptic Fourier descriptor and neural network analysis

Kajpanya Suwansukho, King Mongkut's Institute of Technology Ladkrabang (Thailand); Sarun Sumriddetchajorn, National Electronics and Computer Technology Ctr. (Thailand); Prathan

Buranasiri, King Mongkut's Institute of Technology Ladkrabang (Thailand)

Recently, we have proposed and developed a single-wavelength spectral-imaging-based Thai jasmine (KDML105) rice identification system that can distinguished KDML105 milled rice from other unwanted rice varieties (e.g., CNT1, PTT1, and HPSL2) with a measured average false acceptance rate (FAR) of 15.6%. To improve the overall FAR in pinpointing the KDML105 milled rice, this paper, rather than considering only the amount of fluorescent signal spatially distributed on the image of milled rice grains, analyzes the shape and size of the image of each milled rice variety especially during the image threshold operation. The image of each milled rice variety is expressed as chain codes and elliptic Fourier coefficients in terms of their semi-major axis, semi-minor axis, and perimeter values. After that, a feed-forward back-propagation neural network model is applied, resulting in an improved FAR of 11% in identifying KDML105 milled rice from the unwanted four milled rice varieties. Other key features include adaptive learning ability and ease of implementation.

8558-12, Session 2

Two-dimensional PCA-based human gait identification

Jinyan Chen, Tianjin Univ. (China); Rongteng Wu, Minjiang Univ. (China)

It is very necessary to recognize person through visual surveillance automatically for public security reason. Human gait based identification focus on recognizing human by his walking video automatically using computer vision and image processing approaches. As a potential biometric measure, human gait identification has attracted more and more researchers. Current human gait identification methods can be divided into two categories: model-based methods and motion-based methods. In this paper a two-Dimensional Principal Component Analysis and temporal-space analysis based human gait identification method is proposed. Using background estimation and image subtraction we can get a binary images sequence from the surveillance video. By comparing the difference of two adjacent images in the gait images sequence, we can get a difference binary images sequence. Every binary difference image indicates the body moving mode during a person walking. We use the following steps to extract the temporal-space features from the difference binary images sequence: Projecting one difference image to Y axis or X axis we can get two vectors. Project every difference image in the difference binary images sequence to Y axis or X axis difference binary images sequence we can get two matrixes. These two matrixes indicate the styles of one walking. Then Two-Dimensional Principal Component Analysis(2DPCA) is used to transform these two matrixes to two vectors while at the same time keep the maximum separability. Finally the similarity of two human gait images is calculated by the Euclidean distance of the two vectors. The performance of our methods is illustrated using the CASIA Gait Database.

8558-13, Session 2

Feature point tracking for incomplete trajectories with multi-view constraint

Kun Pen Wang, Beijing Institute of Tracking and Telecommunication Technology (China)

Feature points tracking is a standard task of computer vision with numerous application in navigation, motion, understanding, surveillance, scene monitoring, and video database management. In an image sequence, moving objects are represent by a set of feature points detected prior to tracking or during tracking. As local image properties of feature points are often unstable, points are treated as indistinguishable, and kinematic constraints are solely used to establish the correspondences. This task, called the correspondence problem,

becomes a complicated problem for a dense set of unrelated feature points.

Methods of feature point tracking are researched mainly concerning image sequence from single camera, and the approaches try to recover real 3D motion from its 2D projection which is an incomplete problem and have limited capabilities in handling incomplete trajectories.

The concept of a cooperative multi-camera ensemble, informally a 'forest' of cameras, has recently received increasing attention from the research community. The problem of associating objects across multiple cameras with overlapping fields of views has been addressed in a number of papers, but most of the methods are based on Bayesian framework, which are complex for practical application. Furthermore, Dynamic scenes with multiple, independently moving objects should be considered where feature points may enter, temporarily disappear, and leave the view field.

A new feature points tracking method is proposed here, which is based on the idea of competing trajectories similar to original three-frame matching procedure. The basic difference is that multi-view constraint is utilized besides the constraint of smooth motion, and the motion is confirmed by a step of bidirectional validation. Every point in frames has two state flags. The linking flag stands for correspondence of points in consecutive frames of single camera, and the matching flag indicates correspondence of points from different cameras at the same time. Cost function based on multi-view constraint and smoothness constraint is formed to obtain the best correspondence of points.

8558-14, Session 3

Baikhao (rice leaf) app: a mobile device-based application in analyzing the color level of the rice leaf for nitrogen estimation

Yuttana Intaravanne, Sarun Sumriddetchkajorn, National Electronics and Computer Technology Ctr. (Thailand)

Nitrogen (N) is one of an important nutrient for the growth of rice crop. As the color level of the rice leaf corresponds to the N status of rice in the field, farmers use a cheap and ease-of-use leaf color chart (LCC) to identify color level of the rice leaf for estimating the amount of N fertilizers needed per rice field. However, the ability of the farmers and degeneration of the LCC color affect the accuracy in reading the rice leaf color level. In this paper, we propose a mobile-device based rice leaf color analyzer called "Baikhao" which means rice leave in Thai. Our key idea is to simultaneously capture and process the two-dimensional (2-D) data scattered from the rice leave and its surrounding reference, thus eliminating expensive external components and alleviating the environmental fluctuation but yet achieving a high accuracy of the key color levels. Our field tests using an Android-based mobile phone show that all important leaf color levels of 1, 2, 3, 4, and 5 can be correctly identified. Additional key features include low cost and ease of implementation with highly efficient distribution through the internet.

8558-15, Session 3

In-line retro-reflective polarizing contrast scope for translucent objects

Sarun Sumriddetchkajorn, National Electronics and Computer Technology Ctr. (Thailand)

We propose a very-low-cost fixed interferential polarizing phase contrast scope suitable for the study of translucent objects. Our key design approach is relied on the arrangement of a circular polarizer sheet, a mirror, and a digital camera in a retro-reflective optical structure. The linear polarizer embedded in the circular polarizer sheet acts as both a polarization beam splitter and a polarization beam combiner. Meanwhile the quarter waveplate inside the circular polarizer sheet functions as a fixed phase plate but without narrowing the field of view of the digital camera. The retro-reflective configuration amplifies the phase difference between the two orthogonal polarized

optical beams twice creating an initial dark background. Experimental demonstration using an off-the-shelf digital microscope with built-in white light emitting diodes and a specified 400x maximum magnification, a circular polarizer sheet, and a mirror shows that onion cells and *Steinernema Thailandense* nematodes can be clearly observed with striking color, high contrast, and three-dimensional appearance.

8558-16, Session 3

Design on imaging system base on FPGA technology for EMCCD

Liu Pan, Beijing Institute of Technology (China)

EMCCD (Electronic Multiplication CCD) is a new type of solid-state imaging sensor. Owing to the unique feature of on-chip multiplication, EMCCD obtains the same level of sensitivity compared with ICCD and EBCCD. Back Illuminated EMCCD further enhanced the sensitivity. With its special performance, EMCCD has various applications on astronomy, aerospace, life science and military. In this article, we design an imaging system by chip CCD-97-00, which is produced by British E2V company. Based on the datasheet of EMCCD-CCD97, FPGA was utilized to generate the timing sequence of EMCCD, but the output voltage of FPGA is 0 to 3.3V, in order to better meet the EMCCD driving specification, the exist driving circuit was substituted by a specialized CMOS driver IC and a separate high voltage driving circuit for level shifting; when we put the driver voltage to the pins of the EMCCD, we obtain standard ccd signal. The EMCCD output analog signal was sampled and converted to digital signal by a CCD signal processor AD9845; The converted CCD digital signal was transmitted to FPGA, then cached in SDRAM and finally displayed on a VGA monitor.

Now the imaging system works well, the chip's effective image size is 512*512 pixels. The frame rate is 7.5Hz, works smoothly and stably, but now it can't be used to observe at low illumination, but what we have done now made a foundation for it.

8558-17, Session 3

A high-definition electronic industrial endoscope based on embedded system

Guang Xu, Liqiang Wang, Zhejiang Univ. (China)

This paper presents a low power high-definition (HD) electronic industrial endoscope based on embedded system. A 1/6 inch CMOS image sensor is used to acquire HD images with 1280 * 800 pixels. The camera interface of A8 is designed to generate images of various sizes and support multiple inputs of video such as ITU-R BT-601/656 standard. Image rotation (90 degrees clockwise) and image process functions can be achieved by CAMIF. The decode engine of the processor can playback or record HD video with speed of 30 frames per second, built-in HDMI 1.3 interface can transmit high definition images to the external display. Image processing procedures such as demosaicking, color correction and auto white balance are realized on a high performance cortex A8 platform. Different functions are selected through OSD settings. An LCD panel displays the real time images. The snapshot pictures or compressed videos are saved in an SD card or transmitted to a computer through USB interface. The size of the camera head is 5*5*15 mm with more than 3 meters working distance. To acquire the clear image the brightness of led can be adjusted by the processor according to the environment. The whole endoscope system can be powered by a lithium battery, with the advantages of miniature, low cost and portability.

8558-18, Session 3

A device designed and improved for frequency decorrelation of speckle in multimode fibers

Hongyuan Fu, Harbin Engineering Univ. (China)

Changes in environmental conditions can cause modal noise, but frequency instability of the laser source can also cause such noise under the right conditions. To avoid this case, the frequency changes have to be less than the frequency decorrelation interval. The frequency dependence of speckle is determined by the spread of time delays associated with the various paths contributing to speckle at any given point. The frequency change required to decorrelate a speckle pattern at the end of a fiber is therefore approximately the reciprocal of the width of the impulse response of the fiber. In this paper, a device, for frequency decorrelation of speckle at the end of a fiber in the comparison experiment, was designed and improved based on a theory of time delays in propagation through multimode fiber. By control the frequency of a diffuser driven by an external motor in the device, the frequency decorrelation interval of speckle in fiber can be control. The experiment simulated the practical situation with the CCD to receive star lights based on light from lab experiment and suppressed the speckle pattern received from a large core fiber by different diffuser in speckle suppression devices. The experimental results, analysed by MATLAB, showed that speckle contrast and the speckle spot in the patterns treated by the device decreased obviously. This device was demonstrated to be effective to speckle suppression and image analysis in astronomy.

8558-19, Session 3

Extended depth-of-field for visual systems: an overview

Yufu Qu, Liyan Liu, BeiHang Univ. (China)

The depth of field (DOF) determines the field of view along the optical axis in visual system. In this paper, we classify the existing extended depth of field (EDOF) technology of visual system into the following four types: (1) Simple improvement (Neither add optical elements nor use image restoration). The DOF is extended by changing the elements or parameters of the optical imaging system such as reducing the aperture of the imaging lens. However, the extension ratio of the DOF of this method limited, and furthermore, the luminous flux and the signal-to-noise ratio are reduced in the system. (2) Image restoration (Use image restoration only but not add optical elements). The DOF is extended by altering the parameters of the system to capture images repeatedly. The large DOF is obtained with the aid of digital image processing technology. The representative technology consists of focus variation, aperture variation, defocus and DOF superposition, all of which need multiple imaging and spend longer time (3) Element adding (Add optical elements only but not use image restoration). The DOF is extended by modifying the optical imaging system including optical tomography microscope and digital holographic microscope, leading to the complication of its structure. (4) Computational photography (Add optical elements and use image restoration). By adding an element in the system, the blurred images that are not sensitive to defocus is captured firstly. Then the image restoration is applied to render the blurred images sharp, resulting in DOF extension. Based on the location of the additional elements, the computational photography is divided into three types: light source, diaphragm and focal plane. Among them, the type of diaphragm is composed of mask plate, phase plate, grid focal lens and light field imaging. The mask plate contains gray, ring multi-ring, modified uniformly redundant array (MURA), hole, Levin and Veeraraghavan. Since the computational photography has an advantage of simple implementation, large extension ratio of DOF, small luminous flux loss and big signal-to-noise ratio, it becomes the leading direction of the research and application in the future.

8558-20, Session 4

VLC-based indoor location awareness using LED lights and image sensors

Seok-Ju Lee, Sung-Yoon Jung, Yeungnam Univ. (Korea, Republic of)

Recently, indoor LED lighting can be considered for constructing green infra with energy saving and additionally providing LED-IT convergence services such as visible light communication (VLC) based location awareness and navigation services. For example, in case of large complex shopping mall, location awareness to navigate the destination is very important issue. However, the conventional navigation using GPS is not working indoors. Alternative location service based on WLAN has a problem that the position accuracy is low. For example, it is difficult to estimate the height exactly. If the position error of the height is greater than the height between floors, it may cause big problem. Therefore, conventional navigation is inappropriate for indoor navigation. Alternative possible solution for indoor navigation is VLC based location awareness scheme. Because indoor LED infra will be definitely equipped for providing lighting functionality, indoor LED lighting has a possibility to provide relatively high accuracy of position estimation combined with VLC technology. In this paper, we provide a new VLC based positioning system using visible LED lights and image sensors. Our system uses location of image sensor lens and location of reception plane. By using more than two image sensor, we can determine transmitter position less than 1m position error. Furthermore, our positioning system also can be used in outdoor environment such as intelligent transport system (ITS) thanks to its higher positioning accuracy than GPS. Through numerical analysis, we verify the validity of the proposed VLC based new positioning system using visible LED lights and image sensors.

8558-21, Session 4

Vision communications based on LED array and imaging sensor

Jong-Ho Yoo, Sung-Yoon Jung, Yeungnam Univ. (Korea, Republic of)

In this paper, we propose the brand new communication concept, called as "vision communications" based on LED array and image sensor. This system consists of array LED as a transmitter and digital devices which include image sensor such as CCD and CMOS as receivers. In order to transmit data, the proposed communication scheme simultaneously uses the digital image processing and optical wireless communication schemes. Therefore, the novel cognitive communications scheme is possible with the help of recognition techniques used in vision system. By increasing data rate, our scheme uses LED array consisting of several multi-spectral LEDs. Because each LED can emit multi-spectral optical signal such as visible, infrared and ultraviolet light, the increase of data rate is possible similar to WDM and MIMO skills used in traditional optical and wireless communications. In addition, this multi-spectral capability also makes it possible to avoid the optical noises in communication environment. In our vision communication scheme, the data packet is composed of sync data and information data. Sync data is used to detect the transmitter area and calibrate the distorted image snapshots obtained by image sensor. By making the optical rate of LED array be same with the frame rate (frames per second) of image sensor, we can decode the information data included in each image snapshot based on image processing and optical wireless communication techniques. Through field test based on practical test bed system, we confirm the validity of the proposed vision communications based on LED array and Image sensor.

8558-22, Session 4

Designing and implementing a miniature CMOS imaging system with USB interface

Chenyun Yao, Liqiang Wang, Bo Yuan, Zhejiang Univ. (China)

Although CMOS cameras with USB interface are popular, their sizes are not small enough and working lengths are not that long enough when used as industrial endoscope. Here we present a small-sized image acquisition system for high-definition industrial electronic endoscope based on USB2.0 controller CY7C68013, which is composed of a 1/6 inch CMOS image sensor with resolution of 1 Megapixels. Using slave FIFO mode, signals from the CMOS image sensor are put into computer through the USB interface for processing, storage and display. LVDS technology is used for image data stream transmission between the sensor and USB controller to realize a long working distance, high signal integrity and low noise system. The maximum pixel clock runs at 48MHz to support for 30 fps for QSXGA mode or 15 fps for SXGA mode and the data transmission rate can reach 36 megabytes per second. The imaging system is simple in structure, low-power, low-cost and easy to control. Based on multi-thread technology, the software system which realizes the function of automatic white balance, brightness, hue and saturation adjustment with the method of establishing the corresponding relationship between YUV data and RGB data is also designed.

8558-23, Session 4

Design and implementation of non-linear image processing functions for CMOS image sensor

Purnawarman Musa, Univ. de Bourgogne (France) and Univ. Gunadarma (Indonesia); Sunny A. Sudiro, Institute of Informatics Management and Computer Jakarta (STI&K) (Indonesia); Eri P. Wibowo, Suryadi Harmanto, Univ. Gunadarma (Indonesia); Michel Paindavoine, Univ. de Bourgogne (France)

Today, solid state image sensors are used many applications like in mobile phones, video surveillance systems, embedded medical imaging and industrial vision systems. These image sensors require the integration in the focal plane (or near the focal plane) of complex image processing algorithms. Such devices must meet the constraints related to the quality of acquired images, speed and performance of embedded processing, as well as low power consumption. To achieve these objectives, low-level analog processing allows extracting the useful information in the scene directly. For example, edge detection step followed with a local maxima extraction will facilitate the high-level processing like objects pattern recognition in a visual scene. Our goal was to design an intelligent image sensor prototype achieving high-speed image acquisition and non-linear image processing (like local minima and maxima calculations). For this purpose, we present in this article the design and test of a 64x64 pixels image sensor built in a standard CMOS Technology 0.35 μ m and including non-linear image processing. The architecture of our sensor, named nLiRIC (non-Linear Rapid Image Capture), is based on the implementation of an analog Minima/Maxima Unit. This MMU calculates the minimum and maximum values (non-linear functions), in real time, in a 2x2 pixels neighbourhood. Each MMU needs 42 transistors and the pitch of one pixel is 40 μ m. The total area of the 64x64 pixels is 11mm². Our tests have shown the validity of the main functions of our new image sensor like fast image acquisition (1K frames per second), minima/maxima calculations in less than one ms.

8558-24, Session 5

A fast mode decision algorithm for multiview auto-stereoscopic 3D video coding based on mode and disparity statistic analysis

Cong Ding, Xinzhu Sang, Tianqi Zhao, Binbin Yan, Junmin Leng, Jinhui Yuan, Ying Zhang, Beijing Univ. of Posts and Telecommunications (China)

Abstract--Multiview video coding (MVC) is essential for applications of the auto-stereoscopic three-dimensional displays. Because MVC inherently contains more visual data and adopts exhaustive variable size mode decision, multiple reference frame selection is used to significantly improve high compression efficiency at each macroblock(MB). However, the computational complexity of MVC encoders is tremendously increased. Fast algorithms are very desirable for the practical applications of MVC. Based on joint early termination, the selection of inter-view prediction and the optimization of the process of Inter8x8 modes by comparison, a fast macroblock mode selection algorithm is presented. Firstly, each macroblock is checked whether the rate-distortion(RD) cost of Skip mode is below a predefined 'low' threshold or above the 'high' threshold, to make an early termination or narrow the candidate modes. If neither, Inter16x16 mode will be checked. Then, by utilizing Inter16x16 mode prediction results, the disparity estimation of other Inter modes is guided to bypass the unnecessary inter-view prediction. Finally, by comparing the cost of Inter16x16 with Inter8x8 mode, we can predict the more likely situation of actual motion. Thus, the unlikely candidate modes will be excluded further. As compared to the full mode decision in MVC, the experiment results show that the proposed algorithm can reduce up to 78.13% on average and maximum 90.21% encoding time with a little increase in bit rates and loss in PSNR.

8558-25, Session 5

Stereo correspondence of contour using dynamic programming

Junqin Lin, Dayuan Yan, Xiaoming Hu, Qiaona Xing, Bo Yang, Beijing Institute of Technology (China)

Stereo correspondence is one of the most active research areas in stereo vision. In order to solve the problem of large similar gray-scale region areas and the time-consuming in the dense reconstruction, a novel correspondence algorithm, in which the contour of stereo pairs is extracted to reconstruct the scene, is discussed in this paper. Canny algorithm is selected to extract the contour for it can get a complete, continuous and single-pixel outlines, which is superior to the traditional edge detection algorithms such as Sobel operator, Laplace operator and so on.

A noisy disparity map might be produced if the disparity is solved by using traditional matching algorithms (such as SAD, census, etc.) which choose the optimal disparity for each pixel individual. To reduce the noise which will influence the accuracy rate of stereo matching, a stereo matching algorithm applying on the contour based on the dynamic programming is proposed in the paper. Based on the reasonable and commonly assumption that the disparity of the scene is always smooth, each disparity is constrained to with the values of its neighbors' disparities, in which its neighbors mean the adjacent pixels along the same contour of the image. The searching scale could be reduced as well. As the Dynamic Programming algorithm is applied on the contours with the disparity constrain, the optimal disparity which has the minimum cost along the contour will be obtained.

Since the sum of points that need to be computed are greatly reduced by the edge detection and the disparity is optimal by the Dynamic Programming, the algorithm has a faster speed than dense reconstruction and a higher matching-rate.

8558-27, Session 5

Generation of fractal Chinese characters based on IFS

Zhengbing Zhang, Wei Zhang, Yangtze Univ. (China)

The theory of iterated function systems (IFS) has been used in generating fractal graphics. In this paper, a method is proposed to generate fractal Chinese characters with IFS. Each Chinese character generated with this method is actually the attractor of an IFS, therefore it has the property of self-similarity. A Chinese character is usually composed of a number of strokes. In most cases, one stroke can be modeled with only one affine mapping, but in some special cases, one stroke is divided into two or more parts and modeled with two or more mappings in order to make every mapping be contractive. The finite set of the contractive affine mappings that model all the strokes of the whole character construct the IFS for that Chinese character. It is important to determine the affine mapping coefficients for each stroke. The symbol X is used to denote the square area with its upper-left corner at $(0, 0)$ and lower-right corner at $(1, 1)$, while the symbol C is used to denote the Chinese character to be modeled with an IFS, w_n ($n = 1, 2, \dots, N$) to denote the affine mappings that model C , and S_n ($n = 1, 2, \dots, N$) to denote the strokes or stroke parts corresponding to w_n . Suppose C is included in X , then w_n maps X into S_n . For each affine mapping, there are 6 coefficients, which are calculated by solving matrix equation with three pairs of corner points in X and S_n . Formulas to find out the coefficients of w_n are deduced in this paper. After the coefficients of all the affine mappings for a Chinese character have been determined, the random iteration algorithm is used to show the corresponding fractal Chinese character. The experimental results show that the generated fractal Chinese characters are self-similar and beautiful.

8558-28, Session 5

New algorithms based on data reorganization for three-dimensional point cloud data partition

Meinan Li, Qun Hao, Yong Song, Beijing Institute of Technology (China)

With the development of 3-D imaging techniques, three dimensional point cloud partition becomes one of the key research fields. In this paper, two data partition algorithms are proposed. Each algorithm includes two parts: data re-organization and data classification. Two methods for data re-organization are proposed: dimension reduction and triangle mesh reconstruction.

The distribution of 3-D point cloud is massy and disordered in the space. Dimension reduction investigates the x and y boundary of the data, divides the data into x - y cubes, then the depth data is stored in 2-D matrix like gray image. Triangle mesh reconstruction describes the data in 3-D grid. The triangulation algorithm is based on dominating edge of point cloud data.

Following the dimension reduction, the algorithm of data classification is based on edge detection of depth data. The edge detection algorithms of gray images are improved for depth data partition. As to the triangulation method, the data partition is realized by region growing, starting from several points, judging the depth-related property of the all the points through the triangle grid.

The simulation result shows that the two methods can achieve point cloud data partition of standard template and real scene. The result of standard template shows the total error rates of the two algorithms are both less than 3%.

8558-26, Poster Session

Target contour extraction for shipborne active range-gated imaging

Chao Liu, Xinwei Wang, Yan Zhou, Yuliang Liu, Institute of Semiconductors (China)

A shipborne ranged-gated night vision system which can achieve target finding, target tracing and ranging improves the ability of navigation, positioning and obstacle avoidance for nocturnal operated ships. However, shortcomings such as the vague edges of ranged-gated images and complex backgrounds outside the target impede the accuracy of ranging and the exact target tracing. Therefore, target (ships) acquisition is of great importance for shipborne night vision system to avoid the interference of waves, islands and buoys. A digital image processing algorithm is developed for the mentioned night vision equipment above. After image preprocessing like denoising, target contour is extracted using Canny edge detection algorithm based on self-adapted Otsu threshold segmentation. Furthermore, on account of the vague edges especially for range-gated images, edge thinning, edge connection and morphologic methods are implemented to ameliorate the acquired contour. The entire pixels of the ROI (region of interest) are needed for ranging, hence, pixels inside the contour are collected utilizing horizontal-vertical traverse and Zigzag traverse. After single and multiple targets (mainly ships) from range-gated imaging equipment being all tested, target contour and inner pixels can both be acquired through this algorithm.

8558-34, Poster Session

An effective method of eliminating ghosting in image mosaic

Shurui Zhao, Univ. of Electronic Science and Technology of China (China)

Image mosaic is useful for a variety of tasks in both vision and computer graphics. Image fusion method directly affects the stitching effect. If there are moving objects in the images, the same object may add together after fusion and cause ghosting. A fusion method which can effectively eliminate the exposure difference and ghosting is essential to image mosaic.

The method of optimal seam can eliminate integrated ghosting. But the optimal seam may include individual error points and its overall strength is the smallest. The line is incorrectly taken as the optimal seam. So the ghosting may still exist.

In order to avoid the impact of error points an improved optimal seam based on feature point is proposed in this paper. The scale invariant feature transform (SIFT) and the random sample consensus (RANSAC) are used to ensure the detected feature points are accurate. The improved optimal seam is different from the original optimal seam regards the point has the smallest guidelines value as extended direction this paper regards the feature point as the extended direction. The feature point's strength value should have an appropriate weight value. In this way it can avoid the error points and dynamic elements. Both sides of the optimal seam have exposure differences, an image fusion method should be taken to achieve smooth and natural mosaic. Poisson fusion method can achieve the synthesis of the fragment, thereby maintaining a continuous transition between the two different fragments. So Poisson fusion is used to eliminate exposure difference in this paper. Experimental results show that the proposed method can effectively eliminate the ghosting and achieve seamless mosaic.

8558-36, Poster Session

Calculating method for the brightness of spatial objects in engineering

Tang Jia, Gao Xin, Beijing Institute of Tracking and Telecommunication Technology (China)

Calculating the ground illumination of the space objects is the necessary way to calculate the objects brightness from reflecting sunlight. The ground illumination of the space objects are dependent on the sunlight direction and observation direction, that is in direct proportion to the integral of $\cos\theta_1\cos\theta_2$. θ_1 is the angle between the target surface element normal and the sunlight incident direction. θ_2 is the angle between the target surface element normal and the observation direction.

The integral of $\cos\theta_1\cos\theta_2$ is different to difform object. Integral complexity increases with the increase in the complexity of the surface shape. This paper introduces a simple way through vector integral to calculate of $\cos\theta_1\cos\theta_2$. $\cos\theta_1$ is represented by the sunlight incident direction vector and the target surface element normal direction vector. $\cos\theta_2$ is represented by the observation direction vector and the target surface element normal direction vector. In this way, the integral expressions is changed from angle cosine integral into the integral for the direction vector ,that simplifies the complexity of the integral largely. As an example, the object is used to illustrate the process of vector integral method. The results in this way are same as that indicated in literature. The characteristic of vector integral method is processing in the right-angle coordinate so that doesn't be limited by geometric form of the space objects. The rule of selecting a system of coordinates is ease to calculate. According the selected system of coordinates and the right-angle integral surface (xoy, xoz or yoz), the expression of integral is different .

8558-44, Poster Session

Research on system modeling and data reconstruction for spatial coding compressive spectral imaging

Yuheng Chen, Xinhua Chen, Yiqun Ji, Jiankang Zhou, Weimin Shen, Soochow Univ. (China)

Compressive spectral imaging is a kind of novel spectral imaging technique that combines traditional spectral imaging method with new concept of compressive sensing. Spatial coding compressive spectral imaging realizes snapshot imaging and the data cube dimension reduction by successive modulation, dispersion and aliasing of the light signal. It reduces acquisition data amount, increases imaging signal-to-noise ratio, realizes snapshot imaging for large field of view and has already been applied in the occasions such as high-speed imaging, fluorescent imaging and so on. In this paper, the physical model for single dispersion spatial coding compressive spectral imaging is built on which the data flow procession is analyzed and its reconstruction issue is concluded. The existing sparse reconstruction methods are investigated and the specific module based on the two-step iterative shrinkage/thresholding algorithm is built so as to execute the imaging data reconstruction. A regularizer based on the total-variation form is included in the unconstrained minimization problem so that the smooth extent of the spectral data cube can be controlled by altering its tuning parameter. To verify the system modeling and data reconstruction method, a simulation imaging experiment is carried out, for which a specific imaging scenery of both spatial and spectral features is firstly built. The mean square errors of the whole-band reconstructed spectral images under different regularization tuning parameters are calculated so that the relation between imaging quality and the tuning parameter is revealed, which contributes to corresponding parameter optimization.

8558-45, Poster Session

LDPC codes in wireless optical communication application

Xiangxiang Chang, Univ. of Electronic Science and Technology of China (China)

We introduced and analyzed the basic principles of LDPC codes and the techniques of coding and decoding in detail. Also we applied the LDPC code in the wireless optical communication system, built the model of the system, simulated and analyzed the application, and proved the improvement of the performance of wireless optical communication finally. In the case of weak turbulence, the coding gain of LDPC with 5 iterations is 3 dB higher than uncoded system's when the bit error rate is . In the case of strong turbulence, the bit error rate of system with 5 iterations LDPC is 2 orders of magnitude lower than uncoded one. And with the number of iterations increased, the improvement of the system will become more apparent.

8558-46, Poster Session

A real-time TV logo tracking method using template matching

Zhi Li, Xinzhu Sang, Binbin Yan, Beijing Univ. of Posts and Telecommunications (China); Junmin Leng, Beijing Information Science & Technology Univ. (China)

This paper presents a fast and accurate TV Logo detection algorithm aiming at both semi-opaque and opaque logos. The algorithm can be divided into two individual steps. Firstly extract logo templates from several video streams containing target TV Logos. A revised effective time averaging method is proposed to attain preprocessed logo images. The background can be erased entirely if sufficient frames are processed. Then noise eliminating and smoothing is processed on these logo images using median and mean filter separately. The edge detection on them results in logo templates. Secondly track logos in real time video streams. A tracking window is used for searching the logos. The cross correlation coefficient is calculated as the matching criterion by moving logo templates within the window. The maximum coefficient is chose to compare with a predefined threshold. If it is beyond the threshold, the logo is judged that it appears in the frame and vice versa. Our algorithms are carried out and tested. 12 video streams from 12 broadcasting station are selected, including 7 semi-transparent logos (CCTV1, CCTV2, CCTV7, CCTV10, CCTV11, CCTV12, CCTV-music) and 5 opaque logos (HNTV, HBTU, BTU, TJTV, NMGTU). The resolution definition of the video stream is 768*576. Each stream lasts 30 minutes. The templates are extracted using the corresponding video file recorded from the broadcast stream. The matching accuracy can be up to 99%. The time to process a frame is less than 15ms. The frame rate of video stream is 30fps, namely the time interval between two frames is 30ms. It is fast and accurate enough for the real time application.

8558-47, Poster Session

Imaging reconstruction based on improved wavelet denoising combined with parallel-beam filtered back-projection algorithm

Zhong Ren, Guodong Liu, Zhen Huang, Jiangxi Science and Technology Normal University (China)

The image reconstruction is a key step in medical imaging(MI) and its algorithm's performance determinates the quality and resolution of reconstructed image. Although some algorithms have been used, filter back-projection (FBP) algorithm is still the classical and commonly-used algorithm in clinical MI. In FBP algorithm, filtering of original projection data is a key step in order to overcome artifact of the reconstructed image. Since simple using of classical filters, such as Shepp-

Logan(SL), Ram-Lak(RL) filter have some drawbacks and limitations in practical situation, especially for the projection data polluted by non-stationary random noises. So, an improved wavelet denoising combined with parallel-beam FBP algorithm is used to enhance the quality of reconstructed image in this paper. In the experiments, the reconstructed effects were compared between the improved wavelet denoising and classical Donoho's threshold denosing functions and others (directly FBP, mean filter combined FBP and median filter combined FBP method). To determine the optimum reconstruction effect, different wavelet decomposition scales, different wavelet bases combined with three filters were respectively tested. Experimental results show the reconstruction effect of improved FBP algorithm is better than that of others. Comparing the results of different algorithms based on two evaluation standards (i.e. mean-square error (MSE), peak-to-peak signal-noise ratio (PSNR)), it was found that the reconstructed effects of the improved FBP based on db2 and RL filter at decomposition scale 2 was best, its MSE value was less and the PSNR value was higher than others. Therefore, this improved FBP algorithm has potential value in the medical imaging.

8558-48, Poster Session

Study on thickness measurement of multi alkali photocathode

Xiaofeng Li, Qiang Lu, North Night Vision Technology Co., Ltd. (China)

In this paper the optical properties and spectral reflectance characteristics of multi alkali photocathode were illustrated and spectral reflectance curve of multi alkali photocathode were measured. The shape of spectral reflectance curve is irregular compared with ordinary optical film. The reason is that the cathode layer absorbs light. Interference peak of spectral reflectance curve is the results that the reflection light on the interface between the glass and the cathode layer and the reflection light on the interface between the cathode layer and vacuum interference together. According to interference theory, if two beam light reflected by the cathode film have the optical path difference of even times the $\lambda/2$, interference enhancement peak on spectral reflection curve will appear. Similarly, if two beam light reflected by the cathode film have the optical path difference of odd times the $\lambda/2$, interference decreased peak on spectral reflection curve will appear. According to the interference theory and peak wavelength on spectral reflection interference curve the cathode film thickness of the super second generation image intensifier can be calculated out. The thickness is about 191nm, and increased by 38% compared with the second generation image intensifier. Determination of thickness simply by observing cathode film color was not an accurate method. Practice has proved that, the method to calculate the cathode film thickness by using spectral reflectance method is simple and effective. If the spectral reflectance were monitored during the process of cathode production, then the thickness of cathode layer would be able to control precisely, and the cathode study would be more in-depth, cathode sensitivity would be further improved.

8558-49, Poster Session

Age estimation using active appearance model combine with local texture features

Chunhua Xie, Zhenming Peng, Univ. of Electronic Science and Technology of China (China)

Image based age estimation is a new challenging research topic in computer vision field. Large efforts have been devoted by researchers in recent years. However finding an appropriate age feature representation remains an open problem.

In this paper, we focus on the age feature representation method. The active appearance model (AAM) is widely used to build the age features. The original AAM contains a statistic model of shape and a gray level

appearance of texture. But it only encodes the gray-level information and lack of enough texture features to encode the wrinkles.

To overcome the drawbacks of AAM, a novel age estimation method using AAM combining with local texture features is presented. The multi-scale local binary pattern (MLBP) is served as the local texture descriptor to get the rotation invariant texture features. Build the statistic shape model, and sample the MLBP features instead of gray-level information to build the new texture model, and then apply PCA analysis to combine the shape and MLBP texture model to finish building the combined AAM model. In this way, both global face features and local texture features are used to provide enough aging information. The support vector regression (SVR) is used to estimate the facial age. The face aging data set FG-NET is used, which contains 1002 face images of 82 people with age ranging 0-69 years. Experimental results demonstrate the AAM combined MLBP method performing a lower mean-absolute error (MAE) and high accuracy of estimation comparing to other method results.

8558-50, Poster Session

Target tracking using multiple templates based on maximum pixel count criterion

Jie Pu, Zhenming Peng, Univ. of Electronic Science and Technology of China (China)

Image matching plays an important role for target tracking in image processing filed. It has been widely used in image fusion, target detection, target positioning and image reconstruction, etc. There are many correlation or distance criterions for image matching, such as mean absolute difference (MAD), mean square difference (MSD) and normalized cross correlation (NCC) algorithm, but the existing algorithms usually have high computationally expensive and affected easily by noises and distortion in images. A method of target tracking using multiple templates based on maximum pixel count (MPC) criterion is presented in this paper.

The key issue of MPC criterion is counting the number of similar points. However, we can't make sure which the best matching image is when there is two or more sub-image having the same number of similar points. So a new template matching algorithm which considers not only the number of similar points but the error is proposed. While the sub-images have the same number of similar points, it would choose the best matching sub-image by calculating the summation of the error. Meanwhile, the original template is divided into five small templates to patch the problem that single template is affected easily by geometric distortion. Because the small divided template has fewer pixels than the original template, geometric distortion just affects the relevant small template and the final result will be obtained by comprehensive use of the other templates without the effect of distortion. The experimental results show that the proposed algorithm which combines the improved MPC criterion with the multiple divided templates is accurate, effective and feasible for target tracking.

8558-51, Poster Session

Compound algorithm for restoration of heavy turbulence-degraded image for space target

Liang-liang Wang, Ru-jie Wang, Ming Li, Beijing Institute of Tracking and Telecommunication Technology (China); Zi-qian Kang, Heibei Communication Design & Consultation Co. Ltd (China); Xiao-qin Xu, Xin Gao, Beijing Institute of Tracking and Telecommunication Technology (China)

Restoration of atmospheric turbulence degraded image is needed to be solved as soon as possible in the field of astronomical space technology. Owing to the fact that the point spread function of turbulence is unknown, changeable with time, hard to be described

by mathematics models, withal, kinds of noises would be brought during the imaging processes (such as sensor noise), the image for space target is edge blurred and heavy noised, which making a single restoration algorithm to reach the requirement of restoration difficult. Focusing the fact that the image for space target which was fetched during observation by ground-based optical telescopes is heavy noisy turbulence degraded, this paper discusses the adjustment and reformation of various algorithm structures as well as the selection of various parameters, after the combination of the nonlinear filter algorithm based on noise spatial characteristics, restoration algorithm of heavy turbulence degrade image for space target based on regularization, and the statistics theory based EM restoration algorithms. The intelligent combination of various algorithm structures is accomplished to achieve their superiority. In order to test the validity of the algorithm, a series of restoration experiments are performed on the heavy noisy turbulence-degraded images for space target. The experiment results show that the proposed compound algorithm can achieve detail preservation simultaneously, which is effective and practical.

8558-52, Poster Session

Depth field problem in electronic image stabilization

Chen Huang, Beijing Institute of Tracking and Telecommunications Technology (China)

For electronic image stabilization EIS process of the image sequence, the target scene in different depth of image field have different motion vectors to the dithering caused by imaging system moving. There is not a compensation amount can stable both close-range and long-range target scene, namely the depth of field problem in electronic image stabilization. The past electronic image stabilization algorithm by solving the global motion vector filtering and compensation, and this could not effectively solve the depth of field problem. This article analysis of the depth of field problem by the optical imaging model, use the Harris corner detector algorithm to detect the target scene feature points and feature matching, calculation of the different depth of field motion vector of target scene. Proposed a motion vector compensation method based on electronic image stabilization image quality assessment. Compensate the image after assign value for different depth of field motion vector of target scene, according to assess the image inter-frame differential map and peak signal-to-noise ratio of these two indicators. To adjust the distribution of motion vector assign values based on the results of the assessment feedback. For the assessment of electronic image stabilization image quality is a visual optimization process, we take a local optimal solution to optimize the value to assign. Experimental results show that for the target scene in different depth of image field the motion vector compensation effect in the optimization of the value is better than the global motion vector compensation.

8558-53, Poster Session

Method of Sun scene simulation based on active optical control system for solar occultation measurement

Fei Yu, Zhe Lin, Xiao-jun Kang, Beijing Institute of Space Mechanics and Electricity (China); Ling-Qin Kong, Yuejin Zhao, Beijing Institute of Technology (China)

During the detection of the atmosphere material, sun is used as light source for spectrum analysis of light through atmosphere with detectors on the satellite. However, due to the inhomogeneity of the atmosphere in the air, the shape of sun through the atmosphere of different heights is very different. In the process of changing height in the atmosphere, the gray image of sun is not only an irregular circle, and even is divided into different parts, and the intensity of sunlight through clouds at

different altitudes even has a difference of a thousand of times. Thus, when the light intensity, shape and location of sun in the image keep changing, it is critical for obtaining and following the position of the strongest sunlight accurately.

In the paper, a novel method of sun scene simulation for observation of the sun through the atmosphere is presented. The method based on the active optical control system, is used in sun scene simulation with the variation of light intensity, shape and position. The continuous variation of light intensity, shape and position of sun can be calculated with computer, and the computer can also be used to output solar brightness of simulation to the industrial projector and to control micro-deformable mirror with 109 channels, for simulating the shape and position of sun. The method has a simple theory and is easy to be realized. Industrial projector can output solar brightness accurately with the difference of a thousand of times, and Micro- deformable mirror has the correct and rapid response to control signals for ensuring the accuracy and real-time sun scene simulation.

8558-54, Poster Session

Digital image information hiding based on compressive sensing and double random-phase encoding technique

Lu Pei, Institute of Optics and Electronics (China) and Shihezi Univ. (China) and Graduate Univ. of Chinese Academy of Sciences (China); Zhiyong Xu, Institute of Optics and Electronics (China); Xi Lu, 34th China Electronics Technology Group Co. (China); Xiaoyong Liu, Sichuan Univ. (China)

With the increase of the importance of information security, the information hiding system based on optical encryption is widely used because of the possibility of high speed parallel encryption of 2-D image data. A typical image information hiding method with advantages of optical implementation and high robustness is based on double random-phase encoding technique. For an intercepted image, however, analyzing the probability of hidden information is feasible by a statistical detection method. In this paper, an image information hiding scheme based on Compressive Sensing and double random-phase encoding is proposed which is meaningful due to the high computational complexity of cracking. Firstly, we utilize the characteristics of Compressive Sensing, dimensional reduction and random projection, to sample a digital image, where the obtained measured values with low data volume passed through measurement matrix are considered important or unimportant equivalently and loss of a few can still perfectly reconstruct the original signal. Then, the measured values are re-encrypted by double random-phase encoding technique with smaller random phase masks. In order to increase the system security and make the keys easy to custody, the measurement matrix and the random phase masks are generated by the sequence of irrational number. At the received terminal, the original image information is reconstructed approximately by Orthogonal Matching Pursuit algorithm. Numerical experiments show that this method has following features: low data volume for hiding and high information security.

8558-55, Poster Session

Image process technique used in a large FOV compound eye imaging system

Axiu Cao, Sichuan Univ. (China) and Institute of Optics and Electronics (China); Lifang Shi, Institute of Optics and Electronics (China); Ruiying Shi, Sichuan Univ. (China); Qiling Deng, Institute of Optics and Electronics (China); Chunlei Du, Chongqing Institute of Green and Intelligent Technology (China)

Because of the unique optical scheme for imaging and a huge potential for medical, industrial and military applications, compound eyes with wide field of view (FOV) have attracted a great deal of research interest.

In recent years, many research groups have developed studies about artificial compound eyes, but the researches only focus on the design and fabrication. For practical implementation of compound eyes with wide FOV, the requirement of image process techniques based on multiple optical channels is evident. In this paper, an imaging system contained 19 lenses based on compound eyes with FOV of 112 degrees has been designed, and the study of the image process techniques has been presented.

By analyzing the FOV relationship between the system and each lens, the arrangement of the lenses can be designed. By researching the relationship between the lens position and the corresponding image geometrical shape to realize large FOV detection, an image process technique is proposed. The sub-image captured by each lens is processed and projected onto a spherical surface. All the sub-images on the spherical surface can be assembled to form a large FOV image. The process and projection methods are studied in the manuscript. By researching the relationship between the image spherical and traditional plane display, the spherical image is extended onto a plane for better visual effect. Corresponding image optimization methods are studied to obtain better image quality. To verify the above methods, experiments are carried out based on the designed compound eye imaging system. The results show that an image with FOV over 112 degrees can be acquired while keeping excellent image process quality.

8558-56, Poster Session

An artificial compound eye system for large field imaging

Yan Liu, Sichuan Univ. (China) and Institute of Optics and Electronics (China); Lifang Shi, Institute of Optics and Electronics (China); Ruiying Shi, Sichuan Univ. (China); Xiaochun Dong, Qiling Deng, Institute of Optics and Electronics (China); Chunlei Du, Chongqing Institute of Green and Intelligent Technology (China)

With the rapid development of science and technology, optical imaging system has been widely used, and the performance requirements are getting higher and higher such as lighter weight, smaller size, larger field of view and more sensitive to the moving targets. With the advantages of large field of view, high agility, and multi-channels, compound eye is more and more concerned by academia and industry. In this work, an artificial spherical compound eye imaging system is proposed, which is formed by several mini cameras to get a large field of view. By analyzing the relationship of the view field between every single camera and the whole system, the geometric arrangement of cameras is studied and the compound eye structure is designed. By using the precision machining technology, the system can be manufactured. To verify the performance of this system, experiments were carried out, where the compound eye was formed by seven mini cameras which were placed centripetally along a spherical surface so that each camera points in a different direction. Pictures taken by these cameras were mosaiced into a complete image with wide field of view. The results of the experiments prove the validity of the design method and the fabrication technology. By increasing the number of the cameras, larger view field even panoramic imaging can be realized by using this artificial compound eye.

8558-57, Poster Session

Motion target detection based on the Fourier descriptors of the fractal edge in complex environment

Jing Liang, Zhenming Peng, Univ. of Electronic Science and Technology of China (China)

Detection of moving targets in moving background is a difficult problem in the field of computer vision, throughout the past few years the

method of target detection can be divided into offline machine learning and online features cumulating. But the first method needs a priori model of the specific target through extracting the unique features of trainings, which is difficult to meet the requirements of the complex scenes. So this paper focused on the online features cumulating.

In this paper, a novel motion target detection method based on the Fourier descriptors of the fractal edge is presented. Because the carpet fractal algorithm has good anti-noise performance, and be able to get a continuous edge with the high scale, so it's very applicable to detect the artificial targets. Then get binarization of the features with the maximum entropy threshold segmentation, through labeling targets and removing small area noise targets, the result contains stationary and moving artificial targets. In order to distinguish them, the elliptic Fourier descriptors are used to describe the binary shape features of the artificial targets between multi-frames, establish the links of multi-frame target Fourier descriptors and count the frequencies of descriptors, the frequencies can decide which one is the moving target and which is not. Experiment found that only use the edge information of the high scales, and eliminate the Logarithm, which greatly reduce the computational. Compared to other feature detection and accumulation algorithms, this proposed algorithm is much simpler and well suited for complex environment.

8558-58, Poster Session

Improving videometric precision with adaptive optics based on stochastic parallel gradient descent algorithm

Junfeng Cui, Sanhong Wang, Taiyuan Satellite Launch Ctr. (China); Guangwen Jiang, Haotong Ma, National Univ. of Defense Technology (China)

In a videometric system, there are many factors can induce the dynamic optic aberrations such as vibration, temperature variation and atmospheric turbulence. Because the dynamic aberrations can't be calibrated and amended, they will degrade the videometric system's precision. However, adaptive optics (AO) technique has been widely used to correct for wavefront distortions in astronomy, vision science and laser. So adaptive optics technique is proposed to correct for the optic aberrations (include dynamic and static) in the videometric system. Since there are simple structure and low cost, the adaptive optics system based on stochastic parallel gradient (SPGD) algorithm will be used to improve the videometric precision. In such an adaptive optics system, a deformable mirror is controlled by the SPGD algorithm to optimize a scalar beam quality metric. According to the algorithm, statistically independent small random perturbations are simultaneously applied to all the control channels of the deformable mirror in each iteration step, and the stochastic approximation of the corresponding gradient component of the beam quality metric is subsequently measured. So the convergence speed of this algorithm is faster than that of the conventional gradient descent algorithm. A videometric system with adaptive optics based on SPGD algorithm was modeled numerically in this paper. Then, videometric experiments with aberrations and with aberrations been corrected for by adaptive optics based on SPGD algorithm were numerically conducted to compare the measurement accuracies of the two cases. The results show that the adaptive optics system can effectively improve the videometric system's precision.

8558-59, Poster Session

The control technique of delay-time jitter from the echo-transponder satellite laser ranging

Jian-ting Li, Beijing Institute of Tracking and Telecommunication Technology (China)

Because of the familiar R2 dependence of signal strength on range, and overcoming the prohibitively large R4 losses like the conventional reflecting satellite laser ranging (SLR), the operational distance of the echo-transponder satellite laser ranging is much farther. The echo-transponder SLR can be used for satellite ranging at the great distance, and even for the deep-space probe ranging. The echo-transponder SLR uses the laser transponder instead of the retro-reflector on satellite, and implements the ranging by means of echoing the ranging signal from the master station. However, the ranging precision of the echo-transponder SLR is reduced, because the jitter of the additional delay-time occurs in the process of the transponder's response. The principle of laser echo transponder was introduced, the causes of delay-time and its jitter were analyzed, and the control technique of delay-time jitter in the response was studied. An experimental platform of the laser echo responder was fabricated, in order to validate the availability of the control technique of delay-time jitter, and to detect the control accuracy of the delay-time jitter. As the experimental result indicated, the delay-time jitter of the laser echo transponder could be controlled effectively within 1 ns, thereby it was determined that the corresponding ranging precision was less than 15 cm, if the laser transmitter was suitably selected, and the techniques about the precise temperature control, the power automatic control, the precise Q-switched, and the accurate detection of pulse time were reasonably put to use in the system design of the laser echo transponder.

8558-60, Poster Session

Robust object recognition based on HMAX model architecture

Yongxin Chang, Institute of Optics and Electronics (China) and Univ. of Electronic Science and Technology of China (China); Zhiyong Xu, Chengyu Fu, Institute of Optics and Electronics (China); Chunming Gao, Univ of Electronic Science and Technology of China (China)

In this paper, we describe in detail the hierarchical model and X (HMAX) model of Riesenhuber and Poggio. The HMAX model, accounting for visual processing and making plausible predictions founded on prior information, is built up by alternating simple cell layers and complex cell layers. We generalize the principal facts about the ventral visual stream and argue hierarchy of brain areas to mediate object recognition in visual cortex. Then, in order to obtain the futures of object, we implement Gabor filters and alternately apply template matching and maximum operations for input image. Finally, according to the target feature saliency and position information, we introduce a novel algorithm for object recognition in clutter based on the HMAX architecture. The improved model is competitive with current recognizing algorithms on standard database, such as the UIIC car and the Caltech101 database including a large number of diverse categories. We also prove that the approach combining spatial position information of parts with the feature fusing can further promotes the recognition rate. The experimental results demonstrate that the proposed approach can recognize objects more precisely and the performance outperforms the standard model.

8558-61, Poster Session

An improved algorithm applied to electronic image stabilization based on SIFT

Lu Dai, Yuejin Zhao, Xiaohua Liu, Liquan Dong, Bangze Zeng, Beijing Institute of Technology (China)

Electronic image stabilization, a new generation of image stabilization technology, obtains distinct and stable image sequences by detecting inter-frame offset of image sequences and compensating by way of image processing. As a high-precision image processing algorithm, SIFT can be applied to object recognition and image matching, however, it is the extremely low processing speed that makes it not

applicable in electronic image stabilization system which is strict with speed. Against the low speed defect of SIFT algorithm, this paper presents an improved SIFT algorithm aiming at electronic image stabilization system, which combines SIFT algorithm with Harris algorithm. Firstly, Harris operator is used to extract the corners out of two frames as feature points. Secondly, the gradients of each pixel within the 8x8 neighborhood of feature point are calculated. Then the feature point is described by the main direction. After that, the eigenvector descriptor of the feature point is calculated. Finally, matching is conducted between the feature points of current frame and reference frame. Compensation of the image is processed after the calculation of global motion vector from the local motion vector. According to the experimental results, the improved Harris-SIFT algorithm is less complex than the traditional SIFT algorithm as well as maintaining the same matching precision with faster processing speed. The algorithm can be applied in real time scenario. More than 80% match time can be saved for every two frames than the original algorithm. At the same time, the proposed algorithm is still valid when there are slightly rotations between the two matched frames. It is of important significance in electronic image stabilization technology.

8558-62, Poster Session

A SIFT feature based registration algorithm in automatic seal verification

Jin He, Tianjin Univ. of Technology and Education (China); Tiegen Liu, Tianjin Univ. (China)

Accurate image registration is the key premise of image analysis based automatic seal verification. In this paper, a SIFT (Scale Invariant Feature Transform) feature based registration algorithm is presented to prepare for the seal verification. The similarities and the spatial relationships between the matched SIFT feature points are proposed for the registration of MS (model seal) and SS (sample seal). SIFT features extracted from the binary MS and SS images, which have the characters of rotation invariance, advanced stability and uniqueness, are matched. False matches produce larger errors if using the least square estimation in the registration of MS and SS. To further enhance the accuracy and reliability, the false matches are eliminated by RANSAC (Random Sample Consensus) algorithm. The position relationship of correct SIFT matches is accurately estimated by RANSAC, and the homography matrix between the MS and SS is constructed and named Hs, which defines the positional correspondence between each pair of corresponding points in MS and SS. The theoretical homography is H. The accuracy of registration is evaluated by the Frobenius norm of H-Hs. In experiments, translation, filling and rotation transformation are applied to seals with different shapes, stroke number and structures. The maximum value of the Frobenius norm of their H-Hs is not more than 0.03. The results prove that this algorithm can accomplish accurate registration of MS and SS, which is invariant to translation, filling, and rotation transformation, and there is no limit to the seal shapes, stroke number and structures.

8558-63, Poster Session

A method of contrast enhancement processing on wide-bits image

Xiang Peng, Zhiyong Xu, Institute of Optics and Electronics (China); Xiaoping Qi, The Institute of Optics and Electronics (China)

In order to obtain high-quality images in a project, modern cameras with wide-bits (12, 14 or 16 bits width) are usually used to acquire enough original information. Nevertheless, some kinds of data selection and transform processing are necessary to display such images on a PC (8 bits width). Besides, the output image should include both high general contrast and clear details. This paper proposed a method with two major steps: for the first step is on the basis of partially

overlapped sub-block histogram equalization (POSHE), and change the way of equalizing sub-block image, separate each sub-block recursively with different gray ranges. The next step is taking a kind of pseudo-color processing based on HIS space to enhance the visual effects, so that the image has rich layers and consistent with human's perception. Experimental results show that the algorithm could keep the local details and the mean of the original brightness at the same time, enhanced the image effectively. Considered the adaptability on different scenarios, different objectives, and a reasonable amount of time complexity, this method could adapt the requirements of practical engineering applications.

8558-64, Poster Session

Bayer image parallel decoding based on GPU

Rihui Hu, Zhiyong Xu, Institute of Optics and Electronics (China)

In the photoelectrical tracking system, Bayer images were decompressed in traditional method, which is CPU-based. However, it was too slow when the images become large, for example, 2Kx2Kx16bit. In order to accelerate the Bayer image decoding, this paper introduces a parallel speedup method based on NVIDIA's Graphics Processor Unit (GPU) which supports CUDA architecture. The decoding procedure can be divided into three parts: the first is serial part, the second is task-parallel part, and the last is data-parallel part including inverse quantization, inverse discrete wavelet transform (IDWT) as well as image post-processing part. For reducing the execution time, the task-parallel part run in the CPU in the form of parallel pipeline. The data-parallel part could advance its efficiency through executing on the GPU as CUDA parallel program. The optimization technics include instruction optimize, stream asynchronous technology optimize, texture memory and shared memory conflict avoid. In particular, it can significantly speed up the IDWT by rewriting the 2D (Two-dimensional) serial IDWT into 1D parallel IDWT. Through experiments with 1Kx1Kx16bit Bayer image, data-parallel part was 10 times faster than CPU-based implementation. Finally, a CPU+GPU heterogeneous decompression system was designed. The experimental result shows that it could achieve 4 to 5-fold speed increase compared to the CPU serial method.

8558-65, Poster Session

Non-solid hardware three dimensions display

Junewen Chen, Chung-Hua Univ. (Taiwan)

Screen display is the final and essential apparatus of all the modern 3C products. And now we have many excellent displays in LCD, OLED, FED, and 3D screen displays et. al.. Although the display and the projection display could be simplified to a small rolling sheet or a piece of paper only, but still all of those displays are solid matters.

We have developed a non-solid type spatially empty three dimensional display. In a suitable volume of the space, we had theoretically analyzed and demonstrated the aerial and the fluid dynamics of a stream that when the system is in operation, can be the excellent screen of the projection display. The physical layout is designed and demonstrated to realize the 360 degree surrounding display of the object. With matching numerical image data normalization, any sampling model and the actual person can be displayed with various outfits to be visualized in 360 degree surrounding display and the interactive pose as well. This kind of interactive and addable image display is demanded even more in many presentation and remote virtual show.

We have in this article present the results of non-solid type spatially empty three dimensional display.

8558-66, Poster Session

Analysis of the effect on optical equipment caused by solar position in target flight measure

Shunhua Zhu, Haibin Hu, Beijing Institute of Tracking and Telecommunication Technology (China)

Abstract: Optical equipment is widely used to measure flight parameters in target flight performance test, but the equipment is sensitive to the sun's rays. In order to avoid the disadvantage of sun's rays directly shines to the optical equipment camera lens when measuring target flight parameters, the angle between observation direction and the line which connects optical equipment camera lens and the sun should be kept at a big range, The calculation method of the sun's azimuth and altitude to the optical equipment at any time and at any place on the earth, the equipment observation direction model and the calculating model of angle between observation direction and the line which connects optical equipment camera lens are introduced in this article. Also, the simulation of the effect on optical equipment caused by solar position at different time, different date, different month and different target flight direction is given in this article.

8558-67, Poster Session

Target azimuth estimation for automatic tracking in range-gated imaging

Yinan Cao, Xinwei Wang, Yan Zhou, Institute of Semiconductors (China)

Active range-gated imaging is widely used in long-range surveillance, target detection, as well as salvage and rescue at sea, which is due to its ability of range-finding and good performance in severe condition. However, target tracking is not only in need of range but also azimuth, which is necessary to make 3D coordinate of target. This paper presents a target azimuth estimation method for range-gated imaging system, aiming at obtaining essential information for vision-based automatic tracking. Due to the noise and low contrast of range-gated image, median filter and histogram equalization are used. Then the self-adapted region growing method is performed to make the segmentation of target and background. After segmentation, morphologic transformation methods will be taken in order to delete false targets. With pixels of target extracted from the image, the centroid will be derived. Next the pinhole camera model is applied to work out the azimuth coordinate. Since the focus length of camera is needed in the formula, an NC (Numerical Control) zoom module is developed. In this module, a sliding potentiometer is connected to the focus motor in camera, which serves as a feedback of the focus length. To read the focus length and control the focus motor, an MCU (with AD converter) is used. Once the target azimuth information is obtained, the pan-tilt control unit can track the target bit by bit automatically.

8558-68, Poster Session

Object class recognition based on compressive sensing with sparse features inspired by hierarchical model in visual cortex

Lu Pei, Institute of Optics and Electronics (China) and Shihezi Univ. (China) and Graduate Univ. of Chinese Academy of Sciences (China); Zhiyong Xu, Institute of Optics and Electronics (China); yu huapeng, chang yongxin, the Institute of Optics and Electronics, Chinese Academy of Sciences (China) and Graduate University of Chinese Academy of Sciences (China); shao jianxin, Normal College, Shihezi University (China)

According to models of object recognition in cortex, the brain uses a hierarchical approach in which simple, low-level features having high position and scale specificity are pooled and combined into more complex, higher-level features having greater location invariance. At higher levels, spatial structure becomes implicitly encoded into the features themselves, which may overlap, while explicit spatial information is coded more coarsely. In this paper, the importance of sparsity and localized features in a hierarchical model inspired by visual cortex is investigated. As in the model of Serre, Wolf, and Poggio, we first apply Gabor filters at all positions and scales; feature complexity and position/scale invariance are then built up by alternating template matching and max pooling operations. In order to improve generalization performance, the sparsity of basis functions is increased. Similarly, within computational neuroscience, adding sparsity constraints on the number of feature inputs and feature selection is critical for learning biologically plausible model from the statistics of natural images. Then, a universal dictionary of features that could handle the recognition of most object categories is designed. By means of compressive sensing theory and sparse representation algorithm, object class recognition is implemented quickly and efficiently. The method is test on the large Caltech dataset of images from 101 object categories and the UIUC car database. The success of this approach suggests a plausibility proof for the object class recognition in visual cortex.

8558-69, Poster Session

Multi-limit unsymmetrical MLIBD restoration algorithm for adaptive optics image

Yang Yang, Information Engineering Univ. (China)

No Abstract Available

8558-70, Poster Session

ENAS-RIF algorithm for image restoration

Yang Yang, Bo Chen, Information Engineering Univ. (China)

Image of objects is inevitably encountered by space-based working in the atmospheric turbulence environment, such as those used in astronomy, remote sensing and so on. The observed images are seriously blurred. The restoration is required for reconstruction turbulence degraded images. In order to enhance the performance of image restoration, a novel enhanced nonnegativity and support constraints recursive inverse filtering (ENAS-RIF) algorithm was presented, which was based on the reliable support region and enhanced cost function. Firstly, the Curvelet denoising algorithm was used to weaken image noise. Secondly, the reliable object support region estimation was used to accelerate the algorithm convergence. Then, the average gray was set as the gray of image background pixel. Finally, an object construction limit and the logarithm function were added to enhance algorithm stability. The experimental results prove that the convergence speed of the novel ENAS-RIF algorithm is faster than that of NAS-RIF algorithm and it is better in image restoration.

8558-71, Poster Session

Space debris photometric observation weather impact analysis and processing verification

Xiao-qin Xu, Beijing Institute of Tracking and Telecommunication Technology (China)

Photometric variation curve of space debris can provide basic target identification information. Photometric original data of space target obtained by photometric observation is the photon flow value within the atmospheric layer, which is affected by atmospheric conditions,

observation equipment, detector performance, etc. The influences of the weather are the most direct cause among these factors. Processing results of debris photometric data which are obtained by us show that photometric variation curve of target fragment is smooth and regular in the case of metering night, while which is irregular in the night, which is unsuitable to measure photometric. In addition, it can't distinguish what is the reason of abnormal photometric variation, which may be the weather or the other reasons. Further analysis results show that synchronous monitoring the weather means are available, which can obtain stable photometric variation curve of background fixed star, if compare it with the photometric variation curve of the main observed object, we can test and verify the influence factors of the photometric variation in real time at night when it's unsuitable for photometric measurement.

8558-72, Poster Session

A fast star image extraction algorithm for autonomous star sensors

Xifang Zhu, Feng Wu, Xu Qingquan M.D., Changzhou Institute of Technology (China)

Star sensors have been developed to acquire accurate orientation information in recent decades superior to other attitude measuring instruments. A star camera takes photos of the night sky to obtain star maps. An important step to acquire attitude knowledge is to compare the features of the observed stars in the maps with those of the cataloged stars using star identification algorithms. To calculate centroids of the star images before this step, they are required to be extracted from the star maps in advance. However, some large or ultra large imaging detectors are applied to acquire star maps for star sensors with the development of electronic imaging devices. Therefore, star image extraction occupies more and more portions of the whole attitude measurement period of time. It is required to shorten star image extraction time in order to achieve higher response rate. In this paper, a novel star image extraction algorithm is proposed which fulfill the tasks efficiently. By scanning star map, the pixels brighter than the gray threshold are found and their coordinates and brightness are stored in a cross-linked list. Data of these pixels are linked by pointers, while other pixels are neglected. Therefore, region growing algorithm can be used by choosing the first element in the list as a starting seed. New seeds are founded if the neighboring pixels are brighter than the threshold, and the last seed is deleted from the list. Next search continues until no neighboring pixels are in the list. At that time, one star image is extracted, and its centroid is calculated. Likely, other star images may be extracted, and then the examined seeds are deleted which are never considered again. A new star image search always begins from the first element for avoiding unnecessary scanning. The experiments have proved that for a 1024²1024 star map, the image extraction takes nearly 16 milliseconds. When CMOS APS is utilized to transfer image data, the real-time extraction can be almost achieved.

8558-73, Poster Session

No-reference blur assessment based on entropy and PCNN for restoration images

Jinping He, Beijing Institute of Space Mechanics and Electricity (China); Jiansheng Chen, Guangda Su, Tsinghua Univ. (China)

In practical problems, there are usually no clear counterparts as reference to evaluate restoration results. So no-reference blur assessment is very important and necessary. In this paper, we propose an objective measure named as Edge Factor (EF) to appraise image blurring.

The fundamental rationale is that blurring effect is much more perceptible in edge transition zones. If extent of blurring becomes heavier, the edge transition zones overlap more seriously to neighboring flat areas. Then some part of edge transition fields fuse into their

neighboring flat areas. So, the pixel number of edge transition zones will decrease. We define the pixel number ratio of the edge transition zones to the whole image as EF.

In order to count edge pixel number, the point-base entropy (PE) is utilized to transform ramp edges into roof edges to identify the edge transition zones, and an entropy image is generated. Then Pulse Coupled Neural Network (PCNN) is used to the above entropy image to segment edge pixels out.

Root Mean Square (RMS) is full-reference and more convincing. Comparing RMS, we test the proposed method on images which are blurred with different convolution kernels. Experimental results show the monotonic consistency of EF and RMS. The proposed method is further compared with some common edge detection algorithms to demonstrate the effectiveness of combining PE with PCNN.

8558-74, Poster Session

Impact and application of echo broadening effect on three-dimensional range-gated imaging

Xinwei Wang, Yan Zhou, Yuliang Liu, Institute of Semiconductors (China)

Three-dimensional range-gated imaging (3DRGI) firstly proposed in the 2000s is a relatively new technique in 3D imaging. It has large potential in underwater imaging, intelligent surveillance, spatial obstacle avoidance and aircraft design due to its long range detection, high spatial resolution and effective work through obscurants such as fog, camouflages or water. 3DRGI has been quickly developed with three approaches based on depth scanning (3DRGI-DS), range intensity profile (3DRGI-RIP) and gain modulation (3DRGI-GM). In fact, all 3DRGI approaches are deduced from slicing images formed by active range-gated imaging. However, in active range-gated imaging there is an inherent echo broadening effect (EBE) which affects the range intensity profile of slicing images, and thus the impact of the effect on 3DRGI should be investigated in order to optimize 3DRGI. In this paper, we give the spatiotemporal-correlation model of EBE which can directly display its generation mechanism. Under the spatiotemporal-correlation model, three typical range intensity profiles of EBE are illustrated under different temporal parameters of laser pulse and gate pulse. A head zone and a tail zone exist in both sides of the range intensity profile. Our research demonstrates that EBE should be suppressed in 3DRGI-DS and 3DRGI-GM and utilized in 3DRGI-RIP. In 3DRGI-DS, the laser pulse width had better equal the gate time. In 3DRGI-GM, the laser pulse width should be much smaller than the gate time. In 3DRGI-RIP, the laser pulse width and the gate time should be designed according to the detailed algorithm of 3D reconstruction.

8558-75, Poster Session

Fast range estimation based on active range-gated imaging for coastal surveillance

Qingshan Kong, Institute of Semiconductors (China); yinan cao, CAS, semi (China); xinwei wang, youwan tong, yan zhou, yuliang liu, cas (China)

Coastal surveillance is very important because it is useful for search and rescue, illegal immigration, or harbor security and so on. Furthermore, range estimation is critical for precisely detecting the target. Range-gated laser imaging sensor is suitable for high accuracy range especially in night and no moonlight. Generally, before detecting the target, it is necessary to change delay time till the target is captured. There are two operating mode for range-gated imaging sensor, one is passive imaging mode, the other is gate viewing mode. Firstly, the sensor is passive mode, only capturing scenes by ICCD, once the object appears in the range of monitoring area, we can obtain the course range of the target according to the imaging geometry/projecting

transform. Then, the sensor is gate viewing mode, applying micro second laser pulses and sensor gate width, we can get the range of targets by at least two continuous images with trapezoid-shaped range intensity profile. This technique enables super-resolution depth mapping with a reduction of imaging data processing. Based on the first step, we can calculate the rough value and quickly fix delay time which the target is detected. This technique has overcome the depth resolution limitation for 3D active imaging and enables superresolution depth mapping with a reduction of imaging data processing. By the two steps, we can quickly obtain the distance between the object and sensor.

8558-76, Poster Session

A comparative study of temporal phase analysis in dynamic speckle interferometry

Hao Zhang, Tianjin Univ. (China)

Dynamic speckle interferometry has been applied to measure vibration or continuously-deformation. As a promising technique, temporal phase analysis has been applied to dynamic speckle measurement. In temporal phase analysis, an interferogram sequence is obtained by a high speed camera during object movement. And the phase is extracted from the temporal signal.

In this paper, some classical and recently proposed temporal phase retrieving techniques, such as windowed Fourier transform, wavelet transform, Hilbert transform, circle fitting in complex plane, are comparatively studied. The advantage and drawback of each algorithm are discussed and evaluated in experiments.

8558-77, Poster Session

Research and implementation of real time image restoration based on phase diversity

Quan Zhang, Changhui Rao, Institute of Optics and Electronics (China); Zhenming Peng, Univ. of Electronic Science and Technology of China (China); Hua Bao, Institute of Optics and Electronics (China)

Phase diversity (PD) can be used not only as a wave-front sensor but also a post-detection image processing technology. It makes use of the methods of optimization and image processing, which can jointly estimate the phase aberration and image with the focused and the additional defocused image of the same extended object, however, its computations have been perceived as being too burdensome and it is difficult to increase the speed of PD to achieve its real time application on a PC platform. In this paper, we analysed the basic theory and mathematical model of phase diversity algorithm. Based on signal estimation theory and optimization theory, we have derived the cost function of phase diversity method and solved the large-scale optimization problem using a limited memory BFGS algorithm. By comparing the current mainstream computational-hardware, so we chose the multi-core DSP platform to improve the performance of PD algorithm. In addition, we used a modified way to the PD object function which is more easily to deserialize by using DSP. The experiment results indicate the adopted method is effective to complete the real-time image restoration.

8558-78, Poster Session

Suishu character recognition based on genetic fuzzy C-means algorithm

Xu-Guo Zhou, Fang Dong, Jian Xu, Guizhou Industry Polytechnic College (China)

Suishu character is the very valuable historical and cultural heritage, but the character recognition system of Suishu is almost a blank. At

Present, there is no system research about Suishu character recognition in china. In this paper, the genetic fuzzy C-means algorithm is presented on based Suishu character feature, meanwhile, the precision of segmentation is further improved by using characteristic information to fuzzy reasoning; Genetic algorithm operator applying in shuishu character segmentation is analyzed and designed in detail, and the genetic algorithm is improved to increase convergence speed and avoid local optimal solution; A neural network classifier is designed for suishu character recognition; The software system is realized using suishu character recognition by VC.

8558-79, Poster Session

On-line object tracking method based on co-training

Jianhong Lai, Zhenming Peng, Univ. of Electronic Science and Technology of China (China)

The tracking method based on Co-training framework considers the object tracking as a semi-supervised learning problem. Error accumulation of the classifier can be effectively avoided in long-term tracking with this method. However, this method needs a large number of examples to do off-line training with classifier before tracking.

This paper proposes a new on-line tracking method based on Co-training framework. First of all, the object is selected as a bounding box in the first frame, then the bounding box is amplified and we sampling in it with constant step. The regions surrounding with the object are added to the positive examples; the regions of background are added to the negative examples. In order to increase the number of positive examples, we do randomizing affine deformation with original positive examples. After that, two independent AdaBoost classifiers are established with the two features, Normalized Moment of Inertia (NMI) and Histogram of Oriented Gradient (HOG). After that, every position around the object in previous frame is selected as alternative position of the object in current frame. For every position, two confidence coefficients are calculated by the two classifiers. After weighting them, the maximum position is selected as the tracking position of the object in current frame. The two classifiers exchange their examples of maximum and minimum confidence coefficients to each other to update. Experimental results demonstrate, the on-line tracking method based on Co-training framework can work robustly in long-term tracking and the drift of tracking can be effectively avoided.

8558-80, Poster Session

Adaptive bilateral filter for extended object imaging in adaptive optics system without a wavefront sensor

Huizhen Yang, Huaihai Institute of Technology (China)

Extended object imaging is degraded not only by the atmospheric turbulence but also imaging system noise. The noise in image will affect the value of image quality criteria and further affect the correction capability of adaptive optics (AO) system without a wavefront sensor. Therefore, the imaging noise must be processed in order to the correction effect of AO system. Bilateral Filter (BLF) can maintain the image edge and filter noise of image at the same time. Appropriate parameters are one of the key to removing the noise successfully for BLF. It is necessary to change the size of parameters adaptively as the noise level varies. We call such BLF as Adaptive BLF (ABLF).

An AO system with Stochastic Parallel Gradient Descent (SPGD) algorithm and a 61-element deformable mirror is simulated to restore the image of a turbulence-degraded extended object and the gray level variance function acted the optimized object by control algorithm. Considering the noise level is unknown in practice, we discuss the way of estimating it and then analyze the relationship of parameters with the noise level. During AO correction, after the noise level being estimated and parameters being established based on above method,

the performance metric is calculated according to the image filtered by ABLF. Different level noise and different aberrations are chosen to testify the validity of AO with ABLF. Numerical simulation results verify the method is effective and the correction capability of AO with ABLF is improved more obviously than that of AO without filter or with BLF.

8558-82, Poster Session

An improved electronic image stabilization algorithm

Yantao Zong, Xiaoyu Jiang, Academy of Armored Force Engineering (China)

Electronic Image Stabilization use digital image processing technology to eliminate the jitter of the image in order to gain a clear and stable video image sequences. Image motion model is the basis of parameter estimation, filtering and compensation. Currently, the main model include translation model, imilarity model, affine model and perspective model. The more of the parameters of the model, the more accurate of the image motion, but the solution time is longer. To improve the of electronic image stabilization algorithm, a variety of image motion model is studied. The relationship between image shaking and camera motion is deduced based imaging model. The physical cause of image transformation models is indicated. Design a self-adaptive multi-model electronic image stabilization algorithm, which can choose translation model or affine model and the corresponding motion estimation method automatically, by computing the shaking amplitude of image sequences when camera is working. The experimental result shows that this algorithm can achieve high precision stabilization to image sequences, and enhance the abilities of applicability and real-time of electronic image stabilization algorithm.

8558-83, Poster Session

A novel contour detection method

Rongteng Wu, Minjiang Univ. (China)

Contour detection plays an important role in computer vision. The importance of building up computational models for the perception of contours goes beyond the sole understanding of the human visual system. It is a difficult task for us to accurately detect contour of various image. But contour detection is needed in many practical applications of computer vision.

In this paper, we present a novel contour detection method. This globalization method is run on a boundary posterior probability detector $P_b(x, y)$ of image. The detector is derived from the local image brightness, color, and texture channels of each image pixel (x, y) . To build contour detector, the gradient magnitude G is defined according to a norm. The information of brightness, color and texture of image is used to generate gradient G and detector. For grayscale image, only brightness channel is used. Otherwise, the texture channel of image need to be defined by assigned an integer id. Using a clustering algorithm, each pixel will have only one integer id. Moreover, multiscale cues is used and combined with the three channels to generate G and detector.

To introduce globalization machinery, spectral clustering is used. By using the intervening contour cue, a sparse symmetric affinity matrix is generated and as the spectral clustering stage input. Then generalized eigenvectors of the system is obtained from spectral partitioning. The information from different eigenvector is combined into response spectral component of the detector to generate globalization information. Finally, the paper shows the experiment results of the globalization multiscale cues detector compared with other current detectors.

8558-84, Poster Session

Wavelength calibration of imaging spectrometer using atmospheric absorption features

Jiankang Zhou, Yuheng Chen, Xinhua Chen, Weimin Shen, Soochow Univ. (China)

Imaging spectrometer is a promising remote sensing instrument widely used in many fields, such as hazard forecasting, environmental monitoring and so on. The reliability of the spectral data is the determination to the scientific communities. The wavelength position at the focal plane of the imaging spectrometer will change as the pressure and temperature vary, or the mechanical vibration.

It is difficult for the onboard calibration instrument itself to keep the spectrum reference accuracy and it also occupies weight and the volume of the remote sensing platform. Because the spectral images suffer from the atmospheric effects, the carbon oxide, water vapor, oxygen and solar Fraunhofer line, the onboard wavelength calibration can be processed by the spectral images themselves. In this paper, wavelength calibration is based on the modeled and measured atmospheric absorption spectra. The modeled spectra constructed by the atmospheric radiative transfer code. The spectral angle is used to determine the best spectral similarity between the modeled spectra and measured spectra and estimates the wavelength position. The smile shape can be obtained when the matching process across all columns of the data. The present method is successfully applied on the Hyperion data. The value of the wavelength shift is obtained by shape matching of oxygen absorption feature and the characteristics are comparable to that of the prelaunch measurements.

8558-85, Poster Session

Restoration of nondiffracting image based on multiple copy images and retinex

Xing Zhong, Hubei Univ. of Technology (China)

An image restoration algorithm based on Retinex theory was proposed to enhance the image contrast and details for the imaging system of nondiffracting beams. The proposed algorithm applied the multiple copy images (MCI) superimposed on the multiple images which the system photographed to remove the additive white noise of the image. Then the processed image will be further processed by the multi-scale Retinex (MSR) to get the target image. Comparing with the single MCI or MSR algorithm, the algorithm of MCI combination with the MSR can get well contrast and clear edge contour. Then the image subjective visual characteristic was promoted obviously. And it has been demonstrated by experiment. Thus, the method applied to the imaging system of the nondiffracting beams for image restoration can meet the imaging and on-line testing requirements.

8558-86, Poster Session

Point target detection based on nonlinear spatial-temporal filter in infrared image sequences and its analysis

Wei Zhang, Jinnan Gong, Chunjiang Bian, Qingyu Hou, Harbin Institute of Technology (China)

In this paper, we address a problem of detecting weak point target with low velocity in infrared sequences evolving cloud clutter. Consider moving objects are viewed at a long range with an infrared electro-optical system, a dim point with slow moving speed is appeared as target in sequences. Therefore, its energy is not clearly distinguished between background clutter, evolving cloud in particular. Former methods based on temporal processes either have a poor performance or limit the

minimum speed. They are not suitable for detect weak target which signal-to-clutter (SCR) less than 3 with a low moving velocity.

To solve this problem, a method based on nonlinear spatial-temporal filter is proposed and analysis its performance. First of all, a temporal filter for detecting point target called triple temporal filter (TTF) is introduced. Since theoretical analysis shows that TTF has a poor performance under temporal noise, a nonlinear spatial-temporal filter by neighbor pixels in prior and posterior frames, which takes every possible target trace account to suppress noise before coming into recursion. Then TTF output by positive and inverse sequence order form nonlinear spatial-temporal filter fuse with linear principle is put forward, which called bilateral TTF in this paper. Finally after analyzing the performance of the proposed method, a principle of control parameter settings is built. The results of experiment shows that compared to original TTF, the proposed method achieves a higher signal-to-clutter ratio gain, which is effectively detecting dim target when target signal-to-clutter down to 2.5 or lower with a low moving velocity.

8558-87, Poster Session

Ship target segmentation and detection in complex optical remote sensing image based on component tree characteristics discrimination

Wei Zhang, Research Center for Space Optical Engineering, Harbin Institute of Technology (China); Chunjiang Bian, Xiao Zhao, Qingyu Hou, Jinnan Gong, Harbin Institute of Technology (China)

Automatic ship target recognition in optical remote sensing image has great application value. With the improved resolution of optical satellite images, the outstanding advantages of the ship target classification and recognition in ship investigation, shipping monitoring is attracting the attention of marine monitoring department and domestic - foreign scholars. Under the application background of sea-surface target surveillance based on optical remote sensing image, automatic sea-surface ship target recognition with complicated background is discussed in this paper. The technology this article focused on is divided into two parts, feature classification training and component class discrimination. First, the real ship targets and false targets are selected from remote sensing images as training sample, and their feature parameters are extracted. Then the parameters are chosen with DB Index criterion and a Fisher is used for classification training. Second, analyzing target/background characteristics of satellite remote sensing images with ocean background, an image segmentation method based on the component tree is presented, and suspected targets are obtained by using area - gray (A-L) threshold criteria, then they are input to the trained Fisher classifier to recognize the ship target. Experimental results show that the method discussed in this paper can deal with complex sea surface environment, and can avoid the interference of cloud cover, sea clutter and islands. For the panchromatic images from QuickBird and OrbView, the detection probability of our method is 97.44% and 88.64% respectively. The method can effectively achieve ship target recognition in complex sea background.

8558-88, Poster Session

Template matching and registration based on edge

Qingyu Hou, Lihong Lu, Chunjiang Bian, Wei Zhang, Jinnan Gong, Harbin Institute of Technology (China)

Image matching aided navigation determines the original matching area on the real time image according to template matching, and then determines the real time position and attitude of vehicle accurately using the registration between them to achieve the evaluation of

precise geometric transformation. Therefore, the final precision of aided navigation is determined by the precision of image matching and registration. Considering that the consistency of heterogeneous image feature and the real-time of algorithm, the edge is regarded as the feature of matching and registration. A novel edge template matching measure is proposed based on the point set correlation, termed Weighted Voting Accumulation Measure (WVAM). This measure is capable of resisting the interference of noise and the similarity region and can achieve matching location of template edge in heterogeneous image. On this basis, image registration algorithm based on the steepest descent of the likelihood function is proposed. The likelihood function of edge sets registration is established on the basis of Gauss Mixture Model (GMM) of point sets. In order to achieve the registration between the template and matching area, and resolve the optimum transformation parameter by using the steepest descent method, the likelihood function is regarded as objective function and the affine transformation parameter is regarded as the optimization variance. And the experimental results illustrate WVAM has better characteristic in terms of global single and local gradient than LTS-HD (Least Trimmed Square Hausdorff Distance). Meanwhile, compare to the SIDT feature points registration algorithm, the results proved that the validity of proposed algorithm.

8558-89, Poster Session

The simulation for the temporal characteristic of the microchannel plate

Houzhi Cai, Jinyuan Liu, Xiang Peng, Shenzhen Univ. (China)

Microchannel plate (MCP) gated framing camera is a powerful diagnostic tool for two-dimensional, time-resolved imaging and time-resolved x-ray spectroscopy in the fields of laser-driven inertial confinement fusion and fast Z-pinch experiments. Understanding the behavior of the MCP as used in such camera is critical to understanding the data obtained. The subject of this paper is a Monte Carlo computer code we have developed to simulate the temporal characteristic of the MCP. By simulating the electron cascade in the MCP, the relationship between the MCP temporal resolution and the ratio of its thickness to the channel diameter (L/D ratio) is obtained. The transit time and the transit time spread (TTS) simulations of the MCP are also presented. The simulated results show that the transit time and the TTS of the MCP are increased with the L/D ratio increase while the channel diameter of the MCP is 10 μm .

8558-90, Poster Session

Multichannel serial-parallel analog-to-digital converters based on current mirrors for the high-performance image multi-sensor systems

Vladimir G. Krasilenko, Vinnitsa Social Economy Institute (Ukraine); Aleksandr I. Nikolskiy, Alexander A. Lazarev, Vinnitsa National Technical Univ. (Ukraine)

The paper considers results of designing and modeling of analogue-digital converters (ADC) based on current mirrors for the multi-sensor systems with parallel inputs-outputs. Such ADC, named as multichannel serial-parallel analog-to-digital converters based on current mirrors (M SP ADC CM). Compared with usual converters, for example, reading, a bit-by-bit equilibration, and so forth, have a number of advantages: high speed and reliability, simplicity, small power consumption, the big degree of integration in linear and matrix structures. We discuss aspects of design of M SP ADC CM for Gray and binary codes. We offered, investigated and simulated M SP ADC CM with 6, 8 and more bits for Gray and binary codes. Each channel of the overall structure of M SP ADC CM consists of several base digit cells (ABC). For low power consumption only one such ABC (less than 20 CMOS) and an analog memory block are used for the each channel. Base digit cells (???) of

such M SP ADC CM are serial-parallel connected. The ABC consists of 20-30 CMOS transistors and one photodiode. The ABC has low supply voltage (1-3.3)V and maximum currents values of 10-40 μA . Therefore such new principles of realization high-speed low-digital M SP ADC CM allow reaching a time of transformation less than 20-30nS at 5-8 bits for binary and Gray codes and general power consumption is 1-5mW. The quantity of cascaded ??? depends on number of bits n of multi-bits ADC, and provides quantity of levels of quantization equal to $N=2^n$. Such M SP ADC CM has low power consumption $\leq 3-5\text{mW}$ even at high supply voltage (3-7)V, and good dynamic characteristics (frequency of digitization even for 1,5 μm CMOS-technologies is 40 MHz and can be increased 10 times) and high accuracy ($?$ quantization=156,25nA for $L_{\text{max}}=10?$ A). The range of conversion of optical signals, taking into account sensitivity of modern photo-detectors, is 20-200 ?W. For low power consumption version of ADC based on only one ABC and an analog memory block the general power consumption is 50-100 μW . The ADC with serial output bits has no more than 40 CMOS transistors. The M SP ADC CM opens new prospects for realization linear and matrix (with picture operands) micro photo-electronic structures which are necessary for neural networks, digital optoelectronic processors, neural-fuzzy controllers, and so forth.

8558-91, Poster Session

Noise of CCD reduction based on three-D noise model

Hui Lin, Li-Li Liu, Xi'an Institute of Optics and Precision Mechanics (China)

During the measuring of laser near field distribution With scientific grade CCD process, due to the existence of various noises, which will influence the measurement data degree of confidence. in addition, when using the near field image to calculate contrast of near-field optical , require an accurate assessment of effects which science CCD noise brings, and according to the kind of noise to using different methods to reduce it. In this paper, the author aimed at the scientific grade CCD which using in laser parameter measuring system using 3-D noise model, analysed the noise characteristics of CCD, and classified the CCD noise into temporal noise and spatial noise, then analysed above two which created in the scientific grade CCD measurement processing , and using different methods to reduce noise to get rid of impact in measurement.

8558-92, Poster Session

An image threshold based on Burr distribution

Xiaohong Xie, Rongteng Wu, Minjiang Univ. (China)

Thresholding is a simple and efficient tool for image segmentation. The aim of thresholding image is to segment image into two opposite classes, namely object and background. It is important to accurately fit the unknown probability density functions of background or object. The generalized Guassian distribution model is often used to characterize the statistical behavior of a multimedia signal, and applied in fitting probability density functions of a signal. But, in practically, the probability density function of lots of data source may be inherently non-Gaussian. So simply using the generalized Guassian distribution model cannot describe the data accurately. This paper will use Burr distribution to fit the probability density of histograms of the background and object. Burr distribution is widely used in fitting curves of reliability distribution for it is more flexible than Weibull distribution and its three-parameter form is more generalized than log-logistic distribution. To resolve the estimation difficulty in the Burr distribution model, the expectation maximization algorithm is used. The expectation maximization algorithm starts from a set of selected appropriate parameters' initial values, and then iterates the expectation-step and maximization-step until convergence. The experiment results show that the Burr distribution could depicts quite successfully the probability

density function of a significant class of image, and comparatively the method has low computing complexity.

8558-93, Poster Session

Evolution of the square pattern in dielectric barrier discharge

Yongjie Wang, North China Electric Power Univ. (China); Lifang Dong, Hebei Univ. (China)

Dielectric barrier discharge (DBD) is a kind of nonequilibrium gas discharge, which has been well known for its widespread industrial applications, such as ozone generation, biomedical applications, polymerization process, surface treatment and plasma display panels. Recently, much attention has been paid to DBD due to various kinds of pattern formation, including square, hexagon, spiral, and concentric-ring pattern. In addition, DBD has the unique advantage of light emission feature, which leads to the fact that the spatiotemporal dynamics of patterns can be studied with the optical method. Especially, the intensified charge-coupled device (ICCD) camera is always used to study the evolution of the discharge in DBD.

In this paper, the square pattern is obtained under small boundary condition in DBD. The spatiotemporal dynamics of the square pattern is investigated by the ICCD camera for the first time. The ICCD camera is triggered by a generator of rectangular pulses, which is synchronized directly by the discharge current signal. By varying the delay between the discharge current and the opening of the ICCD's gate, we can track the temporal evolution of the discharge. Each image is taken during one single discharge current pulse of 200ns and not overlapped with the images in other cycles. It is found that there are two discharge current pulses in each half cycle of the applied voltage. The square pattern is an interleaving of two transient sublattices, which appears at different times. In two consecutive half cycles of the applied voltage, the temporal evolution of the two sublattices is inverted. The results show that the wall charges play an important role in the evolution of the square pattern.

8558-94, Poster Session

CT/MR medical image fusion based on fuzzy algorithm

Weidong Lai, Hebei Univ. (China); Xiaojun Wang, North China Electric Power Univ. (China)

The use of imaging as an assay in the medical fields, such as computer tomography (CT), magnetic resonance (MR), ultrasound, etc., relies on either manual interpretation, or algorithms developed specifically for the image type and subject. Automated, robust, and quantitative image analysis methods are in great demand. The translating accuracy achieved from the images extensively depends on the quality of images. But it is unfortunate that the medical images, such as CT, MR etc., are often limited by the isolated features in respective image, which is ascribed to its unique image acquisition technique. For many applications, the information directly provided by single medical images is incomplete. In order to enhance the diagnostic accuracy, image fusion is the fundamental process when aiming at interpreting integrated medical information. In this paper, the combined wavelet transform and fuzzy fusion algorithm is put forward to extract and fuse the features of CT and MR images. After discussion of the defects from ordinary fusion methods, the 3-level wavelet transformation is proposed for extract image features, based on the consideration that the image edge signal exists in high frequency wavelet domain and the local details in low domain. Furthermore, the high frequency wavelet coefficients of CT and MR images are fused by manipulating the respective coefficients according to the local variance, while the low frequency coefficients are fused by fuzzy rule proposed in this paper. The most important factor in the proposed fusion rule is the fuzzy density between the respective CT and MR coefficients, which is put

forward by analyzing the statistic characteristic of such coefficients. By adjustment of the coefficients of the different wavelet domain, the edges and the details from CT and MR are fused and preserved. Simulation indicates that the combined algorithm can effectively fuse the medical images, and the information entropy is calculated to compare the different fuzzy density rule. The combined algorithm proposed in this article can be integrated in medical image analyzing software to obtain higher accuracy for symptom interpretation and multisource fusion.

8558-95, Poster Session

Restoration of ultrasound image based on novel morphology operator

Xiaojun Wang, North China Electric Power Univ. (China); Weidong Lai, Hebei Univ. (China)

Information detection and recognition of nidus have been playing important roles during clinical pathology, which can not only be attained through the general reports such as auscultation, palpation and thermometric analysis, but also by the advanced multi-images from the X-rays, CT (Computerized Tomography), MR (Magnetic Resonance) as well as US (Ultrasound), etc.. Since the medical images can expose the inner structure of the body without significant damages to human body, the medical images have been accepted as the major diagnostics supports in modern clinical medicine. Though all medical images have essential meaning for acquiring the nidus information, the ultrasound technique can be easily generalized in low cost, especially in the developing countries. Ultrasound has increasingly been used as first aid response for emergency cases. Furthermore, ultrasound is acted as remote diagnosis means where teleconsultation is required. Due to the complex composition of human body organs and the air bubble environments, the ultrasound images are inevitably deteriorated by noises from variance sources to generate the echo texture, speckle noise and weak edges. In order to enhance the signal as well as heightening the diagnosis accuracy, many algorithms have been investigated and practiced. From morphology viewpoint, the ultrasound image is constructed by pixels with grey levels image presented as different gradient magnitude. Image morphological segmentation is important for clinically computer vision that aims to segment the image into physically meaningful regions. In this paper, the ultrasound image is analyzed that the edge of tissue is formed as continuous pixels, with the noise points presenting as discrete variability pixel. Based on such analysis, modified Susan operator is proposed by judging the validity of the edges, and extracting the ultrasound information through noise background. The window width and window format of Susan operator is adjusted, with the weight in window matrix also optimized, to the edge detection resolution. As comparison, the traditional filter method, such as differential operators, the median filtering algorithm as well as wavelet transformation is also practiced. Results show that the SUSAN edge detector finds image features by using local information from a pseudo-global perspective. And the proposed method is superior to other methods in both noise reduction and detail preservation. The proposed algorithm can be integrated in expert system for ultrasound analyzing.

8558-96, Poster Session

The effect of chromatic background for luminance contrast-sensitivity function

Li Song, Ningfang Liao, Shuwen Dong, Ting Liao, Weigui Hu, Kai Lin, Beijing Institute of Technology (China)

In the study of human contrast sensitivity, it is mainly measured in three channels: luminance, red-green and yellow-blue. It is based on the assumption that the luminance signal and the chromatic signal are independent. However, there have some results shown that there may be some internal relation between the luminance signal and the chromatic signal. Therefore we study the effect of chromatic

background on luminance contrast-sensitivity function (CSF). We selected three background-grey, orange and yellow-green from CIE 17 color center and the mean luminance of these colors are 29.6 cd/m², 30.6 cd/m² and 33.2cd/m², which are approximately equal. We use CRT monitor display the rectangular stripe. In order to let the minimum contrast is below 0.003, the dither technology was used in producing rectangular stripes. The minimum contrast we produced is 0.0025. Every rectangular stripe has six spatial frequencies, they are 0.4, 1, 2, 3.5, 7 and 14 cycles/degree (cpd). The psychophysical method of limits is used in the experiment, 5 observers, who have normal vision and test of vision are all over 1.0, participated in the experiment. The results of experiment show that the luminance contrast sensitivity on chromatic background is lower than the luminance contrast sensitivity under grey background. We finally used two mathematics models-Barten model and Movshon model to fit the psychophysical data. Fitting result show that Movshon model is better than Barten model, especially for the chromatic background. Both of the models have deviation in the high spatial frequency part.

8558-29, Session 6

Probability voting and SVM-based vehicle detection in complex background airborne traffic video

Bo Lei, Huazhong Institute of Electro-Optics-Wuhan National Lab. for Optoelectronics (China); Qingquan Li, Wuhan Univ. (China); Zhijie Zhang, Chensheng Wang, Huazhong Institute of Electro-Optics-Wuhan National Lab for Optoelectronics (China)

This paper introduces a novel vehicle detection method combined with probability voting based hypothesis generation (HG) and SVM based hypothesis verification (HV) specialized for the complex background traffic video captured by the camera on an airborne platform. In the stage of HG, a statistic based road area extraction method is applied and the lane marks are eliminated by morphological operations. Remained areas are clustered by different area growth method according to whether the processed scene is a high or low velocity scene. Then the canny algorithm is performed to all of the clustered areas to detect edges. Every pixel in these edges votes for a square area which is presumed to contain the center of a vehicle. This voting strategy is designed to detect rectangle objects in the scene. The vote of every pixel is counted to form a voting image, and the center of a possible vehicle always takes a high value, which indicates a vehicle hypothesis. In the stage of HV, every possible vehicle area is rotated to align the vehicle along the vertical direction, and the vertical gradients and the horizontal gradients of them are calculated, which are projected to the horizontal direction and vertical direction respectively. In order to perform classification, several features are defined, which include the length and width of possible vehicle, peaks of the vertical projection, etc. SVM is adopted to classify vehicle and non-vehicle. The proposed method has been applied to several kinds of traffic scenes, and the experiment results show it's effective and veracious for the vehicle detection of the given scenes.

8558-30, Session 6

Silhouette extraction from human gait images sequence using cosegmentation

Jinyan Chen, Yi Zhang, Tianjin Univ. (China)

Gait based human identification is very useful for automatic person recognize through visual surveillance and has attracted more and more researchers. A key step in gait based human identification is to extract human silhouette from images sequence. Current silhouette extraction methods are mainly based on simple color subtraction. These methods will have a very poor performance when the color of some body parts is similar to the background. In this paper a cosegmentation based human silhouette extraction method is proposed. Cosegmentation is

typically defined as the task of jointly segmenting "something similar" in a given set of images. We can divide the human gait images sequence into several steps and every step consist of 10-15 frames. The frames in human gait images sequence have following similarity: every frame is similar to the next or previous frame; every frame is similar to the corresponding frame in the next or previous step. The progress of cosegmentation based human silhouette extraction can be described as follows: Initially only points which have high contrast to background are used as kernel points, then every kernel point will grow using the image similarity information. We define a global energy function G to constraint the growth of the kernel point. The definition of G consider the constraint of the maximum size of a human, the maximum frames count in one step and the Markov random field modeling. Experimental result shows that our method has a better performance comparing to traditional human silhouette extraction methods.

8558-31, Session 6

An Adaboost based approach for ship detection in remote sensing images

Junli Yang, Jiang Zhiguo, BeiHang Univ. (China)

In this work, we address the problem of ship detection in remote sensing images, which is crucial in ocean surveillance, marine traffic security, sea pollution monitoring, and protection against illegal fisheries and oil discharge. Remote sensing images exhibit highly complicated background and contextual information. Most state-of-the-art ship detection methods suffer from long detection time, high false detection rates and unsatisfying detection rates.

We present a machine learning approach for real-time ship detection in remote sensing images that is extremely rapid and can achieve high detection rates. In the approach we use a boosted cascade of simple classifiers under the Adaboost framework. First, in the AdaBoost based learning process, which is carried out off-line to speed up the detection process, we pick a small number of critical features from a large feature pool and acquire highly efficient classifiers. Second, to implement the multi-direction and multi-scale detection, we need to collect corresponding training samples to train a classifier in each orientation and scale, which is a time consuming work. To save the training data collection time, we train a classifier in only one direction and turn the testing image direction in every 10 degrees to be detected by the classifier, and superpose the detection results in all the orientations. Then a clustering method is used to get the final detection result. As for the multi-scale implementation, the similar principle is employed, in which the only difference is to lessen the testing image. Thirdly, to make the feature calculation faster, we employ an image representation called Integral Image which largely simplifies the Haar feature computation. At last, the introduction of "cascade" allows us to combine increasingly complicated classifiers, which can quickly discard the background regions and spend more computation on promising ship-like regions.

The proposed method was tested on Google earth images containing ships or ship plumes. The experimental results show that our method has good performance in detection accuracy and convergence speed.

8558-32, Session 6

Bottom-up attention based on C1 features of HMAX model

Huapeng Yu, Zhiyong Xu, Chengyu Fu, Institute of Optics and Electronics (China); Yafei Wang, Univ. of Electronic Science and Technology of China (China)

This paper presents a novel bottom-up attention model only based on C1 features of HMAX model, which is efficient and consistent. Although similar orientation-based features are commonly used by most bottom-up attention models, we adopt different activation and combination approaches to get the ultimate map. We compare the two different operations for activation and combination, i.e. MAX and SUM, and we

argue they are often complementary. Then we argue that for a general object recognition system the traditional evaluation rule, which is the accordance with human fixations, is inappropriate. We suggest new evaluation rules and approaches for bottom-up attention models, which focus on information unloss rate and useful rate relative to the labeled attention area. We formally define unloss rate and useful rate, and find efficient algorithm to compute them from the original labeled and output attention area. Also we discard the commonly adopted center-surround assumption for bottom-up attention models. Comparing with GBVS based on the suggested evaluation rules and approaches on complex street scenes, we show excellent performance of our model.

8558-33, Session 6

Normalization of the collage regions of iterated function systems

Zhengbing Zhang, Wei Zhang, Yangtze Univ. (China)

Fractal graphics, generated with iterated function systems (IFS), have been applied in broad areas. The generated graphics is actually the attractor of the IFS. Since the rectangle regions containing the attractors for different IFS may be different, it is impossible to respectively show the attractors of different IFS in a same region on a computer screen using one program without modifying the display parameters. A method is proposed in this paper to solve this problem by normalizing the collage regions of IFS. An IFS is defined as a finite set of contractive affirn mappings. The fixed point is calculated for each mapping, and the minimum rectangle region containing all the fixed points is called as the characteristic rectangle of the IFS. The symbol X is used to represent the unit square with the upper-left corner at $(0, 0)$ and the lower-right corner at $(1, 1)$. The collage region of an IFS is defined as the minimum rectangle that contains all the quadrangles transformed from X by its affirn mappings. Proposed algorithm: (1) A transform $T(0)$ determined according to the characteristic rectangle of the IFS and X is used to modify the IFS coefficients so that the characteristic rectangle of the resulted IFS, denoted by $IFS(0)$, changes toward X ; (2) If the collage region of $IFS(i)$ is represented with $R(i)$, then a transform $T(i+1)$ determined according to $R(i)$ and X is used to modify the coefficients of $IFS(i)$ so that $R(i+1)$ of the resulted $IFS(i+1)$ changes toward X , where i goes from 0 up until the required result is obtained. Experimental results demonstrated that the collage region of any IFS can be normalized to the unit square with the proposed method.

8558-35, Session 7

A subpixel motion estimation approach based on phase correlation

Hui Yu, Huazhong Univ. of Science and Technology (China); Fusheng Chen, Zhijie Zhang, Chensheng Wang, Huawang Chen, Huazhong Institute of Electro-Optics-Wuhan National Lab for Optoelectronics (China)

Image registration is a process of overlaying two or more images of the same scene and differing from each other due to displacement, rotation, scaling, etc. Image registration is a crucial step in various image fusion tasks, such as super-resolution. For the success of image super-resolution reconstruction, it is essential to find out high accurate subpixel motion estimation between images in the input sequence. This paper proposes a frequency domain-based motion estimation algorithm for the under-sampled infrared images. Only the pure translational motion is considered, because the rotation and scaling estimation can be converted into the translational motion estimation using the log-polar transform. The proposed algorithm is based on the phase-only correlation which is defined as the inverse Fourier transform of the normalized cross power spectrum. The signal peak of phase-only correlation shall locate at the coordinate which is the number of transformed pixel between the two images. Because of the use of discrete Fourier transform and the subpixel displacement, the signal peak is not always concentrate in the integer

coordinates. This paper proposes a method using the signal adjacent to the signal peak to estimate its location. Because the low resolution images are undersampled and have aliasing effect, the performance of conventional registration methods decreases. This paper presents a method to eliminate the influence of aliasing. Excellent results have been obtained for subpixel translation estimation of synthetic image sequence. The algorithm is also compared to other algorithms. The error analyses show that the proposed algorithm is more robust and have higher precision.

8558-37, Session 7

An illumination and affine invariant descriptor for aerial image registration

Zhaoxia Liu, Yaxuan Wang, Yu Jing, Jing Zhao, Dalian Univ. of Foreign Languages (China); Jingjing Wang, Liaoning Police Academy (China)

An illumination and affine invariant descriptor is proposed for registering aerial images with large illumination changes and affine transformation, low overlapping areas, monotonous backgrounds or similar features. Because K -nearest neighbors (K -NN) graph and the corresponding adjacent graph are invariant to affine transformation, in this paper, they are used for generate the triangle region with initial matched result by Scale-Invariant Feature Transform (SIFT). In order to improve the accuracy, three means of region growth, which is invariant to affine transformation, is applied to boost small and slender triangles. Then a new triangle area based illumination and affine invariant descriptor is defined to describe the triangle regions and measure their similarity. The descriptor is the combination of MultiScale Autoconvolution (MSA) and multiscale retinex (MSR). In the description, illumination invariant is obtained by MSR removing the illuminance of the image, and reflective image is obtained and replaces the original image. Then MSA, which comes from the idea that the corresponding regions have the same intensity distribution and their mathematic expectations are invariant to affine transformation, is applied to describe the triangle regions obtained from reflective image. The performance of the descriptor is evaluated with optical aerial images and the experimental results demonstrate that the proposed descriptor is more distinctive than MSA and SIFT.

8558-38, Session 7

Manifold representation of multi-view images

Haopeng Zhang, Zhiguo Jiang, Junli Yang, BeiHang Univ. (China)

Images of the same object lie on a low-dimensional manifold in the visual space. The manifold that multi-view images of an object lie on can be called view manifold. learning such manifold could be very helpful to multi-view object detection, classification, and viewpoint estimation. In this paper, we use view manifold to represent viewpoint variation of multi-view images in the embedding space. The view manifold can be obtained by current manifold learning methods, such as Isomap, LLE, LE, etc., with proper image features as inputs. In order to evaluate the performance of the learned view manifolds, we firstly analyze the topological property of these manifolds using some mathematical measures, and then learn a generative model that can map from the manifold representation to visual inputs for arbitrary view image synthesis and viewpoint estimation. We did experiments on both synthesized dataset and real dataset which contained images with 1D or 2D viewpoint variation. Five popular manifold learning methods were used in our experiments with different kinds of image features as inputs. Experimental results show that manifold representation can effectively describe the viewpoint variation of multi-view images, and perform successfully on arbitrary view image synthesis and viewpoint estimation.

8558-39, Session 8

Tire x-ray image belt-ply defect feature recognition method based on Gabor wavelets

Qiang Du, Qingdao Mesnac Co., Ltd (China) and Tianjin Univ. (China)

A novel method was developed for belt-ply defect feature recognition of tire X-ray image which is characterized as overlapped textures. Tire X-ray image contains complex texture which is caused by overlapped multi belt-ply, it is difficult to get defect information around the location of complex texture. The spectrum of each belt-ply texture are separable due to different location of each dominant frequencies corresponding to different belt-ply in 2D frequency space, 2D Gabor wavelet is used to separate the spectrum which belongs to different belt-ply texture, after extracting different belt-ply texture of tire X-ray image, each result single texture image is calculated through grey level statistic on vertical orientation to get a 3D model which contains detail defect information, such as texture location, orientation and bend level status. The experiment results show that every belt-ply texture can be separated accurately, and the recognized texture features are accurate and help estimate tire defect correctly according to the result 3D model.

8558-40, Session 8

A three-dimensional cursor used in binocular stereo vision

Hong Jiang, Bo Yuan, Liqiang Wang, Zhejiang Univ. (China)

A three-dimensional (3D) cursor, which is used to locate an object in the binocular stereo vision system and measure the distance from the object to camera, was proposed in this paper. The 3D image is composited of one left-image and one right-image captured by the binocular cameras and is displayed in a 3D liquid crystal TV. The left-cursor, whose position is controlled by the mouse, is generated and constrained in the left-image. Then, the matched point in the right-image with the current position of mouse in the left-image is detected by an effective key-point matching algorithm, and the right-cursor is generated on this matched point. At last, the left-cursor and right-cursor are mixed to a 3D cursor, which is able to select the target in the 3D image; meanwhile the distance is calculated by the parallax between the pair points. The above algorithm for generating the 3D cursor was realized using the own program compiled by C sharp language. The effect of 3D cursor was tested in the self-build binocular stereo camera. The results show that the 3D cursor is distinct to select the target accurately and the real-time distance measurement is realized. Moreover, our method is low-cost with little requirements for hardware.

8558-41, Session 8

Steganography based on human visual system with wet paper codes

Zhihong Chen, Tianjin Univ. (China); Lili Cao, Tianjin Univ. of Technology (China)

Steganography algorithms are often on the basis of different cover images types, transform domain and so on to design different embedded measures, which is to achieve the best performance, such as high capacity, low visibility and high robust.

Wet paper code is a complex model which mainly used in the field of image coding. This paper is based on the researches of wet paper code model and human visual system, and constructs a new steganographic method. Firstly we design a new select channel in steganography. Through the calculation of local mean square value for all wavelet subbands in 2x2 neighborhood and the corresponding

average variance for low frequency sub-band, the secret bits can be guaranteed to be embedded in the regions which is not sensitive for human eyes. Secondly a secret key matrix is proposed and shared by the sender and receiver with the seeds of random number generator. We try to find a suitable vector, which multiplied by the matrix equals to the secret bits vector. And all the values in the suitable vector are adaptively embedded into wavelet coefficients of image subbands with wet paper code. Secret information receivers do not need to know the specific method of secret writing, just do a simple matrix multiplication operation and can extract the secret information, which in many ways to improve the security of the steganographic algorithm. Finally, the experiments show that the method has good visual invisibility and resistance against active steganalysis attacks.

8558-42, Session 8

A visible/infrared gray image fusion algorithm based on the YUV color transformation

Zhu Jin, Weiqi Jin, Jiakun Li, Li Li, Beijing Institute of Technology (China)

Color fusion technology is one of the typical technologies that has been emphasized in domestic and foreign countries by fusing multiband images into a color image. It's suitable for observation and target detection. Effective visible and thermal infrared color fusion algorithms have been proposed now. We have successfully run the natural sense of color fusion algorithm in DSP and FPGA hardware processing platform real-time. However, according to different needs, gray-scale video fusion technology has its own unique applications.

Based on the natural sense of color image fusion algorithm of the visible and infrared, we have studied a based on the YUV color passed visible / infrared gray image fusion algorithm. Firstly we do a YUV color fusion (Threshold of weighted fusion and color transfer of the reference image). Then we output the brightness of the fusion (Y channel) as gray-scale fusion images. This algorithm for image fusion is compared with regular fusion algorithms: the weighted average, the Laplace Pyramid and the Haar basis wavelet. Selected objective evaluations for fusion are information entropy, joint entropy, cross entropy, root mean square error, peak signal to noise ratio and mutual information. The objective and subjective comparing results show that this algorithm compared to the traditional usual algorithm has most advantages.

On the basis of the Matlab simulation, the algorithm is implemented on a DSP hardware image processing platform real-time with the TI's chip (TMS3200M642) as the kernel processor. It makes natural sense of color fusion and gray fusion for visible light (low level light) and thermal imaging integrated. Users are convenient to choose model of the natural sense of color fusion or gray fusion for real-time video imaging output according to their needs. It provides a flexible choice for the application of high-performance visible/infrared fusion imaging system.

8558-43, Session 8

Liver hydatid CT image segmentation based on localizing region active contours method and modified parametric active contour model

Jianjun Chen, Murat Hamit, Yanting Hu, Xinjiang Medical Univ. (China); Yanting Hu, College of Medical Engineer Technology of Xinjiang Medical University (China)

Liver hydatid is a high incidence endemic disease in XinJiang and CT Image segmentation of focal area has important role in clinical diagnosis. Based on CT imaging features of this disease, localizing region active contours method and modified parametric active contour model is proposed. The presented technique is is very suitable for localization active contour energy and our segmentation framework can make accurate segmentation of focal area. by using known intensity information into the image model incorporating modified parametric active contour model, it can handle problems where the interi or exterior of the image of Liver hydatid has a highly inhomogeneous intensity distribution. Its feature term is computed locally. This property allows the algorithm to segment nonhomogeneous objects. We reduce the method sensitive to initialization through the modified parameters and evaluate the algorithm from subjective and objective aspects on different patients' CT slices. By comparing our algorithm segmentation to ground-truth manual segmentation, the results show the effectiveness of our method to segment liver and hydatid lesion.

Tuesday - Wednesday 6 -7 November 2012

Part of Proceedings of SPIE Vol. 8559 Information Optics and Optical Data Storage II

8559-4, Poster Session

A novel high-speed opto-electronic hybrid correlator for recognition and tracking

Jinggao Sui, Xiaoya Zhang, Wusheng Tang, ChenCheng Feng, Jia Hui, National Univ. of Defense Technology (China)

Opto-electronic hybrid correlator can realize the combination of electronic flexibility and high speed of optical computing, so it has widely potential applications in high speed optical information processing system, especially recognition and tracking system. But the opto-electronic conversion speed and the positioning accuracy of correlation peak constrains the performance of this system. This paper first proposes an idea that PSD (Position Sensitive Device) can be applied in optical correlation peak detection instead of traditional CMOS sensor. It is displayed by experimental data that this system can attain a correlation calculation speed of 20,000 frames per second, which indicates that the system can satisfy high speed demands of target recognition and tracking. Through optimal design of Fourier lens, the size, shape and intensity of the correlation peak spot have been optimized to satisfy the positioning accuracy requirement of PSD. Because the property of PSD can lead to nonlinear displacement error of the correlation peak, a new correlation peak compensation algorithm is brought up to compensate the error. The experimental results indicate that positioning accuracy of correlation peak can be promoted five times compared with the original outcome, which reduces the influence of nonlinear displacement error of the correlation peak on this recognition and tracking system sharply. In conclusion, a high speed and high accuracy recognition and tracking system has been realized based on the opto-electronic hybrid correlator.

8559-17, Poster Session

Recognizing and recording the tone of people and others' language to promote development of work, life, and science, and to promote administration of social security

Xu Han-You, Workers' Hospital of Nanyang Textile Corp. (China)

Objective: In this paper, the author outlined a new breakthrough creation of project for information and computer science. Which use the modern information and computer science to solve the present problem which the computer has not recorded all the tone and the words at the same time when the people are speaking.

Method: Summarize the modern information and computer science. Create the new breakthroughs project of computer science.

Results: The author outlines, by developing a new technology project to recognize the people's speaking and their tone and characters, at the same time, transmit the recognizing into computer with their tone and characters and store the tone and characters of the speaking information. Therefore, any people's speaking could be recorded into the computer with their characters of tone at the same time.

Conclusion: This is a breakthrough creation project for information and computer science. When the breakthrough creation came into reality. The revolution movements of science could be induced. The life, work, and security and other active things of mankind could be more easy and wonderful. There were much too harvesting in economical and practical gaining. And there were also much too harvesting in social development. So there are lots of chances waiting us to make her true in the near future when the paper of the new breakthrough creation for information and computer science is published and accepted for application. Because recognizing and recording the tone of people' language and his characters of the speaking information are different from each other. Like the fingerprint, the public security and other

practical gaining could be great.

The breakthrough technology project of computer science can be used for recognizing and recording the tone of language of other biology, and their characters of the speaking or voice information, apart from people'.

8559-18, Poster Session

Hydrogen bonded supramolecular azopolymers: A media for multilayered and polarization-multiplexed data storage based on two-photon process

Daqiao Hu, Yanlei Hu, Wenhao Huang, Qijin Zhang, Univ. of Science and Technology of China (China)

A two-photon induced high density information storage is demonstrated in hydrogen bonded supramolecular azopolymers. Supramolecular azopolymers are prepared through strong hydrogen bonding interaction between pyridine moiety of poly (4-vinylpyridine) (P4VP) and phenol moiety of 4-nitro-4'-hydroxyazobenzene (AzoOH). The content of azo chromophore is tuned easily and it can achieve a high concentration as 69.4wt% in P4VP (AzoOH)1.0 complexes. FT-IR spectrum verifies the hydrogen bonding has formed between them. High quality films of the supramolecular P4VP (AzoOH)1.0 complexes are obtained by spin-coating. A multilayered optical recording medium using the supramolecular azopolymer and a transparent film has been developed for two-photon recording. The thicknesses of the photosensitive layers and the transparent layers are 500nm and 12 μm, respectively. A linearly polarized Ti:Sapphire femtosecond pulsed laser (wavelength: 800 nm, pulse duration: 80 fs, and repetition rate: 80 MHz) is used as a recording beam to induce anisotropy, and the recorded information is readout by transmission microscope with a polarized white light. Multilayered and polarization-multiplexed data storage has been demonstrated by using the method. The capability to combine both advantages of these distinct techniques in supramolecular azopolymer films makes it a novel media for higher optical data density.

8559-19, Poster Session

Simulation results of optoelectronic photocurrent reconfigurable (OPR) universal logic devices (ULD) as the universal circuitry basis for advanced parallel high-performance processing

Vladimir G. Krasilenko, Vinnitsa Social Economy Institute (Ukraine); Aleksandr I. Nikolsky, Alexander A. Lazarev, Vinnytsia National Technical Univ. (Ukraine); Taras E. Magas, Vinnitsa Social Economy Institute (Ukraine)

The conception of construction of the family of the offered optoelectronic photocurrent reconfigurable (OEPR) universal or multifunctional logic devices (ULD) consists in the use of a current mirrors realized on 1.5 μm, 0.35 μm, 65nm technology CMOS transistors. Presence of 18-40 transistors, 1÷5 photo-detectors makes the offered circuits quite compact and allows their integration in 1D and 2D arrays. In the presentation we consider the whole family of the offered circuits, show the simulation results and possible prospects of application of the circuits in particular for time-pulse coding for multivalued, continuous, neural-fuzzy and matrix logics. The simulation results of the NOT, AND, OR, OR-NOT, XOR optoelectronic photocurrent logical elements (OEPL) and OEPR ULD on the 1.5 μm, 0.35 μm, 65nm technology CMOS transistors showed that the level of logical unit can change

from 20nA, 50nA, 500nA 1?A to 10?A for low-power consumption variants and from 20-500nA to 1-10?A for high-speed variants. We have developed schemes OPR ULD which realize the universal binary logic from optical signals. They have subpixel a configuration from 2x2 elements, consist of a small amount of photo diodes (4) and transistors (18), have low power consumption <1μW-5mW, high productivity and realize the basic set of operations of continuous logic with time pulse representation of processed signals. Modeling of such cells in OrCad is made. It is confirmed that all set of possible functions will be realized such OEPL and OEPR ULD by a simple photo-tuning. Such base cells are integrated into arrays 32?32 and allow reaching productivity 10¹² CL-logic operations/sec. The results of design of optoelectronic processors (OEP) with used ULD as base cells for 1D and 2D computing mediums are considered in the chapter. We consider and show that the OEP and all principal components of OEP can be implemented on the basis of optoelectronic photocurrent logical elements (OEPL) and OEPR ULD.

8559-20, Poster Session

Pattern recognition by Mach-Zehnder joint transform correlator with binary power spectrum

Chengyu Liu, Chulung Chen, Weichih Liao, Sihliang Fu, Yuan Ze Univ. (Taiwan)

We propose a construction of the Mach-Zehnder joint transform correlator with binary power spectrum for target recognition, and apply liquid crystal spatial light modulators to this system. In addition, we utilize the minimum average correlation energy method and multi-level quantized reference function. The constructed reference function is designed to be implemented at the input plane. Numerical result is presented.

8559-21, Poster Session

Optical correlation recognition research of low light level target based on lifting wavelet transform

Qibo Zhang, Su Zhang, Wensheng Wang, Changchun Univ. of Science and Technology (China)

Optical correlation technology is an important application in target recognition field, which can apply Joint Transform Correlator to achieve target recognition.

For the low light level target with low contrast and background noise interference, using optical correlation method may reduce the recognition ratio and lead to the correlation peak not sharp in the optical experiment. In order to solve the problem, the wavelet transform applied to low light level target image processing is an effective method. However, the traditional discrete wavelet transform based on convolution has large amount of calculation, high computational complexity and large storage space requirements. Lifting wavelet transform is used to solve this problem successfully.

This paper proposes a new algorithm-adaptive directional lifting based on wavelet transform. Low light level image enhancement and edge extraction are applied in this algorithm. Firstly, low light level image is decomposed into two layers by using adaptive directional lifting based on wavelet transform. The angle of prediction is divided into nine parts. Secondly, through the lifting wavelet transform the 2-D image signal can be decomposed into low-frequency part and the high-frequency part at different scales. The weight of the low frequency coefficients is increased and the weight of the high frequency coefficients is decreased. Low light level image enhancement can be achieved. Lastly, wavelet coefficients after enhancement are fused at various scales. The edge extraction is completed by determining the local modular maximum of the fusion wavelet coefficients. This method can make the

target edge information more prominent and suppress the background noise in the low light level target image.

The optical experiment results show that the optical correlation recognition based on lifting wavelet transform can recognize low light level target effectively and raise the low light level target recognition ratio.

8559-23, Poster Session

Distorted target recognition based on Canny differential operator combined with MACH filter

Jiyang Shang, Yu Zhang, Qibo Zhang, Wensheng Wang, Changchun Univ. of Science and Technology (China)

The image pattern recognition, as a fast and accurate method of targets identification and location, not only be used as target identification and location means of industrial robots and production line automation control in industrial production, but also can be used as missile terminal guidance in the military area. Therefore, image pattern recognition gets more and more people's attentions. But up to now, image pattern recognition is still unable to accurately recognize the distorted targets (the targets rotated in plane or scale changed), which has restricted the development of the image pattern recognition. In order to solve the problem of inaccurate recognition for distorted target in cluttered background among the image pattern recognition, the Canny differential operator is used to optimize the Maximum Average Correlation Height (MACH) algorithm. The distorted (scale and rotation etc) target images and the training images are edge extracted by Canny operator. The training images are used to synthesize MACH filter. The low frequency information of the distorted target images and the filter is enhanced by Canny edge extracted. Then the MACH filter is used to filter the edge extracted distorted target image. Thereby, the distortion tolerance of the MACH filter is expanded. By this method, which the edge extraction combines with frequency domain filtering, the influence of the distortion for the image pattern recognition is eliminated. In order to prove the feasibility of this distortion target recognition method and determine the distortion tolerance, a lot of computer simulation experiments have been made with the Canny differential operator and MACH filter. As an example, in the recognition range, the arbitrary three rotation planes and scale plane are selected to be tested. The experimental results show that the position of the detected target and the position of its output correlation peak have an explicit corresponding relationship. By this way, the scale distortion tolerance is 0.84~1.56 times; the rotation distortion tolerance can reach up to 80 degrees. For the targets of exceeding the distortion tolerance range, the intensity of correlation peak becomes weaker and weaker, but some of the targets can still be identified.

8559-24, Poster Session

Multi-limit unsymmetrical MLIBD image restoration algorithm

Yang Yang, Information Engineering Univ. (China)

A novel multi-limit unsymmetrical iterative blind deconvolution (MLIBD) algorithm was presented to enhance the performance of adaptive optics image restoration. The algorithm enhances the reliability of iterative blind deconvolution by introducing the bandwidth limit into the frequency domain of point spread (PSF), and adopts the PSF dynamic support region estimation to improve the convergence speed. The unsymmetrical factor is automatically computed to advance its adaptivity. Image deconvolution comparing experiments between Richardson-Lucy IBD and MLIBD were done, and the result indicates that the iteration number is reduced by 22.4% and the peak signal-to-noise ratio is improved by 10.18dB with MLIBD method. The performance of MLIBD algorithm is outstanding in the images restoration the FK5-857 adaptive optics and the double-star adaptive optics.

8559-25, Poster Session

Gain and phase dynamics in strained quantum well semiconductor optical amplifiers

Cui Qin, Xinliang Zhang, Wuhan National Lab. for Optoelectronics (China)

gain and phase dynamic characteristics in the compressive, unstrained and tensile strained quantum well (QW) semiconductor optical amplifiers (SOAs) are theoretically investigated via a detailed model. The traveling wave rate equation model includes ultrafast effects due to the carrier heating and the spectral hole burning. The carrier heating effect can be described by coupling carrier temperature equation to carrier and photon density equations. Based on the calculation of energy band structure, the effects of compressive and tensile strain on the differential gain and the derivative of refractive index change are investigated. The peak of the differential gain spectrum shifts to shorter wavelength in the tensile strained structure. In the SOA operation wavelength region, the value of the derivative of refractive index change is obvious enhanced in the compressive strained structure. The characteristics of the differential gain and the derivative of refractive index change have significant influence on the gain and phase recovery dynamics in QW SOAs. The different strained QW SOAs are examined with pump-probe technique via simulation. By comparing the gain and phase recovery dynamics in three different types of SOA samples, it is demonstrated that the compressive QW SOA shows the fastest gain recovery rate and the largest phase change. In addition, the ultrafast recovery process due to the carrier heating effect can be enhanced significantly in the tensile QW SOA. The study can provide reasonable guidance for thorough understanding and proper design of QW SOAs, which are used in all-optical signal processing based on cross gain modulation and cross phase modulation.

8559-26, Poster Session

A GRIN medium coupler and its application in light beam spot conversion

Ning Wang, Fangkui Sun, Harbin Institute of Technology (China); Lixue Chen, Harbin Institute of Technology (China); Lequn Li, Harbin Institute of Technology (China)

GRIN (Gradient refractive index) medium with a lateral sech refractive index variation, can make normal-incident light beam gradually curve to the medium with a larger refractive index, and periodically converge the light beam to a point smoothly and continuously. This property of GRIN medium can be used as a coupler to realize a mode spot size conversion. This paper mainly discuss the transmission property of Gaussian light beam in a sech GRIN medium by numerical simulation. There are three situations for the variation of the half-width of the Gaussian beam waist, including periodic convergence, collimation transmission with a constant incident waist half-width and periodic divergence. SOI waveguide is widely used in the photonic integrated circuit, but coupling problem between an optical fiber and the sub-micrometer waveguide is still a challenge to be solved in a practical optical communication system. To achieve a high coupling efficiency between single mode optical fiber and single mode SOI slab waveguide, which suffer a great light beam coupling loss for the mismatch of the spot size. The GRIN medium coupling structures are designed as a coupler, with symmetric refractive index distribution and asymmetric refractive index distribution. The single mode optical fiber has a mode-field diameter of 10 μm , and the symmetric slab SOI waveguide has a core thickness of 0.25 μm . The insertion loss calculated in theory are 1.35dB and 1.56dB respectively, which has a significant improvement in coupling loss, compared with the 30dB coupling loss caused by direct butt-joint transmission.

8559-28, Poster Session

Optical correlation tracking of low contrast target based on wavelet threshold segmentation

Su Zhang, Youjian Wang, Qibo Zhang, Wensheng Wang, Changchun Univ. of Science and Technology (China)

Target tracking has a wide application in varieties of domains and has a rapid development at home and abroad, so the research on target tracking is more valuable in recent years. In this paper hybrid optoelectronic joint transform correlator (HOJTC) is implemented for tracking the target, which is considered as one of the most effective methods.

But in practical application, the low contrast character of the target and the moving distortion problems between the target and the template may cause the phenomenon of low recognition ratio of HOJTC. In order to solve this problem, a kind of wavelet-based threshold segmentation method is applied to increase the contrast. Through this algorithm the histogram of the image is firstly decomposed into wavelet coefficients at every scale with wavelet basis function Sym4. And then according to segmentation norm and wavelet coefficients, the thresholds can be chosen from the approximate histogram. Finally use these thresholds to segment the image into ideal areas. In addition, for the moving distortion problem, taking temporal state of the target as the template can realize the template update.

To prove this method, many tracking experiments of low contrast targets have been performed with optical correlation method. As an example a low contrast target "tank" (the gray contrast is less than 2%) is presented. The tracking result shows that the brightness of the correlation peaks is enhanced and the target recognition ratio is increased. The conclusion can be drawn that applying this algorithm in optical correlation method can implement the low contrast target tracking successfully and this algorithm provides an available solution to low contrast target tracking.

8559-29, Poster Session

Optical isolator based on surface plasmon polaritons

Wanyuan Liu, Fangkui Sun, Lixue Chen, Bowen Li, Harbin Institute of Technology (China)

Optical isolator is a necessary passive optical element in modern optical communication system. The common optical isolator is based on Faraday rotation and it has been become a mature technology. The size of the common optical isolator is about several centimeters, which is not suitable for the optical integrated circuit. The Surface Plasmon Polaritons(SPP) is caused by the oscillation of electrons and its wave propagates at the interface of a metal and a dielectric. SPP is a slow wave and its wavelength is about one tenth of the excitation light. For this reason, it can be used in optical elements to solve the problem of optical integrated circuit.

A new optical isolator mode which is based on the theory of SPP has been designed. A dielectric waveguide and a SPP waveguide are formulated. And there is a gap in the middle of the core in the dielectric waveguide. Low refractive index material is filled into the gap and the total reflection is satisfied at the interface of the two materials. Magneto-optic material is contained in the two waveguides and the two waveguides are stacked together. For the phase matching of the two waveguides and the total reflection at the gap, the light couples from the dielectric waveguides into the SPP waveguides. With the help of the SPP, the light passes the gap successfully and couples into the dielectric waveguide again. However, there is a different situation at the reverse direction. For the effect of the magnetic field, the permittivity of magneto-optic material has been changed and this caused the phase mismatching of the two waveguides. So effective coupling is not able to finish between the two waveguides. With the total reflection at the

gap of the core, the light cannot traverse the mode, and the aim that reflected light should be isolated is achieved. The insertion loss value is 1.72dB when the light traverses through the optical isolator in forward direction. In the reverse direction, the isolation value is 34.14dB. And this result is better than the common magneto-optical isolator.

8559-30, Poster Session

All-optical programmable logic arrays using SOA-based canonical logic units

Lei Lei, Jianji Dong, Yu Yu, Xinliang Zhang, Wuhan National Lab. for Optoelectronics (China)

All-optical programmable logic arrays (PLAs) based on canonical logic units (CLUs), i.e., minterms and maxterms, are presented. We experimentally demonstrated the full set of two-input and three-input minterms as well as maxterms using the cross-gain modulation in semiconductor optical amplifiers (SOAs). Maxterms can be easily obtained based on minterms. Correct and clear temporal waveforms are achieved for all the canonical logic units. The measured extinction ratios of two-input and three-input CLUs reach to ~ 15 dB and ~ 11 dB, respectively. Based on the CLUs, both sum-of-products (SOP) and product-of-sums (POS) formed PLAs are exhibited. Four important logic functions, including multiplier, multiplexer, demultiplexer and decoder, are presented as examples to show that the canonical logic units-based programmable logic array (CLUs-PLA) can be reconfigured to perform different logic functions. Compared with the reported schemes, our proposal features several improvements and advantages. (1) A programmable OR array is not required for SOP-formed PLA since the products are canonical minterms, and arbitrary combinational logic function can be demonstrated by adding the canonical minterms directly. (2) The absolute and complementary data patterns which are necessary for the PLA can be easily obtained through the preprocessing. (3) The CLUs with different number of inputs are achieved using the most efficient and simple nonlinear effect XGM in SOA. (4) Maxterms can be easily obtained based on minterms, and the reconfigurability and scalability of the system are largely enhanced compared to our previous work. (5) Both SOP and POS formed CLUs-PLA are proposed, and the simple structures composed of SOAs and passive filters make them have a great potentiality to be largely integrated.

8559-1, Session 1

Photonic crystal fiber Raman sensors (Invited Paper)

Claire Gu, Univ. of California, Santa Cruz (United States)

Hollow core photonic crystal fibers (HCPCF) employ a guiding mechanism fundamentally different from that in conventional index guiding fibers. In an HCPCF, periodic air channels in a glass matrix acts as reflectors to confine light in an empty core. As a result, the interaction between light and glass can be very small. Therefore, HCPCFs have been used in applications that require extremely low non-linearity, high breakdown threshold, and zero dispersion. However, their applications in optical sensing, especially in chemical and biological sensing, have only been extensively explored recently.

Besides their well-recognized optical properties the hollow cores of the fibers can be easily filled with liquid or gas, providing an ideal sampling mechanism in sensors. Recently, we have demonstrated that by filling up a HCPCF with gas or liquid samples, it is possible to significantly increase the sensitivity of the sensors in either regular Raman or surface enhanced Raman scattering (SERS) applications. This is because the confinement of both light and sample inside the hollow core enables direct interaction between the propagating wave and the analyte, as opposed to other types of fiber Raman/SERS probes that rely on the evanescent wave interaction with the analyte.

In this talk, we report our recent works on using HCPCFs as a platform

for Raman or SERS in the detection of low concentration greenhouse gas (ambient CO₂), biomedically significant molecules (e.g., glucose), and bacteria.

8559-3, Session 1

Method for measuring retardation of infrared wave-plate by modulated-polarized visible light

Ying Zhang, Beijing Univ. of Posts and Telecommunications (China) and Minzu Univ. of China (China); Feijun Song, China Daheng Group, Inc. (China)

The wave-plates in the infrared spectral region are important polarized elements for modern optical communication technology, astronomical observation field, etc. We propose a new method for precisely measuring the optical phase retardation of infrared wave-plates using modulated-polarized visible light. An instrument is set up for measurement: collimated laser beam goes through a polarizer, an electro-optic modulator, the wave-plate to be measured, a Babinet-Soleil compensator, an analyzer, and finally incident upon the detector. A sinusoid voltage with frequency f_0 is applied to an electro-optic modulator to produce a modulated-polarized light. A Babinet-Soleil compensator is employed to make the phase delay compensation. A photo-detector detects light passing an analyzer. A signal processor selects only the fundamental frequency and the double frequency and shows the output signal on an oscilloscope. The zero and 2π positions are identified when the oscilloscope shows a sinusoidal function with frequency $2f_0$. The compensation from zero to 2π without wave-plate is called instrumental constant $C(\lambda)$. We measured several $C(\lambda)$ for different λ lasers and then produce a relation line. When the wave-plate which need to be measured is put in the instruction, the zero occurs when the compensator completely compensates for the wave-plate. By simple calculating, we get the results of measuring the phase retardation at 1064nm of a half wave-plate using 632.8nm and 532nm laser. It is apparent that the measurement precision is less than and repetitive precision is within 0.3%. The measurement precision of the instruction is almost constant in the visible range.

8559-5, Session 2

Power flow study in subwavelength plasmonic apertures and antennas (Invited Paper)

Byoung-ho Lee, Il-Min Lee, Seung Yeol Lee, Seoul National Univ. (Korea, Republic of)

Plasmonic subwavelength hot spot generation is an important issue for data storage and sensing. The singular points of time-average power flow in electromagnetic fields, which correspond to the saddle or vortex of time-averaged Poynting vector fields, can be used as qualitative parameters to understand the behavior of energy flow of electromagnetic systems. Near the presence of such singular point, the power flow lines show drastic change in their directions and magnitudes, of which effect determines the characteristic of the energy flow through the system. In general, such singular points compose very complicated patterns near the edges of the metallic structures but tend to converge to regular patterns when observed far from the structural abruptions. As a result, in many subwavelength plasmonic systems such as plasmonic antennas or metallic slits, we can find a rough relation between the power transmission efficiency or field enhancement nature and the behavior of the singular points by observing near the structural abruptions such as the slit or aperture openings or the rod ends.

In this study, we investigate the relation between the singular points in power flow in subwavelength plasmonic slit and antennas and other physical characteristics such as the field enhancement or power

transmission efficiencies. The parameters we are interested in are the relative locations of and the strength of the Poynting vector fields near the singular points, especially around the geometric edges of the metallic structures. By investigating the power flows near isolated or periodic slits and antennas, we hope to provide another view of understanding the physics in those structures.

8559-6, Session 2

The workpiece surface intelligent tracing based on support vector machine in laser remanufacturing

Nan Yang, Tianjin Univ. of Technology (China)

In laser remanufacturing, the laser beam need to point the normal direction of the workpiece surface in order to keep constant radiation area and constant energy density. This is a key point for forming accuracy. However, the shapes of the workpieces are arbitrary, and it's difficulty to obtain the normal vector directly according to the 3D surface data of the workpiece which could be obtained by 3D laser scanning system. So, the 3D data of the workpiece surface should be processed based on the nonlinear regression analysis firstly. Support vector machine (SVM) is chosen for the nonlinear regression analysis, because it has good capability and it could overcome "over-fitting". The normal vector could be caculated based on the kernel function used in SVM. It's rare to find the report that choosing SVM as a machine learning method in laser remanufacturing process.

8559-7, Session 2

Light multinary computing: the evolution from electronic binary computing

Jaime Arago, Freelance (Spain)

Next-generation optical communication and optical computing imply an evolution from binary to multinary computing. Light multinary computing encodes data using light components in higher orders than binary and processes it using truth tables larger than Boolean ones. This results in lesser encoded data that can be processed at faster speeds. We use a general-purpose optical transistor as the building block to develop the main computing units for counting, distributing, storing, and logically operating the arithmetic addition of two bytes of base-10 data. Currently available optical switching technologies can be used to physically implement light multinary computing to achieve ultra-high speed communication and computing.

8559-8, Session 3

Compact digital holoscope with dual wavelength (Invited Paper)

Jianglei Di, Jianlin Zhao, Anand Krishna Asundi, Nanyang Technological Univ. (Singapore)

Digital holography allows fast, nondestructive, full-field 3D measurement of reflecting as well as transmitting objects. It is a well-established two-step method of digital recording and numerical reconstruction of the full complex field of wavefront. It has found applications in diverse fields, such as micro-optics and MEMS metrology, cell imaging and particle characterization. However, for quantitative phase measurement there is 2? by phase ambiguities that limit measurements of optical path lengths to the wavelength of the illumination light. For continuous profiles, phase unwrapping is used to overcome the phase jumps. One approach is to use a synthetic wavelength using two lasers with different wavelengths. This synthetic wavelength would depend on the wavelengths of the two sources and thus can be tuned by selecting appropriate sources. In this paper, this

concept is integrated into the compact digital holoscope which provides the system with the capability of measuring over a range of step heights from the nanometer to the micrometer realm. Applications of the system for both transmission and reflecting geometries are discussed.

8559-9, Session 3

Dynamic resource-aware routing and frequency slots allocation in SLICE using adaptive modulation with consideration of both BER requirement and distance

Lei Wang, Min Zhang, Beijing Univ. of Posts and Telecommunications (China)

Proposed in this paper is a dynamic resource-aware routing and frequency slots allocation scheme with consideration of both BER requirement and distance adaptive modulation (RA-BERR-DA) for spectrum-sliced elastic optical path networks (SLICE).By dynamically considering the available frequency slots, the modulation complexity of a computed least crowded route can be adjusted.Physical topology used in the experiment is a 7?7 mesh network with one server, 49 nodes and 84 dual links between nodes. We performed numerical simulations using OMNET++ to compare the blocking rate and the frequency slots occupation of RA-BERR-DA with those of DA. O-OFDM adopted in this paper generates 8 subcarriers and the frequency slot width is set as 12.5GHz. There are two basic modules in the simulation: SERVER, which is in charge of computing route and deciding modulation format; NODE, which is in charge of assigning resources. Backward Reservation Protocol (BRP) in wavelength routed WDM networks is used and the difference is that the reserved resources are not wavelengths but slots. Four slots will be assigned if the modulation format is QPSK and two slots for 16QAM. We apply first fit (FF) algorithm to choose slots. The dynamic connection requests follow as the Poisson process and the source-destination node pair is generated randomly from all the nodes. The holding time of each connection follows a negative exponential distribution.

8559-10, Session 3

Dynamic wavelength, priority, and bandwidth assignment (DWPBA) for long-reach hybrid WDM/TDM-PON based on multi-thread scheduling

Yuqin Xie, Min Zhang, Beijing Univ. of Posts and Telecommunications (China)

Hybrid WDM/TDM-PON as a key solution is a smooth evolution of the passive optical network to Next-Generation Passive Optical Networks (NG-PON). In order to combine the capacity of metro and access networks, it is desirable to propose the Long-Reach (LR) PON, and the propagation delay is proved to be the obstacle during the upstream resource allocation.

In this paper, an enhanced multithread based on Multi-Point Control Protocol (MPCP) was presented for the hybrid LR WDM/TDM-PON by transmitting separate data messages and REPORT messages on the different channels for upstream transmission along with broadcasting the GATE messages on the single channel to the ONUs. This algorithm exploits the benefits of having multiple processed running simultaneously as well as the joint scheduling and grant sizing methods to improve the channel utilization, and reduce the packet delay. This scheme is also to support the Quality of Service (QoS) requirements of different applications in typical access networks.

In the discription part of the algorithm,wo will give illustrative example for scheduling method under joint scheduling and grant sizing,and detailed algorithm process.This model is simulated under OMNeT++. Then,the result analysis will be given.

Simulated results is used to prove that the DWPBA outperforms the traditional DBA in channel utilization and packet delay.

8559-11, Session 3

Holography display with LED illumination based on phase-only spatial light modulator

Yan Zhao, Liangcai Cao, Qingsheng He, Guofan Jin, Tsinghua Univ. (China)

A new holography display technology based on a phase-only spatial light modulator (SLM) is proposed. The normal use of LD light source led to the inevitable speckle noise introduced by the coherence of the laser beam. Some algorithms and special diffractive optical elements have been proposed to reduce the speckle noise. In this paper, a selected LED light source was used in the holography display system to replace the LD light source. The temporal coherence and spatial coherence of the LED were studied. Though the temporal coherence of LED is short, the spatial coherence of the light field can be improved by optimizing the optical paths such as decreasing the emitting area of the light source and so on. A high-power LED with a narrow band-width was selected. An algorithm to generate computer-generated hologram for the SLM based on partially coherent light was proposed. The phase-only holograms for the display were computed using the partially coherent light algorithm. Then the phase holograms were uploaded to the SLM. LED was used as the light source to illuminate the SLM uniformly, and the reconstructions can be observed by naked eye. It is demonstrated that LED is an accepted light source for holographic display. The reconstruction results showed that the speckle noise and multiple reflections were eliminated when LED was used as the light source.

8559-12, Session 4

Vector wave recording techniques for optical data storage (*Invited Paper*)

Toyohiko Yatagai, Daisuke Barada, Utsunomiya Univ. (Japan); Suganda Jutamulia, Univ. of Northern California (United States)

Optical recording techniques utilizing vector wave characteristics potentially have high data transfer rate characteristics because a vector wave has two complex amplitude components and they can be temporarily and spatially modulated. In this paper, two types of vector wave recording techniques are introduced. In these techniques, polarization-sensitive media are required. The one is dual-channel polarization holography. In dual-channel polarization holography, two superposed images can be simultaneously recorded. The two images are transferred by two orthogonal polarization components of a signal beam. The signal beam is superposed by a reference beam and illuminated on a polarization-sensitive medium. Furthermore, holographic multiplexing techniques can be applied. For optical data storage, coded images are used. Two coded images are displayed on two spatial light modulators (SLMs). The other is retardography that is a recording technique of retardation between orthogonal polarization components. The retardation can be generated by using objects with retardance. In order to record a coded image, parallel-aligned liquid-crystal SLM (PAL-SLM) can be used. The PAL-SLM can modulate the phase of a linear polarization component with the azimuth parallel to the liquid crystal orientation axis. Retardography can be regarded as a kind of inline polarization holography without beam splitting. The modulated polarization component and another component are regarded as a signal beam and a reference beam, respectively. Therefore, holographic multiplexing can be applied. In this study, it is confirmed that coded images are recorded in multiple using these vector wave recording techniques. From the results, these techniques can be expected for optical data storage.

8559-13, Session 4

Novel holographic recording in phenanthrenequinone-doped poly(methyl methacrylate) photopolymer and its applications (*Invited Paper*)

Shiuan Huei Lin, June Hua Lin, Ken Y. Hsu, National Chiao Tung Univ. (Taiwan)

In this paper, we report our investigations on two novel holographic recordings in phenanthrenequinone-doped poly(methyl methacrylate) photopolymer, including polarization holographic recording and two-wavelength holographic recording. For polarization holographic recording, we demonstrate that a polarization grating can be recorded in such material using two orthogonal polarization beams. The best experimental results show that the diffraction efficiency of the hologram reaches to ~40 %, and the dynamic range of material (M#) is 1.82 by using two orthogonal circularly polarized recording beams. For two-wavelength holographic recording, we demonstrate that a volume hologram can be recorded at 647-nm in a 2-mm thick sample by use of a gating illumination at 325-nm. The experimental results show that the diffraction efficiency of hologram reaches to ~30%, suggesting as holographic medium with selective recording property. Some applications on optical information storage using two recording mechanisms will also be demonstrated.

8559-14, Session 4

Fundamental study on hybrid phase-coding and spatial multiplexing for holographic data storage

Wei Song, Shiquan Tao, Dayong Wang, Beijing Univ. of Technology (China)

In terms of noise suppression, orthogonal phase-coding multiplexing has particular advantage. So the hybrid phase-coding and spatial multiplexing (PCSM), which incorporates orthogonal phase-coding multiplexing into spatial-multiplexing, has been considered recently.

In the preliminary research on PCSM, the position selectivity of phase-coded reference beam has been proved, but high quality storage of high-resolution data pages has not yet demonstrated. The encoded reference beam contained many plane sub-beams, and the interference between the phase-coded sub-beams was ignored in the analysis of the early work. For implementation of high density and high quality data storage with PCSM, a thorough study on the fundamentals of PCSM, including the general principle and the optimized configuration, is necessary.

In this paper, we investigate some fundamental aspects starting with numerical calculation of the complex Fourier spectrum of an orthogonal phase coded reference beam. The results showed that there is a complex and serious fluctuation in both intensity and phase distribution if a Fourier transform configuration is used for reference beam.

Moreover, the phase is no longer binary (0 or π), but varying continuously between $-\pi$ and π ; this may reduce the phase orthogonally and is not desired for PCSM. Also the additional intensity distribution will influence the quality of the beam.

In order to maintain phase-only modulation and orthogonally in the reference beam pattern, we suggest that the phase modulator should be imaged to the recording plane. Deeper researches on the principle and configuration are still in progress.

8559-15, Session 4

Experimental verification of hologram generation using intensity images

Ni Chen, Jiwoon Yeom, Keehoon Hong, Jae-Hyun Jung, Byoungcho Lee, Seoul National Univ. (Korea, Republic of)

Digital holography is one of powerful methods for three-dimensional displays. However, it generally needs a complicated interference experimental setup which also induces some problems in the hologram reconstruction, such as the DC term problem and the twin image problem. We proposed a method for generating digital hologram from three diffracted intensity images. An object is illuminated by a plane wave and three diffracted intensity images are captured by a charged coupled device (CCD) along the wave propagation axis. By calculating the amplitude and phase distribution from the intensity images using the transport of intensity equation (TIE), we can obtain the wave front of the object at the center intensity image plane, i.e., the Fresnel hologram of the object.

We already verified this method by numerical simulation. In this paper, we do experiments to verify the proposed hologram generation method. In the experiment we use simple setup with a laser and a CCD. The captured images are used to calculate the hologram after some preprocessing. The reconstruction verifies that the proposed method works. We also compare the proposed method with conventional digital holography that records the hologram by interferometry. Both simulation and experiments verify that the proposed method has no twin image problem. Additionally, because the TIE works well under partially coherent illumination, we also do an experiment that uses partially coherent light source instead of laser to verify the partially coherent illumination requirement of the method. The partially coherent light source enables the reduction in the hologram recording cost. In summary, our proposed method is advanced in the recording and reconstruction compared to the conventional method of digital holography.

8559-16, Session 4

Multiplexed holographic gratings recorded by 405nm laser in polymer film containing spirooxazines

Shencheng Fu, Changchun Univ. of Science and Technology (China); Shiyu Sun, Northeast Normal Univ. (China); Wenling Sang, Bo Sun, Changchun Univ. of Science and Technology (China); Xintong Zhang, Yichun Liu, Northeast Normal Univ. (China)

In this rapidly evolving age of information, there has arisen the need for high-density and rapid access memory system. To date, some investigations on photochromic spirooxazines have been carried out in synthesis, reaction mechanism, optical switch and memory etc. However, little attention has been the multiple holographic recording by blue violet laser in spirooxazine doped polymer films, which will be practically used for recording high-density hologram on the media in the future. In this paper, the multiplexed holographic gratings were recorded and probed in spirooxazine doped PMMA films by the blue-violet laser (405nm) and the He-Ne laser (632.8nm), respectively. Accompanied by rotating the storage media, two sets of holographic gratings were recorded at the same point in the sample. It was found that the growth rate of the holographic grating recorded later was lower than that of the earlier one. To better understand the multiple holographic grating formation mechanisms, the single holographic grating dynamics was also recorded. The diffractive signal intensity increased sharply and then decreased to a constant value. A theoretical description of overlapped isomerization gratings agrees well with experimental results. The obtained fitting parameters indicated that the decreased population of spirooxazine molecules results in the longer response time and the lower contrast of the later recorded grating. Due to the long life of the isomerization gratings, the holographic interference fringes with the period of ~500nm were clearly observed by Confocal Laser Scanning Microscope. By optimizing experimental condition, holographic gratings with full angle multiplexing are supposed to be formed.

Conference 8560: LED and Display Technologies II

Tuesday 6 –6 November 2012

Part of Proceedings of SPIE Vol. 8560 LED and Display Technologies II

8560-1, Session 1

Organic spintronics developed from organic light-emitting diodes

Bin Hu, The Univ. of Tennessee (United States)

Inter-molecular excited states are essentially inter-molecular electron-hole pairs with tunable electric and magnetic dipoles in organic semiconducting materials. It has been experimentally observed that inter-molecular excited states are sensitive to a low magnetic field (< 100 mT). We have found from magneto-capacitance studies that inter-molecular excited states can exhibit an intrinsic coupling between electric permittivity and magnetic permeability. The intrinsic coupling between permittivity and permeability provides a promising mechanism to realize excited states-based organic spintronics with magnetic field-dependent optic, electronic, and optoelectronic functions by using inter-molecular excited states. The magneto-electric studies have indicated that inter-molecular excited states have mutually controllable electric and magnetic dipoles. Therefore, electric and magnetic polarizations can resonantly respond to an incident electromagnetic field in a coherent manner. The photoinduced EPR measurements have shown that inter-molecular excited states can magnetically change electric polarization. The photoinduced permeability measurements have indicated that inter-molecular excited states can electrically change magnetic polarization. Furthermore, we have experimentally demonstrated that using inter-molecular excited states forms a new mechanism to de-couple electrical and thermal conductivities, normally un-available in natural materials, for the development of thermoelectric devices. This presentation will present recent progress on inter-molecular excited states-based organic spintronics.

8560-2, Session 1

Investigation of color-stable deep red-emitting OLEDs and transparent LiF:Al composite cathodes (*Invited Paper*)

Qu Bo, Peking Univ. (China); Chao Gao, Xi'an Modern Chemistry Research Institute (China); Zhijian Chen, Lixin Xiao, Qihuang Gong, Peking Univ. (China)

A novel soluble terpolymer (P8FO-Th-BT) containing 9,9-dioctylfluorene, thiophene, and 2,1,3-benzothiadiazole units were synthesized by Still coupling reaction. The single layer and multi-layer organic light emitting diodes (OLEDs) based on P8FO-Th-BT was fabricated. A deep red-emission device with the configuration of ITO/ poly(3,4-ethylenedioxythiophene)-polystyrene sulfonate (PEDOT:PSS)/P8FO-Th-BT:N,N'-Di(3-methylphenyl)-N,N'-diphenyl-(1,1'-biphenyl)-4,4-diamine (TPD) (weight ratio being 1:1)/2,9-dimethyl-4,7-diphenyl-1,10-phenanthroline (BCP, 15nm)/ tris(8-hydroxyquinoline) aluminum (Alq3, 15nm)/ LiF(5Å)/Al(150nm) was obtained, and the maximum luminance was measured to be 226 cd/m² at the bias voltage of 10V. The electroluminescent peak located at 708nm, and the spectrum covered both the red and infrared regions. Moreover, the CIE chromaticity coordinates of the device were inalterable when the bias voltage varied, which was beneficial to the application on display.

The performance of OLEDs also depended on the electrical and optical properties of the electrodes. Therefore, a transparent and electrical conductive layer comprising LiF and Al was designed and obtained. The composite layer was characterized using transparency spectroscopy and sheet resistance measurement. When the ratio of LiF:Al reached 4:4, the sheet resistance and transmittance of the composite layer were 573 Ω/\square ; and 55.5% (at 532nm), respectively. Transparent organic light-emitting diodes (TOLEDs) employing LiF:Al composite layer as cathodes were fabricated and the electroluminescent properties of the TOLEDs were investigated. When the composite cathode had the equal contents

of LiF and Al, the TOLED showed acceptable electroluminescent behavior of both top and bottom emission and the total maximum current efficiency (summed from both top and bottom emission) of the TOLED was calculated to be 2.34 cd/A.

8560-3, Session 1

Optimal spectrum design of OLED indoor lighting

Shih-Jie Dai, National Chung Cheng Univ. (Taiwan); Hsiang-Chen Wang, National Chung Cheng Univ. (Taiwan) and National Chung Cheng Univ. (Taiwan)

When the efficiency of OLEDs reached Fluorescent's brightness level, the OLED is becoming mature. With good surface characteristic of light-emitting, low power and diversity of color distribution, OLEDs has used on the panel backlight or special lighting. The study of white OLED's spectra for indoor lighting are rarely discussed. In this study, we collected dozens of OLED's spectra and recombined new spectrum for indoor lighting. The images after new illuminant design can be display by multi-spectral imaging technology. Finally, we discuss some methods for specifying color-rendering properties of OLEDs such as CRI, CQS, and FCI to prove the optimal spectrum of indoor lighting.

8560-4, Session 2

A simple, low-cost and portable LED-based multi-wavelength light source for forensic application

Wee Chuen Lee, Univ. Sains Malaysia (Malaysia); Bee Ee Khoo, Universiti Sains Malaysia (Malaysia); Ahmad Famhi Lim bin Abdullah, Univ. Sains Malaysia (Malaysia)

Forensic light sources (FLS) have been used frequently in crime scene investigation as a scanning tool for crime scene evidence, such as gunpowder residue, semen, bloodstain, saliva and urine. There were several FLS reported in literature, such as Polilight®, Lumatec Superlite 400, PolirayTM, Bluemaxx BM500 and high intensity LED. LED-based light sources are low in cost and flexible in design. Moreover, LED technologies have been well developed recently, where several types of wavelength LED can be used for light source design. From literature, near UV light (300-400nm) and blue (450nm) light are useful for detecting semen, urine and saliva stains, while 415nm light is useful for bloodstains detection. In this paper, a simple, low cost and portable LED-based multi-wavelength light source for forensic application is proposed. The proposed multi-wavelength light source is able to supply near-UV, blue and 415nm lights from the same point of source and direction, without utilizing any light guide, such as optical fiber. Each type of LED array was mounted separately on the different surfaces of a holder. DC motor was used to rotate the holder for directing the selected LED array to face the object. The proposed design is low in cost, easy to be manufactured, user-friendly and comparable to the other expensive FLS, such as Polilight® PL500 and Crime-lite®2, in terms of detectable dilution of bloodstains.

8560-5, Session 2

Optimized LED spatial apodization and locations for spatial uniformity in enclosed space

Chung-Jen Ou, Chong -Jei Huang, Yu-Yuan Liu, Hsiuping

Institute of Technology (Taiwan)

Spatial uniformity and related photometric/radiometric quantities are very important for optical engineering. Various optical programs had been developed to deal with the calculation and analysis procedure. Optimization and the cost effectiveness are the major difficulties to solve complicated problems. In this paper, we demonstrate the level 1 approach to solve the specific spatial photometric distribution problems by using the spreadsheet program. Base on the transient between the near field area source and the far field point source approach, a reliable illuminating spreadsheet is developed for LED and various kinds of lamp device. Since there is no ray tracing required, the algorithm is fast and simple.

The angular apodization of the LED or lamp can be determined and optimized by simply using the spreadsheet program. Unpredicted solutions are found in several arrangements, demonstrate the possibilities and the effectiveness of the present method. Discussion on the colour mixing and the scattering model of the LED/lamp device is also provided.

8560-6, Session 2

High efficient tandem blue fluorescent organic light-emitting diodes based on C60/NPB:MoO₃ interconnecting layer

W T Bi, M X Wu, Y L Hua, Tianjin University of Technology (China)

Tandem OLEDs(device A) is the same as single-unit device(device B), in which p-bis(p-N, N-diphenyl-amino-styryl) benzene(DSA-ph) was used as blue emitting layer and 1,3,5-tri(phenyl-2-benzimidazole) benzene(Bphen) was used as ETL. Our experiment results indicate that the luminance of the tandem device is basically equal to that of the single-unit device, but the current density of the tandem device is much less than that of the single-unit device under a same luminance. A excellent interconnection layer to effectively charge transport of tandem OLEDs is generally very important. If C60 and NPB:MoO₃ contacted each other, a common Fermi level throughout both layers is required by equilibrium. Therefore, under the external electric field, the electrons may tunnel through from occupied HOMO level of NPB:MoO₃ to unoccupied LUMO level of C60. Then these electrons will immediately be driven away from the interface by the external electric field and injected into EML. In summary, the current efficiency of device B attains 33.8 cd/A at current density of 72.9 mA/cm², which is almost 2.5 times higher than that of the single-unit device A (13.5 cd/A) measured at current density of 68.9 mA/cm². This result indicates that LiF/Ca/C60/NPB:MoO₃/MoO₃ functioned as an effective TL.

8560-7, Session 3

Embed an irregular linear Fresnel lens into a simple empty chamber to let a medium or large edge lighting LED backlight module be thin, lightweight, low-cost, and possess high effect of light rays guiding

Wen-Gong Chen, Yung Ta Institute of Technology & Commerce (Taiwan)

We propose a new and effective Light Guide Plate, called Empty Chamber Fresnel Lens Light Guide Plate (ECFL-LGP), for a medium or large scale Backlight Module. It consists of a simple Empty Chamber and several sets of irregular linear Fresnel lenses. Due to the reasons that the structure of the Empty Chamber is simple and a Fresnel lens is thin and cheap, our ECFL-LGP will own lower cost than the traditional LGP. On the other side, the irregular Fresnel lens in our ECFL-LGP will work better than the traditional LGP about the effect of light rays guiding because its irregular linear groove angles can be evolved in

terms of the optimization requirement on illumination and uniformity. To insure the reliability of the simulated system, we will apply TracePro optical package and its macros into our Genetic Algorithms to let all optical elements become the real entities of evolution programs. Furthermore, to consider the feasibility of evolution programs, it is necessary to divide a medium or large scale of Backlight Module into several small divisions to reduce the number of evolved groove angles. However, how many sets of irregular linear Fresnel lenses are necessary and how to design them will be complicated and technical.

8560-8, Session 3

First principles calculations of electronic and optical properties of Zn_{1-x}(TM)_xO (TM=Mg,Cd)

Peng Chen, South China Normal Univ. (China)

The paper present study of the electronic and optical properties of Zn_{1-x}(TM)_x (TM=Mg,Cd), through density function theory (DFT) based on first-principles method. The calculation indicate that the band gap of Zn_{1-x}Cd_xO narrows as result of the increasing concentrations of Cd. The paper shows that the Zn 4s and Cd 5s electron states broadens to low energy states and that the O2p electron states broadens to high energy states with increasing Cd-doping concentrations. The paper advances a possible theoretical mechanism of Cd-doped regulating Bands gap. Optical property of Zn_{1-x}(TM)_x (TM=Mg,Cd) is presented in the paper.

8560-9, Session 3

Improvement of light extraction efficiency of GaN-based flip-chip light-emitting diodes by double-side patterned sapphire

Xiaoqing Du, Guangming Zhong, Weimin Chen, Xiaohua Lei, Xianming Liu, Chongqing Univ. (China)

The flip-chip light-emitting diodes (LEDs) are very suitable for high power and high brightness applications due to the effective heat dissipation. In flip-chip LED sapphire not only acts as substrate for GaN layer growing, but also as light exit surface. Since the refractive of sapphire (n=1.67) is obviously more than air, the total reflection at the light exit interface would happen, which seriously reduces the light output and light extraction efficiency (LEE) of LEDs. Light-exit surface texturing has been the most effective and simplest one to improve LEE. To make the surface structure controllable, a regular pattern should be preferred. Furthermore, double-side pattern should be more effective than single-side pattern in improvement of LEE.

In this work, we propose a double-side patterned sapphire structure to enhance LEE of flip-chip LEDs. Using Monte Carlo simulation method, the impacts of sapphire substrate thickness, single-side pattern, double-side pattern, pattern shapes and sizes on LEE were analyzed. The simulated results show that compared to no-patterned and single-side patterned LEDs, double-side patterned LEDs have highest output at the same chip size and sapphire thickness. By optimizing the size and shape of pattern pixel the LEE for double-side pattern could reach at more than 50%.

Using silicon oxide as mask membrane, double-side patterned sapphire were processed by the standard lithography and reaction-ion-etching (RIE) technology. The LEDs with patterned sapphire were packaged. The optical and electrical characteristics of the fabricated LEDs will also be discussed. The measured light outputs of LEDs verified our predicted effects.

8560-11, Session 3

Design and fabrication of a controllable haze diffuser film

Zongbao Fang, Heng Zhang, Xiaohong Zhou, Linsen Chen, Soochow Univ. (China)

Plastic diffuser films have been widely used in various applications with LCD devices such as notebooks, TVs, monitors, and lighting systems, etc., for beam shaping, brightness homogenizing, and light scattering. For different applications, the properties of the diffuser films will be chosen according to the realized functions, such as the transmittance, the haze, and the divergent angle etc. In general, the diffusers can be classified into two types: the particle-diffusing type diffuser and the surface-relief type. As the mainstream product, the first relies on the transparent beads inside the plastic films or plates to scatter light, which has not realized the special function such as customized transmittance and haze etc. The second relies on the microstructures on the surface of the plastic films or plates to scatter light, which can be designed according to the customized requirements by optical simulation software. However, the present fabrication process is difficult to realize it under low cost condition. In this paper, we will show a complete process including design and fabrication for a customized diffuser film with different haze and transmittance. The micro-sphere structure will be utilized in the design process, and the relationship between the optical properties and the structure parameter and its distribution will be investigated. The roll to roll UV curing process will be used for fabrication the diffuser film based on PET material. The molding for UV curing is the nickel sheet with thousands of microstructures fabricated by laser etching process. Finally, the uniformity and optical properties of diffuser films will be tested by surface profiler, and haze meter.

8560-12, Poster Session

TDDFT investigation and design for fluorescent molecules with push-pull structures

Lin Tao, Beijing Jiaotong Univ. (China)

The electronic and geometrical structures of the ground and excited states of six fluorescent emitters, namely 3-(dicyanomethylene)-5,5-dimethyl-1-(3-[9-(2-ethyl-hexyl)-carbazol]-vinyl) cyclohexene (DCDHCC), DCDHCC2, 3-(dicyanomethylene)-5,5-dimethyl-1(4-diphenylamino-styryl) cyclohexene (DCDPC), DCDPC2, 3-(dicyanomethylene)-5,5-dimethyl-1-(4-[9-carbazol]-styryl)cyclohexene (DCDCC), and 3-(dicyanomethylene)-5,5-dimethyl-1-(4-dimethylamino-styryl) cyclohexene (DCDDC) which were specifically designed for organic light-emitting diodes (OLEDs), were studied using density functional theory (DFT) and time-dependent DFT (TDDFT) in conjunction with polarizable continuum models (PCMs). Five hybrid functionals, PBE0, M06, BMK, M062X, and CAM-B3LYP, were used and compared. The experimental spectra of the molecules in acetone solvent were precisely reproduced with the BMK functional. The ionization potential and the electron affinity were calculated to access the properties of the molecules in charge injection. It was found that, when double π -bridges and acceptors were used, the emission of emitters red-shifted to the optimal emitting region. Two brand new molecules, DCDDC2 and DCDDC2, which are the double-branched counterparts of DCDCC and DCDDC, respectively, have been designed. The calculated properties of DCDCC2 and DCDDC2 in spectra and charge injection suggested that they would be as effective in their capacities as fluorescent emitters as the above six emitters.

8560-13, Poster Session

BaAl₂S₄:Eu thin films sputtered by complex target with spark plasma sintering BaS:Eu pellets

Dongpu Zhang, Beijing Institute of Technology (China) and Beijing Space Technology Development and Testing Ctr. (China); Wei Xue, Zhinong Yu, Beijing Institute of Technology (China)

Europium doping barium thioaluminates thin films are sputtered by Al complex target embedded with BaS:Eu pellets sintered by spark plasma sintering (SPS). Thin films are deposited by RF-sputtering with complex target. BaAl₂S₄ is found in each thin film sample while BaAl₄S₇ appears in the samples only if the amount of BaS:Eu pellets is more than 3. Oxidizing products are BaAl₂O₄, BaSO₄ and Al₂O₃. The amounts of barium thioaluminates including BaAl₂S₄ and BaAl₄S₇ will increase while the one of Al₂O₃ and BaS decrease if more BaS:Eu pellets are embedded in the target during sputtering. Elements analysis is carried out by EDS. The Al/Ba ratio in thin films will approach 2.0 with more pellets existing in target. PL spectra of thin films are measured and analyzed. The most obvious emission peak in each spectrum is located at about 470nm which corresponds to the 4f65d1²4f7 transition of Eu²⁺ in BaAl₂S₄ lattice. The emission peak will approach 470nm as more pellets are embedded in complex target. As a result, it can be concluded that increasing the amounts of BaS:Eu pellets in complex target is an efficient way to achieve better Eu doping barium thioaluminates thin film.

8560-15, Poster Session

A semi-analytical approach for LED secondary lens design

Chung-Jen Ou, Hsiuping Univ. of Science and Technology (Taiwan)

Based on the geometric optics, the author proposed an analytical approach for LED secondary lens design. The starting point for the secondary lens is the base profile (first surface) near the LED die, where the entrance angle of the LED ray can be calculate according to the given profile. Later, the complicated profile is generated according to the required exit angle of the ray on the second surface, which complete a mathematical mapping relationship between the spatial apodization of the LED die to the angular apodization to both the near field and the far field terms. In this report, the author demonstrates the profiles in the analytical form with iterative and non-iterative form. The numerical solutions for the two forms are compared to the required spatial apodization pattern, and the issues of the advantage and limitations of this novel method is provided. Most important of all, the present method can combine with the analytical description of the LED electrodes, such that improved the performance of the optimization process and solved part of the non-uniformity problems.

8560-16, Poster Session

Energy transfer under applied electric field in doped PLED by transient spectra

Lingchuan Meng, Yanbing Hou, Longfeng Lu, Beijing Jiaotong Univ. (China)

We report enhanced Förster energy transfer from phosphorescent iridium(III)bis(4', 6' -difluorophenylpyridinato)tetrakis(1-pyrazolyl) borate (Fir6) to fluorescent tetraphenylanthracene (rubrene) in dual doped PVK:Fir6:rubrene(100:10:0.3 in wt.) thin film under a increased electric field, the PL lifetime of Fir6 decreased from 708ns to 557ns at applied voltage from 0V to 20 V and according intensity of transient spectra declined from 8.8 to 7 in arbitrary unit. The electroluminescent (EL) spectra with different electric field of device of ITO/PEDOT:PSS(30

nm)/ PVK:Fir6:rubrene(100:10:0.3 in wt.)/ 2,9-dimethyl-4,7-diphenyl-1,10-phenanthroline (BCP) (10 nm)/tris(8-hydroxyquinoline)aluminum (Alq3) (20 nm)/LiF (1 nm)/Al was given. The intensity of Fir6 was decreasing meanwhile that of rubrene was increasing as the applied voltage increasing, that also indicate the enhanced Förster energy transfer from Fir6 to rubrene. The mechanism for the enhanced Förster energy transfer was discussed from energy level. The LUMO of Fir6 and rubrene have a little difference, so the enhanced Förster energy transfer was considered from reduced energy gap of HOMO of Fir6 and rubrene. Technique method, PL transient measurement was obtained by excited the device with 5ns laser pulse wavelength at 355nm meanwhile applying a reverse ac voltage pulse on device and then coupling the emission through a filter into monochromator which connect to a PMT(photomultiplier tube), at last the signal in PMT was extracted into a oscilloscope. The ac voltage source was connected with laser trigger by a time delay to synchronize ac voltage output with laser pulse. We use the ac voltage pulse but dc voltage to prevent the device breakdown at high voltage.

8560-17, Poster Session

A new uniform chromaticity diagram based on CIE1931 (x, y)

Yusheng Lian, Ningfang Liao, Beijing Institute of Technology (China); Xiuze Wang, Institute of Science, Information Engineering University of PLA (China); Jing Liang, School of Light Industry and Chemical Engineering, Dalian Polytechnic University (China); Jiajia Wang, Beijing Institute of Technology (China)

With the rapid development of the new display techniques including color LED display and laser display, the color fidelity reproduction techniques for cross-media and color display quality of the new display technology become more and more important. The uniform color space is the key of color fidelity reproduction and new display technology. In these early uniform color spaces, the uniformity of lightness is quite well, but the performance of the chromaticity has not won great satisfaction. Therefore the establishment of a genuine uniform chromaticity diagram is actually still an important work for both the basic research in color science and the application of the new color display technology. In this paper, according to the properties and distribution of Macadam ellipses on the CIE1931 (x, y), a new uniform chromaticity diagram named (U, C) obtained by using the coordinate translation and non-linear compression along radius direction with the aid of the iterative algorithm. Compared with CIE 1931 (x, y), the uniformity of (U, C) is obviously improved. Moreover, it appears to perform as well as or better than these chromaticity diagrams in the IPT and CIECAM02-UCS color spaces.

8560-18, Poster Session

TEM sample preparation and characterization of the group-III nitrides: common problems and solutions

Xiao-Dong Yang, Xiamen Univ. (China)

The breakthroughs in material growth technology and device technology of group-III nitrides, and the emergence of light emitting diodes have advanced the semiconductor solid state lighting. As an important characterization technique for the micro-nano semiconductor materials, transmission electron microscopy (TEM) has been widely employed to analyze the surface morphology, microstructures, crystalline quality and other crystal characteristics of the group-III nitrides. It also can make qualitative analysis of elemental composition. However, stringent requirements for the TEM sample preparation, especially for the hard and fragile semiconductor materials, and the discrimination of image data validity are still critical problems. In this article, some common problems and the solution methods for the

TEM microstructure characterization and EDX analysis are raised and addressed in detail.

8560-19, Poster Session

Effect of the projection lens on speckle contrast measurement in laser projection displays

Mei-Fang Xu, Wenhong Gao, Yunbo Shi, Pengfei Zhao, Jun Liu, North Univ. of China (China); Xuyuan Chen, Vestfold University College (Norway) and North Univ. of China (China)

Laser speckle is an important concern, as it degrades image quality. Typically, one or multiple speckle reduction techniques are employed in laser displays to reduce speckle contrast. Likewise, speckle contrast issues need to be carefully evaluated in designing laser displays under different usage scenarios. In this paper, a laser projection display system that uses moving small diffuser for speckle reduction is set up. We demonstrate the effect of the resolution cell of the projector lens on speckle contrast measurement under the scenarios of free-space, imaging with different projector-detector geometry configurations. The result shows that suppression of subjective speckle is much more difficult than that of objective speckle. The former depends on the ratio of the resolution cell size of the detector and the projection optic at the screen, while the later is sensitive to illumination variation due to its good transfer from the illumination to the screen. Low speckle projection system based on those mechanisms realized the speckle reduction from 36.59% to 2.75% by removing the projector lens.

8560-20, Poster Session

Quantum efficiency measurement of luminescence glasses for white LED

Xiangkun Dong, Xiaoqing Du, Yulong Liu, Linjiao Ren, Lei Jin, Xiaohua Lei, Weimin Chen, Chongqing Univ. (China)

Compared with the traditional light source, white LEDs play an important role in lighting area with its advantages in energy-efficient, environmental protection, small volume, longer lifetime and so on. Luminescence glasses as an important part of white LEDs, its luminescent properties affect the LEDs' luminous flux, color coordinate and so on, therefore it is necessary to study and measure the luminescent glasses' properties. The quantum efficiency is a major parameter of luminescent materials which can characterize the skill strength of excitation energy converted to luminous energy. Accurate measurement of the quantum efficiency can evaluate the luminescent properties of the luminescent glasses, which provides an important basis for quality improvement of the luminescent material.

Luminescence glasses have transparent and anisotropic characteristics, for this reason, we adopted an integrating sphere with 20cm diameter which was connected to a CCD Spectrometer to measure and calibrate the fluorescence spectra of the sample. We designed and built the quantum efficiency measurement system. The system included four key parts, which were the selection of test light source, the design of the integrating sphere, the design of sample special fixture and the choice of the grating spectrometer. Various components play different key role in the measurement of quantum efficiency. We investigated the system in the design and selection of various components parts, discussed the principle of measurement and put forward the calculation method.

Using the test system to measure YAG aluminum magnesium fluorescent ceramic glass and compared with the literature values. By measuring, the quantum efficiency for YAG fluorescent glass was calculated to be 31% based on the absolute spectral power distribution, it was coincided with the literature. And finally, we analyzed the system error.

8560-21, Poster Session

The thermal effect of PLEDs by Raman spectra

Zhe Qin, Jian Wang, Ya jun Chen, Civil Aviation Univ. of China (China); Cun zhou Zhang, Nankai University (China)

Raman spectra and infrared imaging systems are used for the study of internal temperatures of PLEDs. The aim is to measure the temperature and investigate the thermal degradation of PLEDs with different current densities. Raman intensity is proportional to the number of molecules in the next higher vibration energy level, and accurate internal temperature of PLEDs at thermal equilibrium can be calculated with the ratio of anti-stokes to stokes Raman intensity by Boltzmann equation. With the current density of PLED going from 0 mA/cm² to 169 mA/cm², it is found that the internal temperature of PLED increases accordingly. When the temperature comes to the glass transition temperature (T_g) of the emission layer, there is a phase change in it and the layer becomes free state as liquid, which is not stable. Local disfigurement in the emission layer results in short circuit between the cathode and the anode of a PLED, and the luminescence of PLED fails. At the same time, we also use the infrared imaging camera and thermal resistance to detect the surface temperature of PLED. As a results, with the current density grows, the temperature differences between the emission layer and surface become bigger. Therefore, Raman spectra is considered as a good method for detecting temperatures of thin-film semiconductor devices.

8560-22, Poster Session

Design of freeform LED lens with large light deflection angle for road lighting application

Shaoyun Yin, Xiuhui Sun, Chongqing Institute of Green and Intelligent Technology (China); Yiming Pan, Liangping Xia, Institute of Optics and Electronics (China); Jinglei Du, Sichuan Univ. (China); qiling deng, Institute of Optics and Electronics (China); Chunlei Du, Chongqing Institute of Green and Intelligent Technology (China)

LED owes the virtues of high efficacy, small size, better color rendering, long life and environmental friendliness, and it is considered as the fourth generation of lighting source. However, the radiation distribution of LED devices is usually Lambertian type, and they cannot be used directly in many applications. The ray deflection angle of the free-form surface lens, which is the mainstream of secondary optical elements for various applications, is seriously restricted due to the Fresnel reflection loss. In this paper, a method for designing freeform lens associated with a tilting aspheric is presented to achieve large deflection angle. Using this design method, a Cree-xp-e LED road lighting lens for length L=30m, road width W=12m, tilt angle $\theta = 15^\circ$ is designed and manufactured. The experimental results show that the overall road surface luminance uniformity is as high as 0.7 and the glare factor is less than 2%. This design method greatly expands the light deflection capacity of the traditional free-form surface LED lens, and it also can be widely used in the design of LED road lighting lens and other illumination applications where large light deflection angle is needed.

8560-23, Poster Session

Epitaxial lateral overgrowth on the air void embedded SiO₂ mask for InGaN light-emitting diodes

Sang-Mook Kim, Korea Photonics Technology Institute (Korea, Republic of)

We fabricated In_xGa_{1-x}N multiple quantum well (MQW) light-emitting

diodes (LEDs) on air void embedded SiO₂ mask. Firstly, a 30 nm-thick GaN nucleation layer and 2 nm-thick unintentionally doped GaN layer were grown on the c-face sapphire substrates by using a metalorganic chemical vapour deposition (MOCVD) system. A normal lithography, metal evaporation, and lift-off process were used to fabricate the SiO₂ mask and silver (Ag) embedded SiO₂ mask. Then, the conventional InGaN MQW blue LED structures were grown on the different substrates under identical growth conditions. It is well shown that the Ag was volatilized in the high temperature MOCVD growth process and that was formed air void by the energy dispersive X-ray spectroscopy images was carried out in scanning transmission electron microscopy (STEM) mode. The light output power (at 20mA) of the LED using epitaxial lateral overgrowth on the SiO₂ mask and LED with the air void embedded SiO₂ mask are enhanced compared with that of the conventional LED. Furthermore, LED with the the air void embedded SiO₂ were shown the notable increase than the LED with the SiO₂. The enhancement of the LED with the air void embedded SiO₂ mask could be explained by the increment of light scattering and improvement of quantum efficiency by reducing the dislocation.

8560-24, Poster Session

Preparation and characterization of Eu³⁺ ion in Mg-substituted tricalcium phosphate phosphors

Tsung-Yuan Chang, National Taiwan Ocean University, Keelung (Taiwan); Hsiu-Mei Lin, Tai-Yuan Lin, National Taiwan Ocean Univ. (Taiwan)

Photoluminescence investigation of Eu activated Mg-substituted tricalcium phosphate (β -TCMP) phosphors were prepared by solid-state reaction. The structure and emission spectra were well characterized by X-ray diffraction (XRD) and photoluminescence (PL) techniques. PL excitation spectra of β -TCMP:Eu³⁺ phosphors shows the excitation peaks ranging from 350 to 400 nm due to 4f⁷→4f⁶ transitions of Eu³⁺ ions. PL emission spectra of Eu³⁺ ion under 394 nm excitation shows PL emission peaks at 593 nm (orange-yellow) due to 5D₀→7F₁ transitions and 612 nm (red) due to 5D₀→7F₂ transitions. The excitation and emission spectra show that all the Eu³⁺ doped β -TCMP samples can effectively emit the light excited by UV light. The red-emitting β -TCMP:Eu³⁺ phosphors may be efficient photoluminescent materials for solid-state lighting phosphors.

8560-25, Poster Session

The variation laws of mutual coherence function in laser projector with moving diffuser for speckle reduction

Gaoming Li, Yishen Qiu, Hui Li, Fujian Normal Univ. (China)

The variation laws of mutual coherence function in laser projector with moving diffuser for speckle reduction are studied based on the partly coherent theory. We take the magnification of lens and its spread function into consideration, it gives us a method to weigh the speckle reduction and the loss of optical energy while using the moving diffuser for speckle reduction, and it points out the selection of diffuser slice for laser display.

Conference 8561: Advanced Sensor Systems and Applications V

Monday - Tuesday 5 -6 November 2012

Part of Proceedings of SPIE Vol. 8561 Advanced Sensor Systems and Applications V

8561-1, Session 1

Laser spectroscopy applied to environmental and medical research

Sune Svanberg, Lund Univ. (Sweden) and South China Normal Univ. (China)

Applied laser-based diagnostic methods as developed and pursued at the Atomic Physics Division, Lund University, are illustrated. The fields of application range from environmental monitoring including cultural heritage assessment to biomedical applications. General aspects of laser-based methods are non-intrusiveness, high spectral and spatial resolution, and data production in real-time. Different applications are frequently generically very similar irrespective of the particular context, which, however, decides the spatial and temporal scales as well as the size of the optics employed. Thus, volcanic plume mapping by lidar and optical mammography are two manifestations of the same principle, as is fluorescence imaging of a human bronchus using an endoscope and the scanning of a cathedral using a fluorescence lidar system. Recent applications include remote lidar-based monitoring of insect and bird migration, and gas monitoring in scattering media (GASMAS). The latter technique was employed as a new diagnostic tool for studying materials including ceramics, but also for diagnostics of human sinus cavities and new-born babies, as well as for assessing the integrity of food packages.

8561-2, Session 1

Thermal stability solutions for optical current sensor using thermoelectric method (*Invited Paper*)

Shuping Wang, Univ. of North Texas (United States); Xiaoling Yang, Beijing Union Univ. (China); Abdullaziz Alahmari, Univ. of North Texas (United States)

Compared to conventional current transformers (CTs) optical current sensors (OCSs) have many advantages including electrical isolation, zero hysteresis, large bandwidth, and light weight. Temperature stability is one of the major obstacles that prevent the application of OCSs to power industry. Specifically, the Verdet constant of the optical material used in an OCS based-on the Faraday effect is a function of temperature. Therefore the rotation of polarization of the light passing through the optical material in the OCS, which measures the magnetic field induced by the current under test, will be affected by the temperature variations. In this paper a simple yet effective method using thermoelectric effect and software to compensate temperature drift of an OCS based-on the Faraday effect is demonstrated. The temperature of the optical material is constantly monitored by a self-excited thermoelectric component. The resolution of 1°C and accuracy of $\pm 0.3^\circ\text{C}$ in temperature range from -40 to 80°C can be achieved. With the accurate temperature information the Verdet constant of the optical material can be achieved by looking up a table of temperature vs. Verdet constant that is experimentally obtained and stored in a memory. The magnetic flux density (thus the current under test) with temperature correction can then be calculated. An OCS based-on Faraday effect has been fabricated and tested. The results from the OCS with temperature compensation are compared with those without compensation. High temperature stability has been achieved.

8561-3, Session 1

An experimental study on detection of load application onto an optical fiber by means of changes of a speckle pattern

Makoto Hasegawa, Muneki Kawahara, Chitose Institute of Science and Technology (Japan)

In order to investigate possibility of utilizing speckle patterns to be observed in an output light spot from an optical fiber due to external disturbance for sensing application, a certain load was applied onto an optical fiber through which laser beams emitted from a laser diode were propagating, and changes in speckle patterns in the output light spot from the optical fiber were observed. The obtained results showed that when load was applied onto the optical fiber via a flat plate placed over the fiber, no significant changes were recognized in the speckle pattern. However, in the case where the optical fiber was placed so that corrugated bending of the fiber was induced via load application caused by ridges formed on the flat plate, the number of speckles in the pattern decreased upon load application of certain degrees onto the optical fiber. By employing other structures with ridges of difference configurations and dimensions provided so that a contact area between the ridges and the optical fiber was changed, certain influences were confirmed. Specifically, the larger the contact area between the ridges and the optical fiber was, the more significantly the number of speckles in the pattern decreased upon load application. From these results, there is a possibility of utilizing changes to be observed in speckle patterns formed in an output light spot from an optical fiber for sensing of load application onto the optical fiber by employing configuration in which ridges of appropriate dimensions are disposed against the optical fiber.

8561-4, Session 1

Rotation phenomena of speckle patterns observed in an output light spot from an optical fiber and its applicability for sensing application

Makoto Hasegawa, Yusuke Takahashi, Muneki Kawahara, Chitose Institute of Science and Technology (Japan)

When coherent light beams, i.e., laser beams are incident on one end of an optical fiber, transmitted to another end to exit from there so as to form an output light spot on a screen, non-uniform intensity distribution called speckle patterns is often recognized in the output light spot. The authors have confirmed that when a multimode optical bare fiber is placed in a loop onto a support plate, the speckle patterns in the output light spot appear to rotate while rotating the support plate. In this paper, even when an optical fiber was placed in a U-shape, instead of a loop, onto the support plate, the similar rotation of speckle pattern was observed. Furthermore, it was confirmed that a distance between the optical fiber placed in parallel at the edge of the support plate provides certain influences on the observed rotating characteristics of the speckle patterns. Thus, the pattern rotation seems to be caused by upward and downward displacements of the optical fiber at the edge of the support plate. In addition, even in the case where a jacket-covered and connector-attached optical fiber was placed in the U-shape on the support plate and a laser diode was employed as a light source, similar speckle pattern rotation was recognized. Such rotation phenomena of speckle patterns were observed with satisfactory repeatability, and therefore, there is a possibility of employing these phenomena for sensing purpose.

8561-5, Session 1

Rock mass acoustic emission detection using DFB fiber lasers

Wenzhu Huang, Institute of Semiconductors (China) and Shijiazhuang Tiedao Univ. (China); Huaixiang Ma, Shijiazhuang Tiedao University (China); Wentao Zhang, Fang Li, Institute of Semiconductors (China); Yanliang Du, Shijiazhuang Tiedao Univ. (China)

A systematic study of rock mass acoustic emission detection using distributed feedback (DFB) fiber grating lasers is presented. In this, the dynamic strain sensitivity of the DFB fiber grating laser in different coupled modes is calibrated by a comparison method. The ultra-narrow line width of the DFB fiber grating laser will result in a low equivalent noise level when using a fiber optic interferometric demodulation. A minimum detectable strain of 10-12@900 Hz is achieved in the experiment. Furthermore, the acoustic emission directional characteristics of the DFB fiber grating laser are investigated by two kinds of analyzing method. In the first experiment, the relationship between the wavelength drift and the angle of a continuous acoustic emission source is determined. In the second experiment, the relationship between the percentage of wavelet packet energy and the angle of impact response is established. Their acoustic emission directional characteristics make them suitable for determining principal strains and the direction of propagation of acoustic waves. Finally, three DFB fiber grating lasers are used in the array and the acoustic waves is detected, which shows that the fiber laser array is suitable to use for acoustic emission source location. Because of these advantages, such as anti-electromagnetic interference, high sensitivity, small physical size, the ability to multiplexed and directional characteristics, the DFB fiber grating lasers will provide a practical and advanced measurement means in large civil structural health monitoring.

8561-6, Session 1

High performance four-element DFB fiber laser hydrophone array system

Zhihui Sun, Li Min, Shandong Academy of Sciences (China); Xiaolei Zhang, Shandong Univ. (China); Jiasheng Ni, Yingying Wang, Jinyu Wang, Meng Wang, Chang Wang, Shandong Academy of Sciences (China); Jun Chang, Shandong Univ. (China); Gangding Peng, The Univ. of New South Wales (Australia)

A high performance four-element DFB fiber laser hydrophone array system has been developed and tested. The system has the advantages of low noise floor ($<10^{-6}$ pm/Hz^{0.5}@ 1 KHz) and wide bandwidth (10Hz~10 KHz). The theory analysis, design, development and test of the system are demonstrated in detail.

The wavelength of four-element DFB fiber lasers is 1530.1nm, 1532.9nm, 1537.0nm and 1539.0nm respectively. The parameters of each fiber laser such as relative intensity noise, frequency noise and linewidth are measured. Their influences on fiber laser hydrophone performance are analyzed. Four DFB fiber lasers are multiplexed in a single fiber, and then separated by a four channel DWDM with 200GHz spacing.

DFB fiber laser hydrophone sensitivity enhancement and packing are introduced. Acoustic pressure sensitivity is enhanced up to 115dB re Hz/Pa. Frequency response is achieved with a fluctuation of ± 4 dB from 32Hz to 1 kHz.

Interferometric interrogation method is adopted to realize high resolution fiber laser wavelength shift demodulation. Unbalanced Michelson interferometer and digital phase-generated carrier (PGC) demodulation are adopted. Michelson interferometer is well-built, and its performance such as fringe visibility, acoustic and vibration isolation effect are tested. Two kinds of PGC demodulation algorithms such as

differential-and-cross-multiplying (DCM) and the arctangent approaches are adopted. The digital PGC demodulation performance parameters like wavelength resolution, total harmonic distribution (THD), signal to noise and distortion (SINAD) and linearity is given.

Four-element DFB fiber laser hydrophone array system performance is tested and its noise equivalent pressure (NEP) is below sea state zero (SS0).

8561-7, Session 2

Double clad fibers for optical endomicroscopy applications (*Invited Paper*)

Ming-Jun Li, Corning Incorporated (United States)

Nonlinear optical endoscopes utilizing two-photon process have emerged as one of the best non-invasive means of fluorescence microscopy for early stage disease diagnosis. Compared with the single-photon microscopy, the two-photon microscopy offers inherent optical sectioning property, a great penetration depth and flexible optical spectra accessibility.

One of the key components for nonlinear microscopy is optical fiber. Although a standard single mode fiber can be used to deliver a laser beam to the target, it is not suitable for collecting the signals back due to the low numerical aperture and small core size. To increase the light collection efficiency, a double clad fiber structure has been proposed. Key requirements for double clad fibers include single mode core for pump light delivery, high numerical aperture inner cladding for signal collection efficiency and low background noise.

In this paper, we present double clad fibers that are suitable for nonlinear microscopy applications. We will discuss design considerations and process for making double clad fibers. We have made double clad fibers that are designed for the pump laser wavelengths at 800, 1060, 1310 and 1550 nm. We will present actual fiber results and examples for two-photon endomicroscopy applications.

8561-8, Session 2

Photonic crystal cavity Sensor integrated with microfluidic channel in the visible region (*Invited Paper*)

Lei Zhang, Tun Cao, Kai Rong Qin, Wei Ping Yan, Dalian Univ. of Technology (China)

Photonic crystal(PhC)has been used to detect (bio) chemical complexes due to its ultrasmall size and the potential to make the full on-chip integration with sources and detectors, so-called lab on a chip. Particularly, it can also operate as lasers to decrease the detection level. In this work, we numerically study a two-dimensional(2D) L3 PhC nanocavity integrated with a microfluidic channel by using 3D Finite Difference Time Domain(FDTD) method. The proposed L3 structure is a PhC slab with a triangular lattice on a GaN substrate, having a lattice constant of $a=235$ nm, a slab thickness of $0.9a$, a hole diameter of $d=0.6a$ and a refractive index of $n=2.45$. The cavity is created by missing three linearly aligned air holes (L3 type) with the first nearest-neighbouring holes displaced by a distance of $s=0.21a$ in the middle to maximize the Q-factor.

Sensing is performed by measuring the wavelength shift of the PhC cavity resonant peak due to the change of refractive-index distribution inside and around the PhC caused by the introduction or the adsorption of material. Since the change of resonant peak in the PhC is extremely sharp, a high sensitivity is expected. We observe the resonant peak at 597nm for the structure with air overlaid. We then simulate the PhC cavity with water ($n=1.33$) and two immersion oils ($n=1.48$ and $n=1.518$). The minimal wavelength change $\Delta\lambda=5.2$ nm results in an index change $\Delta n=0.15$. Wavelength shifts of 35nm/RIU for the structure.

8561-9, Session 2

A novel fiber optic microphone with three flexural disks

Ran Tao, Anhui Univ. (China)

In this paper, we present a novel fiber optic flexural disk acoustic sensor utilizing the resonance of flexural disks to get a high sensitivity at the wanted frequency range. Three flexural disks of different resonance frequencies are used as sensing elements, and the pressure induced strain in the flexural disks bonded with optical fiber is detected by the Mach-Zehnder interferometer.

8561-10, Session 2

Single-helix chiral long period fiber gratings for wavelength-interrogated liquid level sensing

Li Yang, Yunfei Wu, Univ. of Science and Technology of China (China)

Single-helix Chiral Long Period Fiber Grating (S-CLPG) has the similar wavelength-selectivity to conventional Long Period Fiber Grating (LPG). It is fabricated by twisting an eccentric-core single-mode fiber with a twist pitch less than 1mm at the melting state, and is desired for sensing applications owing to its stability even in high radiation environment where conventional LPG fabricated by photosensitive effect becomes unstable. To get a thorough understanding of spectral characteristics of S-CLPG in response to surroundings, we develop coupled-mode formalism for multimode couplings among LP₀₁ mode and LP_{1n} modes in the structure, and do simulations on its transmission spectra when it is partially immersed in a liquid with refractive index lower than that of cladding. Simulation results indicate that the attenuation dips corresponding to the multimode couplings in the transmission spectrum would shift continuously and monotonically as liquid level changes. We can thus develop a liquid level sensor based on wavelength interrogation, which is beneficial to avoid sensitivity deterioration caused by power instability in power interrogation for most conventional LPG-based liquid level sensing. Then we demonstrate a sensitivity of about 20 nm wavelength shift in sensing alcohol level from 0 to 13 mm. In addition, we identify that the sensitivity can be improved with a thinner fiber cladding or when the refractive index of the sensing liquid is closer to that of the cladding.

8561-11, Session 2

Self-phase modulation in a nonlinear single-mode fiber Fabry-Pérot cavity with high intensity pulsed laser injection

Haiyan Chen, Cong Chen, Lilin Chen, Yangtze Univ. (China)

Single-mode fiber Fabry-Perot (FP) cavity ring-down spectroscopy (CRDS) has attracted attention due to its applications in aerospace, military, petrochemical, transportation, building and structural monitoring, chemical, and biomedical sectors. There are some kind of cavity structure such as fiber FP interference, fiber Bragg gratings, and a fiber loop. However, the methods above do not consider the birefringence in a single-mode fiber and the difference of the ring-down time caused by the two polarization modes. Recently, a modified CRDS method called cavity ring-down beat spectroscopy (CRDBS) was proposed to study the minute birefringence in a fiber and all-optical clock recovery. In our previous work, we did some researches on CRDBS in a single-mode fiber FP cavity, and took a try to photonic generation of microwave/millimeter-waves and pressure sensor. However, we did not discuss the effect of fiber nonlinearity.

In this presentation, we propose a nonlinear single-mode fiber FP

cavity, in which CRDS is researched theoretically, and the relationship expression between output electric field amplitude and nonlinear phase shift is derived. Numerical results demonstrates that the output performance of nonlinear single-mode fiber Fabry-Perot cavity includes three phases: build-up, stability, and ring-down phase, output power is inversely proportional to the power in cavity, when the power in cavity is larger than 2W, the stable time for output signal with instability becomes longer, but the effect of self-phase modulation on CRD time is ignoring.

8561-12, Session 2

Characterization of Mach-Zehnder interferometer-based photonic crystal fiber sensors

Amine Ben Salem, Ahmed Dhib, Rim Cherif, Mourad Zghal, SUP'COM (Tunisia)

Recently, extensive researches in chemical and biochemical sensing applications have been devoted to the development of evanescent-field-based optical fiber sensors. These sensors exploit the fractional power propagating in the evanescent field in order to analyze the specimen's properties surrounding the waveguide. Sensors based on Mach-Zehnder interferometers (MZI) offer great potential with their phase sensitivity to the refractive index (RI) variation and allow the development of highly-sensitive robust sensors.

In this work, we propose a new design of MZI structure assembled with two arms composed of 400nm-diameter-hole-modified silica photonic crystal fibers (PCFs) and immersed in solvent solution. The proposed design is found to enhance considerably the sensitivity. One PCF-arm is used as reference and kept isolated from the specimen. The other PCF-arm is considered as sensing arm exposed to the specimen with a certain sensitive-area-length. A highly-sensitive versatile interferometry technique is used to determine the phase shift from both arms and consequently the specimen's information can be retrieved. The proposed sensor was first tested when considering the specimen to be analyzed with different concentrations for a probing light of 325nm. The sensitivity of detecting the benzene solutions in water reaches 9 rad/ μm which is much higher compared to what was achieved in photonic nanowires [1,2]. Then, the detection of corn oil into olive oil is achieved with high sensitivity of 14.7 rad/ μm demonstrating that the sensor is capable of detecting a RI variation of 4×10^{-7} in only 1-mm sensitive-area-length. Thus, the proposed MZI-based PCF-sensor shows to be very attractive for compact, flexible and high sensitive biochemical sensing.

[1] J. Lou, L. Tong, and Z. Ye, "Modeling of silica nanowires for optical sensing," *Opt. Express* 13, 2135-2140 (2005).

[2] P. H. Wu, C. H. Sui, and B. Q. Ye, "Modelling nanofiber Mach-Zehnder interferometers for refractive index sensors," *J. Mod. Opt.* 56, 2335-2339 (2009).

8561-13, Session 3

Phase shifted FBG fabricated with arc discharge erasing technique (*Invited Paper*)

Yuanhong Yang, Xiaozhe Zhang, Xuejing Liu, BeiHang Univ. (China)

Phase Shift Fiber Bragg Gratings (PSFBGs) has unique transmission spectrum which has a narrow transmission line in the normal stop band. This characteristic has great potential for laser, sensing and filtering application. There has been a huge effort in improving their fabrication techniques. PSFBGs have been fabricated with a UV-writing technique by using of a specially designed phase mask incorporating the required phase shift, by translating the fiber or the phase mask when the writing-beam is scanned, by post processing uniform FBGs with UV post-exposure and etching the fiber cladding.

In this work, a Arc Discharge Erasing (ADE) post processing technique

was studied and taken to fabricated PSFBG. The FBG ADE effect was demonstrated experimental first and useful parameters was obtained. Based this technology, the capability and fabrication technique was investigated and the full control of the spectral characteristics of the PSFBG, including the position, reflectivity and bandwidth of the phase shift peak was demonstrated. To get optimum technique parameters, many experimental fabrications were done and the characteristic curves under different discharge electric current, times and position were gotten and the effect of original FBG length and the annealing processing were investigated experimentally. With this technique, the in-line erbium doped fiber PSFBG fabricating system was built and the single mode DFB fiber laser was achieved with line width less than 1 kHz.

8561-14, Session 3

A novel method for design and development of magnetic motor based on thermal energy

Nithin Goona, National Institute of Technology, Goa (India)

This paper presents the study on the variations in thermal and magnetic properties of permanent magnets with temperature gradient from cryogenic to room temperature. The concept of adiabatic demagnetization gives the basic idea on variation in temperature of paramagnetic substances due to the application of magnetic field. The present work is on the variations in magnetic fields due to change in temperatures of ferromagnetic substances, which is the reverse process of adiabatic demagnetization. Adiabatic demagnetization explains conservation of energy, and this holds good everywhere, including reverse process of adiabatic demagnetization. The study on thermal conductivity of ferromagnetic material at cryogenic temperatures gives the amount of thermal energy being transferred from or to the surroundings and hence gives the variations in magnetic fields due to temperature changes. The objective of this project is to obtain temperature gradient of samarium cobalt permanent magnets from room temperature to cryogenic temperatures. The thermal conductivity verses temperature curve gives necessary information about thermal properties. The thermal properties of samarium cobalt rare earth permanent magnet help in understanding the variations in its magnetic fields. As samarium cobalt rare earth permanent magnet do quite well at cryogenic temperatures, this study is much useful in future applications of permanent magnets at cryogenic temperatures. Numerous references report the successful use of samarium cobalt to temperatures as low as 2 K.

8561-15, Session 3

Monitoring system for high steep slope based on optical fiber sensing technology

Feng Li, Yanliang Du, Shijiazhuang Tiedao Univ. (China); Wentao Zhang, Institute of Semiconductors (China); Baochen Sun, Shijiazhuang Tiedao Univ. (China); Fang Li, Institute of Semiconductors (China)

Landslide is typical geo-hazards which causes serious threat to the human lives and infrastructures. It's meaningful to develop an early warning system to avoid landslide disasters. In this paper, a real time monitoring system, based on optical fiber sensing technology, was designed to track the health status of slope. Through effective encapsulation, optical fiber grating stress gauge, optical fiber grating inclinometer and optical fiber grating anchor, corresponding surface deformation monitoring, internal displacement monitoring and anchor axial force monitoring respectively, were demonstrated. A light switch (1?4) was introduced to expand the demodulation equipment to 16 channels, which can meet the capacity of more than 200 FBGs. Based on the driving circuit, different channels can be switched to complete demodulation. Through the multiparameter monitoring network, remote and real-time monitoring of the slope can be realized, providing a reliable guarantee for the slope safety.

8561-16, Session 3

Fabrication and sensing characteristics of tilted long-period fiber gratings

Rui Wu, Yunqi Liu, Na Chen, Fufei Pang, Tingyun Wang, Shanghai Univ. (China)

Tilted long period fiber gratings (TLPFs) have attracted more and more attention because their many novel properties, such as stimulating the coupling between core fundamental and homonymous or reverse direction high-order cladding modes, polarization character. We demonstrated experimentally the fabrication of TLPFGs with different tilt angles and period by CO₂ laser. The experimental results reveal that the LPFs written with different tilt angles have quite different transmission spectra and the coupling coefficient of low-order cladding modes is higher than that of high-order ones. The tilted refractive index modulation enhances the coupling coefficient between the core fundamental mode and cladding mode. We wrote the non-titled LPFs with equivalent grating pitches in the same single-mode fiber. The experimental results of the comparison between the TLPFG and corresponding equivalent LPGA show that the TLPFGs' mode coupling is almost same with the equivalent non-titled fiber gratings, while the writing efficiency of the TLPFGs is much higher and the CO₂ laser energy needed is much lower. We also tested refractive index sensitivity of TLPFGs and the equivalent non-titled fiber gratings. The experimental results indicated that tilted LPGA has higher refractive index sensitivity than the corresponding equivalent LPGA. The TLPFG could be widely used in optical communication and fiber sensors.

8561-17, Session 3

Highly sensitive temperature measurement based on polymer-coated single-mode-multimode-single-mode fiber structure

Linlin Xue, Yujuan Zhang, Di Che, Qijin Zhang, Li Yang, Univ. of Science and Technology of China (China)

Recently, sensing applications of multimode interference in the single-mode-multimode-single-mode (SMS) fiber structure has attracted much attention. All-fiber sensors based on the structure own the advantages of low cost and easy fabrication, in addition to the common advantages as an optical fiber sensor, such as immunity to electromagnetic interference, resistibility to harsh environments and compact size. A sensitivity of about 10pm/oC was demonstrated in temperature measurement, and it was enhanced to about 30pm/oC by using a bent form. Here we present a novel way to greatly enhance the sensitivity by replacing the cladding of the silica multimode fiber with a polymer coating. The polymer we used is Poly (MMA-co -TFEMA), whose thermo-optic coefficient is about 50 times higher than that of silica. In this paper, we first analyze the transmission characteristics of the polymer-coated SMS fiber structure by using the mode expansion method, and present optimizations of design parameters such as the length of multimode fiber and refractive index of the polymer. Then we fabricate polymer-coated SMS fiber samples for experiments. By monitoring wavelength shift of valleys in transmission spectrum resulting from multimode interference, a measuring sensitivity of about 700pm/oC is obtained, 20 times higher than the reported highest one based on the structure to the best of our knowledge. With the present desirable coating technique, we believe that this simple structure is promising in high sensitive temperature sensing and measurement.

8561-18, Session 3

Experimental investigation of birefringence of solid core polarization maintaining photonic crystal fibers

Weiqian Duan, Yuanhong Yang, Xing Zhang, Miao Ye, BeiHang Univ. (China)

Photonic Crystal Fiber (PCF) is a sort of micro structure fiber actually. Many unique characteristics, such as endless single mode, small mode field diameter and bend loss insensitive, etc. can be realized with special structure design. A solid core polarization maintaining PCF (PM PCF) was made by destroying the isotropy of the circular cross-section and desired birefringence can be obtained with special parameters. This PM PCF made of pure SiO₂ material and theoretically analysis shown it may have nearly temperature-independent birefringence which is very important for many sensing application. In this paper, we characterized the temperature and operation wavelength sensitivity of birefringence of a commercial polarization maintaining photonic crystal fiber as a typical case first. The temperature dependence of birefringence due to two main factors, namely temperature-induced variations of the refractive index of the glass and the thermal expansion of the fiber in transvers directions, were investigated and simulated in detail. The simulation result shown that the birefringence temperature susceptibility can be described as a second-order polynomial of Δn (distance between small holes) and zero sensitivity to temperature may be obtained at optimum structure parameters with desired operation wavelength. The PM PCF structure parameters measurement setup and the birefringence measurement setup were built. The structure and birefringence of five PM PCFs were measured with different operation wavelength under different temperature environment experimentally and the relationship of different parameters was analyzed and some design rules were summarized. The experimental result agrees with theory analysis well and the nearly temperature-independent birefringence of solid core PM PCF can be realized with optimum structure parameters with certain operation wavelength.

8561-19, Session 4

The fabrication of nanostructures CIGS thin film solar cell (*Invited Paper*)

Li-Hsi Chen, Xusun-Yu Yu, National Chung Cheng Univ. (Taiwan); Hsiang-Chen Wang, National Chung Cheng Univ. (Taiwan) and National Chung Cheng Univ. (Taiwan); Jian-Hung Lin, Chia-Chen Hsu, Chien-Chao Tsiang, National Chung Cheng Univ. (Taiwan)

When the incident light meets the interface between air and electrode layer, reflection occurs from difference of refractive indices. Reflection means the loss of the light, which is absorbed to solar cell and generates electric power. In order to prevent the reflection, some kind of anti-reflection methods need to be developed. Surface anti-reflection treatment can be categorized to 4 different techniques including surface texturing, single-layer interference coating, multi-layer coating and moth-eye structure forming. Among them, moth-eye effect, introduced by Bernhard, caused gradual change in refractive index by forming nano-sized patterns on the surface. Thus the reflection of incident light can be minimized over the whole spectra range. In this study, we used laser interference lithography technique to produce nanostructures on Copper Indium Gallium Selenide solar cells. The CIGS solar cell is a kind of thin film solar cell, and it has the best conversion efficiency of the thin film solar cells. We fabricate 500nm of nanoholes on the CIGS film and arrange in cubic structure and hexagonal structures. Finally, we discuss the gaining degree of optical efficiency.

8561-20, Session 4

Optical voltage sensor using single Fresnel rhomb Bi₄Ge₃O₁₂ crystal

Changsheng Li, BeiHang Univ. (China); Rong Zeng, Tsinghua Univ. (China)

In conventional polarimetric voltage-sensing scheme, an additional quarter wave plate generally is needed to provide a proper optical bias, and it will induce extra measurement errors due to polarization axis mismatch and temperature effect, etc. Among various used quarter wave-plates, the right angle prism-based wave-plate is distinguished because its quarter wave phase retardation is produced by the total inner reflection of the light wave passing through the prism. However, this prism-based wave plate still is a separate element from the voltage sensing crystal, and there exists some issues related to light coupling and reflection, etc.

In this paper, a novel optical voltage sensor is proposed that uses single Fresnel Rhomb bismuth germanate (Bi₄Ge₃O₁₂, BGO) crystal as both voltage sensing element and quarter wave plate. Therefore, the quarter wave optical phase bias is provided by the sensing crystal itself, any additional quarter wave plate is not necessary for the proposed voltage sensor that consists of one Fresnel Rhomb BGO crystal and two prism polarizers. The voltage sensing principle is theoretically analyzed in detail, and its feasibility is demonstrated by related experiments. DC voltage in the range of +10V~+2200V was measured and the standard error of the linear fitting slope for experiment data was less than 4.9x10⁻⁶. AC voltage with 50Hz industrial frequency was also measured within 2000V, and related standard error was less than 1.8x10⁻⁵.

8561-21, Session 4

Sub-pixel algorithms on linear-array detector grating spectrometer

Chuan Qin, Jianlin Zhao, Dexing Yang, Biqiang Jiang, Northwestern Polytechnical Univ. (China)

The optical signal interrogation techniques play an important role in fiber Bragg grating (FBG) sensing areas. Unlike the traditional OSA, which is unstable, low speed and bulk because of its mechanical scanning parts, linear-array detector grating spectrometer draw more attention recently. However, most of the array-detectors, especially, those within the IR range have limited pixels which lead to poor resolution. In this paper, the spectrum of Gauss apodized FBG is analyzed by using transfer matrix method, and the basic principles of sub-pixel curve fitting algorithms including mass center, Gauss and full-width-at-half-maximum (FWHM) are discussed. Based on this, simulation and experimental results are given to compare the three curve fitting algorithms. The results reveal that in simulation, mass center fitting method with an accuracy of 13pm while in experiment, FWHM fitting method with an accuracy of 23pm provides a better match to the actual curve. The research achievements have been applied on the prototype of linear-array detector grating spectrometer and have potential market in portable FBG interrogation field.

8561-22, Session 4

A geometric algorithm for space optical imaging system based on topological mapping relationship

Zhang Zhi, Zhou Feng, Ning-juan Ruan, Beijing Institute of Space Mechanics and Electricity (China)

Space imaging system is affected by micro-vibration of satellite platform on orbit. Therefore, image quality is degraded by variance of attitude angle. High resolution image is easily smeared by motion error of satellite. However, it is very hard to find the error source on the space environment accurately. According to studying geometry model of space camera, the transform relationship between object plane and image plane is put up. Firstly, the paper analyses attitude error and motion source of TDI camera on orbit. Then, the transform matrix is analyzed between earth coordinate and image plane coordinate. The geometry model contains in-out orientation elements. Secondly, imaging procedure of TDI space camera is simulated. Different modes of micro-vibration are added into imaging model in order to simulate jitter on the image. Multi-mode micro-vibrations are simulated on the line of sight at same time. And then the experiment simulation is based on three axis. Imaging procedure of TDI space camera is simulated based on physical character of imaging system. Different images are simulated by changing number of TDI. Various motion errors of satellite are comprised in geometry model. Hereafter, the geometry distortion of pixel position is calculated on image plane. The measurement accuracy of geometry distortion is sub-pixel scale. Afterwards, the corresponding simulated image will be generated if the motion parameters of space imaging system are fixed. Finally, the boundary condition is analyzed. Over passing this extent, image quality will be obviously degraded by changing error amount of motion. The result is good for analyzing parameters of satellite platform and guiding design of remote sensor.

8561-23, Session 5

Planar optical microring resonators used as biosensors: design of polymer compared to semiconductor based waveguides (*Invited Paper*)

Rene Landgraf, Fraunhofer-Institut für Photonische Mikrosysteme (Germany) and Technische Univ. Dresden (Germany); Toni Haugwitz, Robert Kirchner, Andreas Finn, Technische Univ. Dresden (Germany); Frank Deicke, Fraunhofer-Institut für Photonische Mikrosysteme (Germany); Wolf-Joachim Fischer, Technische Univ. Dresden (Germany) and Fraunhofer-Institut für Photonische Mikrosysteme (Germany)

Due to their small footprint and high sensitivity to biological molecule binding, planar optical microring resonators gained high interest for use as optical biosensors. Typically, these microring resonators are made of semiconductor based material and are manufactured by time-consuming lithography and etching steps. Semiconductor based waveguides have high refractive indices, and thus, a high refractive index contrast between core and cladding. In this case, due to strong mode confinement, substrate leakage is a comparably minor issue and bending loss becomes relevant only at small bending radii of less than 10 μm . The main loss is determined by surface scattering, and thus, semiconductor based curved waveguides are designed to have very smooth sidewalls.

If polymer materials are used, as in this work, microring resonators can be cost-efficiently manufactured by nanoimprint lithography. The resulting larger polymer waveguide diameters facilitate in- and out-coupling, and polymer surfaces allow using established surface biofunctionalization techniques. For polymer waveguides, due to the small refractive index contrast, surface scattering loss is a minor issue, but bending loss is dominant due to the low mode confinement. In this

work, design guidelines for polymer microring resonator waveguides are given and compared to semiconductor based waveguides. 3-D FDTD simulation results, including coupling factors and ring waveguide losses, are presented for various relevant waveguide cross-sections. Results are compared with analytic calculations. The effects of nanoimprint manufacturing will be discussed. First measurement results are presented.

8561-24, Session 5

A sensitive refractive-index sensor with a microstructure metamaterial

An Yang, Jiangsu Normal Univ. (China); Changchun Yan, Jiangsu Normal Univ. (China) and Nanyang Technological Univ. (Singapore)

We design a micro-structure metamaterial which has a good capability of the realization of sense of refractive indexes and is different from other sense structure. The metamaterial consists of a large metallic split ring and a metallic small one located on the surface of a substrate. The two split rings have a common axis and surrounded by a specific material. By simulating resonance behaviors of the structure with a finite element method, we find the resonance frequency as a function of refractive index of the specific material, which is used as a refractive-index sensor. We also studied the effect of the substrate thickness and the aspect ratio of the split rings on the resonance. Analyzing all kinds of effect, we propose a set of optimized parameters which effectively enhance the sensitivity of the sensor. An evident advantage of such a sensor is that it can easily be integrated with the other elements due to its miniaturization, which constitutes a complete functional device.

8561-25, Session 5

Sensitivity limits of guided modes in silicon integrated waveguide-based sensors

Oleg Zero, Norwegian Univ. of Science and Technology (Norway); Astrid Aksnes, Norwegian Univ of Science and Technology (Norway)

The material characteristics of silicon, and especially the high index contrast offered by the silicon-on-insulator (SOI) platform offers the potential for building sensors that are both sensitive, extremely compact and compatible with the CMOS fabrication. Due to the high degree of light confinement in silicon, a minute geometrical perturbation can result in a considerable change to the effective refractive index of a guided mode, hence enabling a potential sensing mechanism. However, when analyzing the sensitivity limits of typical integrated photonic components, such as microring resonators or integrated Mach-Zehnder interferometers, the ultimate sensitivity of a sensing device is often dictated and limited by the device's overall surface area. In principle, the existence of a set of multiple guided modes might, however, allow improving the sensitivity without increasing the device's size.

The aim for the study is to investigate the achievable sensitivity in different geometrical configurations related to traditional integrated photonic components. Utilizing numerical modeling tools based on finite elements method (e.g. COMSOL), the sensitivity limits of such a structure are investigated in terms of small geometrical changes and effective index response. Furthermore, the possible enhancement to the sensitivity that is related to simultaneous multiple mode coupling is discussed and various geometries are analyzed by means of 2- and 3-dimensional simulations and a representative structure based on (multi-) mode coupling is presented.

8561-26, Session 5

Lidar observations of the urban aerosols: case study on the air quality in China

Zhenyi Chen, Anhui Institute of Optics and Fine Mechanics (China)

Two measuring campaigns were performed in the downtown of Guangzhou in South China and Shijiazhuang in North China in 2010 and 2011, to investigate the concentration and distribution of urban aerosols. Polarized LIDAR (MPL) operating at 532 nm were employed to track the spatial and temporal aerosol distributions. PM10 concentrations of particles and the wind profile lidar were continuously monitored within the Lidar observing region. The results illustrate that the aerosol types can be estimated based on the depolarization ratio. And we found the aerosol concentrations within the lower troposphere and found the daily aerosol cycles. In both Guangzhou and Shijiazhuang measuring sites, we observed the cases with increased aerosol concentration, associating with the presence of point sources of particulate matter. Furthermore, the back trajectories from Hysplit are also used to identify the pollution sources.

8561-28, Poster Session

A fiber-optic flexural disk microphone of high sensitivity

Ran Tao, Ran Tao, Xuqiang Wu, Qifa Zhang, Sheng Huang, Benli Yu, Anhui Univ. (China)

A fiber-optic flexural disk microphone is developed to detect acoustic signals in the air. It consists of a Mach-Zehnder interferometer with an optimized sensing arm of 7.93 m. The disk's resonance frequencies and their influence on the microphone's sensitivity are investigated. The microphone's frequency response is measured in the frequency range from 100 Hz to 5 kHz and the average phase sensitivity is about -120.7 dB re 1rad/1Pa.

8561-29, Poster Session

Simulation analysis and theoretical model of electro-optic modulator in Rayleigh BOTDA

Hu Wang, Yongqian Li, Huan Li, Qinghe He, North China Electric Power Univ. (China)

The system based on Rayleigh Brillouin optical time domain analysis can work with the non-destructive way only by using one-laser, one-ended and single fiber, modulating pulse base and pulse at the same time by using electro-optical modulator (EOM) based on intensity is the key technology for this system to obtain continuous light and pulsed light. A new modulation method is analyzed theoretically and simulated by using a pulse generator connected to the bias port of EOM and a microwave signal connected to the RF port of the EOM to modulate pulse base and pulse simultaneously. The best operating point problem of Rayleigh BOTDA system by using EOM is discussed, the continuous light and pulsed light of Rayleigh BOTDA system are obtained by simulation, the theoretical basis for the analysis and design of different structures of stimulated Brillouin distributed sensing system is provided.

8561-31, Poster Session

Characteristics analysis of coating layer power distribution of Eccentric Core Optical Fiber

Liu Jianxia, Harbin Engineering Univ. (China) and College of Electronic & Information, Heilongjiang Institute of Science & Technology (China); Yuan Libo, Harbin Engineering Univ. (China)

Eccentric Core Optical Fiber belongs to a kind of special Optical fiber. The centre axis of core does not coincide with clad. Because of the special physical structure more energy than the conventional fiber exists in the form of evanescent wave field and will result in higher sensitivity. The energy distribution will be influenced when the change of the coating refractive index. When the external environment causes the change of the coating refractive index, it may be detected by observing the output spot size of Eccentric Core Optical Fiber.

In practical many optical fibers are made up of poly-regions in each of which the refractive indices are homogeneous. Since 1970 Clarricoats etc presented firstly the matrix method to analyze the poly-regions fiber. Suematsu etc have done much more research. However, the previous research in the area is restricted to analyze characteristics of the poly-regions circular optical fiber. In this paper, analyze characteristics of double-cladding coating layer propagation properties of Eccentric Core Optical Fiber. Firstly, base on the mode theory of the double-cladding step-type circular optical fiber and make use of the Conformal Transformation to obtain propagation properties of Eccentric Core Optical Fiber. Present the general characteristic equations according to the Optical Network concept. Secondly, take Eccentric Core Optical Fiber for example, make use of above theory, numerical calculate to LP01 mode in different eccentric distance and excitation wavelength. Offer η -V characteristic curve in different conditions. Study the relationship between the core-region energy distribution and eccentric core distance, working wavelength and coating refraction index of Eccentric Core Optical Fiber. Finally, compare the energy distribution of Eccentric Core Optical Fiber and circular optical Fiber.

The above revolution will provide an important theoretical foundation to the applications of Eccentric Core Optical Fiber.

8561-32, Poster Session

A method for improving Rayleigh-BOTDA system performance

Yongqian Li, Hu Wang, Huan Li, Qinghe He, North China Electric Power Univ. (China)

In this paper we describe and implement a long-range Rayleigh Brillouin optical time domain analysis (Rayleigh-BOTDA) system using Simplex optical pulse coding techniques, for temperature or strain measurement, in order to overcome the trade-off between the spatial resolution and measurement accuracy and achieve a higher signal-to-noise ratio (SNR). The composition method of Simplex coding is discussed, the physical mechanism for Brillouin scattering process in this system is analyzed and an approximate mathematical model of Rayleigh-BOTDA system based on transient coupled wave equations of stimulated Brillouin scattering (SBS) is proposed. Based on the foregoing work, the theoretical analysis of Simplex coding applied to Rayleigh-BOTDA system is presented, and the system performances in time and frequency domain are simulated numerically by Matlab. Simplex coding using 63 bit codeword provide up to 6 dB SNR improvement, allowing for temperature or strain measurements with 1 m spatial resolution over 10 km of standard single-mode fiber. The simulation results show that the method can improve both the SNR and measurement accuracy of the system without degrading the spatial resolution.

8561-33, Poster Session

Research on fiber Bragg grating based on nano-fiber

Nuan Jiang, Zhengtong Wei, Yongming Hu, National Univ. of Defense Technology (China)

Fiber Bragg grating sensors have been attracted more attention due to its excellent advantages, such as small size, light weight, low cost, immunity to electromagnetic interference, multiplexing and so on, which offer a widely application in optical sensing and communication field. Following the appearance of nano-fiber, it is imperative to develop the manufactured technology of nano-fiber devices, nano-fiber Bragg gratings are the important passive device among these. In this paper, we present a new method to fabricate the nano-fiber Bragg grating. In our theoretical analysis, effective refractive index of nano-fiber is a significantly parameter affected by the diameter of fiber, which determined the Bragg wavelength. A nano-fiber Bragg grating was fabricated through successive improvement of manufactured technology.

8561-35, Poster Session

Localized surface plasmon resonance properties of I-shape Ag/SiO₂/Ag nanoparticles

Juanyi Liu, Zhejiang Ocean Univ. (China); YuLiang Liu, Lili Li, Yaner Feng, QiuLiang Zhao, School of Electromechanical Engineering of Zhejiang Ocean University (China)

The plasmon resonance of I-shape Ag/SiO₂/Ag nanocube was studied using finite difference time domain numerical calculations. The result shows that I-shape nanocube exhibits higher extinction intensity due to its more "hot spots" compared to single layered metal nanoparticle. At the same time, a higher refractive index sensitivity which increases about 100 nm/RIU for single nanoparticle and about 65 nm/RIU for nanoparticles array respectively can be obtained. This structure holds a great potential in the application of bio/chemical sensing.

8561-36, Poster Session

The frequency mixing impact analysis of the light intensity noise with modulation signals in phase generated carrier (PGC) demodulation method

Jiaolong Yu, Jiaolong Yu, Anhui Univ. (China)

In order to improve the measurement resolution of laser Doppler interferometer, the noise of the system need to suppress, which the light intensity noise have a greater effect on the performance of the interferometer. By analyzing the impact of the light intensity noise inherent in the relaxation oscillation noise to the mixing signal of phase generated carrier (PGC) demodulation, arriving at a conclusion that the Low-frequency part of the light source intensity noise have a greater impact on the signal to noise ratio of PGC demodulation, and the phase carrier modulation signal have achieved the noise spectrum of the relocation. Optoelectronic negative feedback program is proposed to achieve effective suppression of the Low-frequency light source intensity noise and laser relaxation oscillation peak, which reduce the influence of the mixing of the light source intensity noise, furthermore the system signal to noise ratio (SNR) is improved.

8561-37, Poster Session

A structured light vision sensor for discrimination of failure laser radar data caused by multiple reflections of laser beam

Xiao Kang, Wei Zhu, Li Tian, KeJie Li, Beijing Institute of Technology (China)

Laser radar is widely used for obstacle detection. The emitted laser beam from the laser radar is reflected by the obstacle; laser radar receives the echo and processes the data by means of a time of flight calculation to get the position and size information of the obstacle. When obstacle is complex or the terrain is fluctuant, multiple reflections of laser beam often happen. Obstacle's position and size information obtained by the laser radar data in this situation are error. Hence how to discriminate these failure laser radar data caused by multiple reflections of laser beam is a key and difficult issue. A structured light vision sensor is proposed for the failure laser radar data discrimination which is composed of a point light source laser, fast piezoelectric ceramics steering mirror and high sensitivity industrial camera. Spots emitted by the laser are projected to the steering mirror and are formed the line structured light through the fast mirror swing. The image of the light stripe distortion which caused by the obstacle is obtained by the camera. Position and size information of the obstacle are obtained through fast image processing. When multiple reflections of laser beam happen, position and size information obtained by the structured light vision sensor and laser radar are different significantly. The conflict and contradiction of information is used for the discrimination of failure laser radar data. Experiment results show that the sensor can discriminate the failure laser radar data at the accuracy rate of 92%.

8561-38, Poster Session

A method for improving the performance of Brillouin echo system

Yongqian Li, Huan Li, Hu Wang, Qinghe He, North China Electric Power Univ. (China)

The high spatial resolution can be achieved in the traditional Brillouin echo system. Generally, the upper sideband of the CW light is eliminated before it enters into the fiber in this system, only the lower sideband interacts with the pulse light, but this system exists pump depletion, and the sensing length is limited. An improved method of distributed optical fiber sensing based on Brillouin echo is studied in this paper, a double sidebands signal of optical carrier suppressed (OCS) which includes the Stokes light and anti-Stokes light is produced by the modulation of the electro-optic modulator (EOM) with the technology of optical suppressed carrier modulation, and the Stokes and anti-Stokes light interact with the pulse light respectively, and the processes of Brillouin gain and loss occur simultaneously, as the pump light power is the dominate factor limiting the sensing length, based on the improved configuration, the pump almost unchanged. The distributed Brillouin signal are received by subtracting the two side bands of the OSC Stokes light, and the transient coupled wave equations of stimulated Brillouin scattering (SBS) are deduced by a time domain perturbation method, and the transient solution is also obtained. The improved Brillouin echo system compared with the traditional Brillouin echo system by Matlab simulation, the results show that a higher signal-to-noise ratio has been obtained in the improved sensing system, and the sensing distance of the system can be increased effectively with improving the spatial resolution and measurement accuracy.

8561-39, Poster Session

Use of bending of a single SMS fiber structure for measurement of temperature sensing

Yujuan Zhang, Qijin Zhang, Univ. of Science and Technology of China (China)

A simple temperature sensor based on a bent single mode-multimode-single mode (SMS) fiber structure fastened on polymer base plate is proposed and experimentally investigated. The surrounding refractive index (RI) is higher than that of the silica multimode fiber and the leaky structure is formed. Thus RI changes with temperature will lead to change of output intensity without wavelength shift. We set up a simple experiment to demonstrate that change the curvature of proposed SMS fiber structure will result in central wavelength shift. The proposed SMS fiber structure is put into oven thermostats and utilizes changing temperature to control the curvature of SMS fiber which is induced by expanding of polymer base plate. The shifts of central wavelength are measured at temperature range from 60 to 75 °C. The proposed temperature sensor offers sensitivity of 3.9 nm/°C, which is significantly higher than that of a normal straight SMS structure (10 pm/°C) or a grating-based fiber structure (FBGs:10 pm/°C, LPG:100 pm/°C).

8561-41, Poster Session

Ultra-long distance distributed fiber-optic system for intrusion detection

Dongsheng Tu, Zhaogong Jiang, Ningbo Nuoke Electronic Technology Development Co., Ltd. (China); Shangran Xie, Tsinghua Univ. (China); Shangjin Ren, Ningbo Nuoke Electronic Technology Development Co., Ltd. (China); Min Zhang, Tsinghua Univ. (China)

This paper research an ultra long distance distributed fiber-optic intrusion detects system based on bidirectional mach-zehnder interferometer. The system has a narrow linewidth laser source and a low noise photodiode amplify module at the each end of the interferometer. The laser source is amplified by a high power EDFA, then input into the mach-zehnder interferometer, and receive at the other end of the fiber. When an intrusion event is act on the fiber, the interference signal is different from the background. The other two communication fibers are used to transmit and receive the high speed synchronous codes. When system detects an intrusion event, recording the codes of the two ends. By measuring the time difference of intrusion signal caused by the event after high speed signal process, the location of the event along the sensing fiber is determined. The challenges of this system are to reduce the nuisance alarm rate and enhance the locating accuracy at ultra long distance. At the present experimental result, system implement the sensing length up to 100km, and the locating accuracy is one thousand of the full length.

8561-42, Poster Session

Characteristics of in-fiber Mach-Zehnder interferometer formed by lateral offset splicing

Xiujuan Yu, Ge Li, Shengchun Liu, Jintao Zhang, Xuefeng Chen, Liying Zhang, Heilongjiang Univ. (China); Yanbiao Liao, Tsinghua Univ. (China)

We present an in-fiber Mach-Zehnder type interferometer (MZI) in single mode fiber based on lateral offset splicing technique. The MZI relies on the interference between the fundamental core mode and a co-propagating cladding mode. To build an in-fiber MZI, we need

one element or device which excites two co-propagating modes and another one to recombine them. In our case, the excitation and recombination of modes is realized by two cascaded lateral offset splicing joints. The effects of the lateral offset amount, the interferometer cavity length, and the fusion splicing parameters on the property and performance of the in-fiber MZI were investigated experimentally. By choosing an appropriate lateral offset amount, the MZIs with good interference fringe contrast and low insertion loss can be fabricated. Several in-fiber MZIs with different interferometer lengths were built and it is found that the interference peak wavelength spacing is inversely proportional to the interferometer length L. The potential applications of the proposed in-fiber MZI were further investigated as temperature and strain sensors.

8561-43, Poster Session

Analysis on the performances of multiple parameters measurement base on the distributed optical fiber sensing system

Lei Qin, Wei Liu, Capital Normal Univ. (China)

With the rapid development of distributed optical fiber sensing technology, it has become a hot research issue. Distributed optical fiber sensors can simultaneously measure temperature and pressure information along the fiber distribution, which is usually continuous change in time and space. The distributed optical fiber sensing technology based on Rayleigh scattering and Raman scattering studies have tended to be mature, and gradually move toward practical. The distributed optical fiber sensing technology based on Brillouin scattering has a later start, but because of its the higher measuring accuracy, range and spatial resolution for temperature and strain compared with those of the other sensor technology, it has been extensive attention and research. In 2009, A. Wosniok and his partner in Germany report on the development of a distributed optical fiber monitoring system for strain and temperature detection along single-mode fibers, in which the sideband technology and digital filter are adopted in order to lower the shift influence and increase the frequency range.

In this letter, the distributed optical fiber sensing system based on Brillouin scattering is built, while maintaining precision, and multiple physical parameters are detected at the same time. The key technology and method are used to improve the signal receiving and processing capability.

8561-44, Poster Session

Distributed feedback fiber laser strain sensor with high sensitivity in a wide frequency range

Xiaolei Zhang, Shandong Academy of Sciences (China); Gangding Peng, The Univ. of New South Wales (Australia); Chang Wang, Zhihui Sun, Jiasheng Ni, Yingying Wang, Shandong Academy of Sciences (China)

A compact high-sensitivity distributed feedback (DFB) fiber laser strain sensor with length of only 56 mm is investigated. The intrinsic performances including optical efficiency, intensity noise of bare DFB fiber laser are tested before packaging. Theoretically the deformation in acoustic pressure field of DFB fiber laser with or without packaging can be simulated by finite-element method. Based on the simulation results a polyurethane spindle-like structure is applied for fiber laser packaging. By use of an imbalance Michelson interferometer and a standard optical phase demodulator, the frequency response of DFB fiber laser before and after packaging is tested in a vibration liquid sound field and compared to standard PZT hydrophone. The experimental results show that the prestress on bare fiber laser affects the frequency response rather than strain sensitivity; the frequency sensitivity of packaged DFB

fiber laser hydrophone is about $113\text{dB}\cdot\text{re}\cdot\text{Hz}\cdot\text{Pa}^{-1}$ at 1 kHz, which is 55 dB higher than bare fiber laser under the same prestress. It is remarkable that in a quite wide frequency range from 10 Hz to 10 kHz, it has a rather flat frequency response with about 18dB fluctuation.

8561-45, Poster Session

Surface plasmon resonance sensor based on grapefruit photonic crystal fiber filled with silver nanowires

Zhang Lei, Shijiazhuang Univ. of Economics (China)

The Photonic crystal fiber (PCF) has attracted more attentions for its flexible structure design and excellent optical performance, and it has become a new focus in the fiber optical research domain, particularly prominent in the research areas of fiber sensor. In recent years, many scholars put forward photonic crystal fiber (PCF) based SPR sensors. The sensing mechanism is through coupling the leaky core mode to the plasmon to achieve resonance sensing. The use of the photonic crystal fiber, with its flexible design, makes it easy to equate the effective index of the core mode to that of the material under test. Thus phase matching condition between the core mode and the plasmon can be easily achieved at the required wavelength and then resonance occurs.

In this letter, surface plasmon resonance sensors based on grapefruit-type photonic crystal fiber filled with silver nanowires have been analyzed through the finite element method (FEM). The regularity of the resonant wavelength changing with refractive index of the sample has been numerically simulated, and resonant wavelength detection as well as intensity detection sensitivity has also been discussed. The surface plasmon resonance sensing properties of PCF based on different nanowires structures are numerically simulated; Numerical results show that excellent sensing characteristics of the structure can be achieved as the radius of the silver nanowires is 150nm, with both spectral and intensity sensitivity in the range of $4?10^{-5}$ ~ $5?10^{-5}$ RIU.

8561-46, Poster Session

Discrete multi-target on-off states detection and location with optical fiber sensing system

Nian Fang, Lutang Wang, Zhaoming Huang, Chen Liu, Shanghai Univ. (China)

Multiple-target sensing is the development trend of the optical fiber sensing technology. People hope to employ a single sensing system to detect all targets needed. In many applications, alarms are usually necessary. In addition, some sensing systems are aimed to monitor the state changes of the targets, for example, a door being opened or closed. When multiple targets located at different places are required for their state detections, a sensing system capable of detecting on-off states of discrete multi-targets and their locations will be demanded. We present such an optical fiber sensing system composed of multiple cascaded 1x2 fiber couplers (FCs). Each FC is connected to a reflective optical switch sensor (ROSS). It can remotely detect on-off states of multiple ROSSs, as well as accurately and rapidly locate the ROSSs in alarm states. By detecting the various intensities of pulsing light reflected by each ROSS, their on-off states can be monitored. The ROSSs in alarm states can be located by directly measuring the reflected light pulse intensity at corresponding time axis or the declined peaks of short-time cross-correlation of reflection pulse train during adjacent optical pulse period in noisy case. The simulation results with the same and different ROSS intervals show that the detection and location methods proposed are feasible and effective. The discretely distributed ROSSs optical fiber sensing system can be used to detect and locate various kinds of physical and chemical parameters at the same time, which reflect state changes of the ROSSs. Although the proposed system is similar to the optical time domain reflectometry (OTDR), it has lower cost and better real time performance than OTDR.

8561-47, Poster Session

Camera calibration external parameters amendments in vision measuring

Yexin Zhao, Naiguang Lv, Xiaoping Lou, Beijing Information Science & Technology Univ. (China)

In the field of vision measuring, camera calibration is a necessary precondition of the three-dimensional measurements. Especially, in binocular vision measurement system, the calibration accuracy plays a vital role on the reconstruction of 3D objects coordinates, therefore, camera calibration is researched. The main content of the paper is that the system model of camera calibration, principles as well as procedures in some traditional calibration methods is discussed; in addition, the problem of external parameters calibration is found and some effective amendments to it is made to achieve a better calibration results. The article is mainly divided into four parts to discuss. Firstly, the principles, steps and system model of the camera calibration was described; Secondly, the common methods for external parameters calibration was discussed, the inadequacies which cycling conditions restrict external parameters calculation and make it not be optimized fully in the optimization process was elaborated, then a new amended method was designed to solve the above shortcomings, according to optimized internal parameters and part-optimized external parameters, cycling condition was re-selected and external parameters was calculated with Least Squares Method, thus effective corrected values was obtained so that the calibration accuracy of the external parameters can be improved. Thirdly, binocular vision system calibration experiments was carried and detailed comparison of the calibration accuracy before and after the correction of external parameters was made, it has been found that standard deviation, variance and the maximum error of three-dimensional reconstruction after the correction of external parameters is less than the calibration error before the correction; Finally, the summary on research was given.

8561-48, Poster Session

A new AD device application in the CCD signal process system

Su Lei, Beijing Institute of Space Mechanics and Electricity (China)

A new Analog-Digital (AD) device is introduced in this paper, which is newly applied on the signal process circuit of the high resolution remote sensing Charge-Coupled Device (CCD). Base on the signal process circuit, the hardware and software design was introduced. In hardware, the new AD had two selectable operated modes which are CDS mode and S/H (Sample Hold) mode. And the new AD output had LVDS transmission. The AD's output was transferred to the FPGA whose IO pin was designed in special mode to receive the LVDS mode data. The frequency of the LVDS data transmission should achieve over 320 Mhz. In software, the software program was designed in VHDL language with Xilinx FPGA to provide the driving signals to the AD and other devices, to handle the data and signals which were received from the AD and other devices in the signal process circuit. The program was introduced in brief chart and the program was divided in three main function modules. The three modules were illustrated one by one with their own figures. The different operate modes of the AD's registers should be selected in the program and the main function of the AD's main registers' were validated and introduced. The image was got by using this signal process system and was analyzed with the MatLab software. According the Analysis this new AD signal process circuit had low noise and high signal to noise ratio which was compared to the contemporary circuit system.

8561-49, Poster Session

Measurement and analysis on infrared imaging system performance under libration

Wang Jing, Ji ming, Xi'an Institute of Applied Optics (China)

The stabilization-aiming system is the important component element of the precision strike tactical weapon system. Helicopter stabilization-aiming system is librated strongly because of the strong libration resulted by the engine and airscrew during the helicopter flight, which affect seriously the performance of the electro-optical system, and the viewing distance is an important performance of the electro-optical system, so the problem how the helicopter libration affects the viewing distance of the electro-optical system is badly in need of solution. A method of measuring dynamic MRTD of infrared imaging system is advanced in this paper, the relation between helicopter libration quantity and viewing distance is analyzed utilizing MRTD. The experimental installation is designed and developed, The libration of helicopter stabilization and aiming system is simulated by experimentation, the infinity dynamic object is formed, based on this object, the test images and data are gotten, and in order to get the MRTD of infrared imaging system under libration, the test image and data are analyzed by image processing and statistical methods. Experimentation result shows that measurement of dynamic MRTD can be achieved commendably utilizing the advanced method and experimental facilities, which establishes basement for estimating the viewing distance effect from libration in the laboratory.

8561-50, Poster Session

Multiplexing of double cladding fiber sensors for bending sensor

Libo Wu, Fufei Pang, Zhenyi Chen, Tingyun Wang, Shanghai Univ. (China)

Double cladding fibers (DCF) have been researched comprehensively for sensor applications. Through evanescent wave coupling, cladding modes can be excited resonantly in the DCF. The transmission of the DCF presents a band-reject filtering spectrum. According to the shift of the transmission spectrum, many sensors have been developed including the parameters of bending, temperature, refractive index, strain and so on. However, since the transmission spectrum has a relative large bandwidth, it is difficult to multiplex such sensors in wavelength domain. In this paper, a multiplexing technique of DCF sensors is proposed and demonstrated for bending sensor network. A time-division multiplexing system with four DCF sensors in parallel is adopted in the experiment. We can control the optical path difference of the four sensing branches reasonably to separate the four sensing signals. To demodulate the sensing signals we adopt an edge filtering technique, and a DFB laser pulse light source is used. As the DCF is used as bending sensor, the resonant wavelength shifts to short wavelength and the amplitude of that also changes when the bend degree is deepening. According to the edge filtering effect, the shift of the resonant wavelength results in the variation of the intensity of the transmission light received by the detector. Through this property we can get the bending information. The results show that the multiplexing sensor system can have a good monotony when the curvature from 0 to 1.8m^{-1} . This time-division multiplexing system can provide a large multiplexing capacity due to the high spatial resolution.

8561-51, Poster Session

Study on an ammonia sensor with high sensitivity in farmland based on laser absorption spectroscopy technology

Ying He, Yujun Zhang, Liming Wang, Kun You, Yanwei Gao, Anhui Institute of Optics and Fine Mechanics, CAS (China);

Anning Zhu, Wenliang Yang, Institute of Soil Science, CAS (China)

High nitrogen fertilizer input is the main manner to maintain the high-yield crops in farmland in China. The average application quantity of nitrogen fertilizer in China is significantly higher than some developed countries in the world. However, the nitrogen fertilizer utilization efficiency is very low. Thus, high sensitivity sensing and on-line monitoring ammonia concentration were needed to quickly acquire the soil nutrient information and to get the nitrogen fertilizer utilization efficiency. A high sensitivity ammonia concentration sensor used in farmland has been developed based on Tunable Diode Laser Absorption Spectroscopy (TDLAS) technology, high frequency modulation technique and long optical path technique. TDLAS is a method to obtain the spectroscopy of gas molecule single absorption line in the characteristic absorption spectrum region as the characteristic of the distributed feed back (DFB) laser with narrow line width and tunability. A sensor array formed with three ammonia concentration sensors by distributed sensing technique was used for ammonia volatilization experiment in a wide range of farmland. It was verified that the performance consistency of the three ammonia sensors was good and the sensor array realized the regional ammonia concentration monitoring. Continuous measurement results showed that the ammonia concentration influenced by the volatile source location, wind direction, weather and other factors, and it was positively correlated with the ammonia volatilization rate. The ammonia sensor array is suitable for continuously ammonia volatilization monitoring in a wide range of farmland environment with its high sensitivity, rapid response time without gas sampling.

8561-52, Poster Session

A pressure sensor based on high-birefringence fiber loop mirror

Tiancong Xu, Shuyang Hu, Dongmei Bai, Beijing Univ. of Technology (China)

Recently, high birefringence fiber loop mirror (HiBi-FLM) has been widely used in gain flattening of erbium-doped fiber amplifiers, multiwavelength and wavelength-switched fiber lasers, demodulation of fiber Bragg grating sensors and dispersion compensation. Because the stress-induced high birefringence fiber (such as Panda fiber) is sensitive to temperature and strain, HiBi-FLM can be used as sensor. In this paper, a pressure sensor based on high-birefringence fiber loop mirror is proposed and demonstrated in the first time. Part of the HiBi-fiber is pasted on the out surface of a ring rubber gasbag that is inflated and elastic, and this part will serve as a sensitive probe to measure the pressure. When outside pressure changes, the volume of the gas in the ring rubber gasbag changes and it makes the strain of the high-birefringence fiber vary. The relationship between shift of the resonant wavelength (peak wavelength) and pressure is discussed and experimentally researched. The formula of the relationship between the resonant wavelength shift and pressure change is derived and it shows that the shift is approximately proportional to pressure change. Moreover, The sensing range and sensitivity can be adjusted by setting the initial inner gas pressure. Experimental results show that the sensitivity is $1.63 \times 10^{-3} \text{nm/Pa}$. This sensor also has many advantages such as high sensitivity, polarization independent, easy manufacture, low cost.

8561-53, Poster Session

Design of semiconductor ice box cooled by solar power supply

Jie Hou, Hebei Univ. of Science and Technology (China); Shiquan Qiao, Jun Zuo, Hebei University of Science and Technology (China); Shuwang Chen, Hebei Univ. of Science and Technology (China)

A design of deepfreeze box is introduced in the paper, which is supported by solar power supply. The box is constituted by four major parts. There are a solar power panel, a solar charge controller, a hermetic box and a series of semiconductor frigorific pieces. The solar power panel collects solar energy through the Photovoltaic effect. The solar energy is stored in storage battery after being regulated by the DC/DC converting circuit of the solar charge controller. The charge controller circuit contains over-charging circuit, over-discharging circuit, short circuit, overload circuit and reversed polarity protection circuit. The storage battery then supplies power to the deepfreeze box. The solar charge controller can automatically track the maximum power point in terms of the solar intensity. The cooling system is made up of semiconductor frigorific pieces, whose power is exclusively provided by solar energy. The whole device is small and portable, and can be applied in some areas of environmental protection and energy saving.

8561-54, Poster Session

Bending characteristics of long-period fiber grating with a over-coupled resonant wavelength

Chunying Guan, Xiaozhong Tian, Harbin Engineering Univ. (China)

The characteristics of LPFG fabricated using high-frequency CO₂ laser pulses exposure in conventional fibers have been well researched in numerous previous literatures. In comparison with other fabrication methods, high-frequency CO₂ laser pulses exposure has many unique advantages, including high efficiency, low cost, low insert loss and easily repetitive exposure. The bending responses of such a LPFG depend strongly on the bending direction, and this character may solve the problem of cross-sensitivity between bending and other measured parameters.

In present paper, a special CO₂-induced LPFG is fabricated in the single mode fiber. There are two resonant peaks in the wavelength range of 1000-1700nm, one of which is over-coupled while the other is not. The grating period is 500 μm and the number of period is 50. We stop the exposure when the amplitudes of two resonant peaks are nearly equal. The bending character of this LPFG is experimentally studied in detail. The results show that the distance between the two resonant wavelengths has a periodic behavior along its circular directions. Under a specific bending direction, the distance between the two resonant wavelengths increases, while under the opposite bending direction, the distance between the two resonant wavelengths decreases. Also the distances between the two resonant wavelengths change nearly linearly against the curvature under the two bending direction mentioned above. The bend sensitivities under these two bending directions are 7.19nm/m and 3.13nm/m, respectively. In addition, with further bending under the direction which makes the distance increases, the over-coupled peak split into two peaks, which has not been found in normal uncover-coupled LPFG.

8561-55, Poster Session

FDMA/TDMA hybrid MAC protocol for wireless sensor network

Qi Qi, Hong Wu, Lei Ji, Beijing Institute of Technology (China)

An efficient MAC protocol is one of the keys for long-time working and high-efficiency communication of WSN. In this paper, we develop a new MAC protocol that based on hybrid FDMA/CDMA technology with three-jump network for achieving long-distance and low power about data transmission. This protocol combines the advantages of both FDMA and TDMA. The communication of cluster heads is based on FDMA technology which can decrease the crosstalk between different frequency and the cluster heads can identify each other easily; the inter cluster communication is based on TDMA technology to achieve basic time synchronization. Then the time synchronization of the network

was obtained. At the same time, the three-jump network increased the range of communication system and reduced the power. The protocol adopts cluster head rotation mechanism, pick the higher power nodes as the cluster head that that drifted higher over the life of the whole network. The design uses CC1120 as the wireless transceiver chip, MSP430FR5739 as main control chip, because MSP430FR5739 belongs to ferroelectric memory which can preserve data better. A typical representative of competition-based periodic sleep MAC protocol for wireless sensor network is S-MAC. Compared with the traditional S-MAC protocol, TH-MAC has the advantages of low crosstalk between frequency, low power and low latency. This algorithm is suitable for the large-scale collection of data and information about industry and agriculture and has an extensive range of applications.

8561-56, Poster Session

Theoretical study of the fiber nonlinear polarization sensing based on whispering gallery modes

Rui Yang, Hai-peng Jin, Yunnan Univ. (China)

The optical circular micro-cavity has been applied in highly sensitive sensors because of its whispering gallery modes (WGMs) with very high Q quality and very small mode volume. Fiber was a kind of optical circular micro-cavity structure, in which WGMs were excited in its cross section by evanescent field. The spectral position of the WGMs shifted in response to the change of correlative refractive index.

However, electromagnetic field in optical fiber was limited within two dimensions at wavelength range. As a result, intense light power density enough to excite the nonlinear interaction was easy to obtain in fiber. The nonlinear polarization interaction caused by strong incidence light field or external field results in slight change of refractive index of the fiber. It was the WGMs of fiber to detect this slight change of refractive index. Therefore it provides an observable sensing method for studying the nonlinear refraction effect of fiber.

In this paper, basing on the quantum model of WGMs in cylindrical optical micro-cavity, resonance spectral shift equation which indicates the variation on spectral position of WGMs with refractive index of fiber's dielectric was derived using quantum perturbation theory. Hence, the refractive index changes caused by the nonlinear effect of fiber were reflected through the observable resonance frequency shift. The calculation showed that a sensitivity of approximately 50 nm per RIU (refractive index unit) was achieved due to the extremely high Q factor associated with the WGM.

8561-57, Poster Session

A HBF strain sensor with piezoelectric ceramic based on Sagnac LM

Lidan Yin, Li Wang, Beijing Univ. of Technology (China)

The fiber sensors have the advantages of high sensitivity, light weight, small size, resistance to electromagnetic interference and corrosion resistance. Because the HBF sensors have the better characters than traditional ones, so in real life, HBF sensors have been more widely used, especially strain sensors are used in the monitoring of buildings and bridges. In the experiments, due to the sensing characters of Sagnac LM, especially in the temperature sensors experiments, the trough (or peak) of each intervention is not completely overlap, which is a zero error, so the experimental data generally take the distance of the wavelength shift, rather than specific wavelength of the trough (or peak) data. It's more difficult to compare the data of every experiment. The strain sensor can be used to compensate the zero error in the experiments.

This article about HBF strain sensing characters is divided into three parts.

The first part, study the stress-sensing characters of high birefringence

and calculate the corresponding theoretical data and stimulate the graph, in the 0 - 120V (providing to piezoelectric ceramic) and wavelength shift (nm), in theory.

The second part, compare the experimental graph with theoretical graph and compare the difference between elliptical fiber and Panda fiber.

The last part, apply the HBF strain sensor to optical fiber temperature sensing experiments, predict the compensated voltage to zero error, which exists between the foregone experiment and this experiment when the voltage is zero, before this tested experiment and compare the predicted data and experimental data.

8561-58, Poster Session

PH sensor using fiber Bragg grating based on swelling of hydrogel

Xiaohua Lei, Chongqing Univ. (China); Bo Dong, Jianmin Gong, Anbo Wang, Virginia Polytechnic Institute and State Univ. (United States); Weimin Chen, Chongqing Univ. (China)

The pH value is a very important parameter in environment monitoring. When the area under investigation is quite large, pH measurement at multiple points is preferred.

Because hydrogel, which is a blend of PVA (vinyl alcohol) and PAA (acrylic acid) polymer, is sensitive to pH value, many pH sensors based on hydrogel were developed. One type of pH sensor is based on hydrogels which are coated directly onto optical sensors. For this kind of sensors, Hydrogel coating is prone to separate from the fiber sensors; therefore this method is not very reliable. But fiber sensors are easy to be multiplexed, so this type of pH sensor is easy to be fabricated for multi-points monitoring. The other type of pH sensor is based on swelling of hydrogels which is transferred to deflection of a micro-mechanic structure and then the deflection is detected by other sensors. For this type of sensor, hydrogel and other sensors are not connected, so it is more sensitive and reliable, but hard to be fabricated for multi-points monitoring.

Here we proposed a new pH sensor based on pH sensitive hydrogel swelling detection by a fiber Bragg grating, which combines advantages of those two methods. The deflection of a silica membrane due to pH value change induced hydrogel swelling is measured by the center wavelength shifts of a fiber Bragg grating epoxied on the membrane. The relation between center wavelength shifts of the fiber Bragg grating with the hydrogel swelling behavior was studied experimentally. Around 100pm shift of the fiber Bragg grating center wavelength was observed when the pH value was changed from 4 to 7 or from 7 to 10 by using pH standard solutions, which fundamentally proved the feasibility of this method for pH detection.

8561-59, Poster Session

Study of a novel micro-displacement measurement system based on chromatic confocal technology

Xiaofei Liu, Wenyi Deng, Chun-Hui Niu, Boshi Jin, Beijing Information Science & Technology Univ. (China)

A chromatic confocal system for measuring micro-displacement is designed and its performance is studied in the paper. First, the measurement principle of the system is introduced, and an actual measurement system is built based on chromatic confocal technology. Second, Gaussian fitting algorithm is used to fit every group of experimental data in order to obtain the peak spectral response curve, and to obtain the wavelength corresponding to the peak. The LM algorithm (Levenberg-Marquardt algorithm) is presented to solve the parameter vector of Gaussian function. The peak position parameter stands for the corresponding wavelength of every peak of the spectral response curve. And then, the calibration to the experimental system

is performed by using dual-frequency laser interferometer, so as to find corresponding relationship between peak wavelengths and displacements of the reflecting mirror. With the quadratic polynomial fitting method, the corresponding relation is described to get the benchmark curve. The linearity is calculated according to the calibration curve and the benchmark curve. Finally, precision analysis about the measurement system is described, aiming at such factors affecting the measurement accuracy as light source, pinhole diameter, resolution of the spectrum analyzer, the optical lens design and optimization method, the data processing method, the calibration method, etc. The experimental results indicate that the measuring range of the chromatic confocal system is 20mm, and the measuring precision can reach 10 μ m, the linearity is relatively good. And it is proved that the designed system can satisfy the rapid displacement measurement requirements with very high precision.

8561-60, Poster Session

An experimental study about humidity sensors based on tapered optical fibers

Xinghu Fu, Guangwei Fu, Weihong Bi, Yanshan Univ. (China)

In order to ensure the normal living and production, it is necessary to monitor air moisture content in different environment, including air conditioning, sterilizers, nutritional products manufacturing, and so on. Optical fiber sensors present advantages such as small size, immunity to electronic magnetic fields, high sensitivity, etc. Moreover, they can be used to detect the humidity induced refractive index changes. Thereby, a humidity sensor is proposed for detecting air moisture content based on tapered optical fiber. According to optical energy transmission theory, the sensing mechanism of humidity sensor is described by analyzing the evanescent field around the sensing fiber. The relationships between the dimensions and spectral characteristics of the taper have been analyzed, respectively. The results show that the taper shape is important for designing a humidity sensor and the spectral characteristics variation can reflect the evanescent field intensity. A straightforward experiment is performed to prove the wavelength dependence of the sensitivity. It is mainly composed of an ASE broadband source, an optical circulator, a tapered optical fiber and a spectrum analyzer. The fitting curves can be obtained by comparing the characteristic wavelengths and humidity, and the errors are also given. The humidity is analyzed in different air moisture content. The humidity measurement resolution is 1% as the measuring range varies within 50-95%. The characteristic wavelengths have a blue shift and decrease as increasing humidity. Thus, the high dynamic performance can allow this sensor to be used for humidity monitoring in time.

8561-61, Poster Session

A novel safety light curtain system using a hemispherical mirror

Yusuke Kenjo, Ryosuke Suzue, Huimin Lu, Kohei Miyata, Shiyuan Yang, Seiichi Serikawa, Kyushu Institute of Technology (Japan)

Light curtain systems are used to detect intruders in various cases and places. However, it is necessary to adjust the position of the light detecting element accurately in order to receive the irradiating laser light. We propose a new type safety light curtain system that uses a hemispherical mirror and an LED in this research. A hemispherical mirror can reflect irradiating lights surroundings of 180° in the vertical direction and 360° in the horizontal direction. So that even if an LED is arbitrarily set up, the LED irradiating light can be reflected by the hemispherical mirror, when the LED is at a position that is higher than the hemispherical mirror, and the light detecting element can receive the LED irradiating light. In the case that the light of LED is intercepted when an intruder passes between the LED and the hemispherical mirror, the output voltage of the light detecting element decreases. We can set a proper threshold voltage value of the detecting element to judge

whether an intruder passes or not. Our system uses a microcomputer to judge the output voltage of the receiving element with the threshold voltage value and the LED output light is modulated by 10kHz in order to avoid the influence of the surrounding turbulence light. Our experiment succeeded to detect intruder using the proposed system without accurate light axis setting.

8561-62, Poster Session

A single-photon detector without cooler

Bing Zhou, Fu-yu Huang, Dong-sheng WU, Jie Liu, Shijiazhuang Mechanical Engineering College (China)

Avalanche photodiode (APD) single-photon detector, which has been the research pivot of single photon detection technology, has the advantage of high quantum efficiency, low power consumption, large performance spectrum range, small volume, low operating voltage and so on. In the detection, APD usually works in Geiger mode and the bias voltage is higher than avalanche voltage. But when the temperature rise, the avalanche voltage would become higher and the diode's noise would rapidly increase around the avalanche voltage. Therefore APD single-photon detector is usually cooled by using fluid nitrogen or thermoelectricity cooling to stability APD's work circumstance temperature to ensure avalanche voltage stabilization and also deduce detector noise and enhance the SNR. The adoption of cooler increases system complexity and restrict the serviceable range of the detector.

One type of single-photon detector that without cooler, which is mainly consisted by noise voltage control circuit and precise pulse width detection circuit, is presented. The noise voltage control circuit is using the characteristic the noise rapid increase in avalanche voltage. The detector signal after forward and video amplifier is measured. When noise voltage exceed a certain range, the bias voltage would be decreased; when noise signal minished, the bias voltage would be increased. So the bias voltage of APD is dynamically fixed by certain voltage. When the avalanche voltage changes with the temperature, the noise character nearby avalanche is resemble. So the bias voltage could be stabilized based on noise character. The detector's output SNR would descend greatly if there was no cooler, and the phonon avalanche signal would not measured efficiently by the tradition extent detection. Considering the difference of time width between photon avalanche signal and noise signal, the precise pulse width detection circuit is designed. It can filter the narrow noise signal and only detect photon avalanche signal which has larger pulse width efficiently.

8561-63, Poster Session

Surface plasmon resonance sensor based on multihole optical fiber with TiO₂ layer

Chunying Guan, Di Gao, Harbin Engineering Univ. (China)

The surface plasmon resonance (SPR) is defined as the physical process that surface plasmons which propagating at the metal/dielectric interface are excited. The surface plasmons are extremely sensitive to even small changes of the refractive index of the dielectric. The fiber optic SPR sensor is a unique combination of optical fiber technology and SPR technology. In the past few decades, because of the advantages of high sensitivity, small size and real-time monitoring, the optical fiber SPR sensor has been widely applied in biochemical detection, environmental and food testing, structural health monitoring.

A novel SPR sensor based on the multihole optical fiber is proposed and numerically characterized in present paper. The six air holes in the multihole fiber are firstly covered by a thin gold film which supports the surface plasmons, and then coated with a uniformed titanium dioxide layer which is used to facilitate spectral tuning of the device and protect the gold film. The finite element method is used to analyze the characteristics of the surface plasmon resonance sensor. The effects of the size of fiber core and the air holes, the pitch between air holes, the thickness of the gold film and titanium dioxide layer on the sensor

are investigated, and the sensitivity of proposed sensor is also given. The results indicate that the resonance wavelength shifts to longer wavelength and the resonance peak broadens when the thickness of gold film increases, and the spectral tuning of the resonance can be more efficiently realized by changing the TiO₂ layer thickness. The resonance wavelength is also sensitivity to the refractive index of the liquid analyte, while the resonance wavelength doesn't move basically when the fiber core size, the pitch between air holes, and the size of air holes vary. The maximal sensitivity of the proposed sensor reaches to 10⁻⁴/RIU.

8561-64, Poster Session

Effects of diameter on characteristics of a long-period fiber grating

Xiaobei Zhang, Zhaohui Yin, Yang Li, Fufei Pang, Yunqi Liu, Tingyun Wang, Shanghai Univ. (China)

As a transmission type fiber passive device, the long-period fiber grating (LPFG) has been greatly applied in optical fiber communication and sensing fields. LPFGs are sensitive to variety of the surrounding medium, while the sensitivity can be enhanced by reducing the fiber diameter through tapering or thinning the fiber using the flame torch, laser and chemical etching.

In this paper, effects of diameter on characteristics of a LPFG are presented, such as the coupling coefficient, refractive index (RI) sensitivity, resonant wavelength and the shape of attenuation dips. By numerical simulations, the couplings between the core mode and the HE, EH cladding mode increase as the fiber diameter decreases. EH cladding mode increases faster than that of HE cladding mode. When the fiber diameter reduces to a certain dimension, coupling of EH cladding modes are analogous to HE cladding modes. Therefore, the coupling of EH cladding mode must be taken into account. Moreover, comparing with LPFGs in common fiber, the depths and bandwidths of the attenuation dips of LPFGs in thinner fiber vary faster as functions of the grating period, the grating number, and the RI modulation depth due to the increases of the couplings coefficients.

The resonant wavelength shifts to the shorter wavelength and the RI sensitivity is greatly enhanced when reducing the fiber diameter. Therefore, we can utilize the higher sensitivity of high-order cladding mode at a suitable wavelength by thinning or tapering the fiber. Furthermore, the sensing resolution and the cladding mode can also be selected by controlling the fiber diameter. We also find that the RI sensitivity of LPFG increase as a function of the exponential shape when the external RI increasing to the cladding RI whatever the fiber diameter is.

8561-66, Poster Session

The implementation of zero-phase high-pass filtering in interferometric fiber-optic hydrophone system

Yaowen Xiao, Tsinghua Univ. (China)

We need high-pass filtering in interferometric fiber-optic hydrophone system. In this paper, two methods of zero-phase high-pass filtering are introduced. The two methods are based on infinite impulse response (IIR) filter and frequency filtering alternatively. The forward and reverse filtering, as the name suggests, is filtering the input data in sequence and in reverse successively. And according to the order of the operations, the method can be divided into two sub-methods. One is FRR, which means forward filter, reverse filter, reverse output. And the other is RRF, which means reverse filter, reverse filter, forward output. Both FRR-method and RRF-method can completely eliminate the influence of the nonlinearity of the phase-response to achieve the zero-phase filtering. Frequency method means doing filtering in frequency domain directly. We get the frequency-domain representation by using Discrete Fourier Transform (DFT). As to the frequency range we

want to filter out, we simply make it zero. Then we use Inverse Discrete Fourier Transform (IDFT) to get the time-domain representation of the output data. Both the two methods can shorten the data processing time compared to finite impulse response (FIR) filter on the expense of memory cost, which is also discussed in this paper.

8561-67, Poster Session

Experiments research on motion detection accuracy of joint transform correlator

Guang Lin, Qi Li, Huajun Feng, Zhihai Xu, Zhejiang Univ. (China)

Typical JTC includes laser sources, Fourier lenses, image sensors, spatial light modulators, and etc., and this article discusses the influence factor on JTC motion detection accuracy. The shapes, brightness uniformity of the correlation peak were closely related to the detection accuracy, and the former has more significant influence than the latter. As the same time we found in experiments, the laser power level has an important influence on the detection results: the laser power level of input image influences the graph of power spectrum, and changes the last shape of correlation peak image. The image quality first rises and then reduces as the power rises; the laser power level of the output power spectrum affects the collected correlation pattern, and changes the SNR of the correlation peak image. The image quality first rises and then reduces as the power rises, too. The effectiveness of these conclusions is verified among different input images during this paper.

8561-68, Poster Session

The design of multi-parameter detection platform of drinking water based on two-electrode voltammetry

Yazhuo Li, Jiali Wei, Xiaoping Wang, Zhejiang Univ. (China)

A novel detection and analysis platform which is based on two-electrode electrochemical voltammetry system has been developed for multi-parameter measurement of drinking water. There are three unit in this platform, multi-sensor unit, hardware system unit and control and processing software unit. After choosing detection objects on computer, the control and processing software unit can control the hardware system unit apply corresponding potential on appropriate working electrode automatically. Currents can be collected on counter electrode and sent to computer for data processing. The multi-sensor unit contains Ti, Pt, Au, etc. noble metal electrodes as working electrodes and a large area ringlike stainless steel was as counter electrode. Comparing with conventional three-electrode voltammetry system, reference electrode has been eliminated in this platform by mechanical improvement of sensor array. This platform has been employed on detection of two common parameters in drinking water, electric conductivity (EC) and concentrations of heavy metal ions. In EC measurement, bipolar pulse with high frequency has been applied on Pt working electrode. In heavy metal ion of lead detection, staircase wave stripping voltammetry was applied on Ti working electrode. This detection platform owns high mechanical strength sensor, low maintenance requirements and easy to use, it could be used for drinking water quality monitoring in laboratory or industry locale.

8561-69, Poster Session

Gas detection system using off-axis cavity enhanced absorption spectroscopy

Wei-dong Zhou, Zhiwei Wu, Zhejiang Normal Univ. (China)

Abstract: A real-time, on-line trace gas detection system based on high-resolution off-axis cavity enhanced absorption spectroscopy (OA-CEAS) technology was developed by employing a high finesse

optical cavity and a tunable external cavity diode laser (ECDL) system. The performance of the system was demonstrated by using the carbon dioxide as the sample gas. Both high resolution and medium resolution spectra of the detected gas can be recorded. The vibration-rotational spectra of CO₂ molecule at room temperature was obtained in the wave number range of 6450~6530 cm⁻¹, which has a medium resolution and can be used to compare with the standard database of CO₂ line and to identify the existence of the CO₂ in the gas mixture. While a high resolution spectra of CO₂ can also be recorded, and be used to evaluate the relationship between the spectral line intensity, line-width and the gas concentration. Using the high resolution spectrum of the CO₂ molecule weak absorption line of 6358.65cm⁻¹, a sensitivity of 1.98×10⁻⁷ cm⁻¹ was achieved by using the detection system, and can be used for pollution gas detection in the environment.

8561-70, Poster Session

A new type fiber-optic accelerometer

Chang Yang, Tianjin Univ. (China); Hongpu Zhou, Min Zhang, Tsinghua Univ. (China); Fajie Duan, Kai Wang, Tianjin Univ. (China); Yanbiao Liao, Tsinghua Univ. (China)

A novel all-metal fiber-optic accelerometer based on Michelson interferometric configuration is proposed by using mass blocks and flexible reed structure. The axial direction of the sensing arm is configured to be parallel to the direction of acceleration, which directly transform the applied acceleration to fiber deformation in axial direction, which increases the acceleration sensitivity of the sensor. The reed serve as a transducer, by alternating which the sensor's performance can be improved. And metal material is adopted to enlarge sensor's applied range. Using the reed of 1mm thick and the mass block of 208g, the acceleration sensitivity of 556rad/g(55dB) is achieved by this structure. In the case of 10⁻⁵rad noise floor, the minimum detectable acceleration is 20ng.

8561-71, Poster Session

The research and implementation of mobile sink for the regional information monitoring system based on WSN

Biyao Shen, Hong Wu, Beijing Institute of Technology (China); Lei Ji, BEIJING SHIDAIJINPU S&T DEVELOP CO.,LTD (China)

As a new area of research, Wireless Sensors Network (WSN) has played a significant role in regional information monitoring area for its potential practical value. However, the promotion of WSN has been limited because of its short lifetime. In a traditional multi-hop WSN, the nodes close to the static Sink easily suffer the energy failure for transmitting large amounts of extra data. This leads to an "energy hole" phenomenon in WSN and finally causes the early death of the whole network. To solve this problem, a mobile Sink was brought in to balance the energy consumption of the whole network. This Mobile Sink Wireless Sensors Network (MSWSN) has recently received a lot of attention from the research community. Based on this view, the paper presents a design proposal of a mobile Sink used in regional monitoring area. To achieve the design requirement, the hardware platform is designed based on a LM4F232H5QD ARM Cortex-M4 processor and the driver program and applications are designed based on embedded real time operation system μC/OSIII. This mobile Sink could not only transmit data, but also calculate its location through a 3-axis analog accelerometer and then reveal the information of its current location through OLED. Compared with traditional WSN, MSWSN shows appealing characteristics of providing longer network lifetimes and the flexibility to adapt dissemination strategies according to applications' requirements and has proved to be more efficient.

8561-72, Poster Session

The study of intelligent temperature measurement based on optic fiber

Xiaoqiao Xing, Yuexiang Peng, Beijing Univ. of Technology
(China)

The Sagnac loop mirror of high birefringence fiber is developing greater more than other fiber because it has the advantages of high precision, wide spectrum and simple structure in applications.

In this paper, general theory of Sagnac loop mirror of high birefringence fiber is presented. Since Sagnac loop mirror of high birefringence fiber is more sensitive to its environmental temperature, an intelligent temperature measurement system based on Sagnac loop mirror of high birefringence fiber is designed. A 1550nm-laser is used as source light going through the high birefringence fiber Sagnac loop mirror. The amplitude of output beam is converted into electrical signals with Photo-Diode (PD), and the signal is collected by the MCU to complete the analog-digital conversion. After calibration, the temperature is calculated, and then shown on LCD displayer. Various parts of the electronic measurement system are introduce in details, containing MCU C8051F020 microcontroller, its internal AD-convert, calibration program and measurement program of temperature. In addition, the paper also introduces the structure and working principle of the high birefringence fiber Sagnac loop mirror system. The fiber optic temperature measurement system is compact, solid with good portability, as well as independent real-time analysis of data processing capability. It's provides a good preliminary basis for implementation the new fiber-optic temperature measurement system. And this system has broad application prospects of a good practice. The arrange of temperature measurement is from 30°C to 50°C with accuracy $\pm 0.2^\circ\text{C}$ in recent research experiment.

Conference 8562: Infrared, Millimeter-Wave, and Terahertz Technologies II

Monday - Wednesday 5 -7 November 2012

Part of Proceedings of SPIE Vol. 8562 Infrared, Millimeter-Wave, and Terahertz Technologies II

8562-1, Session 1

Review of THz wave air photonics (*Invited Paper*)

Xi-Cheng Zhang, Univ. of Rochester (United States)

Summary

THz wave air photonics involves the interaction of intense femtosecond laser pulses with air. The very air that we breath is capable of generating and detecting THz field strengths greater than 1MV/cm and useful bandwidth from 0.1 THz to over 10 THz. Remote broadband THz wave sensing is feasible.

Introduction

Laser-induced-gas-plasma can be used to generate intense, coherent, broadband, and highly directional THz waves through a nonlinear optical process. Moreover, plasma in ambient air or other selected gases can be used as a THz wave sensor. One technique, termed THz air biased coherent detection (THz-ABCD), provides superior bandwidth (0.1 to 40 THz), detection sensitivity (heterodyne method), and frequency resolution (MHz).

Here we review THz wave generation and detection techniques, sensing methodologies, applications for material classification, remaining challenges, and future opportunities for this rapidly evolving area of research that transcends the "gap" once existing between optics and electronics.

THz wave air photonics

Fig. 1a illustrates this all-optical process for the generation and detection of THz waves by using an air emitter and sensor, the system is called as THz air-biased-coherent-detection (THz ABCD). The laser-induced air plasma, shown as a bright spot in Fig. 1b, emits a very intense, highly directional, ultra-broadband THz field. Similar to the widely used generation and detection of THz waves in electro-optic crystals by second-order optical nonlinearity, the THz waves can be detected by the third-order optical nonlinearity in air.

Challenges, Limitations, and Opportunities

Although laser air photonics technology has opened new possibilities for application, many areas remain for improvement. Remote sensing and standoff detection with THz waves could be considered one of the most challenging topics in THz sensing. Due especially to strong water vapor attenuation in the THz frequency range and insufficient THz power, broadband THz sensing has been limited to short distances (a few meters). The generation of air-plasma near the target(s), through laser excitation, provides one approach to remote detection. The THz-ABCD method offers broadband sensing capabilities, but the THz-induced second harmonic signal cannot be easily collected from either a backwards or sideways direction. It is also necessary to provide a high voltage local oscillator bias that cannot be readily placed near the remote target for coherent detection.

While remote THz wave generation (>100 meters) is realistic, coherent remote sensing remains extremely challenging. Currently, the only known solution is to use a two-color laser field to generate air-plasma near the target, measuring THz wave information indirectly through THz-field-induced changes in plasma fluorescence or acoustics. THz air-plasma detection through THz radiation enhanced emission of fluorescence (THz-REEF) or THz enhanced acoustics (TEA), in contrast to nearly all other THz wave sensing methods, enables omnidirectional signal collection, and significantly mitigates the problem of THz absorption by atmospheric moisture. Although both remote generation and detection have been demonstrated separately, it remains to combine these laboratory demonstrations to realize real world THz remote spectroscopy of explosives or other hazardous materials.

Using an intense laser with mJ pulse energy for many practical applications is also a challenge. The focusing of high intensity optical pulses over long distances with precision, and practical control of the THz amplitude and phase at these ranges has not yet been

demonstrated. While some applications such as sensing in remote atmospheric locations may be feasible, public safety must also be considered. These limitations are motivation for improvements to this technology, and/or alternative solutions for remote THz spectroscopy. In the future, we have to address scientific and technical concerns, provide guidelines and solutions to satisfy safety issues, and develop further approaches that make use of THz wave air photonic systems and their unique abilities.

Conclusions:

Recent observations that THz radiation is able to modulate both the fluorescence and acoustics of laser-induced plasma in air, means that THz-REEF or TEA not only present feasible solutions toward remote THz wave detection, but also open exciting new areas of basic research. The fluorescence technique could, for example, exploit the Stark effect to directly measure rectified THz fields inside of a filament core, providing evidence of potentially enormous field strengths that are unable to be probed directly. Furthermore, acoustic techniques could make it possible to study solids or liquids with high absorption coefficients by indirectly studying changes in a sample's acoustic properties under illumination of high-field THz radiation.

Reference:

B. Clough, J.M. Dai, and X.-C. Zhang, *Materials Today*, review paper, Jan., 2012.

8562-2, Session 1

Optimization of receiver parameters of an optical array receiver for deep-space optical communication during Earth-Mars conjunction phase (*Invited Paper*)

Ali Javed Hashmi, National Univ. of Science and Technology (Pakistan); Ali Asghar Eftekhar, Ali Adibi, Georgia Institute of Technology (United States); Farid Amoozegar, Jet Propulsion Lab. (United States)

NASA deep-space ventures so far have relied upon a global Radio Frequency (RF)-based Deep-Space Network (DSN) to capture the communications signal returns from distant planets. The current RF technology is unable to fulfill the demands of such ventures due to constraints like huge free space loss and limited available spectrum in RF region of Electromagnetic spectrum. In this paper, we present the channel modeling, optimization of various receiver parameters, and link analysis of a deep-space optical communication link between a spacecraft at Mars and an Earth based optical array receiver, during Earth-Mars conjunction phase. The simulation results show that optimization of link parameters is essential to maximize the performance of an already power-starved deep-space optical communication link. The calculations of achievable data rates show that optical communication systems operating at 1.06 (IR frequency) can provide an order of magnitude greater bandwidth compared to the current RF technology. This paper presents the analytical results during Earth-Mars conjunction phase, which represents the worst case channel conditions for an optical communication link between Earth and Mars.

8562-3, Session 1

Study of terahertz spectroscopy using an infrared FTS system

Shaoliang Li, Kangmin Zhou, Wenying Duan, Zhenhui Lin, Qijun Yao, Shengcai Shi, Purple Mountain Observatory (China)

Fourier transform spectroscopy (FTS) is a measurement technique widely used in characterizing the spectrum of light sources and the frequency response of detectors. Some “ghost” spectral lines, however, are often observed in measured Fourier transform spectra, such as high-frequency harmonics of the light source due to multiple reflections in the measurement system and unexpected high frequency lines owing to low-frequency interferences in the data acquisition. Here we study the effects of multiple reflections and low-frequency interferences on the THz spectra measured by a Fourier transform spectrometer for different THz sources and detectors. Multiple reflections happen mainly because there are several metal planes such as the detector front part, signal source output plane in the FTS system. During the Fourier transform process the reflected signals are treated as normal signal so that “harmonics” can be witnessed on the final spectra. Details are given in the theoretical inductions part, together with a diagram illustration. Later, we identify the several factors in simulation based on the theoretical assumption to match the experiments’ results. Finally, corresponding experiments are designed to figure out quantitatively the contribution of the several planes to the final result in our system. Low-frequency interferences are generally introduced by the peripherals such as read-out circuits. As shown in the theoretical induction, low-frequency noises coupled with the sampling frequency will form apparent high-frequency signals in the final spectra. An artificial low-frequency “noise” is introduced as reference to identify the relationship between the sampling frequency and the interference frequency. Experimental and simulation results will be presented.

8562-4, Session 1

Design of 800x2 low-noise readout circuit for near-infrared InGaAs focal plane array

Zhangcheng Huang, Huang Songlei, Jiexiong Fang, Shanghai Institute of Technical Physics (China)

InGaAs near-infrared focal plane array (FPA) have important applications in space remote sensing. A design of 800x2 low-noise readout integrated circuit (ROIC) with pitch of 25 μ m is presented for a dual-band InGaAs FPA. The thermal noise of input-stage amplifier which is the major noise source in ROIC is reduced by increasing the load capacitor and a bias voltage in the range of ± 5 mV is obtained by optimizing the transistors in the input-stage amplifier. The circuit has been fabricated with 0.5 μ m 5V mixed signal CMOS process. Test results show that ROIC noise is less than 1E-4 V with dynamic range larger than 84 dB, and a dual-band 800x2 InGaAs focal plane array with D^* above 1E12 cmHz^{1/2}/W is obtained after interfaced with InGaAs chips.

8562-5, Session 1

Shifting media for terahertz carpet cloak and overlapped effects

XiaoFei Zang, YiMing Zhu, Bin Cai, Univ. of Shanghai for Science and Technology (China)

Based on transformation optics and complementary media (folded geometry), levitative carpet cloak and overlapped effects (anti-mirror effects) can be realized. In normal case, the levitative carpet cloak is limited by the shape of the invisible object, and the early folded geometry method can just make two objects with different shapes appear as only one. Here, based on transformation optics and finite element simulations we propose an anisotropic but homogeneous

shifting media. It includes a free region between the complementary media and compressive region that can shift an object from original place to another place with variable distance in terahertz (THz) region. As a result, an arbitrary shaped object levitated on a flat perfect electric conductor ground and covered with the shifting media cannot be detected, leading to the levitative and shape-independent carpet cloak. Furthermore, overlapped effects such as making two separated objects with the same shape appear as only one, can be also realized by using this kind of shifting media.

8562-6, Session 2

Computer processing of image captured by the passive THz imaging device as an effective tool for its de-noising (*Invited Paper*)

Vyacheslav A. Trofimov, Vladislav V Trofimov, Lomonosov Moscow State Univ. (Russian Federation); Yuan-meng Zhao, Chao Deng, Xin Zhang, Cun-lin Zhang, Capital Normal Univ. (China)

We demonstrate real-time computer code improving significantly the quality of nosed images captured by the passive THz imaging system. The code is not only designed for a THz passive device: it can be applied to any kind of such devices and active THz imaging systems as well. The performance of current version of the computer code is greater than one image per second for a THz image having more than 5000 pixels and 24 bit number representation. Processing of THz single image produces about 20 images simultaneously corresponding to various spatial filters. We develop original spatial filters which allow one to see objects with sizes less than 2 cm. For images with high noise we develop an approach which results in suppression of the noise after using the computer processing and we obtain the good quality image.

With the aim of illustrating the efficiency of the developed approach we demonstrate the detection of the liquid explosive, ordinary explosive, knife, pistol, metal plate, CD, ceramics, chocolate and other objects hidden under opaque clothes. The results demonstrate the high efficiency of our approach for the detection of hidden objects and they are a very promising solution for the security problem.

8562-7, Session 2

A new approach of graph cuts based segmentation for thermal IR image analysis (*Invited Paper*)

Sumit Chakravarty, SGT, Inc. (United States)

Thermal Infra Red images are one of the most investigated and popular data modalities whose usage has grown exponentially from humble origins to being one of the most extensively harnessed imaging forms. Instead of capturing the radiometry in visible spectra, the thermal Images focus on the near to mid Infrared spectra thereby producing a scene structure quite different from their visual counterpart images. Also traditionally the spatial resolution of the infra red images has been typically lower than traditional color images. The above reasons have contributed to the past trend of minimal automated analysis of thermal images wherein intensity (which corresponds to heat content) and to a lesser extent spatiality formed the primary features of interest in an IR image.

In this work we extend the automated processing of Infra red images by using an advanced image analysis technique called Graph cuts. Graph cuts have the unique property of providing global optimal segmentation which has contributed to its popularity. We side step the extensive computational requirements of a Graph cuts procedure (which consider pixels as the vertices of graphs) by performing preprocessing to obtain a short list of candidate regions. Features extracted on the candidate regions are then used as an input of the graph cut procedure. Appropriate energy functions are used to combine traditionally used

graph cuts feature like intensity feature with new salient features like gradients. The results show the effectiveness of using the above technique for automated processing of thermal infrared images especially when compared with traditional techniques like intensity thresholding.

8562-8, Session 2

Research on a project of the new airborne polarization hyperspectral imager

Huan Li, Jia ZHAO, Feng Zhou, Xu-ling LIN, Hai-bo Zhao, Beijing Institute of Space Mechanics and Electricity (China)

Polarization hyperspectral imagers combine polarization technology, spectral technology and imaging technology, get both the image of the target and the polarization and spectrum of the pixel to recognize the materials on the objects, have broad applied foreground on airborne remote sensing domain. That arrests extensive attention abroad.

Polarization hyperspectral imagers are compared with conventional hyper-spectral images, added polarization function, improve the capability on two aspects.

One is on account of the spectrum is divided into a lot of parts on a hyperspectral imager, several nanometer as usual, that results the energy collected by each pixel reduced, and restricted by signal-to-noise ratios (SNR). However, the low SNR affects the image observed, but polarization is not sensitive to the light, and it can get good image on the condition of low SNR.

The other is that hyper-spectral imager is not sensitive to observing angle, whereas polarization is much difference on the different position. Therefore when the conventional hyper-spectral imager can't get good recognition, we could make use of the polarization hyperspectral imaging to recognize farther.

This paper brings hyperspectral technology and polarization image together. On the basis of geometrical optics theory and polarization theory, puts forward a new polarization hyper-spectral Imaging technology. That could get hyper-spectral information and whole Stokes elements spectral from the object on the measuring the power spectral from the modulator only one time, and that raise the ability of recognition greatly. The paper carries out a project to the new airborne polarization hyperspectral imager.

8562-9, Session 2

Remote measuring system for infrared spectral features using hollow fiber probe

Yu-jing He, Yi-Wei SHI, Fudan Univ. (China)

Infrared hollow fibers provide a low-loss transmission media in a wide spectral range for active remote measuring system for infrared spectral features, which core is air or vacuum with simple structure and fabrication, flexibility, and low infrared transmission loss. especially in the infrared part it has a lower, flat transmission losses, thus, makes infrared transmission and telemetry possible.

Infrared probes composed of different hollow fibers were designed, fabricated, and optimized according to their transmission properties. Remote measuring system using the probe was set up with a Fourier Transform Infrared Spectrometer (FTIR). Infrared spectral features were measured for films such as polycarbonate (PC) and Poly vinylidene fluoride (PVDF), as well as liquid-phase films such as ethanol and toluene. Quantitative measurements were carried out for the mixed liquid of ethanol and toluene using the characteristic absorption peak of toluene at the wavenumber of 1605cm⁻¹. The system can be used in remote sensing of spectral features for solid and liquid phase films.

8562-78, Session 2

Design of dual-color ROIC with double sharing capacitor

Jie Zhou, Rui Jun Ding, Lei Gao, Guo-Qiang Chen, Pan Wang, Li-Chao Hao, Shanghai Institute of Technical Physics (China)

A readout integrated circuit (ROIC) for 320 x 256 middle-and long-wave infrared focal plane arrays is studied in this paper. This circuit operates in integrating-while-reading (IWR) mode with the frame rate higher than 100fps. A novel DI structure is used for signal acquisition of middle wave while BDI structure for long wave. It is common that trade-offs exist between chip area and performances in integrated circuits design. In order to getting high injection efficiency for BDI structure with small area, a four-transistor amplifier with the gain of 82dB is designed here. The charge handling capacity of the integrating capacitor is also a key performance parameter when considering the noise and the large middle-wave and long-wave photocurrent (up to 5nA and 100nA, respectively). A structure named double sharing capacitor (DSC) presented in this paper will be an effective solution to getting a large capacity in the limited 50 um x 50 um pitch area. DSC means that each sampling capacitor has two kinds of shares. One is between the sampling capacitor and another sampling capacitor in the adjacent pixel. The other is between the sampling capacitor and the holding capacitor in the same pixel. By adopting the 0.35um 1P4M mixed signal process, the DSC architecture can make the total effective charge handling capacity as high as 70Me- per pixel with 3V output swing. According to the simulation result, this circuit works well under 5V power supply and achieves 2.5MHz data transmission rate, more than 95% linearity. Its total power consumption is 110mW.

8562-10, Session 3

Terahertz supercontinuum generation from metal foil (*Invited Paper*)

Cunlin Zhang, Capital Normal Univ. (China)

The interaction of intense ultrashort femtosecond laser with plasma induced by metal targets can generated high power terahertz (THz) supercontinuum. In our experiment, four kinds of metal foil (Ru, Pt, Au, and Ti) were pumped by a p-polarized 1kHz, 800nm, 2.6mJ, and 50fs Ti-sapphire laser beam, the intensity of pump laser is below 20W/cm², and we can get more than 64?J intense single THz pulse, and the maximum spectrum was distributed from 0.3 to 149THz which get from Ru foil as shown in figure 1. The radiated THz supercontinuum were obtained by a Michelson interferometer in room temperature. We found the THz power as a function of thickness of samples, the power and incident angle of pump laser. Usually, we can get the maximum THz power from the 200nm-thick foil at about 40°incident angle. In addition, the THz supercontinuum were broadening when we increased the pump laser power. Finally, we measured the radiated THz energy in different direction around sample, and the results show that the THz emission angular distribution is a typical dipolar emission pattern. We consider that the THz radiation is generated via the acceleration of photoelectron which produced by laser-produced plasma of metal foil target.

8562-12, Session 3

A scheme format conversion from NRZ-OOK to QPSK/16QAM signal based on XPM in SOA-MZI

Yueying Zhan, Min Zhang, Mingtao Liu, Lei Liu, Xue Chen, Beijing Univ. of Posts and Telecommunications (China)

A scheme of format conversion between OOK signal and optical quadrature phase shift keying (QPSK)/16-ary quadrature amplitude

modulation (16QAM) signal based on cross phase modulation (XPM) effect in semiconductor optical amplifiers (SOA) is proposed. Theoretical analysis and simulations of the format conversion scheme are conducted to validate the feasibility of the proposal. In this proposal, When the NRZ-OOK1 data and NRZ-OOK2 data "1" or "0" at the same time, the gain compression of the SOA is obtained the maximum value or minimum value, and then the RZ clock pulse signal after passing through SOA has the phase of " π " or "0" due to the changes of carrier density. On the other hand, when the NRZ-OOK1 data is "1" while NRZ-OOK2 data is "0", and the gain compression is half of the maximum value, the phase of clock pulse is " $\pi/2$ ". However, the NRZ-OOK1 data is "0" while NRZ-OOK2 data is "1", and the phase of clock pulse is " $-\pi/2$ ". Therefore, the QPSK signal is converted based on XPM effect in an SOA. The 16QAM signal can be converted by the superposition of two QPSK signals which the amplitude of QPSK2 is doubled compared to QPSK1. The performance and the optimal design of the 10Gbit/s format conversion system under various key parameters of SOAs are evaluated and discussed. The receiver sensitivity of the converted QPSK signal and 16QAM signal after detected is 27.5dBm and -24dBm with BtB at BER of 10⁻⁹, respectively. Simulation results present useful to enable interconnection between backbone network and access network.

8562-13, Session 3

A robust MAP-based method for infrared image super-resolution

Hui Yu, Huazhong Univ. of Science and Technology (China);
Fusheng Chen, Zhijie Zhang, Huawang Chen, Huazhong
Institute of Electro-Optics-Wuhan National Lab. for
Optoelectronics (China)

Spatial resolution of digital images is limited due to optical/sensor blurring and detector site density. In many imaging systems, the detector array is not dense enough to adequately sample the scene with the desired field of view. And this is particularly true for infrared focal plane array. Because of the huge cost of improving the sensor manufacturing techniques that can directly increase spatial resolution of infrared imaging system, super-resolution technology is considered as a good approach to obtain high resolution image. Among the available reconstruction frameworks, the maximum a posterior (MAP) model based on Bayesian principle is widely used. Motion estimation is the first step which is implemented by using image registration algorithm. The subpixel accurate motion estimation is crucial, otherwise the reconstruction results may be worse than that is obtained by using interpolation directly. In this paper only pure translational motion is considered. Then an approach that can update the image smoothness is used as the prior knowledge, and the reconstructed HR image will become blurry; conversely, the noise will not be effectively restrained. After that, a method based on the U-curve is proposed to choose the regularization parameter adaptively. The reasonable iteration number of the linear equations extracted from MAP algorithm and the suitable number of input low-resolution images are also presented in this paper. The proposed algorithm has been verified using a synthetic infrared image sequence, and the reconstructed HR images are shown in the end. The experiment results and error analysis show that the proposed approach is robust and effective.

8562-15, Session 4

Dimmable VLC demonstration systems based on LED (Invited Paper)

Seongsu Lee, Sung-Yoon Jung, Yeungnam Univ. (Korea,
Republic of)

Recently, there have been many attempts to converge LED with IT technology. Among them, Visible Light Communication (VLC), which is the convergence of illumination and communication, has emerged. In VLC system, both lighting and communication can be simultaneously

implemented. By considering both terms together, VPPM (Variable Pulse Position Modulation) modulation scheme is proposed by the IEEE 802.15 standard group. It uses binary PPM (Pulse Position Modulation) for communication and PWM (Pulse Width Modulation) for dimming control. In this paper, we introduce the implementation of VLC demonstration system based on VPPM modulation scheme. By changing the pulse width of VPPM signal, we can support 25%, 50% or 75% dimming. In addition, our VLC demonstration system provides new power system using solar cell. By receiving the VPPM modulated visible light signal in the receiver end, we turn on the receiver power and start system operation to decode the transmitted signal. By using ATmega128 8bit Micro Controller Unit (MCU) by ATMEL and Cree Q3 of XLamp XP-E LEDs, our system provides about 2.1kbps data rate with 2.5kHz optical rate in more than 30cm distance. By implementing DM S/W, we show the bit error rate (BER) and achievable data rate (BER) of our demonstration system.

8562-16, Session 4

Study of fractional-order surface plasmons in terahertz frequencies (Invited Paper)

Yu-Ping Yang, Central Univ. for Nationalities (China)

Recently, a new type of extremely sharp resonant lines between the fundamental surface plasmon (SP) modes of a hole array fabricated on high-resistivity silicon wafers in "optical contact" with thick silicon plates was reported and identified as fractional-order surface plasmons (FSP). However, the physical mechanisms of the FSP resonances has not been studied more rigorously.

Here, based on the study of a 1D metallic grating, we show experimentally that the FSP resonances are caused by the gap reflection of the zero-order and the first-order diffracted beams back to the 1D or 2D grating, where there is a partial reflection into the forward zero-order direction, thereby causing the sharp interference peaks identified as the FSP resonances.

Furthermore, even when the gap is eliminated and the associated FSP oscillations on the 0-order transmitted pulse disappear, we shown that two very strong, much delayed, chirped, and long-lasting pulses are observed after the second reflected pulse. In the frequency domain, these two strong and fast-ringing structures correspond to the bandwidth ranges between the [0, 1] and [0, 2] surface plasmon modes and the range above [0, 2], respectively. A physical optics ray analysis provides an intuitive understanding of these new four-step (reflection, diffraction, total reflection, and diffraction) pulses, caused by fractional-order surface plasmon type beam coupling.

8562-17, Session 4

A photonic approach to microwave/millimeter-wave frequency measurement with extended range based on phase modulation

Xuiyou Han, Nuannuan Shi, Meng Wang, Yiyang Gu, Mingshan Zhao, Dalian Univ. of Technology (China)

The instantaneous frequency measurement (IFM) of the input unknown microwave signals is critical importance for modern radar warning receivers in the field of electronic warfare. With the frequencies of modern radar systems ranging from sub-gigahertz to millimeter-wave, the conventional electrical IFM implementations may not meet the requirements of wide operating frequency range and nearly real-time response. The photonic techniques overcome these limitations due to the advantages of wide bandwidth, low loss, light weight, and immunity to electromagnetic interference.

In this paper, a photonic approach to IFM with extended range based on phase modulation is presented. For the phase modulated microwave over fiber transmission, the microwave signal can be recovered with the

conversion of phase modulation to intensity modulation. The detected microwave signal power is affected by the microwave frequency, fiber dispersion and the optical wavelength. In the proposed measurement system, two optical wavelengths and two segment dispersion fibers are used to construct the frequency-dependent amplitude comparison functions (ACFs). Several ACFs can be jointly utilized to determine the microwave frequency without ambiguities beyond a monotonic region of the conventional one ACF. Then the measurable range of microwave frequency can be extended and the resolution can be improved by selection of ACF with sharp slope. The operation principle of the photonic approach is illustrated and the preliminary experiment results show that the frequency from 12 GHz to 18 GHz can be measured within ± 0.2 GHz errors. The further research is being conducted and the results will be presented on the coming conference.

8562-18, Session 4

Signal model and jamming characteristics of a 35GHz millimeter-wave FMCW SAR

Wen Yu, Beijing Institute of Tracking and Telecommunication Technology (China)

In the field of airborne remote sensing the combination of compact frequency-modulated continuous wave (FMCW) technology and synthetic aperture radar (SAR) paves a way for the development of the lightweight, cost-effective, high-resolution miniaturized millimeter imaging radar, which is suitable for small platforms such as unmanned vehicles(UAV) in military and civil use.

Compared with the conventional pulsed SAR, the continuous platform motion during the transmission of a sweep and the reception of the corresponding echo will induce serious Doppler frequency shift as a reconstructed image distortion effect. That means, in FMCW SAR, the so-called stop-and-go approximation is no longer valid because of the relatively long sweeps which the FMCW SAR transmits. Based on the analysis of the signal model, a data processing algorithm by introducing a new frequency term is proposed to compensate this Doppler shift in order to complete the imaging process. Through point targets simulation of a 35GHz millimeter-wave FMCW SAR, the validity of the model and the efficiency of the processing algorithm are demonstrated without extra computation load.

As for military use, the technology of FMCW SAR jamming should always be considered. Regarding of the complexity and the difficulty of FMCW SAR jamming, a novel semi-matching interference solution is presented in this paper to obtain part of the processing gain after the dechirp-on-receive configuration, resulting in a wide spread spectral bandwidth and badly degraded resolution. Considering of the FMCW SAR characteristics, several experiments are made to seek significant jamming conclusions, which is an innovative exploration.

8562-19, Session 5

Spatio-temporal characteristics of global atmospheric CO₂ mole fractions (XCO₂) retrieved from remotely sensed data (*Invited Paper*)

Tianxing Wang, Jiancheng Shi, Institute of Remote Sensing Applications (China); Yingying Jing, Yanhui Xie, Institute of Remote Sensing Applications,CAS (China)

Carbon dioxide is the most important greenhouse gas produced by human activities. Global warming induced by atmospheric CO₂ has attracted more and more attention of researchers all over the world. Currently, remotely sensed data are frequently used to map the atmospheric CO₂ globally. Atmospheric CO₂ data retrieved from AIRS, GOSAT, SCIAMACHY over the years of 2009~2011 have been collected as data sources. Unlike GOSAT and SCIAMACHY, the measurements of AIRS correspond only to the layer of free troposphere, thus, the

AIRS CO₂ retrievals are first converted to XCO₂ by incorporating the Carbon Tracker CO₂ profile as well as the averaging kernel of AIRS. Considering the various spatial and temporal differences of these satellite measurements, a matching algorithm has been developed, so that these different sources of CO₂ products can be physically comparable in spatial and temporal scales. The times of retrievals of AIRS and SCIAMACHY are shifted to a uniform reference time (GOSAT overpass time), and CO₂ retrievals with fine spatial resolution are averaged to produce down-scaled values. Based on the processing mentioned above, the relationships of these CO₂ products and their spatio-temporal characteristics are then investigated. The results show that the correlations between them are very weak. Some discrepancies in global CO₂ spatio-temporal characteristics can be detected among these products. Compared to AIRS XCO₂ data, the CO₂ spatial coverage of SCIAMACHY and GOSAT is very limited.

8562-20, Session 5

Development of high efficiency pulse tube cryocoolers for space-borne infrared applications (*Invited Paper*)

Haizheng Dang, Shanghai Institute of Technical Physics (China)

This paper reviews the recent advances in high efficiency pulse tube cryocoolers (PTCs) in Shanghai Institute of Technical Physics, Chinese Academy of Sciences (SITP/CAS). The main motivation is to provide the appropriate active cooling systems with high reliability, low-noise and long life for space-borne infrared applications. Due to the special application field where the power supply is relatively limited and the rejection condition is extremely adverse, the high efficiency of the PTC is especially emphasized and thus becomes the research focus. Three typical geometrical arrangements, U-type, coaxial and in-line, are all involved, while the latter two are stressed on. To date, the single-stage PTC covers a wide temperature range from 25 K to 200 K, and the typical cooling capacities are 4W@60K, 10W@80K and 15W@95K. For the coaxial PTCs, the typical relative Carnot efficiencies at 60 K, 80 K and 95 K achieve 9.6%, 14.4% and 17%, respectively. For the high efficiency in-line PTCs, the much higher relative Carnot efficiencies of 17.7% and 19.2% have been achieved at 80 K and 95 K, respectively. Some typical cryocooler development programs are introduced and a brief overview of the updated data package is presented. The efforts to realize a good adaptability of the PTCs to the adverse rejection conditions are also discussed.

8562-21, Session 5

Readout system for the Terahertz Superconducting Imaging Array (TSIA)

Sheng Li, Jin-Ping Yang, Wen-Ying Duan, Zhen-Hui Lin, Jing Li, Sheng-Cai Shi, Purple Mountain Observatory (China)

Terahertz Superconducting Imaging Array (TSIA) is a project for the development of a large THz direct-detection array for mapping observations. The prototype of the TSIA is an 8x8 pixel direct-detection array operating at the 850 μ m band, incorporating THz superconducting detectors such as kinetic inductance detectors (KIDs) and transition edge sensors (TES). KIDs have the advantage that only a broadband low noise cryogenic amplifier is needed at low temperature for the readout system, and hundreds of pixels could readout simultaneously by the frequency-division multiplexing (FDM) technique. The readout system for a KIDs array is composed of several parts like excitation signal generating, baseband signal acquisition and processing. The excitation signal is a kind of comb signal carrying various frequencies corresponding simply to resonant frequencies of the detectors. It is generated in baseband with a bandwidth covering all KIDs and up-converted to microwave frequency (about several gigahertz) to feed the detectors. With THz radiation, the forward transmission coefficient (S₂₁) of all KIDs varies and the variation can be measured through the

comb signal. Fast Fourier transform spectrometer (FFTS) will be used to acquire and process the baseband excitation signal in real time. Consequently, the radiation intensity can be estimated by monitoring the signal amplitude of the corresponding frequency channels. In this paper we will present mainly the design of an electronic readout system for the 8x8 pixel array. Some preliminary experiment results will also be given.

8562-22, Session 5

Research on the infrared and UV radiation characteristics of ballistic missile tail-flame

Xiao-hu Liang, Beijing Institute of Tracking and Telecommunications Technology (China)

During the ballistic missile boost phase, the tail-frame blowing from the engine spout generates strong radiation in multiple wave bands, which is an important information source for the missile detection and warning. This paper combines the infrared and UV radiation transmission characters with the ballistic trajectory equation and builds the infrared and UV radiation transmission models in boost phase. In ballistic trajectory simulation, we simplify the missile dynamic formulas of the center of mass in boost phase with considering the pitch angle attitude only, design the flight procedure, and adopt the aerodynamic coefficients of "Titan-II" to generate the simulation trajectory using fourth-order Runge-Kutta method. When forming the tail-flame radiation transmission formula, the off-nose angle and the atmosphere transmittance varying with the altitude and wave length are taken into consideration. This paper analyzes the effect on radiation transmission of these factors such as sensor position, missile altitude, missile body attitude, detection wave band and atmosphere attenuation, then gains the received radiation intensity and its time-variant character. The result provides a theoretic foundation for choosing sensor platform and detection wave band. Based on the above working, the infrared and UV background radiation intensity at the sensor is analyzed to compute the received radiation SNR, which gives limits on the sensor sensitivity and the detection capability of weak signal. The results show that the motion character of the missile has different effect in different wave bands and the UV detection can give an earlier warning than the infrared.

8562-23, Session 5

Goos-Hänchen shifts on the air-COC interface in the terahertz region

He Jun, Qingmei Li, Capital Normal Univ. (China)

Transmission properties of terahertz pulses through Asymmetric double split-ring resonators

We demonstrate narrow transmission resonances at THz wavelengths utilizing coupled asymmetric split-ring resonators (SRRs). By breaking the symmetry of the coupled SRR system, one can excite dark resonant modes that are not readily accessible to symmetric SRR structures. Besides, increasing the length of the sides parallel to the polarization of the incident terahertz wave, the resonant frequencies are observed to red shifting. This theoretical simulation will be good reference for the following experience, and these asymmetric metamaterials will promote new avenues to the control of terahertz waves.

8562-37, Poster Session

Rational design of long-wave infrared band for application of the earth surface temperature observation

Yunfei Bao, Hongyan He, Feng Zhou, Beijing Institute of Space

Mechanics and Electricity (China)

The land surface temperature (LST) is very important in determining net radiation, evapotranspiration, and energy balance at the Earth's surface and assessing the status of crops and soils. LST estimation needs to take into account the nonblackness of natural surfaces, their heterogeneity at satellite pixel scale and disturbing effects introduced by the atmosphere. Rational band configuration and sensor performance requirements must also be determined.

For argumentation of feasibility of LST retrieval using 8-10 um infrared band, this paper focuses on band design of long-wave infrared based on theory research. Basis of thermal infrared radiative transfer and atmospheric simulation, the paper analyses atmospheric effect on different long-wave infrared and obtain a preliminary selection of potential spectral channels. Several configurations of long-wave infrared spectral band were selected to perform in Split-Window algorithm. Then the relation of LST retrieval precision and error source were analyzed. Several sources of error must be identified to estimate the total error for LST. We have distinguished three independent error contributions: the error associated with the split-window method; the temperature error due to the emissivity uncertainty; and the radiometric noise error, due to the propagation of the noise equivalent difference of temperature (NEDT).

The analytical results show that the temperature error from split-window algorithm using 10-12.5um is about ± 0.89 K, while the temperature error using 8-10 um is about ± 1.13 K. So the results indicate the scheme of LST retrieval using 8-10 um long-wave infrared is feasibility in scope of needed retrieval precision.

8562-38, Poster Session

The research of remote sensing duststorm with FY-3B three infrared channels

Hui Xu, Tao Yu, Donghai Xie, Jiaguo Li, Institute of Remote Sensing Applications (China); Jibao Lai, State Key Laboratory of Remote Sensing Science, Institute of Remote Sensing Applications (China)

Dust aerosol extinction characteristic shows a significant diurnal cycle which can be used to monitor the dust intensity information. Based on the new generation meteorological satellite of FengYun, this paper proposed a bi-temporal method of remote sensing dust aerosol with infrared channels. Firstly, the dust aerosol extinction diurnal cycle characteristic is discussed within the Infrared spectral range. Secondly, based on the infrared spectral variations difference of dust aerosol, land surface and cloud, the dust aerosol identification method was investigated by this paper. Thirdly, by using the characteristics of infrared extinction and diurnal cycle of dust aerosol, a bi-temporal thermal dust index (BTDI) which can be used to represent the information of dust intensity is derived from the new generation meteorological satellite of FengYun 3B infrared channels(10.8um and 12um) at two different time slots during a day. At last, three months (March to May 2011) BTDI values are evaluated with the corresponding Aerosol Robotic Network (AERONET) data and the result shows that 1. BTDI shows a negative correlation with aerosol optical depth which can well reflect the dust aerosol intensity. 2. BTDI is sensitive to dust aerosol and it will decrease rapidly with the aerosol optical depth increase.

8562-39, Poster Session

Role of soft-collision in terahertz generation in ionizing atoms

Dongwen Zhang, Zhihui Lv, Chao Meng, Zhaoyan Zhou, Zengxiu Zhao, Jianmin Yuan, National Univ. of Defense Technology (China)

We perform a joint measurement by monitoring THz and high-order

harmonic yields in a two-color laser field simultaneously. By correlating their phase-delay dependence, the absolute relative phase dependence of THz yields can be retrieved and it is found that THz yields take maximum at phase delay of 0.8 deviated from the prediction of previous models. By analyzing electron dynamics classically and quantum mechanically, we find that the Coulomb potential of the residual ion can not be neglected. It is shown that laser-assisted soft-collisions of the electronic wave packet with the atomic core induces momentum transfer to the electron affecting the phase dependence of THz yields. The joint measurement of THz and harmonic yields allows us to determine the generation of THz waves in attosecond precision. We show that the hard-collision with the atomic core causes HHG upon recombination, and the soft collision with the atomic core gives rise to THz photocurrents. We expect that the sensitivity of THz yields on Coulomb potential could be used to map atomic fields from within and help the full characterization of the rescattering wave packet, beyond the recombination in HHG and back-scattering in ATI.

8562-40, Poster Session

Single-scan coherent detection with enhanced time resolution for arbitrarily polarized terahertz wave

Zhihui Lv, Zengxiu Zhao, Jianmin Yuan, National Univ. of Defense Technology (China)

The technology of terahertz wave air-biased-coherent-detection (THz-ABCD) using gases as the nonlinear media and utilizes the third-order optical nonlinearities and leading a broad bandwidth fully covering the terahertz gap, has been widely used in THz applications. Utilizing the centrosymmetry of gases, we had reported a scheme of polarization-sensitive THz -ABCD. It directly measures the amplitude and polarization angle of the THz field and provides a same detection bandwidth as the conventional method.

Here we present an enhanced scheme of polarization-sensitive THz-ABCD which can provide about twice broader bandwidth than the conventional method. It uses a probe beam which is modulated in time domain. In our experiment using a 26 fs laser pulse, compared with 0.3-40 THz in conventional scheme, bandwidth coverage from 0.3 to 80 THz has been achieved. It also should have to be noted the terahertz source may also restrict the detection bandwidth. On the other hand, this scheme is also polarization-sensitive. The polarization angle in time domain, as well as the field amplitude, can be achieved with just one single scan. It is expected to reach a high time resolution of few femtoseconds if few cycle laser pulse is employed. The signal-noise-ratio (SNR), however, is much less than that of the conventional method. Several suggestions to improve the SNR have also been indicated in the paper.

8562-41, Poster Session

SBNUC based on constant statistics for VOx uncooled IRFPA and implementation with FPGA

Shudi Wei, Weiqi Jin, Minglei Jin, Chao Xu, Beijing Institute of Technology (China)

The quality of infrared imaging system was limited by the nonuniformity?NU?in the Infrared Focal Plane Array(IRFPA), especially in the uncooled infrared imaging system. Scene based nonuniformity correction?SBNUC?algorithms are widely concerned since they only need the readout infrared data captured by the imaging system during its normal operation. However, there still exists the problem of ghost artifact in the algorithms, and their performance is noticeably degraded when the methods are applied over scenes with lack of motion. In addition, most SBNUC algorithms are difficult to be implemented in the hardware.

In this paper, to reduce the fringe NU in uncooled VOx IRFPA we present a simple and effective SBNUC method based on Constant Statistics in which the fringe NU is reduced by balancing the statistics of the vertical channels. Through analyzing the reason of ghost artifact being brought in in the SBNUC algorithms, our algorithm successfully reduce the ghost artifact that plagues SBNUC algorithms through the use of optimization techniques in the parameter estimation .The advantage of the algorithm lies in its simplicity and low computational complexity. Our algorithm is implemented on a FPGA hardware platform with XC5VSX50T as the kernel processor, the raw infrared data are provided by an uncooled infrared focal plane array of VOx which has fringe NU. Our processing system reaches high correction levels, fringe NU being reduced, the ghost artifact being decreased , which can lay a technical foundation for the following study and applications of high performance thermal imaging system.

8562-42, Poster Session

High-power terahertz quantum cascade laser

Jiayan Chen, Junqi Liu, Tao Wang, Fengqi Liu, Zhanguo Wang, Institute of Semiconductors (China)

In recent years, the terahertz (THz) frequency range (0.1 THz~10 THz) has been concerned because of its great potential applications. With the development of terahertz technique, the "terahertz gap", formed due to the lack of suitable sources to generate steady radiation, has been gradually filled up. However, high-power THz radiation sources are still much desired. Among the various methods of generating coherent THz radiation, quantum cascade laser (QCL) as compact and convenient device is the most promising candidate due to its novel operation principle and attainable performance. Up to now, spectral coverage has been demonstrated from 1.2-5.0 THz (when operated without the assistance of external magnetic field). However, their operation temperature is still limited in the cryogenic range, leading to considerable interest to raise it into thermoelectric coolers' range. At the same time, higher output power is always another most important research goal. High power operation based on resonant-phonon (RP) active region design has been reported. However, considered fault-tolerant space when grown by molecular beam epitaxy (MBE), the bound-to-continuum (BTC) structure is much robust than the RP structures.

In this work, we presented high power THz QCL at about 3 THz based on BTC active region design. At 10 K, corrected by the collection efficiency, the maximum peak power of 137 mW was obtained in pulsed mode. What's more, we firstly introduce monolithically integrated THz QCL array and the maximum peak power of two-device-array increased to 218 mW. In total, the array improves the performance efficiently, implying cheerful prospect.

8562-44, Poster Session

A target recognition method for total reflection terahertz scanning images

Yuan-meng Zhao, Chao Deng, Xin Zhang, Cunlin Zhang, Capital Normal Univ. (China)

The THz region occupies the part of the electromagnetic spectrum between 30?m and 3 mm. THz radiation, which is a form of low level energy naturally emitted from all materials such as rocks, animals and people, doesn't involve any of the harmful radiation like the traditional X-ray. Due to this characteristic, since last two decades, there has been an increased interest in THz imaging for security applications, to uncover concealed weapons, dangerous materials or illegal products on person. Two imaging approaches associated with this technology are active imaging method and passive imaging method. Passive imaging method, without the use of an external illuminator, has the advantage of achieving a good balance between security and civil liberties. Our

work focuses on studying the passive imaging method. From our previous work, we developed a set of passive THz security screening system and got some initial THz scanning images, however, the target recognition ability of the system still needs to be improved. Therefore, the purpose of this paper is to develop an image processing method used in this system for improving the system's target recognition ability. The image processing method includes the following steps. First, the vertical stripes caused by the scanning pattern are filtered by using a variety of masks through methods such as smoothing filtering and median filtering, so that we improve the uniformity of the image. Second, we perform the image interpolation and image sharpening. Third, the person is segmented from the image using the Otsu method, and then we draw the contour outline of the person by means of computing the gradient image. Fourth, the study adopts the watershed algorithm to segment the image region where the possible concealed targets are located. Finally, we optimize the display effect of the target areas by using the pseudo-color enhancement method, image fusion method which involves using a registered visible image, and describing the edges of person and targets through a virtual image. Both the simulation experiment results and the actual system performing results demonstrate the efficacy of our methods. The resulting images can clearly distinguish the human body's edge from the background and display the position of the possible concealed targets. In addition, the shape of the targets can be recognized to a certain extent. We can draw a conclusion that the method introduced in this paper has the capability to help the checkpoint security staff easily detect the concealed targets on person remotely. In the end, we discuss the future research direction which will be to further improve the image resolution.

8562-45, Poster Session

Terahertz spectroscopic investigation of polypeptide and protein

Xiu-Hua Fu, China Jiliang Univ. (China)

With the development of biotechnology, peptides and protein as drugs in clinical become more and more widely. Polypeptide oxytocin, eptifibatide and protein bovine serum albumin and collagen are large bimolecular which had poor stability compared to traditional small molecular of organic medicine. Analysis in their stability of temperature, dehydration, hydration or binding from simple or quickly methods is very important.

In this study, we used terahertz time-domain spectroscopy (THz-TDS) to measure oxytocin, eptifibatide, bovine serum albumin and collagen, and obtained absorption and the refractive spectra of native or heated state in 0.2-1.4THz region at room temperature. The results showed that polypeptide and protein both have strong absorption, but their characteristics were not distinctly, heated protein or polypeptide compared to unheated have distinct difference from each other from absorption spectra, the absorption decreased in heated state. We used Debye model simulated terahertz dielectric spectra of protein or peptide. Experimental results were in good agreement with the simulation. We obtained the Beta relaxation time of different states and conformation changed relaxation time, they had distinct changes in heated. Due to the decrease water in surface layer of protein during thermal, the absorption decreased. The protein of heated had distinct changes compared to small molecules in relaxation time, especially, the high energy of protein. The results proved that the terahertz spectrum technology is feasible in testing protein and peptide that were affected by temperature, which can provide theoretical foundation in the further study about the THz dielectric spectrum of protein and peptide temperature stability

8562-46, Poster Session

Target detection method based on multi-life restrict used in super wide angle infrared starting warning system

Bing Zhou, Fuyu Huang, Jia-ju Ying, Shijiazhuang Mechanical Engineering College (China)

As early as possible discovers the enemy target is the key that seizes the information advantage in the modern war. But the threat present an omni-directional property for the high-tech weapon is applied largely in the modern war, therefore require infrared reconnaissance and warning system to have omni-directional reconnaissance ability. So, the developed country makes greatest efforts to pursue the omni-directional staring electro-optical equipment since the beginning of 90's in last century and make progress continuously. In recent years, infrared equipment with super big field angle appears gradually. In recent years, super angel infrared lens with field angel achieve 135°and 180°appears already, and super airspace staring reconnaissance system based on them being practical gradually.

A moving target will appear as with up-and- down gray scale in sequence images of fish-eye staring system for its sub-pixel imaging attribute. This bring difficult to track correlation for the target's time pertinence reduce too. In allusion to up special problem, put forward adopt nearest correlation method firstly. Add dummy target in tracking maintain process treating the track cross. Endue target multiple life, such as accumulate life in history, per-pixel life and average life, treating the temporary disappearance when target move between pixels. All those method effectually solve the special problem of target time gray scale in fish-eye staring system. Discuss some problems of target track correlation based on sequence images in this kind system. Such as target point register, new target process, nearest correlating process, determine track disappear, track maintain process, and so on.

8562-47, Poster Session

Performance of portable high-resolution Fourier transform spectrometer for trace gas remote sensing

Haoyun Wei, Tsinghua Univ. (China); Dongdong Fan, Beijing Vision Sky Aerospace Technology Co., Ltd. (China); Marc-André Soucy, ABB Analytical Measurement (Canada)

The perturbations of atmospheric composition due to industrial emission, volcanic eruptions and biomass burning are changing the environment and the climax. Observations of these perturbations in the Earth's atmosphere are important in the study of atmospheric chemistry and in the development of models that can predict the possible evolution of this complicated system. Though the conventional sampling measurements provide direct and precise results, the remote sensing measurements using the atmospheric absorption spectrum have advantages in risk-free and long-term monitoring. Fourier Transform Spectrometer (FTS), with its throughput, multiplex, and spectra resolution advantages, has been deployed on various satellites and planetary probes, on balloon gondolas, and on the ground for atmospheric remote sensing. Especially, remote sensing from a satellite platform such as the Atmospheric Chemistry Experiment (ACE) FTS on the SciSat-1, the Infrared Atmospheric Sounding Interferometer (IASI) on the METOP and the Thermal And Near infrared Sensor for carbon Observations (TANSO) on GOSAT can provide a global picture of changes in the atmospheric composition.

In this paper, the concept and performance of a portable high resolution FTS bread board model is reported. With its wide spectral coverage (800cm⁻¹~4000cm⁻¹), high spectral resolution (0.028cm⁻¹), and high SNR(>100:1@atmospheric windows), It is very suitable for atmospheric absorption spectra detection using solar as light source. Some design considerations of the reported FTS are introduced, and its performance, such as the Instrumental Line shape (ILS) and Signal to Noise Ratio

(SNR) are tested. Using the calibrated measurement spectra, total column value of several trace gases are retrieved and discussed.

8562-48, Poster Session

Continuous field measurements of $[\delta^{13}C]$ in water vapor by open-path Fourier transform infrared spectrometry

Wei Wang, university of Science and Technology of China (China) and Anhui Institute of Optics and Fine Mechanics (China); Wenqing Liu, Tianshu Zhang, Anhui Institute of Optics and Fine Mechanics (China)

The measurement of stable isotopes has emerged as a very important tool to understand ecosystem-atmosphere gas exchange and its role in the carbon and hydrologic cycles. The paper describes a seven day field experiment in which an open-path FTIR system was employed to measure the isotope composition of H₂O and CO₂ in ambient air continuously. Mixing ratios of ¹²CO₂, ¹³CO₂, H₁₆OH and HDO were measured simultaneously. We used a three-dimensional sonic anemometer and a temperature and humidity sensor to observe meteorological conditions concurrent with the FTIR measurement. The results suggested that the variations of ¹²CO₂ and ¹³CO₂ were highly correlated, with a obvious diurnal pattern. It was unexpected that time series of $\delta^{13}C$ showed no linear relationship with the variations of carbon dioxide, which was confirmed by the subsequent Keeling plot analysis. The complex geographical environment of the measurement site was likely to make the Keeling assumption break down. On the other hand, the outcomes of H₂O and its isotopes revealed that the variations of H₁₆OH and HDO were also strongly related, both showing a clear diurnal cycle. In this case, although the Keeling assumption appeared to be not well met for the data, the linear relationship between the total mixing ratio H₂O and isotopic composition of existed. The intercept of the linear regression line gave the deuterium isotopic ratio of evapotranspiration source, which is $-110.6 \pm 4.3\%$. The experiment results exhibited the suitability of the open-path FTIR system to long-term and in-situ measurement of isotopes in CO₂ and H₂O.

8562-49, Poster Session

10Gbit/s full-duplex bidirectional RSOA-based WDM PON using Mach-Zehnder interferometer and forward error correction

Weiping Han, Min Zhang, Mingtao Liu, Beijing Univ. of Posts and Telecommunications (China)

In this paper, a 10Gbit/s full-duplex bidirectional WDM PON with RSOA-based colorless ONUs has been designed and demonstrated, which uses Mach-Zehnder Interferometer (MZI) as optical equalizer and applies Forward Error Correction (FEC) to correct burst errors. An effective 10Gbit/s parallel algorithm is designed and implemented to realize the FEC module. DPSK and NRZ are used in the downlink and uplink to reduce the interference. First, we confirm that RS (255,223) decoder is capable of correcting up to at most 16 symbol-errors or 128 continuous bit-errors in a block codeword based on the parity information. Second, we use CW signal in the downstream to drive RSOA with the upstream NRZ signal to test and verify the optical filter capability of MZI which acts as a two-tap optical equalizer in uplink transmission. The measured results show that the received sensitivity of -21.46dBm is obtained with MZI which is about 2dB lower than that without MZI. Lastly, we demonstrate that the fiber length has little impact on the downstream DPSK signal within a range of no longer than 20km. The BER cannot achieve the RS (255,223) threshold whether after 10km or 20km SMF transmission without MZI in the upstream. The received sensitivity of $-25.2\text{dBm}@BER=2.4 \times 10^{-3}$ is obtained in downstream and a better received sensitivity of $-12.68\text{dBm}@BER=2.5 \times 10^{-3}$ is obtained with MZI. In addition, the received sensitivity

could increase by nearly 5dB by using RS (255, 223) code.

8562-50, Poster Session

An experimental 0.2 THz stepped frequency radar system for the target detection

Bangze Zeng, Meiyang Liang, Yuejin Zhao, Beijing Institute of Technology (China); Cunlin Zhang, Capital Normal Univ. (China)

Compared with traditional microwave and millimeter wave radars, Terahertz radar has wide signal bandwidth and a very narrow antenna beam, which is beneficial to the realization of high resolution imaging. And as an instantaneous narrowband and synthetic wideband waveform, stepped frequency radar signal has been widely exploited in many applications, since it allows high range resolution with modest requirements of the system bandwidth. As an instantaneous narrowband and synthetic wideband waveform, stepped frequency radar signal has been widely exploited in many applications, since it allows high range resolution with modest requirements of the system bandwidth. This paper presents the design of a 0.2THz stepped frequency imaging radar system with operating bandwidth of 12 GHz, thus, a theoretical range resolution below 1.25 cm. The simulation of the system is implemented by using system design parameters. An experimental trial has been performed, and one-dimensional range profile of the stationary target is obtained by imaging experiment using THz radar. Results show that the THz radar imaging system could achieve the target detection and centimeter-level range resolution.

8562-51, Poster Session

A reflection sensor based on the Rayleigh anomaly of metallic grating in terahertz wave band

Lingyue Yue, Capital Normal Univ. (China); Jingwen He, Shengfei Feng, Xinke Wang, Wenfeng Sun, Yan Zhang, Capital Normal Univ. (China) and Beijing Key Lab. for Terahertz Spectroscopy and Imaging (China) and Key Lab. of Terahertz Optoelectronics, Ministry of Education (China)

An optical refractive index sensor based on the Rayleigh anomaly of gold grating is demonstrated in terahertz wave band. A pronounced peak due to the Rayleigh anomaly of the gold grating is observed in the reflection spectrum, the center wavelength of which is sensitive to the change in the environmental refractive index on top of the grating. The wavelength of the Rayleigh anomaly reflection peak and the corresponding sensitivity are solely determined by the period of the gold grating, the larger of the period, the longer of the wavelength and the higher of the sensitivity. Therefore, higher sensitivity can be achieved in terahertz wave band. Both theoretical and experimental investigations show that the shape and intensity of the Rayleigh anomaly reflection peaks are determined by the duty cycle of the grating, for the value of the duty cycle about 0.4, the maximum intensity of the Rayleigh anomaly reflection peak was achieved.

8562-52, Poster Session

A novel target LOS calibration method for IR scanning sensor based on control points

Yong-Hong Xue, Wei An, National Univ. of Defense Technology (China); Yin-Sheng Zhang, Tao Zhang, Beijing Institute of Tracking and Telecommunication Technology (China)

Space based IR system uses the information of target LOS (line of sight) for target location. Recent researches show that the measuring precision of target LOS is usually determined by measuring precision

of platform's position and attitude, and deformation of sensor etc. Most methods for improving target location precision are either through improving platform's position and attitude measuring precision or through calibrating the whole image obtained by IR sensor. With the development of measuring technology, it is harder to make a further improvement through measurement of position and attitude of the platform, and the expansion of the sensor view make calibration of the whole image with a larger computation cost. In this paper, a method using control points to calibrate target LOS was proposed. Based on the analysis of the imaging process of scanning sensor of space based IR system, this paper established a modify model of target LOS based on control points, used a bias filter to estimate the bias value of sensor boresight, and finally achieved the mission of target LOS calibration. Different from the traditional calibration method of remote sensing image, the proposed method only made a correction on the LOS of suspicious target, but not established the accurate relationship between the all pixels and their real location, and has a similar calibration performance, but much more lower computational complexity.

8562-53, Poster Session

Numerical simulation of terahertz transmission of bilayer metallic meshes with different thickness of substrates

Guozhong Zhao, Capital Normal Univ. (China)

The terahertz transmission characteristics of bilayer metallic mesh filters with the different thickness of substrates are studied based on the finite difference time domain method. The well-shaped grid, the array of complementary square metallic pill and the cross wire-hole array were investigated. The numerical results show that the well-shaped grid have the function of a high-pass filter, while the square metallic pill array show the function of a low-pass filter, and the cross wire-hole array can be used as a band-pass filter. The substrate fills in the gap between two metallic microstructures. The material and medium thicknesses of substrates have an influence on the terahertz transmission characteristics of metallic microstructures. The simulation results show that the cut-off frequency of high-pass filter and low-pass filter move to low frequency with increasing the thicknesses of medium. The bilayer cross wire-hole array shows two transmission peaks which have the competition effect.

8562-54, Poster Session

Uncooled infrared imaging system based on the filter method with polka-dot beamsplitter

Lin Ding, Beijing Institute of Space Mechanics and Electricity (China); Mei Hui, Beijing Institute of Technology (China); Yiliang Liu, Beijing Institute of Space Mechanics and Electricity (China); Wenjuan Wang, Yuejin Zhao, Beijing Institute of Technology (China)

With the popularization and ripeness of uncooled infrared MEMS system, its advantages such as low-cost, no refrigeration equipment and more reliability have emerged. Compared with electrical method, the optical readout method has advantages like simpler preparation, higher sensitivity. The common filtering methods adopt knife edge and small aperture in the 4f system. However, these methods make the realizing miniaturization system more difficult, and can't remove the background noise effectively. A new filtering method is presented in this paper, this method use Polka-Dot Beam splitter instead of knife edge and small aperture to modulate the incident light.

The Polka-Dot beam splitter filter as a novel kind of spectral component is chosen in this method. The characteristic of this filter is that its coated-to-uncoated surface area has a "polka-dot" type appearance. Incident light can be reflected by the coated area and transmitted through the glass. Therefore the Polka-Dot beam splitter can modulate

the amplitude of incident light for its special structure. The Polka-Dot Beam splitter filter can improve the signal noise ratio (SNA), raise the detection sensitivity and simplify the structure. From the theoretical analysis and experimental results in this paper it can be concluded that the novel method have more advantages compared with the traditional filtering methods.

8562-55, Poster Session

Denosing to the pulsed laser radar return waves based on pulses accumulation and wavelet filter

Xiping Cai, Jianbo Liu, Heilongjiang Univ. (China); Quan Han, Harbin Institute of Technology (China); Wenjiang Dai, Heilongjiang Univ. (China)

Ladar (Laser Radar) is a radar which commonly utilizes the FMCW (Frequency Modulation Continuous Wave) waves or narrow pulses as the modulation regime. Based on the captured return waves, ranges to the target and other information such as characteristic of the target, intensity image, range image and 3D (three dimensional) image of the target may all be obtained. There are many factors which may affect the performance of a laser radar, these include the rationality of the transmitting and receiving optics design, the absorption and scattering of the atmospheric particles to laser, atmospheric turbulence, target's characteristics, signal processing utilized, etc. The method based on advanced signal processing may be applied to increase the signal-to-noise ratio for laser radars. In order to improve the performance of a pulsed laser radar, methods based on wavelet filter and pulses accumulation are investigated. The transmitted pulses and received return waves are modeled for the simulation of signal processing through a filter. It shows that the modeled return waves could be denoised effectively with the wavelet filter 3.9 or db9 if it is on the basis of compulsory denoising. However, under the condition of high fidelity requirement for the waveform, the signal-to-noise ratio may not be increased considerably. Thus, a new filter which is based on the combination of pulses accumulation and a followed wavelet transformer is proposed and studied. The results show that it is preferable to increase the signal-to-noise ratio than any of the two single filters, i.e. pulses accumulation filter and wavelet filter.

8562-57, Poster Session

Measurement and analysis of perceivable signal-to-noise ratio for infrared imaging system with human vision

Xin Liu, Jing Zhao, Honghua Chang, Lin Ma, Xidian Univ. (China)

The perceivable signal-to-noise ratio (SNR) is the basis of performance theoretical model of an infrared imaging system (IRIS) with human vision. The existing triangle orientation discrimination (TOD) performance model assumes that a constant SNR threshold is achieved at some point in the visual processing chain for a detection to occur, which may cause error in the results. In order to improve the precision of the model, we need to obtain the perceivable SNR thresholds changed with the correct discrimination probability of the human eye.

In this paper, the relationship between correct discrimination probability of the human eye and perceivable SNR threshold is studied for different equilateral triangle sizes with specified luminance through combining theoretical calculation with practical experiment. Firstly, the simulation images of triangle patterns with different sizes and thermal contrasts are generated by an IRIS simulation model. System noises and some physical effects are added to each image. Then the perceivable SNRs for these images are calculated by establishing the system theoretical model and the human vision system model. At the same time, the correct probabilities with which the triangle orientation of each test images is just judged are obtained by Four-Alternative Forced-Choice

experiment. Finally, the curves of correct discrimination probabilities changed with perceivable SNRs are fitted for different triangle sizes with specified luminance. The analyses of these results show that these changes are accorded with the psychometric function and the fitting curves become steep with the increasing of triangle size. These data and conclusions are helpful to modify the existing TOD performance model of an IRIS.

8562-58, Poster Session

An 8K FFT architecture for FPGA-based space-borne FTS on-board data processing

Jiaqing Liu, Shanghai Institute of Technical Physics (China)

In-place computation, regularity and parallel FFT algorithms is better for on board data processing with limited resource. To meet 8K or near points of Interferogram inverse fourier transform within 1ms of on board processing requirement. A 8K parallel FFT architecture for FPGA-based is proposed in this paper, which is based on Singleton's parallel FFT algorithm. It contains 8 radix-2 butterflies in parallel and 16 complex data FIFOs to store the input and use as memory storage between stages.

Using Singleton's single butterfly method, the calculated latency for a 8K-point FFT is 26624 cycles. With 8 butterflies parallel, the calculated latency is 6656 cycles. The number of butterflies can be changed to fulfil different calculated latency.

The main function blocks of the 8K parallel FFT Hardware Architecture are: the 8 radix-2 butterflies structure, the 16 FIFOs for the real inputs, the 16 FIFOs for the imaginary inputs, the complex twiddle factor memory storage, the logic controller, and the bit reverse order unit. The radix-2 butterfly based on DSP48E blocks, to improve calculated latency.

The resource utilization of the 8K FFT is shown below. The Xilinx XC5VFX130T is given for comparison (not implemented in it):

Resource Usage XC5VFX130T %

Slices 6812 17280 7.54

DSP48E 32 320 10

BRAMs 32 298 10.7

The 8K parallel FFT has a total latency of 416 μ s while operating at a 16MHz clock which meets the latency requirement of 1ms.

It could have several 8K FFT blocks in one FPGA, which means several Interferograms can be processed parallel at the same time, which is useful for FTS on board processing.

Change the numbers of butterflies, the architecture could have a trade between calculated latency and resource usage.

8562-59, Poster Session

Plasmonic resonance of bowtie antennas and their geometry dependence

Yu-Ping Yang, Minzu Univ. of China (China); Ruilin Dong, Minzu Univ. of Chian (China); Yixuan Nie, Shang Yao, Yucheng Jiang, Jing Meng, Minzu University of Chian (China)

Recently, metallic bowtie antennas have attracted increasing attention because the optical field between two bowtie tips can be enhanced tremendously by the plasmonic resonance and curvature effect of bowtie tips. Studies have shown that the strong field confinement provides a higher spatial resolution and more efficient excitation in the subwavelength-scale regime, which are useful for a variety of applications, such as the surface enhanced Raman scattering, high-density optical storage, and near-field imaging. With extensively increased conductivity of metals in the terahertz regime, the bowtie

geometries are expected to present unique plasmonic properties that were not observed at higher frequencies. In addition, the advantage of exploring such subwavelength structures at terahertz frequencies is that the well-developed lithographic processing allows for precise control over the dimensions of the microstructured bowtie unit cells, which enables systematic and highly reproducible studies of their resonant properties.

Here, in order to provide a guide for the design and optimization of bowtie antennas, their plasmonic properties have been experimentally investigated with emphasis on geometry and gap separation in THz frequencies. Based on numerical simulations, we find that absorbing properties of the periodic bow-tie particles in the terahertz regime are primarily associated with the shape, curvature, gap separation of the bow-tie unit cells.

8562-60, Poster Session

Power-efficient UWB generation based on hybrid of optical fiber link and RF circuits

Jianji Dong, Xinliang Zhang, Dexiu Huang, Yu Yu, Huazhong Univ. of Science and Technology (China)

We propose two simple solutions to generate power efficient UWB waveforms employing an electrical bandpass filter (EBPF) and a fiber link. The fiber link is used to transmit the optical signal in optical domain, and the electrical filter is used to process and generate UWB waveforms. In the first scheme, the arbitrary waveform with enough bandwidth (>10GHz) is converted to power-efficient electrical UWB signal by an EBPF with a passband of 3.1-10.6 GHz, and then intensity modulated onto an optical carrier to form an optical UWB signal, which can be distributed by a fiber link and received by a photodetector (PD). The second scheme is transmitting the optical Gaussian pulse in optical fiber link and received by a PD. Finally the received electrical signal is converted to an electrical UWB pulse by the EPBF. These solutions embody the advantages of both low-loss long-haul transmission of optical fiber and low-cost mature RF circuits.

8562-63, Poster Session

An image processing system design in a new type of infrared imaging technology based on MEMS

Qiang Tong, Liquan Dong, Yuejin Zhao, Cheng Gong, Lei Yang, Beijing Institute of Technology (China)

Compared with the traditional infrared imaging technology, the new type of optical-readout uncooled infrared imaging technology based on MEMS has many advantages, such as low cost, small size, producing simple. In addition to, the theory proves that the technology's high thermal detection sensitivity. So it has a very broad application prospects in the field of high performance infrared detection. The paper mainly focuses on an image capturing and processing system in the new type of optical-readout uncooled infrared imaging technology based on MEMS. The image capturing and processing system consists of software and hardware. We build our image processing core hardware platform based on TI's high performance DSP chip which is the TMS320DM642, and then design our image capturing board based on the MT9P031. MT9P031 is Micron's company high frame rate, low power consumption CMOS chip. Last we use Intel's company network transceiver devices-LXT971A to design the network output board. The software system is built on the real-time operating system DSP/BIOS. We design our video capture driver program based on TI's class-mini driver and network output program based on the NDK kit for image capturing and processing and transmitting. The experiment shows that the system has the advantages of high capturing resolution and fast processing speed. The speed of the network transmission is up to 100Mbps.

8562-64, Poster Session

A reflective optical readout method based on the infrared imaging system

Wenjuan Wang, Mei Hui, Cheng Gong, Liquan Dong, Xiaohua Liu, Yuejin Zhao, Beijing Institute of Technology (China)

The uncooled optical readout infrared imaging system to alter the infrared image directly into a visible image is becoming a hotspot of research recent years. How to reduce the volume and NETD value is a key problem of the optical readout infrared thermal imaging system. In this paper, an effective optical readout method of infrared imaging systems is presented. This method is proposed to design the optical readout system to reflection optical path, and a reflected filter which is complement with traditional filter is used in this method. First, the working principle of this system is described in detail, and length of readout system is calculated. Then the analysis of the characteristics and the working principle of the reflection filter is revealed in this paper. Finally, contrasting experiments have been carried out on reflective filter method and pin-hole filter method, experimental validation of this system is undergone and the feasibility of the system is proved, and NETD value of the system is obtained. Compared with traditional methods, the effective optical readout method could reduce the volume of the system, improve the uniformity of the infrared image, reduce the noise equivalent temperature difference, and improve the detective sensitivity of the infrared imaging systems. The result of experiment is basically consistent with the theory analysis. Compared with traditional pin-hole method, the reflective optical readout method can effectively improve image quality.

8562-65, Poster Session

Optimal design of high frequency readout IC for short-wave IRFPA

Pan Wang, Guo-qiang Chen, Lei Gao, Jie Zhou, Rui-jun Ding, Shanghai Institute of Technical Physics (China)

A novel design of high frequency and low signal ROIC for 512x256 short-wave IR-FPA is presented. This ROIC of a high performance in frame rate can integrate and read out the low signal. Parasitic capacitors and resistances are taken into account. An analog signal chain, which contains CTIA, CDS module, amplifier of charge and complementary output stage, can satisfy the high frequency and low signal application. The improved CTIA can get a gain of 75dB with low power dissipation. The CDS which works well in the previous design is retained. To improve the output voltage range, the amplifier of charge is employed, with which we can amplify the output voltage linearly. The structure for power supplying is changed to strengthen the reliability. The layout has been improved according to the practical test. The simulation and verification are completed both before and after completing the improved layout. The circuit's structure and operation principle are analyzed under the environment of mix-signal, and the result shows that the output dynamic range is over 2.5V, the well capacity is more than 1Me-, the frame rate is 250Hz, the linearity within useful dynamic range is above 99.9 percent, even when the temperature is about 77K. This ROIC is a full-custom flow integrated circuit design. The parasitic parameters are extracted once the layout is finished. Then the design is improved according to the result of post-layout simulation, which leads to the great improvements of most parameters.

8562-66, Poster Session

Infrared and color visible image fusion system based on luminance-contrast transfer technique

Bo Wang, Wenfeng Gong, Chensheng Wang, Huazhong Institute of Electro-Optics-Wuhan National Lab. for Optoelectronics (China)

In this paper, an infrared and color image fusion algorithm based on luminance-contrast transfer technique is presented after careful research on multi-channel and multi-sensor pixel level fusion algorithm. This algorithm shall operate YCbCr transform on color visible image, and obtain the luminance component. Then, the grey-scale image fusion methods like grey-scale weighting average method and pixel comparison method are utilized to fuse the luminance component of visible and infrared image, so that the grey-scale fusion image is acquired. After that, the grey-scale fusion image and visible image are fused to form color fusion image based on inversed YCbCr transform. In this step, the grey-scale fusion image is taken as the luminance component, and the visible image is taken as the color component. This algorithm has the advantages of low computation consumption and natural color effect, but the details appearance is not ideal. To acquire better details appearance, a natural-sense color transfer fusion algorithm based on reference image is proposed by utilizing the mean value and variance transfer of grey-scale reference image. In this way, the luminance and contrast characteristics of reference image transfer to grey-scale fusion image, and the color fusion image quality is improved. Furthermore, a real-time double channel infrared/visible image fusion system based on FPGA is realized. Finally, this design and achievement is verified experimentally, and the experimental results show that the system can produce a color fusion image not only with the natural color appearance similar as the input color visible image, but also with pleasing luminance and contrast.

8562-67, Poster Session

Theoretical and experimental research on recovering absorbance shape with wavelength modulation spectroscopy

Zhimin Peng, Yanjun Ding, Tsinghua Univ. (China); Iijuan Lan, Tsinghua University (China)

The measurement accuracy of absorbance shape directly determines the temperature, pressure, and concentration measurement accuracy in tunable diode laser absorption spectroscopy (TDLAS). However, the traditional direct absorption spectroscopy is easily influenced by particles concentration, laser intensity fluctuations, and baseline-fitting errors that often hamper the accurate determination of absorbance shape. As a result, meeting measurement requirements becomes more and more difficult. In recent years, with the recognition of the power of wavelength modulation spectroscopy (WMS) for highly sensitive measurements, many scientists have applied WMS in a number of areas to measure gas temperature and species concentration, and valuable findings have been obtained. However, the methods applied to measure absorbance shape based on WMS remain to be in the stage of exploration, and an efficient and acceptable method has not yet been developed to date. In the present paper, harmonic expressions were derived based on the absorption spectral and harmonic theories, and we also mathematically proved that the absorbance shape can be directly recovered, when the data of the X and Y axes of odd harmonic are processed by the method established in the current study. In validating the precision of this method, the transitions of NH₃ and CO₂ are selected to recover the absorbance shape using numerical simulation and experimental techniques.

8562-68, Poster Session

Terahertz polarizing beam splitter based on copper grating on polyimide substrate

Mengen Zhang, Xiangjun Li, Wentao Wang, Jianjun Liu, Zhi Hong, China Jiliang Univ. (China)

Terahertz polarizing beam splitter with high extinction ratio, large angular apertures, low attenuation and broadband polarization has recently attracted great interest owing to potential applications in terahertz imaging and spectroscopy. In this article, a terahertz polarizing beam splitter, based on a copper grating on polyimide (PI) substrate, was fabricated by the way of laser induced and non-electrolytic plating. The good polarization characteristics of the splitter in the range of $0^\circ\sim 180^\circ$ polarization are verified experimentally using backward wave oscillator at fixed frequency of 300GHz, and the insertion losses of 0.13dB and 0.32dB are measured for the transmitted and reflected beams, respectively. And the transmitted and reflected powers, normalized to the measured power in the absence of the beam splitter, followed the expected square of cosine relation as a function of polarization angle. The broadband transmission of TM wave of the splitter were also measured by terahertz time-domain spectroscopy, and the extinction ratio larger than 22dB is obtained in the frequency range of 0.2~1.5THz, experiment results were limited by the noise level of the time-domain spectroscopy setup. The theoretical simulation, based on finite element method, was used to discuss the variation of reflection/transmission characteristic and extinction ratio with different grating period or filling factor. According to the simulation results, the smaller grating period or the bigger filling factor would generate the higher extinction ratio but the lower transmittance. The theoretical simulations show a good agreement with experiment results.

8562-69, Poster Session

The design of infrared spaceborne remote sensing signal processing circuit for multi-spectral and multi-focal plane

Tao Liu, Beijing Institute of Space Mechanics and Electricity (China)

With the rapid development of space cameras and remote-sensing application technology, photoelectric sensor of the remote sensing satellite have evolved from the single-spectral, single type, single focal plane to the multi-spectral, multi-type, multi-focal plane integration direction. At present, the manufacturing process of the infrared detector has a larger improvement, but compared to the CCD device, the resolution is still low. In order to improve the resolution of infrared imaging systems, infrared imaging system using jointing multi-focal plane array can increase the resolution of infrared imaging systems. At present, remote sensing satellite equipped with a visible light detector and infrared detector, and design of multi-spectral, multi-type, multi-focal plane imaging circuit has become a new challenge. For multi-spectral, multi-, multi-focal plane imaging characteristics of the circuit system, this paper analysis and design of the FPGA signal processing circuit for multi-spectral, multi-focal plane jointing infrared imaging system, which includes time base correction circuit, infrared detector timing control circuit, multi-channel analog signal delay correction circuit, multi-channel uncertainty calibration circuit, average filtering of over-sampling circuit, multi-channel image data reading and correction circuit. Details the various parts of the design ideas and methods, design, simulation and testing. The test results show that the design is correct and feasible to meet the design requirements.

8562-70, Poster Session

Terahertz multiband filters fabricated by laser induced and non-electrolytic plating

Wentao Wang, Jianjun Liu, Xiangjun Li, Hao Han, Zhi Hong, China Jiliang Univ. (China)

Terahertz resonant devices based on metal-dielectric microstructures can be used for various applications such as spectral imaging, optical modulators, wave-tunable filters and biosensors. In this paper, we report the design, fabrication and characterization of two multiband terahertz bandstop filters. One of the filters is composed of three different square rings, and the other is the combination of individual U- and T-shape. Finite-difference time-domain modeling was used to design the structure of the filters at first. And they were fabricated on polyimide substrates by laser induced and non-electrolytic plating with copper due to its simplicity and flexibility to manufacture metal-dielectric microstructures compared to conventional photolithography. The performance of the fabricated filters was measured using a terahertz time-domain spectroscopy. Three different central frequencies are demonstrated at 0.33THz, 0.68THz and 1.13THz for the square rings filter. And the TU-shaped one shows three distinct resonances at 0.37THz, 0.73THz and 0.96THz. The experimental results are in good agreement with finite-difference time-domain simulations. In order to understand the multispectral response, we analyze the magnetic field distributions of the corresponding resonance frequencies. For the square rings, the three resonance peaks are originated independently from the external, middle and inner square ring, respectively. Accordingly, the first and third order modes of the UT-shaped filter are originated from the individual U- and T-shape, while the second mode is from the interaction between them.

8562-72, Poster Session

Methane gas detection using an intergrating sphere as a multipass absorption cell in mid-infrared band

Huan Xue Wang, Yihuai Lu, Tian Shu Zhang, Anhui Institute of Optics and Fine Mechanics (China)

The reduction of harmful environmental pollutants can have adverse effects on human health, so more and more researchers concentrate their attention on the detection of this pollutants of low concentration. This paper describes a new method of detecting methane concentration. The integrating sphere has an internal coating which is highly reflective in mid-infrared band (over 95%) and was used to input and output methane gas and other interfering gas (For example, water vapor, carbon dioxide and so on). We used a LED (centre wavelength of 3.31 μ m) as a light source and a photodiode as the detector. In order to gain a better reference spectra and improve the accuracy of the measurement, we applied the air filter technology in this experiment. When the concentration of methane gas changed, the optical path length changed with it, which has a linear relationship. Thus, it improved the simplicity and convenience of our experiment largely. The result of the experiment agreed with the basic theoretical model. According to the results of our experiment, signal pulse of 2 mA enable to detect 0.3%v/v of methane at 1cm path. The limit of detection at integration of 1mA signal over 1s is around 18 ppm. The result showed this method is a promising technique for determining the low concentration of methane gas.

8562-73, Poster Session

THz microcavity design using modal method

Xiaoyuan Lu, Xi'an Institute of Optics and Precision Mechanics (China)

No Abstract Available

8562-74, Poster Session

High-frequency analysis on RCS from terahertz conductive targets in free space

Houqiang Hua, Beijing Univ. of Aeronautics and Astronautics (China)

Numerous authors have derived a variety of methods that are used for computing the high-frequency radar cross section (RCS) of complex radar targets in the microwave or lower frequency bands in free space. A variety of RCS prediction software has been widely used for interactive modeling, design, and analysis of aircraft with RCS specifications in the microwave or lower frequency bands, such as XPATCH, CADDSCAT, RESPECT, GRECO, and RANURBS, which are based on the high-frequency techniques and provide an efficient tool to obtain real-time results. But in the scope of the authors' knowledge, it has not been reported that the electrically extremely large conductive targets in free space were calculated by the high-frequency methods in the Terahertz band.

With the development of the electromagnetic and Terahertz technology, the researchers have directed significant attention toward the targets in free space, especially the electrically extremely large perfectly electric conducting (PEC) targets outside the atmosphere or in space in many fields, such as military, astronomy, remote sensing and wave propagation. The scattering fields of the targets in free space could be computed by using the finite-element method (FEM) or finite-difference time-domain methods (FDTD), but they cause some difficulties in the solution procedure. Some researchers try to combine the free space Green's function and the method of moments to consider the electrically extremely large targets in free space, but it also requires more mass storage memory, which results in lower processing speed and computational efficiency.

This paper focuses on the prediction of RCS of conductive targets with electrically extremely large size in the Terahertz band in free space. In order to consider the scattering fields of the electrically extremely large PEC targets in free space, the Green's function was introduced into the conventional physical optics method. Combined with the graphical-electromagnetic computing (GRECO) method, the shadow regions are eliminated quickly by displaying lists technology of OpenGL to rebuild the target, and the geometry information is attained by reading the color and depths of each pixel. The RCS of Terahertz conductive targets can be exactly calculated in free space. The numerical results show that this method is efficient and accurate.

8562-75, Poster Session

Low frequency collective vibrational spectra of zwitterionic glycine studied by density functional theory

Shihua Ma, Institute for THz research, Southeast University (China); Hua Chen, Southeast University (China); YiPing Cui, Institute for THz research, Southeast University (China)

As the simplest protein structural unit and the smallest amino acid, glycine plays an important role in building proteins, constructing of RNA as well as DNAs, and aiding the absorption of calcium in the human body. Considerable efforts have been dedicated to such studies on glycine under various experimental conditions and using different theoretical methods. However, most of the works so far were confined in the mid-infrared spectral region and the research on the low frequency vibration modes is too limited to parallel with the great demand for the rich information that the spectra could provide in this spectral range. Therefore, there are many problems still are open. For example, due to the collective vibrational modes in low frequency spectral range are influenced greatly by the change of structural elements, conformation states and the surrounding environment, some assignments need further confirmation, and some absorption bands were left unassigned, the numbers of the vibrational modes and the

other spectral features in theoretical calculation are quite different from the experimental observations from time to time. Therefore, more attentions and efforts are needed in the FIR spectral range.

In this paper, DFT was employed to calculate the geometric structure and vibrational frequencies of the zwitterionic glycine in FIR region. Detailed assignments of the observed vibrational frequencies are given and the origins of some frequencies are analyzed. The low frequency collective mode of zwitterionic glycine is affected greatly by the intermolecular interaction besides hydrogen bond. At the same time, the low frequency collective vibrations of two more zwitterionic glycines are calculated, and there is more reasonable qualitative agreement between the calculated data of crystalline and observed line positions.

8562-76, Poster Session

Removal of complex-conjugate ambiguity in SDOCT by using phase shiftings

Wenyuan Cai, Zhuqing Jiang, Yujia Wang, Hao-Chong Huang, Yu-Hong Wan, Beijing Univ. of Technology (China)

• Spectral-domain optical coherence tomography (SD-OCT), as a new imaging technique developed rapidly in recent years, has widely prospective applications in clinical medicine, biomedicine and material science due to its high-resolution, high sensitiveness, non-invasion imaging. However, only one half of the imaging depth range is actually effective in the use of SD-OCT due to complex-conjugate ambiguity inherent to Fourier transform of real number data. Consequently, removal of complex-conjugate ambiguity is required to make the full depth range possible and to provide a flexible positioning for a zero plane. In order to resolve the complex-conjugate ambiguity, traditional phase-shifting technique is exploited in the work of image processing. The three-steps or more steps phase shifting method is used by most research, with which two or more phase shift operation is needed in the experiment. However, the image quality with more than three steps phase shifting may be reduced due to more than once operation, and imaging speed is also limited. In this paper, two steps phase-shifting, which only single phase shifting operation is needed, is utilized in digital image processing to resolve the complex-conjugate ambiguity and eliminate the influence of more steps phase-shifting operation on the quality of reconstructed image in FD-OCT. Based on the advantage of single-phase shift operation, quick phase shifting with waveplates or other optical elements is possible, without using a translation stage. The cost of the system may be lowered which makes it more practical. The feasibility and validity of this method is demonstrated by the reconstructed image.

8562-77, Poster Session

Infrared image quality assessment based on fractal dimension method

Zhijie Zhang, Jufeng Zhang, Song Yue, Chensheng Wang, Huazhong Institute of Electro-Optics-Wuhan National Lab. for Optoelectronics (China)

The using and observation experience of users is affected by the quality of infrared images which are collected by infrared imager. The image quality which would decline during the operation procedure as time goes on, and the severe climate is also a significant influence factor for the performance of image processing algorithm and the optimization of system parameters as well. An image quality reduced reference evaluation model is put forward to evaluate the degree of infrared image quality reduction. The image texture roughness is described by fractal dimension which is the denotation of image stability. The detail characteristic of infrared image texture is extracted by the fractal dimension analysis method proposed in this paper as the representation of image quality. The method calculates the fractal dimension of each pixel one by one with a multi-scale window over the entire image to get the corresponding information of adjacent image block. A quality

information image is mapped from the fractal dimension of all pixels to describe the infrared image quality. The parameters of the quality information image combined with the signal noise ratio of original infrared image are adopted as the metric of infrared image quality. The verification experiment of this evaluation shows that the infrared image can be graded by this method very well. As the compromise of full reference evaluation image quality method and no reference image quality evaluation method, this method can be embedded into the image processing system to optimize image processing algorithms and parameters settings, and can also provide reference for fault diagnosis.

8562-79, Poster Session

Optimization for the heating pulse used in infrared thermography non-destructive testing technology

Guo Li, Lichun Feng, Cun-lin Zhang, Capital Normal Univ. (China)

Pulsed-heating infrared thermography non-destructive testing is one of the most common used technology in industrial NDT/NDE. Compared to other theories used in infrared thermography non-destructive testing such as lock-in method, pulse-heating method has an advantage on simple instrument and easy operation while maintains a considerable accuracy. The ways used to produce a heating pulse contain flash lamp, laser, electromagnetic coil, high-temperature object contact, etc. These different ways mainly vary on heating energy and shape of heating pulse. To get an persuasive result, heating energy and width of heating pulse should be adjusted to real testing condition, which mainly depends on depth of defect and thermal conductivity of material. This paper tries to derive a method for a proper chosen of properties of heating pulse. The method is based on theory of thermal wave. First, heating pulse can be decomposed into a series of thermal waves with different spatial frequencies by Fourier transform, each thermal wave will be analyzed to evaluate its effect on creating surface temperature difference, which leads to infrared radiation difference. Then the width of heating pulse will be chosen to make itself contain more effective frequency components. During this process, the shape of different heating pulse should be taken into consideration. Heating energy will also be calculated to get a considerable contrast of infrared radiation. Finally, the effect of this method can be verified by simulation and NDT experiments in this paper. The method in this paper can provide a reference for practical NDT or NDE technology.

8562-81, Poster Session

An improved algorithm based on ROMP used in THz imaging

Ze Li, Xiaohua Liu, Yuejin Zhao, Beijing Institute of Technology (China); Cunlin Zhang, Capital Normal Univ. (China)

In lots of reconstruction algorithms of Compressive Sensing(CS), the reconstructed result of Regularized Orthogonal Matching Pursuit (ROMP) algorithm is better than others, but , the better reconstructed result of the algorithm is based on the fact that the number of iterations is equal to the sparsity of the original image, and the reconstructed result of the image is connected with the number of iterations to a great extent, thus, it's very important to estimate the sparsity of the original image accurately, if the estimated sparsity is larger or smaller than fact, the result of ROMP algorithm will be influenced seriously. To solve this problem, an improved algorithm that based on ROMP was proposed in this paper, in order to determine the best number of iterations automatically and achieve a better reconstructed image, the algorithm determines whether the number of iterations is the best or not by the previous result , instead of estimating the sparsity of the original image. Finally, a series of experiments was done, and the experimental result show that the result of this improved algorithm is better than the result of the previous ROMP algorithm with deterministic iterative number.

8562-82, Poster Session

A signal processing system of infrared remote sensing camera based on oversample and comb filter

Ning Lei, Hua Wang, Zhiyong Wei, Tao Li, Beijing Institute of Space Mechanics and Electricity (China)

Infrared remote sensing camera is a two-dimensional imaging device. The energy distribution of infrared radiation is detected and display using the temperature radiation and emittance differences between the target and the environment. There is variety of noises in the output of infrared detector, such as quantization noise, heat noise, 1/f noise, fix-pattern noise, non-uniformity noise, and so on. The presence of these noises is affected the performance of the infrared image and other processing algorithms. In this paper, a new signal processing system of infrared remote sensing camera is given. This system is used to condition and enlarge the output analog signal of infrared focal plane array. And then, the converted digital signal is processed in FPGA. Finally, the image data is output to data transmission system. The signal processing system is consisted of FPGA, ADC chip, SRAM memory, and so on. Digital low-pass filtering, pixel response non-uniformity correction, data synthesis and the conversion of output data format are implemented in a single FPGA. The SNR is improved by denoising algorithm based on oversample and comb filter, and the non-uniformity of infrared detector is eliminated by real-time correction method based on two-point correction algorithm. This system is easy to implement and can be applied in imaging device widely. The experimental results show the performance of imaging system is improved.

8562-83, Poster Session

High-range resolution profile of terahertz radar

Meiyan Liang, Capital Normal Univ. (China)

Step frequency signal is one of the more commonly used radar signal for high range resolution, it commonly used in radar target recognition. The wavelength of Terahertz signal is shorter than that of microwave, so it is easy to realize the high range resolution. The paper first introduces the step frequency signal to obtain the one-dimensional distance image, and analyzes the principle of high range resolution profiles of step frequency radar. Then, the 0.2THz step frequency radar systems are introduced. Finally, the high resolution range profiles are achieved by the simulation of Matlab. The simulation results show that the step frequency THz radar can reach centimeter level high resolution.

8562-85, Poster Session

A novel 32x1 readout integrated circuit with high dynamic range for IRFPA

Zhuang Miao, Ning Li, Zhifeng Li, Shanghai Institute of Technical Physics (China)

With the fast development of the infrared focal plane arrays (IRFPA) in recent years, the infrared imaging technology has been widely applied in various fields. As an important part of the IRFPA, the readout integrated circuit (ROIC) with wide dynamic range and high sensitivity has become one of the main research areas for the high performance IRFPA. In this paper, a novel 32?1 ROIC with high dynamic range is presented. The ROIC contains a capacitive trans-impedance input amplifier (CTIA integrator), followed by a comparator that set a threshold voltage for comparing the integrating signal. It contains the time-to-threshold information in adding additional dynamic range with a linear voltage ramp input, in addition to the regular integration signal. By the end of integration, if the integration signal is less than the threshold voltage, the integration signal is sampled for readout.

When the integrating signal is reached to the threshold voltage before the end of integration, the ramping voltage is stored and later sampled for readout in representing the signal level and a digital flag is set in recording the event of trigger. Thus, a high level signal can be saved before it saturating the integrator. A test chip of 32?1 ROIC is designed and fabricated with 0.35 μm triple metal, double poly CMOS technology. The chip test results prove correct function of the circuit with 3.3 V power supply. The results of tracing one channel show that the dynamic range increase 58 dB with a 10-bit ADC and the readout clock frequency is up to 10 MHz.

8562-86, Poster Session

A new ROIC with high-voltage protection circuit of HgCdTe e-APD FPA for passive and active imaging

Guoqiang Chen, Shanghai Institute of Technical Physics (China)

HgCdTe electron avalanche photodiode in linear multiplication mode can be used for high speed applications such as active imaging. A readout integrated circuit of e-APD FPA is designed for active/passive imaging system. Cell circuit architecture of ROIC includes a high voltage protection module, a Sample-Hold circuit module and an integrator module which includes a preamplifier and two capacitors. Generally, APD FPA works at high reversed bias such as 10V-15V in active mode, and pixels' dark currents increase exponentially as the reverse-bias voltage is increased. Some cells of ROIC may be short to high voltage because of blind pixels or breakdown of pixels. If there is no protection circuit, these cells will be burnt out, and then the whole ROIC is burnt out. Thus a protection circuit module introduced in every ROIC cell circuit is necessary. Conventional 5V CMOS process is applied to implement the high voltage protection with the small area other than LDMOS in high voltage BCD process in the limited 60 μm ?60 μm pitch area. In integrator module, two capacitors are included with a CTIA input stage to integrate e-APDs' photocurrent, one of them can be shared in two modes in order to save area. The integration time in active mode can be altered by the step of 10ns. A cascode structure is performed as pre-amplifier to reduce the power consumption, area and to void potential instability caused by inaccuracy of MOSFET Model at 77K.

8562-24, Session 6

Double channel mechanically tunable terahertz filter based on parallel plate waveguide cavities (*Invited Paper*)

Lin Chen, YiMing Zhu, Univ. of Shanghai for Science and Technology (China)

Theoretical and experimental works were carried out on a double channel mechanically tunable terahertz filter integrated with parallel plate waveguide cavities. The filter includes two rectangular grooves on upper and bottom plates of waveguide, respectively. The filtered frequency can be linearly tuned by altering the overlap distance between the two rectangle grooves on metal plates together with the Q values. From the experiment, we found the central wavelength can be adjusted from 0.403THz to 0.412THz at low frequency and 0.348THz to 0.366THz at high frequency, and the Q values can reach 46 when the resonant frequency is 0.41THz. Theoretical results show good agreement with experiment.

8562-25, Session 6

Millimeter-wave imaging with frequency scanning antenna and optical arrayed waveguide grating (*Invited Paper*)

Yuntao He, Guoxin Yu, XinYu FU, Yuesong Jiang, Beihang Univ. (China)

A novel millimeter-wave (MMW) imaging method using frequency scanning antenna and optical arrayed waveguide grating is proposed in this paper. The wideband MMW signal processing has been a big problem in the MMW imaging system with frequency scanning antenna. In the proposed method here, the wideband signal collected by MMW frequency scanning antenna is modulated to the optical domain by a phase electro-optical modulator (EOM). The carrier is suppressed and the first side band (FSB) of the modulated optical is transmitted to a special designed optical arrayed waveguide grating (AWG). The AWG could be used to read out each ultra narrow band of the FSR which represents the received wideband MMW signal synchronously. As every narrowband of the received MMW corresponds to every different induced angle, so the real time imaging can be achieved by a simple processing of the output of the AWG.

The principle of the advanced imaging method is analyzed theoretically firstly. A 34~44GHz frequency scanned antenna is then designed carefully with a field of view of 40 degrees for the MMW imaging system. The received wideband MMW signal is amplified with a wideband preamplifier from Cernex Corp. and modulated by a Convege 40GHz phase EOM. An AWG of 1x32 is designed specifically with a channel spacing of 0.3GHz. A simulated imaging system is constructed by the designed results and those components in lab. The designing and simulating demonstrated the feasibility to set up such an imaging system which is progressed.

8562-27, Session 6

A new design of signal processing system for TDI infrared focal plane array

Hua Wang, Tao Li, Xu Wang, Ning Lei, Zhiyong Wei, Beijing Institute of Space Mechanics and Electricity (China)

In this paper, according to the output signal characteristics of TDI(Time Delay Integration) infrared focal plane array, a novel signal processing system based on AC coupling technology is proposed. Firstly, the output signal characteristics of TDI infrared focal plane array are analyzed. The key feature is that the output sequence of signal in each line cycle of TDI detecto is several reset signals followed by a certain number of valid signals, and the level of reset signals is fixed in a given TDI detector. Secondly, the signal processing system based on AC coupling technology is introduced. The designed system is consist of high pass filter circuit, signal condition circuit, differential input analog to digital converting circuit and digital data processing circuit. DC component of output signal from TDI infrared detector is removed by high pass filter circuit. The remaining AC signal is conditioned by signal condition circuit and is converted to digital data by differential input analog to digital converting circuit. The digital DC restoration of valid signals from detector is implemented by digital data processing circuit, which references the digital data of the reset signals. Finally, the designed system is simulated and tested. Simulation and test results show that the novel design idea of signal processing circuit is reasonable and feasible. Compared with the traditional design, the system has the characteristics of high common mode noise rejection, low level drift and low power consumption.

8562-28, Session 6

Aluminum-coated hollow waveguides for the transmission of terahertz radiation

Jing Liu, Jingling Shen, Capital Normal Univ. (China)

We have applied techniques developed for IR waveguides to fabricate Al-coated hollow PTFE waveguide(HPW)s for transmission of terahertz radiation. A wavelength tunable Backward Wave Oscillator(BWO) is used as the THz source. The losses for these hollow-core waveguide are measured by a Pyroelectric detector. Losses at frequencies range from 200GHz to 210 GHz are obtained for 8mm bore, 15/20/30cm long Al HPW. We also test the hollow PMMA waveguide in such range of frequencies. Further simulation is done besides experiments.

8562-29, Session 7

Terahertz super thin planar lens (*Invited Paper*)

Yan Zhang, Capital Normal Univ. (China)

TERAHERTZ (THz) radiation has attracted extensive attentions in the past decades. Many developments have been made in the fields of sources, detector, and applications. However, due to the long wavelength property of the THz radiation, the size of the optical elements for dominating THz beam is quite large. They are not suitable for THz system integration. Based on the diffractive optics theory, the thickness of an element, for example, a lens can be reduced from several millimeters for bulk elements to several hundred micrometers for diffractive optical elements. However, this size is still too large for some applications. Is it possible to reduce the thickness of the THz lens?

A recently published paper presents a possible approach to reduce the thickness of the THz lens further¹. For a V shaped metal antenna, the illuminating radiation will resonate with the charges generated on the surface of metal. By accurately selecting the lengths of two arms and the angle between two arms of the antenna, the amplitude and phase of the resonance wave can be effectively controlled. If the antennas are selected with same resonance amplitude but different phase sampled from 0 to 2π with equal step, one can use these antennas to form arbitrary elements based on the theory of diffractive optics. The size of the antennas is about 1/4 of the wavelength and the thickness of the antennas is only 1/4000 of the wavelength.

The amplitudes and phases of transmitted waveforms of the antennas with different arm lengths and angles have been theoretically calculated using the finite difference time domain method, 8 antennas with same transmitted light amplitude are selected. The phase difference between two adjacent antennas is $\pi/4$. Using the diffractive optics theory, a lens with 4mm focus length for 0.75THz is design and the phase distribution is quantized. The corresponding antennas are selected to generate difference phase difference. The samples are fabricated on a100nm thick gold film on a silicon wafer substrate with the traditional optical lithography method.

The sample is characterized with a THz focusing plane imaging system. The range of the THz radiation is 0.2-2.6THz. The sample is located 4mm away from the detection crystal and under the plane wave illuminating. The waveform at each point on the detection crystal can be achieved via scanning the time delay. After the Fourier transform, the complex amplitude distribution on the focusing plane for 0.75THz can be obtained. The THz wave has been well focused to a point. The FWHM of the focus point is about 400 μ m. The thickness of the lens is only 1/4000 of the illuminating wavelength.

8562-30, Session 7

Atmospheric profiling synthetic observation system at THz (*Invited Paper*)

Qijun Yao, Dong Liu, Jing Li, Zhenhui Lin, Zheng Lou, Shengcai

Shi, Purple Mountain Observatory (China); Hiroyuki Maezawa, Osaka Prefectural University (Japan); Scott Paine, Harvard-Smithsonian Center for Astrophysics (United States)

In this paper, we will introduced a dual-THz-band SIS (Superconductor-Insulator-Superconductor) heterodyne radiometer system developed for the atmospheric profiling synthetic observation system project (APSOS). This THz system is intended to have a durable and compact design to meet the challenging requirements of remote operation. The system as well as its major components such as antenna tipping, quasi-optics, cryogenics, SIS mixers and FFTS backend will be discussed thoroughly. Some scientific simulation focusing on the atmospheric profiling componets at THz bands will also be investigated.

8562-31, Session 7

640x512 InGaAs focal plane array camera for detecting 1.58 μ m absorption spectra of CO₂

Wei Peng, Lei Ding, Xianghua Wang, Shanghai Institute of Technical Physics (China)

This Paper introduces a 640x512 InGaAs focal plane array (FPA) camera for measuring 1.58 μ m absorption spectra of CO₂. To gain atmospheric CO₂ concentration by detecting short wave infrared of reflective sunlight has been demonstrated to be an effective way. A hyperspectral spectrometer is designed to detect 1.58 μ m absorption spectra of CO₂. The spectrometer is a grating spectrometer which is able to response to the spectral range from 1.561 ~ 1.591 μ m with spectral resolution of 0.1nm. For high sensitivity, F number is determined to be 1.8. We designed a 640x512 InGaAs FPA camera coordinating with the grating spectrometer.

The camera integrated a 640x512 InGaAs FPA with a 25 μ m pixel pitch. The 640x512 InGaAs FPA has characteristics of quantum efficiency no less than 65% at wavelength of 1.58 μ m, pixel operability more than 99.91%, two gain modes and three integrate modes. The 640x512 InGaAs FPA is sensitive to 0.9 μ m-to-1.7 μ m short wave infrared (SWIR) band and features a 298 K temperature detectivity, D^* , greater than 5.7×10^{12} cm²·Hz/W. The camera features 3Hz rate (exposure time) and 14-bit output. The FPA's TEC module is controlled to keep the detector core at low temperature. The detector core temperature is going to be adjusted to below 253 K for lower readout noise and dark current. A Universal Series Buses 2.0 (USB2.0) has been used to transmit images and commands. Commands of window size, position, Gain mode and integrate time per frame can be sent by the USB2.0 interface.

8562-32, Session 7

A kind of wide range imaging spectrometer based on deformed Michelson interferometer

Liu Yang, Beijing Institute of Technology (China)

Ultraviolet(UV), Visible and Short-wavelength infrared(SWIR) band Imaging spectrum technology is widely used in various filed such as astronomy, remote sensing, biology, chemistry, etc. This paper will describe a new kind of imaging spectrometer which working band could cover UV to SWIR(250nm-1700nm) just by switching detector and band-pass filter. It is a kind of time modulated Fourier Transform Imaging Spectrometer base on deformed Michelson Interferometer with no moving mirror and one of the mirror rotated a tiny angle from it symmetry position. It could achieve much higher light flux than space modulated type and also without moving part in the interferometer with highly sensitive to external environment. A catoptric imaging lens which called offner system were also be used to ensure there is no chromatic aberration and high resolution during the whole working band. The object lens and beam splitter were made by Fused Silica and the catoptric imaging lens to ensure the whole optical system had high

transmission from 250nm to 1700nm?.

The model of this interferometer will be established in this paper, the window scan and data processing will also be described. Several experiments had been made in different spectral band and the results will be given at the end of this paper. It shows that the imaging spectrometer could obtain and reconstructed spectral data cube correctly in each spectral band, and the resolution of wavenumber is better than 160cm⁻¹ in UV-visible band, better than 60cm⁻¹ in SWIR band.

8562-33, Session 8

THz radiation properties of silver cone antenna arrays (*Invited Paper*)

Mingzhe Hu, Guizhou Univ. (China); Kaijun Mu, Cunlin Zhang, Capital Normal Univ. (China); Ding Zhao, Guizhou Univ. (China)

THz wave finds wide and important applications in drug, bombing and metal danger material detecting, biochemical imaging and food safety detecting. Recently, J.F.Scott et al. reported for the first time that a wide bandwidth THz radiation could be generated by irradiating PZT ferroelectric nanotube array with femto second pulse laser, which can radiate a 2.78THz THz pulse, expanding the THz band gap that traditional semiconductor cannot cover. Moreover, the micrometer or nanometer scale sized antennas possess large surface area and high surface carrier mobility, which will enable a significant improvement of radiated THz power. Therefore, the novel THz radiating technology based on micrometer or nanometer antenna arrays has a potential capability to overcome the present bottleneck of narrow THz bandwidth and low radiation power in traditional electrooptic crystals and photoelectric conductors. In the present work, we set the silver cone antenna and its array antenna as the investigation objects. The THz properties, including the electromagnetic field distribution, of these antennas radiated by the femto second laser were investigated using the moment method and the CST microwave studio software. We designed a single Ag cone antenna and moment method is employed to analyze the solution process of the integrate equation of the irradiated electric field. Results indicate that when the bottom radius of the Ag antenna cone is 5μm and the height of the cone is 22μm, the bandwidth is 7.9~6.8THz at the working frequency of 7.3THz. The radiation gain of the THz electromagnetic wave of the single Ag cone antenna is 22.7dBi under the resistance matching condition. Moreover, the radiation pattern can be effectively improved through combining the single Ag cone antenna into N×N square arrays and the radiation gain can also be enhanced to 42.5dBi.

8562-34, Session 8

Near-field thermal radiation characteristics of metamaterials

Yang Bai, Yongyuan Jiang, Harbin Institute of Technology (China)

In this paper, we theoretically derived the local density of electromagnetic state (LDOS) in vacuum above a semi-infinite metamaterial. Simulated result of permittivity and permeability were used to analyze the LDOS and heat transfer of metamaterial. It showed that p-polarization surface wave is the main contribution to near field enhanced radiation for electrical response; s-polarization surface wave is the main contribution to near field enhanced radiation for magnetic response. The method used and results obtained from this study suggested a convenient way to control the enhanced near field radiation.

8562-35, Session 8

Fast angle catching methods of a millimeter wave radar for hypersonic aircraft

Haibin Zeng, Ying Huang, BITTT (China); Tao Li, EAAF (China); Shasha You, BITTT (China)

Because of its high frequency, a millimeter wave radar will meet angle catching problem for hypersonic aircraft. One hand, antenna beam width of a millimeter wave radar is remarkably narrow comparing with ordinary centimeter wave radar as the same antenna size. On the other hand, Doppler dynamic will be much bigger than that of a lower frequency radar. These two factor make a millimeter wave radar need a fast angle catching method to avoid target fly away antenna beam or too bigger Doppler make signal can not be locked.

In this paper, three kinds of methods are introduced: the first one is the delay-correlation method; the second one is correlation method; the last one is cycle spectrum correlation method. All these three methods need no data demodulation, so they can output angle value quickly. They have different advantages and disadvantages, and are used in different condition.

Delay-correlation method is fit for mono-channel and mono-pulse angle tracking system. The received signal pass a delayer, then correlate with itself. A notable advantage of the method is that it has a very simple structure. But its performance is not very good when SNR is very low. Correlation method is fit for double-channel and mono-pulse angle tracking system. But it can improve the output, reduce the influence of noise. Cycle spectrum correlation method has perfect performance. But it needs much more resource.

This paper introduces theory and performance of these three methods, especially in high dynamic and low SNR condition. Then it points out how to select a method in different condition according to their character.

8562-36, Session 8

A novel quasi-optical subharmonically pumped GaAs diode mixer at 375 GHz

Jie Hu, Zheng Lou, Sheng-Cai Shi, Purple Mountain Observatory (China)

This paper presents the design, characterization, and the fabrication of a novel quasi-optical subharmonically pumped GaAs Schottky diode mixer at 375 GHz. It features the use of two off-axis double-slot antennas to receive the RF and LO signals respectively, aiming to obtain a better coupling efficiency. The mixer circuit together with the antennas is integrated on a silicon extended elliptical lens. The mixer circuit is based on coplanar waveguide design and consists of an anti-parallel Schottky diode pair, harmonic filters and matching networks. In order to achieve good isolations between RF and LO ports, quarter-wavelength resonator directly-coupled bandpass filters are introduced at both RF and LO ports. The IF filter is a seventh order chebyshev lowpass filter with cutoff frequency at 90 GHz, which will be sufficient to block both the RF and LO signals. Conventional harmonic balance simulations in combination with 3D fullwave simulations in HFSS are carried out to analyze the performance of the mixer. Optimal conversion loss is obtained after impedances of the LO and RF ports are matched. A 5 mW local oscillator power is shown to be sufficient to pump the mixer. Finally, measurements at 375 GHz were conducted to verify the performance of the mixer.

8562-80, Session 8

A low-power SAR ADC for IRFPA ROIC

Lei Gao, Ruijun Ding, Jie Zhou, Pan Wang, Guoqiang Chen,
Lichao Hao, Shanghai Institute of Technical Physics (China)

This paper presents a low power ADC for the 512×512 infrared focal plane arrays (IRFPA) readout integrated circuit (ROIC). Our work shows the major structure, the working mode and the simulation result of the readout integrated circuit. The power supply voltage of $0.35\mu\text{m}$ standard CMOS process is 3.3V in this study, and then the dynamic range of the DI (direct injection) input circuit is reached 2V. Successive-approximation-register (SAR) ADC architecture is used in this readout integrated circuit. And each ADC is shared by one column of the IRFPA. This successive approximation ADC is made up of a 13-bit digital-analog converter (DAC), a high resolution comparator and a digital control circuit. The most important part is the voltage-scaling and charge-scaling charge redistribution DAC. In this DAC, charge scaling with a capacitor ladder to determine the least significant bits is combined with voltage scaling with a resistor ladder to determine the most significant bits. The comparator uses three-stage operational amplifier structure to have a 77dB differential gain. The Common-Mode input range of the comparator is 1V to 3V, and minimum resolvable voltage difference is 0.3mV. This SAR ADC has some advantages, especially low power and high speed. The simulation result shows that the resolution of the ADC is 12 bit and the conversion time of the ADC is $6.5\mu\text{s}$, while the power of each ADC is as low as $300\mu\text{W}$. Finally, this SAR ADC can satisfy the request of 512×512 IRFPAs ROIC with a 100Hz frame rate.

Monday - Wednesday 5 -7 November 2012

Part of Proceedings of SPIE Vol. 8563 Optical Metrology and Inspection for Industrial Applications II

8563-1, Session 1

A composite quality-guided phase unwrapping algorithm for fast 3D profile measurement (*Invited Paper*)

Ke Chen, Jiangtao Xi, Yanguang Yu, Univ. of Wollongong (Australia); Limei Song, Tianjin Polytechnic Univ. (China)

Fringe pattern profilometry (FPP) is one of the most promising 3D profile measurement techniques has been widely applied in many areas. A challenge problem associated with FPP is the unwrapping of wrapped phase maps resulted from complex object surface shapes. Although existing quality-guided phase unwrapping algorithms are able to solve such a problem, they are usually extensively computational expensive and not able to be applied to fast 3D measurement scenarios. This paper proposes a new quality-guided phase unwrapping algorithm with higher computational efficiency than the conventional ones. In the proposed method, a threshold of quality value is used to classify pixels on the phase maps into two types: high quality (HQ) pixels corresponding to smooth phase changes and low quality (LQ) ones to rough phase variance. In order to improve the computational efficiency, the HQ pixels are unwrapped by a computationally efficient fast phase unwrapping algorithm, and the LQ pixels are unwrapped by computational expensive flood-fill algorithm. Experiments show that the proposed approach is able to recover complex phase maps with the similar accuracy performance as the conventional quality-guided phase unwrapping algorithm but is much faster than the later.

8563-2, Session 1

An approach to compensate the object movement errors in phase shift profilometry

Lei Lu, Jiangtao Xi, Haiping Du, Yanguang Yu, Univ. of Wollongong (Australia); Limei Song, Tianjin Polytechnic Univ. (China)

Phase shift profilometry (PSP) technique is widely used in 3-D shape measurement for many applications. However PSP needs multiple fringe patterns projected onto the object and reference plane to calculate the phase value, the object must be static when the measurement is taken. If the object moves during the measurement, significantly errors can be introduced to the phase result. Zhang and Yau used a modified two-plus-one phase shift algorithm to alleviate the errors due to motion. Because the phase value only contains in the first two fringe patterns, the measurement error due to motion is less. Wang and Zhang et al. solved for the phase unwrapping errors caused by rapidly moving object. However they still cannot reduce the inherent phase error caused by motion. This paper analyses the relationship between object movement and phase value, and proposes a compensation method for errors caused by two dimensional movement of object. Through the compensation algorithm, the errors caused by two dimensional movement of object can be eliminated. The effectiveness of the proposed technique is tested and verified by both simulations and experiments.

8563-3, Session 1

Multi-frequency sweeping interferometry using spatial optical frequency modulation

Samuel Choi, Osami Sasaki, Takamasa Suzuki, Niigata Univ. (Japan)

The multi-frequency light source such as "optical frequency comb" has been applied to advanced white-light interferometry for surface profile measurement and optical coherence tomography. Recently, it is demonstrated that the interference amplitude and phase distributions produced by sweeping of multiple frequency spacing differ from the white-light fringe produced by the conventional white-light interferometry. The high order amplitude peaks obtained by sweeping of the frequency spacing is a well-known characteristic of the multi-frequency interferometry (MFI). However the characteristic that the interference phase distribution can be controlled independently of the amplitude distribution by shifting of the center frequency is not demonstrated experimentally yet. We investigated the interference phase distribution by means of a novel multi-frequency light source with a spatial frequency filter (SFF) and a sinusoidal phase modulating interferometer (SPMI). This light source generated a quasi-optical frequency comb which varies the frequency spacing and center frequency independently. The zeroth and first order interference amplitude and phase distributions were investigated. The fixation of the phase was observed during the frequency spacing was swept and the center frequency was fixed. The shift of the phase was observed during the center frequency was shifted and the frequency spacing was fixed. The principle of MFI relating to the interference phase and the center frequency was successfully demonstrated.

8563-4, Session 1

Simulation of real-time large-scale absolute distance measurement with a pair of femtosecond frequency comb lasers

Yang Li, Graduate School at Shenzhen, Tsinghua Univ. (China); Qian Zhou, Tsinghua Univ. (China); Kai Ni, Graduate School at Shenzhen, Tsinghua Univ. (China); Guan hao Wu, Tsinghua Univ. (China); Xiaorui Qiao, Graduate School at Shenzhen, Tsinghua Univ. (China)

Absolute distance measurement is essential in large-scale equipment manufacturing and scientific projects. Nowadays, sophisticated equipment manufacture demands for high-precision ranging with a high speed. Femtosecond frequency comb laser makes it possible to determine the distance at higher precision, with its stable interval of frequencies and wide spectral range. However, most of such systems utilized repeat frequency scanning method to realize absolute distance measurement, suffering from the low measurement speed. Fortunately, the ranging method based on a pair of femtosecond frequency comb lasers can potentially resolve such problem.

In the method, one femtosecond laser is utilized as measurement pulses, and another femtosecond laser with a tiny discrepancy in repeat frequency is used to scan the return pulses. The output signals clearly show the phase offset caused by distance. Fourier transformation of the output signals gives frequencies and the corresponding phase offsets, from which we fit a straight line to calculate the distance. Theoretically, such method can realize real-time measurement. But it implies great demands for the data processing system.

We simulated the absolute distance measurement with a pair of femtosecond frequency comb lasers in this paper, and estimated the parameters of data processing system. Analyzing the result of simulation, we gave the suitable bits and sampling frequency of ADC, so as to improve the precision of linear fitting in data processing. And it comes to a conclusion that slow detector with a relatively long response time can be adopted. The possibility of real-time measurement is demonstrated.

8563-5, Session 2

A ball bar based self-calibration technique for 5-axis optical measurement system

Xiaoming Du, Huazhong Univ. of Science and Technology (China) and GE Global Research (China); Jiajun Gu, GE Global Research (China); Kevin G. Harding, GE Global Research (United States)

Micro level accuracy metrology is getting more interesting to modern industry manufacturing, such as high end cutting tools, EDM tooling and so on. Non-contact optical measurement plays an increasing role among industry metrology due to its efficiency on small feature and complex freeform surface measurement capability. System accuracy is essential to such kinds of applications.

This paper presents a ball-bar based self-calibration technique for a 5-axis point laser optical measurement system. The system is composed of a high accuracy laser point sensor and five motion stages X, Y, Z, B, C. A kinematical system model of the 5-axis measurement system is presented to map the stages and sensor readouts to the target position of the object to be measured. With an assumption that each stages' linearity error, straightness errors, angular errors and sensor linearity error have been calibrated or omitted due to high performance hardware selection, the three squareness angles, laser beam direction and rotary axis position and direction of the two rotary stages are well addressed as the model parameters in the system model. Heuristic methods are introduced to separately calibrate the system squareness, beam direction and rotary axis by using different data acquisition approaches over the ball bar. Parameter estimation methods are applied to obtain the system model parameters via the data point cloud of the ball bar. Experimental studies using cylinder bar and ball bar demonstrate that the system achieved an accuracy better than 5 micron.

8563-6, Session 2

A 3D measurement method and its calibration base on the combination of binocular and monocular vision

Dong Li, Jindong Tian, Xin Yang, Shenzhen Univ. (China)

The traditional binocular active vision measurement system consists of two cameras and a projector, which can be regarded to two monocular vision systems composed by the projector and a camera. In this paper, we present a three-dimensional (3D) measurement method based on the combination of binocular vision and monocular vision. The common field of view is reconstructed by a binocular vision system, and the missing data area is filled up by two monocular vision systems. In order to improve the measurement accuracy and unify the three world coordinate systems, a calibration method is proposed. The calibration procedure consists of a binocular vision system calibration, the two monocular vision systems calibration and a globe optimization of the three systems for unifying to a common reference. In monocular vision system calibration, a new method based on virtual target is proposed and used to set up the coordinate relations. We use a projector and two cameras to build a vision system for testing the proposed technique. The experimental results show the calibration algorithm ensures the consistent accuracy in the three systems, which is important for data fusion. And it is clear that the proposed method improves the integrity of measurement results and measuring range efficiently.

8563-7, Session 2

A data processing method to improve the accuracy of depth measurement by binocular stereo vision system

Jia Tang, Ming Zhang, Liqiang Wang, Zhejiang Univ. (China)

It is difficult to achieve accurate calibration of binocular stereo vision system in certain situation. When the system without accurate calibration is used in depth measurement, large systematic errors occur because of coarse calibration. In order to improve the measurement accuracy, we directly calibrate the existed systematic errors after simple calibration steps of the binocular vision system include calibrated the camera's focal length and the distance between two cameras. The depths of the targets located at different distances are measured at three different field of views, which are center field of view, 0.7 field of view and edge field of view. After got the original results, the relationship between the depth errors, the field of views and the distances is analyzed. The error curves for correction are obtained by using the data fitting method, which are used to eliminate the systematic errors and to get the relatively accurate data. We also discuss the factors for causing the error. Based on image processing, a simple matching program is designed to automatically match the feature points at left and right images, and to calculate the depth of the feature points.

8563-8, Session 2

Emission coordinates calibration and precision detecting of 3D measurement system

Honggang Lu, Chunsheng Hu, National Univ. of Defense Technology (China)

We have developed a 3 dimensional deformation optical measurement system, it can be used in the deformation measurement of warship and traking ship. The accuracy of measurement can achieve 3?.

For precision detecting of 3-Dimensions Optical Measure System (OMS), a calibration method of auxiliary coordinate and the optical coordinate base on theodolites has been proposed. The installation method of auxiliary mirrors is elaborated firstly. Installation accuracy of the auxiliary mirrors is detected. Then the influence of Axis-Error of theodolites is analyzed under the condition of our experiment. Base on this work the influence on the OMS's Precision Detecting caused by the misalignment of auxiliary coordinate and optical coordinate is analyzed and calculated. Through our experiments and analysis we find that the coordinates alignment accuracy is no more than 10?. The measuring range of 3-D OMS is $\pm 3?$, on these conditions the precision detecting error of the OMS is no more than 1?. So our method is not only high accuracy but also low requirement for the installation of auxiliary mirrors. This method is also available for other similar work.

8563-9, Session 3

Optical profiler and its applications in industrial measurement and inspection (Invited Paper)

Dong Chen, Bruker Nano Inc. (United States)

Optical profilers have been widely used in many areas of surface measurements and characterizations in the past 30 years. It measures parameters such as step height, surface roughness, films thickness in range from sub-nanometer to micrometers with sub-nanometer resolution and accuracy. In this paper, we will present some of the application oriented 3D measurement techniques using optical profiler

in both R&D lab and industrial production floor. The discussion will target some measurement challenges encountered in optical 3D metrology applications such as resolution enhancement, thin film thickness with rough surfaces, dissimilar material compensation, and high aspect ratio micro-size feature measurement. The industrial applications will include quality controls in precision machining, data storage, HB-LED, semiconductor, lead angle, and others.

8563-10, Session 3

Absolute measurement of optical surface profile with a Fizeau interferometer (*Invited Paper*)

Osami Sasaki, Niigata Univ. (Japan); Akihiro Watanabe, Niigata University (Japan); Samuel Choi, Takamasa Suzuki, Niigata Univ. (Japan)

A method of absolute measurement of optical surface profile in a Fizeau interferometer using a laser diode is proposed. Wavefront aberration in the interferometer causes an undesirable phase distribution in the interference signal. To eliminate this phase distribution, the object surface is shifted in two directions orthogonal to each other and the difference data of the surface profile of the object is obtained. Because the undesired phase distribution does not change by the shifts of the object surface, this phase distribution is eliminated in the difference data which is the difference between the two phase distributions of the interference signal before and after the shift. An absolute surface profile is estimated by representing the object surface with a polynomial function and by solving the difference equations with least-squares method. The object was an 80-mm-diam flat mirror, and the shift amount of the object surface was 4mm in the two directions. The phase distribution of the interference signal was detected with sinusoidal phase-modulating interferometry. The two-dimensional surface profile was represented by a polynomial function with two variables whose degree was less than 4. The coefficients of the terms in the polynomial function were estimated from the difference data with least-squares method. PV (peak-valley) and RMS (root mean square) values of the estimated object surface were 8.9 nm and 1.5 nm, respectively, while their values of the reference wavefront were 46 nm and 4.3 nm, respectively. These experimental results made clear the usefulness of the proposed absolute measurement method.

8563-11, Session 3

Spindle error motion measurement using concentric circle grating and phase modulation interferometers

Masato Aketagawa, Muhummad Madden, Shuhei Uesugi, Takuya Kumagai, Yoshitaka Maeda, Nagaoka Univ. of Technology (Japan); Eiki Okuyama, Akita Univ. (Japan)

In the conventional methods to measure concurrently radial, axial and angular motions of a spindle, complicated reference artifacts with relative large volume (for example, two balls linked with a cylinder) are required. A simple and small artifact is favorable from the viewpoint of the accurate measurement.

This paper describes a concurrent measurement of spindle radial, axial and angular motions using concentric circle grating and phase modulation interferometers. In the measurement, the grating with fine pitch is installed on top of the spindle of interest. The grating is a reference artifact in the method. Three optical sensors are fixed over the concentric circle grating, and observe the proper positions of the grating. The optical sensor consists of a frequency modulated laser diode and two interferometers. One interferometer observes an interference fringe between reflected light from a fixed mirror and 0-th order diffraction light from the grating. Another interferometer observes an interference fringe between ± 2 nd diffraction lights from the grating.

By the combination of the two interferometers, the optical sensor can measure radial and axial displacements of the concentric circle grating simultaneously. By use of the three optical sensors, three radial displacements and three axial displacements of the proper observed position of the grating can be measured. From these measured displacements, radial, axial and angular motions of the spindle can be calculated concurrently. In the paper, a measurement instrument, a novel fringe interpolation technique by sinusoidal phase modulation and experimental results are discussed.

8563-12, Session 3

Automated cylindrical mapper using chromatic confocal measurement

Esmaeil Heidari, Kevin G. Harding, GE Global Research (United States)

Characterization of a surface shape and finish has been vital for the manufacture of precision parts. Overall profile, surface finish and waviness of a part can be measured in two ways, contact and non-contact. In the contact method a stylus is dragged on the surface of a part to measure the profile and texture of the part for quantifying the surface characteristics. Non-contact methods applied to precision metrology include: microscopy, interferometry, chromatic confocal microscopy and laser profiling such as structured light methods. The chromatic confocal method offers flexibility because of its fiber optics probes that can be manipulated to accommodate many sample geometries. This flexibility provides a wide range of possible analysis dimensions such as cylindrical shapes of holes and the potential to provide both surface roughness and shape. This paper will discuss the setup and testing of a system specifically for measuring cylindrical shaped parts and present the performance of the technology as a precision metrology tool.

8563-13, Session 3

Imaging Stokes polarimeter by dual rotating retarder and analyzer and its application of evaluation of Japanese lacquer

Ryota Mizutani, Yukitoshi Otani, Tomoharu Ishikawa, Miyoshi Ayama, Utsunomiya Univ. (Japan) and Utsunomiya Univ. Ctr. for Optical Research and Education (Japan)

Japanese lacquer is a kind of traditional crafts. Its color is black but there are different texture feelings because it is complicated manufacturing process such as repeating steps of japing and polishing with different materials. In this report, we focus polarization properties of surface structures of black Japanese lacquer. All polarization states can be expressed Stokes parameters which consists on four elements of from s_0 to s_3 . These parameters are effective for the evaluation of the state of polarization. As the new approach which is evaluated the state of the surface, we visualize the polarization information of the surface of Japanese lacquer by using an imaging Stokes polarimeter by dual rotating retarder and analyzer. By comparing the degree of polarization, it is possible to evaluate the state of the surface by visualizing of polarization information. Therefore, it can be said that it is effective to evaluate the surface by using the polarization information.

8563-14, Session 4

Phase shift reflectometry for sub-surface defect detection (*Invited Paper*)

Anand K. Asundi, Nanyang Technological Univ. (Singapore); Parthasarathy Sreemathy, Eden Toh, Sook May Watt, Raffles

Girls School (Singapore); Lei Huang, Nanyang Technological Univ. (Singapore)

Sub-surface indentations in a “Magic Mirror” are used as an example of sub-surface defect detection using various methods such as an Optical Microscope, an Interferometer, a Laser Confocal Microscope, the Scanning Electron Microscope and Atomic Force Microscope, and the Phase Shift Deflectometry. The “Magic Mirror” displays an image formed by the sub-surface indentations when the mirror is illuminated by a beam of light such as from the sun. The indentations are formed on a convex surface and are coated with a thin partially reflecting transparent layer and thus no surface irregularities were detected on the surface of the magic mirror using a standard optical microscope. Furthermore the size of the mirror is typically around 100 mm in diameter. Thus the challenge is to measure sub-micron sized defects below a thin layer of reflective coating on a convex surface with a relatively large diameter.

A conventional Fizeau interferometer, an obvious choice did not provide any useful results. Since the surface of the magic mirror is convex, the reference flat used in the interferometer was not the right choice for the reference surface. Due to lack of other reference surfaces, no conclusive results were obtained. A Laser Confocal System also was unable to pick up any information - partly due to the large size of specimen and partially due to the defect causing the light to be reflected outside the imaging objective. The SEM and AFM were too sensitive and measure only a very small area and thus not a suitable choice for this detection.

However, with the use of Phase Shift Reflectometry (PSR), the subsurface dents could be readily detected and measured. PSR is sensitive to the surface slope measurement and hence can readily detect small surface distortions. This was demonstrated in our earlier work wherein PSR was found to be better than the Phase Shift Profilometry for dent identifications. PSR illuminates the specimen with computer generated phase shift sinusoidal fringe patterns. The reflected pattern is recorded and processed using traditional phase shift equations. The resulting phase is then proportional to the surface slope which can be integrated to provide the surface shape of dents. A calibration is necessary to convert the phase information into quantitative depth information. Preliminary analysis indicates that the indentation had depths of the order of a few 100s of nanometers.

8563-15, Session 4

Continuous bucket creep measurement based on moiré

Yi Liao, Robert W Tait, Kevin G. Harding, Wayne C. Hasz, Edward J. Nieters, GE Global Research (United States)

Due to the high temperatures and stresses present in the high-pressure section of a gas turbine, the airfoils, referred to as buckets, experience creep. As gas turbine manufacturers move increasingly toward condition-based maintenance programs whereby the life of a component is assessed to determine its remaining life, the ability to accurately assess creep or other failure modes becomes critical. One approach for measuring creep is the use of moiré imaging. Using pad-print technology, a grating pattern can be printed directly on a turbine bucket. By measuring the change in the moiré fringes, it is then possible to determine creep locally. This paper reviews the development of a prototype system and analysis software for making creep measurements. Using a bench top camera system, measurements of creep in several parts have been taken. As part of these measurements, a sensitivity analysis has been conducted to determine the influence of noise factors on system performance. Finally, the results of creep measurements on test bars have been compared to strain gage measurements, and the results show good agreement between the two techniques.

8563-16, Session 4

Circular gratings' moiré effect for projection measurement in volume optical computerized tomography with two-step phase-shifting method

Jia Wang, Yang Song, Zhen-hua Li, An-zhi He, Nanjing Univ. of Science and Technology (China)

Volume optical computerized tomography (VOCT), which can realize real 3D measurement rather than traditional 2D OCT, has great superiority in quantitatively fully-field measuring the thermo physical parameters of transient flow fields. Among the refractive index reconstruction techniques, filtered back-projection (FBP) method performs better than algebraic reconstruction techniques (ARTs) with higher accuracy and computationally efficient. In order to apply FBP to VOCT, the radial second-order derivative of projection wave front passes through the tested phase object should be obtained firstly.

Our previous study has studied the moiré effect of circular gratings used in projection measurement of volume optical computerized tomography from diffraction theory. The result shows that the moiré fringes contain the radial first-order derivative of projection wave front. Besides, a phase shift which depends on the distance between two gratings exists between the fringes of +1 and -1 diffraction orders.

Consequently, in this paper, a projection device with two circular gratings is established. The light passing through the tested object and two gratings is divided into two optical paths by a prism. Two 4-f systems are used in two paths for filtering +1 and -1 diffraction order light and imaging respectively. Based on which, the phase shift between moiré fringes separately obtained by two paths equal $\pi/2$ by adjusting the distance between two gratings. Thus, based on the accurate analytical expression of moiré fringes, a simple two-step phase-shifting algorithm can be used to extract radial first-order derivative distribution of projection wave front from moiré fringes.

Finally, FBP method is used to quantitatively reconstruct the 3D field.

8563-17, Session 4

High precision absolute distance measurement with the monolithic femtosecond optical frequency comb

Tengfei Wu, Changcheng Institute of Metrology & Measurement (China)

The absolute distance measurement was experimentally demonstrated by using the monolithic femtosecond optical frequency comb in air. Our technique is based on the measurement of second harmonic cross correlation between reference and measurement optical pulses. The second harmonic signal is generated from the difference frequency principle of the monolithic femtosecond optical frequency comb, which simplify the generation process of second harmonic cross correlation. The technique has some advantages, such as compact volume, long term stabilization and low cost et al. The scheme allowing sub-micrometer resolution in large scale measurement by using the monolithic femtosecond optical frequency comb. It will be benefit for future lidar and satellite formation flying mission.

8563-18, Session 5

Small size probe for inner profile measurement of pipes using optical fiber ring beam device (Invited Paper)

Toshitaka Wakayama, Toru Yoshizawa, Saitama Medical Univ. (Japan)

The requirements of inner profile measurement of pipes and tubes become recently larger and larger, and applications of inner profile measurement have rapidly expanded to medical field as well as industrial fields such as mechanical, automobile and heavy industries. We have proposed measurement method by incorporating a ring beam device that produces a circular beam and have developed various probe cameras for different inner profile measurement. To meet request for applying to smaller diameter pipes, we tried to improve the ring beam light source using a conical mirror, optical fiber collimator and a laser diode. At this moment a probe with the size of 5 mm in diameter has been realized.

8563-19, Session 5

Fiber-optic confocal probe with an integrated real-time apex finder for high-precision center thickness measurement of ball lenses

Arnote Somboonkaew, Ratthasart Amrit, Sataporn Chanhorm, National Electronics and Computer Technology Ctr. (Thailand); Boonsong Sutapun, Suranaree Univ. of Technology (Thailand)

Today's optical devices and instruments become smaller and require high-quality optical lenses in a very compact size. Manufacturing and assembling of such high-quality lenses needs a precise quality control for every single lens. One parameter is often measured and monitored during production process is the central thickness of the lens. A precise and non-contact measuring system based on optical techniques is preferred since it does not create any scratches. Among several optical techniques that have been developed a fiber-optic confocal microscopy has been widely used for non-contact measurement due to its high precision, compact size and rapid measurement. However, for small-diameter and large curvature lenses, high-precision instrument is not only the key parameter to achieve an accurate measurement but also the ability to precisely placed the instrument sensing spot at the apex point of the measured lenses. In this paper, we developed a fiber-optic confocal probe with an integrated camera that is used to monitor the beam shape of the reflected light. The integrated camera functions as a real-time apex sensing device. Off-center sensing spot will produces a non-circular image. By analyzing the beam shape of the reflected light spot, we are able to precisely determine the location (both distance and direction) of the focus point of the confocal probe compared to the apex point of the measure lens within $\pm 16.17/30 \pm 15.49$ m accuracy. To demonstrate this concept, we built the new fiber-optic confocal probe and used it to measure the center thickness of 3-mm, 5-mm and 10-mm ball lenses.

8563-20, Session 5

Real-time displacement measurement using VCSEL interferometer

Takamasa Suzuki, Noriaki Yamada, Osami Sasaki, Samuel Choi, Niigata Univ. (Japan)

A displacement sensor (DS) is one of the most important devices used in high-precision manufacturing. It monitors the thermal expansion of a rotating spindle or ball screw, position of cutters, vibrations caused by the misalignment of rotating object, and other such parameters. Such sensors need to be compact and robust against mechanical disturbances in a fabricating process.

There are many types of noncontact DSs such as ultrasonic, capacitance, eddy current, and optical DSs. Optical DSs are easy to use, applicable to most materials, and have high accuracy. Optical DSs are categorized into two types based on the measurement principle used, namely, triangulation and interferometry. Because the resolution of triangulation type DSs is inadequate, interferometry DSs are suitable for ultraprecision machining. However, an interferometer is typically

expensive and unstable because of the mode-hop phenomenon when a conventional Fabry-Perot laser diode is used in it as a light source.

The interferometer we propose herein uses a vertical cavity surface emitting laser (VCSEL). It is superior in terms of the remediation of the mode-hop issue and modulation efficiency. The interference signal is processed with the phase-locked technique. This device allows real-time displacement to be measured. No unstable signals caused by mode-hop were observed in the experiments. Displacement measurements recorded with this device indicate that it has a measurement accuracy of 0.3 micro-m rms and 50 nm rms for displacements of 150 micro-m and 1.2 micro-m, respectively.

8563-21, Session 5

Towards a one step geometric calibration of an optical coherence tomography

Jesús Díaz Díaz, Maik Rahlves, Leibniz Univ. Hannover (Germany); Omid Majdani, Medizinische Hochschule Hannover (Germany); Eduard Reithmeier, Tobias Ortmaier, Leibniz Univ. Hannover (Germany)

In recent years, optical coherence tomography (OCT) has gained increasing interest not only as an imaging system in medicine but also as a measuring device in technical and life science applications. A major requirement for the latter is a high confidence in the validity and realness of the measurements. This article presents a one step 3D landmark-based geometric calibration based on the identification of a parameterized gray-box OCT model. We introduce the complete identification process beginning with a white- and a gray-box OCT model for geometric distortion correction, as well as the - for this purpose explicitly - designed and manufactured calibration standard. It is silicon-made and consists of an array of inverse multilevel pyramids with circular landmarks. The theoretical framework is based on a maximum-likelihood parameter estimation finding the best suitable parameters by minimizing the error between via image processing localized (actual) and real (target) landmark coordinates in the least square sense. For evaluation purposes, common measurement errors in the field of medical surgery such as the Fiducial Registration and Localization Error are compared before and after geometric calibration. Simulation and experimental results show that the proposed methodology reduces systematic errors by more than one order of magnitude. These results affirm the possibility of integrating an OCT in a medical navigation system. Due to its simplicity, the calibration can be carried out directly before a surgical intervention, thus enhancing and assuring the OCT accuracy.

8563-22, Session 5

OCT for industrial applications

Guiju Song, Kevin G. Harding, GE Global Research (United States)

Optical coherence tomography (OCT) was developed at MIT for biomedical imaging in 1990s (1). As a technology capable of producing high-resolution, depth-resolved images of biological tissue, OCT was widely used for the application of ophthalmology and has been commercialized in the market today. This is evidenced by the wide hospital adoption, applications publication by Ocular Surgery News. Benefiting from novel photonics components and devices, the industrial application of the older concepts in OCT can be re-visited with respect to the unique performance and availability. This paper will introduce the fundamental concepts of OCT and discuss its current and potential industrial applications. Specific application of OCT to composite inspection as an NDT tool will be discussed, including the limitations of this method for NDT in general.

8563-25, Poster Session

High-precision sphere diameter determination by phase-shifting interferometry with a frequency-tunable diode laser

Xuejian Wu, Jitao Zhang, Haoyun Wei, Yan Li, Tsinghua Univ. (China)

The Avogadro constant is one of the promising fundamental constants to redefine the SI basic unit "kilogram". The most accurate method to determine the Avogadro constant is the x-ray crystal density method, where the lattice constant, mean molar mass, mass and volume of a perfect silicon sphere are absolutely measured. To redefine the kilogram, the relative uncertainty of the Avogadro constant should be less than 2×10^{-8} , which means that the relative uncertainty of the volume, the largest uncertainty source, should be reduced to 1.7×10^{-8} . The silicon sphere, whose nominal diameter is 93.6 mm, is optically polished with a roundness of less than 100 nm, so that the volume is determined via the diameter measurement. To determine the absolute diameter, the sphere is located in an etalon and the diameter is obtained by subtracting the sum of the two gaps from the etalon spacing. The gaps and the etalon spacing are measured by phase-shifting interferometry with optical frequency tuning. Nowadays, the main uncertainty sources include the laser frequency, interferogram analysis, etalon spacing and sphere temperature. In this paper, a novel phase-shifting interferometer is proposed to improve the diameter measurement uncertainty. A new monolithic etalon with flat references, which is made of ultra-low expansion glass, is applied in this interferometer. On the other hand, a frequency-tunable diode laser is calibrated by an optical frequency comb to generate an arbitrary single optical frequency and the Carré algorithm is used to calculate the phase distribution.

8563-32, Poster Session

Analysis of non-uniformity of irradiance measurement uncertainties of pulsed solar simulator

Yingwei He, Limin Xiong, Haifeng Meng, Dingpu Liu, Jieyu Zhang, Junchao Zhang, National Institute of Metrology (China)

The conversion efficiency measurement accuracy of solar cell is heavily rely on the measurement uncertainty of pulsed solar simulator. The measurement uncertainty assessment method of pulsed solar simulator is widely analyzed and studied. This paper describes uncertainty assessment method of measurement of irradiance non-uniformity which is one of the three most important factors (spectral mismatch, non-uniformity of irradiance and instability of irradiance) influencing pulsed solar simulator measurement uncertainties. An experiment using a real pulsed solar simulator was performed to testify the validity of uncertainty assessment method. The results provide a theoretical and data basis for further analysis of overall uncertainties of solar simulators.

8563-33, Poster Session

Calibration of optical double-triangulation for small-size characteristics workpieces

Yiguang Gu, Xiaoping Lou, Beijing Information Science & Technology Univ. (China)

In order to realize 3D profile measurement of workpieces with small-size characteristics rapidly and precisely, optical triangulation is studied. The measuring accuracy is affected by many factors, such as system structure, surface characteristic of objects and the circumstance. It is

improved in the aspects of structure and calibration in this paper. In the structure, double camera is adopted to reduce the measuring dead zone and improve the impact of the shadow caused by inclined surface of the measured objects. In the calibration, the least-square curving fitting method combined with appropriate error compensation method is selected, based on analyses and comparisons of various calibration approaches.

In this paper, the principle of optical triangulation method is discussed first. The relation between the dependent variable, independent variable and system construction parameters is nonlinear, which makes it difficult to calibrate the optical triangulation system. A least-square curving fitting method is used to reduce the number of calibration parameters and improve the calibration precision. During image processing, appropriate filtering method is applied to preprocess images and grey centroid method is selected to orient light spot center. Linear interpolation method is used to reduce the fitting residual error. At last, the source of the system error is analyzed and some methods are proposed to ensure the precision of optical triangulation system. Experimental results prove the effectiveness of the measuring principle and the reliability of this measuring system.

8563-34, Poster Session

Techniques of thermal state measurement based on blue structure light

Zhang Chi, Zhongwei Li, Yusheng Shi, Congjun Wang, Huazhong Univ. of Science and Technology (China)

To date there hasn't been a satisfactory solution yet for 3D measurement for objects in thermal-state, particularly for large-sized and complex-shaped forgings. Common automatic detection methods include the laser beam projection, the CCD image measurement, the laser scanning and CCD structured light measurement.

This paper proposes to use blue light projection and refit existing DMD projector to increase the light intensity of blue channel and improve the measurement conditions of structured light; use a single CCD camera to reduce system cost, and acquire blue channel data through digital filtration and Bell Interpolation; then complete the measurement of the hot forging by the phase unwrapping algorithm of multi-frequency heterodyne to obtain preferable experimental data.

The whole article including five parts:

1. Composition of Highlighted Blue Light Projection System
2. Principle of 3-D Structured Light Measurement
3. Adaptive Colored Plane Interpolation Algorithm
4. Three-dimensional (3-D) Reconstruction
5. Measurement Experiment and Analysis

This paper outlines the realization of high-brightness projection with blue structured light via reconstruction of the existing projector, to achieve a quick three-dimensional measurement for hot objects in thermal state. Through physical and digital filtration methods, using the single CCD interpolation calculation and technique of temporal phase unwrapping, we can obtain the three-dimensional dynamic data of the hot object at a temperature lower than 800°C. The measurement is higher in accuracy, and the time of each measurement can be controlled within 5s. The experimental facility can meet the requirements for close (about 1.5m) online measurements of thermal state under laboratory condition or at the work site of small forgings. By improving the brightness of the projection device, the online measurement at the casting and forging site in harsh environment is hopeful to be solved.

8563-35, Poster Session

Research of linear CCD on line dynamic detecting raw silk fineness based on FPGA

Fengjiao Liu, Zhou Wang, Soochow Univ. (China)

As a country of major raw silk production and exporter, however, the traditional and inefficient blackboard testing has been used in current raw silk inspection which not only affect the test impartiality, but also greatly reduce the efficiency and accuracy. In order to enhance the competitiveness of raw silk in the international market, a reliable measuring instrument to replace the manual inspection is needed in future industrial field.

A kind of new design scheme has been proposed that aim to realize real time, on line raw silk diameter measurement based on linear CCD (Charge Coupled Device) and FPGA (Field Programmable Gate Array), which possess the advantages of non-contact, high precision, fast response, and good compatibility etc. In this system, the samples of raw silk are placed in parallel light which reflect light through macro imaging is received by CCD image sensor. FPGA chip is easy to configure and use is selected for image signal processing, which is based on hardware parallel processing technology and has a high speed of operation. FPGA is used to achieve a linear CCD driver, the video signal by the CDS (Correlated Double Sampling) configuration and drive, FIFO (First In First Out) memory, data processing.

Firstly, the research on how to improve the precision of the system from theoretical approach to the various functional modules parameter optimization. What's more, effects are solved in instability of the light illumination and raw silk transparency, linear CCD's dark background imaging is chosen to avoid the bright background image easily saturation, the distortion caused by raw silk jitter is eliminated. Lastly, system measurement accuracy reaches to $\pm 1 \mu\text{m}$. Experimental results prove that research programme has certain feasibility and practicality.

8563-36, Poster Session

An optoelectronic system for the in-flight measurement of helicopter rotor blades motions and strains

Youwei Huang, Tsinghua Univ. (China); Weizhen Cheng, Chinese Flight Test Establishment (China); Yan Li, Tsinghua Univ. (China); Wanxin Li, Chinese Flight Test Establishment (China)

An optoelectronic system is developed to measure in-flight the dynamic motions and strains of blades of a helicopter. The motions of the blades, including the flapping, lag and pitch angles, are measured by two-dimensional position sensitive detectors (PSDs) responding to the movements of the light emitting points mounted on blades. The dynamic strains are measured by fiber bragg gratings (FBGs). Test data show that there are good linear relationships between angular motions and the output voltages of PSDs. The angular error is within ± 1 percent over a wide range of flight conditions. The strains measured by FBG are compared with that measured by strain gauge. Good agreements are found between the two methods. The strains measured by FBG are also reproducible, with relative deviation of only 1.22% between twice measurements. It is concluded that the motions and strains can be measured accurately in flight environments.

8563-37, Poster Session

A high speed auto-adaptable system for rail-track detection

Jia Ge, Yunhan Luo, Jun Zhang, Long Guo, Liang Sun, Zhe Chen, Jinan Univ. (China)

Security assurance work is significant in high speed railroad and

track is the fundamental supporting part. Good imaging results are important for inspection of track surface defect, while image distortion problem is frequently occurred in traditional detection systems mainly using constant exposure frequency camera. The system introduced in this paper improves traditional systems by combining a Speed Auto-Adaptable (SAA) system, which mainly consists of a high-speed external controlled camera, a rotary encoder and a signal processing card, to guarantee proper exposure frequency and uniform image quality all the time at variable running speed. This system has a brilliant performance in avoiding image distortion both in laboratory test and practical application, with minimum detection precision of 0.2 mm at relative low speed and theoretically maximum detection speed of about 400 km/h.

8563-38, Poster Session

Three-dimensional inspection and quantitative evaluation of defects in conducting glass using optical coherence tomography

Kung-Min Lin, Feng-Yu Chang, Kuo-En Huang, Jiann-Der Lee, Meng-Tsan Tsai, Chang Gung Univ. (Taiwan)

Optical coherence tomography (OCT) has attracted a lot of attention since 1991 for biomedical and other applications, due to the characteristics such as noninvasive measurement, high-speed imaging, and high resolutions. Furthermore, the conducting glass has been widely used for industrial products, including display devices, solar cells and touch panels. Until now, most proposed approaches for the defect inspection of conducting glass are based on the mechanism of machine vision. However, this technique can only provide defect information on the sample surface and the defects beneath the sample surface cannot be observed with machine vision technique. In this study, nondestructive, three-dimensional imaging technique, OCT, is implemented for optical inspection and quantitative measurement of conducting glasses, which are widely used for the commercially electrical products. With the development of image processing algorithm, the size of the defects can be quantitative evaluated from OCT images. Furthermore, based on the phase information of the OCT interfered signals, the displacement of the single plane can be obtained with nanometer resolution, enabling to inspect the defects of nanostructures, which are not able to be obtained by using machine vision technique. Additionally, an approach is proposed to modify the 2 π ambiguity of the evaluated phase. With the proposed approach, the image artifacts can be greatly improved. Compared with machine vision technique, OCT can be a powerful tool to provide the microstructures at a depth range of 2-3 mm with micrometer resolution and the nanostructures in three dimensions.

8563-39, Poster Session

Simultaneous measurements of atmospheric NO₂ and HONO using IBBCEAS with a near-ultraviolet LED

Liuyi Ling, Anhui Institute of Optics and Fine Mechanics, Chinese Academy of Science (China) and Institute of Electric and Information Technology, Anhui University of Science and Technology (China); Pinhua Xie, Min Qin, Renzhi Hu, Nina Zheng, Fuqi Si, Anhui Institute of Optics and Fine Mechanics, Chinese Academy of Science (China)

High sensitivity simultaneous measurements of atmospheric NO₂ and HONO using incoherent broadband cavity enhanced absorption spectroscopy (IBBCEAS) were developed. A near-ultraviolet light emitting diode (LED) peaked at 372nm was used as light source of the IBBCEAS instrument to measure the absorption of NO₂ and HONO

in the spectral range of 361–378nm. The light emitted from the LED was coupled into a 70 cm long high finesse cavity formed with two high reflectivity mirrors and traveled back and forth between the two mirrors resulting in a long absorption path length. Mirror reflectivity between 358 and 378nm was determined from the changes in transmitted intensity in the cavity filled with pure He and pure N₂ due to the difference between their Rayleigh scattering cross-sections and validated by the absorption of the oxygen collisional pair in pure oxygen in the same spectral range. The maximum mirror reflectivity of 0.99923 was found at about 369nm corresponding to a light path length of 910 m. The air out of our laboratory was pumped into the cavity and the atmospheric absorption spectra were recorded in the absence of atmospheric aerosols by a PTFE filter. Concentrations of NO₂ and HONO in the atmosphere were retrieved by fitting their absorption cross-sections to absorption coefficients deriving from the measured absorption spectra and the average detection limits of 2.9 ppbv for NO₂ and 1.2 ppbv for HONO with an acquisition time of 5 min were achieved. The results demonstrated high sensitivity of this measurement technique based on IBBCEAS, which is a promising technique for measurements of atmospheric trace gases.

8563-40, Poster Session

Preparation and characterization of surface oxide layer on spherical silicon substrate

Wende Liu, Chi Chen, Qiming Fan, National Institute of Metrology (China)

Thermal oxide layer is grown on spherical surface of silicon substrate with respective radius of curvature of 84.6/96.7/120.9mm. Four nominal thicknesses of the oxide layer, i.e., 4/10/50/100 nm, are obtained. The substrate has a spherical surface and a planar bottom surface, both of which are polished. It is such designed that the two sides of the substrate after thermal oxidation can be readily compared and the thin film thickness on the planar side can be used as a reference. With the combination of ellipsometry and X ray method the thin film thickness is characterized. The spot size of the light beam of the ellipsometer is configured to be as small as 0.5*0.7mm so as to minimize the influence of the surface curvature. The calibration line between ellipsometric and X-ray data are obtained, which are compared to results obtained on Si wafer. For characterizing the surface morphology the white light interferometry technique is used. Comparing with past employment of planar Si wafer, the present approach, when applied in accurate determination of Avogadro constant and new definition of weight, can promisingly minimize the influence of the surface curvature to an accepted level, thus further reducing the uncertainty. Finally, the possible application in measuring thin film on curved surface is discussed.

8563-41, Poster Session

Research on the video detection device in the invisible part of stay cable anchorage system

Lin Cai, Guilin Univ. of Electronic Technology (China); Nianchun Deng, Liuzhou OVM Machinery Co., Ltd. (China); Zexin Xiao, Guilin Univ. of Electronic Technology (China)

The cables in anchorage zone of cable-stayed bridge are hidden within the embedded pipe, which leads to the difficulty for detecting the damage of the cables with visual inspection. We have built a detection device based on high-resolution video capture, realized the distance observing of invisible segment of stay cable and damage detection of outer surface of cable in the small volume. The system mainly consists of optical stents and precision mechanical support device, optical imaging system, lighting source, driven motor control and IP camera video capture system. The principal innovations of the device are 1. A set of telescope objectives with three different focal lengths are

designed and used in different distances of the monitors by means of converter. 2. Lens system is far separated with lighting system, so that the imaging optical path could effectively avoid the harsh environment which would be in the invisible part of cables. The practice shows that the device not only can collect the clear surveillance video images of outer surface of cable effectively, but also has a broad application prospect in security warning of prestressed structures.

8563-42, Poster Session

Dynamic measurements by color gratings projection method using two step Fourier transform method

Kazuhide Kamiya, Takashi Nomura, Ami Tanbo, Kimihisa Matsumoto, Toyama Prefectural Univ. (Japan); Hatsuzou Tashiro, Univ. of Toyama (Japan); Shinya Suzuki, Nagano National College of Technology (Japan)

The Fourier transform method is an analytical method for interferograms with a spatial linear carrier. The interferograms with the spatial linear carrier are analyzed to obtain a phase of the interferograms by eliminating the noise from shape components of the interferograms in the Fourier domain. However, when the noise and shape components overlap each other in the Fourier domain, it is difficult to eliminate only the overlapped noise components by using the conventional filtering techniques, such as the bandpass filtering. Therefore, a method is proposed to solve these problems by using two interferograms with slightly different carrier frequencies.

In the proposed method, the Fourier transform of the two interferograms with slightly different carrier frequencies are calculated, respectively. Both Fourier spectra obtained by the Fourier transform of the interferograms contain same noise components. Though the Fourier spectra contain the same shape components, a location of the spectra of shape components is slightly different. By calculating the subtraction of both Fourier spectra, the noise components are removed and inclination components are generated, because the frequency difference between two components are small. We name the proposed method "two step Fourier transpose method".

The validity of the proposed filtering method is confirmed by experiments. In the experiments, two color fringes are projected simultaneously to scatter object. Images of color fringes are acquired by CCD camera under the slow deformation of the scatter object. The images are analyzed by proposed method.

8563-43, Poster Session

Multiple-pulse-train-interference-based measurement of refractive index of air using femtosecond optical frequency comb

Dong Wei, Kiyoshi Takamasu, Hirokazu Matsumoto, The Univ. of Tokyo (Japan)

The traceability of meter is the infrastructure for both scientific and industrial uses. In July 2009, the national standard tool for measuring length in Japan changed from an iodine-stabilized helium-neon (He-Ne) laser to a femtosecond optical frequency comb (FOFC). How to practically perform a distant measurement that is directly linked to an FOFC length standard tool is the most urgent challenge.

One big and basic problem of this challenge is how to achieve a high-accuracy refractive index measurement, because the length is derived from the parameters of air. This paper is intended to give a description to the concept, the principle, and a demonstration of a new temperature technique, called multiple pulse train interference-based (MPTI) method, which was developed for a high-accuracy temperature evaluation. The basic idea of this new technique was that water vapor pressure was recorded based on the interference of multiple pulse trains, and

was found as a distance of a MPPI fringes by the conventional Fourier transformation method.

A demonstration of the proposed method which is the water vapor pressure measurement using a sealed 600-mm cell is presented. From the result of the preliminary experiment, it has been show the possibility that MPPI method can be used for a high-accuracy temperature evaluation.

8563-44, Poster Session

Use of ellipsometer determine the optical properties of the satellite surface coated materials

Yanhui Li, Zhensen Wu, Lu Bai, Xidian Univ. (China)

Ellipsometer enables to characterize optical properties of materials and thin films quantitatively via the measurement of the ellipsometric parameters, Ψ ; and Δ , of the reflected polarized light by specimen. The ellipsometry surgery began to be applied to an increasingly wide range of areas, such as physics, chemistry, materials and biology. The main advantage of the elliptical polarization measurement technique is to measure a long time, take a large wavelength range, the measurement angle, no damage to the sample, measurement results are accurate. By the principle analysis of the ellipsometer, In this paper, ellipsometer is used to measurement electric field component amplitude ratio Ψ ; and electric field component phase difference Δ of the satellite surface coated materials, and then set the angle of incidence and wavelength, the optical constants (refractive index n and extinction coefficient k) and thickness can be obtained. On the measurement results in different incident in a optimization modeling, also has access to more parameters description. The experiments show that the measurement results and fitting results match well within the spectral range 240nm-1200nm range. This paper is offer methods of measurement and modeling for characterize optical properties of materials and thin films.

8563-45, Poster Session

Traceable dual-frequency measurement of Zeeman split He-Ne lasers using an optical frequency comb locked external cavity diode laser

Haoyun Wei, Xuejian Wu, Lei Zhou, Jitao Zhang, Yan Li, Tsinghua Univ. (China)

Heterodyne laser interferometer position measurement systems provide very precise position or distance information for dimensional measurements or motion control, and it is widely used in industrial precision manufacture and inspection system such as the lithography. The core component of the heterodyne laser interferometer is a dual-frequency laser, which can output two Zeeman split frequency with orthogonal polarization. The measured displacement is the multiple of the wavelength, so that the absolute frequency and its stability are the key to keep the accuracy of the heterodyne interferometry. For an accuracy of nanometer scales, the absolute frequency of the dual-frequency laser should be known within 10 MHz, and its relative frequency stability should be within 1×10^{-9} in 1 h averaging time.

Nowadays, optical frequency combs (OFC) provide a robust and simple way for precision optical frequency measurement traceable to the microwave frequency standard. However, due to the characteristic of the two orthogonal polarized beams, it is not easy to measure the absolute frequencies of the dual-frequency He-Ne laser using the OFC directly with high SNR. In this paper, we present a new frequency measurement system for dual-frequency He-Ne lasers using an external cavity diode laser (ECDL). In the proposed system, an optical phase-lock loop is built to lock the ECDL to a fiber-based OFC. After locking, the frequency uncertainty of this tunable, stable, and traceable ECDL

is about 2.7 kHz in 1 second averaging time. Using this ECDL, the stabilities of both the two absolute frequencies and the split frequency are simultaneously evaluated.

8563-46, Poster Session

A new method for phase unwrapping base digital spackle correlation

He Dong, Li Ameng, Xiaoli Liu, Xiang Peng, Shenzhen Univ. (China)

Phase aided three-dimensional imaging and metrology is increasingly used in industrial, technical and medical applications. In this technology, the methods which use the projection of sinusoidal fringe patterns have to face the problem of phase unwrapping. The common methods for phase unwrapping e.g. by the use of multiple spatial frequencies, temporal phase unwrapping methods, or the use of Gray-Code sequences, demand to acquire added image sequences after the wrapping phase gotten by the method of phase-shift sinusoidal fringe. However, in some fields of application, the processing time should be shorter in order to reduce the number of acquiring imaging. In order to solve the above problem we introduce the new method which needs less number of imaging captured. The method just needs to capture four phase shifting images and a digital spackle map projected by projector and acquired by cameras. The wrapping phase can be assured from the above four phase shifting images, mean while, the correlation of each pixel and the projected digital spackle map gotten from the above digital spackle map. We can ensure the wrapping orders of each pixel of camera with the correlation and get the unwrapping phase.

8563-49, Poster Session

Geometric calibration and accuracy assessment of multispectral imager on UAVs

Fengjie Zheng, Tao Yu, Xingfeng Chen, Jiping Chen, Guoti Yuan, Institute of Remote Sensing Applications (China)

Accurate geographical positioning data is critical to UAV quantitative remote sensing research. MCC4-12F, the first UAV multispectral imager in the domestic, is equipped with fisheye lens, a computer-controlled filter wheel and a CCD plane array detector. The approach to perform multispectral imaging is optical filters to separate the electromagnetic spectrum into several passbands. However, some systematic deformations appeared since the optical path is slightly different for image acquisition. Unknown intrinsic parameters and lens optical distortion of the camera will cause serious image aberrations, even leading a few meters or tens of meters errors in ground per pixel. So accurate calibration is necessary for fully assessing corrected images. In this paper, a method on physical model of comprehensive geometric calibration in a 3D test field has been developed and empirically tested using images collected with MCC4-12F. Using space resection algorithm to assess the geometric calibration parameters of the multispectral imager. Then evaluating the accuracy by calculating object space and image point coordinate differences, analyzing impact of different photogrammetric altitudes. Practical geometric accuracy was obtained in Tianjin UAV flight experiments, in order to verify the accuracy and reliability of the calibration parameters. The results showed that theoretical precision were 0.57mm and 0.43mm, object space RMSE were 0.2 and 0.14 pixels in X direction and in Y direction. Image point RMSE was superior to 0.5 pixels. The corrected accuracy validated by ground checkpoints was less than 0.3m. Therefore, the approach presented here was suitable for UAV multispectral imager.

8563-50, Poster Session

Technology of optical azimuth transmission

Honggang Lu, Chunsheng Hu, National Univ. of Defense Technology (China)

In consideration of practical application, the principal of several typical optical azimuth transmission methods are presented. A systematically summary of azimuth transmission method is made for the first time. Four typical methods including Theodolite (including gyrotheodolite) collimation method, Camera series method, Optical apparatus for azimuth method and polarization modulated light transmission method are presented. For these typical azimuth transmission methods, their essential theories are elaborated. The devices, the fields and limitations of these typical methods' are introduced. Theodolite (including gyrotheodolite) collimation method is used in the ground assembly of spacecraft. Camera series method and optical apparatus for azimuth method are used in azimuth transmission between different decks of ship. Polarization modulated light transmission method is used in azimuth transmission of rocket and guided missile. At the last, the further developments of these methods are discussed.

8563-51, Poster Session

Device testing the corner precision of photoelectric shaft angle encoder

Guanyu Wen, Shuang Wang, Changchun Univ. of Science and Technology (China)

To improve efficiency of testing the angle precision of photoelectric shaft encoder, an device can greatly increase the detection efficiency in this paper. and adjust according to actual test detection accuracy. This device used the laser auto-collimation lightpipes and polyhedron, the computer control testing process and dispose the data, directly display test results. Through analysis the test system characteristic and data, find some cause of error factor.

8563-52, Poster Session

Algorithm research of high-precision optical interferometric phase demodulation based on FPGA

Chunxiao Zhi, Xiaojun Zhang, Jinghua Sun, Harbin Engineering Univ. (China)

Optical interferometric phase demodulation algorithm is provided based on the principle of phase generated carrier (PGC), which can realize the optical interference measurement of high-precision signal demodulation, applied to optical fiber displacement, vibration sensor. Modulated photoelectric detection signal is performed by interval 8 frequency multiplication sampling. The samples calculate the phase modulation depth and phase error through a feedback loop to achieve optimum working point control. On the other hand the results of sampling calculate precision of numerical of the phase. The algorithm uses the addition and subtraction method instead of correlation filtering and other related complex calculation process of the traditional PGC digital demodulation, making full use of FPGA data processing with advantage of high speed and parallel; At the same time, the operating speed of the algorithm increases by optimizing the number of sampling points. The experimental results show that: the algorithm of demodulation phase resolution up to $6 \mu\text{rad}$, dynamic range better than 190dB, can run in FPGA as the core system. The algorithm is suitable for application to optical precision measurement such as high-precision displacement, vibration, magnetic field. The demodulation system can get higher speed and precision of measurement.

8563-53, Poster Session

Analysis of solving the point correspondence problem by trifocal tensor for real-time phase measurement profilometry system

Kai Zhong, Zhongwei Li, Yusheng Shi, Congjun Wang, Huazhong Univ. of Science and Technology (China)

With the advancement of DLP technology and powerful hardware, the real-time measurement system based on phase measurement profilometry (PMP) principle has been extensively studied recently. Phase unwrapping for finding point correspondence between cameras or camera and projector is the key technology for 3D calculating in PMP system. In our system three-step phase-shifting algorithm which allows minimum image recording number is used to obtain wrapped phase-map, and our point corresponding method based on trifocal tensor constrain can be directly implement on wrapped phase-map. But many factors can lead to false correspondence, such as number of fringes, images noise, system non-linear response. This paper give a detail analysis on how these factors will affect the point matching process and a feasible method is proposed to reject error candidate points. Furthermore this method is characteristic of pixel-independent, which can speed up by parallel computing technique for real-time applications. Finally this method indicates a good performance in the experiment.

8563-23, Session 6

Industrial surface finish method comparison for fine finish measurements (*Invited Paper*)

Kevin G. Harding, Esmaeil Heidari, Robert W. Tait, GE Global Research (United States); Guangping Xie, Zirong Zhai, GE Global Research (China)

Measurement of surface finish in industrial manufacturing has traditionally been done by means of either visual comparison with reference plates or by the use of contact stylus based profilers. There are many challenges associated with contact profilers such as stability during measurement in an industrial environment, damage and wear of the tip, measurement in tight spaces or on curved surfaces and just the limited amount of data obtained by a linear scan of the stylus. Many alternative methods have become available such as white light interferometry, focus based systems, and even laser scatter. This paper will present the result of testing of the commercially available methods with particular emphasis on the fine surface finishes demanded in today's manufacturing, then present some alternative methods that show strong potential to address some of the challenges mentioned above that are not in wide use today. The analysis will specifically explore some of the physical mechanisms that affect the stylus based measurement, as well as the limitations of many of the optical approaches related to view angle and diffraction limited resolution consequences. The area of confocal imaging method will be specifically explored as how it might be used to obtain more complete data on very fine surface finishes.

8563-24, Session 6

Application of non-contact optical methods for microscale surface metrology

Shihua Wang, A*STAR National Metrology Ctr. (Singapore)

Micro Systems Technologies (MST), MicroElectroMechanical Systems (MEMS) and Micromanufacturing have become synonymous with the design, development, and manufacture of very small devices and systems. Besides continuing effort in developing MEMS-based manufacturing techniques, the latest effort in micro-manufacturing is also applicable to non-MEMS-based manufacturing. Research

and technological development in related field is encouraged by the increased demand on surface metrology of micro-components to be promised development in the scaling down of the traditional macro-manufacturing processes for micro-length-scale manufacturing.

This paper will introduce micro-scale surface metrology at the National Metrology Centre using non-contact optical methods, specifically on the development of a large scanning range laser confocal microscope for calibration and measurement of micro-structures. These structures include dimensional and component surface functional parameters such as material removal/wear, bearing area, cutting tool edge, laser marking, micro-channel in microfluidic device, lens array mould, surface flatness/deformation of super-low reflection (less than 2%) coating surface, low reflection rock surface etc. Corresponding measurement working principle and system design & configuration will be discussed. In addition, some typical applications of laser & white-light interferometry for measuring micro-surface deformation of micro-beam in MEMS accelerometer, membrane in microphone and surface of micro-mirror will also be discussed.

8563-26, Session 6

Image detection of inner wall surface of holes in metal sheets through polarization using a 3D TV monitor

Takamasa Suzuki, Katsunori Nakano, Shogo Muramatsu, Niigata Univ. (Japan); Toshiro Oitate, Totsuka Metal Industry Co., Ltd. (Japan)

An automated inspection system needs to be introduced for sheet-metal working in order to reduce the production cost. For this purpose, we plan to configure a suitable system that uses optical and computerized image processing techniques.

Although a digital camera is a suitable imaging device for this purpose, it captures unnecessary images of the inner hole surface of a hole (hereafter, referred to as the hole surface) in a thick test target. At times, it is difficult to distinguish between the surface of the target and the hole surface. Hence, the unnecessary hole surface images only serve to further complicate the image processing that requires to be performed for edge detection.

We propose an effective technique for optically detecting the hole surface image using the polarization property of a 3D television (TV) monitor. In our technique, a digital camera is used to capture, using a polarizer, an image of the test target placed on the surface of the screen of a TV monitor. The polarized light emitted by the TV monitor illuminates the hole surfaces present in the test target placed on the screen of the monitor. When the polarizer placed in front of a camera lens is adjusted such that the camera captures a dark image for the transmitted light, only the highlighted hole surfaces are visible in the captured image because the light scattered at the hole surfaces is depolarized. This reduces the complexity of performing image processing for edge detection.

8563-27, Session 6

Simultaneous measurement of birefringence magnitude and direction using Wollaston prism

Longhai Liu, Aijun Zeng, Beishi Chen, Lexing Zheng, Huijie Huang, Shanghai Institute of Optics and Fine Mechanics (China)

Measurement of the birefringence magnitude and/or direction attracts many research interests. In existing polarization element rotating methods, the background light and the intensity fluctuation affect the measurement accuracy. For instrumentation, a method of measuring the birefringence magnitude and direction using Wollaston prism is presented.

The light source is a semiconductor laser, whose intensity is sinusoidally modulated. The modulated beam passes through a circular polarizer, the sample and is then split into two sub-beams by a Wollaston prism, whose transmission axes are 0° and 90° . The two sub-beams are detected by a bi-cell detector. The two detected signals are then filtered to get two alternating current signals. Then the Wollaston prism is rotated by 45° , whose two transmission axes are 45° and 135° , and the other two alternating current signals are obtained. By processing the four alternating current signals, the birefringence magnitude and direction can be resolved independent of the intensity.

In experiments, a wedge wave plate was laterally moved to change birefringence magnitude in the range of $0^\circ\sim 90^\circ$. Then the process was repeated at different birefringence direction. The measured birefringence magnitude and direction coincide with the nominal values. The standard deviation of the birefringence magnitude is less than 0.12° . The maximum deviation of the birefringence direction is less than 0.61° . The usefulness of the method is verified.

8563-28, Session 6

Extended depth of field for visual measurement systems

Yanyu Zhao, Yufu Qu, BeiHang Univ. (China)

The field of view of visual measurement systems in the direction of optical axis is determined by the depth of field. While the focus of visual measurement changing from final quality assurance to process test, larger depth of field and faster test speed are becoming increasingly demanding. Therefore, an extended depth of field method based on liquid lens and computational imaging is presented in this paper. The method applies a liquid lens to sweep its focus length within a single detector exposure time, and then a blurred image is obtained through the capturing process. The blurred image is restored to an extended depth of field image based on computational imaging technology. Three contents are included in this paper. First, in the optimization of the optical system, the liquid lens is added to the conventional imaging objective in visual measurement systems, which results in extended depth of field and a nearly constant magnification. Second, the parameters of image acquisition such as the range, speed and time of the liquid lens sweeping and the integration time of the detector, are carefully designed to assure high signal-to-noise ratio and high contrast in visual measurement systems. Third, by modeling the imaging system, we gain the point spread function, after which a deconvolution technique is applied, using the blurred image to restore an extended depth of field image. Experiment results demonstrate that our method can extend the depth of field of the visual measurement system for over 10 times, while the change of the magnification within the depth of field remains less than 1%.

8563-30, Session 7

Temporal phase retrieval in dynamic speckle interferometry by adaptive empirical mode decomposition

Hao Zhang, Tianjin Univ. (China)

As a promising technique, temporal phase analysis has been applied to dynamic speckle measurement. In temporal phase analysis, an interferogram sequence is obtained by a high speed camera during object movement. And the phase is extracted from the temporal phase map.

Hilber transform based analytic algorithm is not trivial with noisy phase map. And the EMD(Empirical Mode Decomposition) algorithm can be performed to put the signal into an appropriate shape for accurate phase computation.

Generally EMD algorithm produces several modes in which only one would be used in phase computation. Traditional approaches would chose the first IMF, which however is not correct.

This paper proposed an algorithm to automatically determine the mode that best fits the shape of input signal. In experiments, the performance of our algorithm was shown.

8563-31, Session 7

Holographic approach to detection of delamination areas in layered polymeric waveguides by means of strain solitons

Irina V. Semenova, Galina V. Dreiden, Ioffe Physico-Technical Institute (Russian Federation); Karima R. Khusnutdinova, Loughborough Univ. (United Kingdom); Alexander M. Samsonov, Ioffe Physico-Technical Institute (Russian Federation)

Laminated structures are widely used now in a wide variety of constructions. The proper functioning of such structures has vital importance especially in automotive and aerospace industries. The major problem in their behaviour is a possibility of a sudden and irreversible delamination caused by various factors. We propose and study a NDT approach to investigate the dynamics of prolonged layered structures based on the propagation and optical (holographic) detection of bulk strain solitons in them.

Being formed, the soliton propagates along the homogeneous wave guide with almost no change of amplitude, shape and velocity. In inhomogeneous wave guides the soliton parameters vary, depending upon parameters of inhomogeneities. We analyze variations in the soliton behaviour in layered wave guides caused by thin cuts, representing delamination, and show that the bulk nonlinear solitary elastic strain waves may provide an opportunity to check quickly the delamination areas even in prolonged layered wave guides.

We present results on experimental observation of the evolution of bulk solitary waves in polymeric 2- and 3-layered waveguides with glassy and rubber-like adhesives used for bonding. Soliton evolution in long delaminated waveguides was recorded using the technique of holographic interferometry. Delamination areas of different length were introduced to study variations in soliton parameters. Variations of soliton amplitude were shown to demonstrate the existence of delamination areas. The formation of complex wave patterns - soliton trains or radiating solitons became an additional evidence of defects in layered waveguides.

Conference 8564: Nanophotonics and Micro/Nano Optics

Monday - Wednesday 5 -7 November 2012

Part of Proceedings of SPIE Vol. 8564 Nanophotonics and Micro/Nano Optics

8564-1, Session 1

New directions for microcavity physics

Kerry J. Vahala, California Institute of Technology (United States)

Over the last ten years there has been remarkable progress in boosting quality factor (Q-factor) in micro and millimeter-scale optical resonators. Chip-based devices have attained Q factors of nearly 1 billion and micro-machined crystalline devices have provided Q factors exceeding 100 billion. The resulting long, energy-storage times combined with small form factors have made it possible to access a wide range of nonlinear phenomena, and has led to new science such as cavity optomechanics. I will review some of these results including optical frequency microcombs, opto-mechanical cooling to the quantum ground state and mechanical amplification by stimulated emission of phonons. Prospects for new technologies will also be discussed.

8564-2, Session 1

Advances in electrically pumped lasing from Ge-on-Si (Invited Paper)

Jurgen Michel, Rodolfo E. Camacho-Aguilera, Yan Cai, Lin Zhang, Marco Romagnoli, Lionel C. Kimerling, Massachusetts Institute of Technology (United States)

Monolithically integrated lasers on a silicon platform have long been a desirable addition to on-chip photonic systems. However, until recently the only viable solutions were based on bonding III-V based semiconductor lasers on silicon waveguides. Several years ago, Germanium (Ge) has been suggested as a gain material for lasing that can be monolithically integrated into a Silicon CMOS flow. More recently, optically pumped lasing has been demonstrated using tensile strained, n-type Ge as the gain medium. Here we will present an electrically pumped Ge laser, using n-type doped Ge with an active carrier concentration above $4 \times 10^{19} \text{ cm}^{-3}$. The Fabry-Perot laser produces more than 1 mW output power and exhibits lasing in a wavelength range from 1520nm to 1700nm. We will discuss the implications of a monolithic lightsource on Si as well as present the most recent results.

8564-3, Session 1

Calculation for gain coefficient dependence on donor density of n+-Ge with considering Auger recombination

Koki Takinai, Kazumi Wada, The Univ. of Tokyo (Japan)

Recently, Ge has attracted strong attention as a gain material for light emitting devices which are compatible with Si-CMOS technology and lasing was achieved by using Fabry-Perot resonator and in situ doped Ge with above $1 \times 10^{19} \text{ cm}^{-3}$. However, lasing by Ge using micro-cavity structure has not achieved. Since micro-cavity has larger scattering and radiation loss than Fabry-Perot, increasing the material gain of Ge is much important to achieve lasing by using several techniques such as quantum dots, tensile-strain and heavily n-type doping. Heavily doping is a promising way and it is eagerly studied how to obtain heavily n-type doped Ge, however, Auger recombination gets increased according to doping level and should be dominant above a specific carrier density, which means there is the most appropriate doping density. We calculated the material gain coefficient of n+-Ge dependence on donor density with considering the decrease of carrier density contributed to Auger recombination. Although the parameters are difficult to determine, Auger coefficient of $1 \times 10^{-30} \text{ cm}^6 \text{ s}^{-1}$

1), spontaneous radiative coefficient of $1 \times 10^{-10} \text{ cm}^3 \text{ s}^{-1}$ and carrier injection of $1 \times 10^{19} \text{ cm}^{-3}$ were assumed. As a result, there was a peak at about $2 \times 10^{20} \text{ cm}^{-3}$ and gain coefficient started to decrease from the point according to the increase of donor density. The peak did not present for calculation without Auger recombination and should be equivalent to the most appropriate donor density under the above assumption. The peak position should shift by the change of the parameters for recombination, so the peak can be at several 10^{19} cm^{-3} .

8564-4, Session 1

Strain induced bandgap and refractive index variation of silicon

Jingnan Cai, Yasuhiko Ishikawa, Kazumi Wada, The Univ. of Tokyo (Japan)

Real time compensation to the temperature fluctuation is on demand for photonic devices applications and the introduction of strain on photonic devices might be a solution. Thus it is necessary to study the strain effect on the behaviors of photonic structures. In this report, a simple flexible structure of silicon micro-beam is designed for the investigation of strain effects on the photonic cavity structures. A finite element simulation shows that by simply bending the silicon micro-beam, strain can be generated on the beam and more than 2.5% of strain can be reached. Experimentally, silicon micro-beams with 2.5 μm in width and 15 μm in length and 250 nm in thickness were fabricated to check the optical behaviors of the micro cavity under strain. The photoluminescence measurement results indicate that with the strain applied, the silicon bandgap can be adjusted from 1.12 eV to about 0.84 eV. A red-shift of Fabry-Perot resonance peak can also be observed to reach up to 18 nm, which is related to a significant 1.4% change of refractive index. Those results prove that by adjusting the strain in the micro cavity, the bandgap as well as the effective refractive index of the micro cavity can be effectively controlled and hence the compensation to temperature fluctuation can be achieved. Our study also demonstrates that rather than other factors, the large change of silicon bandgap and refractive index are induced by the strain. This work indicates that the application of strain in silicon could be a promising way for many photonic applications based on the adjustment of bandgap and refractive index.

8564-5, Session 1

Photoluminescence and electroluminescence of erbium yttrium and ytterbium co-doped Er silicates

Xingjun Wang, Zhiping Zhou, Peking Univ. (China)

In recent years, Erbium (Er) silicates and Yttrium (Y) and Ytterbium (Yb) co-doped Er silicates have attracted intensive investigations due to their efficient luminescence at 1.53 μm . The potential applications are monolithic integrated light emitters or optical waveguide amplifiers for silicon photonics. Compared with traditional Er-doped materials, the Er concentrations of silicates are about 1 to 2 orders of magnitude higher due to the stoichiometric nature of these Er compounds. High gain or strong light emissions may be achieved. Moreover, the Er concentrations of silicates can be easily continuously changed through Y- or Yb co-doping, which is necessary to reduce the deleterious effects for 1.53 μm gain and luminescent efficiencies, such as the concentration quenching and up-conversions due to the neighboring Er ions. The Yb co-doped Er silicates have another advantage than the Y co-doping that is the sensitization effect of Yb for Er, which can enhance the excitation efficiency of Er. In this paper, we summarized our group

recent work about ErYb/Y silicates. We fabricated three kinds of waveguide structure, the strip-loaded, slot and hybrid ErYb/Y silicates waveguides, and the optical amplification was observed in these waveguide structures. In addition, 1.53 μm electroluminescence (EL) in ErYb silicates was also realized using hot carriers' impact excitations of Er ions. The current conduction behavior, EL emissions, and impact excitation cross sections were studied

This work was supported by the Peking University's 985 startup project and National Natural Science Foundation of China Grant No. 60907024.

1. R. M. Guo, X. J. Wang, K. Zang, B. Wang, L. Wang, L. F. Gao, Z. Zhou, *Appl. Phys. Lett.* 99, 161115, 2011.
2. R. M. Guo, B. Wang, X. J. Wang, L. Wang, L. Jiang, and Z. Zhou, *Opt. Lett.*, 37, 1427, 2012.
3. L. Wang, R. M. Guo, B. Wang, X. J. Wang, and Z. Zhou, *IEEE. Photo. Tech. Lett.*, 24, 9000, 2012.
4. B. Wang, R. M. Guo, X. J. Wang, L. Wang, L. Y. Hong, B. Yin, L. F. Gao, Z. Zhou, *Opt. Mater.*, 34, 1289, 2012.

8564-6, Session 1

Emission and optical gain properties of Si slot Er_xY_{2-x}SiO₅ waveguides

Hideo Isshiki, Takayuki Nakajima, Takuya Sato, The Univ. of Electro-Communications (Japan)

High index contrast Si-based slot waveguide is one of key technologies for the heterogeneous integration on a Si chip. The strong optical confinement to the low-index slot, such as Er_xY_{2-x}SiO₅, is expected for guided TM mode. The confinement effect leads to the modification of the optical mode density, resulting in the enhancement of radiative transition. We have fabricated planer Si-slot waveguides with Er_xY_{2-x}SiO₅ slot layers in order to demonstrate the dependence of the radiative emission on guided waveguide modes. The PL fine structure particular to Er₂SiO₅ crystal has been observed through the waveguide structure. We confirmed the enhancement of the TM mode edge emission, and the intensity was about two times higher than that of TE mode. We also demonstrate the fabrication of Er_{0.4}Y_{1.6}SiO₅ waveguide slotted into Si photonic crystal. Strong optical confinement for the C-band is confirmed. 30dB/cm modal gain is achieved in this device by VLS method.

8564-7, Session 2

Carbon nanotubes on silicon for light emission (*Invited Paper*)

Laurent Vivien, Nicolas Izard, Adrien Noury, Institut d'Électronique Fondamentale (France); Etienne Gaufres, Univ. de Montréal (Canada); Xavier Le Roux, Institut d'Électronique Fondamentale (France); Richard Martel, Univ. de Montréal (Canada); M. Tange, Toshi Okasaki, National Institute of Advanced Industrial Science and Technology (Japan)

Single wall carbon nanotubes (SWNTs) have generated a growing interest for several years due to their carbon based 1D structure. The metallic part of them (m-SWNT) as well as the semiconducting part (s-SWNTs) is more and more considered for their future use in microelectronics as electrode or transistor channel. For few years, s-SWNTs are also considered for photonic applications due to their tunable direct band gap in the NIR: optical telecommunications, datacoms and biosensing. To exploit their optical properties, we have developed an efficient technique which selectively extracts semiconducting-SWNTs. These high purified s-SWNTs allow a strong enhancement of the photoluminescence properties at 1.3 μm and 1.55 μm . These advances led to the first demonstration of optical gain in carbon nanotubes of about 180cm⁻¹ at the wavelength of 1.3 μm . The presence of energy threshold in the photoluminescence signal

and linewidth narrowing of the spectra clearly indicate that stimulated emission was obtained. This result is a precursor to obtain nanotube-based laser. Carbon nanotubes have then be integrated in silicon structures to develop a new class of optoelectronic devices. A complete study was carried out which led to the demonstration of the s-SWNTs absorption and emission coupling with evanescent silicon waveguides at a wavelength of 1.3 μm . The emission intensity at the device output was temperature-independent. These results open the door to the development of a new type of silicon photonic devices based on carbon nanotubes.

8564-8, Session 2

Photophysical properties of dendrimer phthalocyanine-functionalized single-walled carbon nanotubes

Hongqin Yang, Dandan He, Dongdong Ma, Yuhua Wang, Jiangxu Chen, Shusen Xie, Yiru Peng, Fujian Normal Univ. (China)

Single Carbon nanotubes (SWNTs) are very promising materials for polymer composites, energy conversion, sensing and biological applications. However, processing SWNTs and integrating them into real application is severely limited by a number of inherent shortcomings such as purification, manipulation and lower solubilities in organic solvents. To improve their solubility and overcome the aggregation, various functionalization strategies including covalent and noncovalent methods, have been explored. Incorporation of light absorbing antenna dendrimer phthalocyanine through a covalent and/or noncovalent linkage with the extended π electron of a carbon nanotube could constitute an ideal supramolecular nanoassembly for generating singlet excited energy and its conversion to chemical energy. In this paper, the photophysical properties of these two novel dendrimer phthalocyanine-functionalized single-walled carbon nanotubes were studied by steady-state fluorescence, time-resolved fluorescence and Raman spectroscopy. The effect of dendron generations on the photophysical properties was compared. Furthermore, the photoinduced electron transfer of these two dendritic phthalocyanine-functionalized carbon nanotubes was studied and compared. The carbon nanotube served as an electron acceptor and the dendritic phthalocyanine served as an electron donor. This study showed that the new dendritic phthalocyanine-functionalized carbon nanotubes could be utilized for subcellular localization and designed as molecular transporters.

8564-9, Session 2

Visibility of few-layer graphene

Yi-Hao Wang, Guan-Huang Wu, Ya-Ping Hsieh, Hsiang-Chen Wang, National Chung Cheng Univ. (Taiwan)

Graphene has emerged to be an exciting material with potential applications. A remarkable feature of graphene is that it is a Dirac solid, with the electron energy being linearly dependent on the wave vector near the crossing points in the Brillouin zone. It also exhibits unusual fractional quantum Hall effect and conductivity behavior. The discovery of the fascinating properties of single-layer graphene has generated much interest in the physical and materials sciences. To distinguish graphene layers become a very important issue. Using the discriminant for each location of the RGB pixel, then calculate the colors of the graphene layers; it can distinguish the different layers of the image thought multi-spectral imaging technology. Therefore this method can save time for material characteristics measurements, such as Raman, TEM, and AFM. We quickly determine the layers of graphene samples from a microscope image.

8564-10, Session 2

New design of As₂Se₃-based chalcogenide photonic crystal fiber for ultra-broadband, coherent, mid-IR supercontinuum generation

Rim Cherif, Amira Baili, Mourad Zghal, SUP'COM (Tunisia)

As₂Se₃ chalcogenide photonic crystal fibers (PCF) exhibit high nonlinearities and present a waveguide suitable for generating broadband supercontinuum (SC) for many applications such as fiber lasers, pulse compression and multi-wavelength optical sources. The optical properties of the fundamental mode in the PCF are accurately calculated in terms of chromatic dispersion, effective mode area and nonlinear coefficient.

In this paper, a new design of PCF is presented by increasing the ratio between d_2 the diameter of the second ring and d_1 the diameter of the inner ring surrounding the core. For the optimization of our structure we fixed d_1 to 1 μm and considered different ratios of d_2/d_1 varying from 0.8 μm to 0.88 μm by steps of 0.02 μm . The proposed fiber possesses an ultra-flattened dispersion curve over a wide wavelength range. The generated SC in such fiber is investigated, which has flat and smooth profile, covers a broad range. We examine the interplay of the nonlinear effects that lead to the construction of the SC as a function of the injected energy and the fiber length. We have found a bandwidth over two octaves coherent SC extending from 2 to 8 μm , by pumping at $\lambda_p = 5 \mu\text{m}$, 100 fs pulses with a relatively low energy of $E = 200 \text{ pJ}$ in only 5 mm fiber length. Supercontinuum generation was mainly attributed to the four wave mixing and the self-phase modulation. The significance of this work is that it provides a new type of mid-infrared coherent SC source with flat shape and broad band.

8564-11, Session 2

Direct patterning of high-resolution and large-area photonic devices by various unique ion-beam lithography approaches

Andre Linden, Raith Asia Ltd. (Hong Kong, China); Sven Bauerdick, Achim Nadzeyka, Raith GmbH (Germany)

Focused ion beam (FIB) systems and combined FIB-SEM microscopes are widely used for sample preparation and various analytical tasks. With the addition of a dedicated pattern generator and lithography software package, these microscopes are applied to some nanopatterning tasks increasingly utilising the focused ion beam as the primary technique. However, given the SEM/ microscope platform supports a tilting stage offering only micro meter positioning accuracy and poor repeatability, nanopatterning applications are usually limited to simple patterns over small areas within one field of view.

Materials like Gold – being very popular for applications in photonics and optics – include special challenges from an ion beam nanopatterning point of view. Due to the very large sputter yield it is difficult to achieve small feature sizes, high aspect ratio structures and a minimum lateral damage. The latter is due to Gold being highly intolerant to collateral beam (tail) damage. On one hand this is a main reason for photonic devices to fail and on the other hand it is a good test for high quality ion beam properties.

Here a novel IBL tool (Ion Beam Lithography, Raith ionLiNE) has been used which overcomes nanofabrication specific limitations of analytical FIB microscopes by utilising a dedicated lithography architecture and an ion column and source optimized for high resolution and large area nanopatterning, over high current performance. This includes in particular a laser interferometer stage, high beam to sample stability as well as enhanced beam current stability, excellent deflection accuracy and true automation capabilities (e.g. for additional positioning correction). These system features resolve the trade-off between the need of high resolution and long patterning time, i.e. by setting up automated over-night processes small currents of only a few pA become applicable to large patterns enabling improved resolution.

We report on the manufacturing of various photonic devices including antennas, photonic crystals, and large resonant arrays by direct milling, including many made in Gold. Results of feature sizes $< 10 \text{ nm}$, on highly topographic samples, of 3-dimensional structures and of long-term processes are presented. Thus the benefits of ion beam patterning and especially the added capabilities of IBL are discussed.

8564-12, Session 2

Sequential phonon excitation in cavity optomechanical system

Xue-Feng Jiang, Yun-Feng Xiao, Peking Univ. (China)

Whispering-gallery-mode (WGM) microcavities, with ultrahigh Q factors and small mode volumes, have attracted increasing interests in extensive applications, e.g., low-threshold lasing [1], nonlinear optics [2], cavity electrodynamics [3-4], cavity optomechanics [5] and miniature sensing [6-7]. Photon circulating in this type of microresonators greatly enhances the energy density inside the microcavities, providing a possible way for the study of the radiation pressure induced mechanical oscillation of the cavity material, i.e., the optomechanics. Once the mechanical oscillation modes are excited, they can couple with the photonic modes of the microresonators. Optomechanics is an interesting phenomenon and it provides a platform for the study of mechanical cooling, macro-quantum states, light storage and other potential fields. Traditional technique to study cavity-optomechanics is locking the laser wavelength to the cavity mode. However, it's complex to operate and hard to excite the high order sideband mode which is important in cooling and heating because pump laser wavelength is far away from the sideband resonant wavelength. Here in this work we report an experimental observation and theoretical analysis of the sequential multi-phonon excitation in an optomechanical system in which a high-Q WGM microtoroid cavity coupled with a fiber taper. With the low-pass filtering, we separate the fast-varying and slowly-varying processes and derive a very clear picture of multi-phonon emission.

We present an experimental observation of sequential phonons emission in an optomechanical system in which a high Q whispering-gallery microtoroid coupled with a fiber taper. Coupling between the phonon modes and the photonic modes leads to more than one resonance dip in the transmission spectrum. It is found that, with increasing input power or taper-cavity coupling strength, more and more phonons can be excited. This may constitute a new way of controlled photon-phonon interaction and is potential for realization of a new class of RF oscillators.

8564-13, Session 2

The effect of aperture layout design on the multi-GHz operation of light-emitting transistors

(Invited Paper)

Chao-Hsin Wu, Peng-Hao Chou, National Taiwan Univ. (Taiwan)

The base current plays a key role in the transistor since its discovery (16 December 1947, Bardeen and Brattain). The base current (IB) separates the low impedance input (emitter) from the high impedance output (collector), thus yielding a "transfer resistor." Recently, III-V semiconductor material has been fabricated as a heterojunction bipolar transistor (HBT) which can operate as a high speed device. The HBT can be modified and operated as a three-port light-emitting device (an electrical input, electrical output, and a third port optical output) by incorporating one or more quantum wells in the base region, thus becoming a heterojunction bipolar light-emitting transistor (LET). In the present work, we have designed different sizes of emitter diameter DE and base diameter DB of InGaP/GaAs LETs in aperture layout design. Through different layout designs, the LETs exhibit different electrical current gain ($\beta = \Delta I_C / \Delta I_B$) and optical light output due to

different carrier recombination processes in the transistor base region. By reducing the lateral emitter size from 18 to 13 μm , τ increases due to the higher injection current densities and better confinement of the radiative recombination in the base region. However, τ decreases when reducing the base diameter from 31 to 22 μm with fixed emitter diameter. The effective carrier recombination lifetime can be estimated from dc analysis and rf measurement (small-signal modulation). We have obtained multi-GHz spontaneous light modulation of LETs, and the device performance is closely related to different layout designs with different device parasitics.

8564-14, Session 2

Theory of phonon assisted secondary emission from a semiconductor quantum dot in the regime of vibrational resonance

Anvar Baimuratov, National Research Univ. of Information Technologies, Mechanics and Optics (Russian Federation); Ivan D. Rukhlenko, Monash Univ. (Australia); Anatoly V. Fedorov, National Research Univ. of Information Technologies, Mechanics and Optics (Russian Federation)

We develop a low-temperature theory of phonon assisted secondary emission from a semiconductor quantum dot, the electronic subsystem of which is resonant with the confined longitudinal-optical phonon modes. Our theory employs a generalized model for renormalization of the quantum dot's energy spectrum, which is induced by the polar electron-phonon interaction. The model takes into account the degeneration of electronic states and allows for several LO-phonon modes to be involved in the vibrational resonance. With these results, we solve the generalized master equation for the reduced density matrix, in order to derive an expression for the differential cross section of secondary emission from a single quantum dot. The obtained expression is then analyzed to establish the basics of optical spectroscopy for measuring fundamental parameters of the quantum dot's polaron-like states.

8564-18, Session 3

High-performance silicon optical modulators (Invited Paper)

Graham T. Reed, David J. Thomson, Frederic Y. Gardes, Youfang Hu, Nathan Owens, Univ. of Southampton (United Kingdom); Kapil Debnath, Liam O'Faolain, Thomas F. Krauss, Univ. of St. Andrews (United Kingdom); Leon J. Lever, Zoran Ikonik, Robert W. Kelsall, Univ. of Leeds (United Kingdom); Maksym Myronov, David R. Leadley, The Univ. of Warwick (United Kingdom); Igor P. Marko, Stephen J. Sweeney, David C. Cox, Univ. of Surrey (United Kingdom); Antoine Brimont, Pablo Sanchis, Univ. Politècnica de València (Spain); Guang-Hua Duan, Alban Le Liepvre, Christophe Jany, Marco Lamponi, Dalila Make, Francois Lelarge, Alcatel-Thales III-V Lab. (France); Jean-Marc Fedeli, Sonia Messaoudene, CEA-LETI (France); Shahram Keyvaninia, Gunther Roelkens, Dries Van Thourhout, Univ. Gent (Belgium)

In this work we present results from high performance silicon optical modulators produced within the two largest silicon photonics projects in Europe; UK Silicon Photonics (UKSP) and HELIOS. Two conventional MZI based optical modulators featuring novel self-aligned fabrication processes are presented. The first is based in 400nm overlayer SOI and demonstrates 40Gbit/s modulation with the same extinction ratio for both TE and TM polarisations, which relaxes coupling requirements to the device. The second design is based in 220nm SOI and demonstrates 40Gbits/s modulation with a 10dB extinction

ratio as well modulation at 50Gbit/s for the first time. A ring resonator based optical modulator, featuring FIB error correction is presented. 40Gbit/s, 32fJ/bit operation is also shown from this device which has a 6 μm radius. Further to this slow light enhancement of the modulation effect is demonstrated through the use of both convention photonic crystal structures and corrugated waveguides. Fabricated conventional photonic crystal modulators have shown an enhancement factor of 8 over the fast light case. The corrugated waveguide device shows modulation efficiency down to 0.45V.cm compared to 2.2V.cm in the fast light case. 40Gbit/s modulation is demonstrated with a 3dB modulation depth from this device. Novel photonic crystal based cavity modulators are also demonstrated which offer the potential for low fibre to fibre loss. In this case preliminary modulation results at 1Gbit/s are demonstrated. Ge/SiGe Stark effect devices operating at 1300nm are presented. Finally an integrated transmitter featuring a III-V source and MZI modulator operating at 10Gbit/s is presented.

8564-19, Session 3

silicon waveguide devices for photonic networks-on-chip (Invited Paper)

Lin Yang, Ruiqiang Ji, Jianfeng Ding, Rui Min, Institute of Semiconductors (China)

With chip multiprocessor continuously requiring more communication bandwidths, metallic-based electrical networks-on-chip (NoC) gradually becomes the bottleneck for improving the performance of chip multiprocessor due to its high power consumption, limited bandwidth and long latency. Silicon-based photonic networks-on-chip is considered as a potential solution to overcome the limitations of its electrical counterpart.

A series of optical devices are required to construct the optical interconnect between two processor cores, such as lasers, modulators, multiplexers, waveguides, de-multiplexers and detectors. Such a point-to-point interconnect is the simplest communication mode. However, for network application environment, the processor core is required to communicate with many processor cores. This function is usually completed by optical router, which is located at each node of photonic networks-on-chip and connects the local processor core with the neighboring nodes.

In this talk, we will review the status of silicon waveguide devices for photonic networks-on-chip and introduce our efforts on these topics. In the first section, we will introduce several critical issues for designing an optical modulator for photonic networks-on-chip. Following these guidelines, we demonstrate a 40 Gbps Mach-Zehnder optical modulator with the extinction ratio of 15 dB. In the second section, we will introduce the guideline for designing an N-port optical router for photonic networks-on-chip. Several five-port optical routers for Mesh photonic networks-on-chip have been demonstrated. By utilizing the periodic filtering property of microring resonator, the data transmission rate is expanded to 100 Gbps for single channel.

8564-20, Session 3

Non-reciprocity in silicon from dynamic modulation (Invited Paper)

Shanhui Fan, Stanford Univ. (United States)

Optical isolators, which suppress all backreflections, are of fundamental importance in large-scale optical information network. Achieving optical isolators on-chip is therefore of great importance for the future developments of silicon photonics. To achieve complete optical isolation, one needs to break time-reversal symmetry or reciprocity. Thus, it is well known that any structures that are linear and static, and that are constructed from materials having a symmetry permeability and permittivity tensor, can not behave as an isolator. In this work, we show that dynamic modulation of silicon structures can function as an effective isolator that reproduces all functionality of conventional

magneto-optical devices. We further show that the phase of the modulation can introduce an effective gauge potential for photons, opening new optical physics for the manipulation of light.

8564-21, Session 3

Active nanoplasmonics (*Invited Paper*)

Anatoly V. Zayats, King's College London (United Kingdom)

Recent advances in nanofabrication and subwavelength optical characterisation have led to the development of a new field of nanophotonics concerned with routing and conditioning of optical signals in scalable and integratable devices. In this context, surface plasmons, the electromagnetic excitations coupled to collective motion of conduction electrons near a metal surface, are emerging as a new optical information carrier that enables signal manipulation and processing on the subwavelength scale. Both surface plasmon polaritons and localised surface plasmons provide the electromagnetic field confinement and enhancement and ability to engineer dispersion by controlling nanostructure parameters. Plasmonic metamaterials play crucial role in the development of novel paradigms such as negative refractive index engineering, superlensing and optical cloaking.

In this talk we will discuss various realisations of plasmonic components for enhancing performance of conventional photonic devices such as (O)LEDs, VCSELs and sensors as well as for development of integrated nanophotonic circuits with particular emphasis on active functionalities such all-optical and electro-optical modulation and amplification of plasmonic signals and dispersion management. These functionalities facilitate possible applications of plasmonics in telecommunication networks, integrated photonics and lab-on-a-chip systems.

8564-22, Session 4

Si photonic crystal waveguide based delay lines (*Invited Paper*)

Ray T. Chen, The Univ. of Texas at Austin (United States)

No abstract available.

8564-23, Session 4

Engineered slot-comb photonic crystal waveguides

Charles Caer, Xavier Le Roux, Eric Cassan, Institut d'Électronique Fondamentale (France)

Slow light in photonic crystal waveguides exhibits peculiar features which provide substantial benefits for enhanced light-matter interactions. It increases the optical path length and the local intensity of light, meanwhile loss issues can be addressed by dispersion engineering of the guided mode. However, silicon nonlinearities are strongly limited by nonlinear losses (e.g. multi-photon absorption, free carrier absorption). This limitation can be overcome when introducing a slot filled by a highly nonlinear material. The slot further provides a stronger confinement of light. We extend the concept of slot photonic crystal waveguides by structuring the slot into a comb, forming Comb Photonic Crystal Waveguides (CPCWs). As reported in our previous works, we show that this comb enhances the light confinement at the narrowest parts. We perform dispersion engineering of the comb to achieve structures supporting high group index bandwidth product, and validate our design by FDTD calculations to study the coupling issue. We then measure the transmission in devices fabricated with 80kV e-beam lithography process. We perform cut-back measurements to investigate the losses, showing that CPCWs have losses are comparable with those of a standard W1 photonic crystal waveguides. Our measurements in a Mach-Zehnder Interferometer allow us to extract high group indices values, enabling us to measure waves

slower than $c/100$. This kind of devices offers promising applications in nonlinear optics.

8564-24, Session 4

Reducing radiation losses of one-dimensional photonic-crystal mirrors in a silica waveguide

Wei Ding, Rongjuan Liu, Zhiyuan Li, Institute of Physics (China)

One-dimensional PhC mirrors are constructed in a single-mode silica slab waveguide with a row of elliptical holes, whose photonic band gap can be quickly attained by eigen-mode calculations. Putting eyes on radiated waves rather than guided modes, we point out that component radiated waves only occur at the interfaces between the feeding waveguide and the PhC mirror section when propagating guided waves impinge on these interfaces. When component radiated beams overlap spatially, the total radiation loss of the PhC mirror periodically oscillates with the increase of the device length. We visualize this process by a simple picture and estimate the total radiation loss via an analytical model. For uniform PhC mirrors, the results of our model agree well with the simulated results in terms of the oscillation period of the total radiation loss, the damping of the oscillation, the initial phase of the oscillation, and the relative intensity of the radiation loss. We further investigate non-uniform PhC mirrors and find that, in contrast to the well-known "impedance-matching" picture, a progressively tapered transition from the feeding waveguide to the PhC mirror does not yield the lowest radiation loss. This surprising result embodies the interferometric nature of the radiation process in a low-index waveguide and clarifies the route of the widely reported "radiation recycling" phenomena. As the refractive index of the waveguide increases, the photonic band gap of the PhC mirror becomes deeper, the interference between component radiated beams gradually diminishes, and the "impedance-matching" picture revives.

8564-25, Session 4

Giant dispersive properties of planar graded photonic crystals

Charles CAER, Xavier Le Roux, Eric Cassan, Institut d'Électronique Fondamentale (France)

The dispersive properties of planar photonic crystals (PhCs) have been envisaged for years. In particular, the superprism effect has been considered to obtain a strong influence of input beam conditions (e.g. wavelength or input angle) on the light group velocity direction, enabling the design and fabrication of on-chip infra-red spectrometers and integrated optical demultiplexers. We extend here the properties of PhCs to the study of graded photonic crystals (GPhCs) made of a two-dimensional chirp of lattice parameters and show that GPhCs enable solving several drawbacks of dispersive PhCs like the beam divergence issues or the need of long preconditioning regions to precompensate beam diffraction effects. The proposed approach is applied to a square lattice air-hole PhC with a gradual filling factor that was fabricated using e-beam lithography and ICP etching techniques. A $0.25\mu\text{m}/\text{nm}$ spatial dispersion is demonstrated for a $60\mu\text{m}$ square GPhC structure in the 1470-1600nm spectral range without noticeable spatial or spectral spreading. Moreover, contrary to PhC superprism structures, a linear dispersion is obtained in the considered wavelength range. It is envisioned that similar GPhC structures could be also used in the mid-infrared wavelengths.

8564-26, Session 4

The temperature influence on the transmission character of a LC full-filled PCF

Jialu Wang, Yongjun Liu, Xiaoqi Liu, Weimin Sun, Harbin Engineering Univ. (China)

Two kinds of full-filled photonic crystal fibers (PCFs) are investigated by experiments. All the air holes of the index-guide photonic crystal fibers are filled with liquid crystal (LC). The light power is launched from the other end of the index-guide photonic crystal fibers. One end of the photonic crystal fibers which is not filled with liquid crystal was connected to the light power, and a part of photonic crystal fiber at the other end was filled with liquid crystal. The filling length of liquid crystal is nearly 5cm. Based on the same test conditions, experiments were carried on the two kinds of photonic crystal fibers. The full-filled part was heated to different temperatures to test the transmission character of the full-filled photonic crystal fibers. When the temperature increased from 30° to 60°, the output light spot gradually turned from a bright spot to a dark one and then faded away. When at 66°, the spot disappeared entirely. At the same time, the whole spectrum also moved towards to the shorter wavelength. After that, the output light power reappeared and became an entire different spot compared to the former spot when the temperature continued increasing. The experiments show that when the temperature is below 66°, the two kinds of fibers have the same performances, but once the temperature is higher than 66°, different phenomena will appear. The reappeared output light spot of smaller air holes presents a circle spot, while the spot of larger air holes shows a ring.

8564-27, Session 4

Optical properties of azo-chromophore attached on the surface of silica photonic crystal

Kwang Sun Kang, Kyungil Univ. (Korea, Republic of)

Optical properties of an azo-dye attached on the surface of the monodisperse silica photonic crystal have been investigated. The azo-chromophore was covalently attached to a 3-isocyanatopropyl triethoxysilane (ICPTES) having isocyanate functional group by a urethane bond formation reaction. The resulting disperse red/ICPTES (DRICP) was attached on the surface of the silica photonic crystal by hydrolysis and condensation reactions. The FTIR spectrum of the resulting product DRICP/silica sphere (DRICPSS) shows no characteristic isocyanate absorption peak at 2270 cm⁻¹ and shows a new absorption peak at 1700 cm⁻¹ corresponding to the C=O stretching vibration. This result indicates the complete reaction between -N=C=O and -OH. The DRICPSS has weak brownish color when it is dried. The color of the DRICPSS changed to intense red when it is wetted in methanol, ethanol and 2-propanol. The near infrared absorption maximum at 788 nm shifted to 718 nm for the DRICPSS after wetting in methanol. This system can be applicable to a sensitive alcohol sensor.

8564-15, Session 5

Si micro- and nano-structures for communication and energy applications (Invited Paper)

Ching-Fuh Lin, Shih-Che Hung, Shu-Chia Shiu, Hong-Jhang Syu, National Taiwan Univ. (Taiwan)

Si is one of the two most abundant materials on earth. In the past decades, Si has been the most important material for electronics. Thus it is also highly desired to use Si for applications in other areas. Here we report the use of Si micro-structures for optical-communications and Si nano-structures for energy applications. Sub-micron Si waveguides

is fabricated on (100) Si substrates using laser reformation technique. This method helps solve the incompatible problem for the integration of optics and electronics on a single Si chip. The typical thickness of the oxide layer on the CMOS transistor layer is below 100nm which, however, creates excessive optical loss due to the light coupling into Si substrate, so conventional Si-photonics need thick-oxide layer. Thus we develop laser reformation technique. High-power pulse laser is used to melt high-aspect ratio Si ridges from regular (100) Si waveguide and form circular-profile structure. Subsequently, thermal oxidation is implemented to oxidize the reformed structure, preventing optical loss due to light coupling to the substrate. For energy applications, Si nanostructures are fabricated using the metal-assisted chemical etching (MacEtch) technique. Si nanostructures could greatly reduce the surface reflection to enhance light harvest. In addition, Si nanowires are further combined with organic materials to form hetero-junction solar cells using low-cost solution process. Furthermore, the Si nanostructures and MacEtch process are refined to form completely single-crystal Si thin film. Thus the material cost of Si solar cells can be potentially reduced to only 1/10 of current ones.

8564-16, Session 5

Brilliant and tunable color by changing pore diameter of metal-coated porous anodic alumina

Jiawen Li, Ping Deng, Zhiqiang Zhu, Wenhao Huang, Univ. of Science and Technology of China (China)

Porous anodic alumina (PAA), with highly ordered microstructures, has attracted much attention due to some unique physical and optical characteristics. In recent years, PAA is also used to obtain different colors by methods such as growing nanowires, tuning pore depth, or sputtering metal on PAA surface. In this paper, we report a simple and precisely controllable method to tune color by changing the pore diameter of PAA. In order to obtain PAA with different pore diameter, we first prepare the PAA membrane by anodization of high purity aluminium foil in acidic solutions in a two step procedure and then immerse the fabricated PAA membrane into phosphoric acid to enlarge pore diameter. The different pore diameters of PAA with same depth are controlled by changing the second anodization time and immersed time in phosphoric acid. After sputtering metal on surface of PAA, the brilliant color can be seen on the surface of PAA. Different colors of PAA film with metal-coated are obtained using this method and colorful patterns are successfully fabricated. The physical models of the original and sputtered PAA are set up and the parameters of model are analyzed by Finite Difference Time Domain (FDTD) method, and the details of the color tuning method are further proposed. It is concluded that the color can cover the whole visible range using this method and color saturation is related to thickness of sputtering metal. This method will have potential use in decoration, color displays and anti-counterfeiting technology.

8564-28, Session 6

Nanowire-based solar cells (Invited Paper)

Xiuling Li, Univ. of Illinois at Urbana-Champaign (United States)

Integrating III-V with silicon (Si) through direct growth at the chip level has been one of the holy grails of III-V semiconductor devices, because it provides opportunities to realize integrated electronics and photonics systems and enable high efficiency multijunction tandem solar cells. The biggest barrier has been that III-V and Si semiconductors do not have the same lattice constants or thermal expansion coefficients, and therefore cannot be stacked on top of each other in a straightforward way without generating dislocations. Because of this, multijunction tandem solar cell structures often consist of layers with graded compositions through metamorphic growth, which inevitably results in lower material quality.

Vertical one-dimensional (1D) nanowire (NW) geometry, on the other

hand, allows a lot more freedom from lattice-matching requirements by dissipating the mismatch strain energy through the vast surface areas. In this talk, we report the realization of ternary III-V ($\text{In}_x\text{Ga}_{1-x}\text{As}$ or $\text{Ga}_x\text{As}_{1-y}\text{Py}$) NWs on Si and other substrates in a wide composition (energy) range through direct heteroepitaxy using metalorganic chemical vapor deposition (MOCVD). We demonstrate monolithically grown axial and radial p-n junctions in the III-V NWs, the interband tunneling diode junctions, as well as the improvement of solar cell efficiency by incorporating III-V NW structures in a planar Si cell.

Nanowire based solar cells fabricated using metal-assisted chemical etching (MacEtch) method will also be presented.

8564-29, Session 6

Morphology effects on the performance of flexible polymer solar cells under bending

Liqu Men, Qiying Chen, Memorial Univ. of Newfoundland (Canada)

Polymer solar cells have been actively pursued recently for their advantages of mechanical flexibility and low cost, which offer the possibility for coating onto flexible substrates, the prerequisite for roll to roll processing. However, the fabrication of multiple layers on flexible substrates exhibits significant technological challenges. In this study, we perform morphology observation of a nanostructured polymer bulk heterojunction flexible solar cell and the effect of morphology change on its photovoltaic performance upon bending. The photovoltaic device consists of poly(3-hexylthiophene) (P3HT) as a donor and [6,6]-phenyl-C61-butyric acid methyl ester (PCBM) as an acceptor, which are prepared on flexible plastic substrate of polyethylene terephthalate (PET) with one of the highly conductive polymers of poly(3,4-ethylenedioxythiophene): poly(styrenesulfonate) (PEDOT:PSS) (for example, PH510) as the anode. We investigate the photovoltaic performance of the flexible solar cells in comparison with solar cells of standard configuration. In particular, we study the morphology changes of the devices to reveal the effects of physical distortion of the cells on the photovoltaic performance of the devices. Morphology observation performed with scanning electron microscopy (SEM) indicates that the quality and morphology of the films become worse after bending with more cracks at significant bending. The SEM images of the individual layers of the device reveal that the morphologies of the PH510 and Al layers are significantly influenced by the bending effect. The photovoltaic performance of a flexible solar cell gradually decreases as the bending angle decreases.

8564-30, Session 6

Mid-infrared chalcogenide photonics (*Invited Paper*)

Juejun Hu, Hongtao Lin, Yi Zou, Lan Li, Okechukwu Ogbuu, Univ. of Delaware (United States); Sylvain Danto, J. David Musgraves, Kathleen Richardson, Clemson Univ. (United States) and Univ. of Central Florida (United States)

Chalcogenide glasses, namely the amorphous compounds containing sulfur, selenium, and/or tellurium, have emerged as a promising material candidate for integrated photonics given their wide infrared transparency window, almost infinite capacity for composition alloying, as well as high linear and nonlinear indices. This talk will review our recent progress on the processing and characterization of integrated photonic devices based on chalcogenide glass materials. We have shown that high optical quality glass films can be prepared using both traditional vacuum deposition as well as emerging solution derived techniques, enabling an entire array of unconventional device architectures both at the telecommunication wavelengths as well as in the 3-6 micron mid-infrared band. The examples include low-loss mid-infrared glass waveguides and resonant cavities on silicon, and robust tunable photonic devices on a flexible substrate platform. We further

demonstrate that these photonic devices constitute the basic building blocks for novel ultra-sensitive chemical sensors with single molecule detection capability, and high performance thermal imagers operating at room temperature.

8564-17, Poster Session

A simple and cost-effective method for fabricating antireflection structure using self-agglomerated metal nanoparticle as etching mask

Xiaoxuan Dong, Su Shen, Renjin Shao, Linsen Chen, Soochow Univ. (China)

Broadband antireflection property is significantly important for many optoelectronic devices, such as solar cells, flat panel displays, and charge coupled devices. Optical interference film stack has been widely used to reduce the reflection on the interface. However, film stack usually works in a specific wavelength bandwidth range and its performance deteriorates with increasing incident angle. Moreover, the material used for coating is limited and thermal mismatch between different coating material is an issue in fabricating such devices. With the rapid development of nanofabrication process, antireflection devices with nanoscale have drawn more and more scientists' attention. The nanostructure-based antireflection devices, with nanopillars, nanocones, nanospheres or nanoholes, can not only increase the transmission efficiently, but also improve the spatial and spectral dispersion characteristics. There are many methods to fabricate such devices, such as electron-beam lithography, laser interference lithography, and nanoimprint lithography etc. Nevertheless, the mentioned approaches suffer from low efficiency, time-consuming and expensive and complicated equipments and processes.

In this paper, a simple and cost-effective method to fabricate antireflection device based on nanoholes was proposed. The main idea is the combination of wet-chemical deposition of silver layer and physical etching on Si substrate. After the wet-chemical deposition, a rapid thermal annealing treatment at the 200°C-400°C was well done to form separate Ag nanoparticle islands owing to the self-agglomerated phenomenon. And then etch the sample with Ag nanoparticle by utilizing ICP technique, in this step, Ag nanoparticle acted as a mask of etching Si substrate. By controlling the etching parameter and etching time, the high performance antireflective structures were achieved. The relationship between each element of experiment and measuring results were further analyzed and discussed.

8564-56, Poster Session

Photonic crystal one-way delay waveguide

Hongliang Ren, Hao Wen, Jia Li, Yali Qin, Zhejiang Univ. of Technology (China); Weisheng Hu, Chun Jiang, Shanghai Jiao Tong Univ. (China)

It is of fundamental important for the coupling between waveguide modes and micro-cavity modes in an integrated optical system based on photonic crystals (PCs). By means of this resonator coupling, channel drop filters (CDF), splitters, switches, and other integrated optical devices can be built. In addition, the micro-resonator systems are developed to control the delay time of optical pulses by many researchers because the realization of all-optical signal processing relies on the ability to delay or store optical pulses. Recently, a PCs one-way waveguide with broken time-reversal has been proposed by, which is similar to the chiral edge states of electrons in the quantum Hall effect. Based on the one-way waveguide, the nature of waveguide-cavity coupling interaction is fundamentally adjusted. We design optical delay lines based on a photonic crystal one-way waveguide, which consists of some point-defect micro-cavities side-coupled to a photonic crystal one-way waveguide. According to the coupled mode theory in time, the transmission spectrum is discussed, and it is

demonstrated that the theoretical result maintains a unity transmission spectrum throughout the entire resonant frequency. Subsequently, the numerical result is calculated by using the finite element method (FEM), which agrees well with the theoretical analysis. As a pulse with a Gaussian profile is launched at the entrance of the waveguide, the structure is calculated by using the finite element method (FEM), and it is verified that the structure can control the delay of optical pulses. Compared with the optical delay lines by introducing the perfect electric conductor (PEC) slabs in the photonic crystal one-way waveguide, the devices have a wavelength-selective characteristic, which are of great significance in optical buffer applications.

8564-57, Poster Session

Analysis of relations between anti-reflective properties and silica structures

Yukun Zhang, Lifang Shi, Qiling Deng, Institute of Optics and Electronics (China); Jinglei Du, Sichuan Univ. (China); Xiaochun Dong, Shaoyun Yin, Chunlei Du, Institute of Optics and Electronics (China)

The paper compares the antireflective properties of three familiar silica structures at the range of the wavelength from 400 nm to 750 nm. The relevant results by finite-difference time-domain method demonstrate that the pyramid array possess the lowest reflection with the same parameters in other structures. Reflection on the structure surface is suppressed effectively resulted from changes in the reflective index caused by variations in the structure height. The reflective index gradient decides the reflection on antireflective structures. In most structures, reflection is stronger than that on the pyramid array, which is affected by the duty ratio on the substrate surface. The pyramid array possessing relatively large duty ratio rather than others can apply sequential reflective index gradient. Therefore, reflection on the pyramid array would be smaller than the other structures. Moreover, the relations among reflection, transmission, and the wavelength have been calculated. The reflection is attenuated with the structure height increasing. When the height is above 200 nm, reflective attenuation on the structure surface gradually gets damped. It indicates that the pyramid array with the height above 200 nm has the better antireflective properties, which is the useful guidance to fabrication of the antireflective structures.

8564-58, Poster Session

Infrared stop-band filter based on a subwavelength structure

Yanqin Song, Chinhua Wang, Yiming Lou, Bing Cao, Soochow Univ. (China)

In this paper, we propose stop-band filter in infrared region using a periodically chirped subwavelength structure. The subwavelength structure is made of a stack of metal and Ge pattern made on a thick metal layer that is deposited a Si substrate. It is found that an appropriately designed microstructure of metal-insulator-metal patches can generate a wideband infrared absorption, resulting in an infrared stop-band filter. Different metallic patch widths existed in a period generate trough in the reflection spectrum at different wavelengths. The full width at half magnitude (FWHM) of the stop-band filter can thus be adjusted by tuning the patch width. The larger the metallic patch width, the wider the bandwidth. The rejection depth of the stop-band was controlled by the metallic and dielectric materials employed and also the thickness of the materials. Under the condition of subwavelength dimension of the structure compared with the working wavelength, it is found that a FWHM of 4 μ m at central wavelength of \sim 10 μ m and 85% isolation depth can be achieved if Cu or Ag grating structures are employed. The results are obtained by FDTD numerical calculation. The proposed structure is helpful to the design of wideband efficient plasmonic absorbers in infrared or THz spectral regions.

8564-59, Poster Session

Effects of grating marks on lithography alignment precision

Jiangping Zhu, Song Hu, Institute of Optics And Electronics (China); Junsheng Yu, Univ. of Electronic Science and Technology of China (China)

In proximity lithography alignment, the method based on moiré fringes, its alignment marks consists of two sets of line gratings with slightly different periods, which are respectively etched on mask and wafer. The relative positions between mask and wafer are analyzed by phase of moiré fringes. And phase of moiré fringes are extracted by Fourier transform method. This alignment technique is capable of determining simultaneously alignment offset of x,y directions and is characterized by high accuracy, high reliability and easy operation, etc. But, the rational design of alignment grating marks parameters for this approach to realize high-precision alignment is of great importance. In order to boost the feasibility of moiré fringes alignment method, effects of a few physical parameters of grating marks on alignment accuracy are deeply investigated by theory reasoning as well as numerical calculation. The results imply that parameters of grating marks, such as period size and ratio, have an important influence on alignment scope and accuracy.

8564-60, Poster Session

Beam splitter with tunable power ratio by a composite structure

Kun Ren, Tianjin Univ. (China); Xiaobin Ren, Tianjin Univ. of Science and Technology (China)

Photonic crystals (PhC) that are periodic dielectric structures are proved to be excellent candidates for controlling an electromagnetic wave. The defects introduced in a perfect photonic crystal can confine the flow of light. Additionally, complex spatial dispersion properties of PhC structures provide mechanism to steer light. The propagation direction is given by the group velocity that is perpendicular to the equal-frequency contour (EFC) of the PhC. In this paper, we present a new method to modulate the direction of wave propagation.

We gradually modify the orientation of dielectric rods in a photonic crystal to investigate the propagation of light. The engineered PC with gradient constitutive parameter in a specific direction is called graded photonic crystal. The continuous bending of wave has been realized. The light guiding relies on the gradual variation of the direction of the group velocity during propagation. The ability to shape the EFC by the structure gradient offers a new way to design optical devices.

A new beam splitter is then designed with a composite constructed by two graded photonic crystals. We find that the incident beam is divided into two output beams by the designed splitter. A Y-shaped beam splitter is achieved. The splitting ability of the beam splitter is discussed further. We demonstrate the power ratio of the two beams can be adjusted easily by changing the location of the input beam.

8564-61, Poster Session

Bending the light by a gradually modulated photonic crystal

Xiaobin Ren, Tianjin Univ. of Science and Technology (China); Kun Ren, Tianjin Univ. (China); Mingcheng Guo, Tianjin Univ. of Science and Technology (China)

Due to their ability to manipulate light at the wavelength scale and their promise in ultra-compact integrated optical circuits, photonic crystals (PhC) have attracted much attention. Straight or bent defect is introduced in a perfect photonic crystal to confine the flow of light. The routing of light depends on the existence of photonic band gap. In this

article, we present a study on the guiding of light by modifying spatial dispersion property of PhC.

Light transport is studied by the use of finite-difference time-domain technique. It's shown that within a frequency window the non-diffraction light propagation can occur. This kind of propagation behavior depends on the self-collimation effect originated from flat shaped dispersion surface of the PhC. The propagation of light under different orientation angle and ellipticity of ellipse is investigated in detail. We find that the orientation of ellipse has an effect on the propagation direction. The degree of controlling light can be tuned by changing the ellipticity. The simulated results are analyzed from the point of equi-frequency contours. Based on the above results, we propose a method to control the flow of light by the use of the graded ellipse rod in PhC. We demonstrate that gradually varying the orientation angle of ellipse can result in smooth change in the light propagation direction. The beam redirection relies on gradual modifications of the PhC structure parameter that gradually change its dispersive properties. This provides a promising way toward designing optical devices for spatial beam routing. We believe that our results suggest a new direction for the realization of photonic crystal light circuits.

8564-62, Poster Session

Pulsed laser deposition of zinc nanostructures and their nonlinear optical characterizations

Yasaman Golian, Asma Motamedi, Mohammad Reza Rashidian Vaziri, Fereshteh Hajiesmaeilbaigi, Univ. of Tehran (Iran, Islamic Republic of)

The field of nanostructured materials has been widely recognized as one of the most promising and rapidly emerging research areas. Optical nonlinearity of metallic nanostructures has attracted much attention because of their fast nonlinear response that can be utilized in making them as potential optical devices. In this work, we report on preparation of Zinc nanostructures using the pulsed laser deposition technique. We have used a Nd:YAG laser (532 nm, 20 ns FWHM and 10 Hz repetition rate) as the ablation source. The laser fluence on the samples was about 1.5 J/cm² and a base pressure of 2e-5 Torr was maintained during the deposition process. The laser ablation was lasted for 30 and 45 min. The linear absorption spectra of the samples were obtained using a UV-Visible spectrometer. Optical absorption spectra show absorption peaks around 297 nm, due to the surface Plasmon resonance (SPR) of Zn nanoparticles. The morphology and the mean size of nanoparticles in the prepared nanostructured films were obtained by Atomic Force Microscopy. The nonlinear absorption coefficient and the nonlinear refractive index of the films were determined using the standard Z-scan technique. To this end, the input beam of a CW Nd:YAG laser (532 nm, 160 mW) was focused by a 19.5 cm lens to obtain a peak intensity of 4.42?10³ W/cm² at the focus. Our measurements indicate positive signs for the nonlinear optical absorption coefficients and refraction indices of the samples. We have also measured the optical limiting and Diffraction patterns of Zinc nanostructured thin samples.

8564-63, Poster Session

Optimized biomimetic antireflection nanostructure for photovoltaic applications

Fei Tao, Jiacheng Chen, Hang Zhou, Peking Univ. Shenzhen Graduate School (China)

Minimizing surface reflection loss is critical when designing high efficiency solar cells. In recent years, biomimetic antireflection nanostructures (such as 'moth-eye' structures), with their extraordinary broadband and omnidirectional antireflection properties, have caught much attention. It has been reported that single side biomimetic nanostructures improved broadband transmission through ITO/glass.

However, reflection from the interface between active region and ITO/glass still remains. In this study, we developed a double-side gradient-index nanostructure, and then examined its reflection spectrum with comparison to different biomimetic nanostructures using a FDTD simulation and effective medium theory. According to our study, any abrupt interface will introduce significant reflection. In order to minimize surface reflection, every abrupt interface should be replaced by gradient-index biomimetic nanostructures, including air/glass interface and active/glass interface. Monolayer of silica spheres serves as double-side gradient-index nanostructures, partially immersed into both sides of glass/ITO/PMMA. Spheres with diameter smaller than light wavelength show excellent antireflection properties. From simulation results, in normal incidence, average reflection rate of double-side AR coating (200nm sphere) is more than 4 times lower than single side AR coating within visible spectrum region (350nm - 850nm). Besides, this method can be widely used because sphere shape is not necessary in this antireflection structure; pyramid and parabolic shape are also applicable to form the AR coatings. Details of how to apply such biomimetic nanostructures in thin film solar cells were also discussed.

8564-64, Poster Session

The role of localized surface plasmon in the THz transmission of metallic rectangular hole arrays

Wei Xiong, Institute of Optics and Electronics (China) and Univ. of Electronic Science and Technology of China (China) and Graduate Univ. of the Chinese Academy of Sciences (China); Jun Yao, Institute of Optics and Electronics (China); Wei Li, Univ. of Electronic Science and Technology of China (China); Jingling Shen, Capital Normal Univ. (China)

We investigate the mechanism of transmission enhancement and the suppression in rectangular aperture arrays at terahertz band. The experimental results and numerical simulations suggest that SPPs propagating along the Al-Si interface lie at the heart of the observed phenomena. We also develop a simple model that explains the behavior of surface waves excitation, propagating and interfering in the array. In this interference model, we suggest there are three parts of radiation involved in the transmission phenomena. (1)First, the hole excites part of the incident radiation into surface wave act as a source of surface wave. Second, parts of the surface wave excited by the holes propagate along the surface of the array and convert to surface wave into free-space radiation. An instinct phase shift between two path of SPPs, which is the key factor in our model, is suggested to π . This interference model gives the direct evidence for role of SPPs in the enhanced optical transmission. This study contributed a better understanding of fundamental physics behind the extraordinary transmission of aperture arrays at THz range and provided a simple method for the THz devices designing.

8564-65, Poster Session

The synthesis of rutile nano-structured TiO₂ composite under low temperature

Lei Zhang, Shijiazhuang Univ. of Economics (China)

As an important inorganic functional material, nanometer-sized TiO₂ has many unique physical and chemical properties. Titania is one of the most effective photocatalyst and widely applied in purification of air and water because of its unique properties.

In order to improve the photocatalytic application of TiO₂, the low-density material such as Pst and beas TiCl₄ is proposed to be the raw carrier, and the nano-structured TiO₂ composite is obtained by combining the sol-gel technology and layer-by-layer self-assembly methods; The pure rutile nano-structured TiO₂ whose diameter is about 0.25μm are prepared under different conditions at low temperature. By

being calcined under 450°C the hollow sphere TiO₂ is prepared and its photocatalytic effect is studied.

8564-66, Poster Session

Simulation and analysis of the transparent and super-hydrophobic micro-nano surface structures

Zhijian Cai, Jianhong Wu, Soochow Univ. (China)

Super-hydrophobicity or “lotus effect” is an attracting feature for surface scientists, for its great potential in anti-fogging, self-cleaning and drag reduction applications. In optical engineering, the surfaces with the characteristics of super-hydrophobicity are also desired by many optical elements in field operation, such as camera lens and vehicle window. Since the micro-nano structure has critical significance for this feature, it's reasonable to design such a functional surface in micron and nanometer scale. However, most optical surfaces also require high transparency to keep the light transmission and imaging ability, which is a contradictive requirement on surface roughness, i.e. hydrophobicity needs rough surfaces but transparency demands smooth ones. It's a big challenge to design a surface with both features of super-hydrophobicity and transparency. This paper used Cassie wettability model to analyze the hydrophobicity on the one-dimensional and two-dimensional periodical structures, and used the finite-difference time domain (FDTD) method to analyze the optical scattering and diffraction properties of the surface. With the simulation and analysis, the design criteria of the transparent super-hydrophobic surface were proposed, and the self-cleaning and imaging ability of such surface were predicted.

8564-67, Poster Session

Absorption spectrum of the PbS doped silica fibers fabricated by ALD and MCVD

Tang Ye, Jianxiang Wen, Yanhua Dong, Tingyun Wang, Shanghai Univ. (China)

Quantum dots (QDs) provide unique advantages in the design of novel optoelectronic devices owing to the ability to tune their properties as a function of size. In order to apply this size effect in fiber optic transmission, various methods on QDs fabrication have already been studied, while the problem remained is that how to activate these QDs in structure like optic fibers.

In this paper, the technique of atomic layer deposition (ALD) is introduced to fabricate PbS doped silica fibers, whose absorption peaks are discovered to be blue shifted from 1230 nm to 920 nm when the number of ALD deposition cycles are varied from 80 to 30 during their preform fabrication. We explain this result by suggesting the PbS doped in fibers are under the 3D quantum confinement, i.e., quantum dots (QDs). Under such assumption, a first approximation of the PbS QDs radius is made by the effective-mass method. According to the wavelength these absorption peaks take place, radius of the PbS QDs inside the fibers are estimated to be decreased from 3.5 nm to 2.8 nm, which is reasonable to the deposition number we have used when preforms are being made.

The method of fabricating PbS doped silica fibers by ALD and MCVD can then be utilized to shift the peaks of fibers' absorption spectrum, and therefore, to enable them being excited at the wavelength one prefers.

8564-69, Poster Session

Focusing of cross-polarized light by plasmonic nanoantenna metasurfaces with phase discontinuities

Jing Lin, Wu Shibin, Institute of Optics and Electronics (??)

An ultrathin metasurface which is constructed with planar arrays of V-shaped nanoantennas is presented to realize the focusing of cross-polarized light. Based on the particular resonance properties of the V-shaped antennas, we can design the amplitude, phase, and polarization state of the scattered light, and then choose the proper antennas to satisfy the desired optical phase discontinuities. Numerical simulation of an illustrative metasurface is performed through finite element method (FEM) and shows agreement with the predesign. In addition, broadband light focusing is also discussed in this article.

8564-71, Poster Session

Dispersive wave generation in As₂S₃ slot waveguide with four zero-dispersion wavelengths

Shaofei Wang, Xianglong Zeng, Jungao Hu, Qianwu Zhang, Tingyun Wang, Shanghai Univ. (China)

Recently, nanophotonic slot waveguides, owing to their abilities of confining light in an embedded low index slot region with high electric field distribution, have attracted great research interests. What's more, dispersion can be freely tailored by using different materials or structural sizes, which can enable a number of interesting optical applications. As₂S₃ has larger nonlinear coefficients in IR wavelength region and strong Raman effects, which benefit the broad supercontinuum and IR generation.

Dispersive wave generation from the emitted solitons perturbed by high order dispersion are promising to generate femtosecond pulses in IR region and achieve the nonlinear wavelength conversion to blue-shift in supercontinuum generation in highly nonlinear microstructure fibers.

In this paper, we present the theoretical design of As₂S₃ slot waveguide that exhibits four zero-dispersion wavelengths and obtain a flattened and low dispersion curve from near-IR to mid-IR wavelength range for about 1800 nm bandwidth. We study the influence of slot waveguide on the total dispersion by choosing the different waveguide dimensions in the nanometer scale. By using a full-vector mode solver, COMSOL, we obtain dispersion of the quasi-TM mode through calculating the effective refractive index as a function of wavelength, thus four zero-dispersion points are located at: 1641nm, 2154nm, 2572nm, 3287nm. The mechanism of generating this kind of concave dispersion profile is mode transition induced by anti-crossing effect.

We also discuss the dispersive wave generation in As₂S₃ waveguide with four zero-dispersion wavelengths. Through numerical simulations under some practical conditions, we demonstrate that a amount of dispersive wave emission occur in As₂S₃ waveguide and the properties of the generated dispersive wave is fairly agree with previous detailed studies, which can be used such as frequency metrology, optical coherence tomography and microscopy.

8564-72, Poster Session

Absorption and microstructure characteristics of the PbS-doped silica optical fiber

Yana Shang, Long Li, Jianxiang Wen, Yanhua Dong, Tingyun Wang, Shanghai Univ. (China)

The microstructures of PbS-doped silica optical fiber have been built

and calculated by Gaussian-03 software. The electronic and optical properties of the local microstructures were investigated by using density functional theory (DFT). In the PbS-doped silica optical fiber material, the microstructures of $\text{PbS}(\text{SiO}_2)_n$ ($n=1-6$) were proposed, and then the initial structures were optimized by using density functional theory at the B3LYP level, with LANL2DZ+d (Pb) and 6-31G basis sets. After this, the stable ground state geometries for $\text{PbS}(\text{SiO}_2)_n$ ($n=1-6$) was obtained. We found that PbS molecule tended to form ring structures with SiO_2 molecules, just like the ring structures existing in the silica. And the gaps between the highest occupied molecular orbital (HOMO) and lowest unoccupied molecular orbital (LUMO) were also calculated for every stable microstructure, which were found to be different from the energy gaps of PbS clusters; Then the absorption characteristics were analyzed, and the excited states of the proposal microstructures in PbS-doped optical fiber materials were calculated by using Hartree-Fock, with the singles configuration interaction (CIS) method, and with the LANL2DZ+d(Pb) and 6-31G basis sets. We found the characteristics of the excited states changed significantly as the geometries of the microstructures changed. The PbS-doped silica optical fiber, which was fabricated by modified chemical vapor deposition (MCVD) and atomic layer deposition (ALD) were measured. Finally, the optical properties of the PbS-doped silica optical fiber measured by the experiments were compared to the results of the theoretical calculation to deduce the possibly existing microstructures in PbS-doped silica optical fiber.

8564-73, Poster Session

Functionalized nano-graphene oxide for cancer targeted imaging and photothermal therapy

Da Zhang, South China Normal Univ. (China)

Integrin $\alpha\beta_3$ is heterodimeric transmembrane receptor, expressed in endothelial cells. It has been extensively investigated as imaging and therapy targets, due to their key roles in angiogenesis, leukocytes function and tumor development and easy accessibility as cell surface receptors interacting with extracellular ligands. Herein we propose an active targeting nanocarrier system based on nano-graphene oxide (NGO) for imaging and photothermal therapy (PTT). The functioned nano-probe based on integrin $\alpha\beta_3$ monoclonal antibody labeled NGO was developed for targeting imaging and killing cancer cells upon 633 nm laser irradiation. The results revealed that the nanoprobe had a high efficiency targeted to the integrin $\alpha\beta_3$ -positive U87-MG cells, with minimal influence on $\alpha\beta_3$ -negative MCF-7 cells, and secure an excellent cell killing efficiency once activated with proper light irradiation with negligible dark toxicity. The feasibility of the graphene oxide, a potential photothermal transduction nanoprobe, may serve as a novel probe for potential cancer targeted imaging and therapy.

8564-74, Poster Session

Photon correlation spectroscopy study of mixture PEG with the AOT microemulsion

Soheil Sharifi, Univ. of Sistan and Baluchestan (Iran, Islamic Republic of)

The correlation function as a function of delay time was study by using photon correlation spectroscopy. The correlation function as a function of delay time shows a single strength exponential for AOT microemulsion with and without PEG. With increase of PEG concentration the delay time is increasing and also shape of correlation function is changing that describe the polydispersity increase with increase of concentration of PEG. In this work, the collective diffusion coefficient is constructing from the correlation function as a function of delay time for the AOT microemulsion mixed with different concentration of PEG. Our results shows increase of PEG concentration slowing down the dynamic of systems.

8564-75, Poster Session

Pauli equation for semiconductor quantum dots photoluminescence kinetics investigation

Vadim Turkov, Mikhail Leonov, National Research Univ. of Information Technologies, Mechanics and Optics (Russian Federation); Ivan D. Rukhlenko, Monash Univ. (Australia); Anatoly V. Fedorov, National Research Univ. of Information Technologies, Mechanics and Optics (Russian Federation)

Optical methods are the most universal techniques for the investigation of semiconductor quantum dots, which allow the determination of the dominant channels of energy and phase relaxation. We employ the kinetic Pauli equation to develop the first generalized model of the pulse-induced photoluminescence from the lowest-energy eigenstates of a semiconductor quantum dot. Without specifying the shape of the excitation pulse and by the assuming that the energy and phase relaxation in the quantum dot may be characterized by a set of phenomenological rates, we derive an expressions for the observable photoluminescence cross section, valid for an arbitrary number of the quantum dot's states decaying with the emission of secondary photons. Our treatment allows for thermal transitions occurring with both decrease and increase in energy between all the relevant eigenstates at room or higher temperature. We illustrate the application of the developed model by considering the processes of resonant luminescence and thermalized luminescence from the quantum dot with two radiating eigenstates, and by assuming that the secondary emission is excited with either a Gaussian or exponential pulse. Analytic expressions describing the signals of secondary emission are analyzed, in order to elucidate experimental situations in which the relaxation constants may be reliably extracted from the photoluminescence spectra.

8564-76, Poster Session

Anomalous size-dependent luminescence decay from PbS quantum dots

Alexander Litvin, Peter Parfenov, Elena Ushakova, Alexander V. Baranov, Anatoly V. Fedorov, Sergey A. Cherevkov, National Research Univ. of Information Technologies, Mechanics and Optics (Russian Federation)

The study is devoted to investigation of size dependence of kinetic and spectral luminescence properties of PbS quantum dots (QDs) in the near-infrared spectral region. Luminescence and absorbance spectra of PbS QDs solutions in the range of 0.8–2 μm are recorded. Radiative lifetimes are measured in the spectral range of 0.8–1.7 μm . Lifetimes lie between 250 ns for the largest QDs and 2.5 μs for the smallest. Lifetimes are close to predicted and Stoke shift is negligible for large QDs. At the same time small dots demonstrate an unusual long lifetimes and Stoke shift reaches 200 meV. These results confirm a presence of the long-live below-gap state. The energy of this state is size-dependent as well as radiative lifetime. Modeling showed that relaxation from this state is dominant for small QDs and is negligible for large dots. This result is in a good agreement with experimental data. Close-packed systems of PbS QDs demonstrate shorter lifetimes and similar size dependence. Red-shift indicates the presence of efficient energy transfer process in the close-packed system.

8564-77, Poster Session

Coherent random fiber lasers in weakly scattering system based on waveguide effect

Zhijia Hu, Qijin Zhang, Univ. of Science and Technology of China (China); Bo Miao, University of Science and Technology of China (China)

Coherent random fiber laser is obtained by end pumping a hollow optical fiber (HOF) filled with a dispersive solution of polyhedral oligomeric silsesquioxanes (POSS) nanoparticles and laser dye pyrromethene 597 (PM597) in carbon disulfide (CS₂). However, coherent random laser can not be observed for the same sample in the quartz cuvette. We analyze coherent random fiber laser in weakly scattering system by using sub-mean-free path regime. We suggest that the coherent feedback is caused by the cooperative effect of light scattering and waveguide effect. To research waveguide effect how to trigger coherent fiber lasing actions, we vary the refractive index of liquid core using the mixed solvent with different ratio of CS₂ and ethanol. Meanwhile, the influence of POSS nanoparticles with different weight concentration to the fiber random laser has been researched.

8564-78, Poster Session

MHz isolated XUV attosecond pulses generation using plasmonic enhancement in asymmetric metallic nanoantenna

Ying-Ying Yang, Institute of Semiconductors (China); Wei Sun, Laboratory of solid state laser sources, Institute of Semiconductors, Chinese academy of sciences (China); Qian-guang Li, Hubei Univ. of Engineering (China); Ling Zhang, Huai-juan Yu, Xue-Chun Lin, Institute of Semiconductors (China)

The asymmetric cross antennas are proposed for the control of the polarization and the selection of the multi-wavelength via varying the ratio of silver nanoantennas. It could generate the XUV pulse in the incidence of arbitrary polarization angle after optimization. The nanoplasmonic field enhancement in this silver cross antennas is fully theoretically investigated for the generation of MHz isolated extreme ultraviolet (XUV) attopulse. Numerical techniques are employed to determine the plasmonic fields in coupled nanoantennas. Within few-cycle laser, optimal conditions of nanoantennas for the production of MHz isolated attosecond pulse of XUV radiation via high harmonic generation (HHG) have been identified and compared. It opens up the possibility for the development of a compact source of XUV pulses with MHz repetition rates and the next generation of the nanophotonic devices.

8564-79, Poster Session

Characteristics of p-GaAs/p-AlxGa1-xAs/GaAs studied by surface photovoltage

Cui Fan, Nanjing Univ. of Science and Technology (China); Gangcheng Jiao, Canglu Hu, Science and Technology on Low-Light-Level Night Vision Lab. (China); Xinlong Chen, Yunsheng Qian, Nanjing Univ. of Science and Technology (China)

A comparative study of semi-insulating GaAs substrate, p-AlxGa1-xAs/GaAs and p-GaAs/p-AlxGa1-xAs/GaAs semiconductor heterojunctions has been done using the surface photovoltage (SPV) spectroscopy in metal-insulator-semiconductor (MIS) configuration. The epilayers were grown by metal organic chemical vapor deposition on the undoped GaAs substrate. The doping level was determined by cyclic voltammetry (CV) measurement at room temperature. SPV spectrums of

the samples were measured in the wavelength range 400nm ~ 1000nm at a modulating frequency of 175 Hz. The mechanism of SPV signals for different structures was theoretically analyzed. Transitions between the surface and bulk of electron-hole pairs (EHPs) generated by absorbed photons were discussed. Which surface space charge region (SCR) dominated contribution to SPV in a certain wavelength range was determined. The SPV signals were calculated in a similar way as the open circuit voltage of an illuminated photodiode. One-dimensional continuity equations forwarded by Moss was adopted for determine the distribution of excess minority carrier density. The parameters of the samples were calculated with different methods. The ideality factor of MIS configuration was investigated for samples with one side polished in air ambient, which was determined by the dependence of the surface photovoltage on incident photon intensity for band-to-band excitation. Normal 'linear SPV' Goodman plot (inverse SPV vs. inverse absorption coefficient) of GaAs substrate was applied for approach the minority carrier diffusion length. The minority carrier drift current of different layers were discussed in detail. At last the minority carrier diffusion length of p-GaAs layer and p-AlxGa1-xAs layer, surface or interface recombination velocity of different structure were calculated.

8564-80, Poster Session

Low loss optical modulator based on slot-loaded waveguide for unmodified CMOS process

Zhiping Zhou, Wei Tan, Qifeng Long, Huaxiang Yi, Feifei Hu, Xingjun Wang, Peking Univ. (China)

How to fabricate silicon photonics devices and electronics devices simultaneously in one shared CMOS process is becoming an urgent issue needed to be solved. Recently, a platform of electronic-photonics integrated circuits (EPICs) is proposed by MIT group, which makes zero infrastructure changes to the existing state-of-the-art CMOS process. However, in the platform of EPICs, polysilicon (poly-Si) layer is a must layer to form modulator. That will result in very high device loss, for example, 50~55 dB/cm for poly-Si waveguide because of high absorption coefficient of poly-Si at optical communication wavelengths.

In this paper, we proposed and demonstrated numerically a novel design of low loss depletion mode modulator based on poly-on-silicon slot-loaded waveguide for unmodified CMOS process. Different from the original design based on poly-on-silicon rib-loaded waveguide in the EPICs platform, slot structure is introduced into the poly-Si region. Taking advantage of confining light in low index region of slot structure, loss induced by poly-Si is significantly reduced. The simulation results show that after introducing slot structure into the poly-rib waveguide, the total loss of modulator phase shifter is largely reduced from 54.2 dB/cm to only 22.9 dB/cm, including 7.1 dB/cm mode loss and 15.7 dB/cm doping loss when slot width is optimized to 250 nm. The design is very simple and makes no change to the EPICs platform. And performances can be expected to be further improved with optimization of other parameters.

8564-81, Poster Session

Fabrication of two-dimensional metallic photonic crystals using colloidal gold nanoparticles

Zhaoguang Pang, Jing Yang, Hebei Normal Univ. (China)

We demonstrate the fabrication of two-dimensional (2-D) metallic photonic crystals (MPCs) using colloidal gold nanoparticles, two different fabrication methods that based on the laser interference lithography and laser interference ablation are employed for the construction of gold nano-dot arrays in square lattice, respectively. The microscopic and spectroscopic properties of the 2-D MPCs are systematically characterized by the scanning electron microscope (SEM) and the angle-resolved optical extinction spectrum

measurements, the strong couplings between the waveguide resonance mode and the particle plasmon resonance of the MPCs imply the success of the fabrication methods, which show potential applications in optoelectronic devices and sensors.

8564-82, Poster Session

Influence of gold nanoparticle size on the trapping performance of optical tweezers

Guang Lu, Harbin Engineering Univ. (China)

Gold nanoparticles are considered to be better probes than the traditional polystyrene nanobeads in nanomaterials and nanobiotechnology. Meanwhile, optical tweezers are very popular tool for manipulation and force measurement in these fields. Gold nanoparticles with different size will receive radiation forces with different scale in optical tweezers. This paper theoretically studies the trapping performance of the optical tweezers for the gold nanoparticle with different size, and finally gives the relation curves between the radiation forces and the radius of the of the particle.

8564-83, Poster Session

Preparation of silver island films with tunable surface plasmon resonance

Wanbing Lu, Wei Yu, Hebei Univ. (China); Xingkuo Li, Liping Wu, College of Physics Science and Technology, Hebei University (China); Xinzhan Wang, Hebei Normal Univ. (China); Guangsheng Fu, College of Physics Science and Technology, Hebei University (China)

Metallic island films exhibit light-induced localized surface plasmon resonance, resulting in selective photon absorption and local electromagnetic field enhancement. Many technological applications using them have been developed such as surface-enhanced spectroscopies, and chemical and biological sensors. In this paper, silver island films are prepared by pulsed laser ablation in vacuum using ns XeCl excimer laser. The effects of the number of ablation pulses, the temperature and time of post-annealing on morphology and surface plasmon resonance feature of the prepared silver island films are investigated by extinction spectra and scanning electron microscopy. It is found that films deposited with a small number of ablation pulses (60 or less), are not continuous, but formed of isolated nearly spherical Ag nanoparticles. With increasing the number of pulses, the mean diameter and the areal density of the nanoparticles increase monotonically. Further increase of the number of pulses, up to 240, quasi-percolated Ag films are obtained, and for 600 pulses or more, continuous films will be formed. Extinction spectra results show localized surface plasmon (LSP) is supported by the silver island films, while propagating surface plasmon (PSP) was supported by the continuous silver films. The LSP of silver island films consists of in-plane and out-of-plane LSP resonance modes. By changing the laser pulse numbers and annealing conditions, the longitudinal and transverse dimensions of silver islands could be adjusted, and then the peak positions and peak widths of in-plane and out-of-plane LSP resonance modes could be effectively controlled.

8564-31, Session 7

High-sensitivity silicon photonic biosensors based on cascaded resonators (*Invited Paper*)

Jian-Jun He, Zhejiang Univ. (China)

Silicon photonic biosensors based on cascaded resonators employing the Vernier effect are shown to be capable of greatly increasing the sensitivity. Two implementation schemes are presented, one using

two cascaded ring resonators, and the other by cascading a Fabry-Perot laser with a silicon ring resonator. Simple intensity interrogation schemes are developed to advance the planar waveguide sensor technology towards low-cost practical applications. Silicon photonic biosensors have great potential for lab-on-a-chip biological analysis. Waveguide sensors based on single microcavity have been extensively investigated. The commonly used sensing scheme is based on wavelength interrogation. An external tunable laser or high-resolution spectrometer is required to measure wavelength shift. The bulky and cumbersome instrumentation offsets the advantage of miniature waveguide devices and increases the overall system cost. A highly sensitive architecture based on two cascaded microring resonators employing Vernier effect was recently proposed and experimentally demonstrated. It can also be operated in intensity interrogation mode using a low-cost broadband source. Due to the Vernier effect, a small variation of the refractive index of an analyte results in a large wavelength shift in the envelope function of the transmission spectrum of the sensor, and consequently a large change in the transmitted power. The refractive index change of the analyte can therefore be derived from simple relative intensity measurement between the output port and the reference port without requiring any spectral measurement. A high sensitivity of 450dB/RIU was achieved experimentally using TE polarization mode, with a Vernier magnification factor of 150. The intensity-interrogated sensing scheme can also be implemented by cascading a Fabry-Perot (FP) laser with a SOI ring resonator. The FP laser serves as the light source as well as the reference comb for the sensing ring. Its sharp emission peaks with high spectral power density results in a higher sensitivity. Preliminary experiments have demonstrated a sensitivity more than twice that of the double-ring sensor.

8564-32, Session 7

Multiple transmission windows in a bilayered metamaterial based on twisted asymmetrically split rings

Ran Liu, Bo Na, Jinhui Shi, Zhengping Wang, Harbin Engineering Univ. (China)

We theoretically investigate electromagnetic resonances of a bilayered metamaterial in the optical frequency range. The metamaterial consists of two stacked split ring resonators with a twist angle spatially separated by a dielectric layer. The results show that multiple narrow-band transmission peaks may be achieved by coupling mutually between two twisted asymmetrical split rings at normal incidence, and manifested transmission properties can be controlled efficiently by regulating geometrical parameters of a unit cell. Our investigation offers an effective way to manipulate the resonant behavior in metamaterials.

8564-33, Session 7

Fano resonance in whispering gallery photonic microcavities (*Invited Paper*)

Yun-Feng Xiao, Bei-Bei Li, Xue-Feng Jiang, Yan Li, Qihuang Gong, Peking Univ. (China)

Whispering gallery photonic microresonators with high Q factors and small mode volumes open a myriad of lab-on-chip applications ranging from fundamental physics to various photonic applications. Here we experimentally reported Fano resonance in a single toroidal microresonator, in which two whispering-gallery modes were excited simultaneously through a fiber taper. By adjusting the fiber-cavity coupling strength and the polarization of incident light, the Fano-like resonance line shape could be engineered and further converted to the electromagnetically induced transparency (EIT) like line shape. The theoretical analysis revealed that both the Fano and EIT resonances originated from an indirect-coupling of two originally orthogonal WGMs, which was mediated by the common fiber taper waveguide.

Furthermore, Fano resonances were observed in a coupled resonator structure in which a low-Q microdisk and a high-Q microtoroid indirectly interact with each other mediated by a fiber taper. The Fano resonance could be controlled to change periodically by adjusting the distance between the two microresonators. The sharp Fano line shape holds great potential in optical switching and sensitivity-enhanced biochemical sensing.

8564-34, Session 7

Study of the spherical lenses as superlens for subwavelength imaging

Qiming Dong, Chaoping Yao, Xiaowei Guo, Univ. of Electronic Science and Technology of China (China)

The imaging resolution of a conventional optical microscope is limited by diffraction to ~ 200 nm in the visible spectrum. Efforts to overcome such limits have stimulated the development of optical nanoscopes using metamaterial superlenses, nanoscale solid immersion lenses and molecular fluorescence microscopy. These techniques either require an illuminating laser beam or have limited imaging resolution above 100 nm. Recently, using optically transparent microspheres as far-field superlenses to overcome the white-light diffraction limit was presented by Wang etc. They experimentally demonstrated 50nm resolution with a magnification factor up to 8, which provides new opportunities to image viruses and biomolecules in real time. Microspheres are placed on the top of the object surface by self-assembly. Microsphere superlenses collect the underlying near-field object information, magnify it (forming virtual images which keep the same orientation as the objects in the far-field) and pick it up by a conventional objective lens.

For real use, however, it is necessary to know the influence on the image quality when the parameters of the nanoscope vary, which is very important to design the imaging setup. For an example, what is the microsphere size allowed to obtain a good image for a fixed nanostructure? In this paper, we numerically investigate the spherical lenses used for imaging nanoscale chrome gratings by using a FDTD technique. The two-dimensional transverse magnetic wave at 400nm is employed to carry out the calculation. The perfectly matched layer absorbing boundary condition is used to efficiently terminate the outer boundary of the computational lattice. The simulations were done as follows. A fixed microsphere size was firstly used for imaging a nanoscale line. After obtaining the focusing nanojets, the refractive index of microsphere was changed to see what the allowed object size at a fixed microsphere is. Then, the microsphere size was changed to understand what the allowed object size for good imaging is. Finally, a triangular array whose feature size well below the diffraction limit was resolved by spherical lenses experimentally.

It is found that the focusing effect is efficiently enhanced with high refractive index and large scale sphere. The internal electric-field peak shifts toward the shadow-side surface of the sphere along the forward direction as the decrease of refractive index of sphere. It finally emerges from the shadow-side surface of the sphere. As the diameter of sphere lenses enlarges, the length of nanojet increases, in contrast, the full width at half maximum waist decreases. The physics mechanisms are presented to explain these phenomena. The waist width and length of nanojets are compared respectively to evaluate the quality of image. At present the imaging experiment is in progress, the imaging results will be given at subsequent paper. In conclusion, the near-field focusing effect of spherical lenses is demonstrated theoretically and experimentally and is believed capable of imaging objects with sizes well below the diffraction limit at visible incident light.

8564-35, Session 7

A compact evanescently-coupled germanium PIN waveguide photodetector

Zhijuan Tu, Kaibo Liu, Huaxiang Yi, Xingjun Wang, Zhiping Zhou, Zhangyuan Chen, Peking Univ. (China)

Germanium photodetectors have attracted much attention for their efficient capability of absorbing near infrared light and its compatibility with CMOS process. They are also the indispensable building blocks in the monolithic silicon photonic integration. High bandwidth, low cost Germanium waveguide photodetectors are urgently needed for high speed monolithic integrated receivers in the optical communication area. In this paper, we demonstrated a compact $1.6 \times 10^{-2} \text{ m}^2$ germanium pin waveguide photodetector on a Silicon-on-Insulator substrate. Germanium with the thickness of 500nm was deposited by Ultra High Vacuum Chemical Vapor Deposition. Our germanium photodetector exhibited a high 3-dB bandwidth of 20GHz at the wavelength of 1.55 μm . A clear open eye diagram at 10 Gb/s was also obtained, although the pulse pattern generator can only provide a 10 Gb/s signal. In addition, the dark current of the photodetector was measured to be 0.66 μA at -1V bias voltage, which is much lower than most of the reported devices.

This work was supported by National High Technology Research and Development Program of China (Grant No. 2011AA010302)

8564-36, Session 8

Simplified modal method of subwavelength gratings (Invited Paper)

Changhe Zhou, Shanghai Institute of Optics and Fine Mechanics (China)

A modal method is concerned with the modes excited, propagating, and coupled out into diffraction orders of a grating. Compared with the well-known rigorous-coupled-wave algorithm (RCWA), the modal method is less recognized. While the RCWA is a pure-numerical method, the modal method reveals a clear physical picture of the modes inside the grating. When a grating has a large period, it usually has too-many modes that are excited and propagating, and its analysis would be too complex. When a grating has a subwavelength period or a close-to-wavelength period, a few propagating modes will be excited. When a few modes are concerned in the analysis, we have a simplified modal method.

We have developed a simplified modal method to explain diffraction due to a deep-etched fused silica grating. Here the "deep-etched" means that the grating has a high ratio of deep-etched depth to the width of the groove. When a deep-etched fused silica grating has a subwavelength period, there are a few (one to two) lower modes that are propagating modes, and higher-order modes are evanescent. We have developed an average effective-index concept to describe a triangular deep-etched grating, and obtained simple analytical equations to describe a three-port beam-splitting grating. These analytical equations are impossible to obtain with the pure-numerical RCWA. We have realized that this simplified modal method is a useful tool for designing a variety of subwavelength deep-etched fused silica gratings for many practical applications.

8564-37, Session 8

Grating imaging scanning lithography for fabrication of large sized grating

Bin Yu, Changhe Zhou, Jia Wei, Shanghai Institute of Optics and Fine Mechanics (China)

Diffraction grating is a high-resolution dispersion optical element. It has been widely used as the key component in optical spectroscopy, telecommunication multiplexing and laser systems, etc. Recently there is a growing demand for large sized diffraction gratings in spectrometers industry, laser fusion facility, and its fabrication method is also a hot topic now. To fabricate large sized gratings, we have developed a grating imaging scanning lithography system. In this technology, the phase grating with jagged edge is used to generate diffractive beams and the spatial filter is used to select ± 1 order diffractive beams. Then two-beam interference on the substrate forms

the grating fringes. At the same time, a 4f-system is used to form an identical image with clear boundary in the interference area. A high precision two-dimensional mobile station, which enables the accurate positioning and move of the substrate, is utilized for complementary cyclical scanning, thus the image stitching errors are effectively eliminated. With this technology, we have fabricated a grating with period of $20\mu\text{m}$ and size of $100\text{mm}\times 100\text{mm}$. In this paper the grating imaging scanning lithography procedure is described step by step. The principles and the experimental results are also explained in detail. With the characteristics of a simple structure, high energy utilization and stability, this new lithography technology should be an efficient way to fabricate large sized grating in the future.

8564-38, Session 8

SOI-based bandwidth-tunable grating filter with a large tuning range

Danhua Wu, Huaxiang Yi, Li Yu, Zhiping Zhou, Peking Univ. (China)

Guided-mode resonance grating filters (GMRGFs) have been of great interest recently. Normally a GMRGF can only function as a narrow or a broadband filter, then property of tunable bandwidth has attracted more and more attentions since several applications require resonant filters with a tunable bandwidth. While a GMRGF with narrow bandwidth can be used in DWDM system and laser devices, a GMRGF with a wide bandwidth can be used in electro-optic modulators, light-matter interfaces, lasers, and detectors. Realization of a resonant waveguide grating filter with property of tunable bandwidth will be of great significance in terms of applications.

An SOI-based bandwidth-tunable filter has been proposed and successfully designed using binary blazed grating. The spectral reflectivity of this grating filter is investigated by Rigorous coupled-wave analysis (RCWA) method. It is demonstrated that the bandwidth of this grating filter can be changed from 0.5nm to 90nm by adjusting the angle of incidence, which is a large tuning range.

When $\theta = 45^\circ$, there is only one transmittance dip in the given wavelength range for both polarization states, which corresponds to a guided-mode resonance, proving that properties of narrow bandwidth is achieved; When θ is changed to 10° , there are two transmittance dips at separate wavelengths for each polarization state, and the distance between either pair is large enough, which makes the bandwidth of this filter become broader. As a matter of fact, when we adjust the angle of incidence, the position where the guided-mode resonance occurs will change correspondingly and this will result in the change of the bandwidth. We can take advantage of this property to design a bandwidth-tunable grating filter. Like using thermal tuning in microring resonator, angle of incidence is regarded as a controllable external factor which could be easily used to change the reflection property of resonant filters. This characteristic makes this device have a large number of potential applications in the laser devices and optical communication systems.

8564-39, Session 8

Modal analysis of a fused-silica three-port beam splitter grating

Wenting Sun, Changhe Zhou, Bin Yu, Shanghai Institute of Optics and Fine Mechanics (China)

A new modal analysis based on the simple mode method and multi-beam interference theory is proposed. Multiple reflection of propagating modes at grating interfaces is considered by introducing equivalent Fresnel coefficients into the diffraction process analysis. Then the proposed modal analysis is applied to design a rectangular-groove fused-silica grating as a three-port beam splitter. The diffraction efficiency expressions are derived in this paper, which are analogous to the results of multi-beam interference of a plane-parallel plate.

Dependence of diffraction efficiencies of the transmission 0th and 1st diffractive orders on the groove depth is obtained with optimized grating period and duty cycle. Compared with the simple mode method, the results based on the proposed modal analysis can match much better with those of rigorous coupled-wave analysis (RCWA), which proves the validity of the new modal analysis method. Moreover, the analysis results give an intuitionistic proof that the ideal 100% diffraction efficiencies of the transmission diffractive orders can't be realized and the transmission 0th order can't be cancelled in low-contrast grating. As the effective refractive indices of diffractive orders are introduced into the diffraction process analysis, this modal analysis is all valid under the usual incidence cases of normal incidence, Littrow mounting, and second Bragg angle incidence. More importantly, the proposed modal analysis provides a more accurate physical image of grating diffraction process, which should be a useful analysis tool for high-density grating.

8564-40, Session 8

Dual structure waveguide grating triplexer based on silicon-on-insulator

Junbo Yang, Xu Suzhi, Xu Jia, Kuo Zhou, National Univ. of Defense Technology (China)

A compact dual-structure waveguide triplexer which consists of two waveguide gratings with different period and fill factor is presented. It not only achieves efficient coupling between single mode fiber and a silicon-on-insulator optical waveguide, but also realizes effectively splitting, especially, for three different wavelengths, i.e. $1.31\mu\text{m}$, $1.49\mu\text{m}$ and $1.55\mu\text{m}$. By appropriate choice of waveguide/grating parameters including thicknesses, periods, height, and fill factor, to optimize the mode matching, and improve coupling efficiency and decrease the value of crosstalk, the coupling efficiency for $1.55\mu\text{m}$ wavelength can reach about 70% for TE polarization light over the 40nm wavelength bandwidth. The crosstalk is about -12dB . Simultaneously, for $1.31\mu\text{m}$ and $1.49\mu\text{m}$, the coupling efficiency is 58% and 40%, respectively. Moreover, the crosstalk of the left and the right branch of waveguide is -10dB and -14dB , respectively.

8564-41, Session 8

Ultra-short silicon MMI duplexer

Huaxiang Yi, Yawen Huang, Xingjun Wang, Zhiping Zhou, Peking Univ. (China)

The fiber-to-the-home (FTTH) systems are growing fast these days, where two different wavelengths are used for upstream and downstream traffic, typically 1310nm and 1490nm . The duplexers are the key elements to separate these wavelengths into different path in central offices (CO) and optical network unit (ONU) in passive optical network (PON). Because MMI have the multimode structure, it has some benefits including large fabrication tolerance, low-temperature dependence, and low-polarization dependence. However, conventional MMI duplexer is too large to be integrated. Here we present a novel silicon duplexer based on cascaded MMI.

Based on the self-image mechanism, the input light can obtain a uniform image through $n\lambda$ self-image-length in the MMI, where n is integer. In such a cascaded MMI duplexer, we made $n=1$ at MMI1, where 1490nm light formed the image at the cross-port. With 1310nm light input, there is no image at the cross-port, because the self-image-length for 1310nm is longer than the one for 1490nm . The MMI2 was placed after the MMI1 to collect the propagation mode for 1310nm . Then the self-image for 1310nm was obtained at the bar-port when $n=1$ also.

The experiment was carried on with the SOI wafer of 340nm top silicon. The spectral of the duplexer was obtained only around 1490nm . The extinct ratio is measured larger than 10dB . Another single wavelength laser was used to provide 1310nm . The extinct ratio for 1310nm is about 13dB .

8564-42, Session 9

On-chip polarization handling for silicon nanophotonic integrated circuits (*Invited Paper*)

Daoxin Dai, Zhejiang Univ. (China)

Silicon-on-insulator (SOI) nanowire provides a very promising way to realize the future large scale nano-photonics integrated circuits because of the CMOS compatibility and the ability for ultrasharp bending. However, SOI nano-PICs usually suffer the issue of severe polarization-dependence due to the giant birefringence. A general solution is using the so-called polarization-diversity technology, which is based on polarization handling with the devices like polarizer, polarization-beam splitter, as well as polarization rotator. On the other hand, polarization handling technologies are also very important for coherent optical communications. In this paper, we give a review for our recent work on silicon polarizers, PBS, as well as polarization rotators. First, small silicon polarizer is presented by utilizing the mode hybridization effect in a straight shallowly-etch SOI ridge waveguide. Second, an asymmetrical evanescent coupling system is presented as a better option than a symmetrical coupling system when used for realizing small PBSs because of the larger bandwidth, smaller foot-print and larger fabrication tolerance. Three types of ultrasmall PBSs based on silicon-on-insulator (SOI) nanowires are proposed and their design rules are given. Thirdly, a novel concept for an ultracompact polarization splitter-rotator is proposed by utilizing mode evolution and mode coupling. An adiabatic taper is introduced to realize the mode evolution from the TM fundamental mode to the first-order TE (TE₁) mode, which is then converted to the TE fundamental mode of an adjacent narrow waveguide through the asymmetrical coupling.

8564-43, Session 9

High-speed optical logic functions using Si-nanocrystal slot waveguides

Jian Wang, Huazhong Univ. of Science and Technology (China)

Optical digital signal processing may be required to overcome the speed limitation of electronics and support necessary functions for future computation and communication fields. Optical nonlinearities are candidates to enable various digital signal processing functions, among which logic gates are building blocks. Besides basic logic operations (AND/OR/NOT/XOR/NOR/NAND/XNOR), advanced logic functions have also gained great interest, such as data selector, Fredkin gate, half-adder, half-subtractor, full-adder and full-subtractor.

Driven by the increasing trend of large-scale integration, it is desirable to achieve logic functions using compact devices. Si-waveguide has attracted increased attention owing to its compactness and CMOS-compatibility. In this scenario, a laudable goal would be to realize advanced logic functions using optical nonlinearities in Si waveguides.

In this paper, we review our recent works on high-speed advanced logic functions by exploiting optical nonlinearities in Si-nanocrystal (Si-nc) slot waveguides. We present Si-nc slot waveguides with the light guided in the low-refractive-index Si-nc slot region sandwiched by high-refractive-index Si regions. The Si-nc slot waveguides show tight light confinement and enhanced nonlinearity. Based on twin degenerate four-wave mixing (FWM) processes, we demonstrate all-optical 160-Gbit/s simultaneous half-adder and half-subtractor using a single Si-nc slot waveguide as well as all-optical 160-Gbit/s data selector and Fredkin gate using two Si-nc slot waveguides. Moreover, based on twin degenerate FWM processes and cross-phase modulation (XPM) induced nonlinear polarization rotation, we demonstrate all-optical 160-Gbit/s simultaneous full-adder and full-subtractor using three Si-nc slot waveguides. Eye diagrams, extinction ratio (ER), quality factor (Q) and eye opening are analyzed to assess the operation performance.

8564-45, Session 9

Plasmon spectroscopy and imaging of individual gold nanodecahedra: a combined optical microscopy, cathodoluminescence, and electron energy-loss spectroscopy study

Viktor Myroshnychenko, Consejo Superior de Investigaciones Científicas (Spain); Jaysen Nelayah, Univ. Paris-Sud 11 (France); Giorgio Adamo, Univ. of Southampton (United Kingdom); Nicolas Geuquet, Facultes Univ. Notre Dame de la Paix (Belgium); Jessica Rodríguez-Fernández, Isabel Pastoriza-Santos, Univ. de Vigo (Spain); Kevin F. MacDonald, Univ. of Southampton (United Kingdom); Luc Henrard, Facultes Univ. Notre Dame de la Paix (Belgium); Luis M. Liz-Marzán, Univ. de Vigo (Spain); Nikolay I. Zheludev, Univ. of Southampton (United Kingdom); Mathieu Kociak, Univ. Paris-Sud 11 (France); F. Javier García de Abajo, Consejo Superior de Investigaciones Científicas (Spain)

The current tremendous interest in the optical properties of metal nanoparticles is due to their ability to host localized surface plasmon excitations in the visible and near-infrared parts of the spectrum. Plasmons can be tailored via the size and morphology of metal nanoparticles. Knowledge and experimental access to the electromagnetic field distributions associated to localized plasmon excitations in metal nanoparticles, with high degree of energy and spatial resolution, are of critical importance in the development of applications such as single-molecule detection, and surface-enhanced Raman scattering.

Here, we demonstrate the combined use of optical dark-field microscopy (DFM), cathodoluminescence (CL), and electron energy-loss spectroscopy (EELS) to study localized surface plasmons on individual gold nanodecahedra. These techniques provide information about plasmon excitations by recording different physical processes: light scattering exerted by the particles on externally incoming light, radiation emission produced by interaction with an electron beam, and energy loss suffered by those electrons. By exciting surface plasmons with either external light or an electron beam, we experimentally resolve a prominent dipole-active plasmon band in the far-field radiation acquired via DFM and CL, whereas EELS reveals an additional plasmon mode associated with a weak dipole moment. We present measured spectra and intensity maps of plasmon modes in individual nanodecahedra in excellent agreement with boundary-element method simulations. Our comparative assessment of the experimental techniques used in this work demonstrates an extremely high capability of electron energy-loss spectroscopy in resolving and imaging surface plasmons in subwavelength metal nanoparticles with unrivalled spatial and energy resolution.

8564-46, Session 9

Impact of emission broadening on plasmonic enhancement with metallic gratings

Xue Feng, Kaiyu Cui, Yidong Huang, Tsinghua Univ. (China)

In particular, the surface plasmon polariton (SPP) is attractive to enhance the spontaneous emission (SE) from active materials due to the larger density of state (DOS) and smaller mode volume comparing with optical wave, namely Purcell effect. Usually, the Purcell factor (PF) is calculated from the reduced form of Fermi's golden rule, where only the DOS and mode volume of photon (or SPP mode) are involved. Obviously, the PFs calculated with reduced form exclude the influence of active material and only evaluate the effect of cavity or SPP waveguide. However, for a practical emitter, the linewidth could not always be ignored. For example, the ensemble emission linewidth of

mass Si-NCs is about 220meV~400meV (90~160nm), which are much wider than the linewidth of the SPP DOS

In this work, the PF of SPP mode on Au-Si₃N₄ grating is calculated with full integration formula of Fermi's golden rule by taking account of the spontaneous emission linewidth from single silicon nanocrystal (Si-NC). The calculated PF is about 1.7~1.4 within the emission range of 1.9~1.6eV. Comparing with the PF value of 266.9~30.1, which is calculated without including the emission linewidth of Si-NC, it could be easily concluded that the impact of rather wide emission linewidth is fatal for applying plasmonic enhancement. To obtain some useful guidelines, we also discuss the necessary linewidth for effective plasmonic enhancement on Si-NCs. It is found that if the emission linewidth could be decreased to several tens of micro-eV, plasmonic enhancement would be helpful.

8564-47, Session 9

Eigenvalue analysis of plasmonic waveguides in layered geometries

Aytac Alparslan, Christian Hafner, ETH Zurich (Switzerland)

Due to the improvements in nanometer scale fabrication techniques, various photonic devices became popular research subjects in theoretical and applied electromagnetics. The analysis of plasmonic (lossy and dispersive) waveguides is one of the subjects that attracts much attention, since they are one of the main building blocks of photonic devices. Waveguides built in or on a multilayered geometry may exhibit extraordinary properties that cannot be observed in standard waveguides or waveguides in free space, e.g. guided wave modes in some layers, surface plasmon polaritons along metallic layers etc. In the analysis of such waveguides, commercial simulation tools exhibit difficulties finding the modes, especially when losses are present. In order to design such structures, a numerical method that can efficiently analyze the effect of layered geometries and losses in waveguides is of huge importance.

The Multiple Multipole Program (MMP) is one of the most accurate simulation tools for the analysis of plasmonic structures. It is a boundary discretization method that uses a set of analytical solutions of the Maxwell's equations (point sources, plane waves, Bessel functions, etc., so called expansions) as an approximation of the electromagnetic fields. In this work, the modified layered geometry Green's functions, i.e. the electromagnetic fields generated by a point source in a layered geometry, are used as an expansion set in MMP. Using these expansions in combination with a sophisticated eigenvalue search, the complex propagation constants of the waveguide modes are determined in an efficient way. In the talk, the derivation of the new expansions and using them in MMP will be discussed. Several numerical examples from OpenMaX, the open-source program that includes the latest MMP version, will be shown and compared with other numerical methods in order to demonstrate the efficiency and advantages of the method.

8564-48, Session 9

Ultracompact racetrack resonators based on hybrid plasmonic waveguides

Liangxiao Tang, Feifei Hu, Zhiping Zhou, Peking Univ. (China)

We propose and analyze a new hybrid plasmonic waveguide composed of a low index layer in between a metal and a high index layer, which can be used to realize a sharp bend with little radiation loss.

First, the effect of the geometrical parameters of the structure on the device is discussed with the help of simulation using finite element method (FEM).

Secondly, bends based on four different kinds of waveguides, hybrid plasmonic waveguide with metal lying outer side of the bend (HPWMOSB), hybrid plasmonic waveguide with the metal layer lying inner side of the bend (HPWMISB), traditional hybrid plasmonic

waveguide (THPW) and traditional dielectric waveguide (TDW), are discussed with finite-difference time-domain method (FDTD). With a small radius $R=0.8\mu\text{m}$, the bends of TDW has significantly larger loss compared to the other three due to its prodigious losses by radiation. What's more, when the radius of the bends decreases, loss of bends based on HPWMOSB increases slowly due to metal absorption loss, while that of the HPWMISB and THPW presents a rapid growth attributed to largely increased radiation loss.

Finally, a racetrack resonator based on HPWMOSB is designed with an outer radius of $0.8\mu\text{m}$ and straight waveguide of $0.89\mu\text{m}$, which presents an extinction ratio of 15.14dB and an insertion loss of 0.98dB. An ultracompact racetrack resonator with an outer radius of $0.5\mu\text{m}$ and straight waveguide of $0.1\mu\text{m}$ is also presented, which has a low transmission loss of 0.25dB and a high extinction ratio of 12.55dB.

8564-49, Session 10

Super-resolution imaging and molecule sensing by plasmonic nanoparticles on AgOx thin film (Invited Paper)

Din Ping Tsai, Ming Lun Tseng, National Taiwan Univ. (Taiwan); Yu-Hsuan Lin, Instrument Technology Research Ctr. (Taiwan); Chia Min Chang, Pin Chieh Wu, Yao-Wei Huang, You Zhe Ho, Ding-Wei Huang, National Taiwan Univ. (Taiwan); Hai-Pang Chiang, National Taiwan Ocean Univ. (Taiwan); Ru-Shi Liu, National Taiwan Univ. (Taiwan); Greg Sun, Univ. of Massachusetts Boston (United States)

In this talk we report the results for the applications of silver oxide thin film (AgOx) on molecule sensing and super-resolution imaging. Under light illumination, Ag nanoparticles can be generated on the AgOx thin film in situ. This photo-induced chemical reduction of AgOx thin film is very useful for the plasmonic applications therefore. For the super-resolution imaging, the focused-laser-generated silver nanoparticles in the AgOx thin film act as a scattering centres for activating the near-field optical imaging process. Localized surface plasmon generated at photo-generated Ag nanoparticles can enhance the near-field optical signals and functions as a probe for recording and readouts. Using this scheme, the 100-nm-diameter polystyrene nanosphere can be resolved by the focused laser beam with a wavelength of 635 nm. This "near-field cover glass slip" can achieve high spatial resolution and similar near-field scanning microscope function with the advantages of a higher scanning rate, less mechanical damage, low costs, and high compatibility with conventional optical microscopy. On the other hand, under light illumination, the plasmonic "hotspot" can be formed at the laser-generated Ag-nanoparticle aggregates, which can be used as the plasmonic substrate for molecule imaging and surface-enhanced Raman scattering measurement. The laser-processed AgOx thin films exhibit broadband enhancement of optical absorption and effectively function as active SERS substrates. Probing of the plasmonic hotspots with dyed polymer beads indicates that these hotspots are uniformly distributed over the treated area. It holds promise as a highly efficient and cost effective approach for applications in imaging and molecular sensing.

8564-50, Session 10

Tunable nano-pattern generation based on surface plasmon polaritons

Chinhua Wang, Fuyang Xu, Yiming Lou, Bing Cao, Soochow Univ. (China)

We present a numerical observation of a tunable 1D and 2D nano pattern generation and photolithography technique based on a surface plasmon resonant cavity formed by a metallic grating and a metallic thin-film layer separated by a photoresist layer. The tuning capability is implemented by varying the cavity length combined with the

polarization of the incident light, from which different surface plasmon interferometric patterns with inherently higher optical resolution than that of conventional surface plasmon techniques are generated in the cavity of photoresist layer. The physical origin of the tunability is analytically confirmed by the dispersion relation derived from the cavity system as well as the interferometric behaviors of the surface plasmon polaritons. The technique opens a new possibility to generate tunable ultra-deep subwavelength patterns by using a fixed diffraction-limited mask with capability of large area, deep exposure depth and flexibility of arbitrary 2D patterns.

8564-51, Session 10

Subwavelength imaging of self-assembled triangular nanoparticles through a silver superlens

Qiming Dong, Chaoping Yao, Xiaowei Guo, Univ. of Electronic Science and Technology of China (China)

Near field perfect imaging technique has received considerable attentions since 2000 when Pendry predicted that a diffraction free image can be produced through a flat slab lens on which SPs are excited and allow propagating and evanescent waves to pass into the recording medium when normal light source illuminates the silver lens through the mask. A lot of numeric simulations and experiments has been done to demonstrate the subwavelength imaging technique, which provides promises for high resolution nanolithography well below diffraction limit.

In most of these early experiments, however, the masks used targeted one dimension(1D) gratings with different periods. As we know, the grating is a periodic object which sometimes results in a frequency-doubled image. It is necessary to investigate the imaging for non-periodic objects. In this paper, subwavelength imaging through a silver superlens structure is performed by using self-assembled triangular particle mask. The schematic of the experimental setup is shown in Figure 1. The setup includes five layers, that is, mask/PMMA/silver/PMMA/recording medium. The mask is made of triangular nanoparticles on a quartz glass and PMMA as the dielectric spacers. The structure size mainly refers to the previous work and we confirmed the silver thickness is 35nm and the spacer thicknesses are 20nm and 15nm, respectively.

The first step in the experiment is fabrication of chromium mask onto a quartz glass substrate. Polystyrene spheres at 430 nm diameter are used for fabricating particle arrays mask by self-assemble method and then deposit a 40 nm thick chrome layer on it. A triangular particle array is formed after removing the PS spheres with an ultrasonic bath for 30 second. The side length of the triangle nanoparticles is 120 nm, about 1/3 of the incidence wavelength. Then, a 20 nm PMMA layer is spin-coated on the mask as the first dielectric spacer. A 35 nm silver layer is deposited on the sample using magnetron sputtering, followed by spin-coating of 15nm PMMA layer as the second dielectric spacer. The resist is spun on a silicon substrate and brought into vacuum contact with the second PMMA layer. Exposure is performed by mounting the superlens structures onto a rigid support that is compatible with a commercial Karl Suss optical mask aligner with 365 nm wavelength.

The resulted image in the photoresist is obtained. Due to the loss of much high frequency information, the particles' tips are rounding. The side length of the imaged triangular particles is about 50nm, which is twice smaller than the original size and about 1/7 of the incidence wavelength. But our experimental results demonstrated that the superlens wavelength imaging of nanoparticles. In future work, we will focus on better control of the imaging quality.

8564-52, Session 10

Ultra-deep subwavelength periodic patterning through multilayered metamaterial microcavity

Jigang Hu, Yongqiang Yu, Chunyan Wu, Linbao Luo, Hefei Univ. of Technology (China); Xiangxian Wang, Hai Ming, Univ. of Science and Technology of China (China)

In this work, we theoretically demonstrate an approach to achieve the sub-20 nm patterns feature sizes at the wavelength of 248 nm with p-polarization, utilizing a designed plasmonic cavity formed by the metallo-dielectric multilayer stacks (MDMS) and a metal layer coated substrate with a chromium mask on the top. This 1-D metamaterial plasmonic cavity enables the periodic SPP interference patterns with the high uniformity and intensity through the high pass filtering of the MDMS and SPP cavity resonance coupling. High resolution ($\sim\lambda/15$) and visibility (~ 1) of patterns have been numerically demonstrated at the cavity bottom, and the period of patterns is better stabilized against the variation of the cavity length in comparison with the conventional grating metal waveguide structure. This proposed ultra-deep subwavelength patterning method offered by the metamaterial cavity system provides a promising route in obtaining the large-area nano-scale patterns with high uniformity and visibility.

8564-54, Session 10

Amplification of surface plasmon polaritons in a methyl orange doped dielectric loaded SPP waveguide

Feng Huang, Hai Ming Yuan, Xiudong Sun, Harbin Institute of Technology (China)

Surface plasmon polaritons (SPPs) have received a significant attention in recent years because of their potential application in photonic devices at the subwavelength scale. Many SPP waveguide designs have been demonstrated, such as the long range SPP waveguide, the dielectric loaded SPP waveguide (DLSPW), metal-insulator-metal waveguide, etc. Being well bounded with small light spot and having small bending loss, the DLSPW has been widely used in waveguide-ring resonators and in-line Bragg grating, and exploited for wavelength selection in the telecommunication range. However, the intrinsic propagation loss of DLSPW leads finite propagation length ($\sim 40\mu\text{m}$) and limits its application. In this paper, we introduced methyl orange doped polymer to DLSPW used as gain medium to amplify the surface plasmon polaritons propagating in this waveguide. The DLSPW also had gratings at its input and output ports to couple in and out DLSPW. Upon the illumination of pump light, the DLSPW propagating in this waveguide was amplified. In addition, we theoretically and experimentally investigated the amplification characteristic. By measuring the power intensity of the output light in different condition, we got the gain factor as functions of the pump energy density, gain medium length and methyl orange doping density. When the pump energy density was higher than a threshold value, the power intensity of the output light was amplified as compared with those achieved without pump light, indicating that the loss of this waveguide was partly eliminate by the gain.

8564-55, Session 10

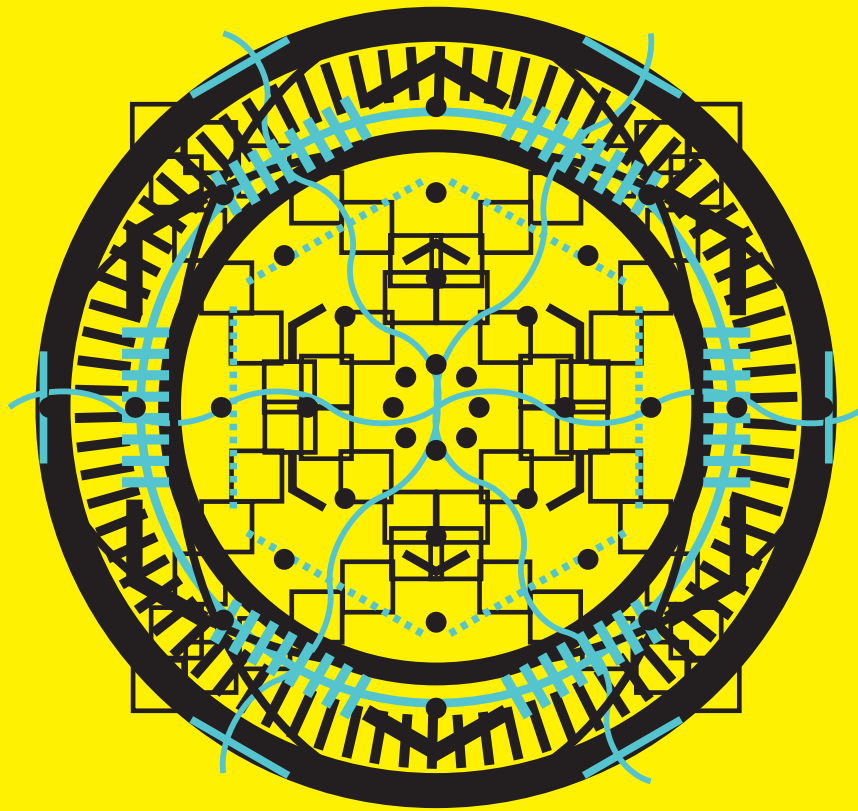
High performance absorber structure using subwavelength multi-branch dimers

Kebo He, Guangyao Su, Peking Univ. Shenzhen Graduate School (China); Zhaoyu Zhang, Peking Univ. (China)

We proposed a type of sub-wavelength multi-branch dimers which exhibit several tunable dipole-dipole-like plasmonic resonances. Three resonances found in a three-branch dimer, and each state corresponding to a unique current distribution on the dimer and that unique current distribution is mostly along one of three branches. On another word, these states are controllable through the design of the geometry which determines the oscillating path of the polarization charges on each resonance state. So, the LSP resonant state can be easily tuned in the dimer.

This unique property is extraordinarily useful to in the application of multi-resonances devices. An ultrathin absorber structure using three-branch dimer was proposed too. As a comparison, both absorptions spectra of the absorber structure with three-branch dimer and that with square dimer of the same area were accumulated. In the calculated wavelength range, there is only one peak showing in the structure with square dimer. However, in the structure with the three-branch dimer, three peaks exist, which certainly broad the absorption range and increase the total absorption as well. The total absorption of the three-branch dimer absorber is about two times of that of the square dimer absorber structure and further improvement can be achieved through the optimization of the structure.

Due to the tunable ability of the dimer, this absorber structure offer an path to fulfill broadband and wavelength tunable within optical frequency device, which could find its application in broadband thin-film thermal emitters, thermophotovoltaic cells, and multi-color filters.



Helping engineers and
scientists stay current
and competitive



Optics &
Astronomy



Biomedical
Optics



Optoelectronics &
Communications



Defense
& Security
Energy



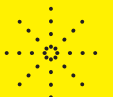
Lasers
Nano/



Micro



Technologies
Sensors



SPIE
Digital
Library

Find the answer
SPIDigitalLibrary.org